Internal Nitro-/Azidoalkyne Redox Processes in Heterocyclic Synthesis and Metal Free McMurry type Coupling

by

Pawan Surendra Dhote
10CC17A26015

A thesis submitted to the
Academy of Scientific & Innovative Research
for the award of the degree of
DOCTOR OF PHILOSOPHY

in

SCIENCE

Under the supervision of

Dr. C. V. Ramana

CSIR- National Chemical Laboratory, Pune

Academy of Scientific and Innovative Research
AcSIR Headquarters, CSIR-HRDC campus
Sector 19, Kamla Nehru Nagar,
Ghaziabad, U.P. – 201 002, India

October-2021

Certificate

This is to certify that the work incorporated in this Ph.D. thesis entitled ***"Internal Nitro-/Azidoalkyne Redox Processes in Heterocyclic Synthesis and Metal Free McMurry type Coupling"*** submitted by ***Mr. Pawan Surendra Dhote*** to the Academy of Scientific and Innovative Research (AcSIR), in partial fulfillment of the requirements for the award of the Degree of ***Doctor of Philosophy in Science***, embodies original research work carried-out by the student. We, further certify that this work has not been submitted to any other University or Institution in part or full for the award of any degree or diploma. Research material(s) obtained from other source(s) and used in this research work has/have been duly acknowledged in the thesis. Image(s), illustration(s), figure(s), table(s) *etc*., used in the thesis from other source(s), have also been duly cited and acknowledged.

Mr. Pawan S. Dhote
Research Student
Date: 04/10/2021

Dr. C. V. Ramana
Research Supervisor
Date: 04/10/2021

STATEMENTS OF ACADEMIC INTEGRITY

I, Mr. Pawan Surendra Dhote, a Ph.D. student of the Academy of Scientific and Innovative Research (AcSIR) with Registration No. 10CC17A26015 hereby undertake that, the thesis entitled "Internal Nitro-/Azidoalkyne Redox Processes in Heterocyclic Synthesis and Metal Free McMurry type Coupling" has been prepared by me and that the document reports original work carried out by me and is free of any plagiarism in compliance with the UGC Regulations on *"Promotion of Academic Integrity and Prevention of Plagiarism in Higher Educational Institutions (2018)"* and the CSIR Guidelines for "*Ethics in Research and in Governance (2020)"*.

Signature of the Student

Date : 04/10/2021

Place : Pune

It is hereby certified that the work done by the student, under my/our supervision, is plagiarism-free in accordance with the UGC Regulations on *"Promotion of Academic Integrity and Prevention of Plagiarism in Higher Educational Institutions (2018)"* and the CSIR Guidelines for "*Ethics in Research and in Governance (2020)"*.

Signature of the Co-supervisor (if any)

Name :

Date :

Place :

Signature of the Supervisor

Name : Dr. C. V. Ramana

Date : 04/10/2021

Place : Pune

CSIR – National Chemical Laboratory

DECLARATION

The research work embodied in this thesis has been carried out at CSIR–National Chemical Laboratory, Pune under the supervision of **Dr. C. V. Ramana**, Organic Chemistry Division, CSIR–National Chemical Laboratory, Pune – 411 008. This work is original and has not been submitted in part or full, for any degree or diploma of this or any other university.

4th October, 2021
Pune

Pawan Surendra Dhote
Organic Chemistry Division
CSIR–National Chemical Laboratory
Pune – 411 008

Dedicated to

My Beloved Family

With Lots of Love

Acknowledgement

Everyone I've known at NCL has had, for better or worse, an impact on my life, and I thank you all for it. Even if you are not specifically named below, know that I am grateful to each and every one of you.

First of all, I would like to express my deep sense of gratitude to Dr. C. V. Ramana for giving me an opportunity for doing my Ph.D under his supervision. His ideas, availability, and the freedom he grants to "see what will happen" with projects has allowed me to both learn and chase after crazy ideas, some of which have wound up in here. I can most certainly say, the intellectual freedom he gave me to explore my own ideas, to write manuscripts, and present research at conferences has helped me grow as an independent researcher. His patience, motivation, enthusiasm, and immense knowledge have helped me a lot during my Ph.D tenure. I could not have imagined having a better advisor and mentor for my doctoral studies. My sincere regards and respect for him will be cherished forever.

My sincere appreciation to my DAC members, Dr. Sailaja Krishnamurty, Dr. Ravindar Kontham, and Dr. Utpal Das for their encouragement, insightful comments and suggestions. I also want to thank Dr. D. S. Reddy (Director CSIR-IIIM, Jammu), Dr. B. L. V. Prasad (Director CENS, Bangalore), Dr. Santosh Mhaske, Dr. Dinesh Sawant and Dr. S. Hotha (IISER Pune) for their help and encouragement. Help from the spectroscopy, analytical and mass group is gratefully acknowledged. I sincerely thank support staff from NMR division especially Mr. Satish Pandole, Mrs. Deepali Jadhav and Mr. Dinesh Shinde, whereas, Mr. Ganesh Sevi (HRMS) for their unhesitant support and assistance. I also thank the former and current HOD, Division of Organic Chemistry and Director, NCL for providing infrastructural facilities.

I am grateful to Dr. Kumar Vanka and Vipin K. Raj for the DFT studies and also for his genuine and valuable suggestions. I also express my profound gratitude to Dr. Srinu Tothadi for introducing me to the field of crystallography, friendly attitude and valuable guidance.

I sincerely acknowledge Dr. Umesh Kshirsagar who taught me the first lessons in Practical Organic Chemistry, from (SPPU) Savitribai Phule Pune University (now shifted to IIT-Indore). Also I'm thankful to my teachers from Dept. of Chemistry, SPPU (M.Sc.), Fergusson College, Pune (B. Sc.) and Shahu's Garden Convent, Nagpur (SSC) for their unique way of teaching & inspiration in my life.

Acknowledgement

The training and support extended by my senior colleagues at the beginning and during my tenure of Ph.D., is worth mentioning, so as to express my thanks to Dr. Suneel Chepuri, Dr. Atul More, Dr. Narendra Reddy, Dr. Ravindra Phatake, Dr. Srinivas Kolluru, Dr. Dinesh Paymode, Dr. Suparna Roy and Dr. Ganesh More. I would also express my gratitude to Dr. Pitambar Patel for valuable suggestions and co-authoring with me for the (OBC) review.

My special thanks to Dr. V. Mullapudi (Babu Sir) and Dr. Rajendra Rohokale (Appa) for introducing me to the field of synthetic methodology. From the countless discussions we had over the years, I have learned so much from them and they have had a great impact on my perception towards organic synthesis and research in general. I would also like to thank Mr. Mahesh Shinde for supporting and encouraging me right from my Masters project to introducing me to the CVR group.

Many thanks to my colleagues Rupali, Anand (Hero), Pushpa, Sibadatta, Shaziya, Swapnil, Kishor (Pund & Thete), Pooja (Sarode & Pawar), Manoj, Harish, Pariksha, Nivedita, Nidhi, also the MSc trainees Shreya, Pandhari, Gauri with whom I shared so many memorable moments during my PhD tenure. I sincerely thank to my NCL friends Dr. Vivek, Rahul, Dipesh, Sangram, Mayur, Kailas, Sairam, Akash, Madhukar, J. Sabne, Digambar, Sagar, and many others for their irreplaceable cooperation.

I express my heartfelt thanks to my family, particularly my parents, sister (Mohini) and brother in law (Gyaneswar), thank you for your love, support, and unwavering belief in me. Whatever I am and whatever I will be in future is because of their enormous blessings, commitments to my ambitions and their selfless sacrifices. Words fall short to thank my niece Khushi for her love during my home visits. I also thank my uncles, aunts, cousins, in–laws and all my relatives for their love, care, support and best wishes. Last but not least, I'd like to express my deepest gratitude to my wife Meena for her love and constant support, for all the late nights and early mornings, and for keeping me sane over the past few months.

I am also thankful to DST-INSPIRE for the financial assistance in the form of a fellowship. Finally, my acknowledgement would not be complete without thanking the Almighty, for the strength and determination to put my chin up when faced with hardships in life.

Pawan S. Dhote

ABBREVIATIONS AND ACRONYMS

General Abbreviations:

aq.	Aqueous
Cat.	Catalytic
Conc.	Concentrated
h	Hour
HRMS	High Resolution Mass Spectrometry
NMR	Nuclear Magnetic Resonance
ORTEP	Oak Ridge Thermal Ellipsoid Plot
rt	Room Temperature

Abbreviations used for

Solvents:

AcOH	Acetic Acid
CH_2Cl_2	Dichloromethane
$CHCl_3$	Chloroform
CH_3CN	Acetonitrile
$DCE/(CH_2Cl)_2$	1,2-Dichloroethane
EtOAc	Ethyl acetate
MeOH	Methanol
PhMe	Toluene
THF	Tetrahydrofuran

General Chemicals:

K_3PO_4	Tripotassium phosphate
MsOH	Methanesulfonic acid
NH_4Cl	Ammonium chloride
Ph_2SO	Diphenyl sulfoxide
$PhI(OAc)_2$	Phenyliodonium Diacetate
PPh_3	Triphenylphosphine
$P(OMe)_3$	Trimethyl phosphite

Lewis Acids:

$Ni(ClO_4)_2$	Nickel perchlorate
$Sc(OTf)_3$	Scandium triflate
$Yb(OTf)_3$	Ytterbium triflate
$Zn(OTf)_3$	Zinc triflate

Silver & Gold Catalyst:

$AgSbF_6$	Silver hexafluoroantimonate
$AgNTf_2$	Silver(I) Bis(trifluoromethanesulfonyl)imide
AgOAc	Silver acetate
$AuCl_3$	Gold(III) chloride
$AuPPh_3Cl$	Chloro(triphenylphosphine)gold
BrettPhosAuCl	Chloro[2-(dicyclohexylphosphino)-3,6-dimethoxy-2′,4′,6′-triisopropyl-1,1′-biphenyl]gold(I)
IPrAuCl	Chloro[1,3-bis(2,6-diisopropylphenyl)1midazole-2-ylidene]gold(I)
JohnPhosAuCl	Chloro[(1,1′-biphenyl-2-yl)di-tert-butylphosphine]gold(I)
$PicAuCl_2$	Dichloro(2-pyridinecarboxylato)gold
XPhos AuCl	Chloro[2-dicyclohexyl(2′,4′,6′-trisopropylbiphenyl)phosphine]gold(I)
$(dppm)Au_2Cl_2$	[μ-(diphenylphosphine-κP)]bis[chlorogold(I)]

Other Catalyst:

$Pd(OAc)_2$	Palladium(II) acetate
$Pd(PPh_3)_2Cl_2$	Bis(triphenylphosphine)palladium(II) chloride
$Pd(CH_3CN)_2Cl_2$	Bis(acetonitrile)palladium dichloride
$PtCl_2$	Platinum(II) chloride
$Rh_2(OAc)_4$	Rhodium(II) acetate dimer

NMR spectral Informations:

br	broad
s	singlet
d	doublet
t	triplet
m	multiplet
q	quartet
quint	quintet
sept	septet
dt	doublet of triplets
ddd	doublet of doublet of doublets
ddt	doublet of doublet of triplets
tt	triplet of triplets

General Remarks

- ✓ All the moisture and air sensitive reactions have been carried out in anhydrous solvents under argon atmosphere in oven-dried glassware. The anhydrous solvents were distilled prior to use: CH_2Cl_2, DCE and DMF from CaH_2; methanol from Mg cake; THF on Na/benzophenone; triethylamine and pyridine over KOH; acetic anhydride from sodium acetate.

- ✓ ^1H NMR spectra were recorded on AV–200 MHz, AV–400 MHz, JEOL AL- 400 (400 MHz) and DRX–500 MHz spectrometer using tetramethylsilane (TMS) as an internal standard. Chemical shifts have been expressed in ppm units downfield from TMS.

- ✓ ^{13}C NMR spectra were recorded on AV–50 MHz, AV–100 MHz, JEOL AL- 100 (100 MHz) and DRX–125 MHz spectrometer.

- ✓ High-resolution mass spectra (HRMS) were recorded on a Thermo Scientific Q-Exactive, Accela 1250 pump and also EI Mass spectra were recorded on Finngan MAT–1020 spectrometer at 70 *eV* using a direct inlet system.

- ✓ Infrared spectra were scanned on FT-IR Bruker Alpha II spectrometer as solution of chloroform and measured in cm^{-1}.

- ✓ All reactions are monitored by Thin Layer Chromatography (TLC) carried out on 0.25 mm E-Merck silica gel plates (60F–254) with UV light, I2, and anisaldehyde in ethanol as developing agents.

- ✓ All evaporations were carried out under reduced pressure on Buchi rotary evaporator below 50 °C unless otherwise specified.

- ✓ Silica gel (60–120), (100–200), and (230–400) mesh were used for column chromatography.

CONTENT

CONTENT

Synopsis Report

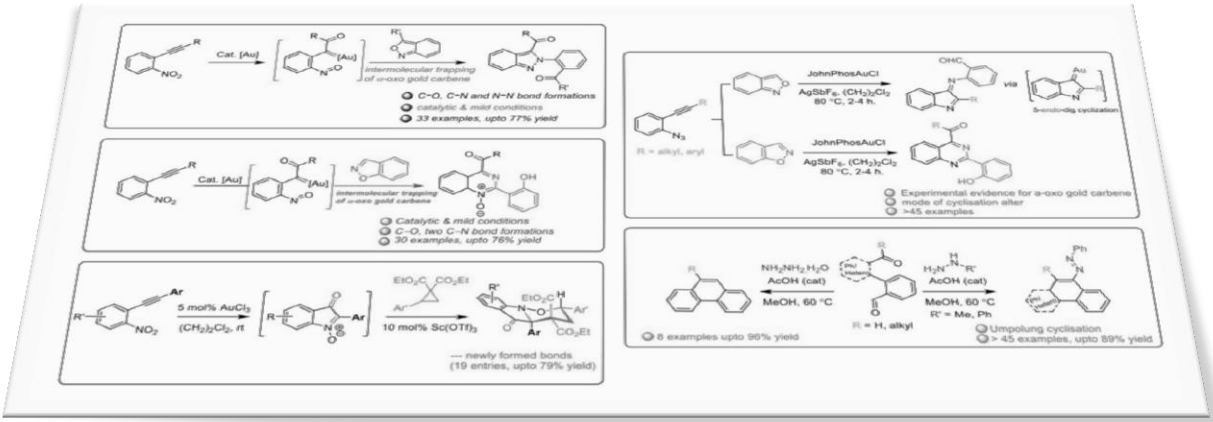

AcSIR	**Synopsis of the Thesis to be submitted to the Academy of Scientific and Innovative Research for Award of the Degree of Doctor of Philosophy in Sciences/ Engineering**
Name of the Candidate	Mr. Pawan Surendra Dhote
Degree Enrollment No. & Date	10CC17A26015; August 2017
Laboratory	Division of Organic Chemistry, CSIR-NCL, Pune
Title of the Thesis	Internal Nitro-/Azidoalkyne Redox Processes in Heterocyclic Synthesis and Metal Free McMurry type Coupling
Research Supervisor/ Co-supervisor	Dr. C. V. Ramana (CSIR-NCL, Pune)

Keywords: **Nitro-alkyne, Azido-alkyne, Donor-Acceptor cyclopropane, Gold catalysis, Cycloisomerisation, McMurry coupling.**

Introduction and Statement of purpose

Gold catalyzed reactions are increasingly emerging in the literature since the past few decades.[1] An interesting class of gold-catalyzed reactions that needs a mention in this context are the involvement of gold-carbenes in these processes. The oxygen (*nucleophilic oxygen atom donors such as nitro, amine-/pyridine N-oxides, nitrone, sulfoxides, and epoxides*) or nitrogen atom transfer (*azides, nitrogen ylides, (benz)isoxazoles and anthranils*) to alkynes catalysed by gold-complexes proceeds *via* an addition−elimination process leading respectively to α-oxo/α-imino gold carbenes.[2] These transformations have been well explored in the synthesis of diverse heterocyclic structures and also in total synthesis.

Objectives

- Catalytic C–N, N–N and C–C bond formations through the interruption of the internal nitroalkyne/azido-redox process with N–centered nucleophiles, especially those that are known to participate in the carbene transfer reactions.
- Switching the mode of cyclisation (*inter-/intramolecular*) of gold catalyzed azidoalkyne reactions by different N-centered nucleophile to synthesize complex heterocyclic

scaffolds of biological significance and expand the utility of these products by synthesizing focused small molecule libraries.

- Isolate and/or provide indirect support for the existence of gold carbene intermediates in the internal nitroalkynes redox processes.
- Catalytic C–N and N–O bond formations *via* Lewis-acid mediated nitroalkyne cycloisomerisation and its cycloaddition with DA- cyclopropanes.
- Expanding the utility of product by showing metal free McMurry type of coupling for the synthesis of polycyclic aromatic compounds.

Methodology

This thesis deals with the development of some novel cascade transformations *via* trapping- or diverting the proposed α-oxo- or imino gold carbenes and these two aspects have been covered respectively in the Chapters 1 and 2. The third chapter deals with reinventions of an old reaction that has been come across by us in the process of exploring the synthetic utility of the compounds resulted during our initial endeavors.

Chapter I: Development of Novel Cascade Reactions *via* Trapping α-Oxo/α-Imino Gold Carbenes

This chapter has been divided into two sections.

Section A. Interrupting the [Au]-Catalyzed Nitroalkyne Cycloisomerization: Trapping the Putative α-Oxo Gold Carbene with 2,1-Benzo[*c*]isoxazole and 1,2-Benzo[*d*]isoxazole:

The gold-catalyzed intramolecular redox cyclization of o-alkynylnitrobenzens documented by Yamamoto is an important discovery that has opened two complementary research domains.[3] Advancing this cyclization with the other metals as well as developing the new methods around the products that result from this reaction is one aspect that has seen growing interest. On the other hand, the idea of generating the α-oxo gold carbenes *via* oxygen transfer to alkynes has established another important aspect in gold-catalysis. Various

developments regard to the internal redox cyclization of nitroalkynes focusing mainly with the gold-complexes and the synthetic methods developed around it from our group and from other groups, albeit providing the details of similar transformations documented with other metals so as the complementary reactivity/diversity of these transformations, has been provided in the introductory part.

This section dealt with the [Au]-catalyzed nitroalkyne cycloisomerization of 2-alkynylnitrobenzenes leading to anthranils that has been interrupted by possible trapping of the postulated intermediate α-oxo gold carbene with an external nucleophile such as 2,1-benzo[*c*]isoxazole (anthranil) and 1,2-benzo[*d*]isoxazole. At the outset, this provided a simple synthesis of highly functionalized 3-acyl-(2-formylphenyl)-2H-indazoles with sequential C−O, C−N, and N−N bond formations and quianozoline N-oxides with sequential one C−O and two C−N bond formations. The control and competitive experiments provided an indirect support for the existence of α-oxo gold carbenes in the [Au]-catalyzed internal redox processes of nitroalkynes.

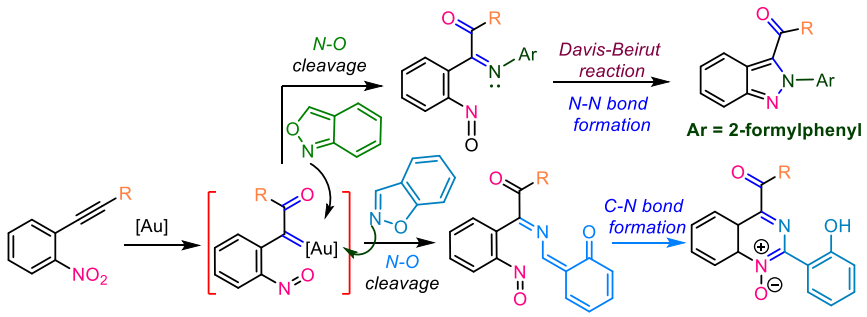

Section B. One-Pot Au[III]-/Lewis Acid Catalyzed Cycloisomerization of Nitroalkynes and [3 + 3] Cycloaddition with Donor−Acceptor Cyclopropanes:

This section deals with the synthesis of a tricyclic pseudoindoxyl scaffold from 2-nitroalkynylbenzenes, comprising of an Au(III)-catalyzed nitroalkyne cycloisomerization leading to isatogen and its highly diastereoselective [3 + 3]-cycloaddition with donor−acceptor cyclopropanes mediated by a Lewis acid. The overall process leads to the sequential C–N and N–O bond formations.

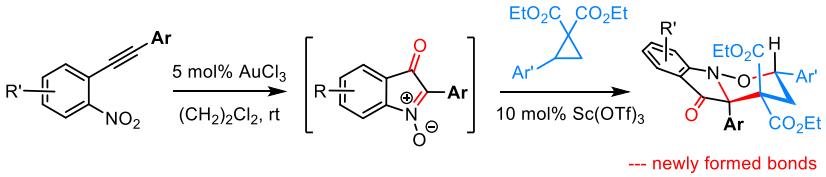

Chapter II: Complementary [Au]-Catalyzed Cyclization of 2-Alkynylphenylazides Directed by Competing Inter- *vs* Intramolecular Nitrogen Tranfer

Toste and co-workers documented the possibility of generating α-imino gold carbenes employing azide as a nitrogen source in the year 2005.[4] This opened up a new avenue in the gold catalysis "gold-catalyzed nitrene transfer reactions", initially employing azides as the nitrogen source. Later, the domain was expanded with the introduction of nitrogen ylides, isoxazoles and anthranils.[2] These reactions have attracted the attention of various research groups across the globe because of their high efficiency in constructing a wide range of nitrogen containing heterocyclic units and all the reactions procced *via* the formation of α-imino gold carbene.[2] In this chapter, we have developed a general convergent method for the synthesis of highly functionalized quinazolines by switching the mode of gold catalyzed cyclisation of 2-Alkynylphenylazides with the known nitrogen-transfer reagent 1,2-benzo[*d*]isoxazole, moreover the synthesis of functionlised indoline-imine scaffolds were also encompassed by trapping the well-known α-imino gold carbene with 2,1-benzo[*c*]isoxazole.

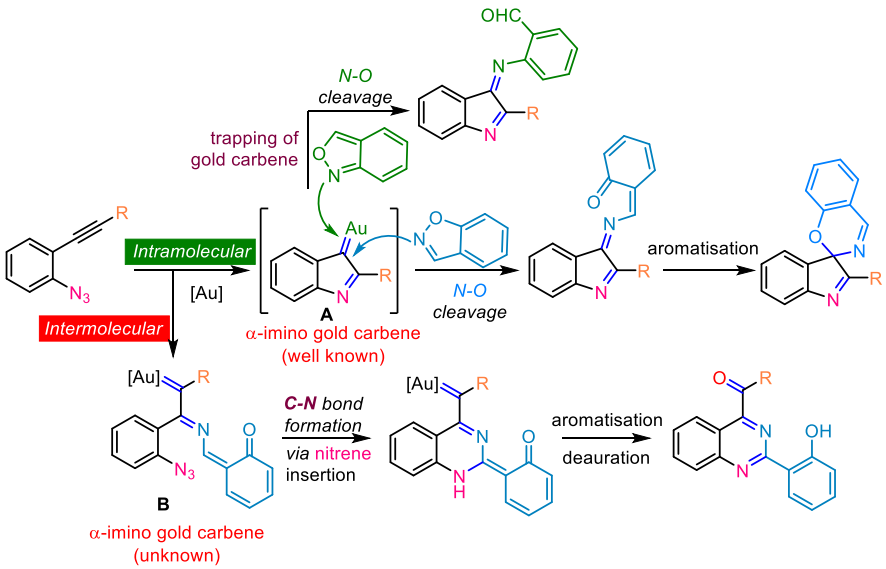

Chapter III: Metal Free McMurry Type Coupling: Synthesis of 2H-indazole π-Conjugated Scaffolds:

The construction of polycyclic aromatic compounds (PACs) containing heterocycle fused π-conjugated systems especially, 2H-indazole π-conjugated scaffolds are of great interest in biological, chemical and materials sciences,[5] which can be achieved by combination of cross-coupling reactions as well as intramolecular C=C bond formation, and has for long, been a pursuit in the synthetic community. Recent decades have witnessed an impressive endeavors in the field of carbonyl olefination that include the Wittig reaction,[6] the Peterson reaction,[7] the Julia olefination[8] and the Tebbe–Petasis olefination.[9] Among these classical olefination methods, for the intramolecular C=C bond formation, the McMurry reaction[10] mediated by low-valent titanium (LVT) reagents is a powerful strategy which can convert dicarbonyl functionality into C=C bonds. As a part of showing the utility of 2H indazole having dicarbonyl functionality, in this chapter, we used the previous reported[11] protocol for the transition metal free intramolecular McMurry type coupling reaction for the synthesis of heterocyclic aromatic compounds especially 2H-indazole π-conjugated scaffolds with an attached azo ring. Interestingly, the crystal structure of synthesized compounds shows elastic property due to weak and strong interaction between the atoms and molecules.

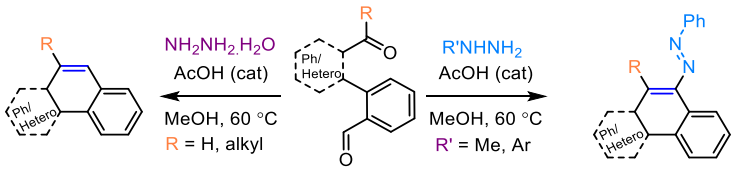

Conclusions

- Succesfully trapped the postulated α-oxo gold carbenes of gold catalysed nitroalkyne cycloisomerisation with external *N*-centered nucleophile such as 2,1-benzo[*c*]isoxazole (anthranil) and 1,2-benzo[*d*]isoxazole for the synthesis of functionlised indazole and quinazoline N-oxides.

- Established a one-pot synthesis of tricyclic pseudoindoxyl core by [Au]-catalysed nitroalkyne cycloisomerisation leading to isatogens and their further [3+3] cycloaddition with donor-acceptor cyclopropanes employing $Sc(OTf)_3$.
- Complementary [Au]-catalysed cyclization reactions of 2-alkynylphenylazides employing external nitrogen-transfer and/or carbene trapping reagents such as 2,1-benzo[*c*]isoxazole and 1,2-benzo[*d*]isoxazole has been developed.
- The Bacon's dicarbonyl coupling reactions employing hydrazine/phenyl hydrazine has been explored for the synthesis of indazolo[2,3-*a*]quinoline and 5-(aryl/alky diazenyl)indazolo[2,3-*a*]quinoline derivatives. The single crystal X-ray diffraction studies revealed 5-(aryldiazenyl)indazolo[2,3-*a*]quinoline derivatives as promissing flexible π-conjugated materials.

Future Directions

- Catalytic C–N, N–N and C–C bond formations *via* the interruption of the internal nitroalkyne/azidoalkyne redox process with other N–/C–centered nucleophiles like alkyne, nitrile, isocyanide, that are known to participate in the carbene transfer reactions.
- Developing intramolecular gold carbene transfer reactions to synthesize complex heterocyclic scaffolds of biological significance.
- Synthesized compound will be further screened for biological activities.

Publications

- Dhote, P. S.; Ramana, C. V. *Org. Lett.* **2019**, *16*, 6221–6224.
- Dhote, P. S.; Ramana, C. V. *Org. Lett.* **2021**, *23*, 2632–2637.
- Dhote, P. S.; Pund, K.; Ramana, C. V. *J. Org. Chem.* **2021**, 86, 10874–10882.
- Dhote, P. S.; Halnor, S. V.; Ramana, C. V. *Chem. Rec.* **2021** (doi.org/10.1002/tcr.202100111).
- Raj, K. V.; Dhote, P. S.; Vanka, K.; Ramana, C. V. *Front. Chem.* **2021** (doi:10.3389/fchem.2021.689780).

- Dhote, P. S; Patel, P.; Vanka, V.; Ramana, C. V. *Org. Biomol. Chem.* **2021,** (doi:10.1039/d1ob01285a)

References

1) Hendrich, C. M.; Sekine, K.; Koshikawa, T.; Tanaka, K.; Hashmi S. *Chem Rev.* **2020**. https://doi.org/10.1021/acs.chemrev.0c00824.
2) (a) Ye, L. W.; Zhu, X.; Sahani, R.; Xu, Y.; Qian, P. C.; Liu, R. S. *Chem. Rev.* **2020**, https://doi.org/10.1021/acs.chemrev.0c00348.; (b) Aguilar, E.; Santamaría, *Org. Chem. Front.* **2019**, *6*, 1513−1540.
3) Asao, N.; Sato, K.; Yamamoto, Y. *Tetrahedron Lett.* **2003**, *44*, 5675−5677.
4) Gorin, D. J.; Davis, N. R.; Toste, F. D. *J. Am. Chem. Soc.* **2005**, *127*, 11260−11261.
5) (a) Harvey, R. G. Polycyclic Aromatic Hydrocarbons, Wiley-VCH, New York, **1997**.; (b) Anthony, J. E. *Chem. Rev.* **2006**, *106*, 5028–5048.
6) Wittig, G.; Geissler, G. *Liebigs Ann. Chem.* **1953**, *580*, 44–57.
7) Peterson, D. J. *J. Org. Chem.* **1968**, *33*, 780–784.
8) Julia, M.; Paris, J. M. *Tetrahedron Lett.* **1973**, *14*, 4833–4836
9) Tebbe, F. N.; Parshall, G. W.; Reddy, G. S. *J. Am. Chem. Soc.* **1978**, *100*, 3611–3613.
10) (a) McMurry, J. E.; Fleming, M. P. *J. Am. Chem. Soc.* **1974**, *96*, 4708–4709. (b) McMurry, J. E.; Krepski, L. R. *J. Org. Chem.* **1976**, *41*, 896–897.
11) Bacon, R.; Bigg, D. *J. Chem. Soc.*, **1974**, 2156–2161.

Chapter I

Development of Novel Cascade Reactions Initiated by Nitroalkyne Cycloisomerisation

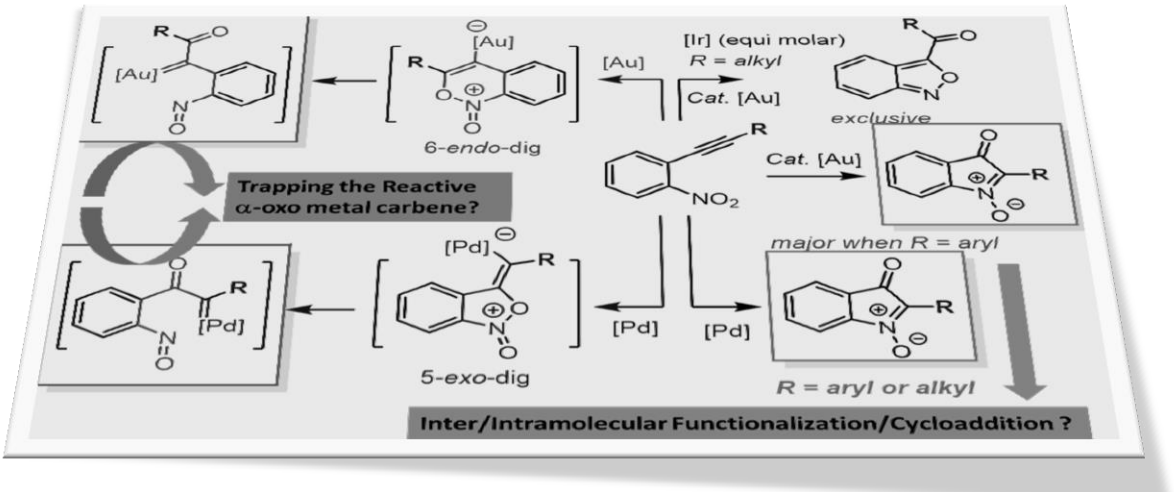

1.0. Introduction

Catalysis with gold-complexes is one of the remarkable areas that emerged in this millenium and has grown exponentially in a short span of two decades keeping its presence in majority of the fundamental reaction classes that are known to be mediated by acids/bases and other metal complexes.[1] This includes simple electrophilic cylizations/cycloisomerisations, rearrangements to diverse cycloadditions, cyclopropanation to glycosidations, oxidations and internal redox processes, aryl couplings and C–H functionalization to name a few. This taken together with the distinct and unprecedented organic transformations that are reported with gold-complexes, the catalytic transformations by gold-complexes have gained popularity as reliable transforms in the retrosynthetic design of target molecules of natural and unnatural origin.[2] Especially, the high carbophilicity/ π-electrophilic activation of gold-complexes has been naively explored in intra and intermolecular functionalization of C–C multiple bonds to forge a wide range of carbocyclic and heterocyclic skeletons in a regi*o*-/stere*o*- and enantioselective manner.[3]

A particularly interesting class of gold-catalyzed reactions is the catalytic internal niroalkyne redox cyclization.[4] The cyclization of *o*-(arylalkynyl)nitrobenzenes reported by Yamamoto and c*o*-workers was one of the early examples for the gold(III)-catalyzed nitr*o*-alkyne redox process - that has provided a practical alternative for the synthesis of 2-aryl-3-ox*o*-3*H*-indole 1-oxide unit (trivially known as isatogens) (Figure F1.1).[5] This indeed opened a new domain in the gold-catalysis that comprises of the gold-catalyzed oxygen atom transfer to alkynes employing nucleophilic oxygen atom donors such as amine-/pyridine N-oxides, nitrone, sulfoxides and epoxides for the generation of reactive α-oxo gold carbene intermediates.[6] Taken together with the α-imino gold carbene intermediates, this has been regarded as an important advancement in the gold catalysis due to versatile transformations these intermediates undergo and the resulting product diversity.[7] In the following sections, described will be a brief compilation of methods that are documented for the nitroalkyne redoxy cyclization until recently, followed by the mechanistic aspects of the gold-catalyzed nitroalkyne cycloisomerization and subsequent synthetic exploration of the gold-catalyzed nitroalkyne cycloisomerization by combining it with the nucleophilic additions and cycloadditions in the synthesis complex heterocyclic scaffolds.

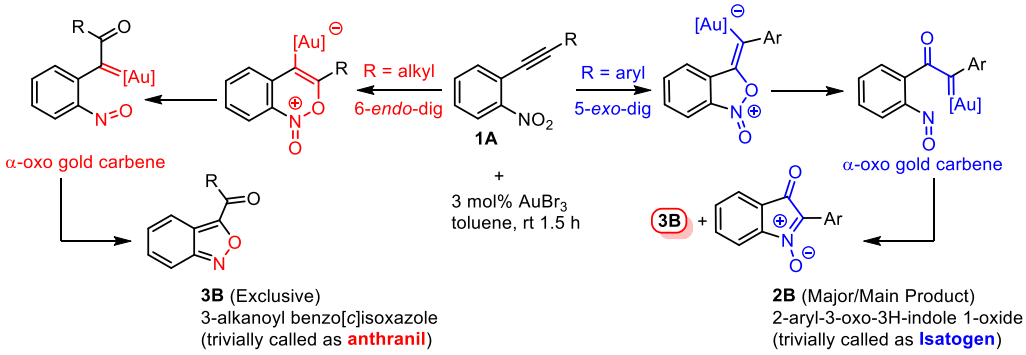

Figure F1.1: *Yamamoto's Gold-Catalyzed Nitroalkyne Cycloisomerization & Substrate Dependent Complementary Cyclization and the Key Reactive α-Nitroso Gold Carbene Intermediates Proposed Later*

2.0. Nitroalkyne Redox Cycloisomerization Leading to Isatogens

2.0.1. Documented Before Yamamoto's 2003 Disclosure

The cyclization of *o*-alkynylnitrobenzens is one of earleist redox processes to be documented in organic synthesis. In dealing with the synthesis of indigo, in 1881, Baeyer reported cycloisomerisation of *o*-nitrophenylpropiolates **4** in cold concentrated sulphuric acid leading to 2-carboxy-3-ox*o*-3*H*-indole 1-oxide **5**. The central bicyclic core of which is trivially called as isatogen (isatin + gen) since they are isomeric to isatin. Later, Pfeiffer and Ruggli have explored this class of compounds systematically and provided some important advancements for the *o*-nitroalkyne cycloisomerization that includes the pyridine-mediated internal redoxycyclization either under photochemical or thermal conditions (Scheme S1.1) or use of nitrosobenzene to promote the cycloisomerization that takes several days to form the isatogens.

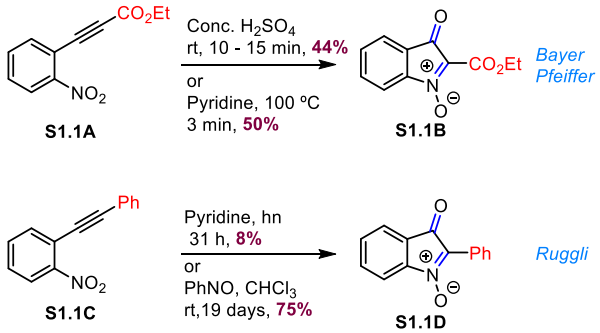

Scheme S1.1: *Acid/Base-Mediated Nitroalkyne Cycloisomerization*

(Baeyer, A. *Ber. Dtsch. Chem. Ges.* **1881**, *14*, 1741–1746.; Pfeiffer, P.; Liebigs, J. *Ann. Chem.* **1916**, *411*, 72.; Ruggli, P.; Casper, E.; Hegedus, B. *Helu. Chim. Acta*. **1937**, *20*, 250)

In 1969, Bond and Hooper revealed that during the preparation of unsymmetrical diaryl acetylenes employing Cu-(I) 2-nitrophenylacetylide **S1.2A** under Castro-Stephens coupling conditions, in some instances, prolonged heating of the reaction in pyridine gave the corresponding isatogens **S1.2C** directly (Scheme S1.2). The yields and the time of the reaction varied with respect to the substituents present on the aryl ring.

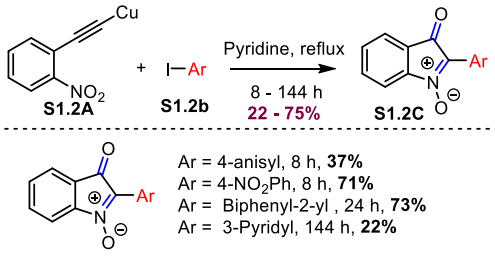

***Scheme S1.2**: A One-pot Castro-Stephen's coupling and Nitroalkyne Cycloisomerization*

(Bond, C.; Hooper, M. *J. Chem. Soc.* **1969**, (*C*), 2453–2460)

On similar lines, Rosen and co-workers recently developed a one-pot protocol that comprises of carrying Sonogashira coupling of *o*-iodonitrobenzene derivatives **S1.3A** with (hetero)arylacetylenes **S1.3B'** in neat triethyl amine and continuing the reaction for 3 – 4 days at rt (Scheme S1.3). This has been applied aptly for the synthesis of various 2-(hetero)aryl isatogens **S1.3C**, however, when alkyl group such a methyl is present on the alkyne end, the corresponding 2-methylisatogen was obtained in poor yields. Although, the role of original [Pd]-catalyst over the cyclization is not very clear, however, the facile nitroalkyne cycloisomerization at rt indicates that the phosphine free Pd(II)-salts resulting after the initial Sonogashira coupling may be responsible. Interestingly, a similar protocol with 6-chloro-5-nitropyrimidine derivatives **S1.3D/S1.3F** required separate heating in neat pyridine to carry the requisite nitroalkyne cycloisomerization.

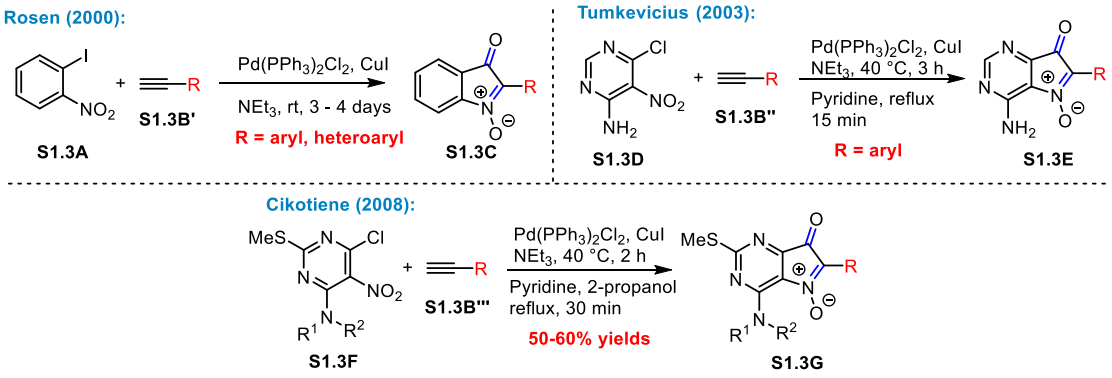

***Scheme S1.3**: One-pot Sonogashira Coupling – Nitroalkyne Cycloisomerization*

(Rosen, G. M.; Tsai, P.; Barth, E. D.; Dorey, G.; Casara, P.; Spedding, M.; Halpern, H. J. *J. Org. Chem.* **2000**, *65*, 4460–4463.; Susvilo, I.; Brukstus, A.; Tumkevicius, S. *Synlett* **2003**, *8*, 1151–1152.; Cikotiene, I.; Pudziuvelyte, E.; Brukstus, A.; *J. Heterocyclic Chem.*, **2008**, *45*, 1615–1620)

2.0.2. Reported After Yamamoto's 2003 Disclosure

In 2009, Soderberg and co-workers reported a regiospecific synthesis of isatins from 1-iodo-2-nitro-benzenes under Pd catalysis (Scheme S1.4). The optimal reaction conditions were 5 mol % $PdCl_2(PPh_3)_2$ in acetone at 60 °C. Both electron rich and well as electron deficient substitutions on aromatic unit were well tolerated. However, only in two cases, the corresponding 2-bromoisatogens were isolated in good yields. Control experiments revealed that switching to dichloromethane with the same catalyst, at reflux gave the bromoisatogen **S1.4C** in excellent yields. Considering this it has been assumed that 2-haloisatogens are involved *en route* to the isatins formation. Interestingly, in the same report, it has been also shown that the attempted conversion of the TMS-alkyne **S1.4D** to corresponding iodoalkyne with $AgNO_3$/NIS gave the isatogen **S1.4E** exclusively.

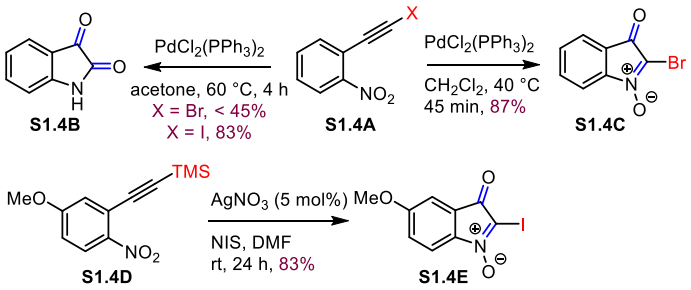

***Scheme S1.4:** Pd-/Ag-Catalyzed Nitroalkyne Cyloisomerizations*

(Söderberg, B. C. G.; Gorugantula, S. P.; Howerton, C. R.; Dantale, S. W. *Tetrahedron* **2009**, *65*, 7357–7363)

In 2015, Harrity and C*o*-workers have generalized the Söderberg's Ag-catalyzed nitroalkyne cycloisomerization of iodoalkynes **S1.5A** employing Cu-catalysts in THF at reflux (Scheme S1.5). Substrates having electron donating group on the aryl unit were compatible under low catalyst loading that is 25 mol % of CuBr.DMS complex, whereas with electron withdrawing groups the reaction underwent slow cyclisation requiring stoichiometric amounts of $Cu(CH_3CN)BF_4$. The utility of these products has been examined by cross coupling of the iodo at C2 position with a wide range of alternative heterocyclic derivatives.

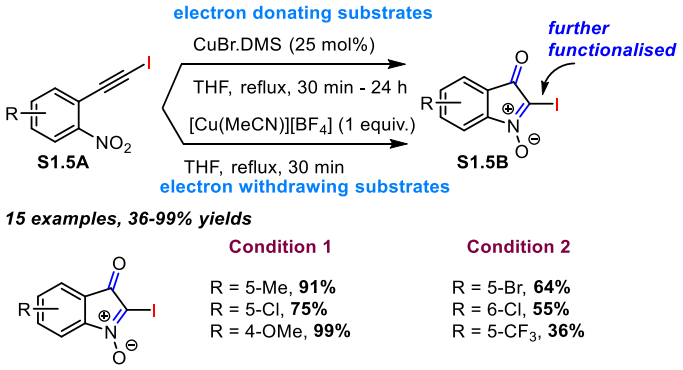

Scheme S1.5: *Cu-Catalysed Cycloisomerisation of 2-Nitrophenyliodoacetylene*

(Maduli, E. J. M.; Edeson, S. J.; Swanson, S.; Procopiou, P. A.; Harrity, J. P. A. *Org. Lett.* **2015**, *17*, 390−392)

In 2018, Song and group developed a copper-catalyzed redox cycloisomerisation of non-prefunctionalized nitroalkynes **S1.6A** for the synthesis of C2-tetrasubstituted indolin-3 ones **S1.6D** with $BrCF_2CO_2R$ **S1.6B** (Scheme S1.6). In this protocol, diboron acts as the reductant, rendering a fluorine-containing non-carbon quaternary centre in mild to excellent yields. Later, the same group employed different radical sources such allyl, benzyl and propargyl bromides to synthesize diverse C2-quaternary indolin-3-ones **S1.6E** (Scheme S1.6).

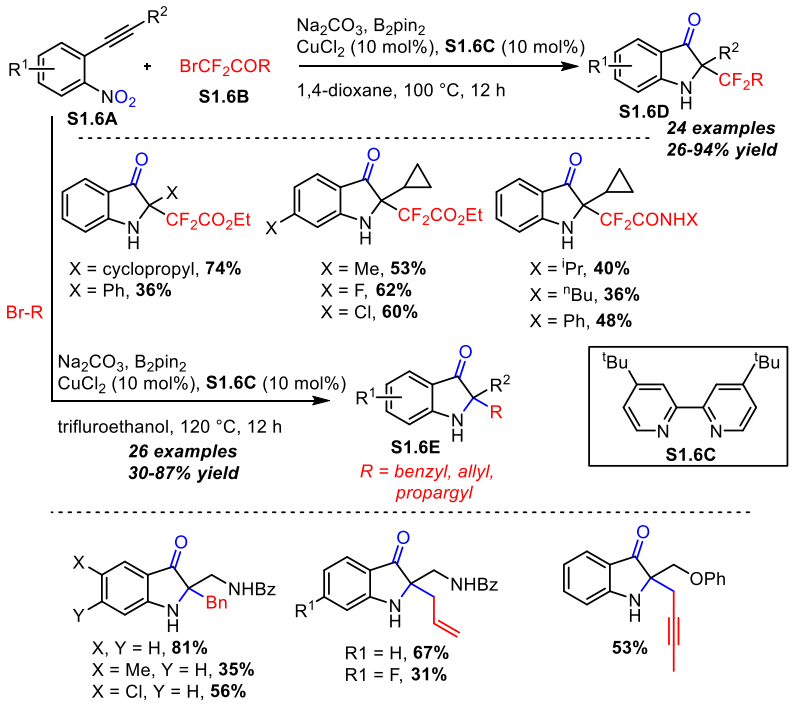

Scheme S1.6: *Cu/B_2pin_2-Catalyzed Redox Cycloisomerisation of o-Nitroalkynes for Synthesis of C2-Tetrasubstituted Indolin-3-ones*

(Fu, W.; Song, Q. *Org. Lett.* **2018**, *20*, 393−396.; Fu, W.; Zhou, Y.; Song, Q. *Chem. Asian J.* **2018**, *13*, 2511–2515)

Following this, Peng's group developed a CuH-catalyzed reductive cyclization of *o*-alkynylnitroarene **S1.7A** for the diasterospecific synthesis of 3- hydroxyindoline **S1.7B** and 2-ary-3*H*-indol-3-one scaffolds **S1.7C** in one pot operation (Scheme S1.7). The standard catalytic operation involved treatment of **S1.7A** in the presence of CuCl/dppf (ligand) (10 mol %) along with $Me(EtO)_2SiH$/LiOMe (4 equiv) at room temperature to deliver 3-hydroxyindoline derivative **S1.7B**. When the reaction was continued with added silica gel at 80 °C for 12 h under O_2 it provided the 2-ary-3*H*-indol-3-ones **S1.7C**. The reaction mechanism involves formation of LCu-H active catalyst that promotes the key nitroalkyne cycloisomerization resulting in the isatogen which upon reduction by hydrosilane furnishes 2-ary-3*H*-indol-3-one, the further reduction of which gives the 3- hydroxyindoline **S1.7B**.

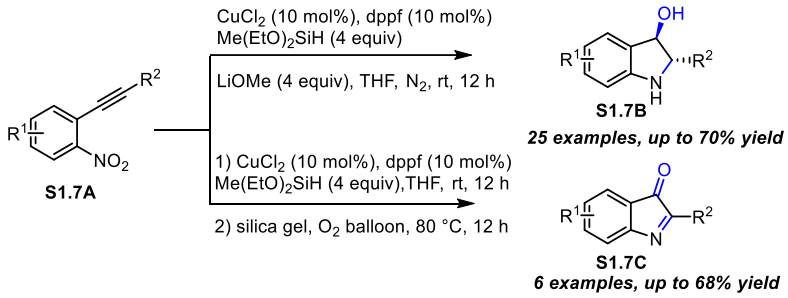

Scheme S1.7: *Cu-H Catalyzed Synthesis of 3-hydroxyindolines and 2-aryl-3H-indol-3-ones*

(Peng, H.; Ma, J.; Duan, L.; Zhang, G.; Yin, B. *Org. Lett.* **2019**, *21*, 6194–6198)

3.0 Gold-Catalyzed Internal Nitroalkyne Redox Cycloisomerization & Involvement of α-Nitroso Gold carbenes

In 2003, Yamamoto and *co*-workers reported a substrate dependent gold(III)-catalyzed cycloisomerization of *o*-alkynylnitrobenzenes **S1.8A**. When the pendant alkyne substituent is aryl, isatogen **S1.8E** was obtained as the major product along with the isomeric benzo[*c*]isoxazole which is trivially known as anthranil **S1.8F**. Interestingly when an alkyl group such as isobutyl is placed on the alkyne, corresponding anthranils were obtained exclusively in good yields. As mentioned above, this is an important development as it is the first report on catalytic internal nitroalkyneredox process to be documented. In addition, it also indicated an alternative possibility with the nitroalkyne cycloisomerization to synthesize anthranils, which otherwise was known to provide the isatogens. An importantly, subsequent findings revealed that this gold-catalyzed internal oxygen transfer to alkynes leads of reactive α-oxo gold carbenes which are otherwise synthesized *via* carbene transfer to the gold complexes.

The initial mechanistic path proposed by Yamamoto is founded upon the addition of the oxygen from the nitro group in a 6-*endo*-dig fashion which results in the formation of **S1.8B**. The resulting Aurate complex undergoes protonolysis to afford **S1.8C** followed by ring opening with water to produce a nitrosobenzene adduct **S1.8D**. At this stage there exist two possibilities for the subsequent dehydrative cyclization, either leading to isatogens **S1.8E** (Scheme S1.8, *path a*) or anthranil **S1.8F** (Scheme S1.8, *path b*). Though this explained the possible paths for the two isomeric products, however it did not account for why these paths are substituent dependent.

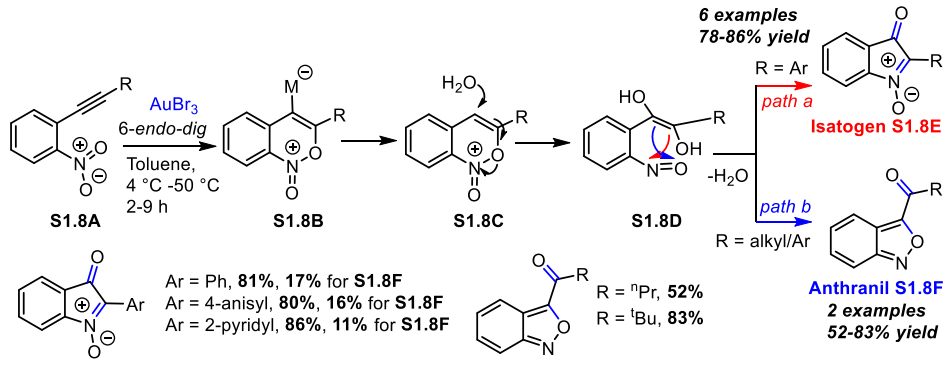

Scheme S1.8: *Gold(III)-Catalyzed Redox Cyclization of o-(Alkynyl)nitrobenzenes*

(Asao, N., Sato, K., Yamamoto, Y. *Tetrahedron Lett.* **2003**, *44*, 5675−5677)

In 2005, Crabtree's group studied the nitroalkyne cycloisomerisation that leads to anthranil **S1.9C** using stoichiometric amounts iridium hydride complex **S1.9A** (Scheme S1.9). With the help of single crystal structural analysis, it has been speculated that there exists an intermediate nitroso stabilized α-oxo iridium(III) complex **S1.9E**, which results after the initial oxygen transfer from nitro to alkyne in a 6-*endo*-dig fashion.

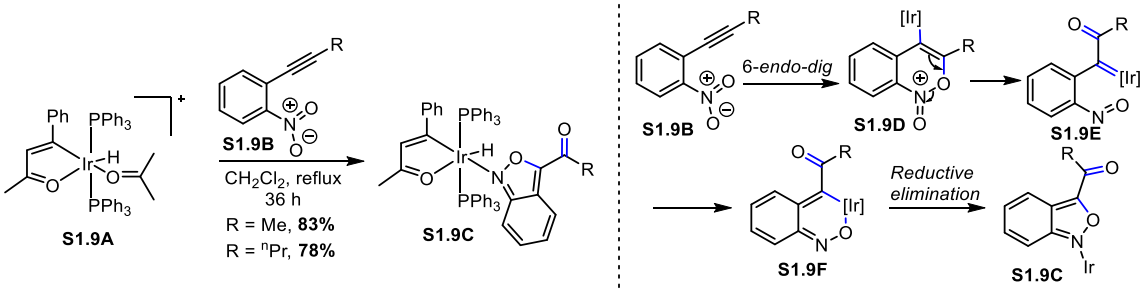

Scheme S1.9: *Iridium(III) Hydride Complex Mediated Nitroalkyne Cycloisomerisation*

(Li, X.; Incarvito, C. D.; Vogel, T.; Crabtree, R. H. *Organometallics* **2005**, *24*, 3066−3073)

In 2010, as a part of total synthesis of Isatisine A, our group speculated about the possibility of a palladium-catalyzed nitroalkyneredox cycloisomerization to synthesize both 2-aryl and 2-alkyl isatogens (Scheme S1.10) and executed successfully with $PdCl_2(CH_3CN)_2$ complex in acetonitrile. Though, our initial hypothesis was a halopalladation of the alkyne and subsequent oxygen transfer from the nitro to vinyl-[Pd] intermediate, however, the detailed density functional theory (DFT) calculations revealed that the reaction path involves the formation of the *α-oxo* palladium carbene **S1.10C** *via* the internal oxygen transfer from nitro to [Pd]-complex alkyne in a 5-*exo*-dig fashion. The intermediate metal carbene subsequently

undergoes 5*n*-electro cyclization leading to isatogen **S1.10D**. Subsequent examination of substrate scope demonstrated this as a general method for the synthesis of 2-aryl and 2-alkylisatogens. Indeed, this has been employed as the key tool in our total synthesis of Isatisine A and Trigonalimine C.[8]

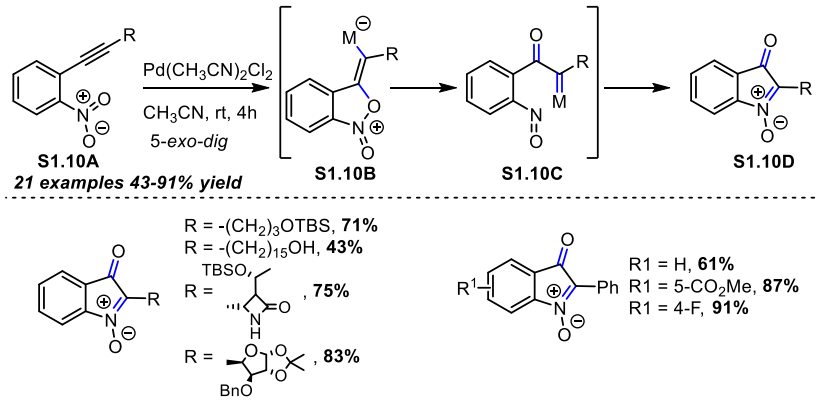

Scheme S1.10: *[Pd]-Catalyzed Nitroalkyne Cycloisomerisation*

(Ramana, C. V.; Patel, P.; Vanka, K.; Miao, B.; Degterev, A. *Eur. J. Org. Chem.* **2010**, 5955−5966)

After a year later, Liu and co-workers reported the gold-catalyzed internal nitroalkyneredox/[3+2]-cycloaddition comprising of 1-ethynyl-2-nitrobenzenes **S1.11A** and alkenes **S1.11B** to form complex azacyclic compounds **S1.11C** in a stereoselective manner (Scheme S1.11).[19] The mechanism for this transformation involves the formation of α-oxo gold carbene **S1.11D** *via* a 5-*exo* dig cyclization and N–O bond cleavage. Next, the resulting gold carbene undergoes internal redox reaction giving the enol core **S1.11E**, which upon [3+2]-cycloaddition with an external alkene **S1.11B** in a concerted *exo*-manner results in the bridged bicyclic compound **S1.11C** in a stereoselective manner. The scope of this cycloisomerization-cycloaddition cascade was demonstrated by using various electron-rich olefins, along with electron-rich and -deficient nitroalkynes. Interestingly, as a part of control experiments, this group revised the mechanism for the formation of anthranil previously reported by Yamamoto, and described the possible involvement of α-oxo gold carbene.

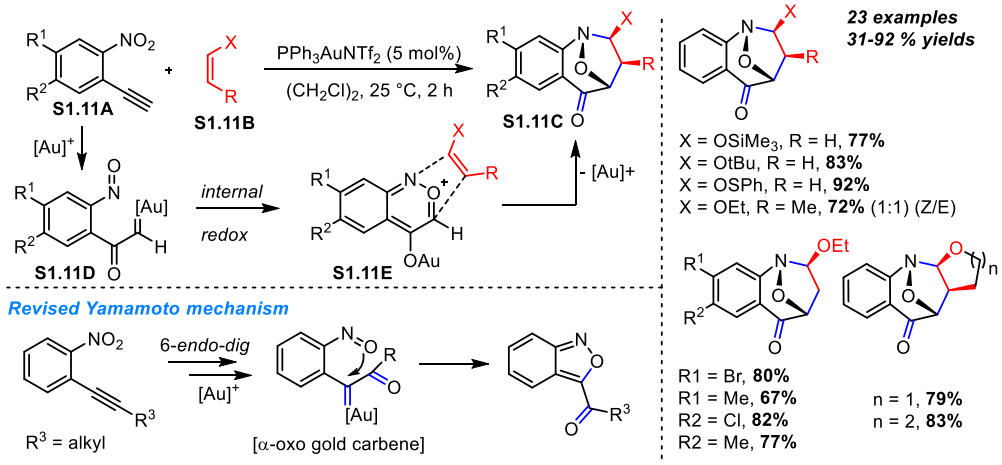

Scheme S1.11: *[Au]-Catalyzed Synthesis of Azacyclic Compounds and Revised Mechanism.*

(Jadhav, A. M.; Bhunia, S.; Liao, H. Y.; Liu, R. S. *J. Am. Chem. Soc.* **2011**, *133*, 1769−1771)

Recently, Xu's group showed that these intermediate terminal α-oxo gold carbenes could be trapped with indoles. This group developed a simple method for the synthesis of 2-indolylisatogens **S1.12C** *via* gold(I)-catalyzed cascade reaction of *o*-alkynylnitrobenzene **S1.12A** with indoles **S1.12B** (Scheme 12). The reaction mechanism proceeds through the formation of gold carbene intermediate **S1.12D** *via* 5-*exo*-dig cyclization of *o*-alkynylnitrobenzene, followed by addition of C3-indole which on internal redox forms enolate and subsequent cyclization yields 2-indolyl derivatives **S1.12C**.

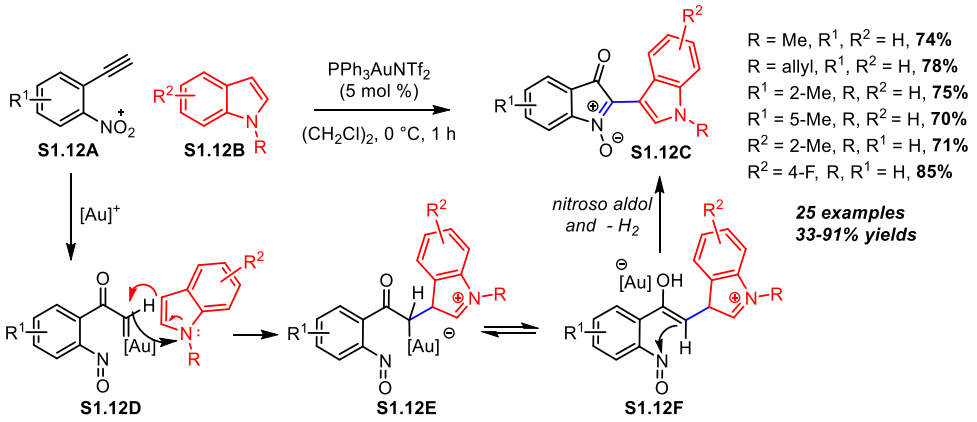

Scheme S1.12: *Gold(I)-Catalyzed Redox Transformation of o-Alkynylnitrobenzene with Indoles*

(Zhou, S.; Liu, Q.; Bao, M.; Huang, J.; Wang, J.; Hua, W.; Xu, X. *Org. Chem. Front.* **2021**, DOI:10.1039/d1qo00134e)

In parallel to Liu's work, our group also speculated the possible involvement of α-oxo gold carbenes during our investigations that are aimed at the possible interruption of these metal catalysed cycloisomerization process with internal nucleophiles such as –OH. As shown in Scheme S1.13, depending upon catalyst employed and the proximity of the –OH group, the formation of the *spiro*-indolin-3-one **S1.13A** and *spiro*-benzoxazinone **S1.13B** was noticed with Pd-complex. Whereas, when $AuBr_3$ employed as a catalyst, in case of substrate **S1.13A'**, the *spiro*-benzoxazinone **S1.13E** and anthranil derivative **S1.13F** were obtained in equal proportion and with **S1.13A''**, *spiro*-benzoxazinone **S1.13H** was obtained exclusively. The diversity in the product formation has explained by possible complementary 5-*exo*/6-*endo* dig cyclizations operating respectively with Pd- and Au-complexes, and the nature of the intermediate nitroso-stabilized metal carbenoids involved in the reaction (Scheme S1.14). The formation of *spiro*-benzoxazinone **S1.13C** with substrate **S1.13A**, has been explained by invoking the possible insertion of carbene across the –OH. However, the products obtained from the $AuBr_3$-cyclization revealed that such trapping of the intermediate α-oxo gold carbene is not operational and the protodeauration is operational at least in case of cycloisomerization of substrate **S1.13A**.

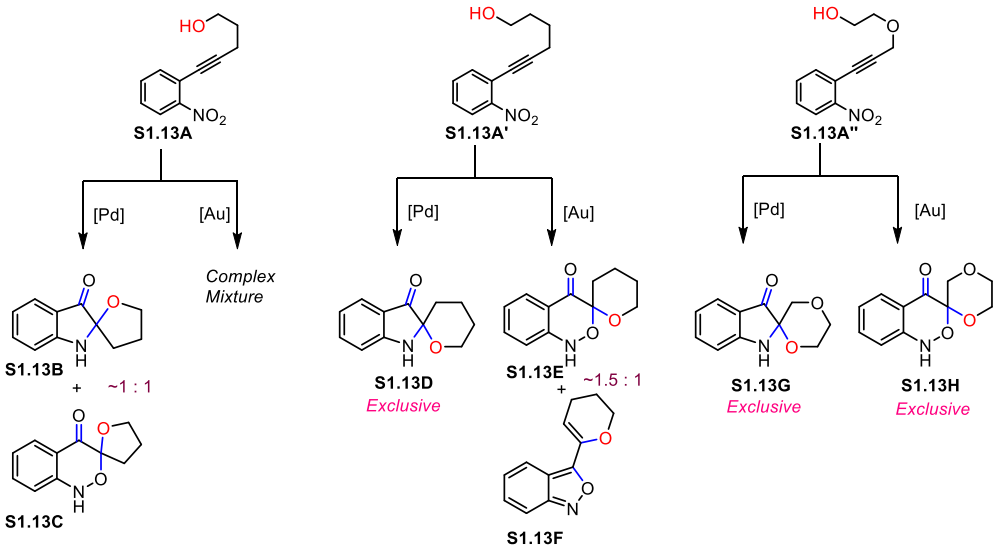

Scheme S1.13: *Interrupting the [Pd]-/[Au]-Catalyzed Nitroalkyneredox Process with Internal Nucleophile*

(Patel, P.; Ramana, C. V. *Org. Biomol. Chem.* **2011**, *9*, 7327−7334)

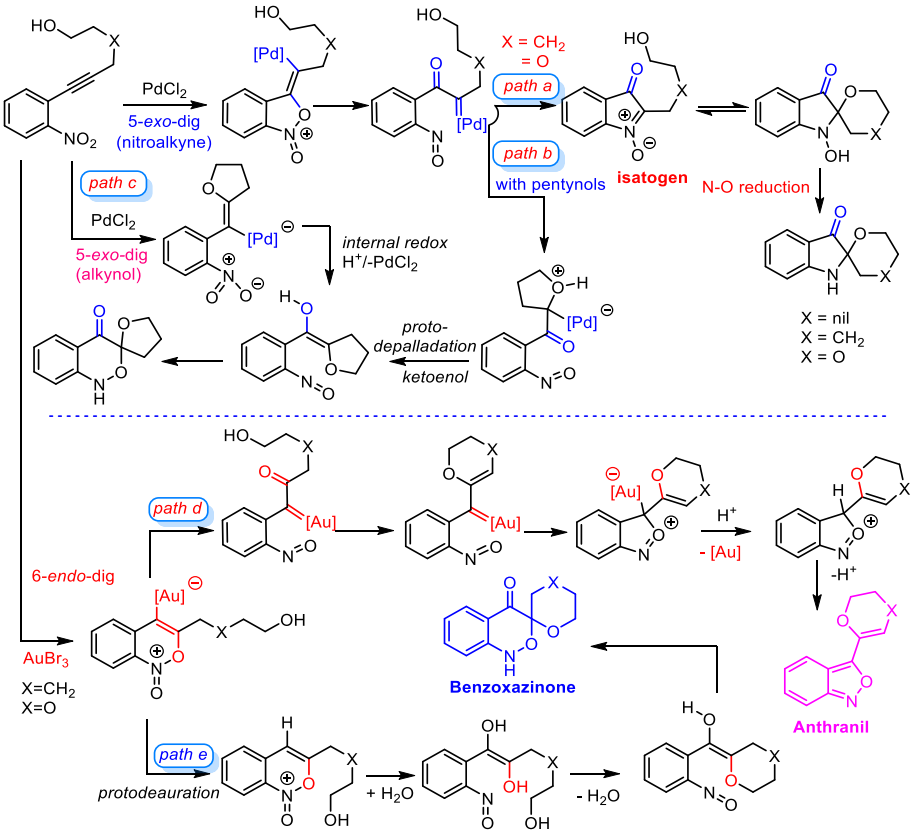

Scheme S1.14: *Mechanism of [Pd]-/[Au]-Catalyzed Nitroalkyneredox Process with Internal Nucleophile*

However, Wang and co-workers documented a similar [Pd]-catalyzed cycloisomerisation of *o*-alkylnylnitrobenzenes **S1.15A** having an internal nitrogen-nucleophile leading to *N,N*'-ketal spiropseudoindoxyl derivatives **S1.15B** (Scheme S1.15). The proposed mechanism consists of a 5-*exo* dig cyclization to isatogens **S1.15C** followed by an intramolecular nucleophilic addition of the amine and subsequent $Mo(CO)_6$-mediated reductive cleavage of N–O bond.

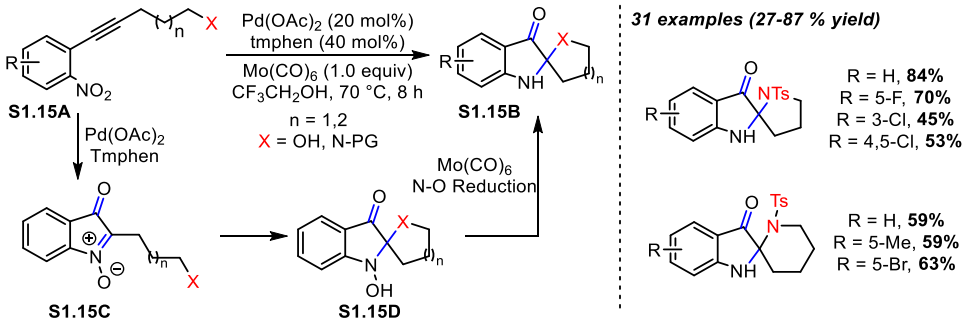

Scheme S1.15: *Synthesis of N,N'-ketal Spiropseudoindoxyl Derivatives*

(Chen, L. W.; Xie, J. L.: Song, H. J.: Liu, Y. X.: Gub, Y. C.: Wang, Q. M. *Org. Chem. Front.* **2017**, *4*, 1731–1735)

4.0. Synthetic Utility of [Au]-Catalyzed Nitroalkyne Redox Cycloisomerization

From the above discussion it is evident that the Yamamoto's report on [Au]-catalyzed nitralkyne cycloisomerization leading to the synthesis of isatogens has reinitiated this area. The ready functionalization of these isatogens at the C2-position either by nucleophilic addition or by cycloaddition generates synthetically demanding 2,2-disubstituted 1,2-dihydro-3*H*-indolin-3-one (trivially known as pseudoindoxyl - a subgroup that bears this name present in the widely distributed indole class of alkaloid) skeleton which is one of the key aspects that has been inspired the researchers. This is evident from the appearance of various Pd, Ag, Hg and Cu-complexes in the pursuit of developing regioselective nitroalkyne cycloisomerizations. Yet, the cyclizations with [Au]-complexes are more attractive since they are facile at rt and the added advantage with the [Au]-complexes is their Lewis acidity that can be used for further functionalization of the resulting isatogens and also a provision to employ other Lewis acids in the same-pot to develop novel cascade and/or one-pot operations. In the following sections, various reports documented in this context are summarized briefly.

4.0.1. Cascade Transformations by Combining the [Au]-Catalyzed Nitroalkyne Redox Cycloisomerization with Nucleophilic Additions

The intermolecular functionalization of isatogens with external nucleophiles such as amino acids and alcohols has been studied in details by Hooper's group (Scheme S1.16). The addition of Grignard reagents or anions derived from the active methylene groups were documented earlier by Marchetti and Greci groups respectively. As a part of the total synthesis of Isatisine A, our group reported the $InCl_3$-mediated addition of C3 of indoles and also a [Au]-catalyzed addition of C2 of indole selectively at the nitrone carbon of the isatogens in the context of the total synthesis of Trigonolliimine C. The reaction of isatogens with allyl- and propargyl bromides under Barbier conditions has been also examined by our group in the context of ongoing total synthesis of Austamide, however, it was not regiospecific (unpublished results).

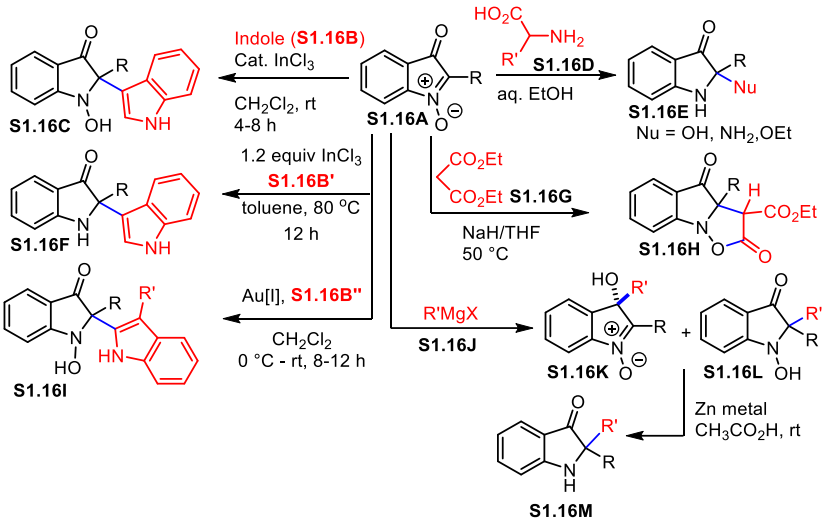

Scheme S1.16: *Nucleophilic Addition to Isatogens*

(Bunney, J. E.; Hooper, M.; *Tetrahedron Let.* **1966**, 3857–3860.; Berti, C.; Colonna, M.; Greci, L.; Marchetti, L.; *Tetrahedron* **1975**, *31*, 1745–1753.; Berti, C.; Greci, L.; Marchetti, L. *J. Chem. Soc. Perkin Trans*. **1979**, 233–236)

A successful merger of [Au]-catalyzed cycloisomerization with indole addition in an asymmetric manner has been accomplished by Jia's group (Scheme S1.17). In 2015, Jia and co-workers documented a gold(III) and chiral phosphoric acid-catalyzed enantioselective construction of N-hydroxyindolin-3-ones **S1.17D** bearing a C2 quaternary stereocenter. In general, *o*-nitroalkyne **S1.17A** and indole **S1.17B** were reacted in the presence of $AuCl_3$ (7 mol %) and chiral phosphoric acid **S1.17C** (10 mol %) in toluene at 0 °C to expedite this redox annulation. Interestingly, the use of 3 Å molecular sieves was found to be important, increasing both yield and enantioselectivity of *N*-hydroxyindolin-3-one derivatives **S1.17D**. In their proposed redox annulation pathway comprises of an initial internal oxygen transfer in a 5-*exo*-dig leading to the α-oxo gold carbene **S1.17E** and subsequent internal cyclization to isatogen **S1.17G** and then nucleophilic attack of indole on the chiral ion pair **S1.17H** to form indoline-3-one derivatives **S1.17D**. Another possibility that comprises of the intermolecular interception of the gold carbene **S1.17E** with indole followed by cyclization has been also invoked; however, control experiments revealed that a stepwise protocol involving isatogen as intermediate was operating.

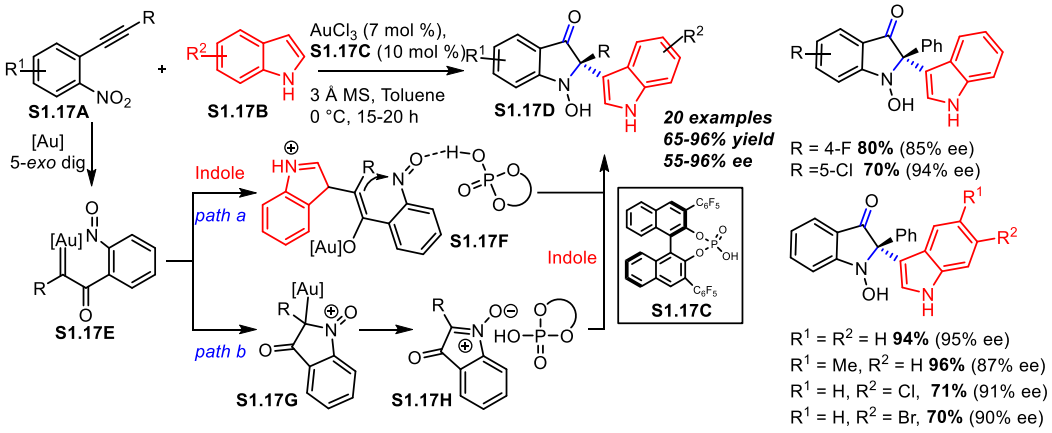

Scheme S1.17: *Asymmetric Addition of Indole to in-situ prepared Isatogens via gold (III) Catalyzed Nitroalkyne Cycloisomerisation*

(Liu, R. R.; Ye, S. C.; Lu, C. J.; Zhuang, G. L.; Gao, J. R.; Jia, Y. X. *Angew. Chem., Int. Ed.* **2015**, *54*, 11205−11208)

4.0.2. Cascade Transformations by Combining the [Au]-Catalyzed Nitroalkyne Redox Cycloisomerization with Cycloaddition Reactions

Though, isatogens are known for more than 140 years, the cycloaddition reactions with isatogens were reported very recently. In 2001, Greci and coworkers have studied the [3+2]-dipolar cycloaddition of 2-phenylisatogen **S1.19A** with maleamide derivatives **S1.19B** (4 equiv) in refluxing toluene (Scheme S1.18). The reactions proceeded smoothly and provided a mixture of *exo*/*endo* isomers **S1.19C** in good yields. Later, in 2003, the same group carried out the cycloaddition of 2-phenylisatogen in neat ethyl acrylate and methyl crotonate, ethyl cinnamate at 80 °C. Interestingly, in case of ethyl acrylate, the cycloaddition was found to be non-selective and delivered the all four possible isomers **S1.19E-E'''**. Whereas with ethyl crotonate or ethyl cinnamate having trans-configuration, the cycloaddition reaction proceeded with complete regio- and stereoselectivity and provided a single product **S1.19G**. The *ab initio* calculations have revealed that the product distribution may be influenced by kinetic rather than thermochemical factors. In 2015, our group documented a one-pot [3+2]-cycloaddition of isatogens with olefins **S1.19I** followed [Ru]-catalyzed redox neutral cleavage resulting in beta-amino ketones or ester **S1.19J** when a vinyl ether was used. Control experiments revealed that the cycloaddition was regio- and stereoselective. Very recently, Liu and co-workers documented an organocatalytic asymmetric formal [3+2] cycloaddition of isatogens with azalactones **S1.19L** to construct

indolin-3-one derivatives **S1.19N**. Whereas, Du and co-workers reported a NHC-catalyzed [3+3]-cycloaddition of isatogen with acryl aldehyde derivatives **S1.19O**.

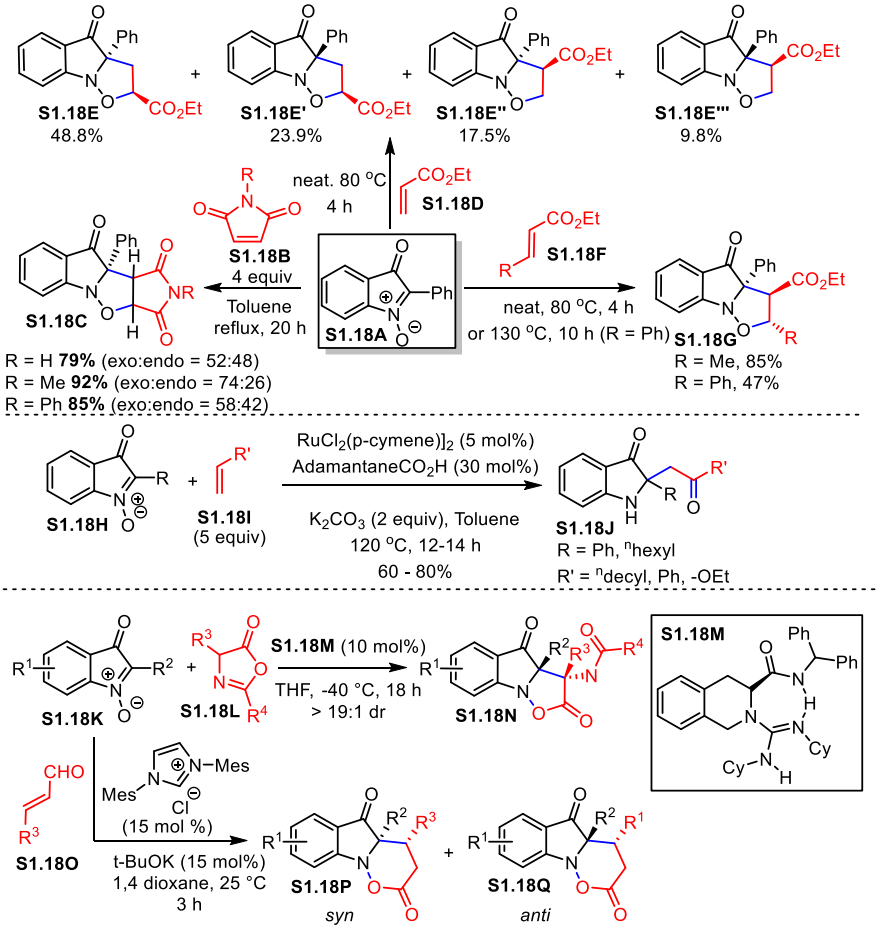

Scheme S1.18: *Documented Cycloaddition Reactions of Isatogens*

(Greci, L.; Tommasi, G.; Bruni, P.; Sgarabotto, P.; Righi, L. *Eur. J. Org. Chem.* **2001**, 3147–3153.; Astolfi, P. Bruni, P.; Greci, L.; Stipa, P.; Righi, L.; Rizzoli, C. *Eur. J. Org. Chem.* **2003**, 2626–2634.; Kumar, C. V. S.; Ramana, C. V. *Org. Lett.* **2015**, *17*, 2870–2873.; Xie, L., Li, Y.; Dong, S.; Feng, X.; Liu, X. *Chem. Commun.* **2021**, *57*, 239–242.; Xu, J.; Hu, S.; Lu, Y.; Dong, Y.; Tang, W.; Lu, T.; Du, D. *Adv. Synth. Catal.* **2015**, *357*, 923–927)

As a part of our ongoing program on total synthesis of Austamide, one of early approaches comprises constructing the tricyclic core by employing a gold-catalyzed nitroalkyne cycloisomerization with intramolecular [3+2]-cycloadditions. However, one major concern was completion between the isatogen *vs* anthranil formation in gold-catalyzed cycloisomerization in general and especially when the substituent on the alkyne end is an alkyl group, the exclusive formation of anthranil. In this context, we hypothesized that the presence of an electron withdrawing group such as nitrogen on a pendant chain should promote the 5-exo mode of

cyclization inter alia isatogen formation. With this proposal, as shown in Scheme S1.19, the gold(I)-catalyzed cycloisomerisation of *o*-nitroenynamides **S1.19A** lead mainly to isatogens **S1.19B** and subsequent regioselective [3+2] cycloaddition with suitably positioned internal olefins yielded products **S1.19C/19D** in moderate to good yields. The regioselectivity in cycloaddition for the construction of tricyclic core depends on varying the chain length of the olefin unit. As such, propargyl-N-allyl derivatives (m, n=1) underwent this 2 step protocol to give isoxazolidines **S1.19C** exclusively whereas with propargyl-N-butenyl (m>1) or increasing the length of carbon before nitrogen atom from the alkyne unit (n>1) provided the [4,2,1]-bridged bicyclic products **S1.19D** with endo-selectivity. The scope of the reaction was proved by varying the substituents on the aryl ring, chain length on olefin unit and different protecting groups.

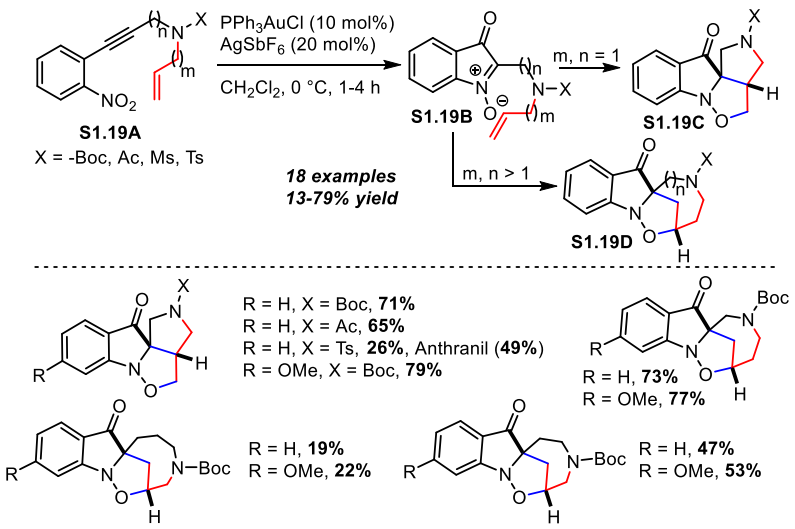

Scheme S1.19: *Gold(I)-Catalyzed Cycloisomerisation of o-Nitroenynamides and Intramolecular [3+2] Cycloaddition with Olefin*

(Kumar, C. V. S.; Ramana, C. V. *Org. Lett.* **2014**, *16*, 4766−4769)

Later, our group proceed to use this approach for the synthesis of Austamide (unpublished results) employing the carboxylate substituted derivative X. However, it has been realized that the cycloaddition proceed with complete *exo*-selectivity resulting in the fused tricyclic core. Control experiments revealed that the presence of carboxylate was responsible for the switching of the regioselectivity during the cycloaddition.

In parallel to our report, Verniest's group reported a similar Au(III)-catalyzed cycloisomerisation of *o*-nitrophenylpropiolamides and subsequent intramolecular dipolar cycloaddition with alkenes affording the tetracyclic core (Scheme S1.20). The strained heterocycle undergoes N-O bond reduction by hydrogenative cleavage which provides the tricyclic C2-spiropseudoindoxyl product **S1.20B** as a single diastereomer. Interestingly, the DFT studies revealed that these transformations do not involve the gold carbene **S1.20D**. A mechanism founded upon the participation amide oxygen in the ring opening *via* the formation of an oxirane core **S1.20E**, which subsequently converts to isatogen **S1.20F** and undergoes intramolecular [3+2]-cycloaddition and hydrogenation transformation to afford the tricyclic C2-spiropseudoindoxyl product **S1.20B**. In the substrate-scope exploration, electron-donating and –halogens on aryl unit, electron-rich and -poor groups on amide nitrogen atom were well-tolerated in this cascade protocol.

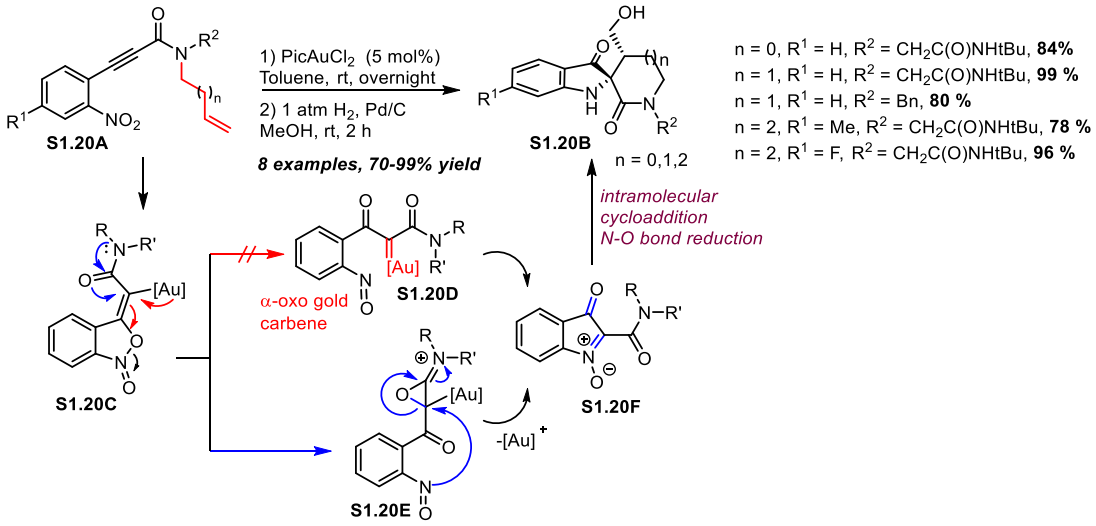

Scheme S1.20: *Gold (III)- Catalyzed Synthesis of Tricyclic core of C2-Spiropseudoindoxyl*

(Marien, N.; Brigou, B.; Pinter, B.; Proft, F.; Verniest, G. *Org. Lett.* **2015**, *17*, 270−273)

In 2018, the same group developed a metal free cascade reaction between 1-dibromovinyl-2-nitro substituted arenes **S1.21A** and secondary amines **S1.21B**, resulting in the formation of spiropseudoindoxyls **S1.21C** in a one pot protocol (Scheme S1.21). The proposed reaction mechanism involves the formation of bromoalkyne, followed by the loss of HBr to form ynamide **S1.21E** through an addition/elimination sequence. This ynamide undergoes two distinct pathways, where *path a* proceeds *via* attack of oxygen of nitro group to β-position of alkyne and subsequent cyclization forms stabilised carbene **S1.21F**, whereas in *path b*, attack of the ynamide

on oxygen of nitro group results in the formation of carbene **S1.21H**. Next, the nucleophilic attack of nitroso nitrogen at the carbene and further isomerisation to afford 2-amino isatogen, followed by intramolecular [3+2] cycloaddition which provide the tetracyclic compounds **S1.21C** in good yields. The QTAIM (quantum theory of atoms in molecules) and ELF (electron localization function) studies revealed that, a single-electron transfer from the nitro group is having an important role in cycloisomerisation process. In the substrate scope exploration, electron-donating and -withdrawing groups on aryl unit, protecting group of amine nitrogen atom, were well-tolerated to construct the respective pseudoindoxyl core.

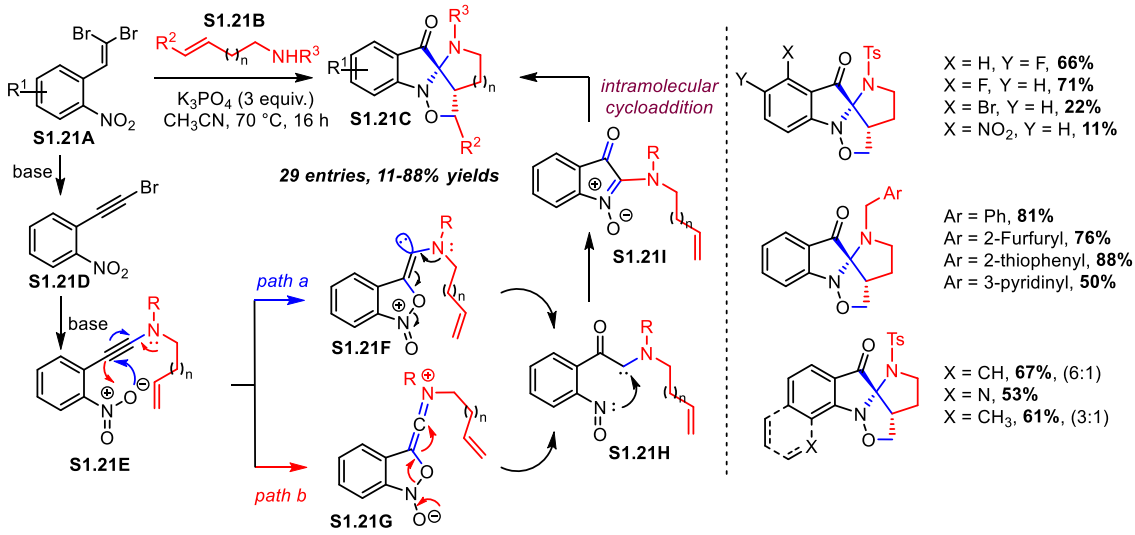

Scheme S1.21: *Metal free Cyclization of o-Nitroaryl Ynamides and Ynamines*

(Marien, N.; Reddy, B. N.; Vleeschouwer, F.; Goderis, S.; Hecke, K.; Verniest, G. *Angew. Chem. Int. Ed.* **2018**, *57*, 5660 –5664)

In 2020, Deng's group demonstrated the Cu(0)/PPh_3-Catalyzed cascade bis-heteroannulation reaction by employing various *o*-nitroalkynes **S1.22A** and methylketoximes **S1.22B** leading to the pharmacologically significant pyrazofused pseudoindoxyl compounds **S1.22C** with broad substrate scope and functional-group tolerance (Scheme S1.22). A standard catalytic operation involved treatment of *o*-nitroalkynes **S1.22A** with methylketoximes **S1.22B** in the presence of Cu metal (50 mol %)/PPh_3 (2 equiv.) to deliver pyrazolo[1,5-a]indolone product **S1.22C**. In a proposed reaction mechanism, first, a nucleophilic attack of the PPh_3 base to an alkyne moiety gives **S1.22E**, and on cyclization/intramolecular charge transfer/deoxygenation gives indol-3-one **S1.22F**. Later, oxidative addition of Cu(0) into the N−O bond of oxime acetate

further undergoes migratory insertion across C=N bond, with final reductive elimination with N–N bond formation to afford **S1.22C**.

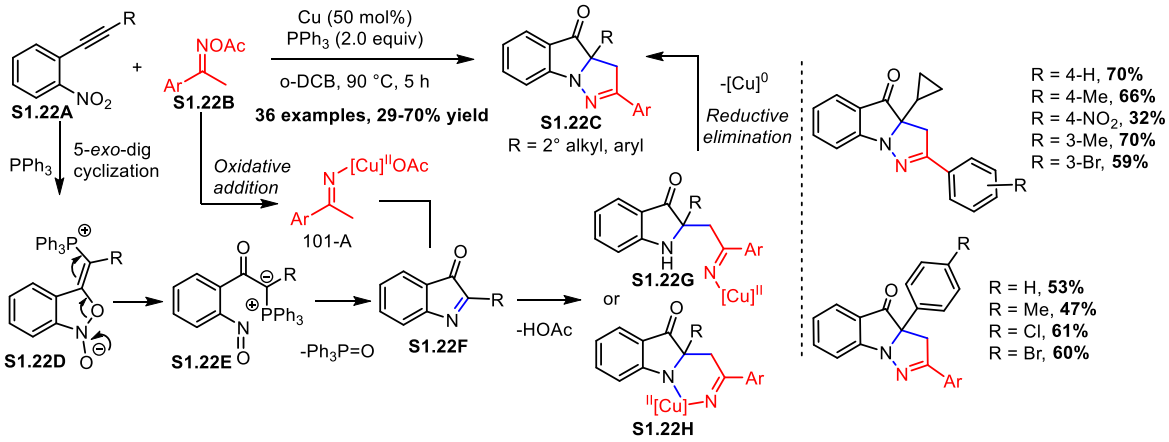

Scheme S1.22: *Cu(0)-Mediated Reductive Bisheteroannulations Reaction*

(H. Meng, Z. Xu, Z. Qu, H. Huang, G. J. Deng, *Org. Lett.* **2020**, *22*, 6117−6121)

5.0. Conclusion

From the above brief introduction, it is evident that the internal redox cyclization of *o*-alkynylnitrobenzenes with metal complexes in general, and with gold complexes in particular, is relatively unexplored, as the efforts are mainly focused on the utilization of end products. The substrate dependent complementary formation of isatogens or anthranils is the unique feature of the gold-complexes. Though it has been speculated that reactive α-oxo gold carbenes are involved in these transformations, it has not yet been fully established in the case of isatogen synthesis, as there are some instances where DFT calculations revealed alternative possibilities. In addition, even the case of the complementary path that provides the anthranil, which revealed the existence of α-oxo metal carbenes in the reaction path, has been relatively unexplored. In this regard, what we have speculated is the possibility of the trapping of the α-oxo gold carbenes intermediates, which have been postulated in the gold-catalyzed redox cyclization of nitroalkynes with external nucleophiles. This is a challenging process, as the external reagent has to compete with the intramolecular 6π-electrocyclization. There were attempts earlier to trap these intermediates with external nucleophiles. However, they were not successful in interrupting their original intramolecular cyclization. However, if successful, it was expected to provide an

indirect support for the nitroso stabilized α-oxo metal carbenes postulated in the internal redox process. Coming to the synthetic potential, the Lewis-acidity of gold complexes allowed post modification of these reactive units *via* nucleophilic additions or cycloadditions. However, the nucleophiles or the dipolarophiles used are limited in number and this domain is still open for further exploration.

Chapter 1, Section A

Interrupting the [Au]-Catalyzed Nitroalkyne Cycloisomerization: Trapping the Putative α-Oxo Gold Carbene with 2,1-Benzo[*c*]isoxazole and 1,2- Benzo[*d*]isoxazole

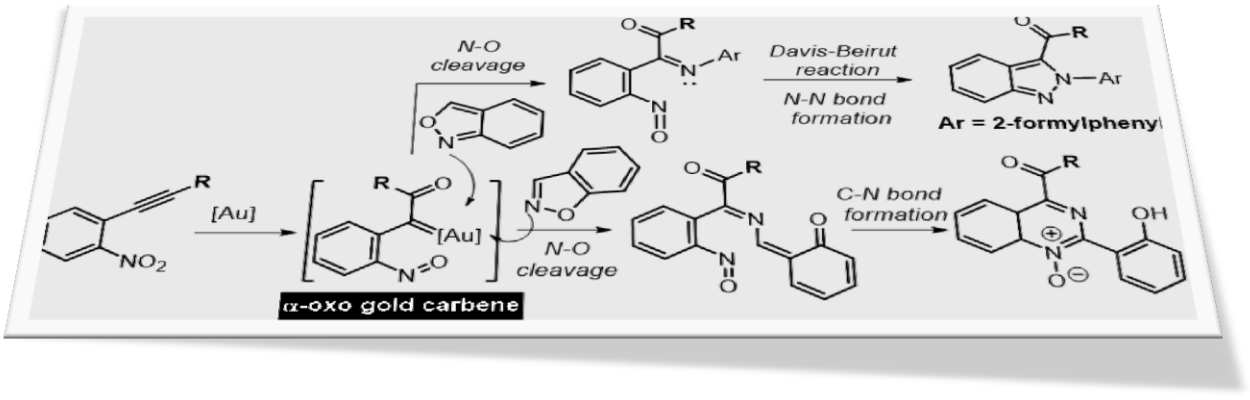

6.0. Introduction

As already described in the introduction, the cycloisomerization of *o*-alkynylnitrobenzenes (trivially known as nitrotolans) leading to isatogens is one of the earliest redox neutral reactions, documented as early in 1881 by Bayer during the course of his classic research on indigo.[9] In 2003, a seminal contribution by Yamamoto's group revealed the possibility of affecting this nitroalkyne cycloisomerization under gold-catalysis (see Scheme S1.8). Importantly, it has been revealed by Yamamoto's group that depending upon the pendant substituent on the alkyne, the nitroalkyne cycloisomerization proceeds in complementary paths leading to either isatogen (when the substituent is aryl) and/or isomeric anthranil (exclusively with alky substituent). By isolating a nitroso-stabilized α-oxo alkyl iridium intermediate, Crabtree's group revealed that the overall process is a metal-mediated internal redox process leading to an α-oxo iridium carbene intermediate (see Scheme S1.9). A similar mechanism even in gold(I/III)-catalyzed nitroalkyne internal redox processes with complementary regioselectivity during the initial oxygen transfer has been extended by Liu (see Scheme S1.11) and our groups as documented in introduction section.

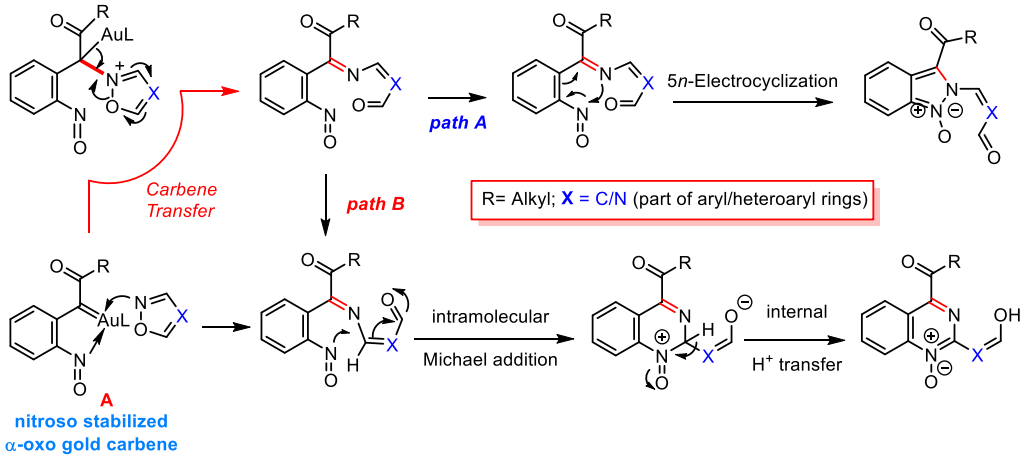

Figure F1.2: *Possible Interruption of Nitroso Stabilized α-Oxo Metal Carbene Intermediate with an External N-based Nucleophile for Intermolecular C-X and X-N Bonds Formation.*

In this section, we speculated on the possibility of trapping the nitroso stabilized α-oxo gold carbene intermediates that are proposed in the catalytic cyclization of *o*-alkynylnitrobenzenes with N-centered nucleophiles. These nitroso stabilized α-oxo gold carbene

intermediates provide a handle for the carbene for exchange with N-centered nucleophiles and also the reactive nitroso group in the proximity, for the subsequent C–N and/or N–X bond formation. Some of the known reagents for the carbene transfer reactions and the expected products are depicted in Figure F1.2 and possible reaction path has been depicted by employing isoxazoles as a representative nucleophile for the carbene transfer. However, in this event, the carbene exchange process has to compete with the original intramolecular cyclization of the α-oxo gold carbene intermediate that leads to anthranil. In order to check the possibilities of trapping the nitroso stabilized α-oxo gold carbene intermediates with N-centered azide nucleophile,[10] which are known to exchange with gold carbenes (Scheme S1.23). It is found that there is no interruption and the nitroalkynes underwent intramolecular cycloisomerisation giving anthranil as a sole product.

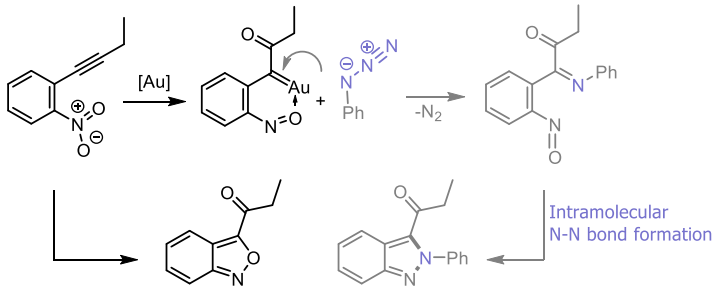

Scheme S1.23: *Failure Interruption of Nitroalkyne Cycloisomerisation with Azides*

With this initial failure, we proceed with the other nitrogen transferring heterocyclic scaffolds such as 2,1 benzo [*c*]isoxazole and 1,2 benzo[*d*]isoxazole, which are popular nitrene transfer reagents and at the same are known to trap the carbene from metal centers leading to imine derivatives with the simultaneous cleavage of N–O bonds.

6.0.1. Literature Report on Trapping of Gold Carbene with 2,1 benzo[*c*]isoxazole (Anthranil)

In 2018, Liu group described the [4+2] annulation of the α-alkyl vinyl gold carbene **S.24D** (cyclic/acyclic) generated from the allene **S1.24A** with anthranil **S.24B** affording the 3,4-dihydroquinoline derivative **S1.24C**. The proposed mechanism comprises of the initial formation of an alkenyl gold carbene **S1.24D** and subsequent carbene transfer to anthranil **S1.24B** leads to

the imine **S1.24G**. The resulting imine undergoes tautomerization followed by carbonyl ene-reaction to afford **S1.24C** (Scheme S1.24).

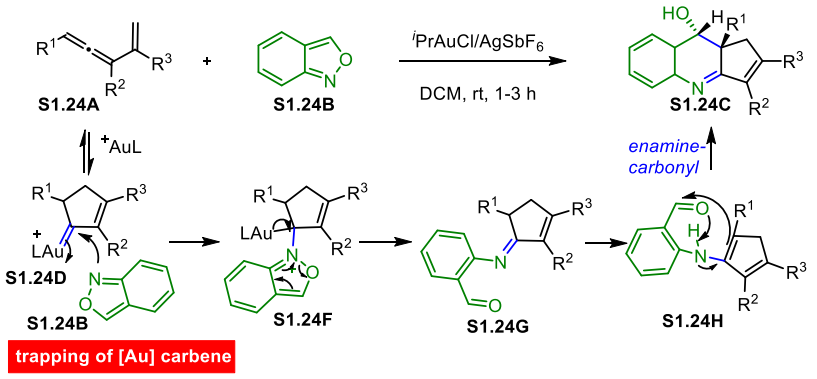

Scheme S1.24: *[4+2] annulation of anthranil with α-alkyl alkenyl gold carbenes*

(Mokar, B. D.; Jadhav, P. D.; Pandit, Y. B.; Liu, R.-S. *Chem. Sci.* **2018**, *9*, 4488−4492)

In 2019, the same group reported the gold-catalyzed annulation of N-propargyl ynamides **S1.25A** in the presence of anthranil **S1.25B** affording a mixture of imine derivative **S1.25C** (which on further acid hydrolysis affords) and hydrolyzed pyrrole product **S1.25D** (Scheme S1.25). In the proposed mechanism, α-imino gold carbene intermediate **S1.25E** formed first, which underwent carbene/alkyne metathesis to generate gold carbene intermediate **S1.25F**. Further, trapping of gold carbene with N-centered nucleophile of anthranil and subsequent aromatization leads to the intermediate imine **S1.25C** which on hydrolysis formed pyrrole product.

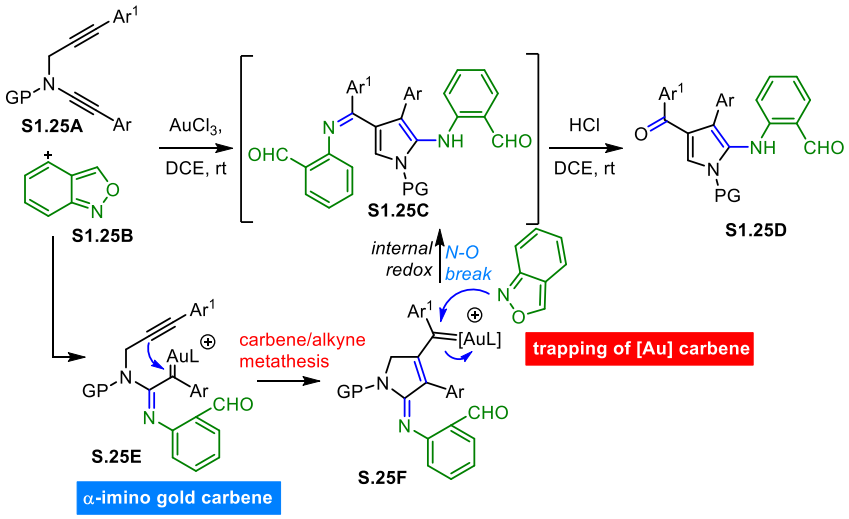

Scheme S1.25: *Gold[III]-Catalysed Annulation between Ynamides and Anthranil*

(Hsu, Y.-C.; Hsieh, S.-A.; Liu, R.-S. *Chem.- Eur. J.* **2019**, *25*, 5288−5297)

In continuation, the same group, reported reaction of internal ynamide **S1.26A** and anthranil **S1.26B** leading to tetrahydro-1*H*-benzo[*b*]azepine scaffold **S1.26C**. The proposed mechanism comprises of the formation of cyclopropyl gold carbene intermediate **S1.26D** which is in resonance with intermediate **S1.26E**, and its further *exo*-(4+3) anulation with anthranil leads to the gold carbene intermediate **S1.26F.** The product **S1.26C** was formed by carbene transfer to another molecule of anthranil (Scheme S1.26).

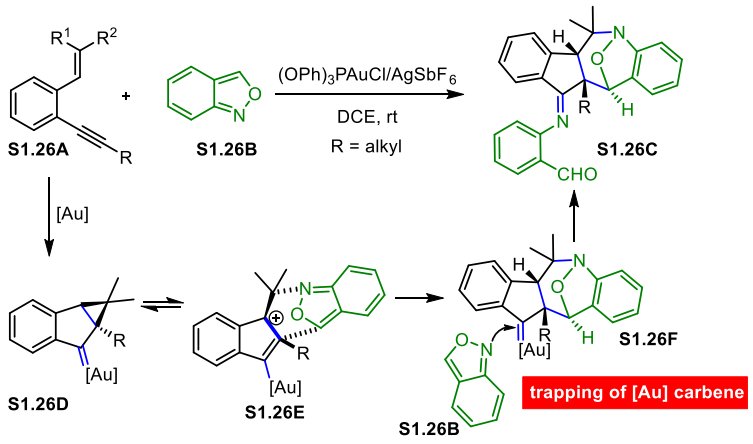

Scheme S1.26: *[4+3] Annulation between Anthranil and 2-Alkynyl-1-alkynylbenzenes and Trapping of Gold Carbene Intermediate*

(Singh, R. R.; Skaria, M.; Chen, L.-Y.; Cheng, M.-J.; Liu, R.-S. *Chem. Sci.* **2019**, *10*, 1201−1206)

6.0.2. Literature Report on Trapping of Gold Carbene with 1, 2 Benzo[*d*]isoxazole

There is only a singular report for the trapping of gold carbene with 1,2 benzo[*d*]isoxazole documented by Liu and coworker in 2019 (Scheme S1.27). The reaction involves the trapping of gold-carbene intermediate **S1.27D** derived from propargyl esters **S1.27A** *via* 1,2-acyloxy migration with 1, 2 benzo[*d*]isoxazole **S1.27B** affording the [5 + 1] annulation products **S1.27C**.

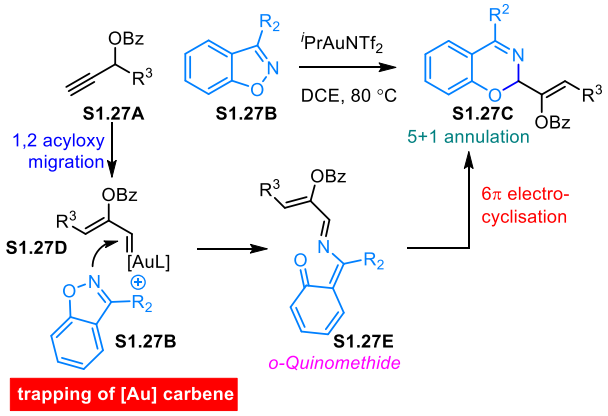

Scheme S1.27: *[5+1] Annulation between 1,2 benzo[d]isoxazole and Gold Carbene from Propargyl Esters*

(Xu, W.; Zhao, J.; Li, X.; Liu,Y. *J. Org. Chem.* **2018**, *83*, 15470–15485)

6.0.3. Our Hypothesis

Having understood that the gold carbene can be trapped with N-centered nucleophiles like anthranil as well as 1,2-benzoisoxazole, we speculated that, if the proposed α-oxo gold carbene intermediates of the nitroalkyne cycloisomerisation is trapped with benzo[*c*]isoxazole **4,** the reaction is expected to provide an imine **B** that should undergo Davis-Beirut cyclization[11] leading to the indazole **5** with simultaneous C–N and N–N bond formations. Whereas, with other N-centered nucleophile benzo[*d*]isoxazole **6**, the reaction is expected to provide the imino-*o*-quinomethide **B'** which on subsequent intramolecular Michael addition of nitroso group to quinomethide followed by aromatisation should lead to the quinazoline N-oxide **7** with simultaneous C–O and C–N bond formations (Figure F1.3).

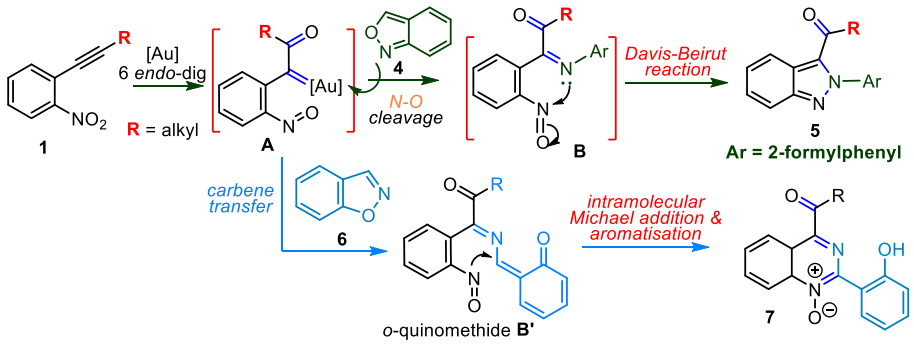

Figure F1.3: *Possible Interruption with an Anthranil and 1,2-Benzo[d]isoxazole leading to Indazoles and Quinazoline N-oxides respectively*

7.0. Part A- Synthesis of 2*H*-indazoles by Interrupting the Nitroalkyne Redox Process by 2, 1-Benzo[*c*]isoxazole

The 2*H*-indazole scaffold is one of the prominent pharmacophores well explored in medicinal chemistry with a good number of approved medicines spanning across a broad range of therapeutic applications.[12] The "Cadogan[13] and Davis-Beirut reactions[11]" that forge a 2*H*-indazole heterocyclic core *via* an intramolecular N–N bond formation are the two important reactions applied in the synthesis of this heterocyclic core. In both the reactions, initially a nitro group undergoes either a reduction or an internal redox process leading to a reactive nitroso intermediate. In the case of the Davis-Beirut reaction, the intramolecular nucleophilic attack and/or a 5-centered 6π-electrocyclization of the nitroso intermediate results in an indazole N-oxide that either under-goes an internal redox reaction or deoxygenation. On the other hand, in the classical mechanism proposed for the Cadogan indazole synthesis, the nitroso intermediate further reduces to a nitrene that adds to the imine, though the possibility of the former process has also been established.[14] Despite their widespread utility, the harsh conditions/reagents employed for generating the reactive nitroso intermediates warrants the availability of milder reagents/conditions that are amicable for sensitive functional/protecting groups.

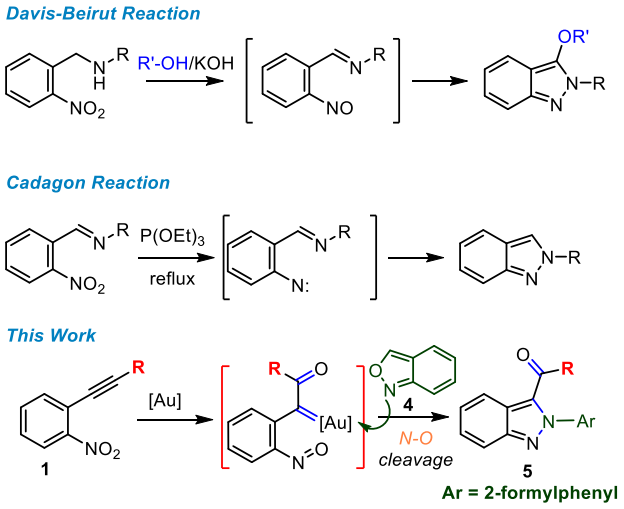

Scheme S1.28: *Indazole Synthesis: Davis-Beirut & Cadagon Reactions and Present Work*

7.0.1. Present Work

To examine these hypothetical possibilities, initially, employing 1-(but-1-yn-1-yl)-2-nitrobenzene (**1a**) as a substrate, we examined its cycloisomerization in the presence of anthranil **4a** following reported conditions using $AuBr_3$ (in toluene) and $Pd(CH_3CN)_2Cl_2$ (in acetonitrile) complexes. As shown in Table 1 (entries 1 and 2), with the palladium complex, isatogen **2a** was obtained exclusively. On the other hand, with the $AuBr_3$, the corresponding anthranil **3a** was mainly obtained with trace amounts of a new product, with the expected mass corresponding to the desired indazole **5aa**.

Next, we studied the reactions with $AuCl_3$, which had shown superior reactivity over $AuBr_3$ in nitroalkyne cycloisomerizations. However, in the prescribed 1,2-dichloroethane solvent, we got a poor conversion, resulting mainly in the formation of the anthranil **3a** in small amounts. Gratifyingly, when we switched to toluene, the uncharacterized product **5aa** that was encountered with $AuCl_3$ was obtained in 54% yield along with the anthranil **3a** (12%). The structure of product **5aa** was established with the help spectral, analytical and single crystal X-ray diffraction studies. In the ^1H NMR spectra of compound **5aa,** about 8 aromatic protons have seen along with an aldehyde proton which confirmed the incorporation of the anthranil moiety and at the same time the N-O bond cleavage. The two protons of the methylene group (CH_2) at alkyne unit shifted to downfield and resonated at δ 3.15 ppm compared to δ 2.50 ppm in the case of starting compound **1a**. The loss of alkyne carbons in the ^{13}C NMR spectrum of **5aa** indicated the modification at the alkyne end. The appearance of two carbonyl carbons at 188.4 and 190.3 ppm and from DEPT spectra confirms that aldehyde carbon resonate at 190.3 ppm (formed *via* N-O bond cleavage of an anthranil group). The constitution of **5aa** has been confirmed as $C_{17}H_{15}N_2O_2$ by the HRMS ($[M+H]^+$) found as 279.1132. Finally, the single crystal X-ray diffraction analysis of compound **5aa** revealed that it was the desired indazole. Importantly, it proved the point that the intermolecular trapping of proposed gold carbene intermediates of nitroalkyne cycloisomerization was possible.

Encouraging with this results, we next proceeded further to improve the yield of the reaction. As shown in Table 1, our initial attempts with changing the solvent were not promising (entries 5–8). This provoked us to explore the other gold(III) and cationic gold(I)-complexes in this pursuit. As shown, in the Table 1 (entry 9), with dichloro(2-pyridinecarboxylato)gold(III)

($PicAuCl_2$, entry 9) the requisite indazole was obtained as a major product in moderate yields. Similarly, with AuCl and with other cationic gold(I)-complexes, the results are not encouraging (entries 10–13). In the majority of the cases, the cycloisomerization leading to anthranil **3a** was the major event, along with the formation of the requisite **5aa**. Gratifyingly, with $AuCl_3$, in toluene, when the reaction was heated to 80 °C, the yield of **5aa** was improved to 57% and the anthranil **3a** was also obtained in 10% yield (entry 14). Finally, when the reaction was carried out by slow addition of **1a** to a solution of **4a** and $AuCl_3$ catalyst at rt, the yield of **5aa** was improved to 69%, and the formation of the cycloisomerization product **3a** was also minimized (entry 15).

Table 1: *Optimisation of the Reaction Condition.*[a]

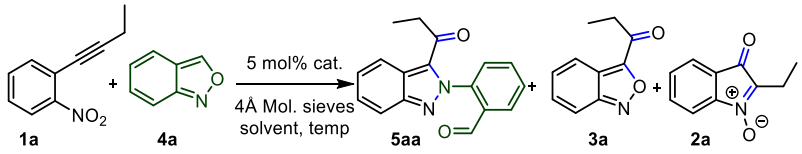

Entry	Catalyst	Solvent	Yield (%)	
			5aa[b]	2a or3a[b]
1	$AuBr_3$	PhMe	trace	64 (3a)
2	$Pd(CH_3CN)_2Cl_2$	MeCN	-	69 (2a)
3	$AuCl_3$	$ClCH_2CH_2Cl$	-	trace (3a)
4	$AuCl_3$	PhMe	54	12 (3a)
5	$AuCl_3$	MeCN	-	-
6	$AuCl_3$	1,4-Dioxane	-	-
7	$AuCl_3$	$PhCF_3$	44	13 (3a)
8	$AuCl_3$	PhCl	49	10 (3a)
9	$PicAuCl_2$	PhMe	42	10 (3a)
10	AuCl	PhMe	35	24 (3a)
11	$PPh_3AuCl/AgSbF_6$	PhMe	26	38 (3a)
12	IPrAuCl/AgOTf	PhMe	20	46 (3a)
13	$(ArO)_3PAuCl/AgNTf_2$	PhMe	27	42 (3a)
14[c]	$AuCl_3$	PhMe	57	10 (3a)
15[d]	**$AuCl_3$**	**PhMe**	**69**	**trace (3a)**

[a]In general, the reactions were carried out with 0.2 mmol of **1a** and 0.22 mmol of **4a** in 2mL of solvent and 5 mol% of catalyst at rt with a reaction time of 3-4 h. [b]Isolated yield. [c]Reaction was carried at 80 °C. [d]Slow addition of **1a** through syringe pump at rt for 4 h.

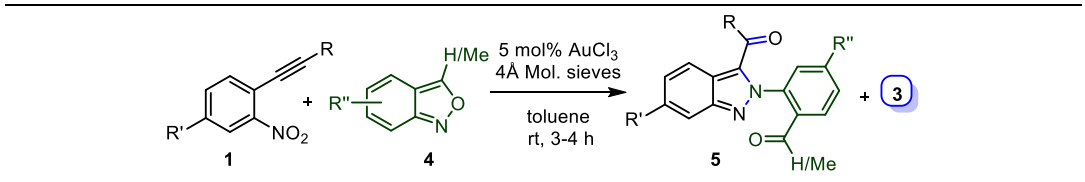

5aa (65%) + **3a** (11%) [R = -Et] **(500 mg Scale)**
5ba (67%) + **3b** (8%) [R = -^{n}Pr]
5ca (64%) + **3c** (12%) [R = -^{n}penty]
5da (65%) + **3d** (20%) [R = -^{t}Bu]
5ea (58%) + **3e** (24%) [R = -$(CH_2)_2$Ph]
5fa (63%) + **3f** (14%) [R = -$(CH_2)_3$OAc]
5ga (68%) + **3g** (8%) [R = -$(CH_2)_3$OTBS]
5ha (31%) + **3h** (56%) [R = -cyclopropyl]

5ac (51%) + **3a** (12%)

5ad (56%) + **3a** (16%) [R = -Et]
5cd (55%) + **3c** (14%) [R = -^{n}penty]
5dd (58%) + **3d** (16%) [R = -^{t}Bu]
5ed (47%) + **3e** (24%) [R = -$(CH_2)_2$Ph]

5ia (47%) + **3i** (20%) [R' = -F]
5ja (56%) + **3j** (16%) [R' = -Me]
5ka (72%) + **3k** (6%) [R' = -CO_2Me]
5la (77%) + **3k** (6%) [R' = -CN]

5jb (39%) + **3j** (20%)

5be (56%) + **3b** (18%) [R' = -H]
5je (64%) + **3b** (14%) [R' = -Me]
5le (71%) + **3k** (10%) [R' = -CN]

5bf (56%) + **3b** (18%) [R' = -H, R = -^{n}Pr]
5ef (54%) + **3e** (14%) [R' = -H, R = -$(CH_2)_2$Ph]
5jf (51%) + **3j** (18%) [R' = -Me, R = -^{n}Pr]

5ab (42%) + **3a** (10%) [R = -Et]
5cb (36%) + **3c** (16%) [R = -^{n}penty]

5kc (68%) + **3k** (6%) [R' = -CO_2Me]
5lc (71%) + **3k** (8%) [R' = -CN]

5bg (71%) + **3b** (10%) [R = -^{n}Pr]
5dg (66%) + **3d** (16%) [R = -^{t}Bu]
5eg (57%) + **3e** (24%) [R = -$(CH_2)_2$Ph]

5jg (60%) + **3j** (16%) [R' = -Me]
5kg (69%) + **3k** (8%) [R' = -CO_2Me]

Incompatable nitroalkyne and anthranil substrates

1m **1n**

R = -Ph (**1o**)
= -OTHP (**1p**)
= -NHBoc (**1q**)

4h

4i

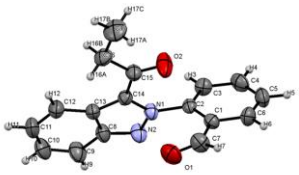

ORTEP Diagram of **5aa**
(Thermal ellipsoids are shown at the 50% probability level)

Scheme S1.29: *Reaction Scope, Limitations and a Single Crystal XRD Structure.*

As illustrated in Scheme S1.29, a wide range of substituted nitroalkynes have been employed to examine the scope of the reaction and to understand how the substituents influence the outcome. Initially, we employed the substrates having different pendant substituents on the alkyne unit. As shown, changing the length of the side chain did not alter the reaction outcome and it was also found that the protecting groups such as *O*-acetyl and *O*-TBS placed on this alkyl chain were intact. Interestingly, with the cyclopropyl substituted alkyne, the intramolecular cyclization was successfully completed, and resulted in the requisite indazole **5ha** as a minor product and the corresponding anthranil **4h** as the major product. For the substrates **5ia**–**5la** having different substituents placed para to the alkyne unit, the outcome of the reaction was influenced. For example, when a carboxylate as well as cyano was present, the yield was 72% (**5ka**) and 77% (**5la**) revealing that the presence of an EWG group at this position had a stabilizing effect on the intermediate gold carbene. In contrast, when the substituent was fluorine, the yield was reduced to 47% (**5ia**), which indicates that sigma-acceptors at this position are not compatible. When a methyl group **5ja** was present at this position, the yield was only 56%. It is noteworthy that the good yield was retained even when the reaction was carried out on 500 mg scale (**5aa**, 65% yield).

Next, we varied the substituents on the anthranil ring. When halogen-substituted anthranils were employed as the substrates, the reactions in general resulted in the corresponding indazoles **5ab**–**5ad** in low to moderate yields depending upon the position of the halogen atom. The yields are poor when the halogen is placed para to the nitrogen. On the other hand, with 5-methyl and 5-carboxymethyl anthranils **4e** and **4f** respectively, the corresponding indazoles were obtained in good to moderate yields. Interestingly, when a methoxy group is placed on the anthranil ring, there was no interception of the original internal nitroalkyne redox process and the corresponding anthranil was obtained exclusively.[15] Next, we examined the compatibility of a C3-methyl substituted anthranil **4g** employing different nitroalkynes. The results are encouraging and the corresponding 2*H*-indazole containing an *o*-acyl group on the pendant aryl ring were obtained in moderate to good yields (**5bg, 5cg**, **5dg**, **5jg** and **5kg**). In this case also, the nitroalkyne **1k** having the carboxylate group gave the best results. On the contrary, the nitroalkyne or the anthranil having methoxy or hydroxyl substitutes on the aryl ring were found to be incompatible and the reactions employing either of these substrates gave mainly the corresponding anthranil derivatives. In addition, when the alkyne end carries a bulky group or an

alkyl chain having electron withdrawing groups, the intramolecular cyclization is facile over the intermolecular carbene exchange, indicating that both steric and electronic factors play important roles.

7.0.2. Utility of Product

To show the utility, the selective homologation of the aldehyde group present in these products has been carried out employing the stable Wittig ylides. The reactions are highly selective and proceed smoothly at rt to provide the corresponding E-olefins **8** and **9** in excellent yields (Scheme S1.30). Coming to the structural assignment of compound **8a**, in the ^{1}H spectrum, the two olefinic protons appeared separately at δ6.34 ppm and δ7.02 ppm, both as doublets with a characteristic trans-olefin coupling constant at J = 16 Hz. In ^{13}C NMR of compound **8a**, these olefin carbons resonated at δ121.4 and δ126.2 ppm, both as doublets. Similar trend was obtained with compound **9a.**

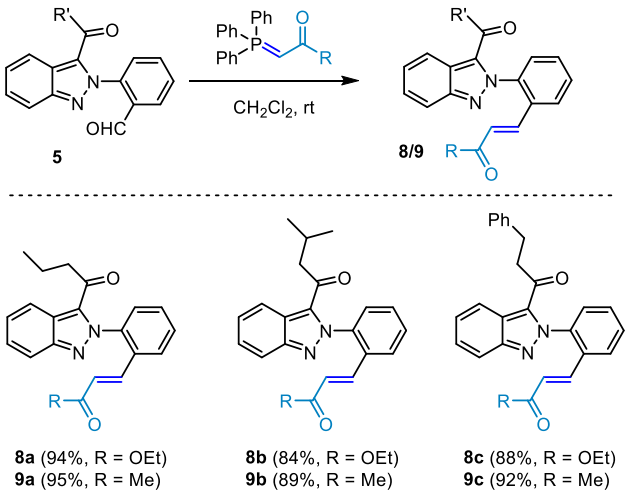

Scheme S1.30: *Selective Wittig Homologation of the Aldehyde group*

7.0.3. Control Experiments

To probe whether this overall process involves the anthranil **3a** as an intermediate, control experiments have been carried out by employing **3a** as a substrate under the optimized conditions in the presence of **4a** (Scheme S1.31, eq. 1). Even after prolonged reaction times, both **3a** and **4a** were intact, thus revealing that the internal redox cascade process was interrupted prior to the formation of **3a** and presumably by the carbene transfer from the intermediate α-oxo

gold carbene to the nitrogen of anthranil **4a**. Next, the concern is about the possible intermolecular functionalization of alkyne with the anthranil **4** leading to a α-imino gold carbene[7a,16] followed by oxygen transfer from the nitro group[17] (Scheme S1.31, eq. 4) and finally the N–N bond formation. As a control, the phenyl substituted nitroalkyne **1r,** when treated with **4a** under the optimized conditions (Scheme S1.31, eq. 2) gave exclusively isatogens **2r** *via* 5-ex*o*-dig cyclization. This indicated that the isomeric α-oxo gold carbene involved in this process prefers the intramolecular cyclization over the intermolecular carbene interception and importantly that the possibility of anthranil addition to the alkyne and subsequent α-imino gold carbene formation is not operational. An additional control experiment was conducted by carrying the reaction in the presence of excess styrene (known/used to trap the gold carbenes).[18] Though, the expected cyclopropane product could not be isolated in reasonable amounts to characterize, however, the LCMS analysis showed its presence in the crude reaction mixture (Scheme S1.31, eq. 3).

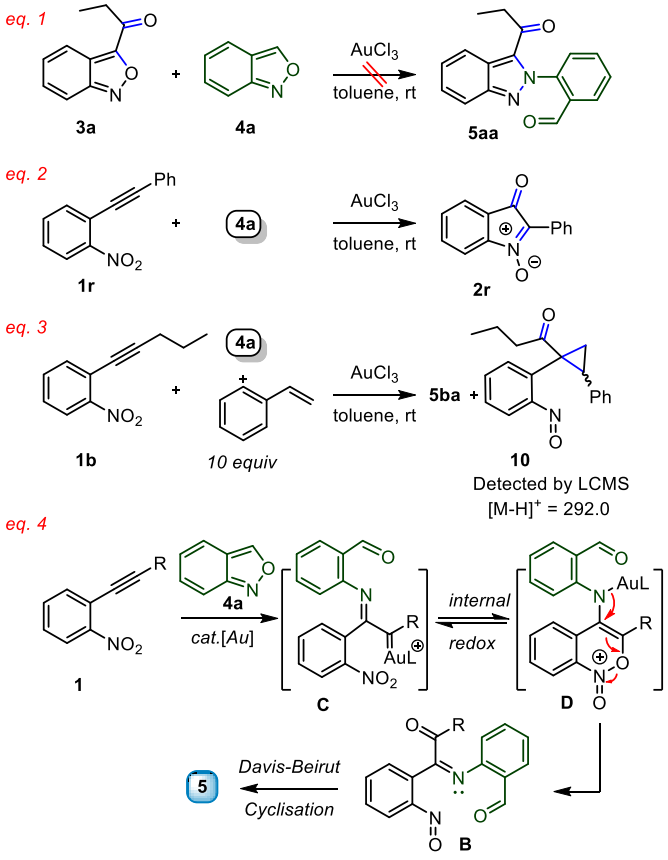

Scheme S1.31: *Control Experiments to Support the Involvement of the α-Oxo Gold Carbene Intermediate (eq.1–eq.3) and Alternative Possibility for the Formation of Indazole (eq.4)*

7.0.4. Competition Experiments

Further, competition experiments were done employing the alkynes **11a**–**11c**, which are known to be functionalized with the anthranil **4a** (leading to an α-imino gold carbene intermediate) under current conditions and also under the conditions\gold-complex reported for the same transformation.[19–21] As shown in Scheme S1.32, the reaction of **1a** and **4a** in the presence of ethynyl cyclopropane (**11a**) under the prescribed conditions and Au[I]-catalyst/Ag-additive catalysts resulted in a mixture of the reported product **12aa** (42%) and indazole **5aa** (12%).[19] When the same reaction was carried out under the current conditions, it provided mainly the indazole **5aa** along with the anthranil **3a**. Similar results were obtained in the competition experiments employing alkynes **11b** or **11c**.[20,21] In general, with the reported complexes, the reaction between the anthranil **4a** and the alkyne **11** is facile and with $AuCl_3$, the nitroalkyne redox process seems to be operating exclusively. Thus, these competition experiments clearly indicate that, unlike with the other complexes, it appears that $AuCl_3$ selectively activates the nitroalkyne **1a** over the competing terminal alkyne and this provides an indirect evidence for an internal oxygen transfer leading to a α-oxo gold carbene intermediate, and subsequent carbene transfer to the nitrogen present in the anthranil **4**.

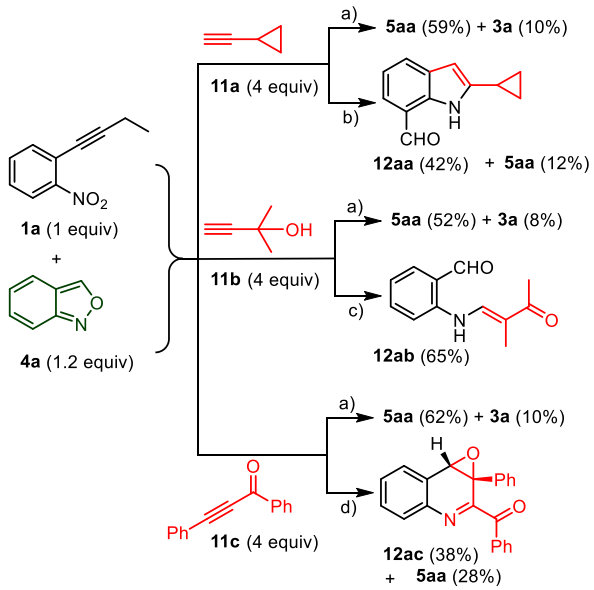

Conditions:- a) $AuCl_3$, Toluene, rt, 3 h; b) IPrAuCl/$AgNF_2$, $Zn(OTf)_2$ $PhCF_3$, 65 °C, 4 h; c) JohnPhosAuCl, $AgNTf_2$, $(CH_2Cl)_2$, rt, 6 h; d) $(PhO)_3AuCl$, $AgSbF_6$, $(CH_2Cl)_2$, 80 °C, 7 h.

Scheme S1.32: *Competition Experiments to Support the Involvement of the α-Oxo Gold Carbene Intermediate*

8.0. Part B- Syntheisis of Quinazoline N-oxides by Interrupting the Nitroalkyne Redox Process by 1,2-Benzo[*d*]isoxazole

Quinazoline N-oxides are relatively unexplored in medicinal chemistry, which is quite surprising, as the parent quinazoline is one of the privileged skeletons in various drug discovery programs and is widely found in various natural products/approved drugs.[22] In general these quinazoline N-oxides are synthesized by *N*-oxidation and there are no general methods documented in the literature for their convergent synthesis (Scheme S1.33).[23] The development of novel synthetic routes to access quinazoline N-oxides is an attractive task using catalytic and mild conditions.

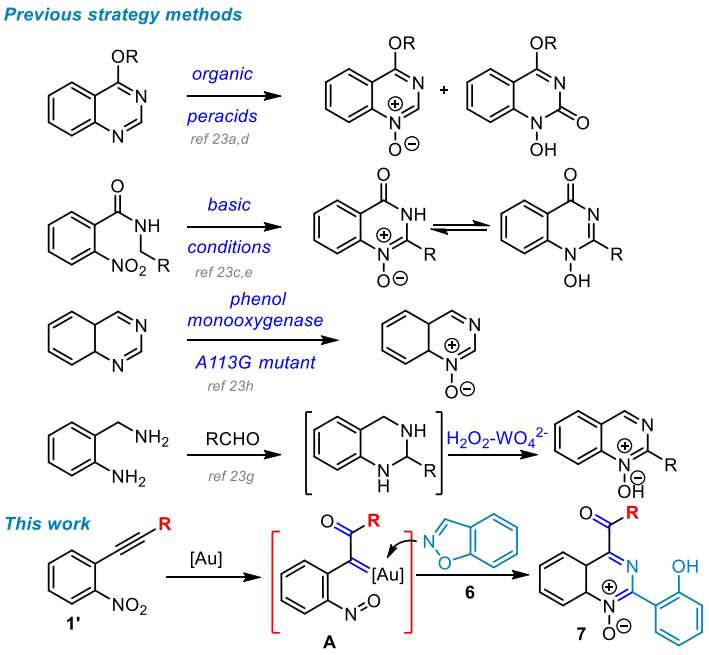

Scheme S1.33: *Synthesis of Quinazoline N-oxides: Reported Methods and Proposed Method via Trapping of the Intermediate α-Oxo Gold Carbenes with 1,2-Benzo[d]isoxazole.*

8.0.1. Present Work

Our initial experiments in this regard started with the nitroalkyne **1a'** and benzo[*d*]isoxazole **6a** as the substrates and examined the gold and palladium complexes that are commonly employed in the internal nitroalkyne redox process. In general, the reaction were carried out employing 1 equiv. of 1-(but-1-yn-1-yl)-2-nitrobenzene (**1a'**) and 1.1 equiv. of benzo[*d*]isoxazole **6a** in suitable solvent at given temperature in presence of 5 mol% of catalyst. Table 2 saliently describes the exploratory experiments that were conducted in this context. When $AuBr_3$ was employed as a catalyst in toluene it afforded the self cycloisomerisation product anthranil **3a** along with the trace amount of a new product with an expected mass corresponding to the desired product **7aa** while the reaction with $Pd(CH_3CN)_2Cl_2$ complex in acetonitrile gave isatogen **2a** exclusively. Next, $AuCl_3$ was employed in 1,2-dicloroethane that results in the formation of anthranil **3a** in trace amounts (entry 3). Gratifyingly, when we switched to toluene as a solvent, it afforded the desired quinazoline N-oxide **7aa** (62%) as major product along with anthranil **3a** (10% yield) (entry 4). Coming to the ^1H NMR spectrum of compound **7aa**, the characteristic phenolic peak (exchanged with D_2O) was seen to resonate at δ 10.41 ppm in addition to the total number of 8 aromatic protons that appeared near the $CDCl_3$ signal. This confirmed the union of 1,2-benzoisoxazole unit with the nitroalkyne *via* N-O bond cleavage. The two protons of the methylene group (CH_2) at alkyne end shifted to downfield (δ 3.41 ppm) when compared to (δ 2.50 ppm) in the case of starting nitroalkyne. The appearance of carbonyl carbon at δ 202.3 ppm proved to be formed by the internal oxygen transfer from nitroalkyne redox process. The constitution of **7aa** has been confirmed as $C_{17}H_{15}N_2O_3$ by the HRMS ($[M+H]^+$) found as 295.1073. Finally, single crystal X-ray diffraction studies revealed the structure of compound **7aa** as the desired quinazoline N-oxide.

Encouraged with this results, next we screened different solvents, however, there is no net increase in the yield of **7aa** (entries 5-8). Changing of gold catalyst and addition of silver salts didn't improve the yields (entries 9-10). In all these cases the anthranil **3a** was obtained in major quantity along with requisite product **7aa** as a minor one. When AuCl was employed as a catalyst, a mixture of **7aa** and **3a** in were obtained in equal proportions (entry 11). Heating the reaction to 80 °C improved the yield of **7aa** nominally (65%, entry 12). The yield of **7aa** was improved further to 73%, when the reaction was carried out by slow addition of **1a'** to a solution of **6a** along with $AuCl_3$. In this case, the formation of cycloisomerisation product **3a** was also

minimized to trace amounts (entry 13). At this stage, the reaction with excess 1,2-benzo[*d*]isoxazole **6a** (3 equiv.) under these conditions has been tried, however, it has not improved the yield of the desired product. A control experiment conducted without gold-catalyst and heating a mixture of **1a'** and **6a** at 80 °C in toluene revealed that both starting compounds are intact and the essential of role of the gold complex for the internal oxygen transfer.

Table 2: *Optimization of the Reaction Conditions.*[a]

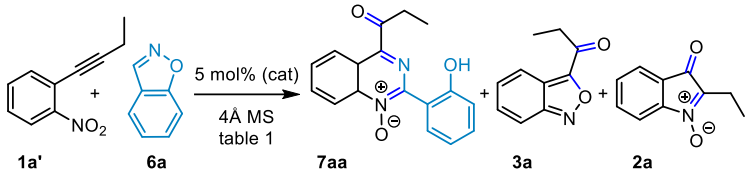

Entry	Catalyst	Solvent	Yield (%)	
			7aa[b]	2a/3a[b]
1	$AuBr_3$	PhMe	trace	64 **(3a)**
2	$Pd(CH_3CN)_2Cl_2$	CH_3CN	-	66 (**2a**)
3	$AuCl_3$	$(CH_2)_2Cl_2$	-	trace **(3a)**
4	$AuCl_3$	PhMe	62	10 **(3a)**
5	$AuCl_3$	CH_3CN	-	-
6	$AuCl_3$	1,4 Dioxane	-	-
7	$AuCl_3$	$PhCF_3$	54	13 **(3a)**
8	$AuCl_3$	PhCl	59	10 **(3a)**
9	$PPh_3AuCl/AgSbF_6$	PhMe	26	32 **(3a)**
10	$PicAuCl_2$	PhMe	44	16 (**3a**)
11	AuCl	PhMe	38	24 (**3a**)
12[c]	$AuCl_3$	PhMe	65	6 (**3a**)
13[d]	**$AuCl_3$**	**PhMe**	**73**	**trace (3a)**
14[e]	$AuCl_3$	PhMe	72	trace (**3a**)
15[c]	--	PhMe	--	--

[a]In general, the reactions were carried out with 0.2 mmol of **1a** and 0.22 mmol of **6a** in 2mL of solvent and 5 mol% of catalyst at rt with a reaction time of 3-4 h. [b]Isolated yield. [c]Reaction was

carried at 80 °C. [d]Addition of **1a** to solution of **6a** in solvent through syringe pump for 4 h. [e]with 3 equiv. (0.66 mmol) of **6a**.

With an optimized conditions in hand, the scope of this reaction has been expanded by employing nitroalkyne substrates with varying substituents on pendant alkyne unit (**1a'–1i'**, **1o'–1r'**) and also phenyl substituted one **1t'**, by placing different substituents para to the alkyne group (**1j'–1n'**) and also by changing the substituents on the 1,2-benzo[*d*]isoxazole counterpart (**6a–6h**). As shown in Scheme S1.34, changing the length of the pendant alkyne unit did not alter the reaction outcome (**7aa–7ca**) whereas; steric hindrance on the alkyne unit had influence on the reaction outcome. For example, with the isobutyl substituent, the yield of the desired quinazoline 1-oxide was reduced to 60% (**7da**) and when a benzyl (**1o'**) and *tert*-butyl (**1r'**) group is present, there was no intermolecular interception and the intramolecular cyclization leading to corresponding anthranils was the main event. Similarly, when propargylic carbons bears an –I group such as –OTHP (**1p'**) or –NHBoc (**1q'**), the reactions led to complex mixture from which a mixture of corresponding anthranil and/or isatogens could be isolated in small amounts. However, when the same groups are present on homopropargylic position are further, their reactions with 1,2-benzo[*d*]isoxazole **6a** proceeded smoothly and provided the corresponding quinazoline oxides in moderate to good yields. The examined scope with these substrates revealed the tolerance for various protecting group such as OAc, OTBS, OTHP, OBn on the alkyl chain under current conditions. In addition, a gram scale reaction was performed under the optimized conditions and it was found that with 2 mol% of $AuCl_3$ the reactions proceed well and provided the desired quinazoline N-oxide **7ba** in 69%. Next, we examined the reactions with the substrates having electron withdrawing/donating groups such as $–CO_2Me$ (**1m'**), $–NO_2$ (**1k'**), –F (**1j'**) and –Me(**1l'**) para to the alkyne unit. Interestingly, with the substrate having the $–CO_2Me$ the best reaction outcome has seen. Whereas with the substrate having the $–NO_2$ group, the intramolecular cyclisation competed well, and resulted in the requisite quinazoline N-oxide (**7ka**) in 34% yield along with the substantial amounts of anthranil/isatogen. With the substrates –F or –Me groups, corresponding quinazoline N-oxides **7ja** (51%) and **7la** (61%) respectively were obtained in moderate yields.

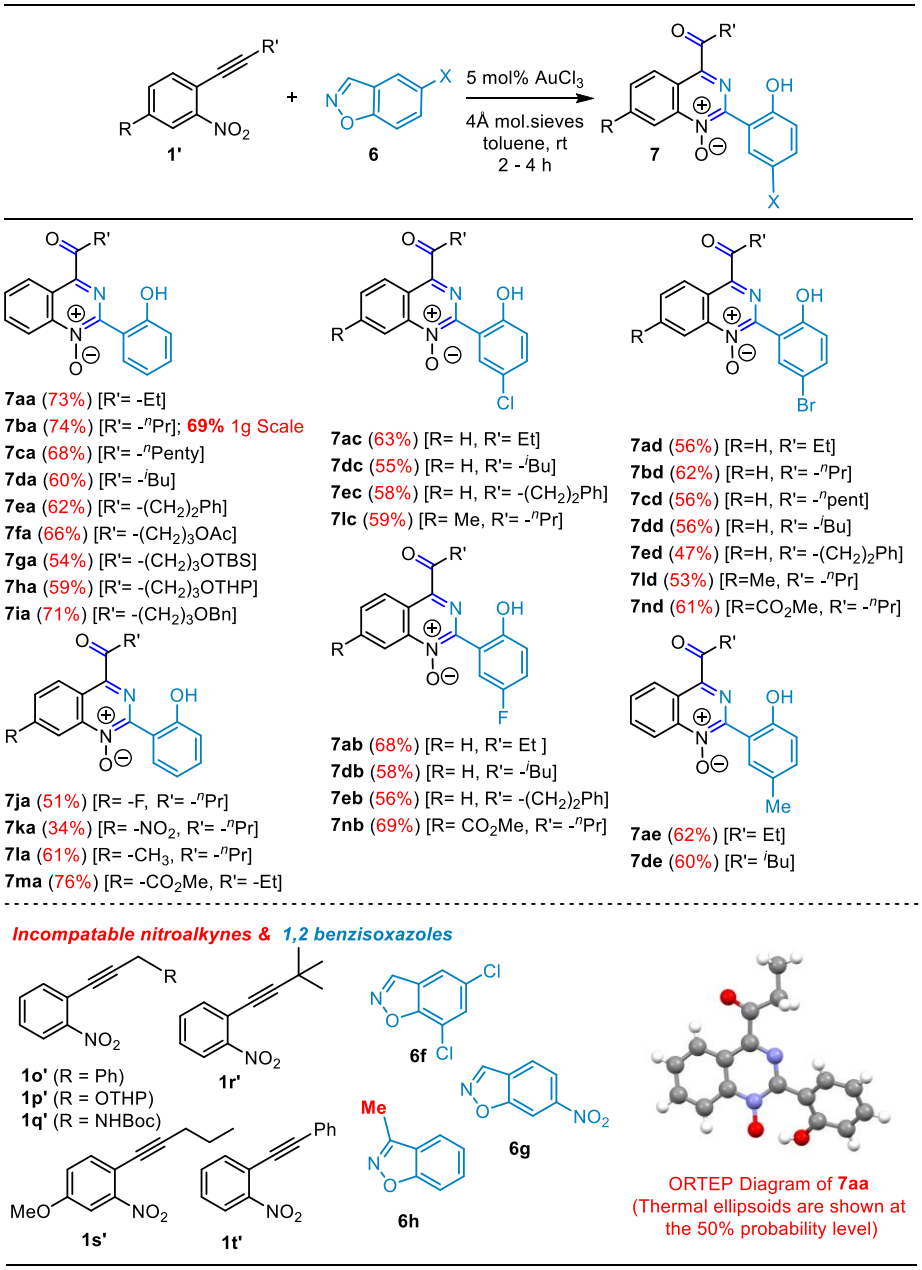

Scheme S1.34: *Reaction Scope, Limitations and a Single Crystal XRD Structure*

Next, the 1,2-benzo[*d*]isoxazoles having substituents such as –F (**6b**),–Cl (**6c**),–Br (**4d**) and also with –Me (**6e**) group have been employed in the current reaction to examine how the electronic nature of the substituent para-to the phenolic oxygen will influence the reaction outcome. In general, the reactions with these four 1,2-benzo[*d*]isoxazole are smooth and provided the corresponding heterocyclic products in moderate to good yields. In addition, the benzo[*d*]isoxazole having 5,7-dichloro (**6f**) or –NO_2 (**6g**) were found to be incompatible and the

reactions with these substrates resulted mainly with the anthranil formation. When 3-methylbenzo[*d*]isoxazole **6h** was used along with **1b'**, the self cycloisomerized product **3b** was obtained exclusively. This indicated that the aromatization step involves the removal of hydrogen atom next to the imine.

8.0.2. Utility of Product

In order to show the utility of product, some of the synthesized N-oxide derivatives have been subjected for N–O bond reduction by using Zn dust in 30% aq. NH_4Cl in THF to afford the corresponding quinazoline derivative in good yields (Scheme S1.35).[24] Coming to the structural elucidation of compound **13a**, in the ^1H spectrum, the phenolic proton appears to be in downfield and found to be resonate at δ 13.50 ppm compared to the phenolic proton of starting material which resonate at δ 10.41 ppm due to hydrogen bonding between N-oxides and phenolic proton. In ^{13}C NMR of compound **13a**, there is slight difference in the chemical shift of aromatic carbons.

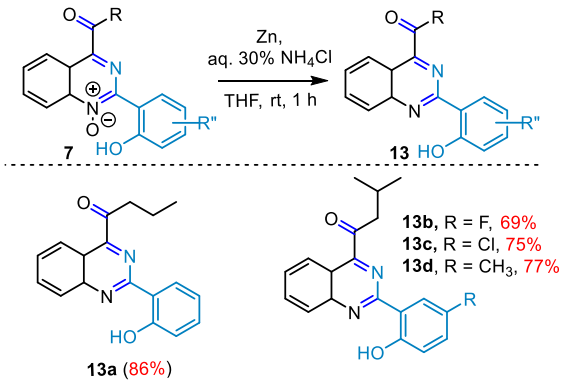

Scheme S1.35: *Functionalisation to Quinazoline Scaffolds.*

8.0.3 Control and Competition Reaction

Having established the generality of the current reaction, we next proceeded further to learn about the possible involvement a α-oxo gold carbene intermediate and carbene transfer to a nitrogen center.[17] As expected, with 2-phenyethynylnitrobenzene **1t'**, there was no interception by the 1,2-benzo[*d*]isoxazoles and the reaction provided exclusively isatogen (Scheme S1.36, eq.1) indicating that the isomeric gold carbene expected from initial internal oxygen transfer (5-

exo-dig) is relatively unstable. In addition, this also provides an indirect support for the initial N–O transfer to the alkyne, as there is an alternative possibility that comprises of competing addition of the benzoxazole nitrogen to the alkyne leading to a α-imino gold carbene and subsequent internal oxygen transfer.[25]

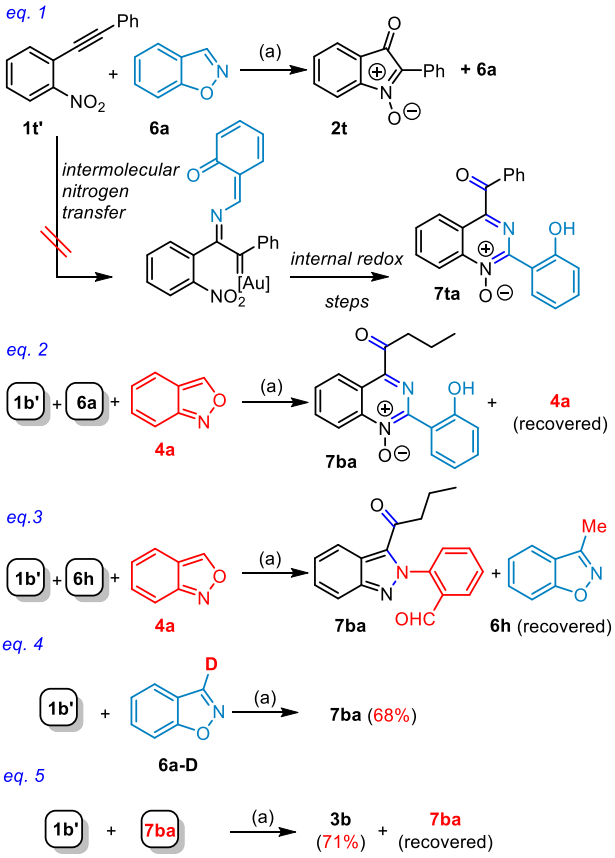

Condition: (a) = $AuCl_3$ (5 mol%), 4Å MS, toluene, rt, 4 h

Scheme S1.36: *Control and Competition Experiments*

Finally, competition experiment comprising of adding the nitroalkyne **1b'** to a equimolar mixture of benzo[*d*]isoxazole **6a** and its regioisomer benzo[*c*]isoxazole **4a** under current conditions resulted in exclusively quinazoline N-oxide **7ba** (71% yield) along with the recovery of **4a** revealing that the N-centered nucleophile of benzo[*d*]isoxazole is more reactive than that of the anthranil (Scheme S1.36, eq.2). Interestingly, when the same competition experiment was carried out with employing 3-methylbenzo[*d*]isoxazole **6h** and anthranil **4a**, the indazole derivative **5ba** was obtained exclusively revealing that the carbene transfer happened selectively to nitrogen of the anthranil over the benzoisoxazole **6h** (Scheme S1.36, eq.3). In addition, it also

ruled out the alternative possibility of forming an α-imino gold carbene followed by the oxygen transfer from nitro group and provided an indirect support for the formation of α-oxo gold carbene intermediate after the initial nitro-alkyne redox cyclization. When deuterated (benzo[*d*]isoxazole-3-d) **6a-D**[26] was employed along with **1b'**, there was no incorporation of the deuterated hydrogen in product **7ba** (Scheme S1.36, eq.4). This indicated that the aromatization step involves the removal of the hydrogen atom next to the imine. Finally, a control experiment comprising of treating a equimolar mixture of o-nitroalkyne **1b'** and the quinazoline *N*-oxide **7ba** under the optimized conditions (in absence of benzo[*d*]isoxazole) has been carried out (Scheme S1.36, eq.5). The cycloisomerised product anthranil **3b** was obtained in 71% yield along with recovery of N-oxide **7ba**. This result suggests that the obtained N-oxide products are stable and that there is no oxygen transfer from these N-oxides to the nitroalkyne that can potentially interrupt the initial nitroalkyne redox cyclization.

9.0. Conclusion

To conclude, a novel methodology for the convergent synthesis of functionalized 2H-indazoles and quinazoline N-oxides has been developed. The overall process comprises of trapping of α-oxo gold carbene with 2,1-benzo[*c*]isoxazole and 1,2-benzo[*d*]isoxazole with the orchestration of sequential N–O bonds cleavage and formation of C–O, N–N bonds in case of 2H-indazole, and C–O, C–N bonds in quinazoline *N*-oxide case. The fine competition experiments between inter- *vs* intramolecular heteroatom addition to alkynes *inter-alia* competition between the formation of α-imino *vs* α-oxo gold carbenes and the unique opportunities with 1,2-benzo[*d*]isoxazoles that is known generate to the α-imino gold carbenes from alkynes, albeit with equal ease to participate in the carbene transfer from the gold-centers. At the outset, the current results provide an indirect support for the proposed nitroso stabilized α-oxo gold carbene intermediate in the nitroalkyne cycloisomerization leading to anthranil. Currently trapping of gold carbenes with various C-centered and N-centered nucleophile for the construction of various heterocycles is undergoing in our lab.

Experimental Section

Part A. General Procedure for the synthesis of 2H-indazole derivatives

In general, all reactions were carried out employing 50 mg of nitroalkyne 1.

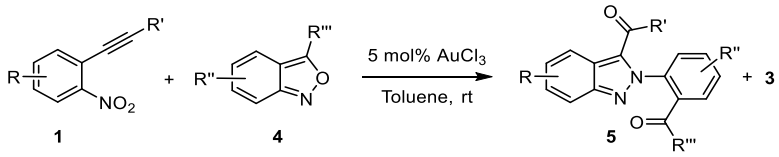

At rt, to a stirred solution of anthranil **4** (1.1 equiv) in anhydrous toluene (1 mL) was added $AuCl_3$ (5 mol %) and 4Å molecular sieves (40 mg), a solution of nitroalkyne **1** (1 equiv) in anhydrous toluene (1 mL) was introduced *via* syringe pump over a period of 4 h. The stirring was continued until the complete disappearance of the starting nitroalkyne as indicated by TLC. The reaction mixture was concentrated under reduced pressure and the resulting crude was purified by column chromatography to afford the products **5** along with the small amounts of anthranil **3**.

2-(3-Propionyl-2*H*-indazol-2-yl)benzaldehyde (5aa)

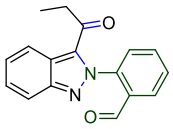

R_f = 0.4 (15% EtOAc in petroleum ether); yield: 55 mg (69%); yellow solid; mp: 134–136 °C; IR (neat) ν_{max} 3775, 2930, 2856, 1674, 1597, 1453, 1199, 758 cm^{-1}; ^1H NMR (500 MHz, $CDCl_3$): δ 1.21 (t, J = 7.2 Hz, 3H), 3.15 (q, J = 7.2 Hz, 2H), 7.43 (dd, J = 0.7, 7.6 Hz, 1H), 7.45–7.51 (m, 2H), 7.71 (t, J = 7.6 Hz, 1H), 7.75–7.79 (dt, J = 1.5, 7.6 Hz, 1H), 7.89–7.92 (m, 1H), 8.02–8.05 (m, 1H), 8.08 (dd, J = 1.9, 7.6 Hz, 1H), 9.49 (s, 1H) ppm; ^{13}C NMR (125 MHz, $CDCl_3$): δ 7.5(q), 35.6 (t), 119.4 (d), 120.5 (d), 122.0 (s), 126.6 (d), 127.2 (d), 127.9 (d), 129.3 (d), 129.9 (d), 131.6 (s), 133.9 (s), 134.2 (d), 143.2 (s), 148.9 (s), 188.4 (d), 190.3 (s) ppm; HRMS (ESI) m/z: $[M + H]^+$ calcd. for $C_{17}H_{15}N_2O_2$: 279.1128 $[M + H]^+$; found: 279.1132.

Procedure for 500 mg scale

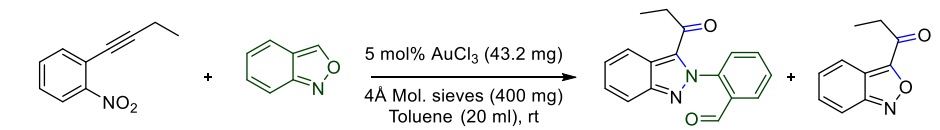

1a (500 mg, 2.85 mmol) **4a** (373 mg, 3.14 mmol) 65% **5aa** (519 mg, 1.86 mmol) **3a** (*12%, 62 mg*)

At room temperature, to a solution of anthranil **4a** (373 mg, 3.14 mmol) in anhydrous toluene (10 mL) and 4Å molecular sieves (400 mg) and $AuCl_3$ (43 mg) was added *o*-nitroalkyne **1a** (500 mg,

2.85 mmol) in anhydrous toluene (10 mL) *via* syringe pump over 6 h. The reaction was stirred at rt until the completion as indicated by TLC. Usual workup followed by purification by column chromatography afforded compound **5aa** (519 mg, 65% yield) as yellow solid.

2-(3-Butyryl-2*H*-indazol-2-yl)benzaldehyde (5ba)

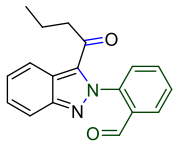

R_f = 0.4 (15% EtOAc in petroleum ether); yield: 52 mg (67%); yellow gum; IR (neat) ν_{max} 2925, 1686, 1589, 1453, 1205, 754 cm^{-1}; ^1H NMR (400 MHz, $CDCl_3$): δ 1.00 (t, J = 7.4 Hz, 3H), 1.76 (sxt, J = 7.3 Hz, 2H), 3.01–3.14 (m, 2H), 7.41–7.45 (m, 1H), 7.45–7.51 (m, 2H), 7.71 (tdd, J = 0.6, 1.3, 7.6 Hz, 1H), 7.77 (td, J = 1.7, 7.6 Hz, 1H), 7.88–7.93 (m, 1H), 8.01–8.05 (m, 1H), 8.06–8.11 (m, 1H), 9.49 (d, J = 0.6 Hz, 1H) ppm; ^{13}C NMR (100 MHz, $CDCl_3$): δ 13.7 (q), 17.0 (t), 44.2 (t), 119.3 (d), 120.5 (d), 122.0 (s), 126.5 (d), 127.2 (d), 127.9 (d), 129.3 (d), 129.9 (d), 131.6 (s), 134.1 (s), 134.2 (d), 143.2 (s), 148.9 (s), 188.4 (s), 189.8 (s) ppm; HRMS (ESI) m/z: $[M + H]^+$ calcd. for $C_{18}H_{17}N_2O_2$: 293.1285; found: 293.1289.

2-(3-Hexanoyl-2*H*-indazol-2-yl)benzaldehyde (5ca)

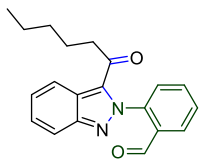

R_f = 0.4 (15% EtOAc in petroleum ether); yield: 47 mg (64%); yellow syrup; IR (neat) ν_{max} 2956, 2868, 1684, 1571, 1458, 1217, 1121, 966, 753 cm^{-1}; ^1H NMR (400 MHz, $CDCl_3$): δ 0.88–0.92 (m, 3H), 1.33–1.37 (m, 4H), 1.67–1.80 (m, 2H), 3.08 (t, J = 7.2 Hz, 2H), 7.40–7.53 (m, 3H), 7.68–7.73 (m, 1H), 7.77 (td, J = 1.7, 7.6 Hz, 1H), 7.87–7.94 (m, 1H), 8.00–8.05 (m, 1H), 8.08 (dd, J = 1.7, 7.5 Hz, 1H), 9.49 (s, 1H) ppm; ^{13}C NMR (100 MHz, $CDCl_3$): δ 13.9 (q), 22.5 (t), 23.2 (t), 31.3 (t), 42.3 (t), 119.3 (d), 120.5 (d), 122.0 (s), 126.5 (d), 127.2 (d), 127.9 (d), 129.3 (d), 129.9 (d), 131.6 (s), 134.1 (d), 143.2 (s), 148.9 (s), 188.4 (d), 190.0 (s) ppm; HRMS (ESI) m/z: $[M + H]^+$ calcd. for $C_{20}H_{21}N_2O_2$: 321.1603 ; found: 321.1598.

2-(3-(3-Methylbutanoyl)-2*H*-indazol-2-yl)benzaldehyde (5da)

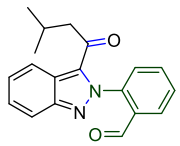

R_f = 0.3 (15% EtOAc in petroleum ether); yield: 49 mg (65%); yellow syrup; IR (neat) ν_{max} 2957, 2883, 1678, 1636, 1569, 1456, 1307, 1212, 962, 892, 824, 748 cm^{-1}; ^1H NMR (400 MHz, $CDCl_3$): δ 0.98 (s, 3H), 1.00 (s, 3H), 2.30 (dt, J = 6.7, 13.4 Hz, 1H), 2.95 (d, J = 6.9 Hz, 2H), 7.42 (dd, J = 1.2, 6.6 Hz, 1H), 7.43–7.51 (m, 2H), 7.68–7.74 (m, 1H), 7.77 (dt, J = 1.7, 7.5 Hz, 1H), 7.88–7.92 (m, 1H), 7.99–8.04 (m, 1H), 8.08 (dd, J = 1.50, 7.50 Hz, 1H), 9.50 (d, J = 0.4 Hz, 1H) ppm; ^{13}C NMR (100 MHz, $CDCl_3$): δ 22.6

(q, 2C), 24.5 (d), 51.1 (t), 119.3 (d), 120.5 (d), 121.9 (s), 126.5 (d), 127.2 (d), 127.8 (d), 129.2 (d), 129.9 (d), 131.6 (s), 134.1 (d), 134.3 (s), 143.2 (s), 148.9 (s), 188.3 (d), 189.6 (s) ppm; HRMS (ESI) m/z: $[M + H]^+$ calcd. for $C_{19}H_{19}N_2O_2$: 307.1447 ; found: 307.1441.

2-(3-(3-Phenylpropanoyl)-2*H*-indazol-2-yl)benzaldehyde (5ea)

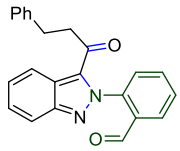

R_f = 0.4 (25% EtOAc in petroleum ether); yield: 41 mg (58%); yellow syrup; IR (neat) ν_{max} 3623, 2932, 1691, 1457, 1362, 1286, 1214, 969, 757 cm^{-1}; ^1H NMR (500 MHz, $CDCl_3$): δ 3.05 (t, J = 7.63 Hz, 2H), 3.45 (t, J = 7.63 Hz, 2H), 7.20–7.26 (m, 3H), 7.28–7.34 (m, 2H), 7.37 (d, J = 7.63 Hz, 1H), 7.41–7.51 (m, 2H), 7.69–7.79 (m, 2H), 7.91 (d, J = 8.39 Hz, 1H), 7.99 (d, J = 8.39 Hz, 1H), 8.09 (dd, J = 1.53, 6.87 Hz, 1H), 9.51 (s, 1H) ppm; ^{13}C NMR (125 MHz, $CDCl_3$): δ 29.4 (d), 43.9 (d), 119.4 (d), 120.4 (d), 122.0 (s), 126.3 (d), 126.6 (d), 127.3 (d), 127.9 (d), 128.4 (d, 2C), 128.6 (d, 2C), 129.4(d), 129.9 (d), 131.6 (s), 133.8 (s), 134.1 (d), 140.5 (s), 143.0 (s), 148.9 (s), 188.4 (d), 188.8 (s) ppm; HRMS (ESI) m/z: $[M + H]^+$ calcd. for $C_{23}H_{19}N_2O_2$: 355.1447; found: 355.1441.

4-(2-(2-Formylphenyl)-2*H*-indazol-3-yl)-4-oxobutyl acetate (5fa)

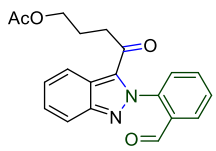

R_f = 0.4 (20% EtOAc in petroleum ether); yield: 45 mg (63%); dark yellow solid; mp: 139–141 °C; IR (neat) ν_{max} 2930, 1672, 1592, 1487, 1452, 1209, 875, 821, 747, 699 cm^{-1}; ^1H NMR (400 MHz, $CDCl_3$): δ 2.04 (s, 3H), 2.05–2.10 (m, 2H), 3.20 (t, J = 7.1 Hz, 2H), 4.15 (t, J = 6.2 Hz, 2H), 7.44 (dd, J = 1.2, 7.5 Hz, 1H), 7.46–7.52 (m, 2H), 7.69–7.75 (m, 1H), 7.77 (dd, J = 1.7, 7.5 Hz, 1H), 7.89–7.94 (m, 1H), 8.01–8.05 (m, 1H), 8.08 (dd, J = 1.6, 7.5 Hz, 1H), 9.51 (s, 1H) ppm; ^{13}C NMR (100 MHz, $CDCl_3$): δ 20.9 (q), 22.5 (d), 38.5 (d), 63.4 (d), 119.5 (d), 120.4 (d), 122.1(s), 126.8 (d), 127.3 (d), 127.9 (d), 129.6 (d), 130.0 (d), 131.6 (s), 133.8 (s), 134.2 (d), 142.9 (s), 148.9 (s), 171.0 (s), 188.4 (d), 188.5 (s) ppm; HRMS (ESI) m/z: $[M + H]^+$ calcd. for $C_{20}H_{19}N_2O_4$: 351.1345; found: 351.1339.

2-(3-(4-((*t*Butyldimethylsilyl)oxy)butanoyl)-2*H*-indazol-2-yl)benzaldehyde (5ga)

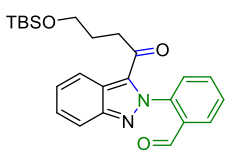

R_f = 0.4 (20% EtOAc in petroleum ether); yield: 45 mg (68%); yellow syrup; IR (neat) ν_{max} 2932, 2857, 1685, 1599, 1460, 1091, 835, 751, 667 cm^{-1}; ^1H NMR (400 MHz, $CDCl_3$): δ 0.05 (s, 6H), 0.90 (s, 9H), 1.90–1.98 (m, 2H), 3.21 (t, J = 7.2 Hz, 2H), 3.68–3.72 (m, 2H), 7.42 (dd, J = 1.0, 7.6 Hz, 1H), 7.45–7.51 (m, 2H), 7.68–7.73 (m, 1H), 7.76 (td, J = 1.7, 7.6 Hz, 1H), 7.91 (dt, J = 1.1, 7.3 Hz, 1H), 8.07–8.12 (m,

2H), 9.49 (d, *J* = 0.5 Hz, 1H) ppm; ^{13}C NMR (100 MHz, $CDCl_3$): δ -5.4 (q, 2C), 18.3 (s), 25.9 (q, 3C), 26.7 (t), 38.8 (t), 61.9 (t), 119.3 (d), 120.7 (d), 122.1 (s), 126.6 (d), 127.3 (d), 127.9 (d), 129.2 (d), 129.9 (d), 131.7 (s), 134.1 (d), 134.1 (s), 143.3 (s), 148.9 (s), 188.3 (d), 189.9 (s) ppm; HRMS (ESI) m/z: $[M + H]^+$ calcd. For $C_{24}H_{31}N_2O_3Si$: 423.2098; found: 423.2104.

2-(3-(Cyclopropanecarbonyl)-2*H*-indazol-2-yl)benzaldehyde (5ha)

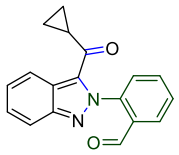

R_f = 0.4 (10% EtOAc in petroleum ether); yield: 24 mg (31%); yellow syrup; IR (neat) ν_{max} 2929, 1674, 1589, 1454, 1362, 1211, 970, 827, 747, 698 cm^{-1}; ^{1}H NMR (400 MHz, $CDCl_3$): δ 1.06–1.13 (m, 2H), 1.26–1.29 (m, 2H), 2.61 (tt, *J* = 4.6, 7.9 Hz, 1H), 7.42–7.46 (m, 1H), 7.46–7.51 (m, 2H), 7.66–7.71 (m, 1H), 7.75 (td, *J* = 1.7, 7.6 Hz, 1H), 7.90 (dt, *J* = 1.1, 7.6 Hz, 1H), 8.08 (dd, *J* = 1.5, 7.6 Hz, 1H), 8.14 (dt, *J* = 1.1, 7.5 Hz, 1H), 9.56 (d, *J* = 0.6 Hz, 1H); ^{13}C NMR (100 MHz, $CDCl_3$): δ 11.9 (t, 2C), 21.3 (d), 119.1 (d), 120.6 (d), 122.6 (s), 126.3 (d), 127.4 (d), 128.0 (d), 128.8 (d), 129.9 (d), 131.7 (s), 134.0 (d), 135.1 (s), 142.8 (s), 148.9 (s), 188.4 (d), 190.3 (s) ppm; HRMS (ESI) m/z: $[M + H]^+$ calcd. for $C_{18}H_{15}N_2O_2$: 291.1134; found: 291.1128.

2-(3-Butyryl-6-fluoro-2*H*-indazol-2-yl)benzaldehyde (5ia)

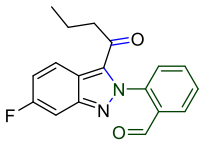

R_f = 0.4 (15% EtOAc in petroleum ether); yield: 35 mg (47%); pale yellow solid; mp: 108–110 °C; IR (neat) ν_{max} 2961, 2863, 1691, 1600, 1456, 1409, 1124, 988, 771 cm^{-1}; ^{1}H NMR (400 MHz, $CDCl_3$): δ 0.98 (t, *J* = 7.4 Hz, 3H), 1.74 (q, *J* = 7.2 Hz, 2H), 3.01 (t, *J* = 7.2 Hz, 2H), 7.26 (td, *J* = 2.4, 9.0 Hz, 1H), 7.42 (dd, *J* = 1.2, 7.7 Hz, 1H), 7.47(dd, *J* = 1.0, 9.0 Hz, 1H), 7.72 (td, *J*= 1.0, 7.6 Hz, 1H), 7.77 (td, *J* = 1.8, 7.5 Hz, 1H), 8.03 (dd, *J* = 4.9, 9.4 Hz, 1H), 8.07 (dd, *J* = 1.6, 7.6 Hz, 1H), 9.53 (s, 1H) ppm; ^{13}C NMR (100 MHz, $CDCl_3$): δ 13.7 (q), 16.9 (d), 44.2 (d), 102.3 (dd, J_{C-F} = 23.2 Hz) 117.8 (dd, J_{C-F} = 10.2 Hz), 119.1 (s), 122.5 (dd, J_{C-F} = 10.2 Hz), 127.9 (d), 129.8 (d), 130.1 (d), 131.5 (s), 134.2 (d), 134.4 (s), 142.6 (s), 148.8 (ds, J_{C-F} = 13.1 Hz), 160.5 (ds, J_{C-F} = 247.8 Hz), 188.3 (d), 189.6 (s) ppm; HRMS (ESI) m/z: $[M + H]^+$ calcd. for $C_{18}H_{16}FN_2O_2$: 311.1196; found: 311.1190.

2-(3-Butyryl-6-methyl-2*H*-indazol-2-yl)benzaldehyde (5ja)

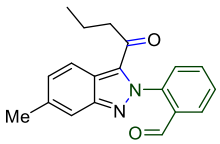

R_f = 0.3 (15% EtOAc in petroleum ether); yield: 42 mg (56%); yellow syrup; IR (neat) ν_{max} 2962, 2873, 1667, 1597, 1454, 1407, 1194, 980, 761 cm^{-1}; ^{1}H NMR (400 MHz, $CDCl_3$): δ 0.99 (t, *J* = 7.4 Hz, 3H), 1.71–1.78 (q, *J* = 7.4

Hz, 2H), 2.53 (s, 3H), 3.05 (t, *J* = 7.2 Hz, 2H), 7.29 (dd, *J* = 1.2, 8.8 Hz, 1H), 7.42 (dd, *J* = 1.0, 7.9 Hz, 1H), 7.64 (d, *J* = 1.0Hz, 1H), 7.66–7.71 (m, 1H), 7.72 (td, *J* = 1.6, 7.6 Hz, 1H), 7.90 (d, *J* = 8.9 Hz, 1H), 8.05 (dd, *J* = 1.7, 7.9 Hz, 1H), 9.48 (s, 1H) ppm; ^{13}C NMR (100 MHz, $CDCl_3$): δ13.7 (q), 17.0 (d), 21.9 (q), 44.1 (d), 117.5 (d), 120.0 (d), 120.4 (s), 127.9 (d), 129.0 (d), 129.4 (d), 129.7 (d), 131.7 (s), 134.0 (s), 134.1 (d), 137.3 (s), 143.3 (s), 149.5 (s), 188.4 (d), 189.8 (s) ppm; HRMS (ESI) m/z: $[M + H]^+$ calcd. for $C_{19}H_{19}N_2O_2$: 307.1441; found: 307.1447.

Methyl 3-butyryl-2-(2-Formylphenyl)-2*H*-indazole-6-carboxylate (5ka)

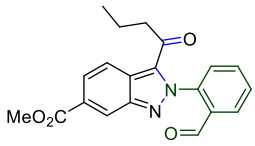

R_f = 0.4 (15% EtOAc in petroleum ether); yield**:** 51 mg (72%); pale yellow gummy solid; IR (neat) ν_{max} 2942, 2864, 1712, 1597, 1420, 1230, 1087, 756 cm^{-1}; ^{1}H NMR (400 MHz, $CDCl_3$): δ 1.00 (t, *J* = 7.4 Hz, 3H), 1.72–1.79 (q, *J* = 7.4 Hz, 2H), 3.08 (t, *J* = 7.2 Hz, 2H), 4.01 (s, 3H), 7.44 (dd, *J* = 1.4, 7.6 Hz, 1H), 7.75 (dd, *J* = 1.4, 7.4 Hz, 1H), 7.78 (dd, *J* = 1.9, 7.5 Hz, 1H), 8.06–8.08 (m, 2H), 8.09 (d, *J* = 1.9 Hz, 1H), 8.64–8.66 (m, 1H), 9.54 (s, 1H) ppm;^{13}C NMR (100 MHz, $CDCl_3$): δ13.7 (q), 16.9 (t), 44.2 (t), 52.5 (q), 120.7 (d), 122.7 (d), 123.7 (s), 125.9 (d), 127.8 (d), 129.2 (s), 130.1 (d), 130.2 (d), 131.4 (s), 134.2 (d), 134.3 (s), 142.5 (s), 148.2 (s), 166.6 (s), 188.3 (d), 189.6 (s) ppm; HRMS (ESI) m/z: $[M + H]^+$ calcd. for $C_{20}H_{19}N_2O_4$: 351.1345; found: 351.1356.

3-butyryl-2-(2-formylphenyl)-2H-indazole-6-carbonitrile (5la)

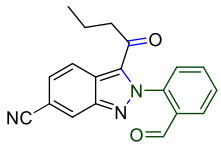

R_f = 0.4 (15% EtOAc in petroleum ether); yield: 57 mg (77%); orange gummy solid; IR (neat) ν_{max} 2922, 1687, 1409, 1191, 980, 762 cm^{-1}; ^{1}H NMR (400 MHz, $CDCl_3$): δ 0.98 (t, *J* = 7.4 Hz, 3H), 1.69–1.79 (m, 2H), 3.02 (t, *J* = 7.2 Hz, 2H), 7.41–7.46 (m, 1H), 7.57 (dd, *J* = 1.3, 8.8 Hz, 1H), 7.79 (ddd, *J* = 1.7, 5.2, 7.5 Hz, 2H), 8.05–8.10 (m, 1H), 8.16 (dd, *J* = 0.9, 8.9 Hz, 1H), 8.32 (t, *J* = 1.1 Hz, 1H), 9.61 (s, 1H) ppm; ^{13}C NMR (100 MHz, $CDCl_3$): δ 13.7 (q), 16.8 (t), 44.2 (t), 110.8 (s), 118.6 (s), 122.5 (d), 122.9 (s), 126.2 (d), 126.5 (d), 127.8 (d), 130.5 (d), 131.2 (d), 131.2 (s), 131.3 (s), 134.4 (d), 141.5 (s), 147.0 (s), 188.3 (d), 189.4 (s) ppm; HRMS (ESI) m/z: $[M + H]^+$ calcd. for $C_{19}H_{16}N_3O_2$: 318.1243; found: 318.1234.

4-Fluoro-2-(3-propionyl-2*H*-indazol-2-yl)benzaldehyde (5ab)

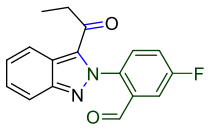

R_f = 0.3 (15% EtOAc in petroleum ether); yield: 36 mg (42%); yellow solid; mp: 89–91 °C; IR (neat) ν_{max} 2981, 1674, 1585, 1453, 1411, 1194, 935, 818, 749 cm^{-1}; ^1H NMR (400 MHz, $CDCl_3$): δ 1.22 (t, J = 7.1 Hz, 3H), 3.17 (q, J = 7.1 Hz, 2H), 7.41–7.45 (m, 2H), 7.45–7.52 (m, 2H), 7.72–7.77 (m, 1H), 7.88–7.92 (m, 1H), 8.00–8.04 (m, 1H), 9.37 (d, J = 2.5 Hz, 1H) ppm; ^{13}C NMR (100 MHz, $CDCl_3$): δ 7.4 (q), 35.6 (t), 115.0 (dd, J_{C-F} = 24.0 Hz), 119.3 (d), 120.4 (d), 121.0 (dd, J_{C-F} = 23.2 Hz), 122.0 (s), 126.8 (d), 127.4 (d), 129.9 (dd, J_{C-F} = 8.7 Hz), 133.5 (ds, J_{C-F} = 10.2 Hz), 134.0 (s), 139.0 (ds, J_{C-F} = 3.6 Hz), 148.9 (s), 161.5 (ds, J_{C-F} = 252.1 Hz), 187.0 (d), 190.2 (s) ppm; HRMS (ESI) m/z: $[M + H]^+$ calcd. for $C_{17}H_{14}FN_2O_2$: 297.1039; found: 297.1034.

4-Fluoro-2-(3-hexanoyl-2*H*-indazol-2-yl)benzaldehyde (5cb)

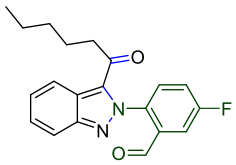

R_f = 0.4 (15% EtOAc in petroleum ether); yield: 28 mg (36%); yellow solid; mp: 94–96 °C; IR (neat) ν_{max} 2955, 2929, 1690, 1596, 1263, 749, 663 cm^{-1}; ^{1}HNMR (400 MHz, $CDCl_3$): δ 0.88–0.93 (m, 3H), 1.31–1.40 (m, 4H), 1.68–1.80 (m, 2H), 3.11 (t, J = 7.4 Hz, 2H), 7.40–7.44 (m, 2H), 7.44–7.53 (m, 2H), 7.75 (ddd, J = 0.9, 2.2, 8.1 Hz, 1H), 7.87–7.94 (m, 1H), 7.98–8.06 (m, 1H), 9.37 (d, J = 2.5 Hz, 1H) ppm; ^{13}C NMR (125 MHz, $CDCl_3$): δ 13.9 (q), 22.5 (t), 23.2 (t), 31.3 (t), 42.4 (t), 115.0 (dd, J_{C-F} = 24.0 Hz), 119.4 (d), 120.4 (d), 120.9 (dd, J_{C-F} = 24.0 Hz), 122.0 (s), 126.8 (d), 127.4 (d), 129.9 (dd, J_{C-F} = 8.7 Hz), 133.5 (ds, J_{C-F} = 7.3 Hz), 134.1 (s), 139.4 (ds, J_{C-F} = 3.6 Hz), 149.0 (s), 161.6 (ds, J_{C-F} = 252.9 Hz), 187.0 (d), 190.0 (s) ppm; HRMS (ESI) m/z: $[M + H]^+$ calcd. for $C_{20}H_{20}FN_2O_2$: 339.1503; found: 339.1510.

2-(3-Butyryl-6-methyl-2*H*-indazol-2-yl)-4-fluorobenzaldehyde (5jb)

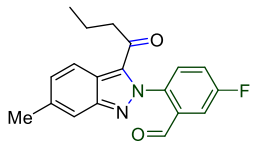

R_f = 0.4 (15% EtOAc in petroleum ether); yield: 31 mg (39%); dark yellow syrup; IR (neat) ν_{max} 2914, 2857, 1780, 1692, 1616, 1383, 1228, 957, 830, 768 cm^{-1}; ^1H NMR (400 MHz, $CDCl_3$): δ 0.98–1.03 (m, 3H), 1.72–1.79 (m, 2H), 2.54 (s, 3H), 3.08 (t, J = 7.1 Hz, 2H), 7.28–7.33 (m, 1H), 7.38–7.45 (m, 2H), 7.63 (s, 1H), 7.70–7.79 (m, 1H), 7.89 (d, J = 8.9 Hz, 1H), 9.36 (d, J = 2.6 Hz, 1H) ppm; ^{13}C NMR (100 MHz, $CDCl_3$): δ 13.7 (q), 17.0 (t), 21.9 (q), 44.2 (t), 114.8 (dd, J_{C-F} =24.0 Hz), 117.6 (d), 119.9 (d), 120.4 (s), 120.9 (dd, J_{C-F} = 24.0 Hz), 129.7 (d), 130.0 (dd, J_{C-F} = 8.7 Hz), 133.5 (ds, J_{C-F} = 7.3 Hz), 134.0 (s), 137.6 (s), 139.6 (ds, J_{C-F} = 3.6 Hz), 149.6 (s), 161.5 (ds, J_{C-F} =

252.9 Hz), 187.1 (d), 189.8 (s) ppm; HRMS (ESI) m/z: $[M + H]^+$ calcd. for $C_{19}H_{18}FN_2O_2$: 325.1347; found: 325.1352.

4-bromo-2-(3-propionyl-2*H*-indazol-2-yl)benzaldehyde (5ac)

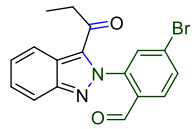

R_f = 0.4 (25% EtOAc in petroleum ether); yield: 52 mg (51%); pale yellow solid; mp: 130-132 °C; IR (neat) ν_{max} 2981, 1673, 1597, 1496, 1409, 1261, 1147, 951, 827, 745, 666 cm^{-1}; ^1H NMR (400 MHz, $CDCl_3$): δ 1.23 (t, J = 7.1 Hz, 3H), 3.19 (q, J = 7.1 Hz, 2H), 7.46–7.51 (m, 2H), 7.60 (d, J = 1.9 Hz, 1H), 7.84 (dd, J = 1.5, 8.4 Hz, 1H), 7.88–7.91 (m, 1H), 7.93 (d, J = 8.4 Hz,1H), 8.00–8.05 (m, 1H), 9.43 (s, 1H) ppm; ^{13}C NMR (100 MHz, $CDCl_3$): δ 7.5 (q), 35.6 (t), 119.4 (d), 120.4 (d), 121.9 (s), 126.9 (d), 127.5 (d), 128.6 (s), 130.2 (d), 130.5 (s), 131.2 (d), 133.3 (d), 134.0 (s), 143.9 (s), 149.2 (s), 187.4 (d), 190.2 (s) ppm; HRMS (ESI) m/z: $[M + H]^+$ calcd. for $C_{17}H_{14}BrN_2O_2$: 357.0233; found: 357.0235.

Methyl 3-butyryl-2-(5-fluoro-2-formylphenyl)-2*H*-indazole-6-carboxylate (5kc)

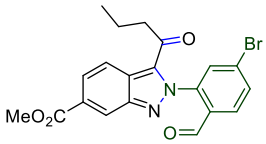

R_f = 0.4 (15% EtOAc in petroleum ether); yield: 59 mg (68%); pale yellow gummy solid; IR (neat) ν_{max} 2955, 2862, 1713, 1585, 1423, 1254, 1232, 984, 828, 756 cm^{-1}; ^1H NMR (400 MHz, $CDCl_3$): δ 1.02 (t, J = 7.4 Hz, 3H), 1.77–1.80 (m, 2H), 3.12 (t, J = 7.2 Hz, 2H), 4.01 (s, 3H), 7.60 (d, J = 1.7 Hz, 1H), 7.87 (dd, J = 1.6, 8.4 Hz, 1H), 7.93 (d, J =8.4 Hz, 1H), 8.06 (dd, J = 1.4, 3.4 Hz, 2H), 8.64 (t, J = 1.0 Hz, 1H), 9.48 (s, 1H) ppm; ^{13}C NMR (100 MHz, $CDCl_3$): δ 13.7 (q), 16.9 (t), 44.1 (t), 52.5 (q), 120.6 (d), 122.8 (d), 123.5 (s), 126.2 (d), 128.7 (s), 129.5 (s), 130.3 (s), 131.0 (d), 131.1 (d), 133.5 (d), 134.3 (s), 143.2 (s), 148.4 (s), 166.5 (s), 187.2 (d), 189.5 (s) ppm; HRMS (ESI) m/z: $[M + H]^+$ calcd. for $C_{20}H_{18}BrN_2O_4$: 429.0444; found: 429.0452.

2-(5-Bromo-2-formylphenyl)-3-butyryl-2*H*-indazole-6-carbonitrile (5lc)

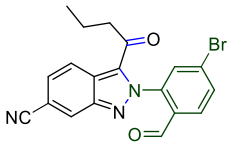

R_f = 0.4 (15% EtOAc in petroleum ether); yield: 66 mg (71%); orange syrup; IR (neat) ν_{max} 2923, 1691, 1586, 1412, 820 cm^{-1}; ^1H NMR (400 MHz, $CDCl_3$): δ 1.01 (t, J = 7.4 Hz, 3H), 1.71–1.84 (m, 2H), 3.08 (t, J = 7.2 Hz, 2H), 7.56–7.62 (m, 2H), 7.91 (s, 2H), 8.14 (d, J = 8.9 Hz, 1H), 8.31 (s, 1H), 9.53 (s, 1H) ppm; ^{13}C NMR (100 MHz, $CDCl_3$): δ 13.6 (q), 16.8 (t), 44.1 (t), 111.1 (s), 118.4 (s), 122.3 (d), 122.6 (s), 126.3 (d), 126.7 (d), 128.8 (s), 130.0 (s), 131.1 (d), 132.0 (d), 133.7 (d), 134.7 (s), 142.2 (s),

147.2 (s), 187.3 (s), 189.3 (s) ppm; HRMS (ESI) m/z: $[M + H]^+$ calcd. for $C_{19}H_{15}N_3O_2Br$: 396.0348; found: 396.0339.

4-Chloro-2-(3-propionyl-2*H*-indazol-2-yl)benzaldehyde (5ad)

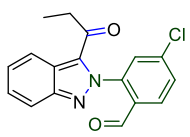

R_f = 0.4 (25% EtOAc in petroleum ether); yield: 50 mg (56%); yellow syrup; IR (neat) ν_{max} 2963, 2869, 1674, 1594, 1454, 1367, 984, 878, 749 cm^{-1}; ^1H NMR (400 MHz, $CDCl_3$): δ 1.23 (t, J = 7.19 Hz, 3H), 3.19 (q, J = 7.1 Hz, 2H), 7.44 (d, J = 1.9 Hz, 1H), 7.46–7.51 (m, 2H), 7.67 (dd, J = 1.6, 8.6 Hz, 1H), 7.88–7.92 (m, 1H), 7.97–8.07 (m, 2H), 9.42 (d, J = 0.5 Hz, 1H) ppm; ^{13}C NMR (100 MHz, $CDCl_3$): δ 7.5 (q), 35.6 (t), 119.4 (d), 120.4 (d), 121.9 (s), 126.9 (d), 127.5 (d), 128.3 (d), 130.2 (s), 130.2 (d), 130.3 (d), 133.9 (s), 140.3 (s), 144.1 (s), 149.1 (s), 187.2 (d), 190.2 (s) ppm; HRMS (ESI) m/z: $[M + H]^+$ calcd. for $C_{17}H_{14}ClN_2O_2$: 313.0738; found: 313.0741.

4-Chloro-2-(3-hexanoyl-2*H*-indazol-2-yl)benzaldehyde (5cd)

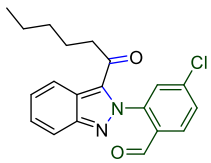

R_f = 0.4 (10% EtOAc in petroleum ether); yield: 45 mg (55%); yellow syrup; IR (neat) ν_{max} 2957, 2927, 2864, 1674, 1598, 1409, 869, 743 cm^{-1}; ^1H NMR (400 MHz, $CDCl_3$): δ 0.89–0.94 (m, 3H), 1.33–1.41 (m, 4H), 1.74 (t, J = 7.4 Hz, 2H), 3.13 (t, J = 7.4 Hz, 2H), 7.43 (d, J = 1.9 Hz, 1H), 7.45–7.52 (m, 2H), 7.67 (ddd, J = 0.6, 1.9, 8.4 Hz, 1H), 7.86–7.93 (m, 1H), 7.97–8.04 (m, 2H), 9.43 (d, J = 0.5 Hz, 1H) ppm;^{13}C NMR (100 MHz, $CDCl_3$): δ 13.9 (q), 22.5 (t), 23.2 (t), 31.4 (t), 42.3 (t), 119.4 (d), 120.4 (d), 121.8 (s), 126.8 (d), 127.5 (d), 128.3 (d), 130.1 (s), 130.2 (d), 130.2 (d), 134.1 (s), 140.3 (s), 144.1 (s), 149.1 (s), 187.2 (d), 189.9 (s) ppm; HRMS (ESI) m/z: $[M + H]^+$ calcd. for $C_{20}H_{20}ClN_2O_2$: 355.1213; found: 355.1208.

4-Chloro-2-(3-(3-methylbutanoyl)-2*H*-indazol-2-yl)benzaldehyde (5dd)

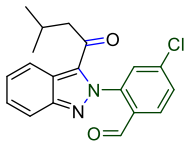

R_f = 0.4 (15% EtOAc in petroleum ether); yield: 49 mg (58%); yellow syrup; IR (neat) ν_{max} 2959, 2871, 1669, 1589, 1457, 1197, 874, 820, 749, 673 cm^{-1};^1H NMR (400 MHz, $CDCl_3$): δ 1.01 (s, 3H), 1.02 (s, 3H), 2.31 (dt, J = 6.7, 13.4 Hz, 1H), 3.00 (d, J = 6.9 Hz, 2H), 7.43 (d, J = 1.9 Hz, 1H), 7.46–7.50 (m, 2H), 7.65–7.69 (m, 1H), 7.87–7.92 (m, 1H), 7.97–8.04 (m, 2H), 9.43 (s, 1H) ppm; ^{13}C NMR (125 MHz, $CDCl_3$): δ 22.7 (q, 2C), 24.5 (d), 51.0 (t), 119.4 (d), 120.4 (d), 121.8 (s), 126.8 (d), 127.5 (d), 128.2 (d), 130.1 (s), 130.2 (d), 130.2 (d), 134.3 (s), 140.3 (s), 144.1 (s), 149.1 (s), 187.2 (s), 189.5 (s) ppm; HRMS (ESI) m/z: $[M + H]^+$ calcd. for $C_{19}H_{18}N_2O_2Cl$: 341.1057; found: 341.1051.

4-Chloro-2-(3-(3-phenylpropanoyl)-2*H*-indazol-2-yl)benzaldehyde (5ed)

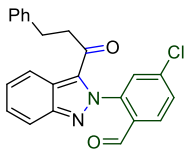

R_f = 0.4 (15% EtOAc in petroleum ether); yield: 37 mg (47%); yellow syrup; IR (neat) ν_{max} 3729, 2860, 1672, 1592, 1486, 1452, 1210, 974, 746, 697 cm^{-1}; ^1H NMR (400 MHz, $CDCl_3$): δ 3.05 (t, J = 7.7 Hz, 2H), 3.44–3.50 (m, 2H), 7.21–7.27 (m, 3H), 7.31–7.34 (m, 2H), 7.37 (d, J = 2.0 Hz, 1H), 7.43–7.51 (m, 2H), 7.67 (dd, J = 1.7, 8.4 Hz, 1H), 7.86–7.91 (m, 1H), 7.93–7.98 (m, 1H), 8.01 (d, J = 8.4 Hz, 1H), 9.42 (s, 1H) ppm; ^{13}C NMR (100 MHz, $CDCl_3$): δ 29.4 (t), 43.9 (s), 119.5 (d), 120.3 (d), 121.9 (s), 126.4 (d), 127.0 (d), 127.5 (d), 128.3 (d), 128.4 (d, 2C), 128.6 (d), 128.7 (d, 2C), 130.1 (s), 130.3 (d), 133.8 (s), 140.3 (s), 140.4 (s), 143.9 (s), 149.1 (s), 187.2 (d), 188.7 (s) ppm; HRMS (ESI) m/z: $[M + H]^+$ calcd. for $C_{23}H_{18}N_2O_2Cl$: 389.1057; found: 389.1051.

2-(3-butyryl-2*H*-indazol-2-yl)-4-methylbenzaldehyde (5be)

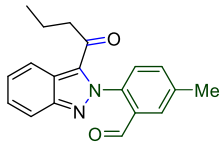

R_f = 0.4 (15% EtOAc in petroleum ether); yield: 45 mg (56%); pale yellow syrup; IR (neat) ν_{max} 2924, 1679, 962, 829, 750 cm^{-1}; ^1H NMR (400 MHz, $CDCl_3$): δ 0.99 (t, J = 7.4 Hz, 3H), 1.69–1.82 (m, 2H), 2.54 (s, 3H), 3.06 (t, J = 7.3 Hz, 2H), 7.31 (d, J = 8.0 Hz, 1H), 7.42–7.51 (m, 2H), 7.53–7.59 (m, 1H), 7.86–7.93 (m, 2H), 7.99–8.07 (m, 1H), 9.46 (s, 1H) ppm; ^{13}C NMR (100 MHz, $CDCl_3$): δ 13.8 (q), 17.0 (t), 21.2 (q), 44.2 (t), 119.3 (d), 120.5 (d), 122.0 (s), 126.4 (d), 127.1 (d), 127.6 (d), 129.6 (d), 131.3 (s), 134.1 (s), 134.8 (d), 140.3 (s), 140.9 (s), 148.8 (s), 188.6 (s), 189.9 (s) ppm; HRMS (ESI) m/z: $[M + H]^+$ calcd. for $C_{19}H_{19}N_2O_2$: 307.1446; found: 307.1441.

2-(3-butyryl-2*H*-indazol-2-yl)-4-methylbenzaldehyde (5je)

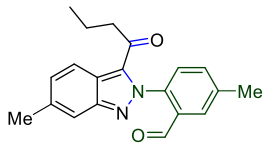

R_f = 0.4 (15% EtOAc in petroleum ether); yield: 50 mg (64%); pale yellow syrup; IR (neat) ν_{max} 2920, 1681, 1270, 805 cm^{-1}; ^1H NMR (400 MHz, $CDCl_3$): δ 0.99 (t, J = 7.4 Hz, 3H), 1.67–1.81 (m, 2H), 2.53 (s, 3H), 2.53 (s, 3H), 3.03 (t, J = 7.2 Hz, 2H), 7.30 (d, J = 8.1 Hz, 2H), 7.54 (ddd, J = 0.6, 2.1, 8.0 Hz, 1H), 7.61–7.65 (m, 1H), 7.86 (dd, J = 0.4, 1.5 Hz, 1H), 7.90 (d, J = 8.8 Hz, 1H), 9.45 (s, 1H) ppm; ^{13}C NMR (100 MHz, $CDCl_3$): δ 13.7 (q), 17.0 (t), 21.2 (q), 21.9 (q), 44.1 (t), 117.5 (d), 120.0 (d), 120.5 (s), 127.7 (d), 129.3 (d), 131.3 (s), 134.8 (d), 137.2 (s), 140.1 (s), 141.0 (s), 149.4 (s), 188.7 (d), 189.8 (s) ppm; HRMS (ESI) m/z: $[M + H]^+$ calcd. for $C_{20}H_{21}N_2O_2$: 321.1603; found: 321.1599.

3-butyryl-2-(2-formyl-5-methylphenyl)-2*H*-indazole-6-carbonitrile (5le)

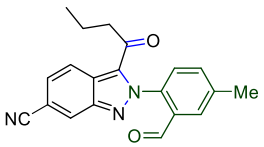

R_f = 0.4 (15% EtOAc in petroleum ether); yield: 55 mg (71%); orange syrup; IR (neat) ν_{max} 2957, 1683, 1409, 1292, 816 cm^{-1}; ^1H NMR (400 MHz, $CDCl_3$): δ 0.98 (t, J = 7.4 Hz, 3H), 1.68–1.79 (m, 2H), 2.57 (s, 3H), 3.01 (t, J = 7.2 Hz, 2H), 7.31 (d, J = 7.9 Hz, 1H), 7.56 (dd, J = 1.3, 8.8 Hz, 1H), 7.58–7.62 (m, 1H), 7.82–7.89 (m, 1H), 8.11–8.20 (m, 1H), 8.31 (s, 1H), 9.57 (s, 1H) ppm; ^{13}C NMR (100 MHz, $CDCl_3$): δ 13.7 (q), 16.8 (t), 21.3 (q), 44.2 (t), 110.7 (s), 118.6 (s), 122.5 (d), 122.9 (s), 126.2 (d), 126.4 (d), 127.6 (d), 130.9 (s), 131.7 (d), 134.8 (d), 135.0 (s), 139.1 (s), 141.1 (s), 147.0 (s), 188.6 (s), 189.5 (s) ppm; HRMS (ESI) m/z: $[M + H]^+$ calcd. for $C_{20}H_{18}N_3O_2$: 332.1399; found: 332.1399.

Methyl 3-(3-butyryl-2*H*-indazol-2-yl)-4-formylbenzoate (5bf)

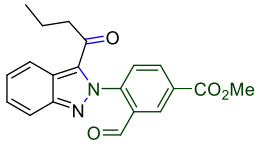

R_f = 0.4 (25% EtOAc in petroleum ether); yield: 52 mg (56%); yellow syrup; IR (neat) ν_{max} 3729, 2354, 1716, 1290, 1190, 808 cm^{-1}; ^1H NMR (400 MHz, $CDCl_3$): δ 1.01 (t, J = 7.4 Hz, 3H), 1.73–1.81 (m, 2H), 3.12 (t, J = 7.2 Hz, 2H), 4.02 (s, 3H), 7.46–7.49 (m, 1H), 7.49–7.53 (m, 2H), 7.88–7.93 (m, 1H), 8.00–8.04 (m, 1H), 8.41 (dd, J = 2.0, 8.3 Hz, 1H), 8.72 (d, J = 1.9 Hz, 1H), 9.54 (s, 1H) ppm; ^{13}C NMR (100 MHz, $CDCl_3$): δ 13.8 (q), 16.9 (t), 44.1 (t), 52.7 (q) , 119.4 (d), 120.4 (d), 121.9 (s), 126.8 (d), 127.5 (d), 128.3 (d), 130.8 (d), 131.7 (s), 134.1 (s), 134.8 (d), 146.3 (s), 149.3 (s), 165.2 (s), 187.6 (s), 189.8 (s) ppm; HRMS (ESI) m/z: $[M + H]^+$ calcd. for $C_{20}H_{19}N_2O_4$: 351.1345; found: 351.1347.

Methyl 4-formyl-3-(3-(3-phenylpropanoyl)-2*H*-indazol-2-yl)benzoate (5ef)

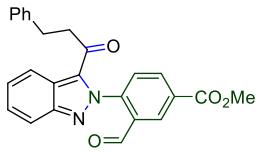

R_f = 0.4 (25% EtOAc in petroleum ether); yield: 44 mg (54%); pale yellow syrup; IR (neat) ν_{max} 2917, 1715, 1293, 1103, 807 cm^{-1}; ^1H NMR (400 MHz, $CDCl_3$): δ 3.05 (t, J = 7.6 Hz, 2H), 3.45–3.51 (m, 2H), 4.02 (s, 3H), 7.20–7.24 (m, 3H), 7.29–7.33 (m, 2H), 7.42 (d, J = 8.1 Hz, 1H), 7.45–7.52 (m, 2H), 7.88–7.92 (m, 1H), 7.95–7.99 (m, 1H), 8.39 (dd, J = 2.0, 8.1 Hz, 1H), 8.72 (d, J = 2.0 Hz, 1H), 9.55 (s, 1H) ppm; ^{13}C NMR (100 MHz, $CDCl_3$): δ 29.4 (t), 43.8 (t), 52.7 (q), 119.4 (d), 120.3 (d), 122.0 (s), 126.4 (d), 126.9 (d), 127.5 (d), 128.3 (d), 128.4 (d, 2C), 128.6 (d, 2C), 128.6 (s), 130.9 (d), 131.7 (s), 133.8 (s), 134.8 (d), 140.4 (s), 146.1 (s), 149.2 (s), 165.2 (s), 187.6 (s), 188.8 (s) ppm; HRMS (ESI) m/z: $[M + H]^+$ calcd. for $C_{25}H_{21}N_2O_4$: 413.1501; found: 413.1494.

Methyl 4-formyl-3-(3-(3-phenylpropanoyl)-2*H*-indazol-2-yl)benzoate (5jf)

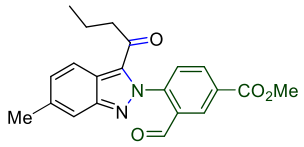

R_f = 0.4 (25% EtOAc in petroleum ether); yield: 46 mg (51%); pale yellow gummy solid; IR (neat) ν_{max} 2354, 1719, 1290, 1188, 808 cm^{-1}; ^1H NMR (400 MHz, $CDCl_3$): δ 1.01 (t, J = 7.4 Hz, 3H), 1.71–1.80 (m, 2H), 2.54 (s, 3H), 3.09 (t, J = 7.3 Hz, 2H), 4.01 (s, 3H), 7.31 (dd, J = 1.3, 8.8 Hz, 1H), 7.50 (d, J = 8.1 Hz, 1H), 7.64 (d, J = 1.1 Hz, 1H), 7.89 (d, J = 8.4 Hz, 1H), 8.40 (dd, J = 2.0, 8.1 Hz, 1H), 8.71 (d, J = 1.8 Hz, 1H), 9.52 (s, 1H) ppm; ^{13}C NMR (100 MHz, $CDCl_3$): δ 13.8 (q), 17.0 (t), 22.0 (q), 44.0 (t), 52.7 (q), 117.6 (d), 119.9 (d), 120.4 (s), 128.4 (d), 129.8 (d), 130.6 (d), 131.5 (s), 131.7 (s), 134.8 (d), 137.7 (s), 146.5 (s), 149.9 (s), 157.5 (s), 165.3 (s), 187.6 (s), 189.8 (s) ppm; HRMS (ESI) m/z: $[M + H]^+$ calcd. for $C_{21}H_{21}N_2O_4$: 365.1501; found: 365.1496.

1-(2-(2-Acetylphenyl)-2*H*-indazol-3-yl)butan-1-one (5bg)

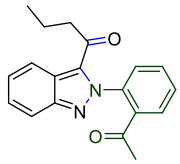

R_f = 0.4 (15% EtOAc in petroleum ether); yield: 57 mg (71%); pale yellow syrup; IR (neat) ν_{max} 2960, 2926, 1687, 1605, 1505, 1363, 1249, 984, 756 cm^{-1}; ^1H NMR (400 MHz, $CDCl_3$): δ 1.00 (*t*, J = 7.4 Hz, 3H), 1.71–1.81 (m, 2H), 2.16 (s, 3H), 3.04 (t, J = 7.2 Hz, 2H), 7.33–7.37 (m, 1H), 7.38–7.46 (m, 2H), 7.61–7.66 (m, 2H), 7.86–7.92 (m, 2H), 7.97–8.06 (m, 1H) ppm; ^{13}C NMR(100 MHz, $CDCl_3$): δ 13.7 (q), 17.0 (t), 28.3 (q), 44.0 (t), 119.2 (d), 120.6 (d), 122.1 (s), 126.1 (d), 126.8 (d), 128.2 (d), 129.2 (d), 129.5 (d), 132.1 (d), 133.4 (s), 135.4 (s), 140.1 (s), 148.6 (s), 190.0 (s), 197.9 (s) ppm; HRMS (ESI) m/z: $[M + H]^+$ calcd. for: $C_{19}H_{19}N_2O_2$: 307.1441; found: 307.1447.

1-(2-(2-Acetylphenyl)-2*H*-indazol-3-yl)-3-methylbutan-1-one (5dg)

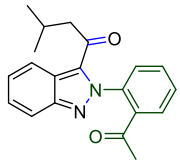

R_f = 0.5 (15% EtOAc in petroleum ether); yield: 52 mg (66%); dark yellow syrup; IR (neat) ν_{max} 2957, 1678, 1602, 1359, 1246, 999, 955, 751 cm^{-1}; ^1H NMR (400 MHz, $CDCl_3$): δ 0.99 (s, 3H), 1.00 (s, 3H), 2.16 (s, 3H), 2.31 (dt, J = 6.7, 13.4 Hz, 1H), 2.93 (d, J = 6.7 Hz, 2H), 7.32–7.36 (m, 1H), 7.40–7.47 (m, 2H), 7.60–7.68 (m, 2H), 7.86–7.92 (m, 2H), 7.97–8.02 (m, 1H) ppm; ^{13}C NMR (100 MHz, $CDCl_3$): δ 22.7 (q, 2C), 24.5 (d), 28.3 (q), 51.0 (t), 119.3 (d), 120.5 (d), 122.1 (s), 126.1 (d), 126.8 (d), 128.2 (d), 129.3 (d), 129.5 (d), 132.1 (d), 133.5 (s), 135.5 (s), 140.1 (s), 148.7(s), 189.8 (s), 197.8 (s) ppm; HRMS (ESI) m/z: $[M + H]^+$ calcd. for: $C_{20}H_{21}N_2O_2$: 321.1598; found: 321.1603.

1-(2-(2-Acetylphenyl)-2*H*-indazol-3-yl)-3-phenylpropan-1-one (5eg)

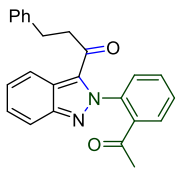

R_f = 0.4 (15% EtOAc in petroleum ether); yield: 42 mg (57%); dark yellow syrup; IR (neat) ν_{max} 2962, 2930, 1705, 1253, 1024, 799, 701 cm^{-1}; ^1H NMR (400 MHz, $CDCl_3$): δ 2.51 (s, 3H), 2.93–3.06 (m, 2H), 3.18–3.29 (m, 2H), 7.15–7.24 (m, 3H), 7.27–7.32 (m, 2H), 7.32–7.37 (m, 1H), 7.37–7.41 (m, 1H), 7.42–7.48 (m, 1H), 7.71–7.77 (m, 2H), 7.86 (d, J = 8.6 Hz, 1H), 7.98 (d, J = 8.6 Hz, 1H), 8.02–8.07 (m, 1H) ppm; ^{13}C NMR (100 MHz, $CDCl_3$): δ 28.1 (q), 29.7 (t), 43.2 (t), 114.6 (d), 117.7 (s), 119.9 (s), 120.9 (d), 126.2 (d), 126.6 (d), 128.4 (d, 2C), 128.6 (d, 2C), 128.9 (d), 130.0 (s), 130.1 (d), 130.2 (d), 131.1 (d), 132.2 (s), 132.9 (d), 135.3 (s), 140.8 (s), 185.1 (s), 197.0 (s) ppm; HRMS (ESI) m/z: $[M + H]^+$ calcd. for: $C_{24}H_{21}N_2O_2$: 369.1603; found: 369.1598.

1-(2-(2-Acetylphenyl)-6-methyl-2*H*-indazol-3-yl)butan-1-one (5jg)

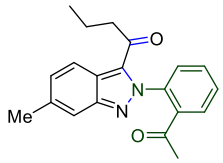

R_f = 0.4 (30% EtOAc in petroleum ether); yield: 47 mg (60%); yellow syrup; IR (neat) ν_{max} 2965, 1679, 1417, 1243, 972, 759, 670 cm^{-1}; ^1H NMR (400 MHz, $CDCl_3$): δ 0.99 (t, J = 7.4 Hz, 3H), 1.71–1.81 (m, 2H), 2.12 (s, 3H), 2.51 (d, J = 0.9 Hz,3H), 3.02 (t, J = 7.2 Hz, 2H), 7.25 (dd, J =1.2, 8.7 Hz, 1H), 7.32–7.36 (m, 1H), 7.58–7.66 (m, 3H), 7.86–7.91 (m, 2H) ppm; ^{13}C NMR (100 MHz, $CDCl_3$): δ 13.8 (q), 17.1 (t), 21.9 (q), 28.3 (q), 44.0 (t), 117.5 (d), 120.1 (d), 120.6 (s), 128.2 (d), 129.0 (d), 129.2 (d), 129.4 (d), 132.0 (d), 133.2 (s), 135.6 (s), 136.9 (s), 140.1 (s), 149.3 (s), 190.0 (s), 198.0 (s) ppm; HRMS (ESI) m/z: $[M + H]^+$ calcd. for: $C_{20}H_{21}N_2O_2$: 321.1598; found: 321.1603.

Methyl 2-(2-acetylphenyl)-3-butyryl-2*H*-indazole-6-carboxylate (5kg)

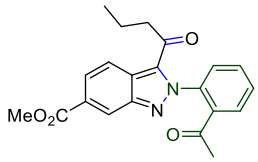

R_f = 0.4 (30% EtOAc in petroleum ether); yield: 51 mg (69%); yellow syrup; IR (neat) ν_{max} 2955, 1713, 1581, 1417, 1258, 984, 828, 756, 659 cm^{-1}; ^1H NMR (400 MHz, $CDCl_3$): δ 0.89–1.03 (m, 3H), 1.68–1.75 (m, 2H), 2.53 (d, J = 0.6 Hz, 3H), 2.87 (t, J = 7.2 Hz, 2H), 3.99 (s, 3H), 7.35–7.45 (m, 1H), 7.68–7.81 (m, 2H), 7.99–8.18 (m, 3H), 8.58–8.66 (m, 1H) ppm; ^{13}C NMR (100 MHz, $CDCl_3$): δ 13.7 (q), 17.2 (t), 28.0 (q), 43.5 (t), 52.5 (q), 117.9 (s), 118.0 (d), 120.8 (s), 121.0 (d), 128.1 (d), 128.1 (s), 129.4 (s), 130.1 (d), 130.2 (d), 131.3 (d), 132.0 (s), 133.0 (d), 135.0 (s), 165.9 (s), 186.3 (s), 196.9 (s) ppm; HRMS (ESI) m/z: $[M + H]^+$ calcd. for: $C_{21}H_{21}N_2O_4$: 365.1496; found: 365.1498.

General Procedure for Wittig homologation

In general, all reactions were carried out employing 50 mg of 2*H*-indazole derivative **5**.

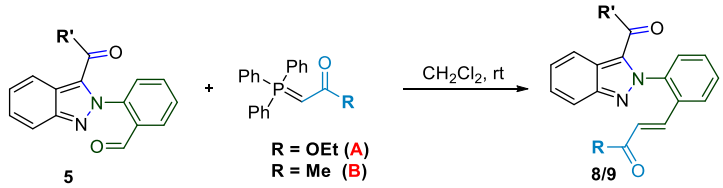

To the stirred solution of aldehyde **5** (1 equiv.) in dry CH_2Cl_2 (2ml) triphenylphosphoranylidine **A/B** (1.5 equiv.) was added in portions. The mixture was stirred at room tempreture until completion of reaction (approx. 8-9 h, checked by TLC), followed by evaporation of solvent. The residue was purified by silica gel column chromatography to afford the product **8/9**.

Ethyl (*E*)-3-(2-(3-butyryl-2*H*-indazol-2-yl)phenyl)acrylate (8a)

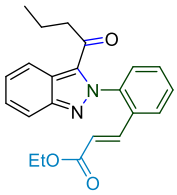

R_f = 0.4 (15% EtOAc in petroleum ether); yield: 58 mg (93%); yellow gum; IR (neat) ν_{max} 1712, 1671, 1173, 980, 751 cm^{-1}; ^1H NMR (400 MHz, $CDCl_3$): δ0.95 (t, *J* = 7.4 Hz, 3H), 1.20 (t, *J* =7.1 Hz, 3H), 1.65–1.79 (m, 2H), 2.96 (t, *J* = 7.1 Hz, 2H), 4.12 (q, *J* = 7.1 Hz, 2H), 6.34 (d, *J* = 15.9 Hz, 1H), 7.02 (d, *J* = 16.0 Hz, 1H), 7.32–7.40 (m, 1H), 7.45 (quin, *J* = 6.8 Hz, 2H), 7.52–7.60 (m, 2H), 7.76–7.84 (m, 1H), 7.90 (d, *J* = 8.0 Hz, 1H), 8.04 (d, *J* = 7.9 Hz, 1H) ppm; ^{13}C NMR (100 MHz, $CDCl_3$): δ13.7 (q), 14.1 (q), 17.0 (t), 44.1 (t), 60.5 (t), 119.3 (d), 120.6 (d), 121.4 (d), 122.1 (s), 126.2 (d), 126.8 (d), 127.0 (d), 127.6 (d), 129.8 (d), 130.4 (d), 131.4 (s), 133.9 (s), 138.2 (d), 141.1 (s), 148.8 (s), 166.1 (s), 189.7 (s) ppm; HRMS (ESI) m/z: $[M + H]^+$ calcd. for: $C_{22}H_{23}N_2O_3$: 363.1703; found: 363.1709.

Ethyl (*E*)-3-(2-(3-(3-methylbutanoyl)-2*H*-indazol-2-yl)phenyl)acrylate (8b)

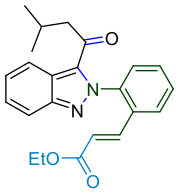

R_f = 0.4 (15% EtOAc in petroleum ether); yield: 52 mg (84%); yellow gum; IR (neat) ν_{max} 1712, 1672, 1282, 1175, 755 cm^{-1}; ^1H NMR (400 MHz, $CDCl_3$): δ0.94 (s, 3H), 0.96 (s, 3H), 1.17–1.24 (m, 3H), 2.26 (dt, *J* = 6.7, 13.4 Hz, 1H), 2.86 (d, *J* = 6.9 Hz, 2H), 4.06–4.18 (m, 2H), 6.34 (d, *J* = 15.9 Hz, 1H), 7.01 (d, *J* = 15.9 Hz, 1H), 7.32–7.38 (m, 1H), 7.40–7.50 (m, 2H), 7.52–7.60 (m, 2H), 7.80 (dd, *J* = 1.9, 7.4 Hz, 1H), 7.88–7.94 (m, 1H), 7.99–8.05 (m, 1H) ppm; ^{13}C NMR (100 MHz, $CDCl_3$): δ14.1 (q), 22.6 (q, 2C), 24.5 (d), 51.1 (t), 60.5 (t), 119.3 (d), 120.6 (d), 121.5 (d), 122.0 (s), 126.3 (d), 126.8 (d), 127.0 (d), 127.6 (d), 129.8 (d), 130.4 (d), 131.5 (s), 134.1 (s), 138.2 (d), 141.2 (s), 148.8 (s),

166.1 (s), 189.5 (s) ppm; HRMS (ESI) m/z: $[M + H]^+$ calcd. for: $C_{23}H_{25}N_2O_3$: 377.1865; found: 377.1865.

Ethyl (*E*)-3-(2-(3-(3-phenylpropanoyl)-2*H*-indazol-2-yl)phenyl)acrylate (8c)

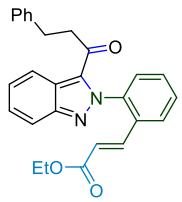

R_f = 0.4 (20% EtOAc in petroleum ether); yield: 53 mg (88%); yellow gum; IR (neat) ν_{max} 1710, 1672, 1173, 975, 750 cm^{-1}; ^1H NMR (400 MHz, $CDCl_3$): δ 1.18 (t, J = 7.1 Hz, 3H), 2.99 (t, J = 7.7 Hz, 2H), 3.27–3.36 (m, 2H), 4.10 (q, J = 7.1 Hz, 2H), 6.33 (d, J = 16.0 Hz, 1H), 7.01 (d, J = 16.0 Hz, 1H), 7.14–7.18 (m, 2H), 7.18–7.22 (m, 1H), 7.23–7.26 (m, 1H), 7.26–7.31 (m, 2H), 7.36–7.47 (m, 2H), 7.48–7.59 (m, 2H), 7.79 (dd, J = 7.7, 1.4 Hz, 1H), 7.85–7.91 (m, 1H), 7.97 (d, J = 8.3 Hz, 1H) ppm; ^{13}C NMR (100 MHz, $CDCl_3$): δ 14.1 (q), 29.5 (t), 43.8 (t), 60.5 (t), 119.3 (d), 120.6 (d), 121.5 (d), 122.1 (s), 126.2 (d), 126.4 (d), 126.8 (d), 127.1 (d), 127.6 (d), 128.3 (d, 2C), 128.5 (d, 2C), 129.8 (d), 130.4 (d), 131.5 (s), 133.7 (s), 138.1 (d), 140.6 (s), 141.0 (s), 148.8 (s), 166.1 (s), 188.7 (s) ppm; HRMS (ESI) m/z: $[M + H]^+$ calcd. for: $C_{27}H_{25}N_2O_3$: 425.1865; found: 425.1858.

(*E*)-4-(2-(3-Butyryl-2*H*-indazol-2-yl)phenyl)but-3-en-2-one (9a)

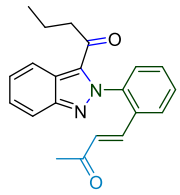

R_f = 0.3 (15% EtOAc in petroleum ether); yield: 54 mg (95%); yellow syrup; IR (neat) ν_{max} 1670, 1612, 1361, 978, 751 cm^{-1}; ^1H NMR (400 MHz, $CDCl_3$): δ 0.95 (t, J = 7.4 Hz, 3H), 1.67–1.77 (m, 2H), 2.09 (s, 3H), 2.95 (t, J = 7.2 Hz, 2H), 6.58 (d, J = 16.1 Hz, 1H), 6.85 (d, J = 16.1 Hz, 1H), 7.34–7.39 (m, 1H), 7.41–7.53 (m, 2H), 7.53–7.65 (m, 2H), 7.82 (dd, J = 1.9, 7.4 Hz, 1H), 7.88–7.95 (m, 1H), 8.01–8.09 (m, 1H) ppm; ^{13}C NMR (100 MHz, $CDCl_3$): δ 13.7 (q), 17.1 (t), 27.7 (q), 44.1 (t), 119.3 (d), 120.7 (d), 122.1 (s), 126.4 (d), 126.9 (d), 127.2 (d), 127.7 (d), 129.7 (d), 129.9 (d), 130.6 (d), 131.5 (s), 134.0 (s), 136.8 (d), 141.3 (s), 148.8 (s), 189.8 (s), 197.6 (s) ppm; HRMS (ESI) m/z: $[M + H]^+$ calcd. for: $C_{21}H_{21}N_2O_2$: 333.1598; found: 333.1603.

(*E*)-4-(2-(3-(3-Methylbutanoyl)-2*H*-indazol-2-yl)phenyl)but-3-en-2-one (9b)

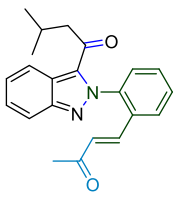

R_f = 0.3 (15% EtOAc in petroleum ether); yield: 50 mg (89%); yellow gum; IR (neat) ν_{max} 1668, 1612, 1362, 1176, 984, 749 cm^{-1}; ^1H NMR (400 MHz, $CDCl_3$): δ 0.94 (s, 3H), 0.96 (s, 3H), 2.09 (s, 3H), 2.25 (dt, J = 6.7, 13.4 Hz, 1H), 2.84 (d, J = 6.9 Hz, 2H), 6.58 (d, J = 16.3 Hz, 1H), 6.84 (d, J = 16.3 Hz, 1H), 7.33–7.39

(m, 1H), 7.43–7.50 (m, 2H), 7.53–7.62 (m, 2H), 7.82 (dd, J = 1.8, 7.3 Hz, 1H), 7.88–7.94 (m, 1H), 8.00–8.08 (m, 1H) ppm; ^{13}C NMR (100 MHz, $CDCl_3$): δ22.6 (q, 2C), 24.5 (s), 27.6 (q), 51.1 (t), 119.3 (d), 120.6 (d), 122.0 (s), 126.4 (s), 126.9 (d), 127.2 (d), 127.6 (d), 129.7 (d), 129.9 (d), 130.6 (d), 131.6 (s), 134.2 (s), 136.8 (d), 141.3 (s), 148.8 (s), 189.6 (s), 197.6 (s) ppm; HRMS (ESI) m/z: $[M + H]^+$ calcd. for: $C_{22}H_{23}N_2O_2$: 347.1759; found: 347.1763.

(*E*)-4-(2-(3-(3-Phenylpropanoyl)-2*H*-indazol-2-yl)phenyl)but-3-en-2-one (9c)

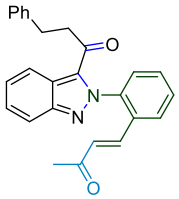

R_f = 0.3 (20% EtOAc in petroleum ether); yield: 51 mg (92%); yellow gum; IR (neat) ν_{max} 2926, 1669, 1606, 1529, 977, 755 cm^{-1}; ^{1}H NMR (400 MHz, $CDCl_3$): δ2.25 (s, 3H), 3.14–3.21 (m, 2H), 3.26–3.34 (m, 2H), 6.51 (d, J = 7.5 Hz, 1H), 6.66 (d, J = 16.4 Hz, 1H), 6.76 (dd, J = 1.1, 7.8 Hz, 1H), 7.15 (td, J = 1.0, 7.6 Hz, 1H), 7.22 (dt, J = 2.0, 7.0 Hz, 1H), 7.29–7.35 (m, 5H), 7.41 (td, J = 1.4, 7.6 Hz, 1H), 7.50 (td, J = 1.0, 7.7 Hz, 1H), 7.58 (d, J = 16.4 Hz, 1H), 7.67–7.77 (m, 2H) ppm; ^{13}C NMR (100 MHz, $CDCl_3$): δ24.1 (t), 27.2 (q), 31.6 (t), 114.2 (d), 118.9 (d), 119.7 (s), 123.9 (d), 124.8 (s), 125.9 (d), 126.3 (d), 127.6 (d), 128.4 (d, 2C), 128.5 (d), 128.5 (d, 2C), 129.7 (d), 130.9 (d), 132.3 (d), 138.8 (s), 140.5 (s), 142.0 (s), 147.0 (s), 149.8 (s), 158.0 (s), 198.2 (s) ppm; HRMS (ESI) m/z: $[M + H]^+$ calcd. for: $C_{26}H_{23}N_2O_2$: 395.1759; found: 395.1780.

Carbene trapping experiment by employing excess styrene:

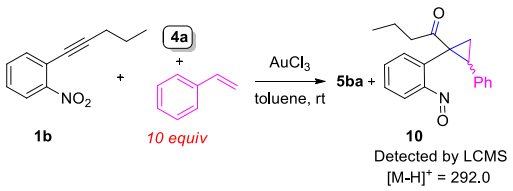

At room temperature, to a stirred solution of anthranil **4a** (1.1 equiv.) in anhydrous toluene (1 mL) was added $AuCl_3$ and 4Å molecular sieves (40 mg), a solution of nitroalkyne **1** (1 equiv) and styrene (10 equiv.) in anhydrous toluene (1 mL) was introduced *via* syringe pump over a period of 4 h. The stirring was continued until the complete disappearance of the starting nitroalkyne or alkyne as indicated by TLC. The product mass was confirmed by LCMS.

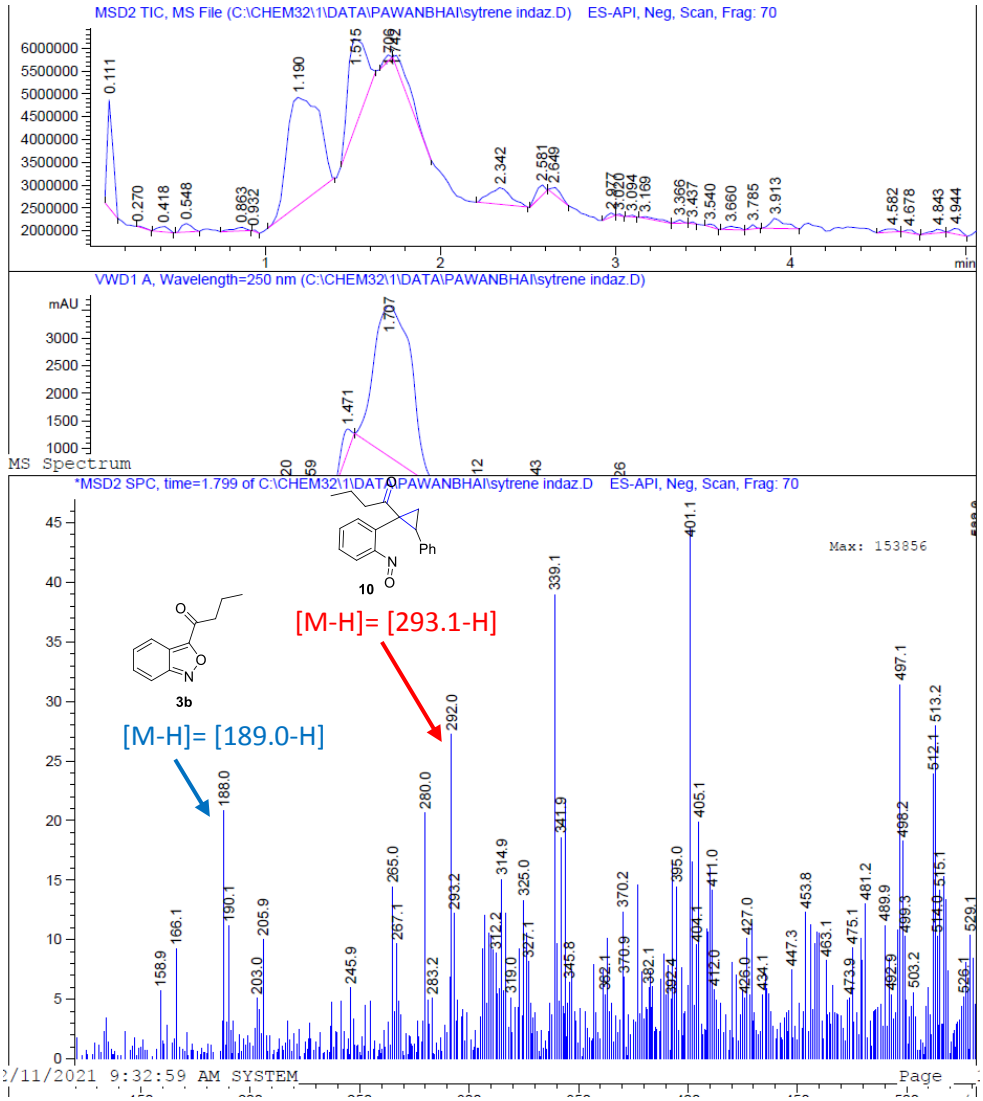
MSD2 TIC, MS File (C:\CHEM32\1\DATA\PAWANBHAI\sytrene indaz.D) ES-API, Neg, Scan, Frag: 70
VWD1 A, Wavelength=250 nm (C:\CHEM32\1\DATA\PAWANBHAI\sytrene indaz.D)
mAU
MS Spectrum
*MSD2 SPC, time=1.799 of C:\CHEM32\1\DATA\PAWANBHAI\sytrene indaz.D ES-API, Neg, Scan, Frag: 70
Max: 153856
10
Ph
3b
[M-H]= [293.1-H]
[M-H]= [189.0-H]
min
Page

Part B. General Procedure for the synthesis of Quinazoline N-Oxides derivatives

In general, all reactions were carried out employing 50 mg of nitroalkyne **1**.

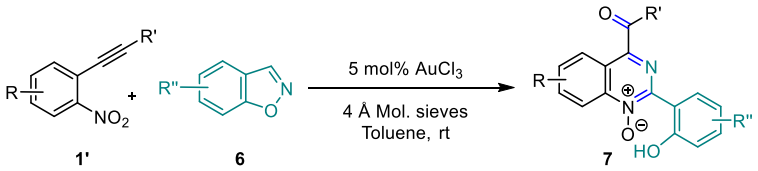

1' **6** **7**

R' = *alkyl*

At rt, to a stirred solution of 1,2-benzo[*d*]isoxazole **6** (1.1 equiv) in anhydrous toluene (1 mL) was added $AuCl_3$ (5 mol %) and 4Å molecular sieves (40 mg), a solution of nitroalkyne **1'** (1 equiv) in anhydrous toluene (1 mL) was introduced *via* syringe pump over a period of 4 h. The stirring was continued until the complete disappearance of the starting nitroalkyne as indicated by TLC. The reaction mixture was concentrated under reduced pressure and the resulting crude was purified by column chromatography to afford the products **7**.

2-(2-hydroxyphenyl)-4-propionylquinazoline 1-oxide (7aa)

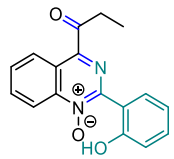

R_f = 0.4 (20% EtOAc in petroleum ether); yield: 61 mg (73%); orange solid; IR (neat)ν_{max} 2975, 2930, 1699, 1530, 1468, 1314, 1252, 1159, 755 cm^{-1}; ^1H NMR (500 MHz, $CDCl_3$): δ 1.31 (t, *J* = 7.2 Hz, 3H), 3.42 (q, *J* = 7.2 Hz, 2H), 7.09–7.22 (m, 2H), 7.58 (ddd, *J* = 1.7, 7.0, 8.4 Hz, 1H), 7.88 (ddd, *J* = 1.2, 7.1, 8.5 Hz, 1H), 8.07–8.15 (m, 2H), 8.87 (d, *J* = 8.7 Hz, 1H), 9.05 (dd, *J* = 0.7, 8.5 Hz, 1H), 10.41 (s, 1H) ppm; ^{13}C NMR (125 MHz, $CDCl_3$): δ 7.8 (q), 33.2 (t), 119.3 (d), 120.1 (d), 120.4 (s), 120.5 (d), 121.2 (s), 127.6 (d), 130.9 (d), 133.0 (d), 133.7 (d), 135.7 (d), 144.6 (s), 148.7 (s), 152.1 (s), 160.3 (s), 202.3 (s) ppm; HRMS (ESI) calcd. for $C_{17}H_{15}N_2O_3$: 295.1077 $[M+H]^+$; found: 295.1073.

2-(2-hydroxyphenyl)-4-propionylquinazoline 1-oxide (7ba)

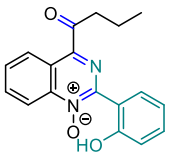

R_f = 0.4 (20% EtOAc in petroleum ether); yield: 60 mg (74%); dark yellow solid; IR (neat)ν_{max} 2975, 2930, 1699, 1530, 1468, 1314, 1252, 1159, 755 cm^{-1}; ^1H NMR (500 MHz, $CDCl_3$): δ 1.08 (t, *J* = 7.4 Hz, 3H), 1.79–1.91 (m, 2H), 3.35 (t, *J* = 7.3 Hz, 2H), 7.10–7.24 (m, 2H), 7.58 (ddd, *J* = 1.7, 7.0, 8.4 Hz, 1H), 7.88 (ddd, *J* = 1.2, 7.1, 8.5 Hz, 1H), 8.06–8.16 (m, 2H), 8.84–8.92 (m, 1H), 9.03 (dd, *J* = 0.7, 8.6 Hz, 1H), 10.41 (s, 1H) ppm; ^{13}C NMR (125 MHz, $CDCl_3$): δ 13.8 (q), 17.4 (t), 41.6 (t), 119.3 (d), 120.1 (d), 120.4 (s), 120.5 (d), 121.2 (s), 127.6

(d), 130.8 (d), 132.9 (d), 133.7 (d), 135.7 (d), 144.6 (s), 148.9 (s), 152.0 (s), 160.3 (s), 201.8 (s) ppm; HRMS (ESI) calcd. for $C_{18}H_{17}N_2O_3$: 309.1239 $[M+H]^+$; found: 309.1248.

Procedure for 1g scale

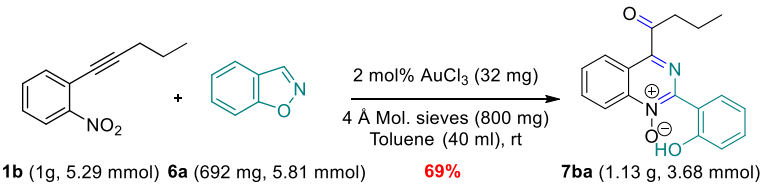

1b (1g, 5.29 mmol) **6a** (692 mg, 5.81 mmol) 69% **7ba** (1.13 g, 3.68 mmol)

At room temperature, to a solution of 1,2-benzo[*d*]isoxazole **6a** (632 mg, 5.81 mmol) in anhydrous toluene (20 mL) and 4Å molecular sieves (800 mg) and $AuCl_3$ (32 mg) was added *o*-nitroalkyne **1b** (1g, 5.29 mmol) in anhydrous toluene (20 mL) *via* syringe pump over 6 h. The reaction was stirred at rt until the completion as indicated by TLC. Usual workup followed by purification by column chromatography afforded compound **7ba** (1.13 g, 69% yield) as yellow solid.

4-hexanoyl-2-(2-hydroxyphenyl)quinazoline 1-oxide (7ca)

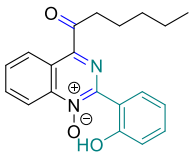

R_f = 0.5 (15% EtOAc in petroleum ether); yield: 53 mg (68%); yellow syrup; IR (neat)ν_{max} 2925, 2858, 1700, 1603, 1533, 1469, 1317, 1251, 1160, 759 cm^{-1}; ^1H NMR (400 MHz, $CDCl_3$): δ 0.94 (t, J = 7.1 Hz, 3H), 1.38–1.45 (m, 4H), 1.82 (t, J = 7.3 Hz, 2H), 3.36 (t, J = 7.4 Hz, 2H), 7.08–7.22 (m, 2H), 7.51–7.65 (m, 1H), 7.83–7.94 (m, 1H), 8.04–8.17 (m, 2H), 8.87 (d, J = 8.7 Hz, 1H), 9.02 (d, J = 8.5 Hz, 1H), 10.42 (s, 1H) ppm; ^{13}C NMR (125 MHz, $CDCl_3$): δ 13.9 (q), 22.5 (t), 23.7 (t), 31.4 (t), 39.8 (t), 119.3 (d), 120.1 (d), 120.4 (s), 120.5 (d), 121.2 (s), 127.6 (d), 130.8 (d), 132.9 (d), 133.7 (d), 135.7 (d), 144.6 (s), 148.9 (s), 152.0 (s), 160.3 (s), 202.0 (s) ppm; HRMS (ESI) calcd. for $C_{20}H_{21}N_2O_3$: 337.1547 $[M+H]^+$; found: 337.1549.

2-(2-hydroxyphenyl)-4-(3-methylbutanoyl)quinazoline 1-oxide (7da)

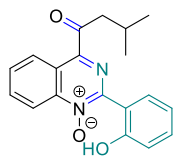

R_f = 0.5 (10% EtOAc in petroleum ether); yield: 48 mg (60%); orange solid; IR (neat)ν_{max} 2958, 1700, 1603, 1534, 1320, 1253, 1163, 762 cm^{-1};^1H NMR (400 MHz, $CDCl_3$): δ 1.06 (s, 3H), 1.08 (s, 3H), 2.38 (dt, J = 6.7, 13.4 Hz, 1H), 3.23 (d, J = 6.9 Hz, 2H), 7.12–7.21 (m, 2H), 7.59 (ddd, J = 1.7, 7.0, 8.4 Hz, 1H), 7.88 (ddd, J = 1.2, 7.1, 8.5 Hz, 1H), 8.06–8.13 (m, 2H), 8.84–8.89 (m, 1H), 8.98–9.03 (m, 1H), 10.41 (s, 1H) ppm;

^{13}C NMR (100 MHz, $CDCl_3$): δ22.7 (q, 2C), 25.2 (d), 48.4 (t), 119.3 (d), 120.2 (d), 120.4 (s), 120.6 (d), 121.2 (s), 127.6 (d), 130.8 (d), 132.9 (d), 133.7 (d), 135.7 (d), 144.6 (s), 149.1 (s), 152.0 (s), 160.3 (s), 201.7 (s) ppm; HRMS (ESI) calcd. for $C_{19}H_{19}N_2O_3$: 323.1390 $[M+H]^+$; found: 323.1388.

2-(2-hydroxyphenyl)-4-(3-phenylpropanoyl)quinazoline 1-oxide (7ea)

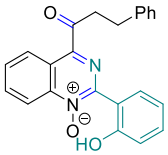

R_f = 0.4 (15% EtOAc in petroleum ether); yield: 46 mg (62%); pale yellow solid; IR (neat)ν_{max} 3016, 2922, 2859, 1699, 1601, 1532, 1488, 1318, 1251, 757, 698 cm^{-1}; ^{1}H NMR (400 MHz, $CDCl_3$): δ3.14 (t, J = 7.5 Hz, 2H), 3.70 (t, J = 7.5 Hz, 2H), 7.09–7.13 (m, 1H), 7.15 (dd, J = 0.92, 8.2 Hz, 1H), 7.18–7.22 (m, 1H), 7.25 (s, 1H), 7.28 (d, J = 4.1 Hz, 3H), 7.56 (ddd, J = 1.8, 7.1, 8.5 Hz, 1H), 7.83–7.88 (m, 1H), 8.03 (dd, J = 1.8, 8.2 Hz, 1H), 8.08 (ddd, J = 1.1, 7.1, 8.7 Hz, 1H), 8.81–8.87 (m, 1H), 9.00 (dd, J = 1.4, 8.7 Hz, 1H), 10.32 (s, 1H) ppm; ^{13}C NMR (100 MHz, $CDCl_3$): δ30.1 (t), 41.3 (t), 119.2 (d), 120.2 (d), 120.3 (s), 120.5 (d), 121.1 (s), 126.3 (d), 127.6 (d), 128.5 (d, 2C), 128.6 (d, 2C), 130.9 (d), 133.0 (d), 133.7 (d), 135.7 (d), 140.5 (s), 144.6 (s), 148.4 (s), 152.1 (s), 160.2 (s), 200.8 (s) ppm; HRMS (ESI) calcd. for $C_{23}H_{19}N_2O_3$: 371.1390 $[M+H]^+$; found: 371.1393.

4-(4-acetoxybutanoyl)-2-(2-hydroxyphenyl)quinazoline 1-oxide (7fa)

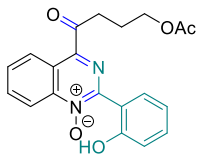

R_f = 0.4 (20% EtOAc in petroleum ether); yield: 49 mg (66%); yellow solid; IR (neat)ν_{max} 2954, 2928, 1726, 1530, 1468, 1239, 1067, 873, 753 cm^{-1}; ^{1}H NMR (400 MHz, $CDCl_3$): δ2.04 (s, 3H), 2.18 (quin, J = 6.7 Hz, 2H), 3.48 (t, J = 7.1 Hz, 2H), 4.24 (t, J = 6.4 Hz, 2H), 7.12–7.21 (m, 2H), 7.59 (ddd, J = 1.7, 7.0, 8.4 Hz, 1H), 7.89 (ddd, J = 1.2, 7.1, 8.5 Hz, 1H), 8.06–8.15 (m, 2H), 8.84–8.89 (m, 1H), 9.07 (dd, J = 0.7, 8.5 Hz, 1H), 10.32 (s, 1H) ppm; ^{13}C NMR (100 MHz, $CDCl_3$): δ20.9 (q), 23.0 (t), 36.1 (t), 63.5 (t), 119.3 (d), 120.2 (d), 120.3 (s), 120.6 (d), 121.2 (s), 127.6 (d), 131.1 (d), 132.9 (d), 133.8 (d), 135.8 (d), 144.7 (s), 148.1 (s), 152.1 (s), 160.3 (s), 171.1 (s), 200.6 (s) ppm; HRMS (ESI) calcd. for: $C_{20}H_{19}N_2O_5$: 367.1288 $[M+H]^+$; found: 367.1284.

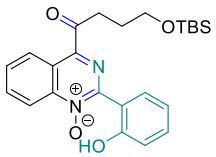

4-(4-((tert-butyldimethylsilyl)oxy)butanoyl)-2-(2-hydroxyphenyl)quinazoline 1-oxide (7ga)

R_f = 0.4 (20% EtOAc in petroleum ether); yield: 37 mg (54%); dark yellow

syrup; IR (neat)ν_{max} 2929, 2860, 1699, 1602, 1531, 1469, 1315, 1252, 1103, 906, 760 cm^{-1}; ^1H NMR (400 MHz, $CDCl_3$):δ0.05 (s, 6H), 0.89 (s, 9H), 2.05 (dt, *J* = 6.5, 13.4 Hz, 2H), 3.47 (t, *J* = 7.2 Hz, 2H), 3.78 (t, *J* = 6.1 Hz, 2H), 7.10–7.15 (m, 1H), 7.16–7.19 (m, 1H), 7.54–7.61 (m, 1H), 7.84–7.91 (m, 1H), 8.07–8.15 (m, 2H), 8.84–8.89 (m, 1H), 9.03–9.09 (m, 1H), 10.42 (s, 1H) ppm; ^{13}C NMR (100 MHz, $CDCl_3$): δ-5.4 (q, 2C), 18.3 (s), 25.9 (q, 3C), 27.0 (t), 36.4 (t), 62.1 (t), 119.3 (d), 120.1 (d), 120.4 (s), 120.5 (d), 121.2 (s), 127.7 (d), 130.8 (d), 133.0 (d), 133.7 (d), 135.7 (d), 144.6 (s), 148.6 (s), 152.1 (s), 160.3 (s), 201.6 (s) ppm; HRMS (ESI) calcd. for: $C_{24}H_{31}N_2O_4Si$: 439.2048 $[M+H]^+$; found: 439.2055.

2-(2-hydroxyphenyl)-4-(4-((tetrahydro-2H-pyran-2-yl)oxy)butanoyl)quinazoline 1-oxide (7ha)

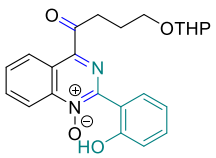

R_f = 0.4 (20% EtOAc in petroleum ether); yield: 42 mg (59%); yellow solid; IR (neat)ν_{max} 2938, 2863, 1700, 1603, 1533, 1316, 1121, 1028, 756 cm^{-1}; ^1H NMR (400 MHz, $CDCl_3$): δ1.43–1.49 (m, 2H), 1.53–1.61 (m, 2H), 1.61–1.76 (m, 2H), 2.14 (quin, *J* = 6.6 Hz, 2H), 3.41–3.59 (m, 4H), 3.82 (ddd, *J* = 3.0, 8.1, 11.1 Hz, 1H), 3.89 (dt, *J* = 6.3, 9.7 Hz, 1H), 4.57 (t, *J* = 3.4 Hz, 1H), 7.13 (ddd, *J* = 1.1, 7.1, 8.1 Hz, 1H), 7.17 (dd, *J* = 0.9, 8.3 Hz, 1H), 7.58 (ddd, *J* = 1.7, 7.0, 8.4 Hz, 1H), 7.88 (ddd, *J* = 1.2, 7.1, 8.5 Hz, 1H), 8.07–8.15 (m, 2H), 8.85–8.90 (m, 1H), 9.06 (dd, *J* = 0.7, 8.6 Hz, 1H), 10.42 (s, 1H) ppm; ^{13}C NMR (100 MHz, $CDCl_3$): δ19.6 (t), 24.4 (t), 25.4 (t), 30.6 (t), 36.8 (t), 62.4 (t), 66.5 (t), 98.9 (d), 119.2 (d), 120.1 (d), 120.4 (s), 120.5 (d), 121.2 (s), 127.7 (d), 130.8 (d), 133.0 (d), 133.7 (d), 135.6 (d), 144.6 (s), 148.7 (s), 152.0 (s), 160.3 (s), 201.5 (s) ppm; HRMS (ESI) calcd. for: $C_{23}H_{25}N_2O_5$: 409.1758 $[M+H]^+$; found: 409.1757.

1-(2-(2-acetylphenyl)-6-methyl-2H-indazol-3-yl)butan-1-one (7ia)

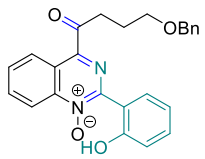

R_f = 0.4 (20% EtOAc in petroleum ether); yield: 50 mg (71%); orange gummy solid; IR (neat)ν_{max} 2925, 2859, 1699, 1603, 1533, 1363, 1104, 749, 693 cm^{-1}; ^1H NMR (400 MHz, $CDCl_3$): δ2.13–2.21 (m, 2H), 3.47 (t, *J* = 6.9 Hz, 2H), 3.62 (t, *J* = 6.0 Hz, 2H), 4.43 (s, 2H), 7.10–7.15 (m, 1H), 7.18 (dd, *J* = 0.9, 8.3 Hz, 1H), 7.20–7.26 (m, 5H), 7.58 (ddd, *J* = 1.7, 7.0, 8.4 Hz, 1H), 7.76–7.82 (m, 1H), 8.06 (ddd, *J* = 1.3, 7.1, 8.7 Hz, 1H), 8.11 (dd, *J* = 1.7, 8.1 Hz, 1H), 8.83 (dq, *J* = 0.6, 8.7 Hz, 1H), 8.91–8.98 (m, 1H), 10.46 (s, 1H) ppm; ^{13}C NMR (100 MHz, $CDCl_3$): δ24.7 (t), 36.8 (t), 69.3 (t), 72.9 (t), 119.1 (d), 120.1 (d), 120.4 (s), 120.5 (d), 121.2 (s), 127.5 (d, 2C), 127.7 (d), 127.8 (d), 128.3 (d, 2C), 130.7 (d),

133.0 (d), 133.7 (d), 135.5 (d), 138.1 (s), 144.5 (s), 148.9 (s), 151.9 (s), 160.3 (s), 201.4 (s) ppm; HRMS (ESI) calcd. for: $C_{25}H_{23}N_2O_4$: 415.1652 $[M+H]^+$; found: 415.1660.

4-butyryl-7-fluoro-2-(2-hydroxyphenyl)quinazoline 1-oxide (7ja)

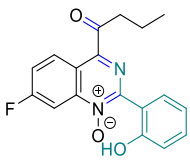

R_f = 0.4 (15% EtOAc in petroleum ether); yield: 40 mg (51%); orange solid; IR (neat)ν_{max} 2962, 1700, 1603, 1536, 1489, 1322, 1252, 1159, 752 cm^{-1}; ^1H NMR (400 MHz, $CDCl_3$): δ1.07 (t, J = 7.4 Hz, 3H), 1.85 (sxt, J = 7.3 Hz, 2H), 3.35 (t, J = 7.2 Hz, 2H), 7.12–7.20 (m, 2H), 7.57–7.65 (m, 2H), 8.10 (dd, J = 1.5, 8.0 Hz, 1H), 8.51 (dd, J = 2.5, 9.3 Hz, 1H), 9.15 (dd, J = 5.6, 9.4 Hz, 1H), 10.30 (s, 1H) ppm; ^{13}C NMR (100 MHz, $CDCl_3$): δ13.8 (q), 17.4 (d), 41.5 (d), 104.8 (dd, J_{C-F} = 26.9 Hz), 118.4 (s), 120.1 (s), 120.3 (d), 120.7 (d), 121.0 (dd, J_{C-F} = 24.7 Hz), 131.2 (dd, J_{C-F} = 10.8 Hz), 133.0 (d), 134.1 (d), 146.5 (ds, J_{C-F} = 12.3 Hz), 148.1 (ds, J_{C-F} = 1.4 Hz), 153.0 (s), 160.4 (s), 165.6 (ds, J_{C-F} = 262.3 Hz), 201.7 (s) ppm; HRMS (ESI) calcd. for $C_{18}H_{16}N_2O_3$: 327.1139 $[M+H]^+$; found: 327.1141.

4-butyryl-2-(2-hydroxyphenyl)-7-nitroquinazoline 1-oxide (7ka)

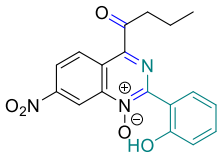

R_f = 0.3 (25% EtOAc in petroleum ether); yield: 26 mg (34%); yellow solid; IR (neat)ν_{max} 2924, 2853, 1695, 1602, 1538, 1465, 1348, 1073, 746 cm^{-1}; ^1H NMR (400 MHz, $CDCl_3$): δ1.09 (t, J = 7.4 Hz, 3H), 1.88 (sxt, J = 7.3 Hz, 2H), 3.38 (t, J = 7.2 Hz, 2H), 7.15–7.22 (m, 2H), 7.60–7.66 (m, 1H), 8.09–8.14 (m, 1H), 8.60 (dd, J = 2.3, 9.3 Hz, 1H), 9.35 (dd, J = 0.5, 9.2 Hz, 1H), 9.66 (dd, J = 0.5, 2.3 Hz, 1H), 9.71 (s, 1H) ppm; ^{13}C NMR (100 MHz, $CDCl_3$): δ13.8 (q), 17.4 (t), 41.4 (t), 115.8 (d), 119.5 (s), 120.6 (d), 120.9 (d), 123.6 (s), 124.2 (d), 130.6 (d), 132.9 (d), 134.6 (d), 145.0 (s), 147.5 (s), 151.4 (s), 153.5 (s), 160.5 (s), 201.1 (s) ppm; HRMS (ESI) calcd. for $C_{18}H_{16}N_3O_5$: 354.1084 $[M+H]^+$; found: 354.1090.

4-butyryl-2-(2-hydroxyphenyl)-7-methylquinazoline 1-oxide (7la)

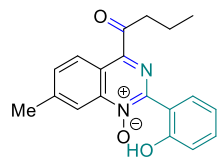

R_f = 0.3 (20% EtOAc in petroleum ether); yield: 48 mg (61%); yellow solid; IR (neat)ν_{max} 2961, 2929, 1702, 1605, 1523, 1488, 1328, 1255, 1165, 756 cm^{-1}; ^1H NMR (400 MHz, $CDCl_3$): δ1.07 (t, J = 7.4 Hz, 3H), 1.85 (sxt, J = 7.3 Hz, 2H), 2.71 (s, 3H), 3.34 (t, J = 7.2 Hz, 2H), 7.10–7.20 (m, 2H), 7.58 (ddd, J = 1.7, 7.0, 8.4 Hz, 1H), 7.69 (dd, J = 1.6, 8.7 Hz, 1H), 8.10 (dd, J = 1.6, 8.0 Hz, 1H), 8.66 (s, 1H), 8.91 (d, J = 8.7 Hz, 1H), 10.57 (s, 1H) ppm; ^{13}C NMR (100 MHz, $CDCl_3$): δ13.8 (q),

17.4 (t), 22.7 (q), 41.6 (t), 118.3 (d), 119.4 (s), 120.1 (d), 120.5 (d), 120.6 (s), 127.3 (d), 132.9 (d, 2C), 133.6 (d), 144.7 (s), 147.9 (s), 148.6 (s), 152.1 (s), 160.3 (s), 202.0 (s) ppm; HRMS (ESI) calcd. for $C_{19}H_{19}N_2O_3$: 500.2068 $[M+H]^+$; found: 500.2068.

2-(2-hydroxyphenyl)-7-(methoxycarbonyl)-4-propionylquinazoline 1-oxide (7ma)

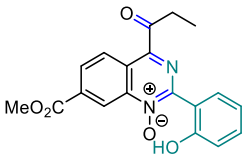

R_f = 0.4 (20% EtOAc in petroleum ether); yield: 58 mg (76%); yellow solid; IR (neat)ν_{max} 2939, 1720, 1605, 1529, 1447, 1281, 1177, 1051 754 cm^{-1}; ^1H NMR (400 MHz, $CDCl_3$): δ1.32 (t, J = 7.1 Hz 3H), 3.42 (q, J = 7.2 Hz, 2H), 4.07 (s, 3H), 6.94–7.00 (m, 1H), 7.12–7.19 (m, 2H), 7.41–7.51 (m, 1H), 7.59 (td, J = 1.5, 7.7 Hz, 1H), 8.10 (dd, J = 1.7, 8.1 Hz, 1H), 8.41–8.46 (m, 1H), 9.14 (d, J = 8.9 Hz, 1H), 9.42–9.46 (m, 1H), 10.14 (s, 1H) ppm; ^{13}C NMR (100 MHz, $CDCl_3$): δ 7.7 (q), 33.2 (t), 53.2 (q), 120.0 (d), 120.4 (d), 120.6 (d), 121.1 (d), 123.0 (s), 128.3 (d), 130.4 (d), 133.0 (d), 134.1 (d), 136.3 (s), 144.6 (s), 148.1 (s), 152.6 (s), 160.2 (s), 165.0 (s), 201.9 (s) ppm; HRMS (ESI) calcd. for $C_{19}H_{17}N_2O_5$: 353.1132 $[M+H]^+$; found: 353.1134.

2-(5-fluoro-2-hydroxyphenyl)-4-propionylquinazoline 1-oxide (7ab)

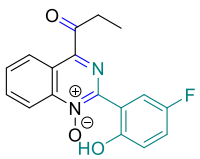

R_f = 0.4 (20% EtOAc in petroleum ether); yield: 61 mg (68%); dark yellow gummy solid; IR (neat) ν_{max} 2236, 1703, 1507, 1432, 1143, 750 cm^{-1}; ^1H NMR (400 MHz, $CDCl_3$):δ1.32 (t, J = 7.2 Hz, 3H), 3.42 (q, J = 7.3 Hz, 2H), 7.12 (dd, J = 4.9, 9.0 Hz, 1H), 7.28–7.34 (m, 1H), 7.78 (dd, J = 3.1, 9.6 Hz, 1H), 7.86–7.96 (m, 1H), 8.12 (td, J = 0.9, 7.9 Hz, 1H), 8.86 (d, J = 8.9 Hz, 1H), 9.06 (d, J = 8.6 Hz, 1H), 10.13 (s, 1H) ppm; ^{13}C NMR (100 MHz, $CDCl_3$): δ7.8 (q), 33.3 (t), 117.7 (dd, J_{C-F} = 25.2 Hz), 119.3 (d), 121.0 (dd, J_{C-F} = 23.6 Hz), 121.3 (s), 121.7 (dd, J_{C-F} = 8.4 Hz), 127.8 (d), 129.3 (s), 131.2 (d), 135.9 (d), 148.7 (s), 150.9 (s), 156.4 (s), 156.4 (s), 159.2 (s), 202.1 (s) ppm; HRMS (ESI) calcd. for: $C_{17}H_{14}N_2O_3F$: 313.0983 $[M+H]^+$; found: 313.0984.

2-(5-fluoro-2-hydroxyphenyl)-4-(3-methylbutanoyl)quinazoline 1-oxide (7db)

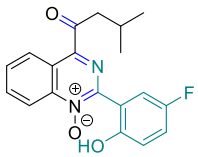

R_f = 0.4 (20% EtOAc in petroleum ether); yield: 49 mg (58%); yellow gummy solid; IR (neat)ν_{max} 2958, 1699, 1535, 1477, 1243, 754 cm^{-1}; ^1H NMR (400 MHz, $CDCl_3$): δ1.07 (s, 3H), 1.08 (s, 3H), 2.33–2.43 (m, 1H), 3.23 (d, J = 6.9 Hz, 2H), 7.12 (dd, J = 4.9, 9.0 Hz, 1H), 7.31 (ddd, J = 3.1, 7.6, 9.1 Hz, 1H), 7.77 (dd, J = 3.1, 9.6 Hz, 1H), 7.90 (ddd, J = 1.2, 7.1, 8.5 Hz, 1H), 8.12 (ddd, J = 1.3, 7.1, 8.7 Hz, 1H), 8.81–8.90

(m, 1H), 9.01 (dt, J = 0.6, 8.5, Hz, 1H), 10.14 (s, 1H) ppm; ^{13}C NMR (100 MHz, $CDCl_3$): δ 22.7 (q, 2C), 25.1 (d), 48.4 (t), 117.6 (dd, J_{C-F} = 25.2 Hz), 119.3 (d), 121.0 (dd, J_{C-F} = 23.6 Hz), 121.3 (s), 121.7 (dd, J_{C-F} = 7.6 Hz), 127.7 (d), 131.1 (d), 135.9 (d), 144.6 (s), 149.2 (s), 150.8 (ds, J_{C-F} = 3.0 Hz), 155.1 (s), 156.4 (ds, J_{C-F} = 1.5 Hz), 157.5 (s), 201.4 (s) ppm; HRMS (ESI) calcd. for: $C_{19}H_{18}N_2O_3F$: 341.1296 $[M+H]^+$; found: 341.1300.

2-(5-fluoro-2-hydroxyphenyl)-4-(3-phenylpropanoyl)quinazoline 1-oxide (7eb)

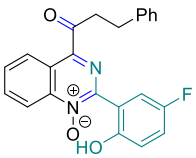

R_f = 0.4 (20% EtOAc in petroleum ether); yield: 43 mg (56%); yellow solid; IR (neat)ν_{max} 3016, 2958, 1699, 1601, 1532, 1488, 1318, 1251, 757, 698 cm^{-1}; ^{1}H NMR (400 MHz, $CDCl_3$): δ 3.17 (t, J = 7.4 Hz, 2H), 3.71 (t, J = 7.4 Hz, 2H), 7.11 (dd, J = 4.8, 9.1 Hz, 1H), 7.15–7.20 (m, 1H), 7.27–7.34 (m, 5H), 7.72 (dd, J = 3.1, 9.6 Hz, 1H), 7.89 (ddd, J = 1.2, 7.1, 8.5 Hz, 1H), 8.11 (ddd, J = 1.3, 7.1, 8.7 Hz, 1H), 8.84 (d, J = 8.4 Hz, 1H), 9.01 (dd, J = 0.7, 8.6 Hz, 1H), 10.05 (s, 1H) ppm; ^{13}C NMR (100 MHz, $CDCl_3$): δ 30.1 (t), 41.3 (t), 117.6 (dd, J_{C-F} = 25.2 Hz), 119.2 (d), 121.0 (dd, J_{C-F} = 23.6 Hz), 121.3 (s), 121.7 (dd, J_{C-F} = 7.6 Hz), 126.3 (d), 127.7 (d), 128.5 (d, 2C), 128.6 (d, 2C), 131.2 (d), 135.9 (d), 140.4 (s), 144.6 (s), 148.5 (s), 150.8 (s), 155.1 (s), 156.3 (ds, J_{C-F} = 1.5 Hz), 157.5 (s), 200.6 (s) ppm; HRMS (ESI) calcd. for: $C_{23}H_{18}N_2O_3F$: 389.1296 $[M+H]^+$; found: 389.1300.

4-butyryl-2-(5-fluoro-2-hydroxyphenyl)-7-(methoxycarbonyl)quinazoline 1-oxide (7nb)

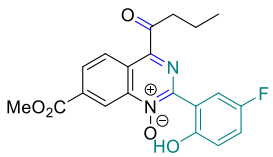

R_f = 0.4 (20% EtOAc in petroleum ether); yield: 54 mg (69%); orange gummy solid; IR (neat) ν_{max} 2959, 1721, 1528, 1235, 1125, 748 cm^{-1}; ^{1}H NMR (400 MHz, $CDCl_3$): δ 1.09 (t, J = 7.4 Hz, 3H), 1.82–1.90 (m, 2H), 3.35 (t, J = 7.2 Hz, 2H), 4.08 (s, 3H), 7.11 (dd, J = 4.8, 9.1 Hz, 1H), 7.31 (ddd, J = 3.1, 7.5, 9.1 Hz, 1H), 7.73–7.79 (m, 1H), 8.44 (dd, J = 1.7, 8.8 Hz, 1H), 9.08–9.17 (m, 1H), 9.40–9.47 (m, 1H), 9.78 (s, 1H) ppm; ^{13}C NMR (100 MHz, $CDCl_3$): δ 13.8 (q), 17.3 (t), 41.5 (t), 53.2 (q), 117.6 (dd, J_{C-F} = 25.2 Hz), 120.4 (s), 121.1 (d), 121.3 (dd, J_{C-F} = 23.6 Hz), 121.8 (dd, J_{C-F} = 8.4 Hz), 123.1 (s), 128.4 (d), 130.7 (d), 136.4 (s), 144.7 (s), 148.2 (s),155.2 (s) 156.4 (ds, J_{C-F} = 1.5 Hz), 157.6 (s), 164.9 (s), 201.3 (s) ppm; HRMS (ESI) calcd. for: $C_{20}H_{18}N_2O_5F$: 385.1194 $[M+H]^+$; found: 385.1196.

2-(5-chloro-2-hydroxyphenyl)-4-(3-phenylpropanoyl)quinazoline 1-oxide (7ac)

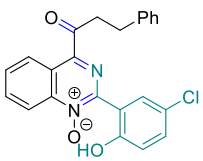

R_f = 0.4 (20% EtOAc in petroleum ether); yield: 59 mg (63%); dark yellow solid; IR (neat)ν_{max} 2932, 1706, 1603, 1532, 1469, 1321, 763 cm^{-1}; ^1H NMR (400 MHz, $CDCl_3$): δ1.31 (t, J = 7.1 Hz, 3H), 3.42 (q, J = 7.1 Hz, 2H), 7.11 (d, J = 8.9 Hz, 1H), 7.51 (dd, J = 2.6, 8.9 Hz, 1H), 7.86–7.96 (m, 1H), 8.05 (d, J = 2.6 Hz, 1H), 8.12 (ddd, J = 1.2, 7.2, 8.6 Hz, 1H), 8.85 (d, J = 8.8 Hz, 1H), 9.01–9.11 (m, 1H), 10.42 (s, 1H) ppm; ^{13}C NMR (100 MHz, $CDCl_3$): δ 7.7 (q), 33.3 (t), 119.3 (d), 121.3 (s), 121.5 (s), 122.0 (d), 125.0 (s), 127.7 (d), 131.2 (d), 131.8 (d), 133.6 (d), 135.9 (d), 144.6 (s), 149.0 (s), 150.8 (s), 158.9 (s), 202.1 (s) ppm; HRMS (ESI) calcd. for: $C_{17}H_{14}N_2O_3Cl$: 329.0687 $[M+H]^+$; found: 329.0691.

2-(5-chloro-2-hydroxyphenyl)-4-(3-methylbutanoyl)quinazoline 1-oxide (7dc)

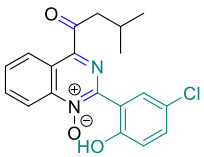

R_f = 0.4 (20% EtOAc in petroleum ether); yield: 48 mg (55%); yellow gummy solid; IR (neat) ν_{max} 2951, 1698, 1535, 1467, 1285, 754 cm^{-1}; ^1H NMR (400 MHz, $CDCl_3$): δ 1.08 (s, 3H), 1.09 (s, 3H), 2.38 (dt, J = 6.7, 13.4 Hz, 1H), 3.22 (d, J = 6.9 Hz, 2H), 7.10 (d, J = 8.9 Hz, 1H), 7.51 (dd, J = 2.6, 8.9 Hz, 1H), 7.90 (ddd, J = 1.2, 7.1, 8.4 Hz, 1H), 8.04 (d, J = 2.6 Hz, 1H), 8.12 (ddd, J = 1.3, 7.1, 8.7 Hz, 1H), 8.81–8.88 (m, 1H), 9.00 (dt, J = 0.6, 8.5 Hz, 1H), 10.43 (s, 1H) ppm; ^{13}C NMR (100 MHz, $CDCl_3$): δ 22.7 (q, 2C), 25.3 (d), 48.5 (t), 119.3 (d), 121.3 (s), 121.5 (s), 122.0 (d), 125.0 (s), 127.7 (d), 131.2 (d), 131.9 (d), 133.6 (d), 135.9 (d), 144.6 (s), 149.3 (s), 150.7 (s), 158.9 (s), 201.5 (s) ppm; HRMS (ESI) calcd. for: $C_{19}H_{18}N_2O_3Cl$: 357.1000 $[M+H]^+$; found: 357.1007.

2-(5-chloro-2-hydroxyphenyl)-4-(3-phenylpropanoyl)quinazoline 1-oxide (7ec)

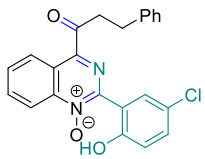

R_f = 0.4 (20% EtOAc in petroleum ether); yield: 47 mg (58%); dark yellow solid; IR (neat)ν_{max} 3018, 2925, 2859, 1703, 1606, 1318, 1251, 740, 689 cm^{-1}; ^1H NMR (400 MHz, $CDCl_3$):δ 3.18 (t, J = 7.4 Hz, 2H), 3.70 (t, J = 7.4 Hz, 2H), 7.10 (d, J = 8.9 Hz, 1H), 7.19–7.23 (m, 1H), 7.30 (d, J = 4.4 Hz, 4H), 7.51 (dd, J = 2.6, 8.8 Hz, 1H), 7.89 (ddd, J = 1.2, 7.1, 8.5 Hz, 1H), 8.02 (d, J = 2.6 Hz, 1H), 8.11 (ddd, J = 1.3 ,7.1, 8.7 Hz, 1H), 8.80–8.86 (m, 1H), 8.99 (dt, J = 0.6, 8.5 Hz, 1H), 10.33 (s, 1H) ppm; ^{13}C NMR (100 MHz, $CDCl_3$): δ 30.3 (t), 41.3 (t), 119.2 (d), 121.3 (s), 121.4 (s), 122.0 (d), 125.0 (s), 126.3 (d), 127.7 (d), 128.5 (d, 2C), 128.6 (d, 2C), 131.2 (d), 131.8(d), 133.6 (d), 135.9 (d), 140.4 (s), 144.6

(s), 148.7 (s), 150.8 (s), 158.9 (s), 200.7 (s) ppm; HRMS (ESI) calcd. for: $C_{23}H_{18}N_2O_3Cl$: 405.1000 $[M+H]^+$; found: 405.1005.

4-butyryl-2-(5-chloro-2-hydroxyphenyl)-7-methylquinazoline 1-oxide (7lc)

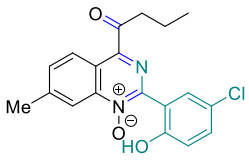

R_f = 0.4 (20% EtOAc in petroleum ether); yield: 52 mg (59%); yellow gummy solid; IR (neat)ν_{max} 2124, 1704, 1367, 1163, 742, 660 cm^{-1}; ^1H NMR (400 MHz, $CDCl_3$): δ 1.09 (t, J = 7.4 Hz, 3H), 1.81–1.91 (m, 2H), 2.72 (s, 3H), 3.33 (t, J = 7.2 Hz, 2H), 7.10 (d, J = 8.9 Hz, 1H), 7.50 (dd, J = 2.6, 8.9 Hz, 1H), 7.72 (dd, J = 1.4, 8.7 Hz, 1H), 8.05 (d, J = 2.6 Hz, 1H), 8.62–8.69 (m, 1H), 8.90 (d, J = 8.6 Hz, 1H), 10.58 (s, 1H) ppm; ^{13}C NMR (100 MHz, $CDCl_3$): δ 13.8 (q), 17.4 (t), 22.7 (q), 41.7 (t), 118.2 (d), 119.5 (s), 121.7 (s), 122.0 (d), 124.9 (s), 127.4 (d), 131.9 (d), 133.3 (d), 133.5 (d), 144.6 (s), 148.2 (s), 149.0 (s), 150.9 (s), 158.9 (s), 201.8 (s) ppm; HRMS (ESI) calcd. for: $C_{19}H_{18}N_2O_3Cl$: 357.1000 $[M+H]^+$; found: 357.1007.

2-(5-bromo-2-hydroxyphenyl)-4-propionylquinazoline 1-oxide (7ad)

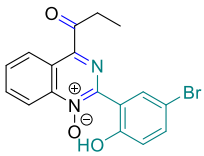

R_f = 0.4 (15% EtOAc in petroleum ether); yield: 60 mg (56%); orange solid; IR (neat)ν_{max} 2926, 2855, 1690, 1601, 1534, 1464, 1251, 1116, 759 cm^{-1}; ^1H NMR (400 MHz, $CDCl_3$): δ1.33 (t, J = 7.2 Hz, 3H), 3.42 (q, J = 7.2 Hz, 2H), 7.05 (d, J = 8.7 Hz, 1H), 7.64 (dd, J = 2.5, 8.9 Hz, 1H), 7.91 (ddd, J = 1.2, 7.1, 8.4 Hz, 1H), 8.12 (ddd, J = 1.3, 7.1, 8.6 Hz, 1H), 8.19 (d, J = 2.5 Hz, 1H), 8.83–8.87 (m, 1H), 9.04 (dd, J = 0.7, 8.6 Hz, 1H), 10.46 (s, 1H) ppm; ^{13}C NMR (125 MHz, $CDCl_3$): δ7.7 (q), 33.3 (t), 112.0 (s), 119.2 (d), 121.3 (s), 122.0 (s), 122.4 (d), 127.7 (d), 131.2 (d), 134.8 (d), 135.9 (d), 136.4 (d), 144.6 (s), 149.1 (s), 150.7 (s), 159.4 (s), 202.0 (s) ppm; HRMS (ESI) calcd. for $C_{17}H_{14}BrN_2O_3$: 373.0182 $[M+H]^+$; found: 373.0185.

2-(5-bromo-2-hydroxyphenyl)-4-butyrylquinazoline 1-oxide (7bd)

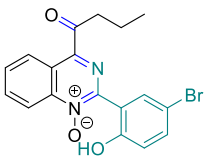

R_f = 0.5 (15% EtOAc in petroleum ether); yield: 63 mg (62%); dark yellow solid; IR (neat)ν_{max} 2925, 2866, 1699, 1600, 1531, 1466, 1323, 1246, 1155, 762 cm^{-1}; ^1H NMR (400 MHz, $CDCl_3$): δ1.10 (t, J = 7.4 Hz, 3H), 1.81–1.93 (m, 2H), 3.34 (t, J = 7.2 Hz, 2H), 7.06 (d, J = 8.9 Hz, 1H), 7.64 (dd, J = 2.5, 8.7 Hz, 1H), 7.91 (ddd, J = 1.2, 7.1, 8.5 Hz, 1H), 8.12 (ddd, J = 1.3, 7.1, 8.7 Hz, 1H), 8.20 (d, J = 2.5 Hz, 1H), 8.82–8.89 (m, 1H), 8.99–9.05 (m, 1H), 10.46 (s, 1H) ppm; ^{13}C NMR (100 MHz, $CDCl_3$): δ13.8

(q), 17.5 (t), 41.7 (t), 112.0 (s) 119.3 (d), 121.3 (s), 122.0 (s), 122.4 (d), 127.7 (d), 131.2 (d), 134.9 (d), 135.9 (d), 136.4 (d), 144.6 (s), 149.2 (s), 150.7 (s), 159.4 (s), 201.6 (s) ppm; HRMS (ESI) calcd. for $C_{18}H_{16}BrN_2O_3$: 387.0339 $[M+H]^+$; found: 387.0344.

2-(5-bromo-2-hydroxyphenyl)-4-hexanoylquinazoline 1-oxide (7cd)

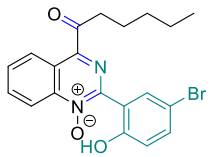

R_f = 0.4 (15% EtOAc in petroleum ether); yield: 53 mg (56%); dark yellow solid; IR (neat)ν_{max} 2927, 2862, 1694, 1600, 1530, 1469, 1251, 1079, 1022, 761 cm^{-1}; ^1H NMR (400 MHz, $CDCl_3$): δ0.93–0.98 (m, 3H), 1.40–1.50 (m, 4H), 1.84 (t, *J* = 7.4 Hz, 2H), 3.35 (t, *J* = 7.4 Hz, 2H), 7.06 (d, *J* = 8.9 Hz, 1H), 7.64 (dd, *J* = 2.5, 8.7 Hz, 1H), 7.91 (ddd, *J* = 1.1, 7.1, 8.4 Hz, 1H), 8.12 (ddd, *J* = 1.1, 7.1, 8.7 Hz, 1H), 8.20 (d, *J* = 2.5 Hz, 1H), 8.82–8.88 (m, 1H), 9.02 (dd, *J* = 0.7, 8.6 Hz, 1H), 10.47 (s, 1H) ppm; ^{13}C NMR (100 MHz, $CDCl_3$): δ13.9 (q), 22.5 (t), 23.9 (t), 31.4 (t), 39.9 (t), 112.0 (s), 119.3 (d), 121.3 (s), 122.0 (s), 122.4 (d), 127.7 (d), 131.2 (d), 134.9 (d), 135.9 (d), 136.4 (d), 144.6 (s), 149.2 (s), 150.7 (s), 159.4 (s), 201.8 (s) ppm; HRMS (ESI) calcd. for $C_{20}H_{20}BrN_2O_3$: 415.0652 $[M+H]^+$; found: 415.0654.

2-(5-bromo-2-hydroxyphenyl)-4-(3-methylbutanoyl)quinazoline 1-oxide (7dd)

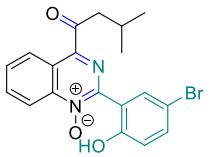

R_f = 0.4 (15% EtOAc in petroleum ether); yield: 55 mg (56%); orange solid; IR (neat)ν_{max} 2958, 2874, 1696, 1599, 1531, 1469, 1373, 1324, 1284, 1244, 1161, 762 cm^{-1}; ^1H NMR (500 MHz, $CDCl_3$): δ1.08 (s, 3H), 1.10 (s, 3H), 2.38 (dt, *J* = 6.6, 13.5 Hz, 1H), 3.22 (d, *J* = 6.9 Hz, 2H), 7.05 (d, *J* = 9.1 Hz, 1H), 7.64 (dd, *J* = 2.7, 8.8 Hz, 1H), 7.88–7.94 (m, 1H), 8.09–8.16 (m, 1H), 8.19 (d, *J* = 3.05 Hz, 1H), 8.85 (d, *J* = 8.4 Hz, 1H), 9.01 (d, *J* = 7.6 Hz, 1H), 10.48 (s, 1H) ppm; ^{13}C NMR (125 MHz, $CDCl_3$): δ22.7 (t, 2C), 25.4 (s), 48.6 (t), 112.0 (s), 119.3 (d), 121.3 (s), 122.0 (s), 122.4 (d), 127.7 (d), 131.2 (d), 134.9 (d), 135.9 (d), 136.4 (d), 144.6 (s), 149.4 (s), 150.6 (s), 159.4 (s), 201.5 (s) ppm; HRMS (ESI) calcd. for $C_{19}H_{18}BrN_2O_3$: 401.0495 $[M+H]^+$; found: 401.0497.

2-(5-bromo-2-hydroxyphenyl)-4-(3-phenylpropanoyl)quinazoline 1-oxide (7ed)

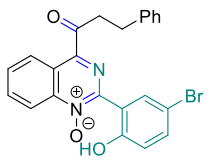

R_f = 0.4 (20% EtOAc in petroleum ether); yield: 44 mg (47%); pale yellow solid; IR (neat)ν_{max} 3016, 2916, 2859, 1699, 1599, 1531, 1467, 1369, 1283, 1152, 758, 698 cm^{-1}; ^1H NMR (400 MHz, $CDCl_3$): δ3.18 (t, *J* = 7.4 Hz, 2H), 3.70 (t, *J* = 7.4 Hz, 2H), 7.05 (d, *J* = 8.7 Hz, 1H), 7.19–7.24 (m, 1H), 7.31 (d, *J* = 4.4 Hz, 4H),

7.64 (dd, *J* = 2.5, 8.9 Hz, 1H), 7.89 (ddd, *J* = 1.2, 7.1, 8.4 Hz, 1H), 8.11 (ddd, *J* = 1.3, 7.1, 8.7 Hz, 1H), 8.17 (d, *J* = 2.4 Hz, 1H), 8.81–8.87 (m, 1H), 8.99 (dd, *J* = 0.7, 8.6 Hz, 1H), 10.38 (s, 1H) ppm; ^{13}C NMR (100 MHz, $CDCl_3$): δ30.3 (t), 41.3 (t), 112.0 (s), 119.2 (d), 121.3 (s), 122.0 (s), 122.4 (d), 126.4 (d), 127.7 (d), 128.5 (d, 2C), 128.6 (d, 2C), 131.2 (d), 134.8 (d), 136.0 (d), 136.4 (d), 140.3 (s), 144.6 (s), 148.7 (s), 150.7 (s), 159.4 (s), 200.7 (s) ppm; HRMS (ESI) calcd. for $C_{23}H_{18}BrN_2O_3$: 449.0495 $[M+H]^+$; found: 449.0504.

2-(5-bromo-2-hydroxyphenyl)-4-butyryl-7-methylquinazoline 1-oxide (7ld)

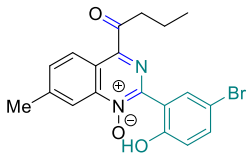

R$_f$ = 0.4 (15% EtOAc in petroleum ether); yield: 52 mg (53%); orange solid; IR (neat)ν_{max} 2962, 2928, 2874, 1701, 1596, 1532, 1468, 1288, 1167, 823, 754 cm^{-1}; ^{1}H NMR (400 MHz, $CDCl_3$): δ1.06–1.12 (m, 3H), 1.82–1.91 (m, 2H), 2.72 (s, 3H), 3.30–3.37 (m, 2H), 7.01–7.08 (m, 1H), 7.60–7.66 (m, H), 7.72 (d, *J* = 8.7 Hz, 1 H), 8.17–8.22 (m, 1H), 8.65 (br. s., 1H), 8.83–8.95 (m, 1H), 10.62 (s, 1H) ppm; ^{13}C NMR (100 MHz, $CDCl_3$):δ13.8 (q), 17.5 (t), 22.7 (q), 41.7 (t), 111.9 (s), 118.3 (d), 119.6 (s), 122.2 (s), 122.4 (d), 127.4 (s), 133.3 (d), 134.9 (d), 136.3 (d), 144.6 (s), 148.3 (s), 149.0 (s), 150.8 (s), 159.4 (s), 201.8 (s) ppm; HRMS (ESI) calcd. for $C_{19}H_{18}N_2O_3Br$: 401.0495 $[M+H]^+$; found: 401.0494.

2-(5-bromo-2-hydroxyphenyl)-4-butyryl-7-(methoxycarbonyl)quinazoline 1-oxide (7nd)

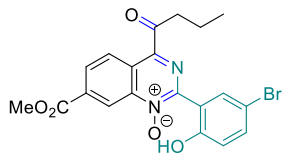

R$_f$ = 0.4 (20% EtOAc in petroleum ether); yield: 55 mg (61%); orange gummy solid; IR (neat)ν_{max} 2959, 2680, 1723, 1567, 1435, 1235, 1132, 815, 755 cm^{-1}; ^{1}H NMR (400 MHz, $CDCl_3$): δ1.10 (t, *J* = 7.38 Hz, 3H), 1.82–1.94 (m, 2H), 3.35 (t, *J* = 7.2 Hz, 2H), 4.08 (s, 3H), 7.07 (d, *J* = 8.9 Hz, 1H), 7.66 (dd, *J* = 2.5, 8.7 Hz, 1H), 8.19 (d, *J* = 2.5 Hz, 1H), 8.44–8.49 (m, 1H), 9.09–9.16 (m, 1H), 9.45 (d, *J* = 1.1 Hz, 1H), 10.11 (s, 1H) ppm; ^{13}C NMR (100 MHz, $CDCl_3$): δ13.8 (q), 17.5 (t), 41.6 (t), 53.2 (q),112.2 (d), 121.1 (d), 121.7 (s), 122.5 (d), 123.2 (s), 128.4 (d), 130.8 (d), 134.8 (d), 136.5 (s), 136.7 (d), 144.6 (s), 148.5 (s), 151.3 (s), 159.4 (s), 164.9 (s), 201.3 (s) ppm; HRMS (ESI) calcd. for $C_{20}H_{18}BrN_2O_5$: 445.0394 $[M+H]^+$; found: 445.0399.

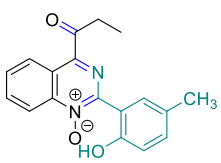

2-(2-hydroxy-5-methylphenyl)-4-propionylquinazoline 1-oxide (7ae)

R$_f$ = 0.4 (20% EtOAc in petroleum ether); yield: 55 mg (62%); dark yellow gummy solid; IR (neat)ν_{max} 2931, 1701, 1530, 1481, 1248, 823, 755 cm^{-1}; ^{1}H

NMR (400 MHz, $CDCl_3$): δ1.32 (t, J = 7.2 Hz, 3H), 2.44 (s, 3H), 3.42 (q, J = 7.2 Hz, 2H), 7.07 (d, J = 8.4 Hz, 1H), 7.39 (dd, J = 2.2, 8.4 Hz, 1H), 7.81–7.91 (m, 2H), 8.09 (ddd, J = 1.3, 7.1, 8.7 Hz, 1H), 8.81–8.90 (m, 1H), 8.98–9.06 (m, 1H), 10.13 (s, 1H) ppm; ^{13}C NMR (100 MHz, $CDCl_3$): δ7.8 (q), 20.7 (q), 33.2 (t), 119.3 (d), 120.0 (s), 120.3 (d), 121.1 (s), 127.6 (d), 129.3 (s), 130.7 (d), 132.6 (d), 134.8 (d), 135.6 (d), 144.6 (s), 148.6 (s), 152.1 (s), 158.1 (s), 202.3 (s) ppm; HRMS (ESI) calcd. for: $C_{18}H_{17}N_2O_3$: 309.1234 $[M+H]^+$; found: 309.1238.

2-(2-hydroxy-5-methylphenyl)-4-(3-methylbutanoyl)quinazoline 1-oxide (7de)

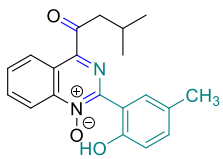

R_f = 0.4 (20% EtOAc in petroleum ether); yield: 50 mg (60%); yellow gummy solid; IR (neat) ν_{max} 2957, 1695, 1531, 1479, 1161, 1067, 751 cm^{-1}; ^{1}H NMR (400 MHz, $CDCl_3$): δ 1.07 (s, 3H), 1.09 (s, 3 H), 2.39 (dt, J = 13.5, 6.8 Hz, 1H), 2.44 (s, 3H), 3.23 (d, J = 6.9 Hz, 2H), 7.08 (d, J = 8.4 Hz, 1H), 7.37–7.42 (m, 1H), 7.84–7.90 (m, 2H), 8.06–8.15 (m, 1H), 8.81–8.92 (m, 1H), 9.00 (dd, J = 0.8, 8.5 Hz, 1H), 10.15 (s, 1H) ppm; ^{13}C NMR (100 MHz, $CDCl_3$): δ 20.7 (d), 22.8 (q, 2C), 25.4 (q), 48.6 (t), 119.3 (d), 120.0 (s), 120.3 (d), 121.2 (s), 127.5 (d), 129.3 (s), 130.7 (d), 132.6 (d), 134.8 (d), 135.6 (d), 144.6 (s), 149.0 (s), 152.1 (s), 158.1 (s), 201.7 (s) ppm; HRMS (ESI) calcd. for: $C_{20}H_{21}N_2O_3$: 337.1547 $[M+H]^+$; found: 337.1548.

General procedure for N-O bond reduction

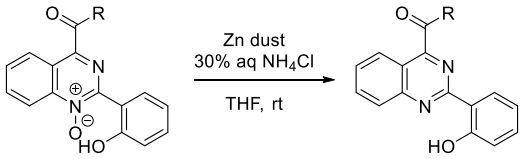

7 **13**

To a stirred solution of **7** in THF at room temperature, Zn dust (2 equiv.) was added followed by 30% aq NH_4Cl solution. The reaction mixture was stirred till the disappearance of the starting material shown by TLC (i.e. 2 h). Then usual workup followed by purification by column chromatography afforded compound **13**.

1-(2-(2-hydroxyphenyl)quinazolin-4-yl)butan-1-one (13a)

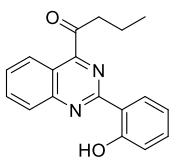

R_f = 0.5 (10% EtOAc in petroleum ether); yield: 41 mg (86%); dark yellow solid; IR (neat)ν_{max} 1703, 1547, 1471, 1254, 760 cm^{-1}; ^{1}H NMR (400 MHz, $CDCl_3$): δ

1.11 (t, *J* = 7.4 Hz, 3H), 1.83–1.95 (m, 2H), 3.37 (t, *J* = 7.2 Hz, 2H), 7.04 (ddd, *J* = 1.2, 7.1, 8.1 Hz, 1H), 7.11 (dd, *J* =0.9, 8.2 Hz, 1H), 7.46 (ddd, *J* = 1.8, 7.0, 8.4 Hz, 1H), 7.68 (ddd, *J* = 1.2, 6.9, 8.4 Hz, 1H), 7.96 (ddd, *J* = 1.4, 6.9, 8.4 Hz, 1H), 8.05 (dq, *J* = 0.6, 8.5 Hz, 1H), 8.59–8.72 (m, 2H), 13.50 (s, 1H) ppm; ^{13}C NMR (100 MHz, $CDCl_3$): δ 13.8 (q), 17.3 (t), 42.1 (t), 117.9 (d), 118.8 (s), 119.0 (s), 119.2 (d), 126.7 (d), 127.3 (d), 128.8 (d), 129.6 (d), 133.5 (d), 135.0 (d), 149.9 (s), 160.3 (s), 160.7 (s), 160.9 (s), 203.5 (s) ppm; HRMS (ESI) calcd. for: $C_{18}H_{17}N_2O_2$: 293.1290 $[M+H]^+$; found: 293.1292.

1-(2-(5-fluoro-2-hydroxyphenyl)quinazolin-4-yl)-3-methylbutan-1-one (13b)

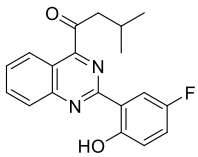

R_f = 0.5 (10% EtOAc in petroleum ether); yield: 33 mg (69%); dark yellow gummy solid; IR (neat)ν_{max} 1707, 1547, 1475, 1248, 760 cm^{-1}; ^{1}H NMR (400 MHz, $CDCl_3$): δ 1.10 (s, 3H), 1.11 (s, 3H), 2.40 (dt, *J* = 6.7, 13.4 Hz, 1H), 3.25 (d, *J* = 6.9 Hz, 2H), 7.05 (dd, *J* = 4.7, 9.0 Hz, 1H), 7.17 (ddd, *J* = 3.2, 7.7, 9.0 Hz, 1H), 7.71 (ddd, *J* = 1.2, 6.9, 8.4 Hz, 1H), 7.98 (ddd, *J* = 1.4, 6.9, 8.4 Hz, 1H), 8.03–8.09 (m, 1H), 8.30 (dd, *J* = 3.2, 9.8 Hz, 1H), 8.62–8.68 (m, 1H), 13.23 (s, 1H) ppm; ^{13}C NMR (100 MHz, $CDCl_3$): δ 22.8 (q, 2C), 24.9 (d), 49.0 (t), 114.7 (dd, J_{C-F} = 25.2 Hz), 118.9 (dd, J_{C-F} = 7.6 Hz), 119.0 (ds, J_{C-F} = 7.6 Hz), 119.1 (s), 120.5 (dd, J_{C-F} = 23.6 Hz), 126.7 (d), 127.4 (d), 129.2 (d), 135.2 (d), 149.8 (s), 154.6 (s), 156.9 (ds, J_{C-F} = 1.5 Hz), 159.8 (ds, J_{C-F} = 3.0 Hz), 160.7 (s), 203.1 (s) ppm; HRMS (ESI) calcd. for: $C_{19}H_{18}N_2O_2F$: 325.1352 $[M+H]^+$; found: 325.1345.

1-(2-(5-chloro-2-hydroxyphenyl)quinazolin-4-yl)-3-methylbutan-1-one (13c)

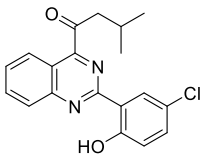

R_f = 0.5 (10% EtOAc in petroleum ether); yield: 36 mg (75%); yellow gummy solid; IR (neat)ν_{max} 1703, 1536, 1462, 1212, 819, 759 cm^{-1}; ^{1}H NMR (400 MHz, $CDCl_3$): δ 1.10 (s, 3H), 1.12 (s, 3H), 2.41 (dt, *J* = 6.7, 13.5 Hz, 1H), 3.24 (d, *J* = 6.9 Hz, 2H), 7.05 (d, *J* = 8.7 Hz, 1H), 7.38 (dd, *J* = 2.7, 8.8 Hz, 1H), 7.68–7.75 (m, 1H), 7.99 (dd, *J* = 1.4, 6.9 Hz, 1H), 8.02–8.08 (m, 1H), 8.58 (d, *J* = 2.7 Hz, 1H), 8.64 (dt, *J* = 0.6, 8.5 Hz, 1H), 13.45 (s, 1H) ppm; ^{13}C NMR (100 MHz, $CDCl_3$): δ 22.8 (q, 2C), 25.0 (d), 49.0 (t), 119.2 (s), 119.5 (d), 119.7 (s), 124.0 (s), 126.7 (d), 127.4 (d), 128.9 (d), 129.2 (d), 133.3 (d), 135.3 (d), 149.8 (s), 159.4 (s), 159.6 (s), 160.9 (s), 203.1 (s) ppm; HRMS (ESI) calcd. for: $C_{19}H_{18}N_2O_2Cl$: 341.1057 $[M+H]^+$; found: 341.1050.

1-(2-(5-methyl-2-hydroxyphenyl)quinazolin-4-yl)-3-methylbutan-1-one (13d)

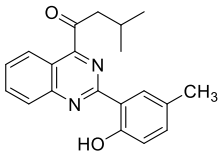

R_f = 0.5 (10% EtOAc in petroleum ether); yield: 37 mg (77%); yellow gummy solid; IR (neat)ν_{max} 1713, 1547, 1467, 1283, 810, 754 cm^{-1}; ^1H NMR (400 MHz, $CDCl_3$): δ 1.10 (s, 3H), 1.12 (s, 3H), 2.40–2.43 (m, 4H {methyl is merged}), 3.25 (d, J = 6.9 Hz, 2H), 7.01 (d, J = 8.4 Hz, 1H), 7.25–7.29 (m, 1H), 7.67 (ddd, J = 1.2, 7.0, 8.3 Hz, 1H), 7.96 (dd, J = 1.4, 6.9 Hz, 1H), 8.01–8.07 (m, 1H), 8.42 (d, J = 1.9 Hz, 1H), 8.62 (dt, J = 0.7, 8.5 Hz, 1H), 13.28 (s, 1H) ppm; ^{13}C NMR (100 MHz, $CDCl_3$): δ 20.8 (d), 22.8 (q, 2C), 25.1 (q), 49.1 (t), 117.8 (d), 118.3 (s), 118.9 (s), 126.6 (d), 127.4 (d), 128.2 (s), 128.7 (d), 129.4 (d), 134.5 (d), 135.0 (d), 150.0 (s), 158.7 (s), 160.6 (s), 160.7 (s), 203.4 (s) ppm; HRMS (ESI) calcd. for: $C_{20}H_{21}N_2O_2$: 321.1603 $[M+H]^+$; found: 321.1591.

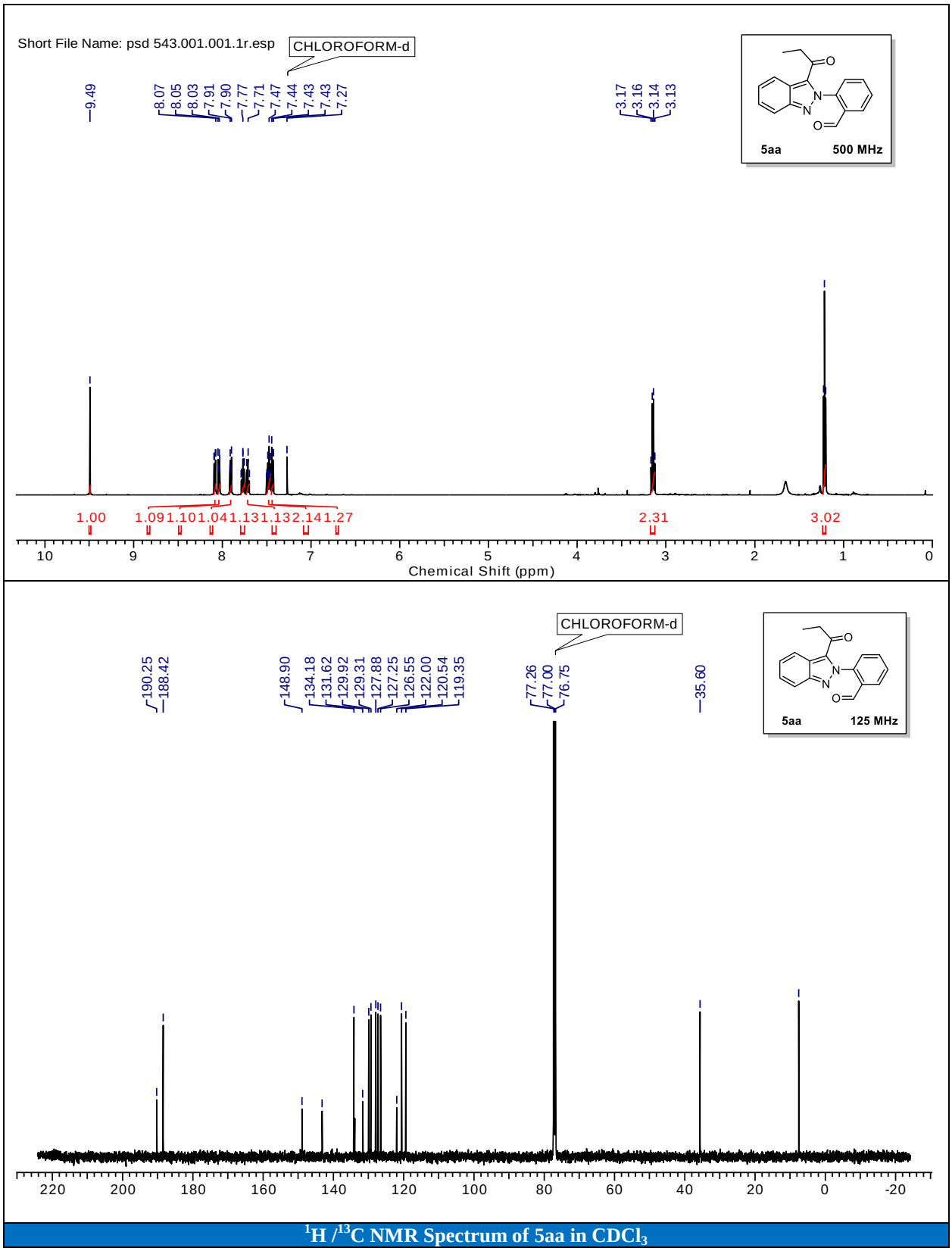

^{1}H /^{13}C NMR Spectrum of 5aa in $CDCl_3$

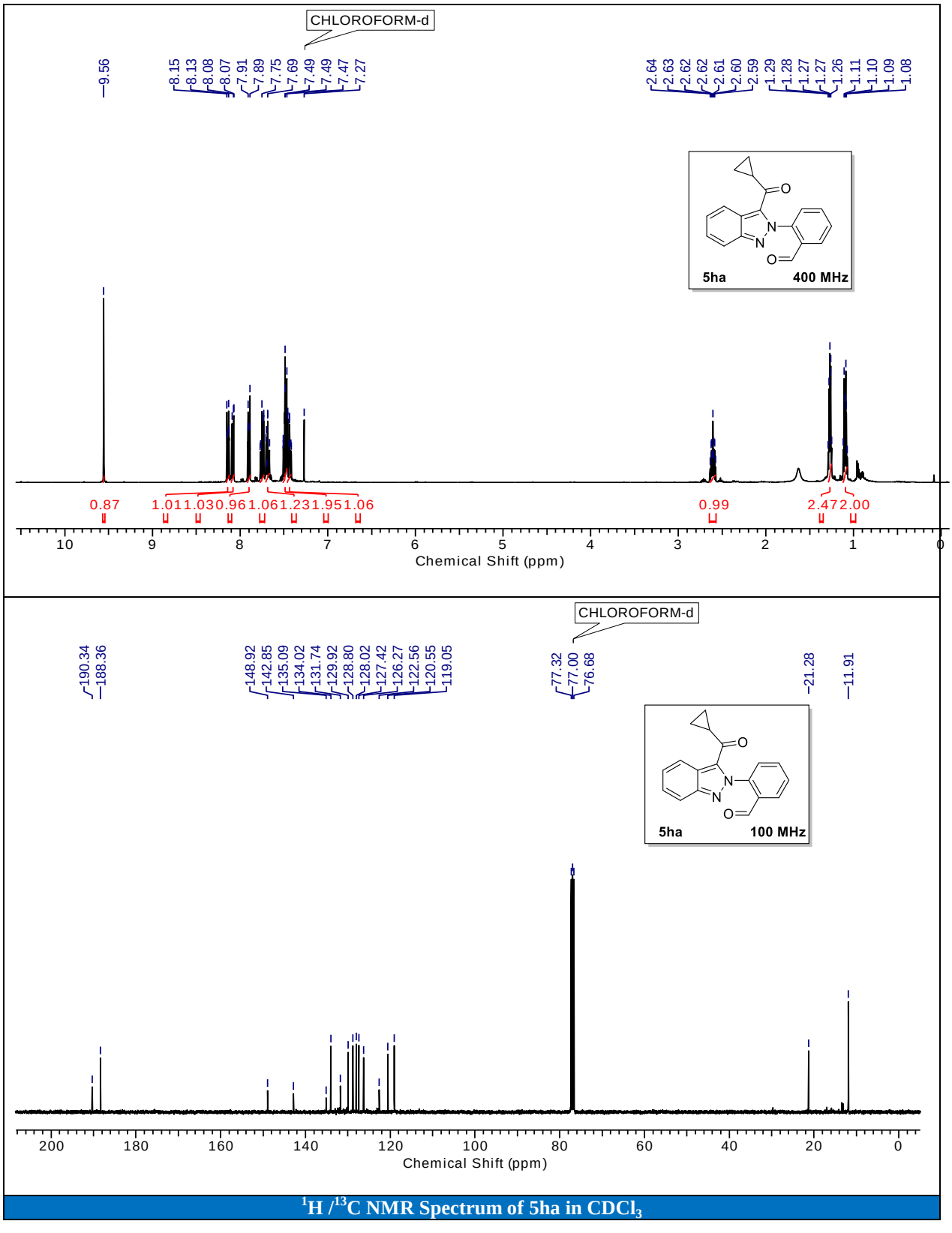

^{1}H /^{13}C NMR Spectrum of 5ha in $CDCl_3$

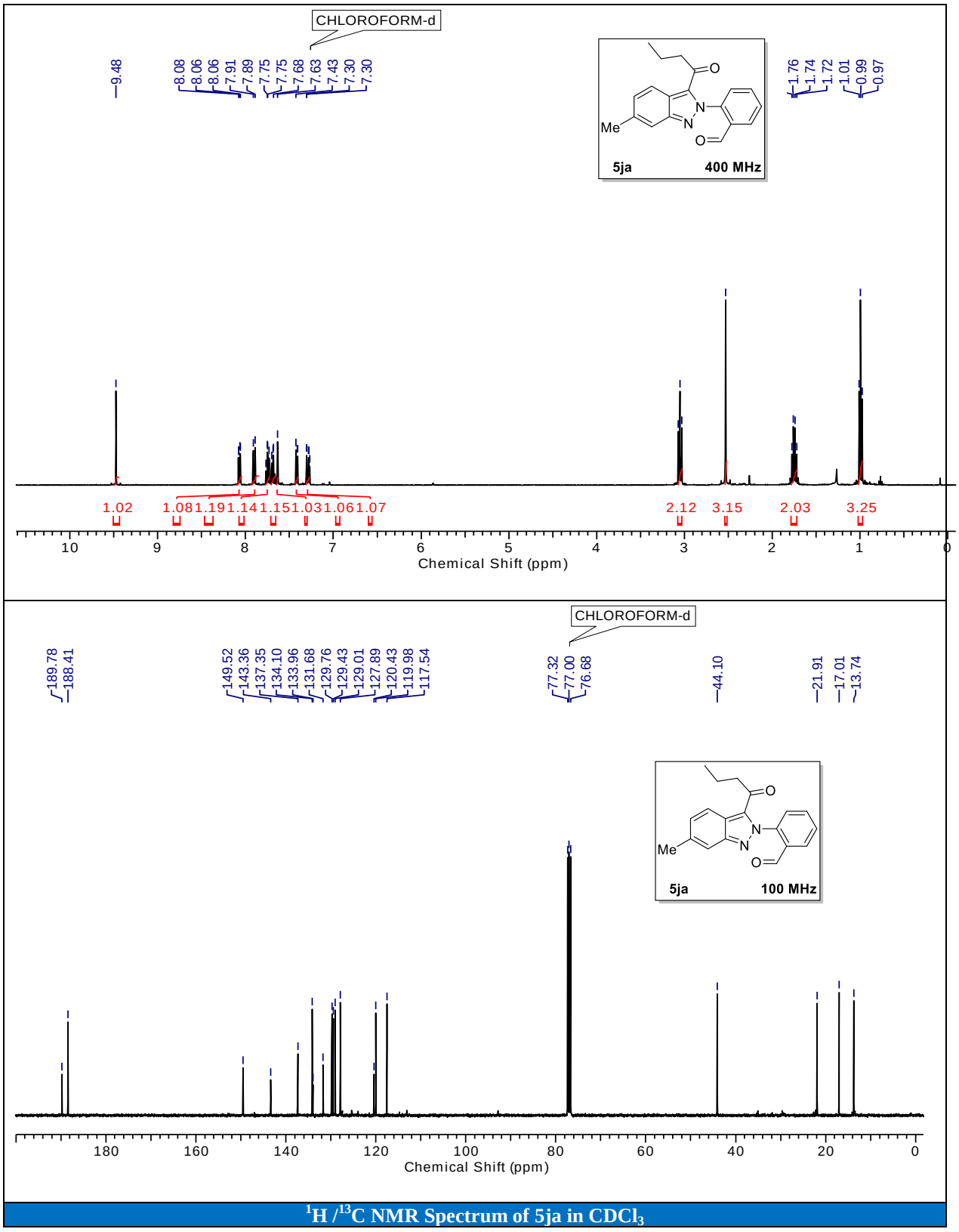

^{1}H /^{13}C NMR Spectrum of 5ja in $CDCl_3$

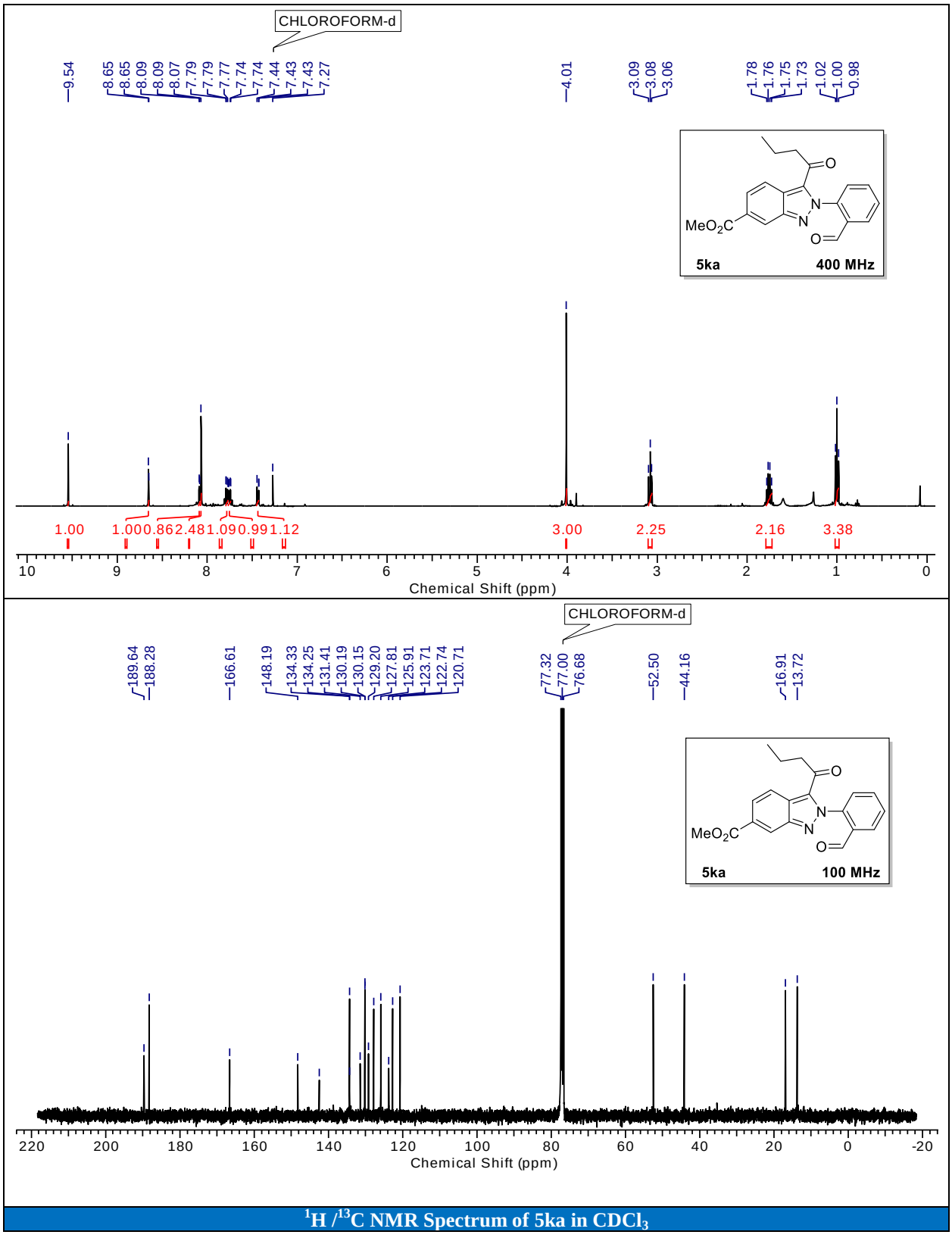

^{1}H /^{13}C NMR Spectrum of 5ka in $CDCl_3$

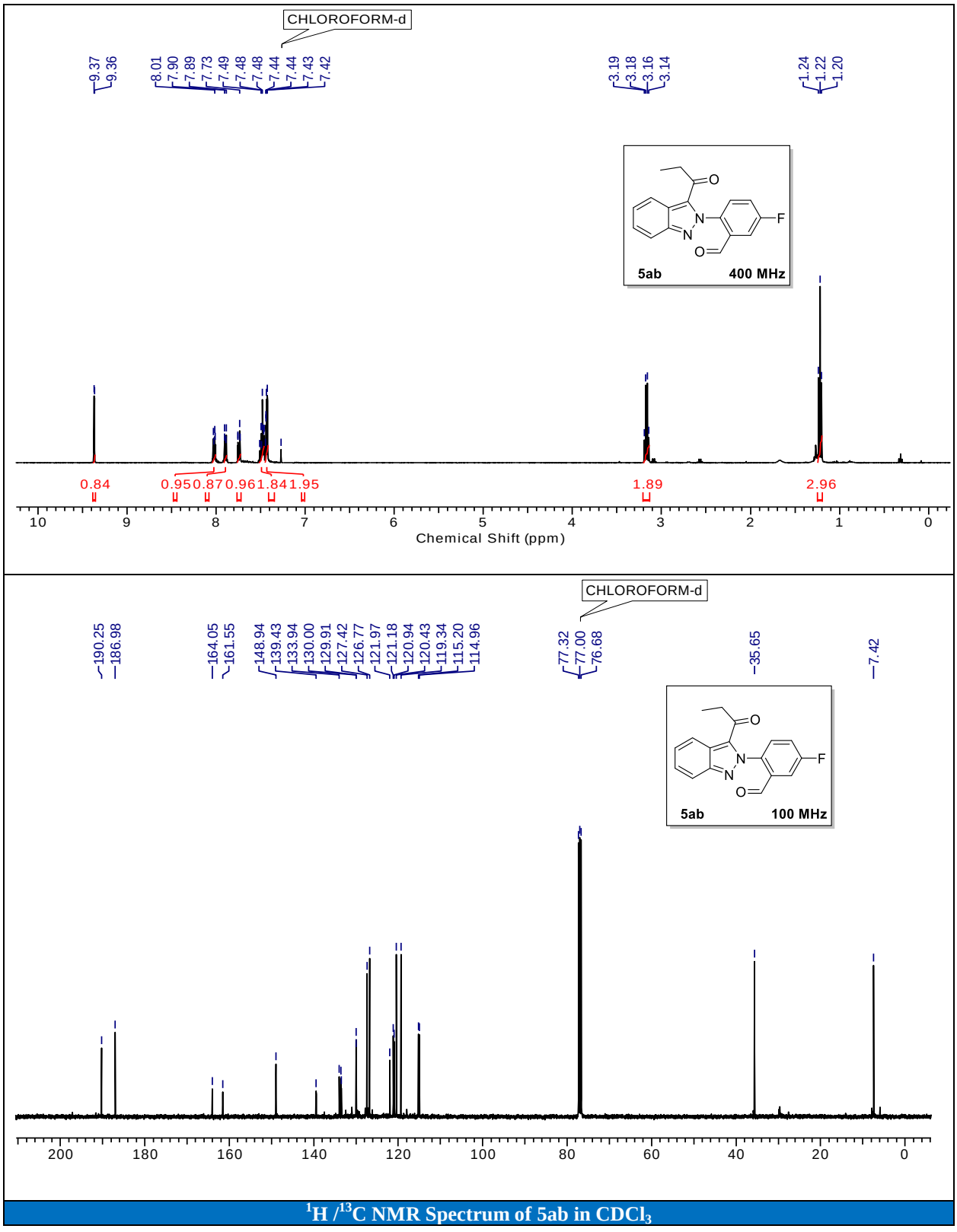

^{1}H /^{13}C NMR Spectrum of 5ab in $CDCl_3$

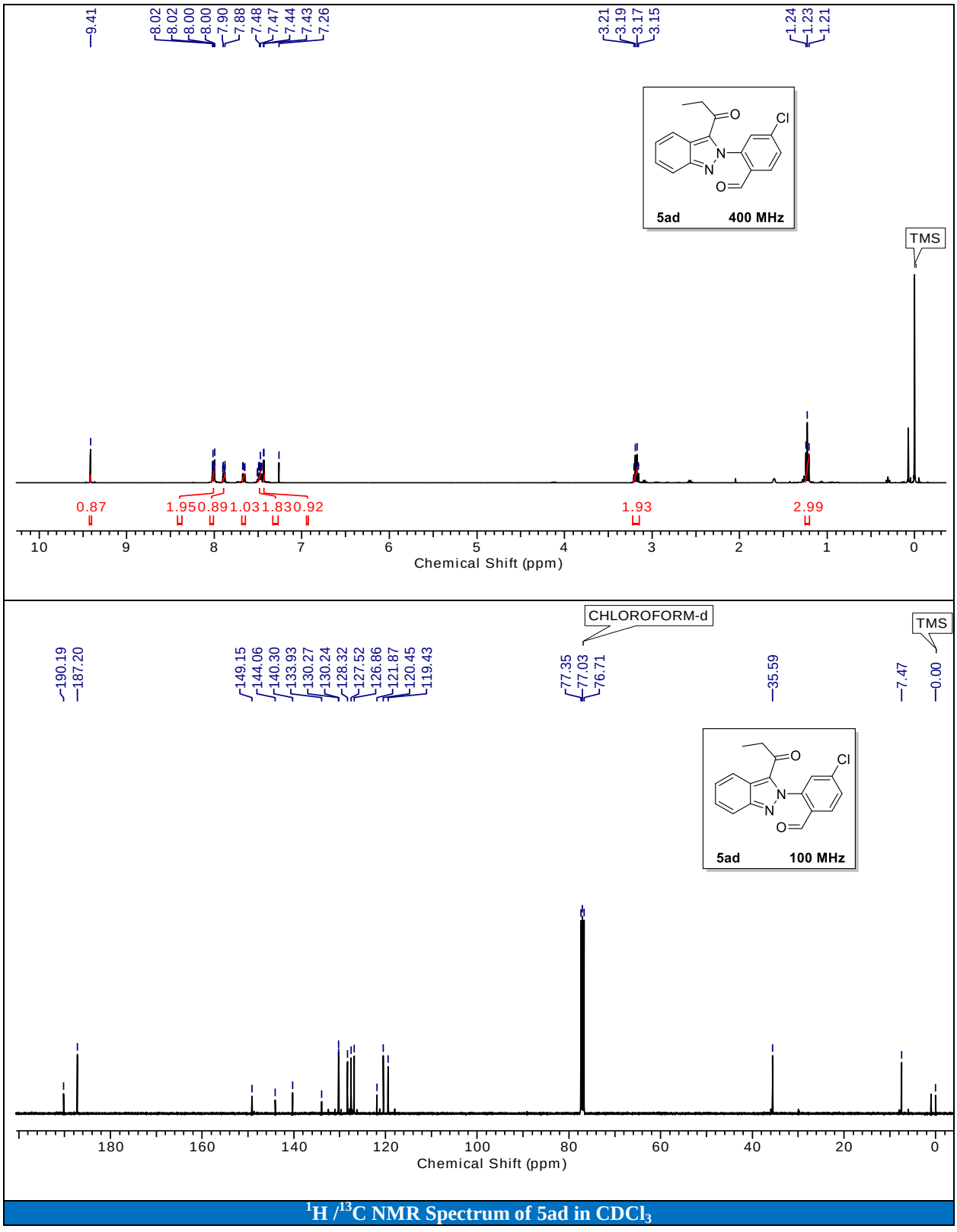

^{1}H /^{13}C NMR Spectrum of 5ad in $CDCl_3$

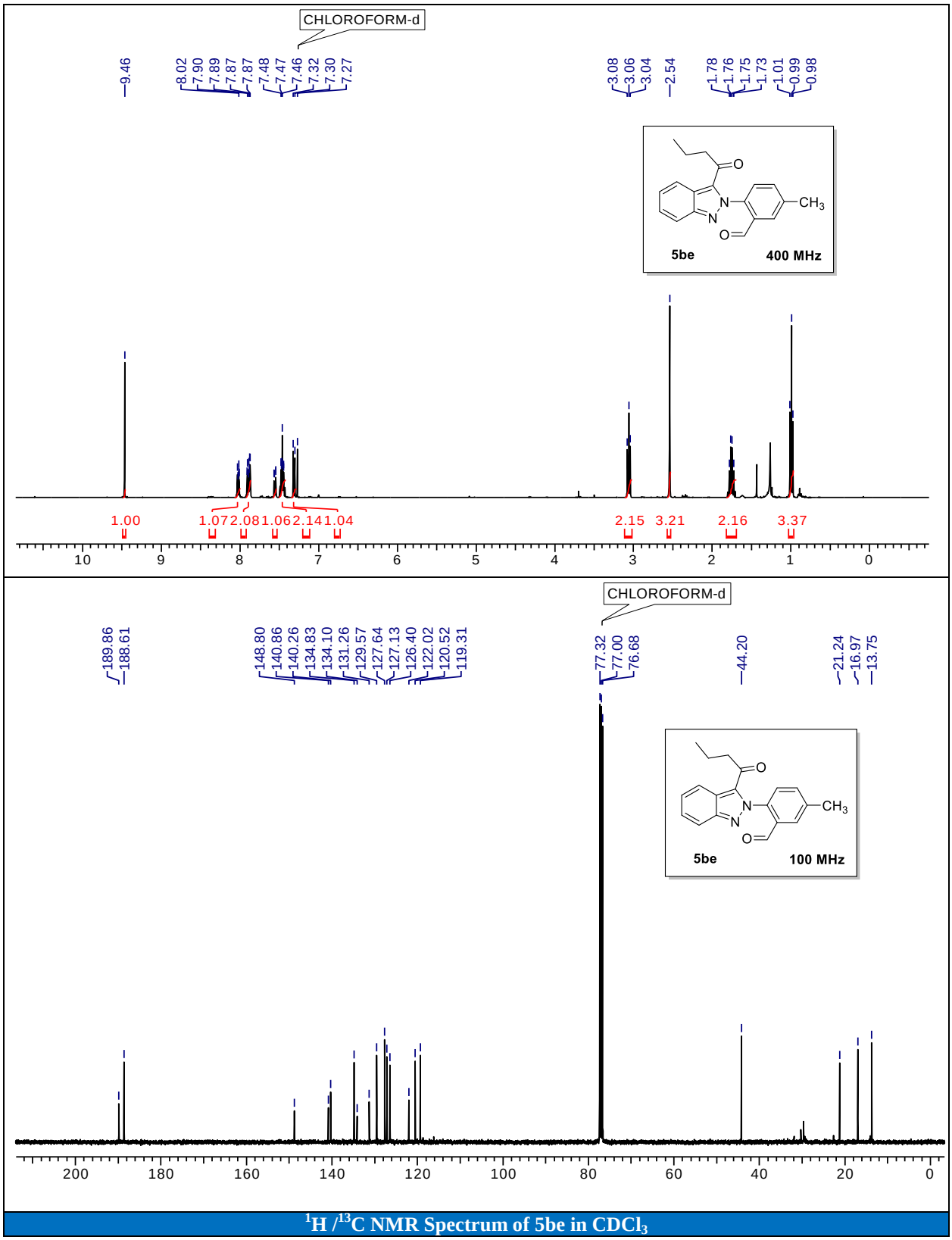

^{1}H /^{13}C NMR Spectrum of 5be in $CDCl_3$

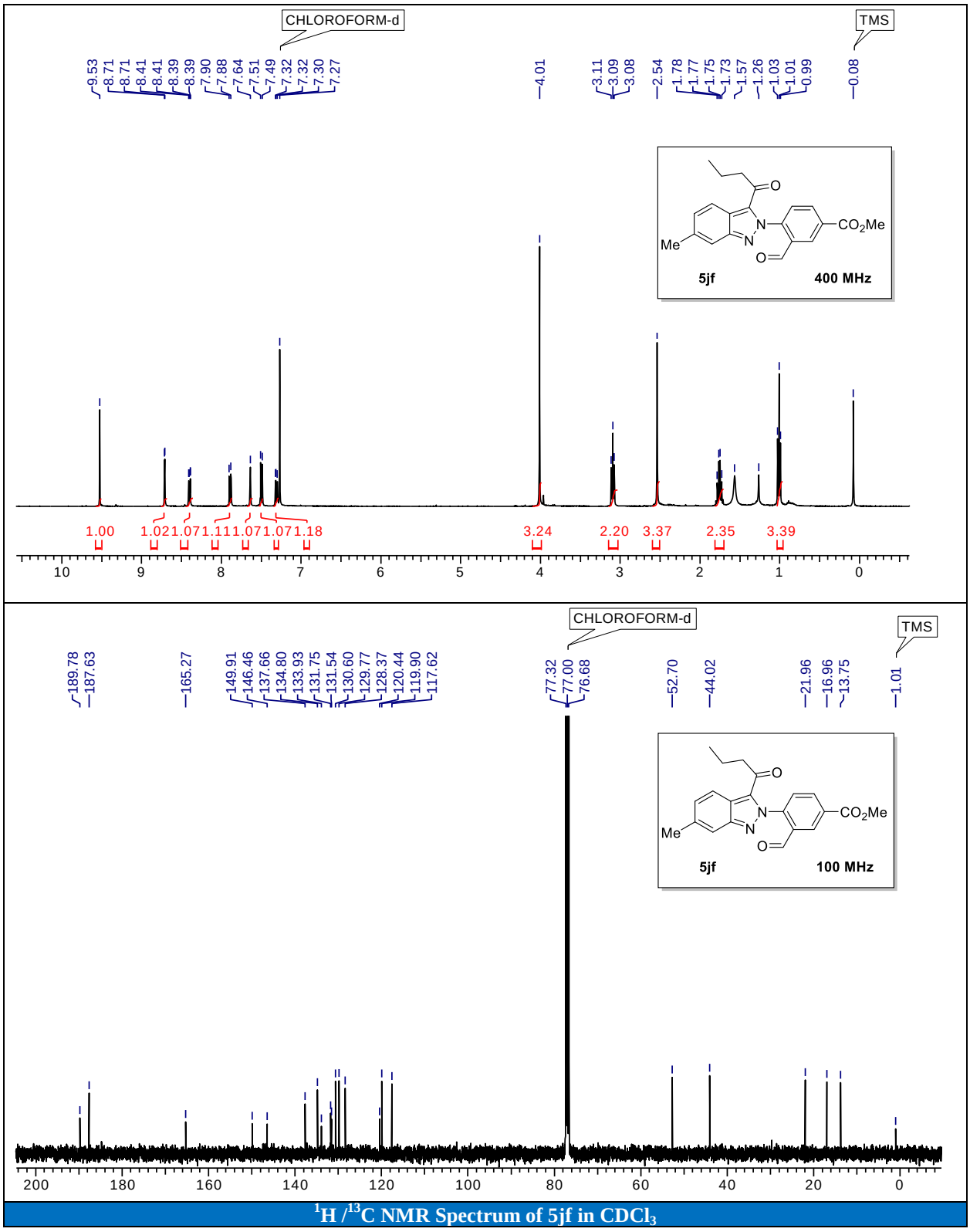

^{1}H /^{13}C NMR Spectrum of 5jf in $CDCl_3$

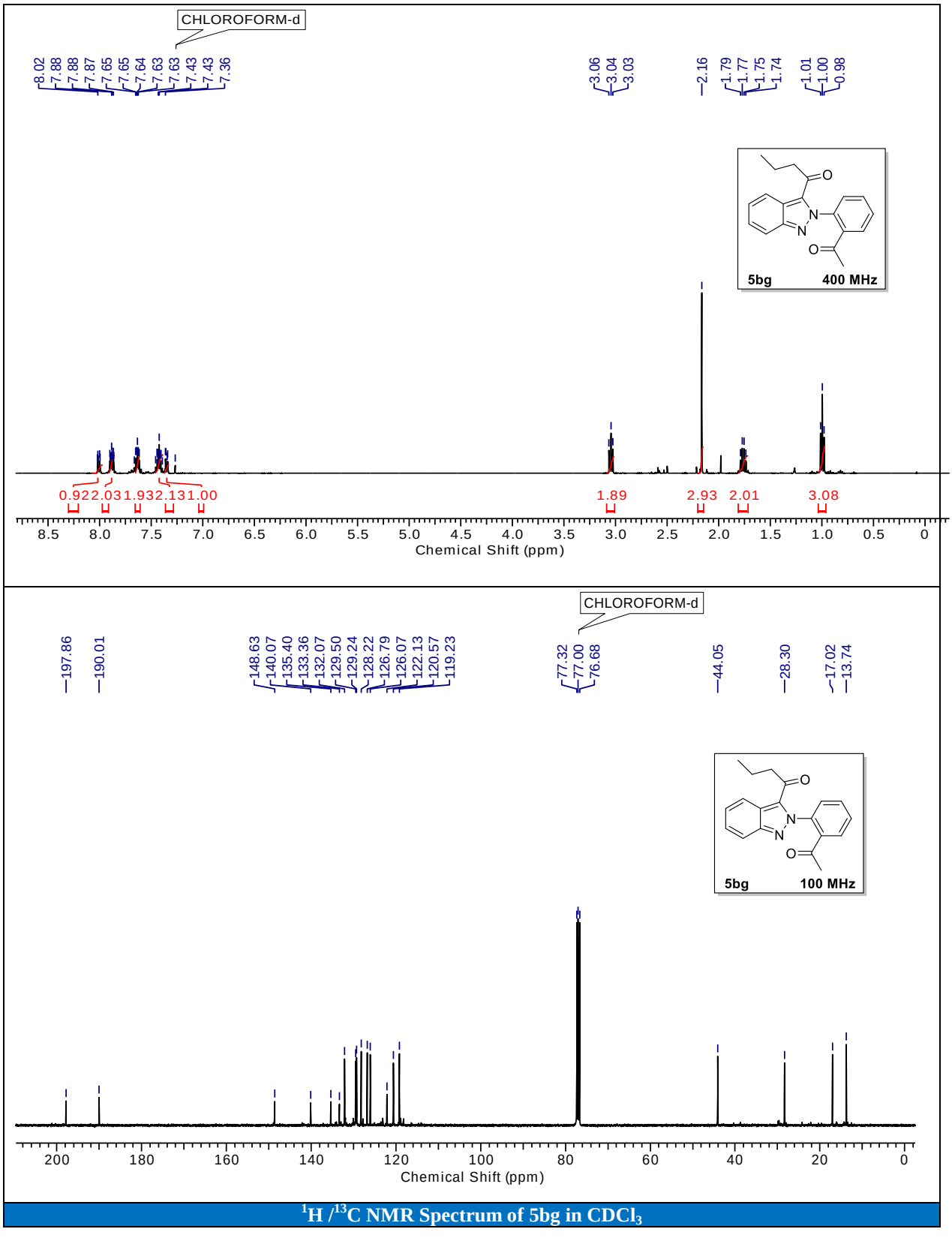

^{1}H /^{13}C NMR Spectrum of 5bg in $CDCl_3$

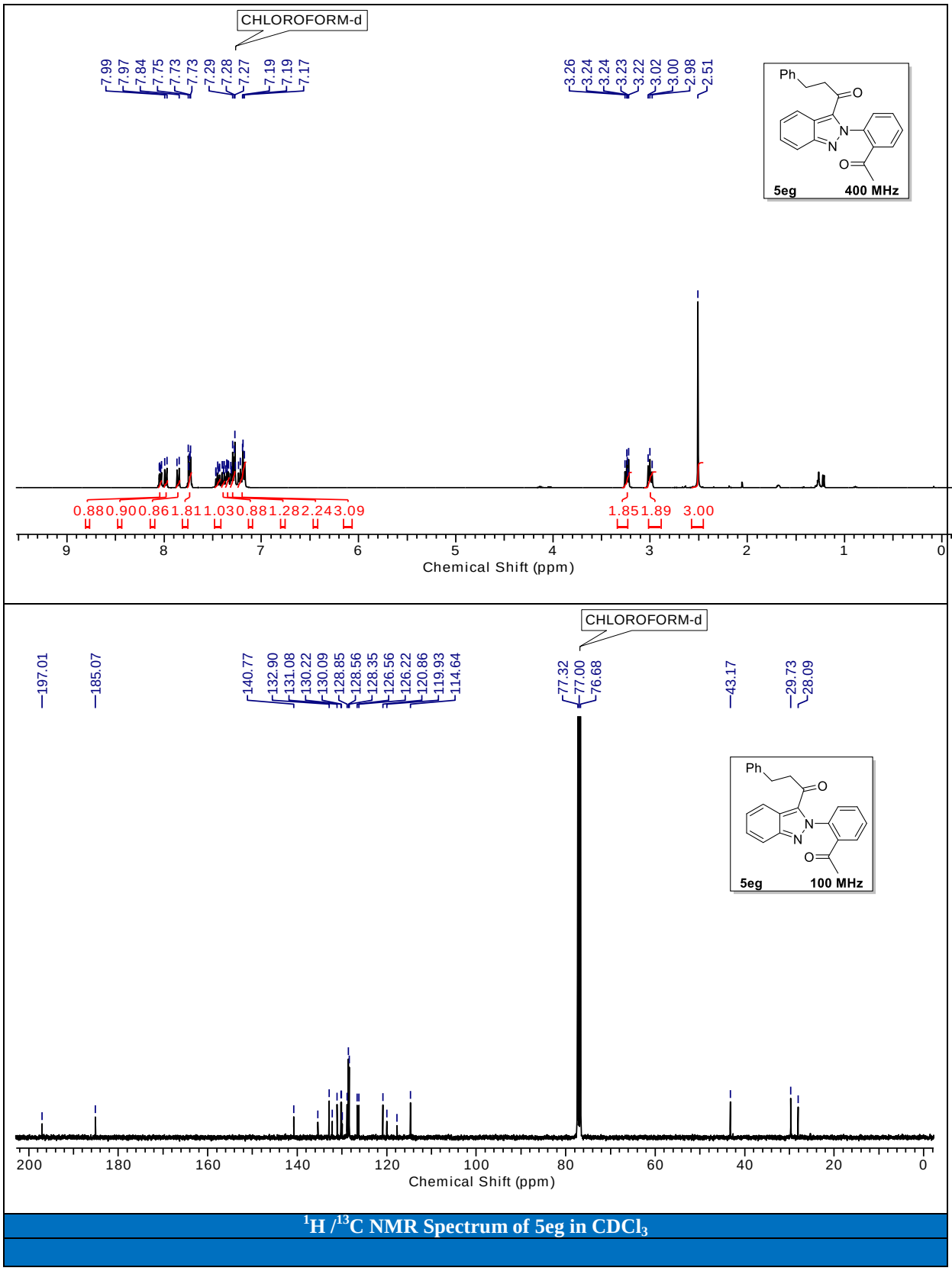

^{1}H /^{13}C NMR Spectrum of 5eg in $CDCl_3$

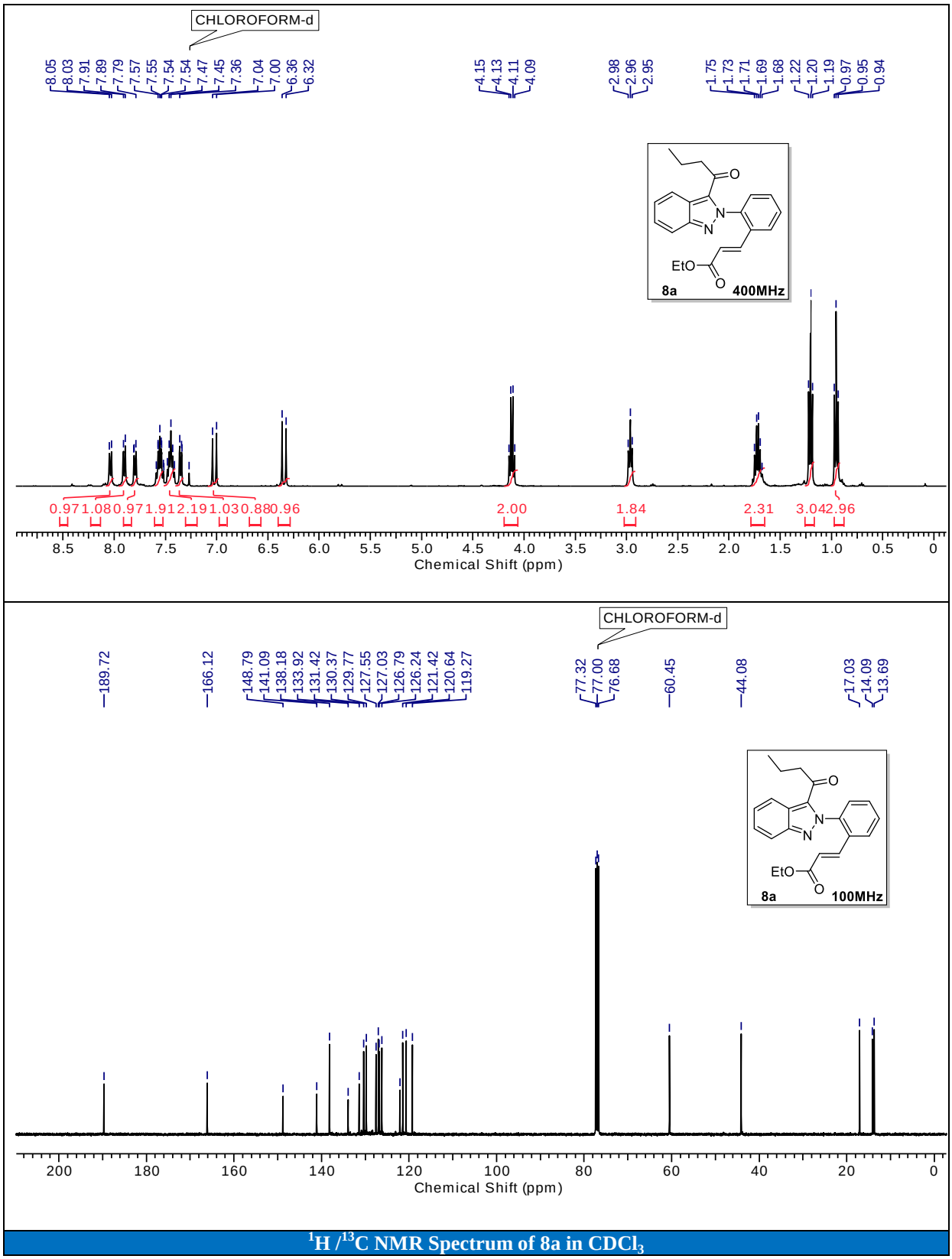

^{1}H /^{13}C NMR Spectrum of 8a in $CDCl_3$

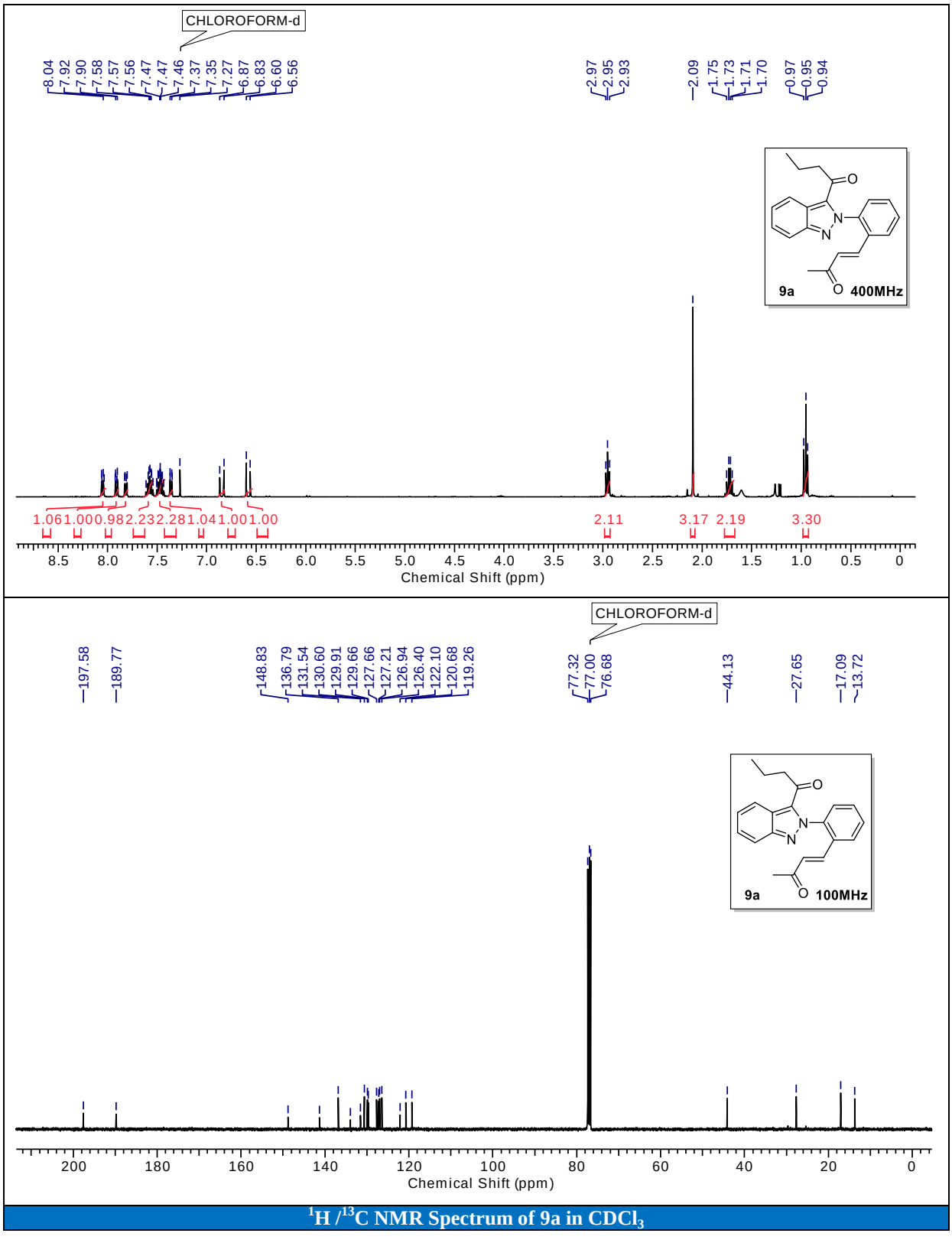

^{1}H /^{13}C NMR Spectrum of 9a in $CDCl_3$

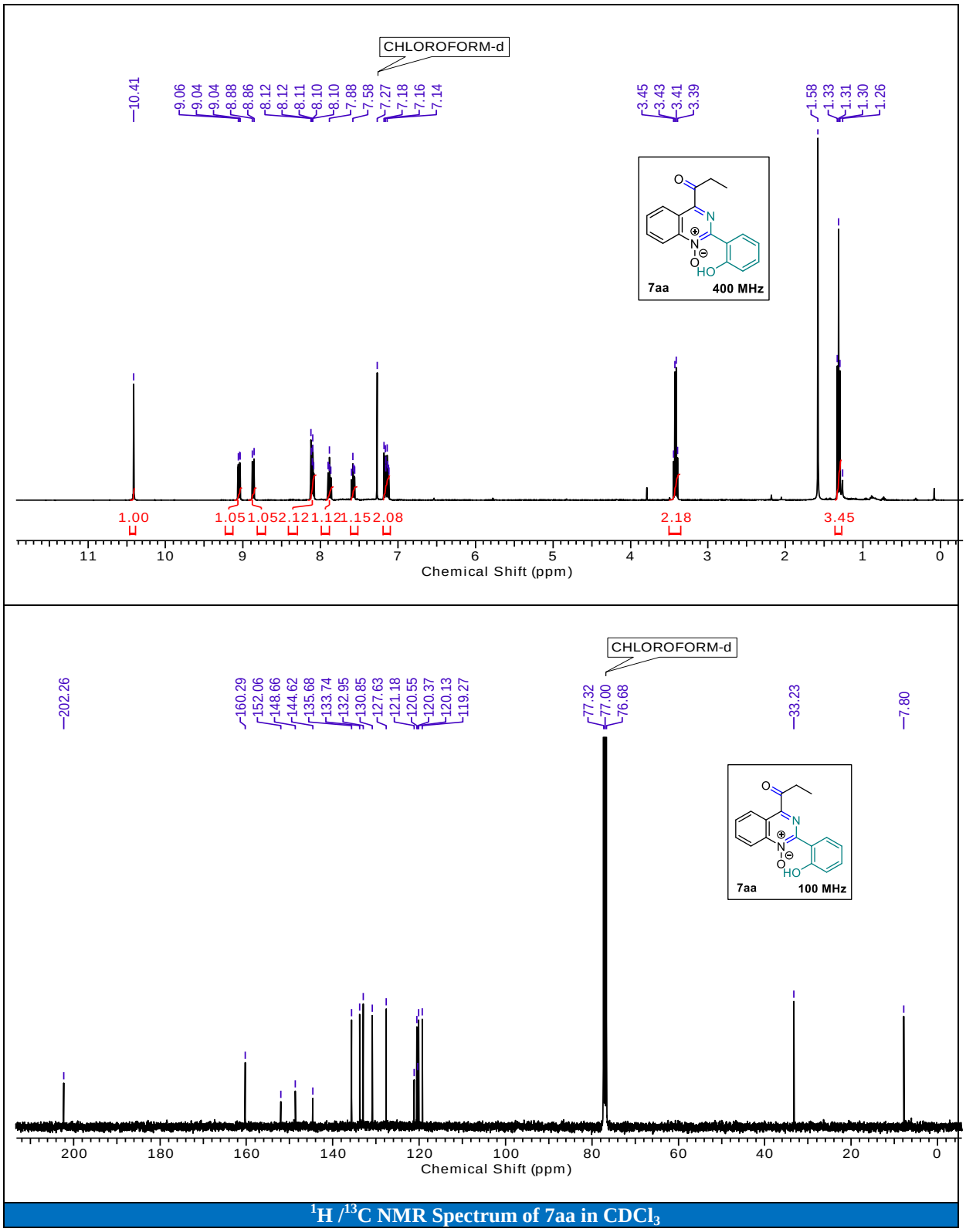

^{1}H /^{13}C NMR Spectrum of 7aa in $CDCl_3$

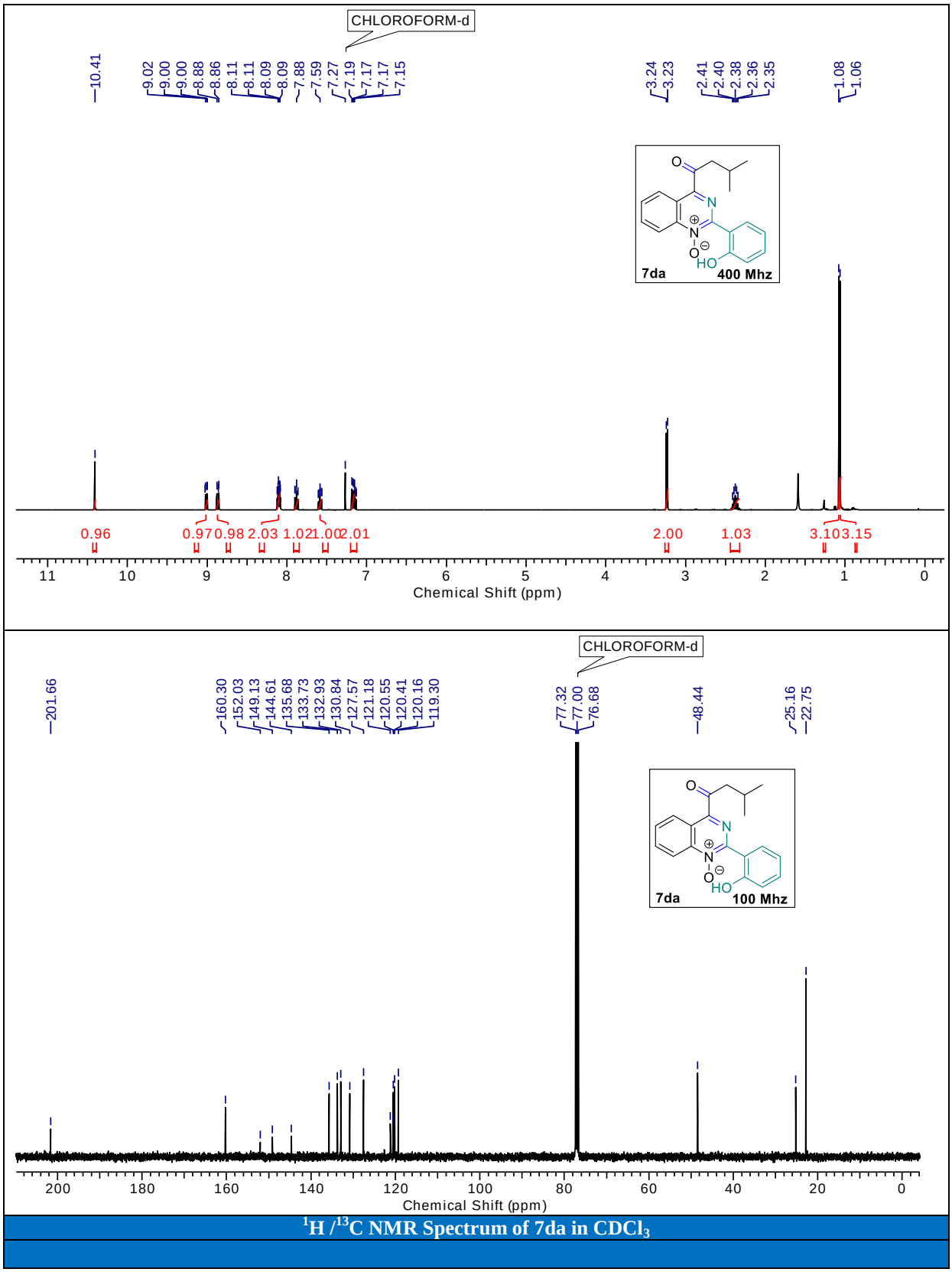

^{1}H /^{13}C NMR Spectrum of 7da in $CDCl_3$

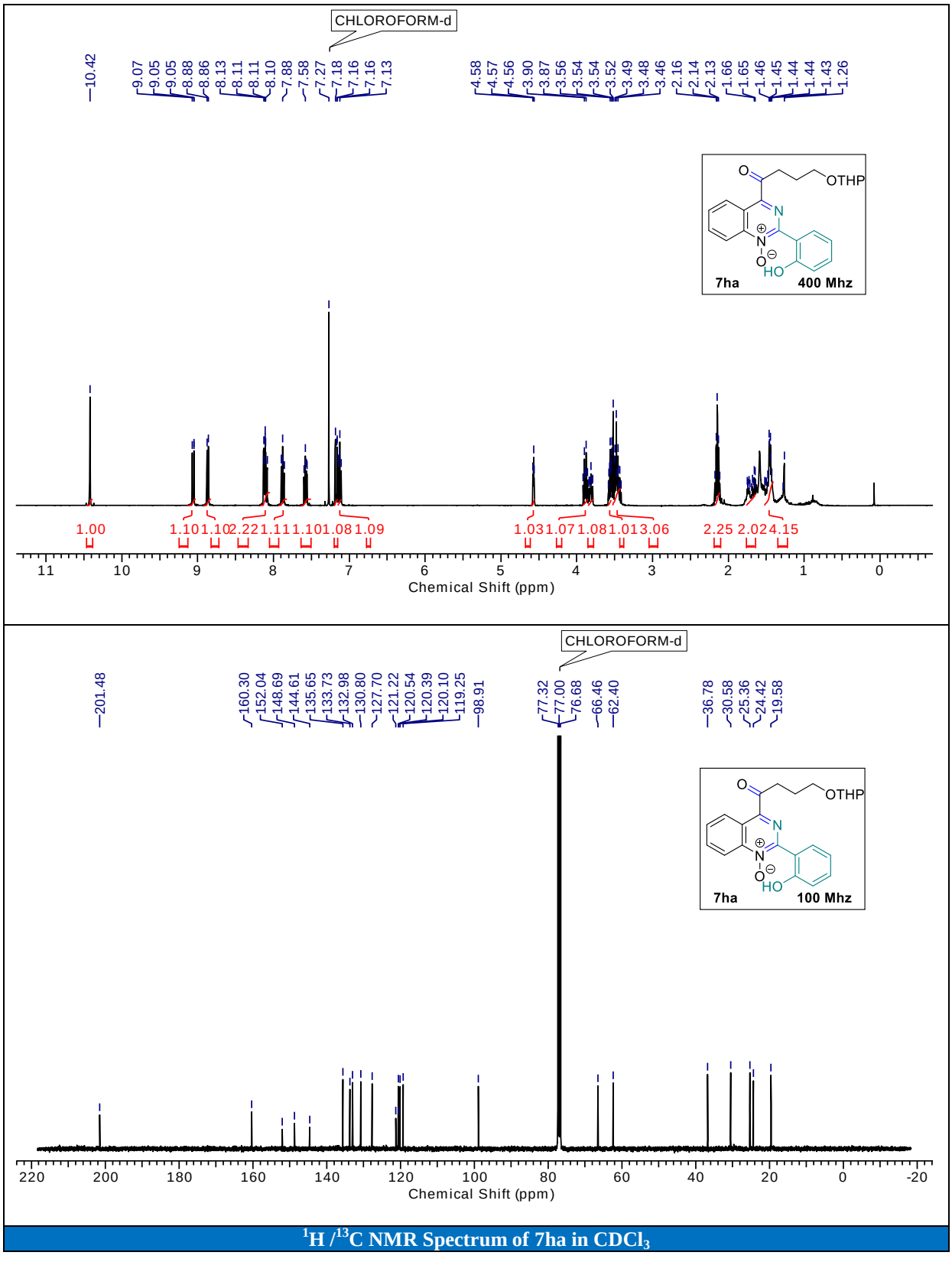

^{1}H /^{13}C NMR Spectrum of 7ha in $CDCl_3$

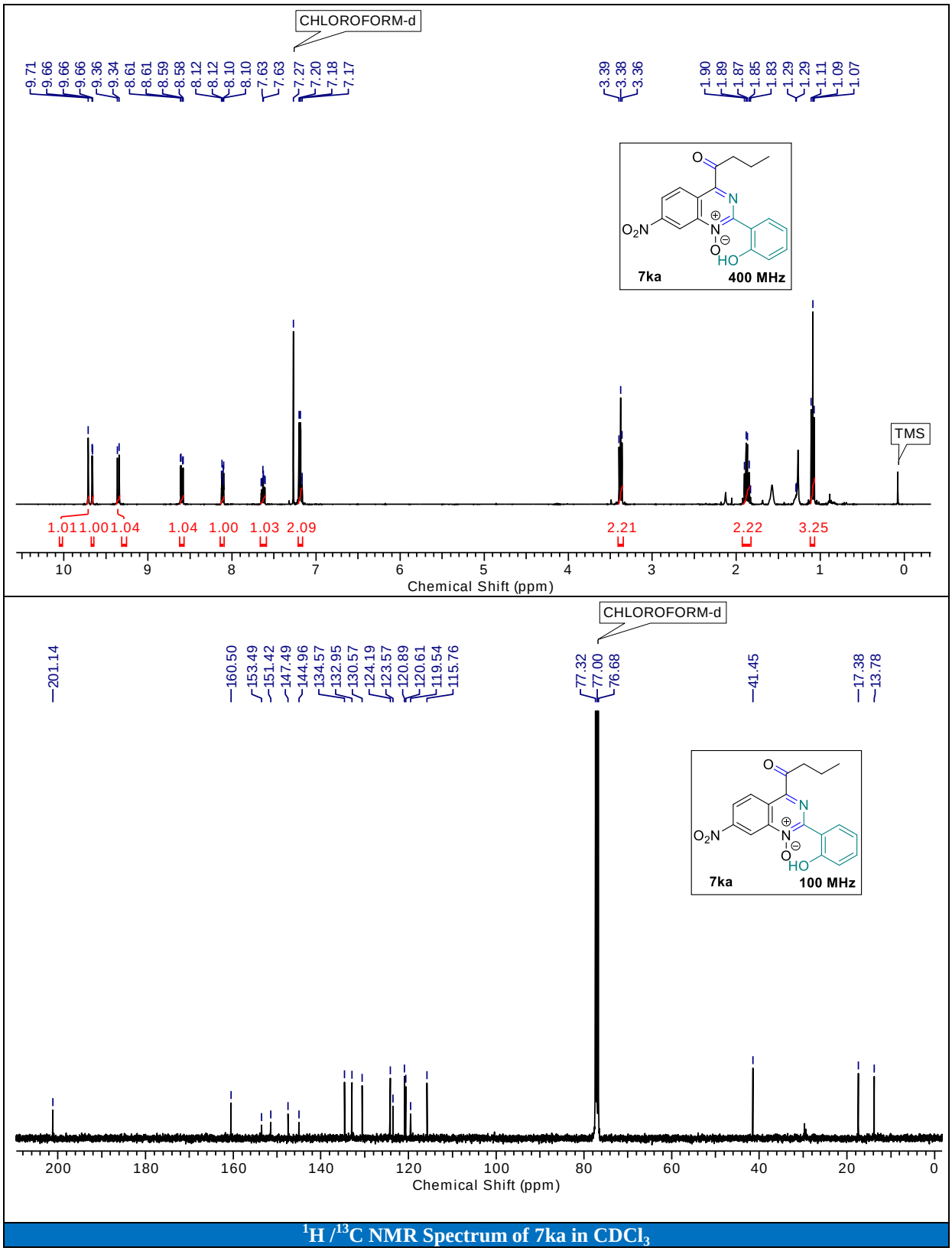

^{1}H /^{13}C NMR Spectrum of 7ka in $CDCl_3$

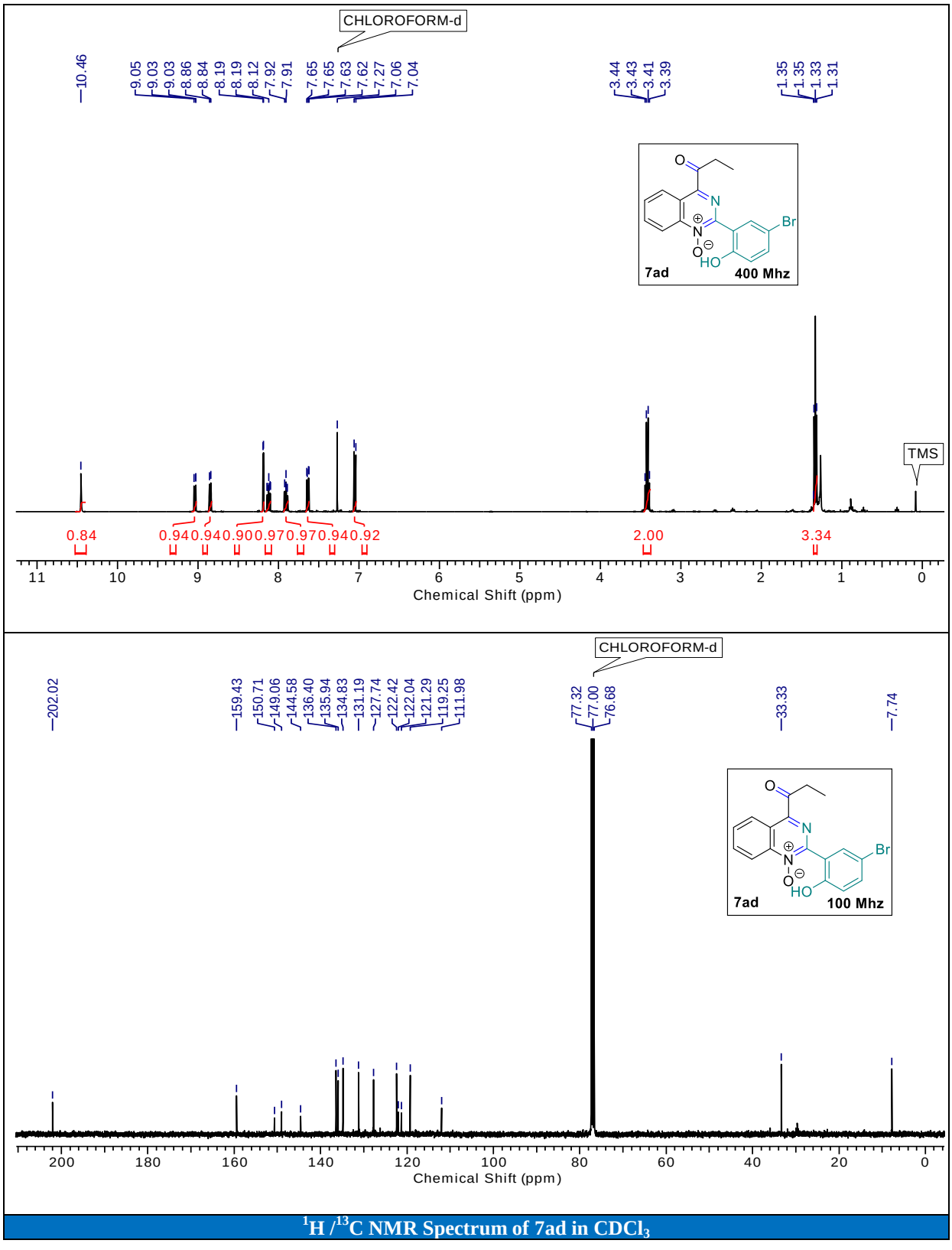

^{1}H /^{13}C NMR Spectrum of 7ad in $CDCl_3$

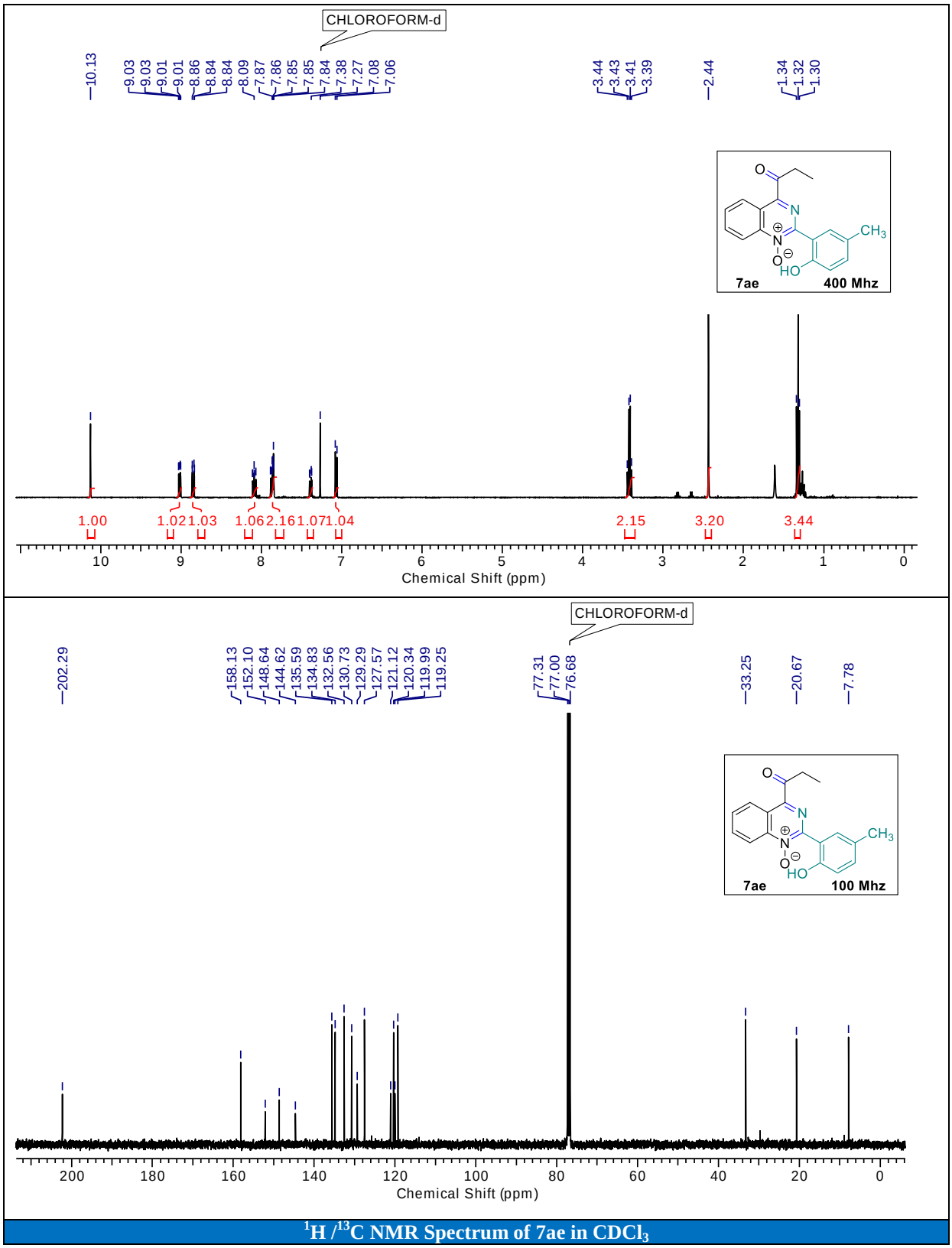

^{1}H /^{13}C NMR Spectrum of 7ae in $CDCl_3$

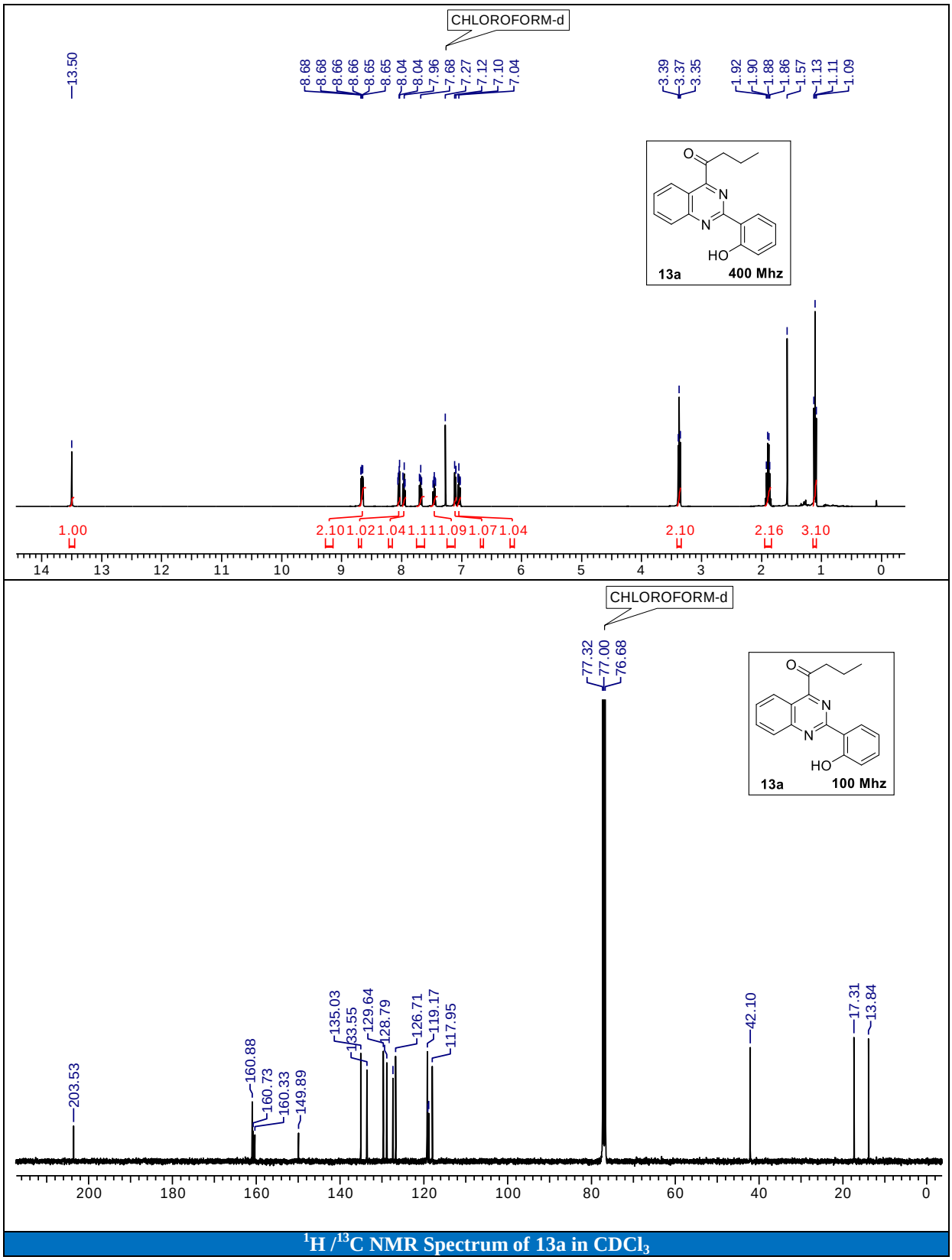

^{1}H /^{13}C NMR Spectrum of 13a in $CDCl_3$

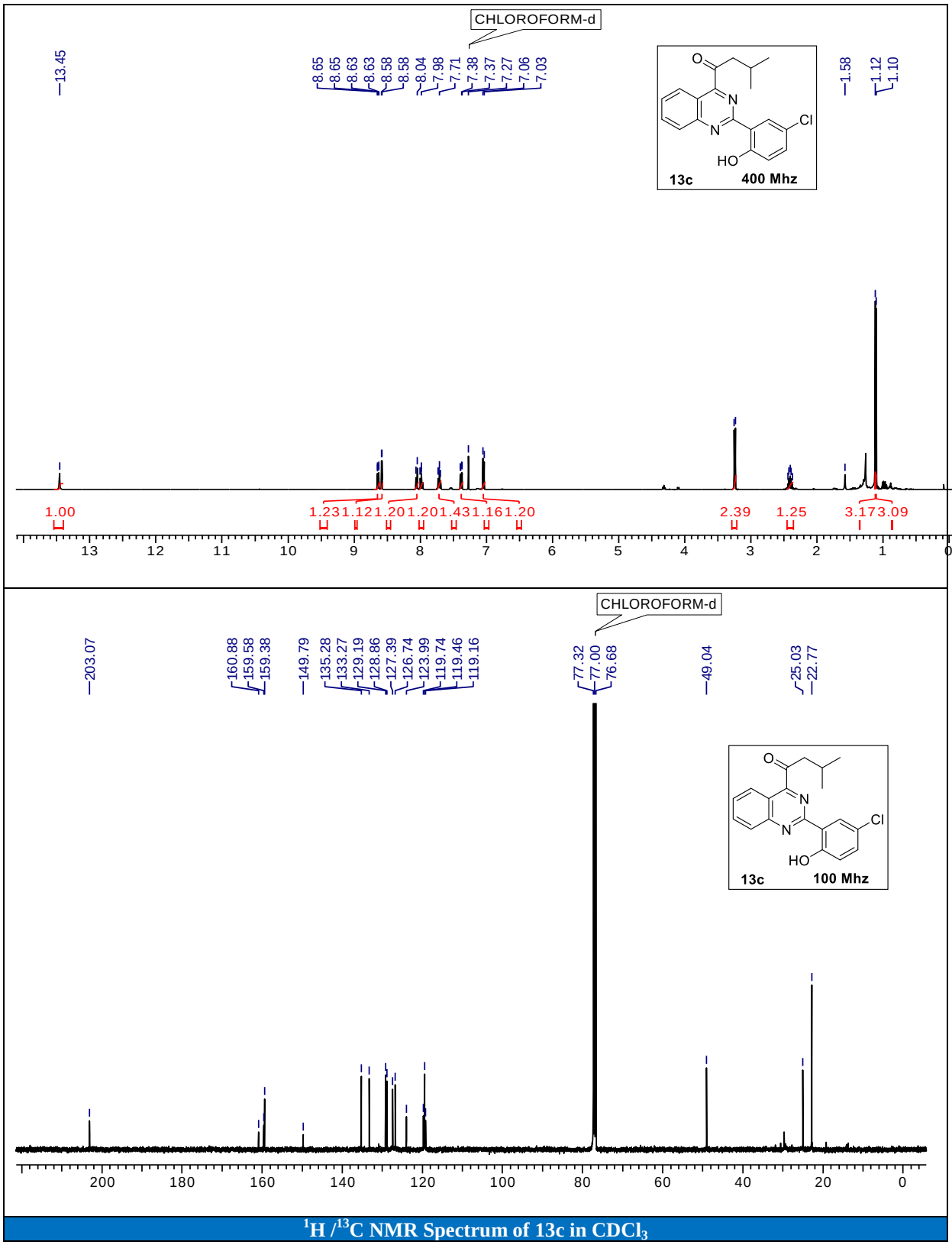

^{1}H /^{13}C NMR Spectrum of 13c in $CDCl_3$

1. Selected reviews on gold-catalyzed reaction: a) Hashmi, S. K. *Chem. Rev.* **2007**, *107*, 3180. b) Hashmi, S. K.; Hutchings, G. J. *Angew. Chem. Int. Ed.* **2006**, *45*, 7896.
2. Selected reviews on gold-catalyzed reaction in total synthesis: a) Rudolph, M.; Hashmi, S. K.; *Chem. Soc. Rev.* **2012**, *41*, 2448. b) Pflästerera, D.; Hashmi, S. K. *Chem. Soc. Rev.* **2016**, *45*, 1331. c) Zhang, Y.; Luo, T.; Yang, Z. *Nat. Prod. Rep.* **2014**, *31*, 489.
3. Selected reviews on gold-catalyzed enantioselective reaction: a) Zia, W.; Toste, D. *Chem. Soc. Rev.* **2016**, *45*, 4567. b) Li, Y.; Li, W.; Zhang, J. *Chem. Eur. J.* **2017**, *23*, 467.
4. Selected reviews on gold-catalyzed internal redox processes: a) Garayalde, D.; Nevado, C. *ACS Catal.* **2012**, *2*, 1462. b) Zhang, L. M. *Acc. Chem. Res.* **2014**, *47*, 877. c) Yeom, H. S.; Shin, S. *Acc. Chem. Res.* **2014**, *47*, 966.
5. Asao, N.; Sato, K.; Yamamoto, Y. *Tetrahedron Lett.* **2003**, *44*, 5675.
6. Xiao, J.; Li, X. *Angew. Chem. Int. Ed.* **2011**, *50*, 7226.
7. a) Aguilar, E.; Santamaría, J. *Org. Chem. Front.* **2019**, *6*, 1513. b) Ye, L. W.; Zhu, X.; Sahani, R.; Xu, Y.; Qian, P. C.; Liu, R. S. *Chem. Rev.* **2020**, DOI: 10.1021/acs.chemrev.0c00348.
8. a) Patel, P.; Ramana, C. V. *J. Org. Chem.* **2012**, *77*, 10509. b) Reddy, B. N.; Ramana, C. V. *Chem. Commun.* **2013**, *49*, 9767.
9. Baeyer, A. *Ber. Dtsch. Chem. Ges.* **1881**, *14*, 1741.
10. Evjen, S.; Fiksdahl, A. *Eur. J. Org. Chem*. **2016**, 2858.
11. Zhu, J. S.; Haddadin, M. J.; Kurth. M. J. *Acc. Chem. Res.* **2019**, *52*, 2256.
12. a) Denya, I.; Malan, S.; Joubert, J. Indazole derivatives and their therapeutic applications: a patent review (2013-2017) *Expert Opinion on Therapeutic Patents* **2018**, *28*, 441. b) Zhang, S. G.; Liang, C. G.; Zhang, W. H. *Molecules* **2018**, *23*, 2783. c) Gaikwad, D. D.; Chapolikar, A. D.; Devkate, C. G.; Warad, K. D.; Tayade, A. P.; Pawar, R. P.; Domb, A. J. *Eur. J. Med. Chem.* **2015**, *90*, 707. d) Janardhanan, J. C.; Bhaskaran, R. P.; Praveen, V. K.; Narayanapillai, M.; Babu, B. P. *Asian J. Org. Chem.* **2020**, *9*, 1410. e) Hassan, A. A.; Aly, A. A.; Tawfeek, H. N. Indazoles: Synthesis and Bond-Forming Heterocyclization in *Advances in Heterocyclic Chemistry*, Vol. *125*, E. F. V. Scriven, C. A. Ramsden, Eds.; Academic Press, Cambridge, **2018**, pp. 235. f) Schmidt, A.; Beutler, A.; Snovydovych, B. *Eur. J. Org. Chem.* **2008**, 4073.
13. Kaur, M.; Kumar R. *Chemistry Select* **2018**, *3*, 5330.

14. Zhu, J. S.; Li, C. J.; Tsui, K. Y.; Kraemer, N.; Son, J.-H.; Haddadin, M. J.; Tantillo, D. J.; Kurth, M. J. *J. Am. Chem. Soc.* **2019**, *141*, 6247.
15. Jadhav, A. M.; Bhunia, S.; Liao, H.-Y.; Liu, R.-S. *J. Am. Chem. Soc.* **2011**, *133*, 1769.
16. Gao, Y; Nie, J.; Huo, Y.; Hu, X. Q. *Org. Chem. Front.* **2020**, *7*, 1177.
17. a) Yeom, H.; Lee, J.; Shin, S. *Angew. Chem. Int. Ed.* **2008**, *47*, 7040. b) Yeom, H. S.; Lee, Y.; Lee, J. E.; Shin, S. *Org. Biomol. Chem.* **2009**, *7*, 4744. c) Wetzel, A.; Gagosz, F. *Angew. Chem. Int. Ed.* **2011**, *50*, 7354.
18. a) Johansson, M. J.; Gorin, D. J.; Staben, S. T.; Toste, F. D. *J. Am. Chem. Soc.* **2005**, *127*, 18002. (b) Lopez, S.; Gomez, E. H.; Galan, P. P.; Oberhuber, C. N.; Echavarren, A. E. *Angew. Chem. Int. Ed.* **2006**, *45*, 6029.
19. Jin, H.; Huang, L.; JinXie, Rudolph, M.; Rominger, F.; Hashmi, S. K. *Angew. Chem. Int. Ed.* **2016**, *55*, 794.
20. Skaria, M.; More, S.;Kuo, T. C.; Cheng, M. J.; Liu, R. S. *Chem. Eur. J.* **2020**, *26*, 3600.
21. Sahani, R. L.; Liu, R. S. *Angew. Chem. Int. Ed.* **2017**, *56*, 12736.
22. a) Mfuh, A. M.; Larionov, O. V. *Curr. Med. Chem.* **2015**, *22*, 2819–2857. b) Khan, I.; Zaib, S.; Batool, S.; Abbas, N.; Ashraf, Z.; Iqbal, J.; Saeed, A. *Bioorg. Med. Chem.* **2016**, *24*, 2361.
23. a) Yamanaka, H. *Chem. Pharm. Bul.* **1959**, *7*, 152. b) Sternbach, L. H.; Kaiser, S.; Reeder, E. *J. Am. Chem. Soc.* **1960**, *82*, 475. c) Tennant, G. *J. Chem. Soc.* C. **1966**, 2285. d) Higashino, T.; Amano, T.; Tamura, Y.; Katsumata, N.; Washizu, Y.; Ono, T.; Hayashi, E. *Chem. Pharm. Bul.* **1972**, *20*, 1874. e) Spence, T. W. M.; Tennant, G. *J. Chem. Soc. Perkin Trans. I.* **1972**, 97. f) Murashima, T.; Tamai, R.; Fujita, K.; Uno, H.; Ono, N. *Tetrahedron Lett.* **1996**, *37*, 8391. g) Coşkun N.; Çetin M. *Tetrahedron* **2007**, *63*, 2966. h) Petkevičius, V.; Vaitekūnas, J.; Vaitkus, D.; Čėnas, N.; Meškys, R. *Catalysts* **2019**, *9*, 356.
24. Schulz, J.; Jašíková, L.; Škríba, A.; Roithová, J. *J. Am. Chem. Soc.* **2014**, *136*, 11513.
25. a) Jadhav, P. D.; Lu, X.; Liu, R. S. *ACS Catal.* **2018**, *8*, 9697. b) Xu, W.; Zhao, J.; Li, X.; Liu, X. *J. Org. Chem.* **2018**, *83*, 15470.
26. Manetsch, R.; Zheng, L.; Reymond, M.;. Woggon, W. D.; Reymond, J. L. *Chem. Eur. J.* **2004**, *10*, 2487.

Chapter 1, Section B

One-Pot Au[III]-/Lewis Acid Catalyzed Cycloisomerization of Nitroalkynes and [3 + 3] Cycloaddition with Donor–Acceptor Cyclopropanes

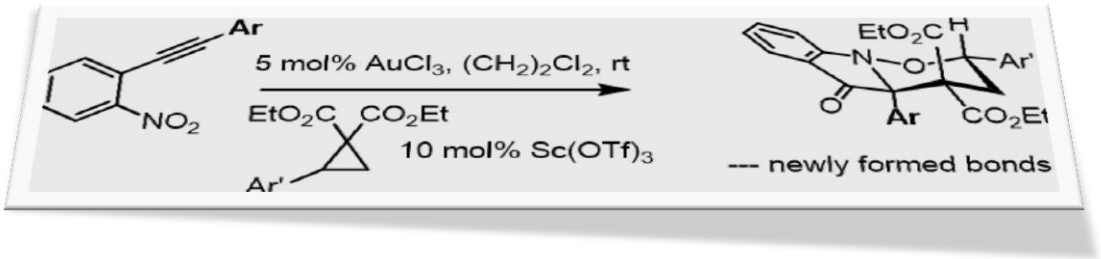

10.0. Introduction

Pseudoindoxyl natural products occupy a special place in the indole alkaloids family because of their fascinating molecular structures and promising biological activities.[1] The term "pseudoindoxyl" has had its own association with the father of indole chemistry, "Adolf Bayer". The word indoxyl (3-hydroxyindole) that was isomeric with oxindole was coined by Bayer in 1883 for an intermediate product of indigo degradation (Figure F1.4).[2] However, as this compound showed the characteristic reactions of both phenol and ketone and since the concept of keto-enol tautomerism had been not yet put forward, due to ambiguity about the position of one of the hydrogen atoms in indoxyl, it was believed that both the enolic and the ketonic forms were two different compounds. In addition to this, it was also strongly believed that the indoxyl occurred solely in the stable enolic form (3-hydroxyindole) and the ketonic form was labile and unstable, and hence this was called as "pseudoindoxyl".

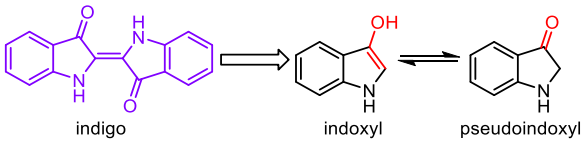

Figure F1.4: *Indigo Degradation leading to Indoxyl and Pseudoindoxyl*

The biosynthesis of these pseudoindoxyl natural products comprises of an oxidative rearrangement of the corresponding indole alkaloids.[3] Indeed, this is one of the key approaches employed in the synthesis of the pseudoindoxyl core.[4] However, the competing formation of 2-oxindole derivatives during the rearrangement and control over the stereochemistry of the newly generated quaternary carbon center are the major concerns.[5] In this regard, alternative approaches for constructing the pseudoindoxyl (2,2-disubstituted 1,2-dihydro-3*H*-indol-3-one) core have been explored.[6] As describe in the introduction, the metal catalyzed cycloisomerization of *o*-nitrotolans and *o*-azidotolans (2nd chapter introduction) and subsequent inter- and intramolecular transformations have emerged as simple and effective tools to create pseudoindoxyl cores. Figure F1.5 depicted the representative natural product having pseudoindoxyl core.

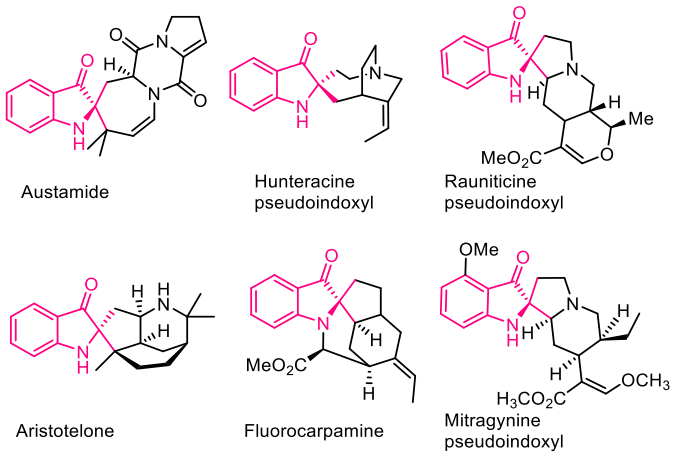

Figure F1.5: *Representative Pseudoindoxyl Natural Products*

10.0.1. Literature Reports on Cycloadditions Reactions of Donor-Acceptor Cyclopropane with Nitrones

The cycloaddition reaction of DA-cyclopropanes is one of the important reactions unveiled during the last decade.[7] The (homo) cycloaddition reactions of DA-cyclopropanes with various dipolarophiles, in general,[8] and with nitrones, in particular, have been well explored in natural products synthesis.[9]

Kerr and co-worker reported the first example of a dipolar homo [3 + 2] cycloaddition reaction between nitrones **S1.37A** and donor-acceptor (DA) cyclopropanes **S1.37B** for the formation of tetrahydro-1,2-oxazines **S1.37C** in good to excellent yields and with complete 1,4-*syn* diastereoselectivity (Scheme S1.37).

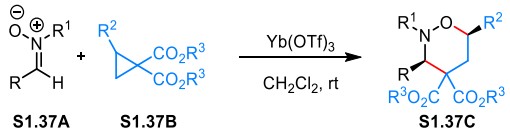

Scheme S1.37: *Kerr's Approach for Homo[3+2] Cycloaddition*

(Young, I. S.; Kerr, M. A. *Angew. Chem. Int. Ed.* **2003**, *42*, 3023–3026)

In 2004, Kerr and co-workers documented a three-component one pot protocol for a facile construction of tetrahydro-1,2-oxazines **S1.38D**. The reaction comprises of generating the unstable nitrones *via* the coupling of hydroxylamine **S1.38B** and aldehyde **S1.38A** and its [3+3] cycloaddition with DA cyclopropanes **S1.38C** (Scheme S1.38). This multicomponent reaction

provides the construction of a various array of tetrahydro-1,2-oxazines **S1.38D** having the core structure of FR900482.

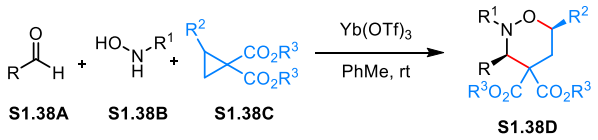

Scheme S1.38: *Kerr's Three Component One Pot Approach for [3+3] Cycloaddition*

(Young, I. S.; Kerr, M. A. *Org. Lett.* **2004**, *6*, 139–141)

In 2005, Sibi and co-workers reported the first asymmetric version of this cycloaddition using bisoxazoline ligand (**S1.39C)** catalyzed by $Ni(ClO_4)_2$. The products are obtained in excellent yields and with high enantiomeric excess, however, the intended dynamic kinetic resolution was found to be indescribable while using racemic cyclopropanes (Scheme S1.39).

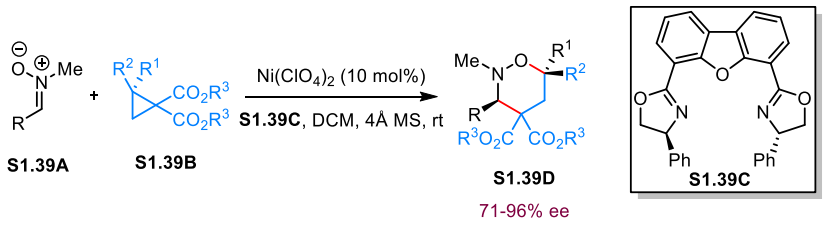

Scheme S1.39: *Sibi's Asymmetric [3+3] Cycloaddition of DA-Cyclopropanes and Nitrones*

*(*Sibi, M. P.; Ma, Z.; Jasperse, C. P. *J. Am. Chem. Soc.* **2005**, *127*, 5764–5765)

In 2007, Tang's group addressed this dynamic kinetic resolution problem by switching the bisoxazoline-Ni^{II} catalyst to a trisoxazoline-Ni^{III} catalyst (**S1.40B**) for asymmetric [3+3] cycloaddition of DA-cyclopropanes with nitrones. As shown Scheme S1.40, both enantiomers of product tetrahydro-1,2-oxazine **S1.40C**/**40C'** could be prepared from racemic DA cyclopropane **S1.40A** by either by a direct cycloaddition with nitrone in the presence of catalytic ligand/$Ni(ClO_4)_2$ (Scheme S1.40, eq. 1) or by a ligand/$Ni(ClO_4)_2$-catalyzed kinetic resolution followed by cycloaddition with nitrone (Scheme S1.40, eq. 2).

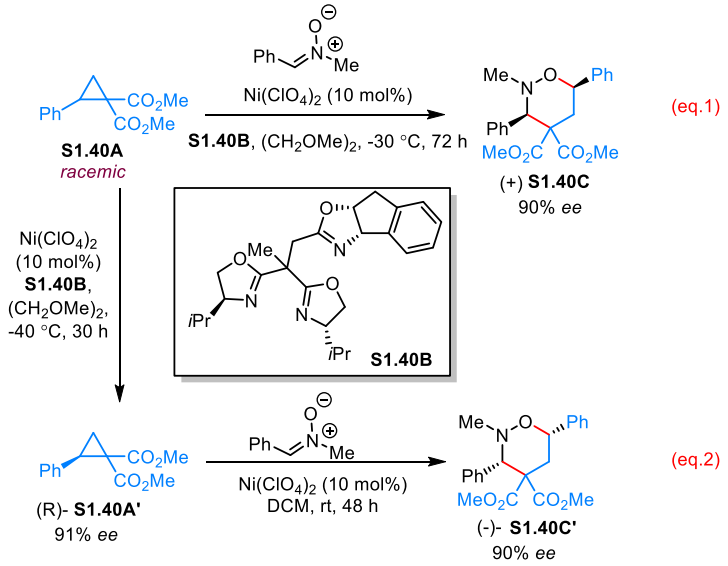

Scheme S1.40: *Tang's Asymmetric [3+3] Cycloaddition of DA-Cyclopropanes and Nitrones*

(Kang, Y.-B.; Sun, X.-L.; Tang, Y. *Angew. Chem. Int. Ed.* **2007**, *46*, 3918–3921)

An additional stereocenters at the C4-position of oxazines were obtained by the simultaneous use of two different acceptor groups. Mattson and co-workers changed one of the ester groups by a nitro group and carried out the desired cycloaddition reaction in presence of boronate urea catalyst **S1.41C** (Scheme S1.41).

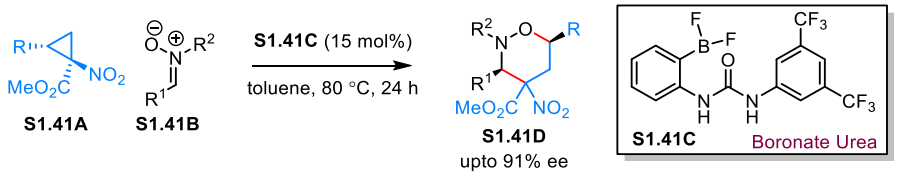

Scheme S1.41: *Mattson's [3+3] Cycloaddition of DA-Cyclopropanes and Nitrones*

(Hardman, A. M.; So, S. S.; Mattson, A. E. *Org. Biomol. Chem.* **2013**, *11*, 5793)

Zhang and co-workers reported the formal [4+3] cycloaddition catalyzed by Au(I) using 1-(1-alkynyl)cyclopropylketones and nitrones for the synthesis furo[3,4-*d*]-[1,2]oxazepine **S1.42F**. Mechanistically, AuI catalyst coordinates to the alkyne with an initial formation of the **S1.42E** by nucleophilic attack of the carbonyl group on the vinyl-Au moiety. This intermediate undergoes subsequent [4+3]-annulation with nitrone **S1.42B** giving the seven-membered

scaffolds. However, when $Sc(OTf)_3$ was employed as a catalyst, the tetrahydro-1,2-oxazines **S1.42C** was obtained exclusively. The complementary reactivity observed in this case has been exaplained by invoking facile coordination of the catalyst with carbonyl group of the alkyne-substituted DA-cyclopropane (Scheme S1.42).

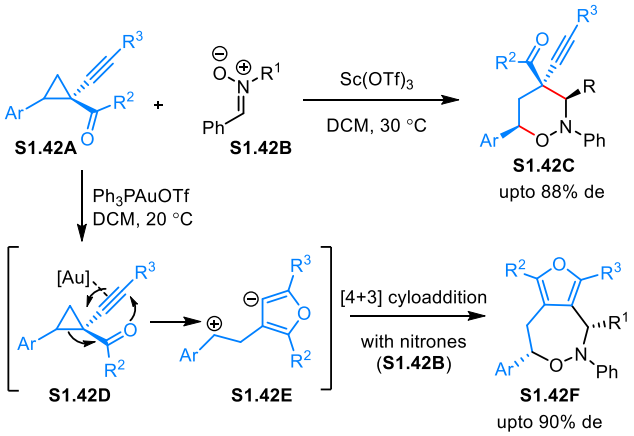

Scheme S1.42: *Zhang's Regioselective Cycloaddition of 1-(1-Alkynyl)cyclopropyl Ketones and Nitrones*

(Zhang, Y.; Liu, F.; Zhang, J. *Chem. Eur. J.* **2010**, *16*, 6146–6150)

In 2013, Loffe and co-workers employed cyclic nitronates **S1.43A** for the formal [3+3] cycloadditions with DA-cyclopropane **S1.43B** to prepare bicyclic nitroso acetates **S1.43C** by employing $Yb(OTf)_3$ as a catalyst (Scheme S1.43).

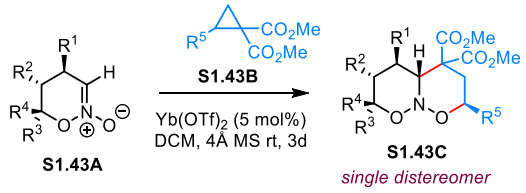

Scheme S1.43: *Loffe's [3+3] Cycloaddition of DA-Cyclopropanes and Cyclic Nitronates*

(Gorbacheva, E. O.; Tabolin, A. A.; Novikov, R. A.; Khomutova, Y. A.; Nelyubina, Y. V.; Tomilov, Y. V.; Ioffe, S. L. *Org. Lett.* **2013**, *15*, 350–353)

10.0.2. Our Hypothesis

As described in the introduction, the cycloaddition reaction of DA-cyclopropane with isatogen has not yet been examined. Considering the fact that the preparation of isatogens from nitroalkynes and the [3+3]-cycloaddition reaction of DA-cyclopropanes require Lewis acids, we assumed that there is a chance of combining both the reactions in one-pot, which would lead to fused tricyclic pseudoindoxyl derivatives.

11.0. Present Work

With these intention in mind, and in order to identify the suitable Lewis acid for the [3+3]-cycloaddition, 2-phenyl- and 2-^{n}pentyl isatogens **1a** and **1b** respectively, as well as commonly employed DA-cyclopropane diethyl 2-phenylcyclopropane-1,1-dicarboxylate (**2a**) have been selected as the suitable partners and screened with the commonly employed $Sc(OTf)_3$ and $Yb(OTf)_3$ for the projected [3+3]-cycloaddition. With both Lewis acids, the cycloaddition reaction of **2a** with **1a** and **1b** was facile at room temperature and provided the corresponding cycloaddition products **3aa** and **3ba** with complete diastereoselectivity. The yields in general were also good and that with $Sc(OTf)_3$ were best. The structure of product **3aa** was established with the help of spectral and analytical data. For example, in the ^{1}H NMR spectrum of compound **3aa**, two ortho protons (nitrone) in the 8.61–8.66 ppm region of compound **1a** were absent and shifted to up field. This indicated that there is a change at the nitrogen center. The presence of 14 aromatic protons as well as the alkyl groups of the ester confirmed that the cycloaddition reaction has been taken place. The protons of methylene group from the DA-cyclopropane were seen to be resonated separately at δ 2.48 (dd, J = 14.6, 3.1 Hz) and at δ 2.55 (dd, J = 14.6, 11.6 Hz). The remaining tertiary proton was appeared at δ 4.96 (dd, J = 11.6, 3.1 Hz). The appearance of a quaternary carbon at 71.6 ppm in the ^{13}C NMR spectrum of **3aa** and a downfield shift of the carbonyl group from 186.7 to 193.0 ppm indicated the loss of conjugation which is present in the isatogen. Further two distinctive ester carbonyl peaks appeared at the δ 167.5, δ 168.6 ppm. Lastly, the constitution of **3aa** has been confirmed as $C_{29}H_{28}NO_6$ by HRMS ($[M+H]^+$) found as 486.1899.

The relative stereochemistry of the newly formed 1,2-oxazine ring has been proposed by considering the previous reports on the cycloaddition with cyclic nitrones where both experimental and theoretical calculations favored a single diastereomer having cis-orientation of the 1,4-phenyl substituents (see Figure F1.6 for the NOESY spectra of cycloaddition product **3eb** synthesized later and the representative nOes observed that support the assigned configuration/conformation).[10] Nonetheless, this early success with the cycloaddition of isatogens with DA-cyclopropanes prompted us to proceed for the examination of the possibility of carrying out nitroalkyne cycloisomerization and cycloaddition in one pot.

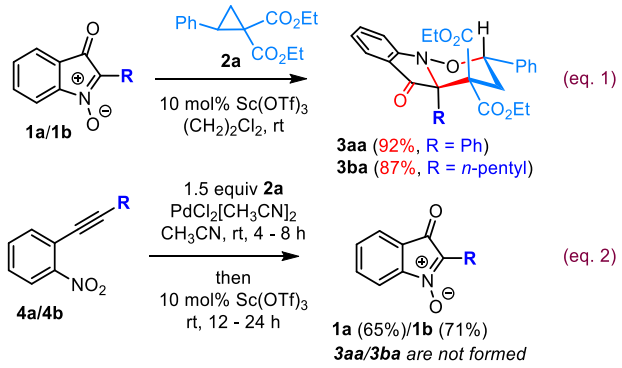

Scheme S1.44: *[3+3]-cycloaddition of 2-phenyl /n-pentyl isatogens* ***1a/1b*** *with DA-cyclopropane* ***2a***

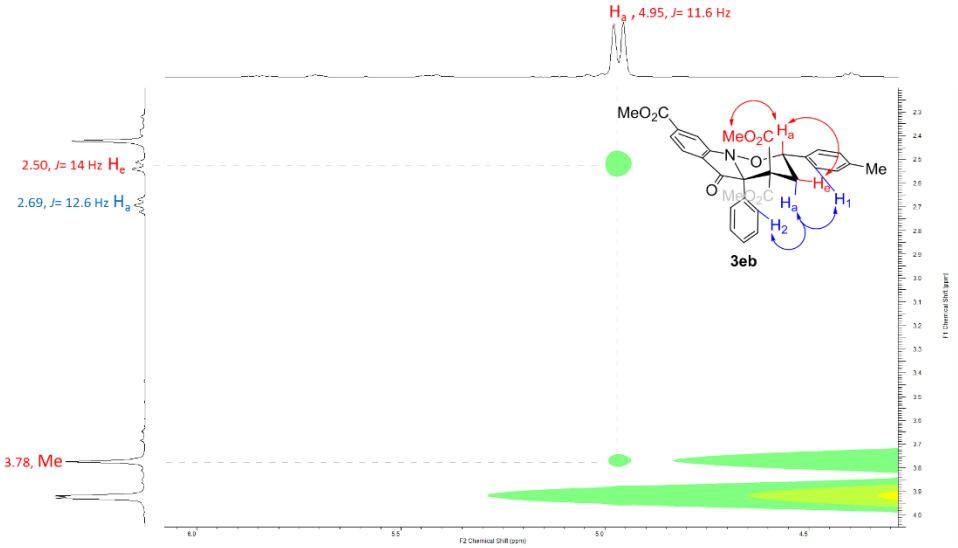

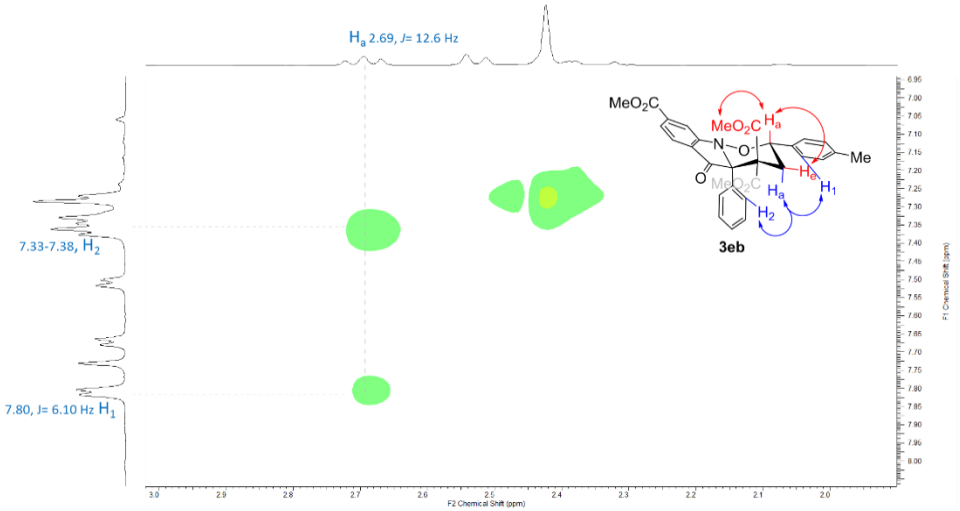

Figure F1.6: *Characteristic through bond and through space interactions that assisted to assign the relative stereochemistry of cycloaddition products*

The nitroalkyne cycloisomerization leading to isatogens has been explored with [Au]- and [Pd]-complexes, though the former has a limitation of requirement of aryl substituent on the other side of alkyne (with simple alkyl substituents, it leads to isomeric anthranil derivatives, see Scheme S1.8 in Introduction section). [Pd]-complexes generally lead to the isatogens (see Scheme S1.10 in Introduction section). Keeping this in mind, the initial studies have been carried out by employing the nitroalkynes **4a/4b** and DA-cyclopropane **2a**. Initial experiments employing $PdCl_2[CH_3CN]_2$ for cycloisomerization and $Sc(OTf)_3$ for cycloaddition have been carried out in acetonitrile at rt. The procedure followed involved the stirring of a solution of nitroalkynes **4a/4b** along with 1.5 equiv of **2a** in the presence of 10 mol% [Pd]-complex in acetonitrile at rt (for 4–10 h), subsequent addition of 10 mol% of $Sc(OTf)_3$ and continued stirring for an additional 12–24 h. As shown in Scheme 1 (eq. 2), in both cases, only corresponding isatogens were isolated. Changing the solvent to dichloromethane hampered the initial cycloisomerization itself. This led us to look at the [Au]-complexes; however, with due consideration of employing only aryl substituted derivatives such as **4b**.

At the outset, $AuCl_3$ has been selected as a catalyst for the nitroalkynes cycloisomerization, given its superior selectivity to provide isatogens over the initially discovered $AuBr_3$ by Yamamoto. Following the prescribed conditions, the cycloisomerization of **4a** has been carried out employing 5 mol% of $AuCl_3$ as a catalyst in CH_2Cl_2 as a solvent at rt. To

our delight, we observed that both nitroalkyne **4a** and cyclopropane **2a** were getting consumed slowly and that the formation of product **3aa** along with the isatogen **1a** took place. The reaction was incomplete even after stirring for 24 h. The product **3aa** was isolated in 48% yield (Table 3, entry 1). The structure of compound were characterized with the help of spectral and analytical data and completely matches with the product in scheme 1 eq. 1. In the ^{13}C NMR of compound **3aa**, the two alkyne carbons of **4a** (at 85.7 and 93.2 ppm) have been replaced with two new quarterly peaks at 71.9 and 193.0 ppm. In addition, benzylic C–H proton of cyclopropane compound **2a** resonating at 32.1 (d) ppm have been replaced with 80.5 (d) ppm in the ^{13}C NMR spectrum of compound **3aa**. These chemical shifts suggested that –CH was connected to the oxygen of nitrone and quaternary peak to the spiro-junction thus indicating a tricyclic system *via* [3+3]-cycloaddition.

Encouraged by this result, initially we looked at the possibility of bringing both cycloisomerization and cycloaddition with $AuCl_3$ alone as catalyst. In this regard, we screened different solvents, different [Au]-complexes and some of the prescribed additives, changing the catalyst from gold to platinum, and increasing the temperature to 60 °C, the results are not encouraging. Only when solvent was switched from dichloromethane to dichloroethane, was the yield improved to 54% with $AuCl_3$ and there was no improvement when the solution was heated to 60 °C in the same solvent. Next, considering the excellent cycloaddition yields of isatogen **1a** with **2a** that we had initially noticed, we looked at the possibility of carrying the [Au]-catalyzed cycloisomerization first and then adding cyclopropane **2a** and $Sc(OTf)_3$ to proceed for the cycloaddition. The results are promising and we obtained the desired **3aa** in 65% yield (Table 3, entry 12). Increasing the temperature of the reaction did not improve the yield. The yield of **3aa** was improved to 71% when the reaction was carried out in the presence of 4Å molecular sieves, at room temperature (Table 3, entry 14).

Table 3: *Optimization of the Reaction Conditions.*[a]

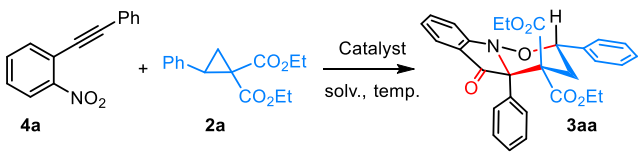

Entry	Cat.1	Additive or Cat.2	Solvent	T (°C)	Yield[b]
1	$AuCl_3$	-	DCM	rt	48%[c]
2	$AuCl_3$	-	1,2-DCE	rt	54%[c]
3	AuCl	-	1,2-DCE	rt	50%[c]
4	$PtCl_2$	-	1,2-DCE	rt	23%[c]
5	$PtCl_4$	-	1,2-DCE	rt	43%[c]
6	$AuCl_3$	-	1,2-DCE	60	55%
7	$AuCl_3$	$AgSbF_6$	1,2-DCE	60	no reaction
8	$AuCl_3$	AgOAc	1,2-DCE	60	42%[c]
9	$AuCl_3$	-	Toluene	rt	no reaction
10	$AuCl_3$	-	Acetonitrile	rt	no reaction
11	$AuCl_3$	-	THF	rt	no reaction
12[d]	$AuCl_3$	$Sc(OTf)_3$	1,2-DCE	rt	65%
13[d]	$AuCl_3$	$Sc(OTf)_3$	1,2-DCE	60	68%
14[d,e]	**$AuCl_3$**	**$Sc(OTf)_3$**	**1,2-DCE**	**rt**	**71%**

[a]*Reaction conditions*: **4a** (0.1 mmol), **2a** (0.15 mmol), catalyst (5 mol %) and additive (10 mol %) in 1.0 mL of distilled solvent for 16 h. [b]Isolated yield after column chromatography. [c]10–35% isatogen recovered. [d]Stepwise addition of DAC and additive or *cat 2*. [e]In presence of 4Å molecular sieves.

Having optimal conditions in hand, the substrate scope of this one-pot cycloisomerization/cycloaddition protocol has been examined by employing different nitroalkynes and DA-cyclopropanes with varying substituents on the aryl rings (Scheme S1.45).The reactions with substrates having electron-donating groups like -Me and -OMe *meta* to the nitro group are smooth, giving the corresponding cycloaddition products **3ca** and **3da** in moderate yields 56% and 74% respectively. Even when there is an electron withdrawing group -CO_2Me, the reaction was facile and provided **3ea** in 75% yield. Next, the nitrotolans having -OMe and -^{t}Bu substituents *para* to the alkyne of pendant aryl ring have been subjected for this

one pot protocol and obtained the corresponding products **3fa** and **3ga** in moderate yields. Later, the scope of DA-cyclopropanes has been explored by employing DA-cyclopropanes **2b**–**2d** that bear different *para*-substituents and the dimethyl 2-(naphthalen-2-yl)cyclopropane-1,1-dicarboxylate (**2e**). In general, the reactions with these four cyclopropanes are smooth and provided the corresponding cycloaddition products in moderate to good yields. In addition, the cycloaddition reactions of 2-^{n}pentylisatogen **1b** has been carried with DA-cyclopropanes **2c** and **2e** to obtain the corresponding cycloaddition products **3bc** and **3be** in 78% and 81% yields.

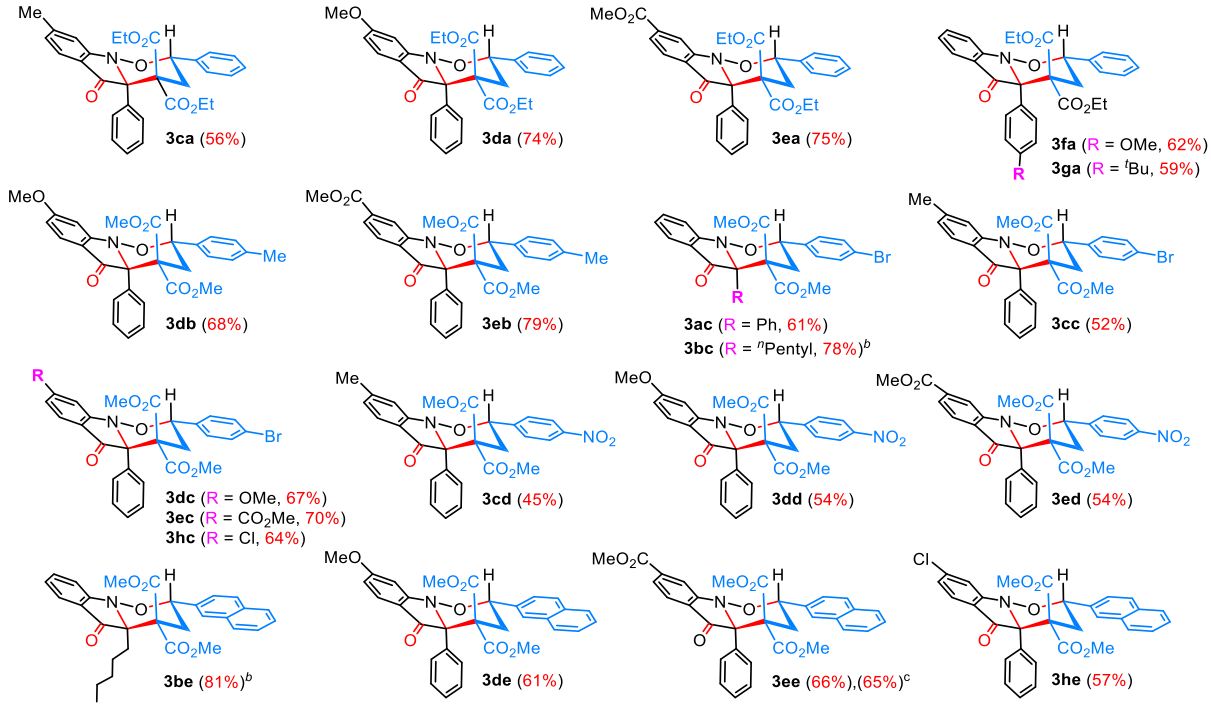

[a]*Reaction conditions*: **4** (1 equiv), **2** (1.5 equiv), $AuCl_3$ (5 mol %) and $Sc(OTf)_3$ (10 mol %); [b]isatogen **2b** was used as the substrate; [c]2 mmol scale, employed 15 mol% $Sc(OTf)_3$.

Scheme S1.45*: Scope of Reactions.*[a]

11.0.1. Competition experiments

As part of expanding the scope of this one-pot protocol, the compatibility of isatogens **1c**–**1e** having functional groups at the propargylic position has been examined (Scheme S1.46). All the three substrates failed to undergo cycloaddition with DA-cyclopropane **2a** under established conditions. The lack of reactivity of substrates **1c**–**1e** may probably be due to the

bulky C2-substituent that hinders the approaching dipolarophile. Interestingly, when the *N*-allyl propargylamide derived nitroakyne **4i** (see Scheme S1.19) was treated with a gold complex along with the **2a**, it was found that after the cycloisomerization, the intermediate isatogen underwent an intramolecular [3+2]-cycloaddition with the pendant allyl group over the intermolecular [3+3]-cycloaddition. On the other hand, when the intermolecular completion experiments were conducted employing equal amounts of electron rich/electron deficient olefins along with DA-cyclopropane **2a**, the [3+3]-cycloaddition dominated the classical [3+2]-cycloaddition of isatogens.

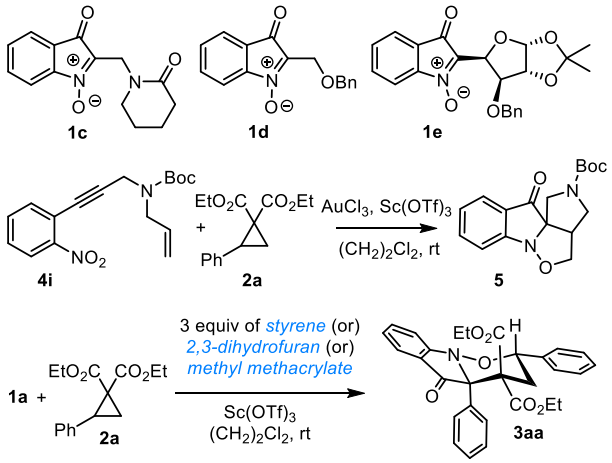

Scheme S1.46: *Limitation of Substituents at C2 and Competition between DA-Cyclopropane and Olefins*

12.0 Conclusion

In conclusion, the [3+3]-cycloaddition of DA-cyclopropanes with isatogens has been examined. In general, the cycloaddition reaction is highly diastereoselective and facile with 2-arylisatogens and also with 2-alkylisatogens. In case of 2-arylisatogens, the preceding Au(III)-catalyzed nitroalkynye cycloisomerization has been successfully combined with the cycloaddition step in one-pot. On the other hand, with 2-alkylisatogens these steps have to be separately conducted and also the cycloaddition is not facile. The functionalized alkyl groups are present at the C2 position of isatogen. Currently, work in the direction of employing this protocol in the synthesis of pseudoindoxyl natural products is under progress.

Experimental Section

General Procedure for one-pot Au[III]-catalyzed nitroalkyne cycloisomerization of 4 and Sc(OTf)$_3$ catalyzed [3+3]*-cycloaddition with DA-cyclopropane 2.*

In general all reactions were carried out employing 50 mg of nitroalkyne **4** or 50 mg of isatogen

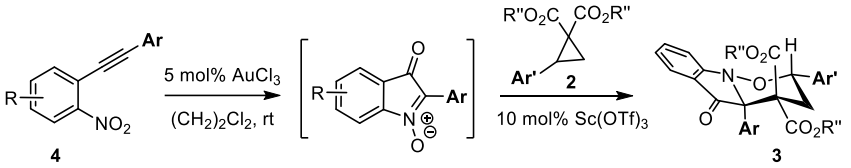

A solution of *o*-nitro alkyne **4** (1 equiv), $AuCl_3$ (5 mol %) in anhydrous 1,2-dichloroethane (4 mL) was stirred at room temperature for 2 h. To this, DA-cyclopropane **2** (1.5 equiv) and 4Å molecular sieves (40 mg) followed by $Sc(OTf)_3$ (10 mol%) were added and continued the stirring for additional 16 h. After completion, as indicated by TLC, the reaction mixture was concentrated under reduced pressure and the resulting crude was purified by column chromatography to procure the cycloadduct **3**.

Procedure for 2 mmol scale

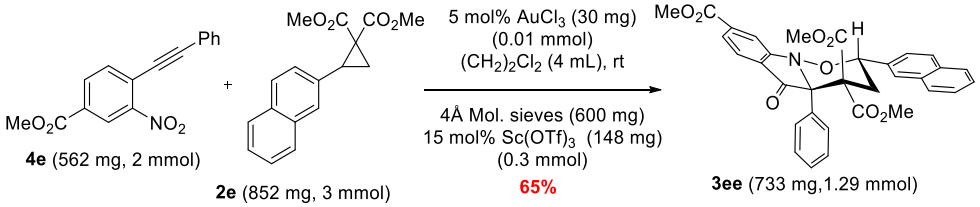

At rt, a solution of nitroalkyne **4e** (562 mg, 2 mmol) in anhydrous 1,2-dichloroethane (20 mL) was treated with $AuCl_3$ (30 mg) and stirred for 2 h. To this, DA-cyclopropane **2e** (852 mg, 3 mmol) and 4Å molecular sieves (600 mg) followed by $Sc(OTf)_3$ (148 mg, 0.3 mmol) were added continued the stirring for additional 8h. Usual workup followed by purification by column chromatography afforded compound **3ee** (733 mg, 65% yield) as yellow syrup.

Diethyl (4aR)-5-*oxo*-2,4a-diphenyl-2,3,4a,5-tetrahydro-4*H*-[1,2]oxazino[2,3-a]indole-4,4-dicarboxylate (3aa)

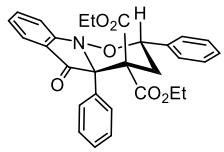

Yellow syrup: yield 77 mg (71%) R_f = 0.4, 15% EtOAc in petroleum ether; IR (neat) ν_{max} 2982, 2928, 1729, 1611, 1476, 1274, 1095, 1016, 950, 753, 700 cm^{-1}; ^1H NMR (400 MHz, $CDCl_3$): δ 1.05–1.19 (t, J = 6.4 Hz, 3H), 1.36 (t, J = 6.4 Hz, 3H), 2.43–2.65 (m, 2H), 4.12–4.26 (m, 2H), 4.26–4.38 (m, 2H), 4.96 (d, J = 10.5 Hz, 1H), 6.74–6.83 (m, 1H), 7.04 (d, J = 7.8 Hz, 1 H), 7.24 (br. s., 3H), 7.39 (br. s., 6H), 7.56 (d, J = 6.9 Hz, 1H), 7.71–7.84 (m, 2H) ppm; ^{13}C NMR (125 MHz, $CDCl_3$): δ 13.8 (q, 2C), 35.7 (t), 50.8 (d), 62.7 (t), 62.3 (t), 62.8 (s), 71.9 (s), 80.5 (d), 108.8 (d), 119.7 (s), 119.8 (d), 124.4 (d), 126.9 (d, 2C), 128.0 (d, 2C), 128.1(d), 128.7 (d, 2C), 128.9 (d), 129.1 (d, 2C) 136.4 (d), 137.9 (s), 154.9 (s), 167.5 (s) 168.6 (s), 193.0 (s) ppm; HRMS (ESI) calcd. for $C_{29}H_{28}NO_6$: 486.1917 $[M+H]^+$; found: 486.1899.

Diethyl (4aS)-5-*oxo*-4a-pentyl-2-phenyl-2,3,4a,5-tetrahydro-4*H*-[1,2]oxazino[2,3-a]indole-4,4-dicarboxylate (3ba)

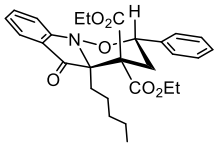

Green syrup: yield 96 mg (87%); R_f = 0.4, 30% EtOAc in petroleum ether; IR (neat) ν_{max} 2957, 1727, 1611, 1456, 1244, 954, 751, 699 cm^{-1}; ^1H NMR (400 MHz, $CDCl_3$): δ 0.71–0.82 (m, 4H), 1.10 (t, J = 7.1 Hz, 3H), 1.14–1.23 (m, 5H), 1.37 (t, J = 7.1 Hz, 3H), 1.81 (dt, J = 8.9, 4.6 Hz, 1 H), 2.34 (dt, J = 13.3, 3.8 Hz, 1H), 2.60 (dd, J = 14.9, 2.3 Hz, 1H), 2.94 (dd, J = 14.9, 11.8 Hz, 1H), 4.08–4.19 (m, 2H), 4.28–4.37 (m, 2H), 4.95 (dd, J = 11.8, 2.3 Hz, 1H), 6.85 (t, J = 7.4 Hz, 1H), 6.94 (d, J = 8.0 Hz, 1H), 7.34–7.53 (m, 6H), 7.65 (d, J = 7.6 Hz, 1H) ppm; ^{13}C NMR (125 MHz, $CDCl_3$): δ 13.7 (q), 13.9 (q), 13.9 (q), 22.2 (t), 23.2 (t), 32.0 (t), 32.9 (t), 36.1 (t), 61.0 (s), 62.0 (t), 62.3 (t), 69.8 (s), 80.8 (d), 108.1 (d), 119.3 (d), 121.4 (s), 123.2 (d), 126.6 (d, 2C), 128.7 (d, 2C), 128.9 (d), 136.3 (d), 137.9 (s), 155.2 (s), 167.9 (s), 168.6 (s), 196.3 (s) ppm; HRMS (ESI) calcd. for $C_{28}H_{34}NO_6$: 480.2381 $[M+H]^+$; found: 480.2372.

Diethyl (4aR)-8-methyl-5-*oxo*-2,4a-diphenyl-2,3,4a,5-tetrahydro-4*H*-[1,2]oxazino[2,3-a]indole-4,4-dicarboxylate (3ca)

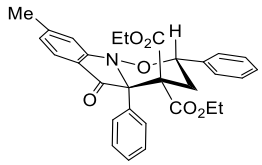

Yellow syrup: yield 59 mg (56%); R_f = 0.3, 15% EtOAc in petroleum ether; IR (neat) ν_{max} 1730, 1617, 1448, 1184, 951, 857, 745, 698, 665 cm^{-1}; ^1H NMR (400 MHz, $CDCl_3$): δ 1.5 (t, J = 7.3 Hz, 3H), 1.36 (t, J = 6.7 Hz, 3H), 2.34 (s, 3H), 2.48 (dd, J = 3.1, 14.6 Hz, 1H), 2.55 (dd, J = 11.6, 14.6 Hz, 1H), 4.17–4.26 (m, 2H), 4.28–4.35 (m, 2H), 4.87 (dd, J = 3.1, 11.6 Hz, 1H), 6.62 (d, J = 7.3 Hz, 1H), 6.89 (s, 1H), 7.25–7.34 (m, 3H), 7.38–7.40 (m, 2H), 7.41 (m, 4H), 7.46 (d, J = 7.9 Hz, 1H), 7.78 (d, J = 7.9 Hz, 1H) ppm; ^{13}C NMR (100 MHz, $CDCl_3$): δ 13.9 (q, 2C), 22.5 (q), 35.8 (t), 62.1 (t), 62.3 (t) ,62.7 (s), 72.1 (s), 80.7 (d), 109.0 (d), 117.3 (s), 121.3 (d), 124.2 (d), 126.9 (d, 2C), 128.0 (d, 2C), 128.0 (d), 128.7 (d, 2C), 128.9 (d), 129.0 (d, 2C), 134.0 (s), 137.8 (s), 148.1 (s), 155.1 (s), 167.5 (s), 168.7 (s), 192.4 (s) ppm; HRMS (ESI) calcd. for $C_{30}H_{30}NO_6$: 500.2068 $[M+H]^+$; found: 500.2068.

Diethyl (4aR)-8-methoxy-5-oxo-2,4a-diphenyl-2,3,4a,5-tetrahydro-4*H*-[1,2]oxazino[2,3-a]indole-4,4-dicarboxylate (3da)

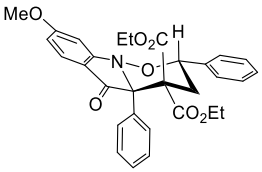

Green syrup: yield 76 mg (74%); R_f = 0.4, 25% EtOAc in petroleum ether; IR (neat) ν_{max} 2982, 1733, 1612, 1495, 1446, 1228, 1097, 953, 854, 823, 755, 700, 665 cm^{-1}; ^1H NMR (400 MHz, $CDCl_3$): δ 1.18 (t, J = 7.6 Hz, 3H), 1.36 (t, J = 7.6 Hz, 3H), 2.45 (dd, J = 2.3, 14.7 Hz, 1H), 2.56 (dd, J = 11.7, 14.7 Hz, 1H), 3.82 (s, 3H), 4.21–4.39 (m, 4H), 4.97 (dd, J = 2.3, 11.7 Hz, 1H), 6.32 (dd, J = 2.3 Hz, 1H), 6.47 (d, J = 2.3 Hz, 1H), 7.26–7.31(m, 3H), 7.40–7.42 (m, 5H), 7.48 (d, J = 8.4, 1H), 7.80 (d, J = 6.9 Hz, 2H) ppm; ^{13}C NMR (100 MHz, $CDCl_3$): δ 13.9 (q), 13.9 (q), 36.0 (t), 55.7 (q), 62.1 (t), 62.3 (t), 62.5 (s), 72.0 (s), 81.1 (d), 91.5 (d), 108.3 (d), 112.3 (s), 126.1 (d), 127.0 (d, 2C), 128.08 (d, 3C), 128.7 (d, 2C), 128.8 (d, 2C), 129.1 (d), 134.2 (s), 137.6 (s), 156.7 (s), 167.3 (s), 167.5 (s), 168.6 (s), 190.9 (s) ppm; HRMS (ESI) calcd. for $C_{30}H_{30}NO_7$: 516.2017 $[M+H]^+$; found: 516.2026.

4,4-diethyl 8-methyl (4aR)-5-*oxo*-2,4a-diphenyl-2,3,4a,5-tetrahydro-4*H*-[1,2]oxazino[2,3-a]indole-4,4,8-tricarboxylate (3ea)

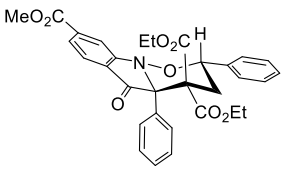

Yellow syrup: yield 73 mg (75%); R_f = 0.4, 25% EtOAc in petroleum ether; IR (neat) ν_{max} 2982, 1722, 1621, 1443, 1243, 1186, 1092, 949, 752, 698 cm^{-1}; ^1H NMR (400 MHz, $CDCl_3$): δ 1.17 (t, J = 6.8 Hz, 3H), 1.39 (t, J = 6.8 Hz, 3H), 2.55 (dd, J = 14.5, 2.3 Hz, 1H), 2.60 (dd, J = 11.4, 14.5 Hz, 1H), 3.90 (s, 3H), 4.16–4.27 (m, 2H), 4.34 (qd, J = 3.2, 7.1 Hz, 2H), 4.97 (dd, J = 2.3, 11.4 Hz, 1H), 7.26–7.32 (m, 3H), 7.42 (s, 5H), 7.45–7.49 (m, 1H), 7.63 (d, J = 7.6 Hz, 1H), 7.69 (s, 1H), 7.78 (dd, J = 2.3, 8.4 Hz, 2H) ppm; ^{13}C NMR (100 MHz, $CDCl_3$): δ 13.9 (q), 13.9 (q), 35.8 (t), 52.5 (q), 62.4 (t), 62.5 (t), 63.1 (s), 72.1 (s), 81.0 (d), 109.2 (d), 120.5 (d), 122.3 (s), 124.3 (d), 126.9 (d, 2C), 128.2 (d, 2C), 128.3 (d), 128.8 (d, 2C), 129.0 (d, 2C), 129.2 (d), 133.1 (s), 137.0 (s), 137.4 (s), 154.1 (s), 166.4 (s), 167.2 (s), 168.6 (s), 192.4 (s) ppm; **HRMS** (ESI) calcd. for $C_{31}H_{29}NNaO_8$: 566.1791 $[M+Na]^+$; found: 566.1778.

Diethyl (4aR)-4a-(4-methoxyphenyl)-5-*oxo*-2-phenyl-2,3,4a,5-tetrahydro-4*H*-[1,2]oxazino[2,3-a]indole-4,4-dicarboxylate (3fa)

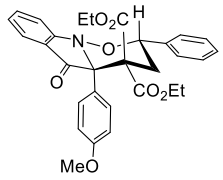

Yellow syrup: yield 63 mg (62%); R_f = 0.4, 25% EtOAc in petroleum ether; IR (neat) ν_{max} 2957, 1728, 1609, 1511, 1249, 951, 893, 746, 697, 664 cm^{-1}; ^1H NMR (400 MHz, $CDCl_3$): δ 1.15 (t, J = 7.2 Hz, 3H), 1.40 (t, J = 7.2 Hz, 3H), 2.52 (dd, J = 14.4, 2.7 Hz, 1H), 2.62 (dd, J = 14.6, 11.7 Hz, 1H), 3.75 (s, 3H), 4.13–4.27 (m, 2H), 4.34 (qd, J = 7.2, 4.2 Hz, 2H), 4.99 (dd, J = 2.7, 11.7 Hz, 1H), 6.76–6.88 (m, 3H), 7.06 (d, J = 8.2 Hz, 1H), 7.36–7.49 (m, 6H), 7.59 (d, J = 7.6 Hz, 1H), 7.71 (d, J = 8.8 Hz, 2H) ppm; ^{13}C NMR (100 MHz, $CDCl_3$): δ 13.8 (q), 13.9 (q), 35.6 (t), 55.1 (q), 62.1 (t), 62.3 (t), 62.6 (s), 71.6 (s), 80.6 (d), 108.8 (d), 113.4 (d, 2C), 119.7 (s), 119.8 (d), 124.4 (d), 125.3 (s), 126.9 (d, 2C), 128.7 (d, 2C), 128.9 (d), 130.5 (d, 2C), 136.3 (d), 137.9 (s), 154.7 (s), 159.2 (s), 167.5 (s), 168.7 (s), 193.1 (s) ppm; HRMS (ESI) calcd. for $C_{30}H_{30}NO_7$: 516.2017 $[M+H]^+$; found: 516.2021.

Diethyl (4aR)-4a-(4-(tert-butyl)phenyl)-5-*oxo*-2-phenyl-2,3,4a,5-tetrahydro-4*H*-[1,2]oxazino [2,3-a]indole-4,4-dicarboxylate (3ga)

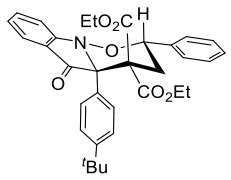

Yellow syrup: yield 57 mg (59%); R_f = 0.2, 20% EtOAc in petroleum ether; IR (neat) ν_{max} 2962, 1730, 1612, 1458, 1241, 1095, 951, 857, 749, 698 cm^{-1}; ^1H NMR (400 MHz, $CDCl_3$): δ 1.13 (t, J = 7.3 Hz, 3H), 1.22 (s, 9H), 1.36 (t, J = 7.3 Hz, 3H), 2.48 (dd, J = 2.6, 14.5 Hz, 1H), 2.58 (dd, J = 11.7, 14.5Hz, 1H), 4.13– 4.23 (m, 2H), 4.27– 4.34 (m, 2H), 4.96 (dd, J = 2.6, 11.7 Hz, 1H), 6.78 (t, J = 7.6 Hz, 1H), 7.03 (d, J = 8.4 Hz, 1H), 7.23 (d, J = 3.8 Hz, 1H), 7.26 (s, 1H), 7.34–7.45 (m, 6H), 7.55 (d, J = 7.6 Hz, 1H), 7.62–7.66 (m, 2H) ppm; ^{13}C NMR (100 MHz, $CDCl_3$): δ 13.9 (q, 2C), 31.2 (s, 3C), 34.4 (s), 35.8 (t), 62.2 (t), 62.3 (t), 62.7 (s), 71.9 (s), 80.8 (d), 108.6 (d), 119.5 (s), 119.6 (d), 124.4 (d) 125.0 (d, 2C), 126.9 (d, 3C), 128.7 (d, 3C), 128.9 (d), 130.4 (s), 136.3 (d), 137.9 (s), 150.7 (s), 154.7 (s), 167.5 (s), 168.7 (s), 193.1 (s) ppm; HRMS (ESI) calcd. for $C_{33}H_{36}NO_6$: 542.2543 $[M+H]^+$; found: 542.2527.

Dimethyl (4aR)-8-methoxy-5-*oxo*-4a-phenyl-2-(p-tolyl)-2,3,4a,5-tetrahydro-4*H*-[1,2]oxazino[2,3-a]indole-4,4-dicarboxylate (3db):

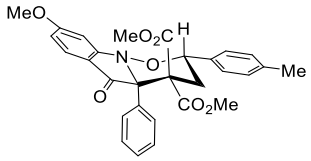

Green syrup: yield 68 mg (68%); R_f = 0.4, 25% EtOAc in petroleum ether; IR (neat) ν_{max} 1735, 1609, 1515, 1495, 1226, 946, 874, 746, 702, 666 cm^{-1}; ^1H NMR (500 MHz, $CDCl_3$): δ 2.38 (s, 3H), 2.41 (dd, J = 2.3, 15.3 Hz, 1H), 2.60 (dd, J = 12.2, 15.3 Hz, 1H), 3.74 (s, 3H), 3.81 (s, 3H), 3.87 (s, 3H), 4.90 (dd, J = 2.3, 12.2 Hz, 1H), 6.32 (dd, J = 2.3, 8.4 Hz, 1H), 6.46 (d, J = 2.3, 1H), 7.26 – 7.31 (m, 5H), 7.32 (s, 2H) 7.47 (d, J = 8.4 Hz, 1H), 7.76 (dd, J = 2.4, 8.4 Hz, 2H) ppm; ^{13}C NMR (125 MHz, $CDCl_3$): δ 21.3 (q), 35.7 (t), 53.1 (q), 53.3 (q), 55.7 (q), 62.5 (s), 71.8 (s), 80.8 (d), 91.5 (d), 108.4 (d), 112.2 (s), 126.1 (d), 127.2 (d, 2C), 128.0 (d, 2C), 128.0 (d), 128.7 (d, 2C), 129.4 (d, 2C), 134.1 (s), 134.3 (s), 139.2 (s), 156.8 (s), 167.3(s), 168.0 (s), 169.1 (s), 190.9 (s) ppm; HRMS (ESI) calcd. for $C_{29}H_{28}NO_7$: 502.1860 $[M+H]^+$; found: 502.1861.

Trimethyl (4aR)-5-*oxo*-4a-phenyl-2-(p-tolyl)-2,3,4a,5-tetrahydro-4*H*-[1,2]oxazino[2,3-a]indole-4,4,8-tricarboxylate (3eb)

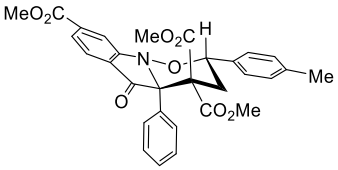

Yellow syrup: yield 74 mg (79%); R_f = 0.4, 30% EtOAc in petroleum ether; IR (neat) ν_{max} 3025, 2953, 1723, 1621, 1435, 1246, 1092, 810, 746, 666 cm^{-1}; ^1H NMR (500 MHz, $CDCl_3$): δ 2.43 (s, 3H), 2.50 (d, J = 14.0 Hz, 1H), 2.69 (t, J = 12.8 Hz, 1H), 3.78 (s, 3H), 3.92 (s, 3H), 3.93 (s, 3H), 4.95 (dd, J =, 11.6 Hz, 1H), 7.28 (d, J = 7.3 Hz, 2H), 7.33–7.38 (m, 5H), 7.50 (d, J = 7.9 Hz, 1H), 7.66 (d, J = 7.9 Hz, 1H), 7.73 (s, 1H), 7.80 (d, J = 6.10 Hz, 2H) ppm; ^{13}C NMR (125 MHz, $CDCl_3$): δ 21.2 (q), 35.4 (t), 52.4 (q), 53.2 (q), 53.4 (q), 63.1 (s), 71.9 (s), 80.8 (d), 109.2 (d), 120.5 (d), 122.1 (s), 124.3 (d), 127.0 (d, 2C), 128.2 (d, 2C), 128.3 (d), 128.9 (d, 2C), 129.4 (d, 2C), 133.0 (s), 134.0 (s), 137.0 (s), 139.3 (s), 154.1 (s), 166.3 (s), 167.6(s), 169. 1 (s), 192.4 (s) ppm; HRMS (ESI) calcd. for $C_{30}H_{27}NNaO_8$: 552.1629 $[M+Na]^+$; found: 552.1631

Dimethyl (4aR)-2-(4-bromophenyl)-5-*oxo*-4a-phenyl-2,3,4a,5-tetrahydro-4*H*-[1,2]oxazino[2,3-a]indole-4,4-dicarboxylate (3ac)

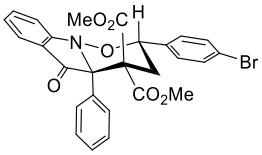

Yellow syrup: yield 73 mg (61%); R_f = 0.4, 15% EtOAc in petroleum ether; IR (neat) ν_{max} 2928, 1735, 1611, 1478, 1246, 1072, 1009, 951, 752, 705 cm^{-1}; ^1H NMR (400 MHz, $CDCl_3$): δ 2.52–2.60 (m, 2H), 3.74 (s, 3H), 3.88 (s, 3H), 4.93 (dd, J = 3.6, 10.9 Hz, 1H), 6.84 (t, J = 7.9 Hz, 1H), 7.09 (t, J = 7.9 Hz, 1H), 7.27 (d, J = 7.3 Hz, 2H), 7.32 (d, J = 8.5, 3 H), 7.46 (t , J = 7.3, 1H), 7.54 (d, J = 8.5 Hz, 2H), 7.59 (d, J = 7.3 Hz, 1H), 7.71 (dd, J = 1.8, 7.94 Hz, 2H) ppm; ^{13}C NMR (100 MHz, $CDCl_3$): δ 35.4 (t), 53.28 (q), 53.43 (q), 62.58 (s), 72.18 (s), 79.75 (d), 109.34 (d), 119.9 (s), 120.5 (d), 123.0 (s), 124.6 (d), 128.1 (d, 2C), 128.3 (d), 128.6 (d, 2C), 129.0 (d, 2C), 132.0 (d, 2C), 133.5 (s), 136.5 (d), 136.8 (s), 154.9 (s), 167.8 (s), 169.0 (s), 193.0 (s) ppm; HRMS (ESI) calcd. for $C_{27}H_{22}BrNNaO_6$: 558.0528 $[M+Na]^+$; found: 558.0515.

Dimethyl (4aS)-2-(4-bromophenyl)-5-*oxo*-4a-pentyl-2,3,4a,5-tetrahydro-4*H*-[1,2]oxazino[2,3-a]indole-4,4-dicarboxylate (3bc)

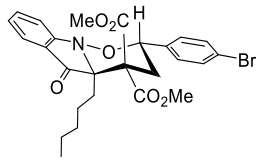

Yellow syrup: yield 95 mg (78%); R_f = 0.4, 15% EtOAc in petroleum ether; IR (neat) ν_{max} 2954, 1734, 1611 1457, 1249, 954, 750, 699 cm^{-1}; ^1H NMR (500 MHz, $CDCl_3$): δ 0.75–0.80 (m, 3H), 1.07–1.25 (m, 6H), 1.79 (td, *J* = 12.7, 4.6 Hz, 1H), 2.23 (dt, *J* = 13.4, 3.7 Hz, 1H), 2.58 (dd, *J* = 2.4, 14.6 Hz, 1H), 2.88 (dd, *J* = 11.6, 14.6 Hz, 1H), 3.66 (s, 3H), 3.87 (s, 3H), 4.92 (dd, *J* = 11.6, 2.4 Hz, 1H), 6.89 (t, *J* = 7.3 Hz, 1H), 6.93 (d, J = 7.9 Hz, 1H), 7.32 (d, *J* = 7.9 Hz, 2H), 7.47 (t, *J* = 7.3 Hz, 1H), 7.57 (d, *J* = 7.9 Hz, 2H), 7.66 (d, *J* = 7.3 Hz, 1H) ppm; ^{13}C NMR (100 MHz, $CDCl_3$): δ 13.9 (q), 22.2 (t), 23.2 (t), 31.9 (t), 32.7 (t), 35.9 (t), 53.1 (d), 53.2 (d), 60.8 (s), 70.0 (s), 79.9 (d), 108.4 (d), 119.8 (d), 121.5 (s), 122.9 (s), 123.3 (d), 128.3 (d, 2C), 131.9 (d, 2C), 136.5 (d), 136.8 (s), 155.2 (s), 168.2 (s), 169.0 (s), 196.2 (s) ppm; HRMS (ESI) calcd. For $C_{26}H_{28}BrNO_6Na$: 552.0922 $[M+Na]^+$; found: 552.0983.

Dimethyl (4aR)-2-(4-bromophenyl)-8-methyl-5-*oxo*-4a-phenyl-2,3,4a,5-tetrahydro-4*H*-[1,2]oxazino[2,3-a]indole-4,4-dicarboxylate (3cc)

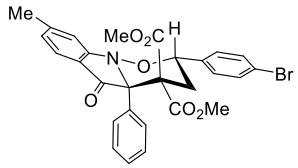

Yellow syrup: yield 60 mg (52%); R_f = 0.4, 30% EtOAc in petroleum ether IR (neat) ν_{max} 2982, 1735, 1615, 1489, 1435, 1246, 959, 943, 821, 751, 703 cm^{-1}; ^1H NMR (400 MHz, $CDCl_3$): δ 2.35 (s, 3H), 2.49–2.53 (m, 2H), 3.74 (s, 3H), 3.87 (s, 3H), 4.93 (d, *J* = 10.3 Hz, 1H), 6.67 (d, *J* = 7.6, 1H), 6.89 (s, 1H), 7.26 –7.28 (m, 3H), 7.29 (d, *J* = 8.0 Hz, 2H), 7.47 (d, *J* = 7.6 Hz, 1H), 7.54 (d, *J* = 7.6 Hz, 2H), 7.70 (d, *J* = 7.0 Hz, 2H) ppm; ^{13}C NMR (100 MHz, $CDCl_3$): δ 22.5 (q), 35.5 (t), 53.2 (q), 53.4 (q), 62.4 (s), 72.4 (s), 79.8 (d), 109.5 (d), 117.6 (s), 121.9 (d), 123.0 (s), 124.4 (d), 128.1 (d,2C), 128.1 (d), 128.5 (d, 2C), 128.9 (d, 2C), 131.9 (d, 2C), 133.7 (s), 136.8 (s), 148.2 (s), 155.2 (s), 167.8 (s), 169.0 (s), 192.3(s) ppm; HRMS (ESI) calcd. for $C_{28}H_{25}BrNO_6$: 550.0860 $[M+H]^+$; found: 550.0858.

Dimethyl (4aR)-2-(4-bromophenyl)-8-methoxy-5-*oxo*-4a-phenyl-2,3,4a,5-tetrahydro-4*H*-[1,2]oxazino[2,3-a]indole-4,4-dicarboxylate (3dc)

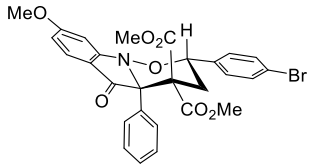

Green syrup: yield 75 mg (67%); R_f = 0.4, 15% EtOAc in petroleum ether; IR (neat) ν_{max} 1735, 1610, 1492, 1437, 1333, 1227, 1072, 947, 873, 822, 750, 703, 666 cm^{-1}; ^1H NMR (400 MHz, $CDCl_3$): δ 2.42 (d, J = 12.8 Hz, 1H), 2.52 (d, J = 12.2 Hz, 1H), 3.75 (s, 3H), 3.83 (s, 3H), 3.87 (s, 3H), 4.92 (d, J = 10.3 Hz, 1H), 6.35 (d, J = 8.5 Hz, 1H), 6.47 (s, 1H), 7.28–7.30 (m, 5H), 7.48 (d, J = 8.5 Hz, 1H), 7.53 (d, J = 7.9 Hz, 2H), 7.72 (d, J = 7.3 Hz, 2H) ppm; ^{13}C NMR (125 MHz, $CDCl_3$): δ 35.7 (t), 53.2 (q), 53.3 (q), 55.7 (q), 62.2 (s), 72.1 (s), 80.2 (d), 92.0 (d), 108.6 (d), 112.5 (s), 123.1 (s), 126.2 (d), 126.3 (d), 128.1 (d, 2C), 128.7 (d, 4C), 132.0 (d, 2C), 133.9 (s), 136.5 (s), 156.7 (s), 167.3 (s), 167.8 (s), 168.9 (s), 190.7 (s) ppm; HRMS (ESI) calcd. for $C_{28}H_{25}BrNO_7$: 566.0809 $[M+H]^+$; found: 566.0812.

Trimethyl (4aR)-2-(4-bromophenyl)-5-*oxo*-4a-phenyl-2,3,4a,5-tetrahydro-4*H*-[1,2]oxazino[2,3-a]indole-4,4,8-tricarboxylate (3ec):

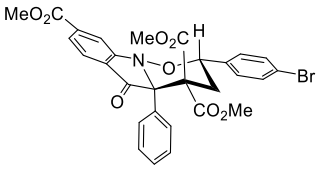

Green syrup: yield 74 mg (70%); R_f = 0.4, 25% EtOAc in petroleum ether; IR (neat) ν_{max} 1722, 1621, 1436, 1246, 1072, 1009, 940, 822, 746, 665 cm^{-1}; ^1H NMR (400 MHz, $CDCl_3$): δ 2.47 (dd, J = 3.1, 14.6 Hz, 1H), 2.53 (dd, J = 11.4, 14.6 Hz, 1H), 3.73 (s, 3H), 3.88 (s, 3H), 3.90 (s, 3H), 4.91 (dd, J = 3.1, 11.4 Hz, 1H), 7.27–7.31 (m, 5H), 7.49 (dd, J = 1.2, 7.8 Hz, 1H), 7.55 (d, J = 8.3 Hz, 2H), 7.63 (dd, J = 0.7, 7.8 Hz, 1H), 7.68–7.72 (m, 3H) ppm; ^{13}C NMR (100 MHz, $CDCl_3$): δ 35.4 (t), 52.5 (q), 53.3 (q), 53.5 (q), 62.9 (s), 72.3 (s), 80.1 (d), 109.6 (d), 121.1 (d), 122.5 (s), 123.2 (s), 124.4 (d), 128.3 (d, 2C), 128.5 (d), 128.6 (d, 2C), 128.8 (d, 2C), 132.0 (d, 2C), 132.9 (s), 136.3 (s), 137.1 (s), 154.2 (s), 166.3 (s), 167.5 (s), 169.0 (s), 192.3 (s) ppm; HRMS (ESI) calcd. for $C_{29}H_{24}BrNNaO_8$: 616.0583 $[M+Na]^+$; found: 616.0568.

Dimethyl (4aR)-2-(4-bromophenyl)-8-chloro-5-*oxo*-4a-phenyl-2,3,4a,5-tetrahydro-4*H*-[1,2]oxazino[2,3-a]indole-4,4-dicarboxylate (3hc)

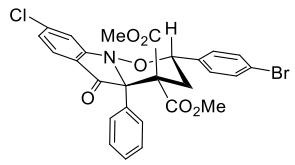

Green syrup: yield 71 mg (64%); R_f = 0.4, 30% EtOAc in petroleum ether; IR (neat) ν_{max} 1734, 1607, 1436, 1245, 1067, 1008, 939, 820, 748, 700 cm^{-1}; ^1H NMR (400 MHz, $CDCl_3$): δ 2.45 (dd, J = 3.4, 14.6 Hz, 1H), 2.53 (dd, J = 11.6, 14.6 Hz, 1H), 3.75 (s, 3H), 3.87 (s, 3H), 4.88 (dd, J = 2.4, 11.6 Hz, 1H), 6.77 (dd, J = 1.8, 8.5 Hz, 1H), 7.03 (d, J = 1.8 Hz, 1H), 7.27–7.33 (m, 5H), 7.49 (d, J = 7.9 Hz, 1H), 7.54 (d, J = 8.5 Hz, 2H), 7.69–7.72 (m, 2H) ppm; ^{13}C NMR (100 MHz, $CDCl_3$): δ 35.4 (t), 53.3 (q), 53.5 (q), 62.7 (s), 71.9 (s), 80.3 (d), 108.5 (d), 117.8 (s), 120.3 (d), 123.3 (s), 125.6 (d), 128.3 (d, 2C), 128.5 (d), 128.6 (d, 2C), 128.7 (d, 2C), 132.0 (d, 2C), 133.1 (s), 136.1 (s), 143.2 (s), 154.8 (s), 167.5 (s), 168.9 (s), 191.3 (s) ppm; HRMS (ESI) calcd. for $C_{27}H_{21}BrClNNaO_6$: 592.0133 $[M+Na]^+$; found: 592.0135.

Dimethyl (4aR)-8-methyl-2-(4-nitrophenyl)-5-*oxo*-4a-phenyl-2,3,4a,5-tetrahydro-4*H*-[1,2]oxazino[2,3-a]indole-4,4-dicarboxylate (3cd)

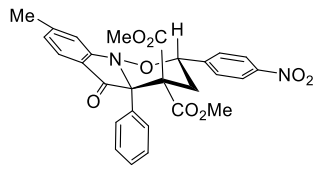

Yellow syrup: yield 49 mg (45%); R_f = 0.4, 25% EtOAc in petroleum ether; IR (neat) ν_{max} 1737, 1615, 1523, 1436, 1347, 1280, 1246, 1092, 850, 751, 702 cm^{-1}; ^1H NMR (400 MHz, $CDCl_3$): δ 2.38 (s, 3H), 2.4 (dd, J = 11.5, 14.6 Hz, 1H), 2.58 (dd, J = 3.6, 14.6 Hz, 1H), 3.75 (s, 3H), 3.87 (s, 3H), 5.09 (dd, J = 3.6, 11.5 Hz, 1H), 6.73 (d, J = 7.8 Hz, 1H), 6.95 (s, 1H), 7.24–7.28 (m, 3H), 7.49 (d, J = 7.8 Hz, 1H), 7.61 (d, J = 8.7 Hz, 2H), 7.65–7.68 (m, 2H), 8.27 (d, J = 9.2 Hz, 2H) ppm; ^{13}C NMR (100 MHz, $CDCl_3$): δ 22.5 (q), 35.5 (t), 53.3 (q), 53.4 (q), 62.2 (s), 73.0 (s), 79.0 (d), 110.6 (d), 118.4 (s), 122.8 (d), 123.9 (d, 2C), 124.5 (d), 127.4 (d, 2C), 128.1(d, 2C), 128.3 (d), 128.8 (d, 2C), 133.5 (s), 145.3 (s), 148.0 (s), 148. 2 (s) 155.4 (s), 167.7 (s), 168. 8 (s), 192. 4 (s) ppm; HRMS (ESI) calcd. for $C_{28}H_{24}N_2NaO_8$: 539.1430 $[M+Na]^+$; found: 539.1420.

Dimethyl (4aR)-8-methoxy-2-(4-nitrophenyl)-5-*oxo*-4a-phenyl-2,3,4a,5-tetrahydro-4*H*-[1,2]oxazino[2,3-a]indole-4,4-dicarboxylate (3dd)

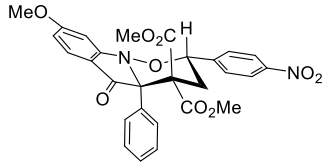

Green syrup: yield 56 mg (54%); R_f = 0.4, 25% EtOAc in petroleum ether; IR (neat) ν_{max} 1737, 1609, 1523, 1440, 1346, 1229, 1095, 950, 849, 751, 701 cm^{-1}; ^1H NMR (400 MHz, $CDCl_3$): δ 2.51–2.53 (m, 2H), 3.77 (s, 3H), 3.84 (s, 3H), 3.87 (s, 3H), 5.09 (dd, J = 3.6, 11.3 Hz, 1H), 6.41 (d, J = 8.5, 1H), 6.51 (s, 1H), 7.31 (d, J = 6.1 Hz, 3H), 7.51 (d, J = 8.5 Hz, 1H), 7.59 (d, J = 7.9 Hz, 2H), 7.68 (d, J = 6.5 Hz, 2H), 8.27 (d, J = 7.9 Hz, 2H) ppm; ^{13}C NMR (125 MHz, $CDCl_3$): δ 36.1 (t), 53.4 (q), 53.6 (q), 55.9 (q), 62.2 (s), 72.8 (s), 79.7 (d), 92.9 (d), 109.2 (d), 113.1 (s), 124.1 (d, 2C), 126.5 (d), 127.7 (d, 2C), 128.3 (d, 2C), 128.4 (d), 128.7 (d, 2C), 133.8 (s), 144.9 (s), 148.2 (s), 156.9 (s), 167.4 (s), 167.8 (s), 168.9 (s), 190.7 (s) ppm; HRMS (ESI) calcd. for $C_{28}H_{25}N_2O_9$: 533.1560 $[M+H]^+$; found: 533.1547.

Trimethyl (4aR)-2-(4-nitrophenyl)-5-*oxo*-4a-phenyl-2,3,4a,5-tetrahydro-4*H*-[1,2]oxazino[2,3-a]indole-4,4,8-tricarboxylate (3ed)

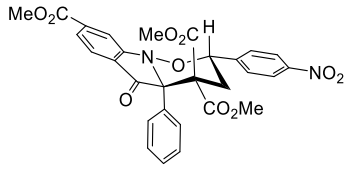

Yellow syrup: yield 54 mg (54%); R_f = 0.4, 25% EtOAc in petroleum ether; IR (neat) ν_{max} 1722, 1621, 1523, 1440, 1246, 1009, 940, 849, 751, 665 cm^{-1}; ^1H NMR (500 MHz, $CDCl_3$): δ 2.48 (dd, J = 11.5, 14.50 Hz 1H), 2.57 (dd, J = 3.1, 14.50 Hz, 1H), 3.76 (s, 3H), 3.90 (s, 3H), 3.91 (s, 3H), 5.08 (dd, J = 3.1, 11.5 Hz, 1H), 7.27–7.31 (m, 3H), 7.55 (dd, J = 1.53, 7.63 Hz, 1H), 7.61 (d, J = 9.16 Hz, 2H) , 7.65 (m, 3H), 7.74 (s, 1H), 8.39 (d, J = 9.16 Hz, 2H) ppm; ^{13}C NMR (125 MHz, $CDCl_3$): δ 35.6 (t), 52.6 (q), 53.4 (q), 53.6 (q), 62.7 (s), 72.8 (s), 79.5 (d), 110.4 (d), 121.9 (d), 123.1 (d), 124.0 (d, 2C), 124.6 (d), 127.5 (d, 2C), 128.4 (d, 2C), 128.6 (s), 128.8 (d, 2C), 132.5 (s), 132.7 (s), 144.6 (s), 148.1 (s), 154.2 (s), 166.2 (s), 167.4 (s), 168.8 (s), 192.1 (s) ppm; HRMS (ESI) calcd. for $C_{29}H_{24}N_2NaO_{10}$: 583.1329 $[M+Na]^+$; found: 583.1321.

Dimethyl (2S,4aS)-2-(naphthalen-2-yl)-5-*oxo*-4a-pentyl-2,3,4a,5-tetrahydro-4*H*-[1,2]oxazino[2,3-a]indole-4,4-dicarboxylate (3be)

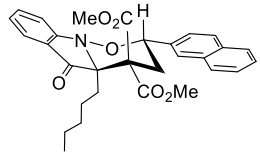

Green syrup: yield 94 mg (81%); R_f = 0.4, 25% EtOAc in petroleum ether; IR (neat) ν_{max} 2954, 1735, 1612, 1457, 1250, 954, 751, 591, 699 cm^{-1}; ^1H NMR (500 MHz, $CDCl_3$): δ 0.77 (t, J = 7.2 Hz, 3H), 1.07– 1.25 (m, 6H), 1.84 (dt, J =12.6, 4.2 Hz, 1H), 2.41 (dd, J = 13.2, 3.8 Hz, 1H), 2.70 (dd, J = 2.7 ,14.9 Hz, 1H), 3.07 (dd, J = 11.8, 14.9 Hz, 1H), 3.69 (s, 3H), 3.88 (s, 3H), 5.13 (dd, J = 2.7, 11.8 Hz, 1H), 6.89 (t, J = 7.4 Hz, 1H), 6.99 (d, J = 8.4 Hz, 1H), 7.48 (t, J = 7.6 Hz, 1H), 7.52–7.62 (m, 3H), 7.68 (d, J = 7.6 Hz, 1H), 7.85–7.99 (m, 4H) ppm; ^{13}C NMR (125 MHz, $CDCl_3$): δ 13.9 (q), 22.2 (t), 23.2 (t), 31.9 (t), 32.8 (t), 35.9 (t), 53.1 (t), 53.2 (t), 61.0 (s), 70.1 (s), 80.7 (d), 108.3 (d), 119.6 (d), 121.5 (s), 123.3 (d), 124.2 (d), 126.0 (d), 126.5 (d), 126.6 (d), 127.8 (d), 128.1 (d), 128.6 (d), 133.1 (s), 133.5 (s), 135.1 (s), 136.5 (d), 155.3 (s), 168.3 (s), 169.1 (s), 196.4 (s) ppm; HRMS (ESI) calcd. For $C_{30}H_{31}NO_6Na$: 524.2044 $[M+Na]^+$; found: 524.2037.

Dimethyl (2S,4aR)-8-methoxy-2-(naphthalen-2-yl)-5-*oxo*-4a-phenyl-2,3,4a,5-tetrahydro-4*H*-[1,2]oxazino[2,3-a]indole-4,4-dicarboxylate (3de)

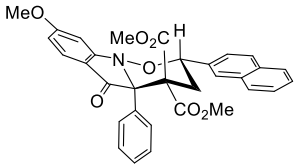

Yellow syrup: yield 65 mg (61%); R_f = 0.4, 25% EtOAc in petroleum ether; IR (neat) ν_{max} 1736, 1611, 1437, 1228, 1095, 946, 821, 750, 703 cm^{-1}; ^1H NMR (500 MHz, $CDCl_3$): δ 2.54 (d, J = 14.5 Hz, 1H), 2.73 (t, J = 12.6 Hz, 1H), 3.79 (s, 3H), 3.82 (s, 3H), 3.88 (s, 3H), 5.13 (d, J = 11.4 Hz, 1H), 6.36 (d, J = 7.6 Hz, 1H), 6.51 (s, 1H), 7.29–7.33 (m, 3H), 7.52 (s, 4H), 7.82 (d, J = 6.5 Hz, 2H), 7.85–7.89 (m, 4H) ppm; ^{13}C NMR (100 MHz, $CDCl_3$): δ 35.7 (t), 53.2 (q), 53.3(q), 55.7 (q), 62.5 (s), 72.0 (s), 81.0 (d), 91.8 (d), 108.5 (d), 112.4 (s),124.4 (d), 126.2 (d), 126.5 (d), 126.6 (d), 126.7 (d), 127.7 (d), 128.1 (d, 2C), 128.2 (d, 2C), 128.6 (d), 128.8 (d, 2C), 133.0 (s), 133.5 (s), 134.1 (s), 134.7 (s), 156.8 (s), 167.3(s), 167.9 (s), 169.1 (s), 191.0 (s) ppm; HRMS (ESI) calcd. for: $C_{32}H_{28}NO_7$: 538.1866 $[M+H]^+$; found: 538.1854.

Trimethyl (2S,4aR)-2-(naphthalen-2-yl)-5-*oxo*-4a-phenyl-2,3,4a,5-tetrahydro-4*H*-[1,2]oxazino[2,3-a]indole-4,4,8-tricarboxylate (3ee)

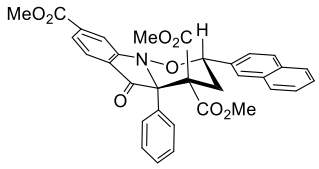

Yellow syrup: yield 66 mg (66%); R_f = 0.3, 25% EtOAc in petroleum ether; IR (neat) ν_{max} 1725,1621, 1437, 1214, 1094, 958, 816, 744, 666 cm^{-1}; ^1H NMR (400 MHz, $CDCl_3$): δ 2.59 (d, J= 14.6 Hz, 1H), 2.73 (t, J = 12.2 Hz, 1H), 3.77 (s, 3H), 3.89 (s, 6H), 5.12 (d, J = 11.6 Hz, 1H), 7.34 (d, J = 6.1 Hz, 3H), 7.49 (d, J = 8.5 Hz, 1H), 7.53–7.58 (m, 3H), 7.64 (d, J = 7.9 Hz, 1H), 7.73 (s, 1H), 7.79 (d, J = 6.1 Hz, 2H), 7.90–7.92 (m, 4H) ppm; ^{13}C NMR (100 MHz, $CDCl_3$): δ 35.5 (t), 52.5 (q), 53.3 (q), 53.5 (q), 63.2 (s), 72.2 (s), 81.0 (d), 109.5 (d), 120.8 (d), 122.4 (s), 124.4 (d), 124.5 (d), 126.4 (d), 126.6 (d), 126.7 (d), 127.8 (d, 2C), 128.1 (d), 128.2 (d), 128.4 (d), 128.7 (d), 128.9 (d, 2C), 133.0 (s), 133.1 (s), 133.6 (s), 134.5 (s), 137.1 (s), 154.2 (s), 166.3 (s), 167.6 (s), 169.1 (s), 192.8 (s) ppm; HRMS (ESI) calcd. for $C_{33}H_{28}NO_8$: 566.1809 $[M+H]^+$; found: 566.1812.

Dimethyl (2S,4aR)-8-chloro-2-(naphthalen-2-yl)-5-*oxo*-4a-phenyl-2,3,4a,5-tetrahydro-4*H*-[1,2]oxazino[2,3-a]indole-4,4-dicarboxylate (3he)

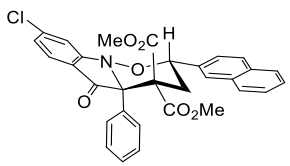

Yellow syrup: yield 60 mg (57%); R_f = 0.4, 25% EtOAc in petroleum ether; IR (neat) ν_{max} 1780, 1734, 1607, 1436, 1245, 1094, 938, 818, 746, 701, 666 cm^{-1}; ^1H NMR (500 MHz, $CDCl_3$): δ 2.56 (d, J = 14.6 Hz, 1H), 2.73 (t, J = 13.4 Hz, 1H), 3.79 (s, 3H), 3.89 (s, 3H), 5.09 (d, J = 11.6 Hz, 1H), 6.76 (d, J = 7.9 Hz, 1H), 7.07 (s, 1H), 7.34 (d, J = 6.7 Hz, 3H), 7.51–7.54 (m, 4H), 7.78 (d, J = 6.7 Hz, 2H), 7.86–7.92 (m, 4H) ppm; ^{13}C NMR (100 MHz, $CDCl_3$): δ 35.3 (t), 53.3 (q), 53.5 (q), 62.9 (s), 71.7 (s), 81.0 (d), 108.3 (d), 117.6 (s), 120.1 (d), 124.3 (d), 125.5 (d), 126.5 (d), 126.6 (d), 126.8 (d), 127.8 (d), 128.1(d), 128.7 (d, 2C), 128.4(d), 128.6 (d), 128.7 (d, 2C), 133.0 (s), 133.2 (s), 133.6 (s), 134.3 (s), 143.2 (s), 154.8 (s), 167.6 (s), 169.1 (s), 191.6(s) ppm; HRMS (ESI) calcd. for: $C_{31}H_{25}ClNO_6$: 542.1365 $[M+H]^+$; found: 542.1379.

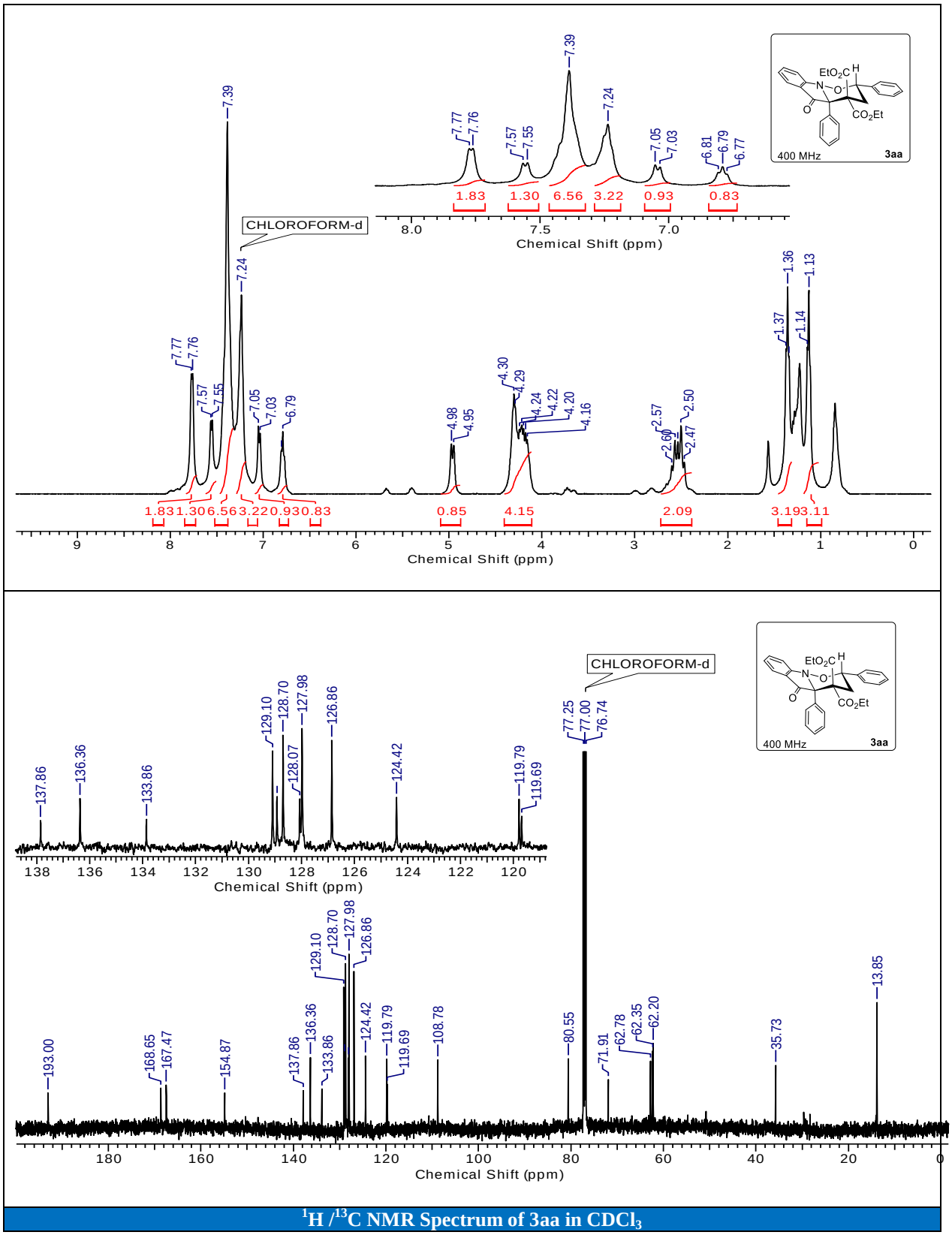

^{1}H /^{13}C NMR Spectrum of 3aa in $CDCl_3$

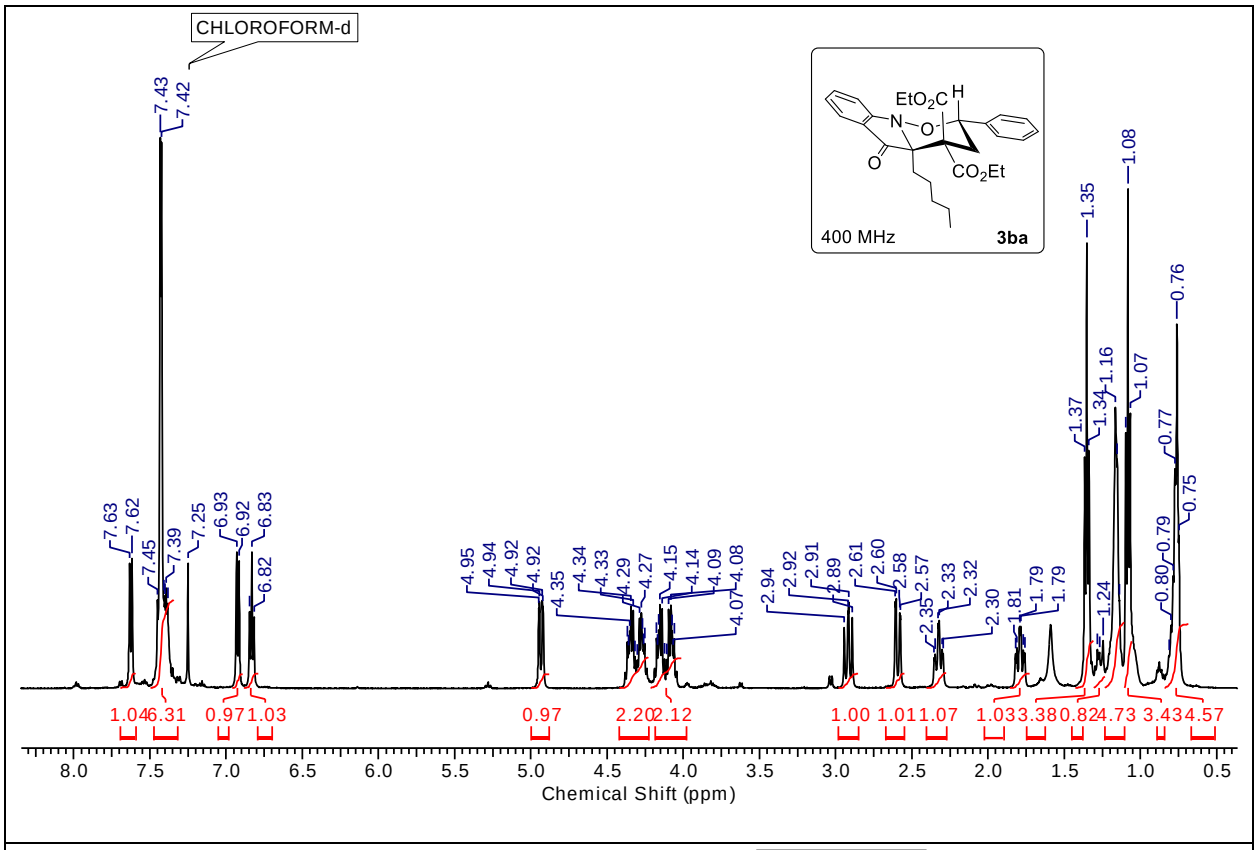

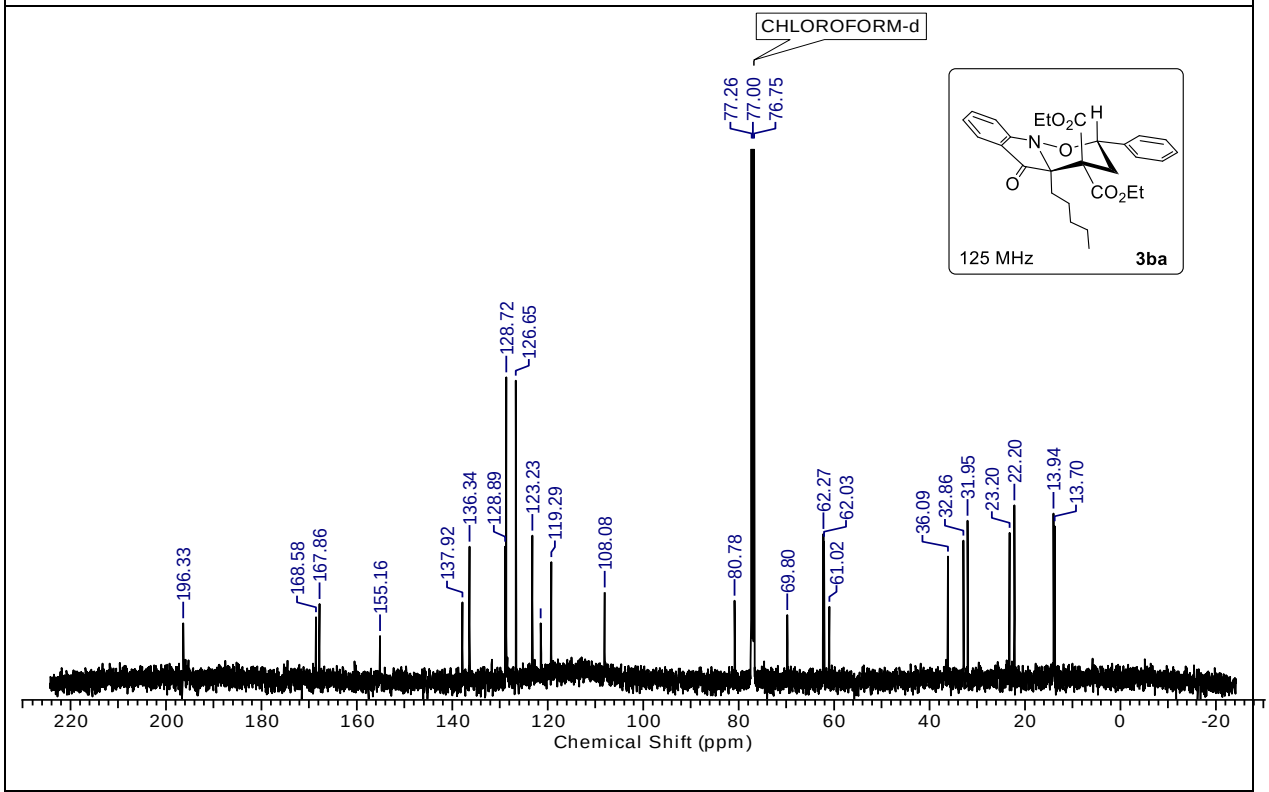

^{1}H /^{13}C NMR Spectrum of 3ba in $CDCl_3$

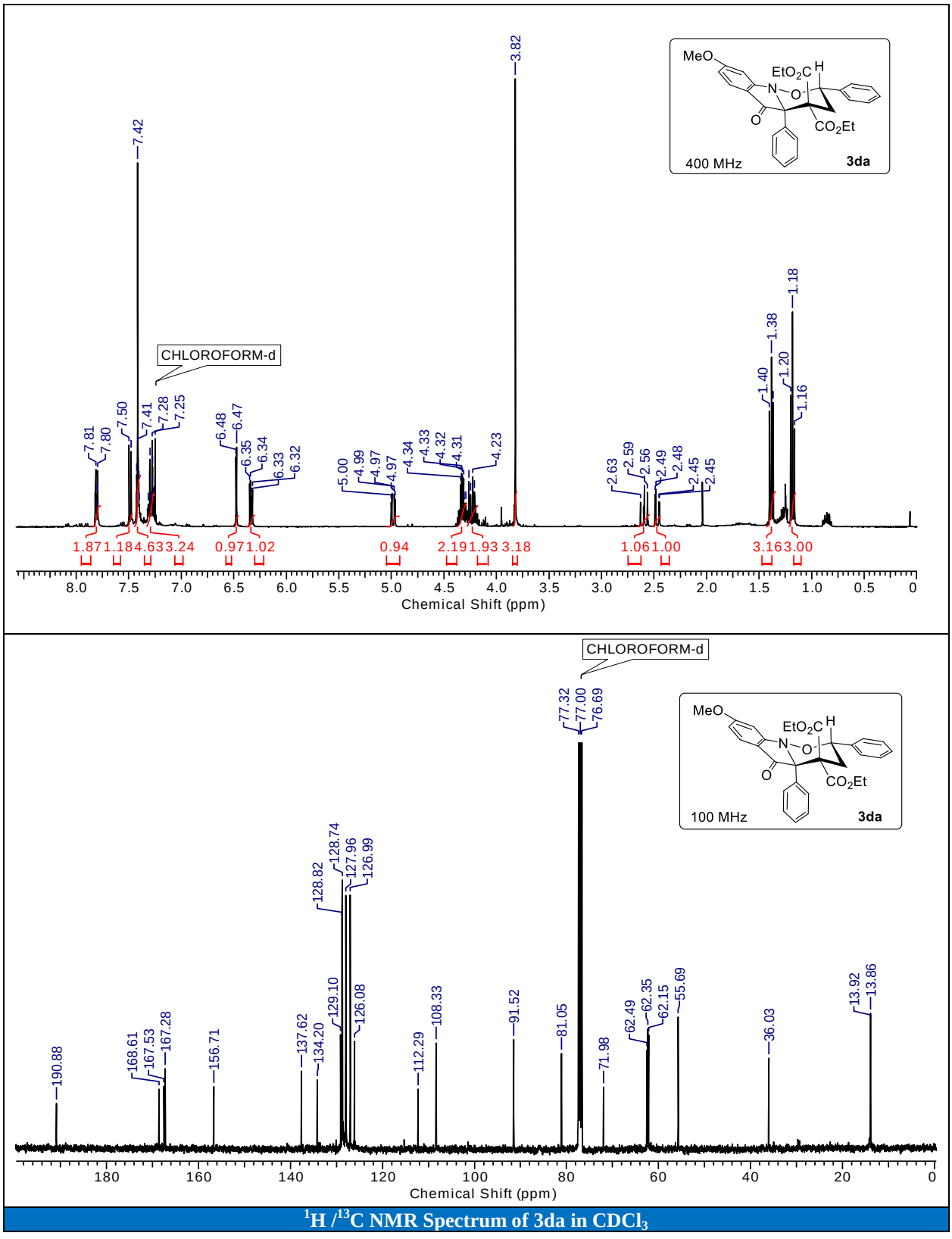

^{1}H /^{13}C NMR Spectrum of 3da in $CDCl_3$

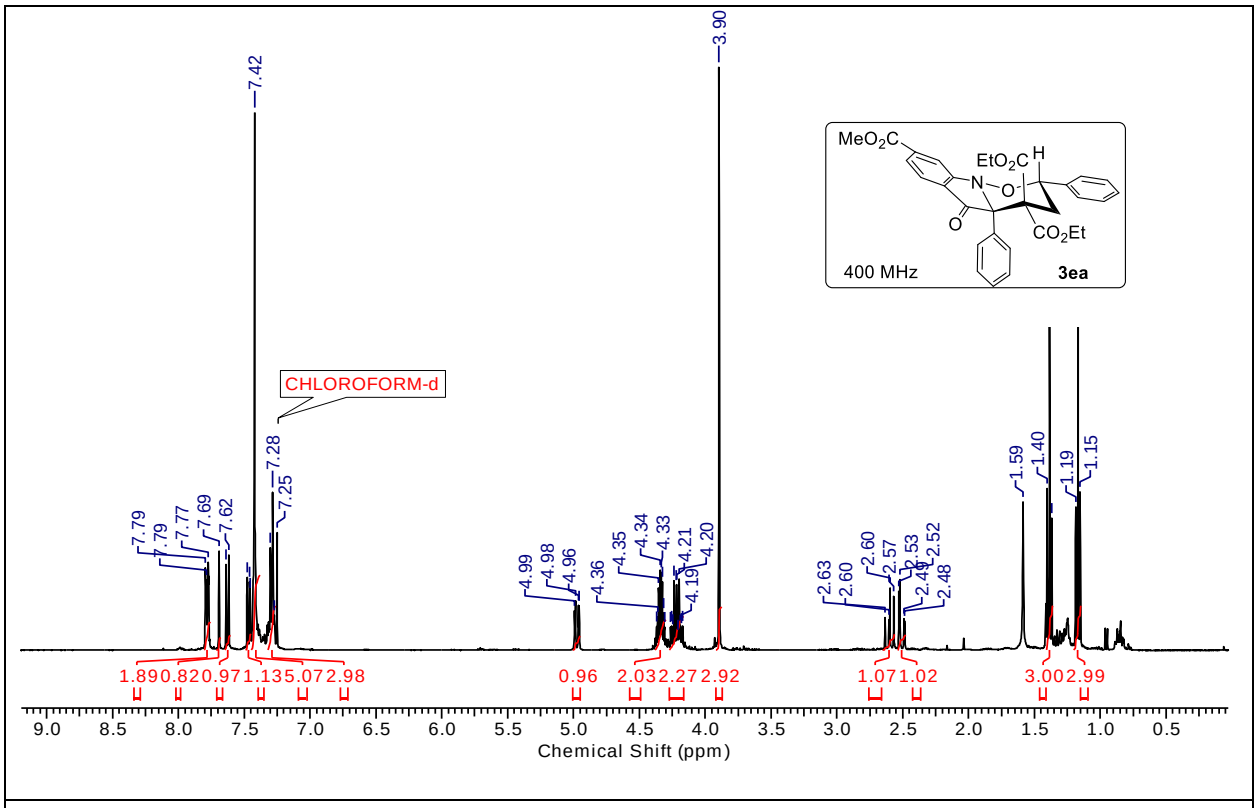

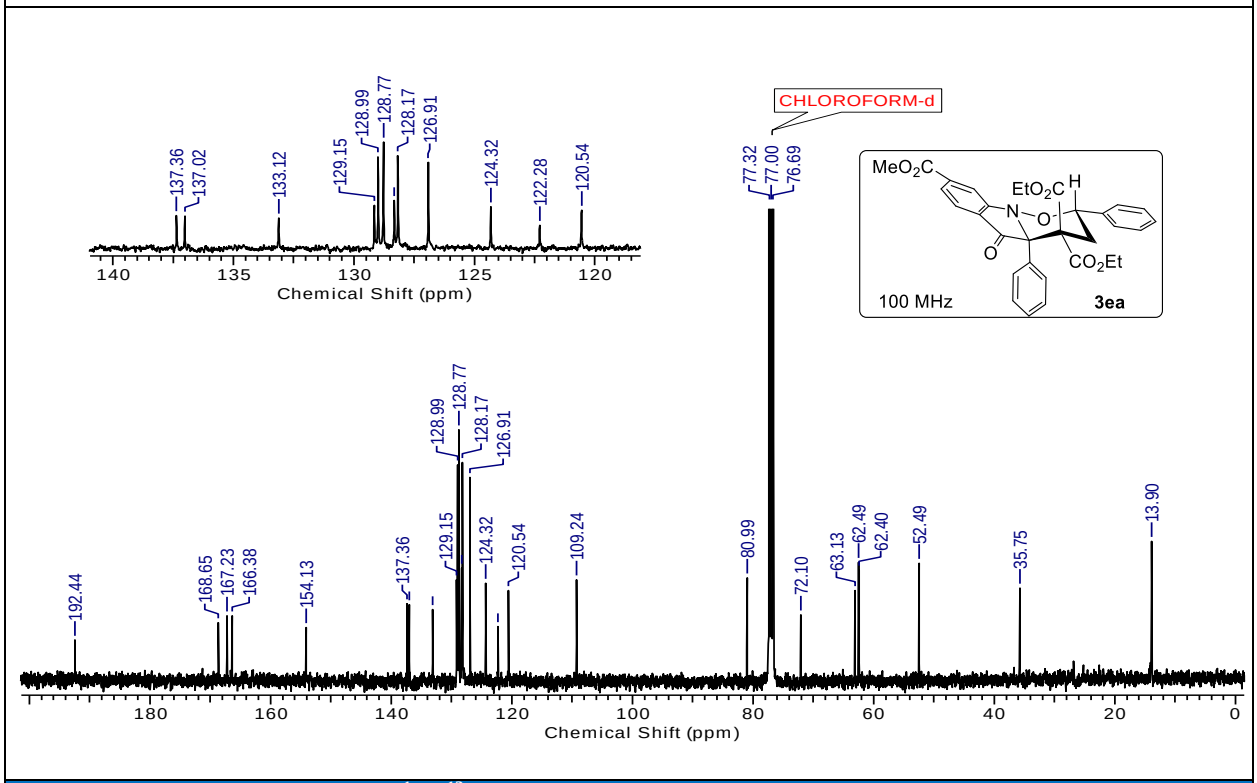

^{1}H /^{13}C NMR Spectrum of 3ea in $CDCl_3$

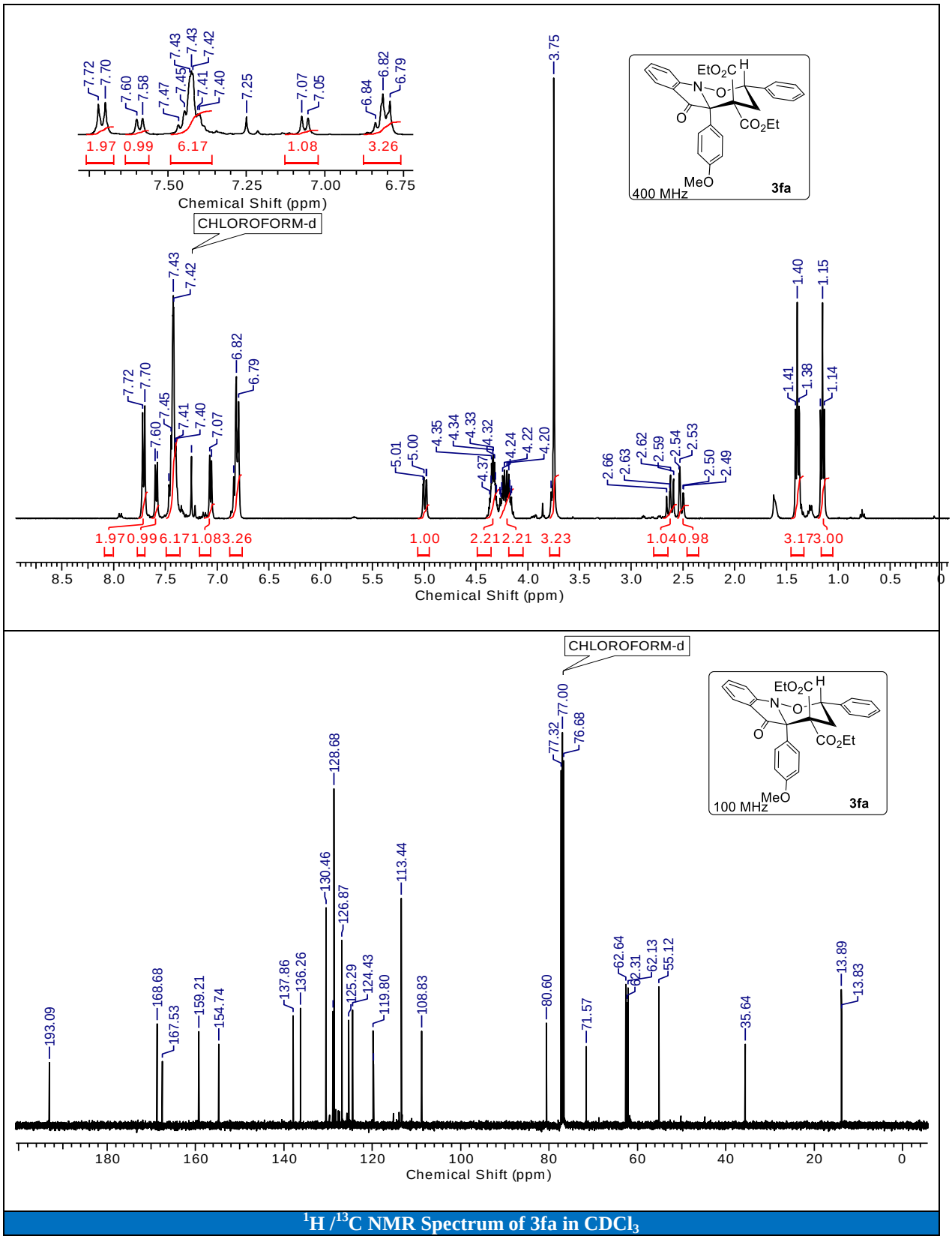

^{1}H /^{13}C NMR Spectrum of 3fa in $CDCl_3$

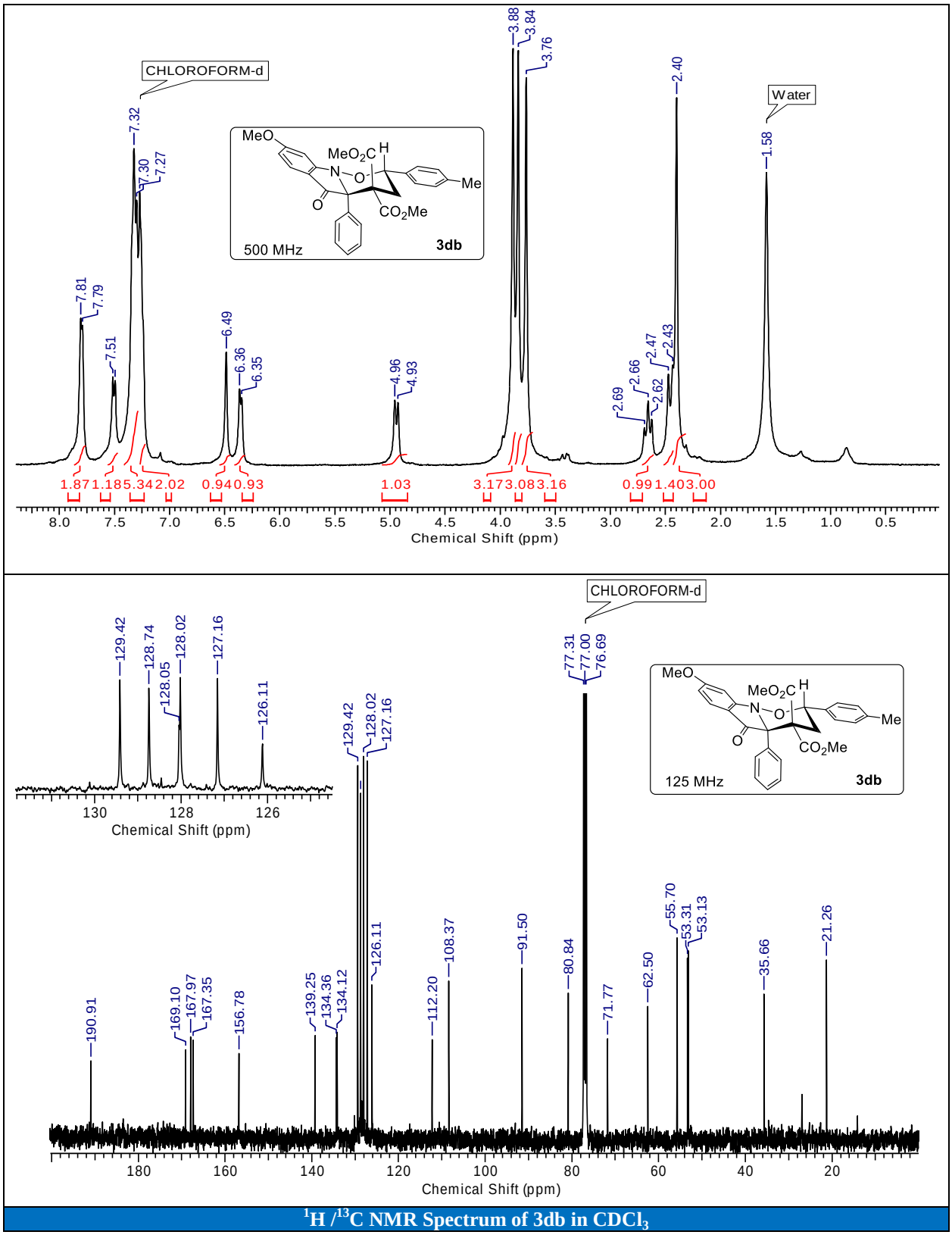

^{1}H /^{13}C NMR Spectrum of 3db in $CDCl_3$

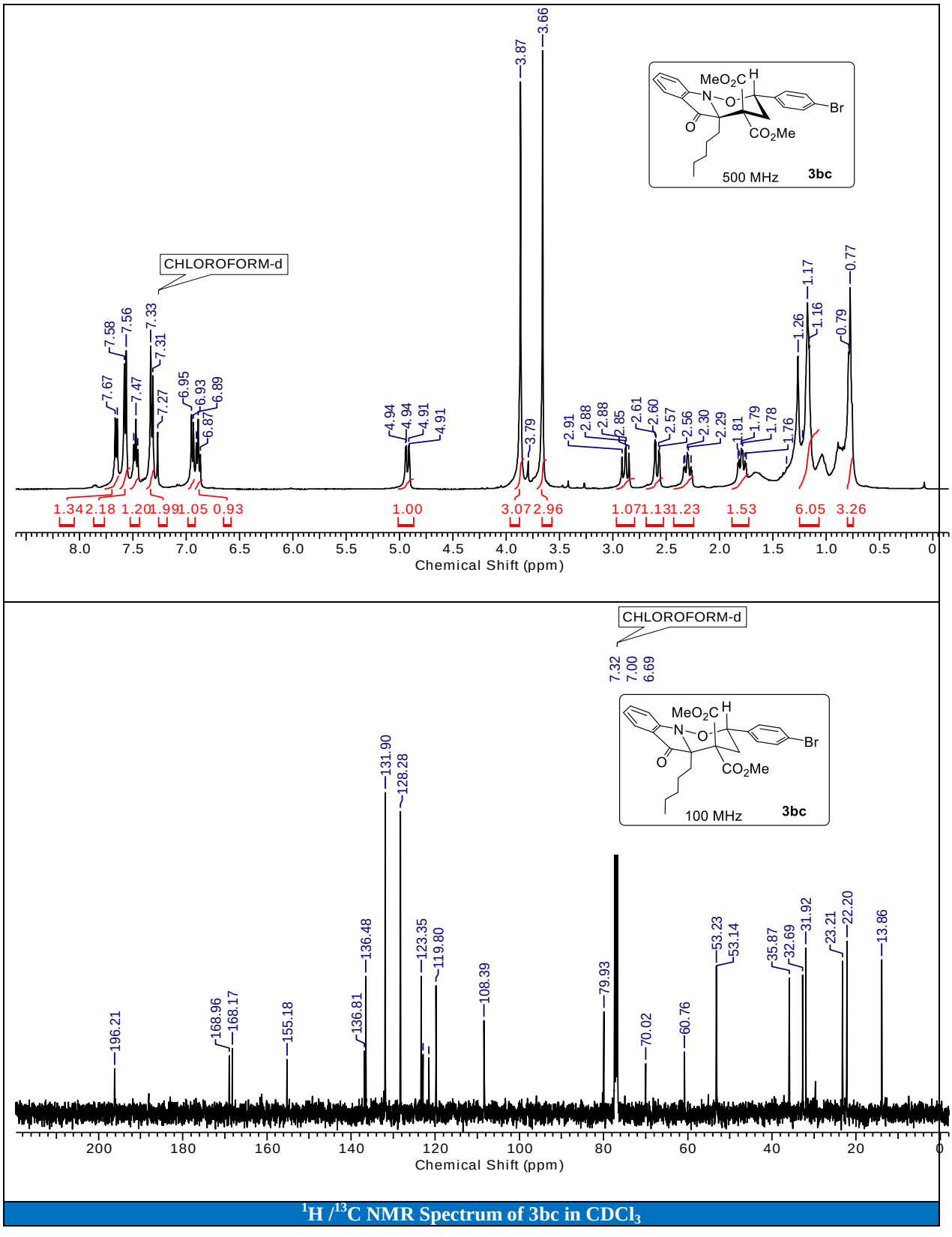

^{1}H /^{13}C NMR Spectrum of 3bc in $CDCl_3$

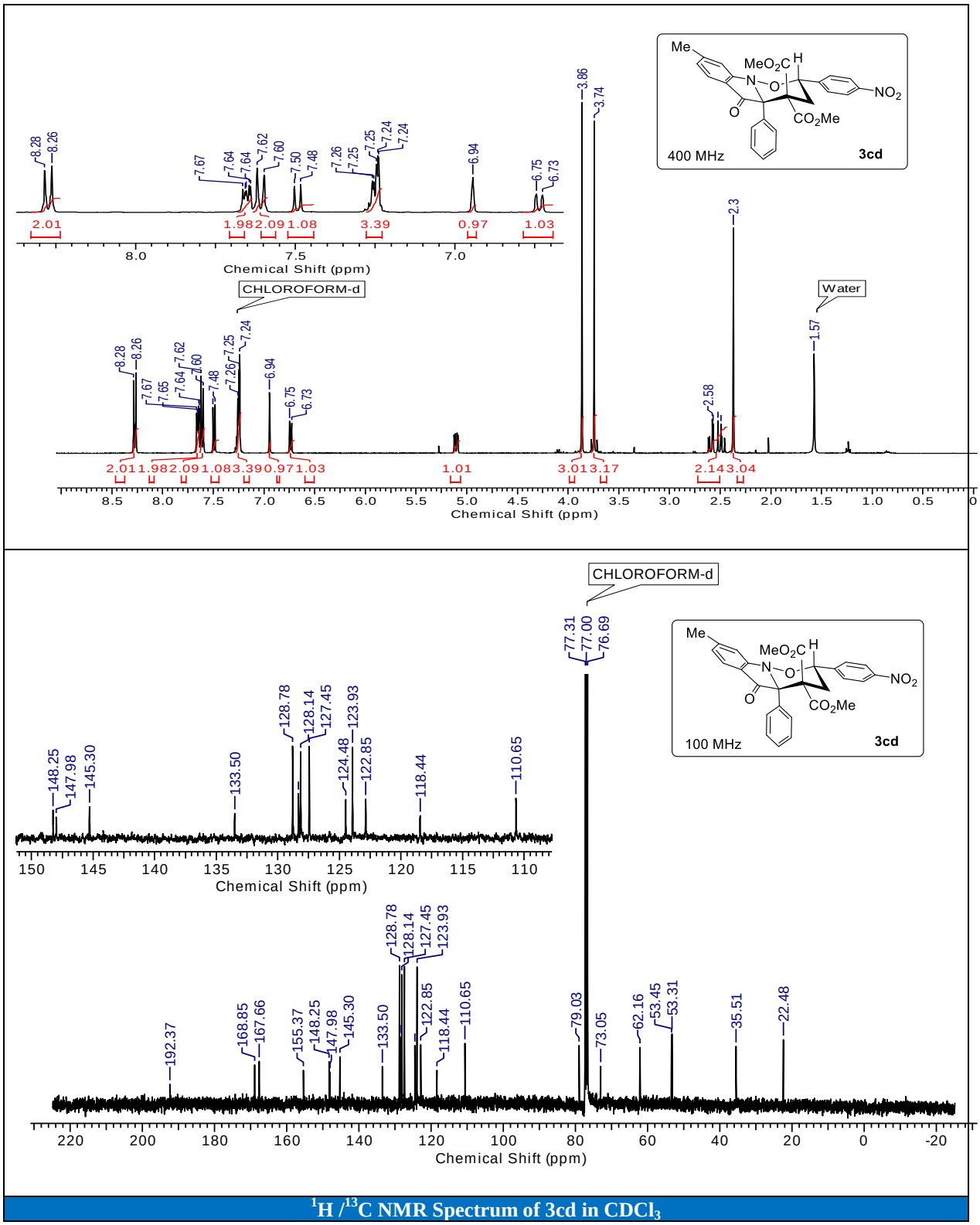

^{1}H /^{13}C NMR Spectrum of 3cd in $CDCl_3$

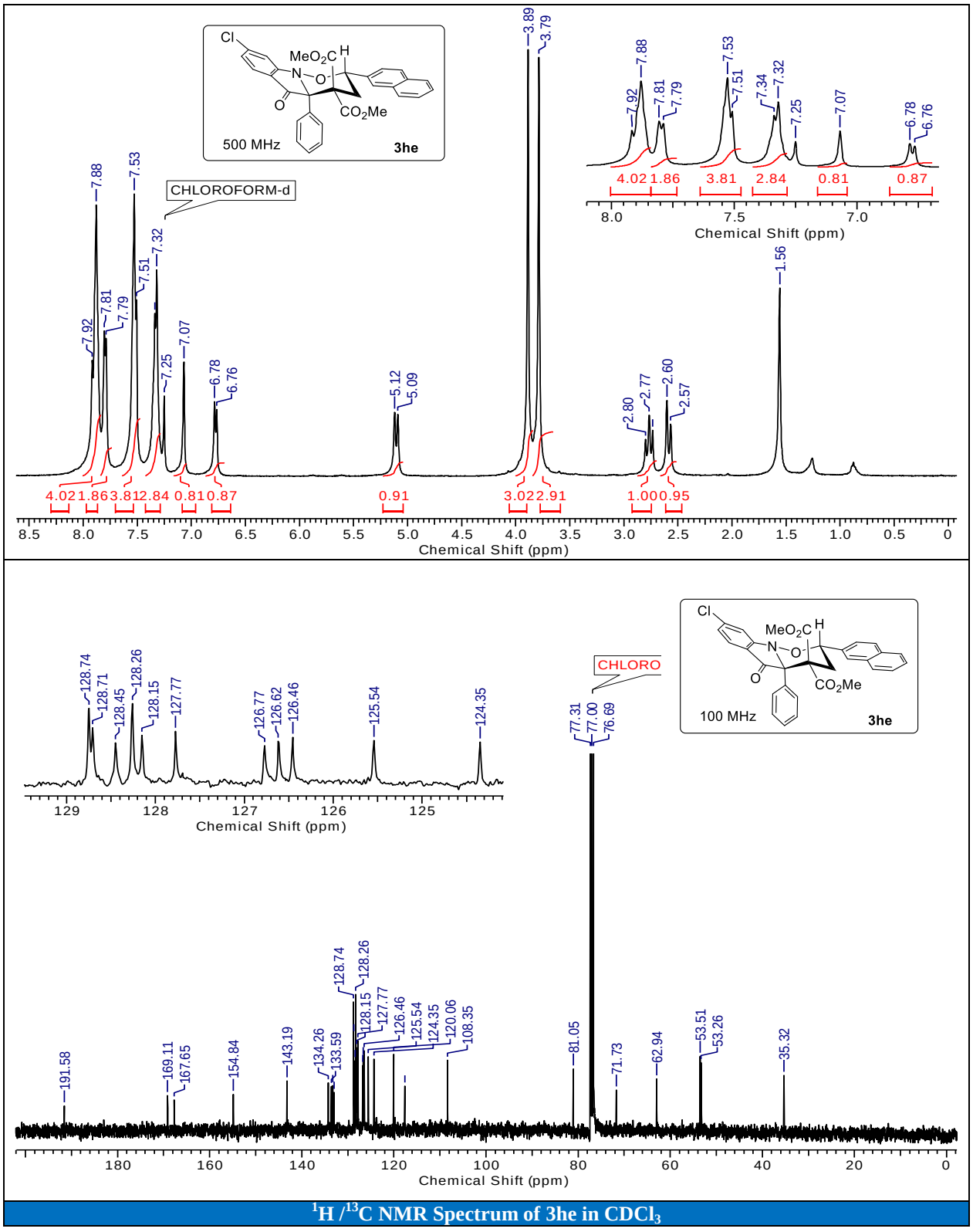

^{1}H /^{13}C NMR Spectrum of 3he in $CDCl_3$

1) a) Steyn, P. S. *Tetrahedron Lett.* **1971**, 3331. b) Burnell, R. H.; Chapelle, A.; Khalil, M. F. *Can. J. Chem.* **1974**, *52*, 2327. c) Phillipson, J. D.; Supavita, N. *Phytochemistry* **1983**, *22*, 1809. d) Bhakuni, D. S.; Silva, M.; Matlin, S.A.; Sammes, P.G. *Phytochemistry* **1976**, *15*, 574. e) Birch, J.; Wright, J. J. *J. Chem. Soc., Chem. Commun.* **1969**, 644.

2) Baeyer, A.; Drewsen, V. *Berichte der deutschen chemischen Gesellschaft*, **1882**, *15*, 2856.

3) a) Witkop, B.; Patrick, J. B. *J. Am. Chem. Soc.* **1951**, *73*, 2188. b) Dolby, L. J.; Rodia, R. M. *J. Org. Chem.* **1970**, *35*, 1493. (c) Saito, I.; Imuta, M.; Matsuura, T. *Chem. Lett.* **1972**, 1173. d) Berti, C.; Greci, L.; Andruzzi, R.; Trazza, A. *J. Org. Chem.* **1982**, *47*, 4895. e) Movassaghi, M.; Schmidt, M. A.; Ashenhurst, J. A. *Org. Lett.* **2008**, *10*, 4009.

4) a) Finch, N.; Taylor, W. I. *J. Am. Chem. Soc*. **1962**, *84*, 3871. b) Hutchison, A. J.; Kishi, Y. *J. Am. Chem. Soc*. **1979**, *101*, 6786. c) Stoermer, D.; Heathcock, C. *J. Org. Chem*. **1993**, *58*, 564. (d) Baran, P. S.; Corey, E. J. *J. Am. Chem. Soc*. **2002**, *124*, 7904. e) Schneekloth, J. S.; Kim, J.; Sorensen, E. J. *Tetrahedron* **2009**, *65*, 3096. (f) Kim, J.; Schneekloth, J. S.; Sorensen, E. J. *Chem. Sci*. **2012**, *3*, 2849.

5) a) Han, S.; Movassaghi, M. *J. Am. Chem. Soc*. **2011**, *133*, 10768. b) Qi, X.; Tambar, U. K. *J. Am. Chem. Soc.* **2011**, *133*, 10050.

6) Ji, Y.; He, X.; Peng, C.; Huang, W. *Org. Biomol. Chem.* **2019**, *17*, 2850.

7) Selected reviews on DA-cyclopropanes in annulation reaction, see: a) Mel'nikov, M.; Budynina, E.; Ivanovaa, O.; Trushkova, I. *Mendeleev Commun*. **2011**, *21*, 293. b) Schneider, T.; Kaschel, J.; Werz, D. *Angew. Chem. Int. Ed*. **2014**, *53*, 5504. c) Grover, H.; Emmett, M.; Kerr, M. A. *Org. Biomol. Chem*. **2015**, *13*, 655.

8) Selected reports on DA-cyclopropane cycloaddition reactions: a) Yu, M.; Pagenkopf, B. L. *J. Am. Chem. Soc.* **2003**, *125*, 8122. b) Carson, C. A.; Kerr, M. A. *J. Org. Chem.* **2005**, *70*, 8242. c) Korotkov, V. S.; Larionov, O. V.; Hofmeister, A.; Magull, J.; de Meijere, A. *J. Org. Chem.* **2007**, *72*, 7504. d) Pohlhaus, P. D.; Sanders, S. D.; Parsons, A. T.; Li, W.; Johnson, J. S. *J. Am. Chem. Soc.* **2008**, *130*, 8642. e) Perreault, C.; Goudreau, S. R.; Zimmer, L. E.; Charette, A. B. *Org.Lett.* **2008**, *10*, 689. f) Goldberg, A. F. G.; O'Connor, N.; Craig II, R. A.; Stoltz, B. M. *Org. Lett*. **2012**, *14*, 5314. g) Zhang, H. H.; Luo, Y.; Wang, H.; Chen, W.; Xu, P.F. *Org. Lett.* **2014**, *16*, 4896. h) Garve, L.; Pawliczek, M.; Jones, P.; Werz, D. *Chem. Eur. J.* **2016**, *22*, 521. i) Preindl, J.; Chakrabarty, S.; Waser, J. *Chem. Sci.* **2017**, *8*, 7112. j) Matsumoto, Y.; Nakatake, D.; Yazaki R.; Ohshima, T. *Chem. Eur. J. 2018*, **24**, 6062–6066.

k) Augustin, A.; Busse, M.; Jones, P.; Werz, D. *Org. Lett.* **2018**, *20*, 820. l) Chagarovskiy, A.; Vasin, V.; Kuznetsov, V.; Trushkov, I. *Angew. Chem. Int. Ed*. **2018**, *57*, 10338. m) Varshnaya. R.; Banerjee, P. *J. Org. Chem*. **2019**, *84*, 1614. n) Petzold, M.; Jones, P.; Werz, D. *Angew. Chem. Int. Ed.* **2019**, *58*, 6225. (o) Xu, P.; Yu, J.; Zhou, F.; Zhou, J. *ACS Catal.* **2019**, *9*, 1820.

9) a) Carson, C. A.; Kerr, M. A. *Angew. Chem. Int. Ed.* **2006**, *45*, 6560. b) Nakadomarin, A.; Young, I. S.; Kerr, M. A. *J. Am. Chem. Soc*. **2007**, *129*, 1465. c) Morales, C.; Pagenkopf, B. *Org. Lett.* **2008**, *10*, 157. d) Karadeolian, A.; Kerr, M. A. *Angew. Chem., Int. Ed.* **2010**, *49*, 1133. e) Zhang, H.; Curran, D. P. *J. Am. Chem. Soc.* **2011**, *133*, 10376.

10) a) Young, I.; Kerr, M. *Angew. Chem. Int. Ed*. **2003**, *42*, 3023. b) Sapeta, K.; Kerr, M. *J. Org. Chem.* **2007**, *72*, 8597. c) Karadeolian, A.; Kerr, M. *J. Org. Chem.* **2007**, *72*, 10251.

Chapter II

Complementary [Au]-Catalyzed Cyclization of 2-Alkynylphenylazides Directed by Competing Inter- *vs* Intramolecular Nitrogen Transfer

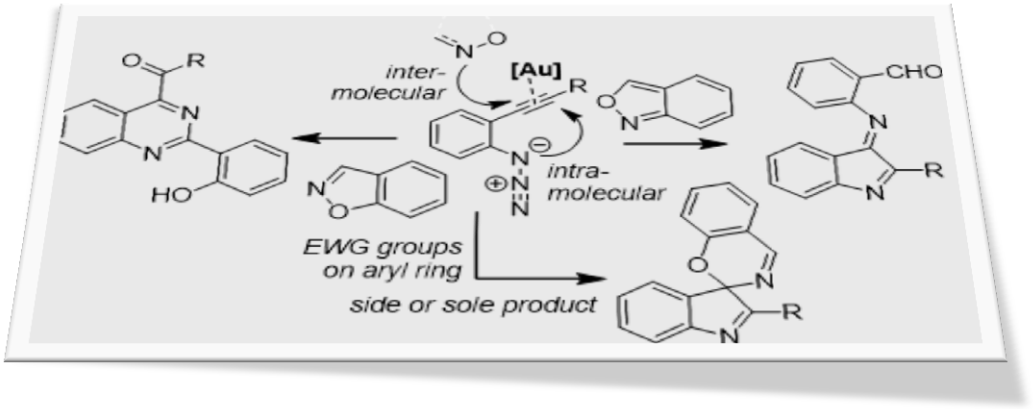

1.0. Introduction

Gold catalysed reactions are increasingly emerging in the literature since the past few decades.[1] The majority of these reactions are based on the propensity of gold to act as a carbophilic Lewis acid in the activation of carbon-carbon multiple bonds, thus allowing the formation of new C–C and C–hetero atom bonds by inter-/intramolecular addition of nucleophiles across the Au-complexed multiple bonds.[2] An interesting class of gold-catalysed reactions that needs a mention in this context are the reactions involving gold-carbenes.[3] When employed, the addition of nitrogen-transfer reagents such as azides, nitrogen ylides, (benz)isoxazoles and anthranils to the gold-complexed alkyne is known to lead to α-imino gold carbenes.[4] Similarly, oxygen atom transfer by employing nucleophilic oxygen atom donors such as nitro, amine-/pyridine N-oxides, nitrone, sulfoxides, and epoxides to alkynes catalysed by gold-complexes is a well-known addition−elimination process that leads to α-oxo gold carbenes.[5] This has been well explored in the synthesis of diverse heterocyclic structures and also in total synthesis.[6]

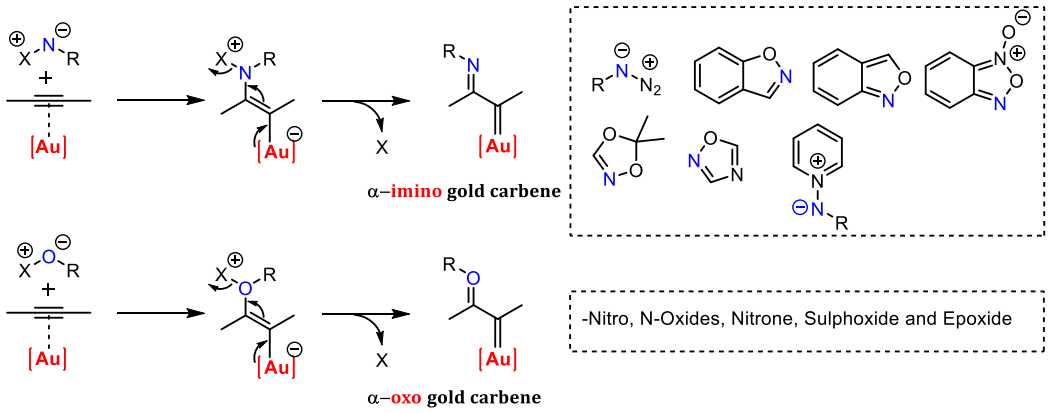

Figure F2.1: *Generation of α-Imino/Oxo Gold Carbenes & Representation of N-/O-Transfer Reagents*

The typical reaction model of gold-catalyzed nitrene transfer or carbene transfer is shown in Figure F2.1. The nitrogen atom within the nitrene-transfer reagent primarily attacks the gold-activated triple bond to generate the vinyl gold intermediate, which further undergoes N−X bond cleavage to form the key intermediate α-imino gold carbene, that areseldom generated from the corresponding α-imino diazo compounds through metal-mediated de-diazotizations of

diazo compounds.[7] These α-imino gold carbene intermediates undergo various transformations which lead to the formation of diverseN-heterocycles throughcarbene transfer, X-H insertion, 1,2-migration, formal annulation, cyclopropanation and skeletal rearrangements, thus making these processes highly versatile.[4d]

The major difference between α-oxo and α-imino gold carbene complexes lies in its structural feature and has been particularly focused upon for better understanding. Thus, the α-oxo gold carbene complexes form O-heterocycles, whereas the α-imino gold carbene complexes lead to N-heterocycles. When considering their chemical behaviors; the electronegativity difference between nitrogen and oxygen atoms (i.e O>N), makes the α-imino gold carbenes less electrophilic as compared to their oxygenatedcounterparts. The last important difference, featuring both chemical as well as structural behavior, is the option of having a substituent at the imino group that would help to modulate and control the reactivity in terms of electronics and/or sterics whichoffers a surplus point of diversity as well as of reactivity when compared to α-oxo gold carbenes

Although α-imino gold carbenes are proposed as key reactive intermediates in many of the cascade reactions and their involvement has been anticipated by computational DFT studies, as per our knowledge, their isolation and/or spectroscopic characterization is found to be understated.

In this part, we will be focusing on the gold-catalyzed nitrene-transfer reactions based on azides leading to α-imino gold carbene complexes in a more comprehensive way by emphasizing their product diversity, selectivity and applicability with the proposed mechanism.

2.0 Gold-Catalyzed Intramolecular Nitrene-Transfer Reactions based on Azides

2.0.1. 1,2-Migration

Toste and co-workers documented the possibility of generating α-imino gold carbenes employing azide as a nitrogen source in the year 2005. This opened a new chapter in gold catalysis which lead to the exploration of "gold-catalyzed nitrene transfer reactions". In this

pioneering work, the authors demonstrated the cyclisation of homopropargyl azides **S2.1A** by using 2.5 mol % $(dppm)Au_2Cl_2$ and 5 mol % $AgSbF_6$ as the catalysts in CH_2Cl_2 as solvent for the synthesis of 1H-pyrrole frameworks **S2.1B** (Scheme S2.1). The proposed mechanism involved the coordination of gold complex with alkyne followed by the intramolecular attack of the nitrogen atom *via* 5-endo-dig mode of cyclisation providing vinyl gold intermediate **S2.1D**. Further, the elimination of nitrogen molecule led to α-imino gold carbene **S2.1E,** which on formal 1,2-H shift/protodeauration and tautomerization produced 1H-pyrroles compounds. Different substituents such as alkyl, aryl, and heterocycles on homopropargyl azide moieties were found to be well-tolerated in this cascade process.

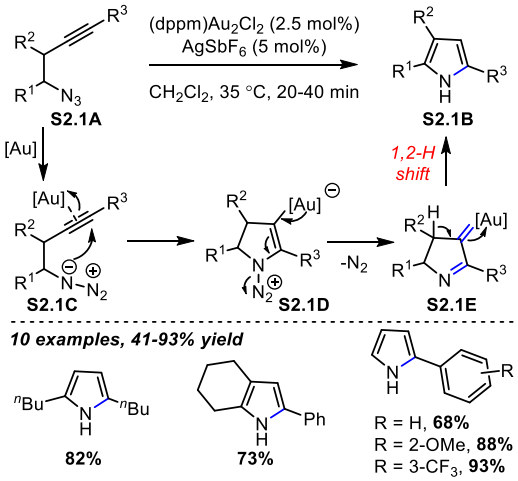

Scheme S2.1: *Gold-Catalyzed Acetylenic Schmidt Reaction of Homopropargyl Azides*

(Gorin, D. J.; Davis, N. R.; Toste, F. D. *J. Am. Chem. Soc.* **2005**, *127*, 11260−11261)

In 2013, Gagosz and co-workers developed an efficient protocol for synthesizing functionalized polysubstituted quinolines **S2.2B** by employing $AuCl_3$ or $IAdAuNTf_2$-catalyzed domino cyclization of acetoxy-tethered 2-alkynyl arylazides **S2.2A** (Scheme S2.2). The proposed mechanism for this cascade involved the coordination of the gold catalyst to the electron rich alkyne moiety followed by 1,3-acetoxy shift, providing allene intermediate **S2.2D**. Then, the nucleophilic attack of the azide group into this gold-activated allene and elimination of N_2 led to the cyclic α-gold carbene **S2.2E,** which further converted into the quinolines **S2.2B** *via* 1,2-shift

of the R^3 group. Electron-donating and electron-withdrawing groups on the aryl ring of 2-alkynyl arylazides as well as acyclic and cyclic systems were well tolerated in this cyclization.

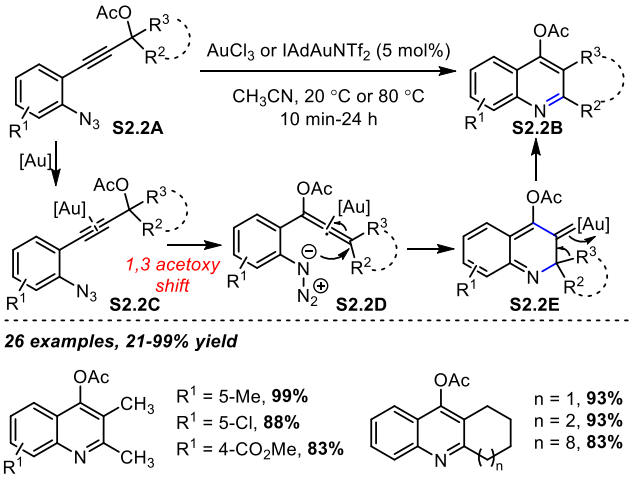

Scheme S2.2: *Gold-Catalyzed Cascade Cyclization of 2-Alkynyl Arylazides*

(Gronnier, C.; Boissonnat, G.; Gagosz, F. *Org. Lett.* **2013**, *15*, 4234−4237)

On similar lines, in 2017, the same group documented the synthesis of 2H-1,3-oxazines **S2.3B.** Mechanistically, a gold-catalyzed 6-*endo-dig* azide-yne cyclization of α-propargyloxy-β-haloalkylazides **S2.3A** led to an α-imino gold carbene **S2.3E,** which on 1,2-Hydrogen shift, furnished oxazines **S2.3B** in 25−96% yields (Scheme S2.3). Reaction scope exhibited that both aryl and alkenyl substituents on α-propargyloxy-β-haloalkylazides **S2.3A** competed well whereas, low yield was attained in the case of R^1 = alkyl substrate.

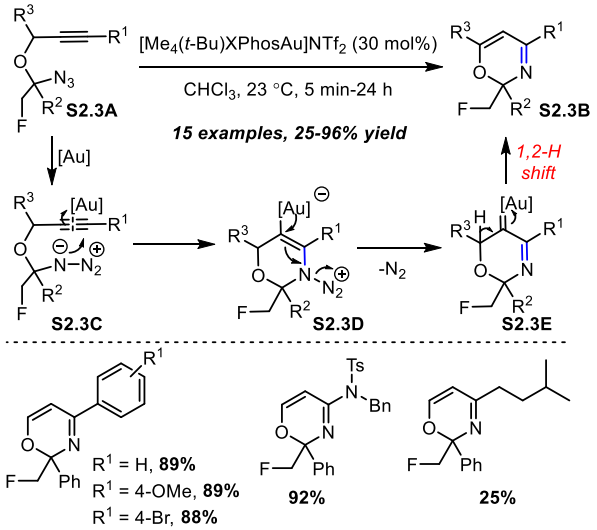

Scheme S2.3: *Gold-Catalyzed 6-endo-dig Azide−Yne Cyclization*

(Lonca, G. H.; Tejo, C.; Chan, H. L.; Chiba, S.; Gagosz, F. *Chem. Commun.* **2017**, *53*, 736−739)

2.0.2. Oxidation

The trapping of α-imino gold carbene intermediates by oxidants was first reported by Toste and coworkers in 2007. As depicted in Scheme S2.4, the reaction of homopropargyl azide **S2.4A** with 10 mol % IPrAuCl/$AgSbF_6$ as the catalyst and 4 equiv. of diphenyl sulfoxide which act as an oxidant in CH_2Cl_2 as solvent at room temperature gives pyrrolone **S2.4B** in 73% yield along with a minor amount of alkyl shift product **S2.4B'**. As far as the mechanism is concerned, the reaction involved the formation of α-imino gold carbene intermediate **S2.4C**, followed by trapping of carbene with intermolecular oxygen atom from diphenyl sulfoxide.

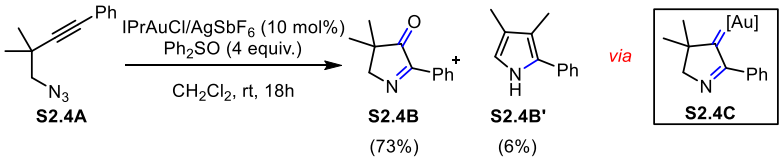

Scheme S2.4: *Oxidation of α-Imino Gold Carbene*

(Witham, C. A.; Mauleón, P.; Shapiro, N. D.; Sherry, B. D.; Toste, F. D. *J. Am. Chem. Soc.* **2007**, *129*, 5838−5839)

2.0.3. X-H Insertion

Until 2011, the homogeneous gold-catalyzed X−H insertion reactions on azides were not explored in the literature. Then, Wetzel and Gagosz reported the first gold-catalyzed tandem O−H insertion followed by Claisen rearrangement cascade reaction. As shown in Scheme S2.5, reaction of 2-alkynyl arylazides **S2.5A** by employing 4 mol % IAdAuNTf$_2$ as catalyst in $(CH_2Cl)_2$ as a solvent, formed α-imino gold carbene intermediates **S2.5D**, that were trapped by an excess of allylic alcohols **S2.5B** *via* O−H insertion, furnishing 3-allyloxyindoles **S2.5E**.Finally, [3,3]-Claisen rearrangement of **S2.5E** yielded diastereoselective indolin-3-ones (**S2.5C**) in moderate to excellent yields. The reaction scope studies revealed that a wide range of 2-alkynyl arylazides having electron-poor or electron-rich substituents and primary and secondary allylic alcohols were well tolerated.

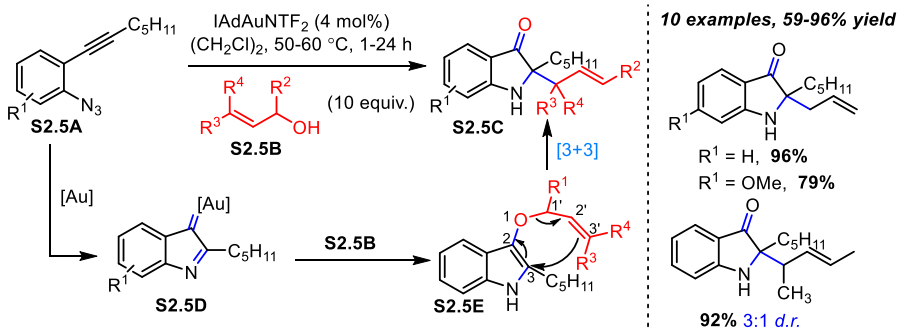

Scheme S2.5: *Gold-Catalyzed Tandem O–H Insertion/Claisen Rearrangement*

(Wetzel, A.; Gagosz, F. *Angew. Chem., Int. Ed.* **2011**, *50*, 7354–7358)

In the same year, L. Zhang and group presented the umpolung reactivity of indole at the 3-position by employing the electron-rich arenes/heteroarenes, such as xylenes, naphthalenes, anisoles, pyrroles, or indoles, as carbon-nucleophiles for gold-catalyzed X–H (C–H and N–H) insertion to α-imino gold carbenes for the formation of versatile indoles **12** (Scheme S2.6). In 2015, X. Zhang and group documented a similar gold-catalyzed cascade reaction of 2-alkynyl arylazides with alkynes providing 3-alkynyl indoles in good to excellent yields.[8]

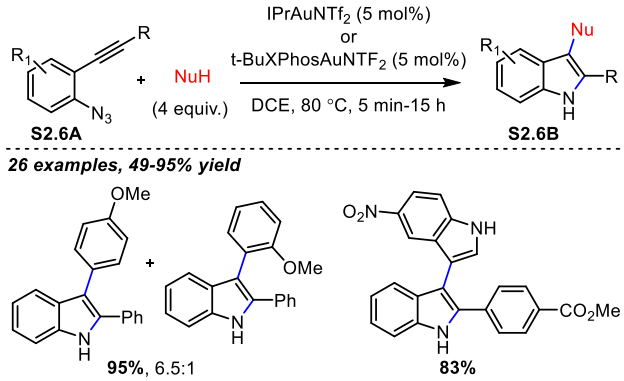

Scheme S2.6: *Gold-Catalyzed Intermolecular X–H Insertion of α-Imino Gold Carbenes*

(Lu, B.; Luo, Y.; Liu, L.; Ye, L.; Wang, Y.; Zhang, L. *Angew. Chem., Int. Ed.* **2011**, *50*, 8358–8362)

Along with intermolecular X–H insertion into α-imino gold carbenes, an intramolecular X–H insertion was also shown by Ye and co-workers in the year 2015. The intramolecular X–H(O–H and N–H) insertion of α-imino gold carbenes **S2.7C** obtained *via* gold-catalyzed cascade cyclization of (azido)ynamides **S2.7A** for the synthesis of [1,4]-oxazino[3,2-b]indoles or 1H-pyrazino[2,3-b]indoles **S2.7B** was demonstrated (Scheme S2.7). Mechanistically, the

reaction proceeds *via* 5-endo-dig mode of cyclisation to form α-imino gold carbene intermediate **S2.7C**, which subsequently underwent intramolecular X-H insertion.

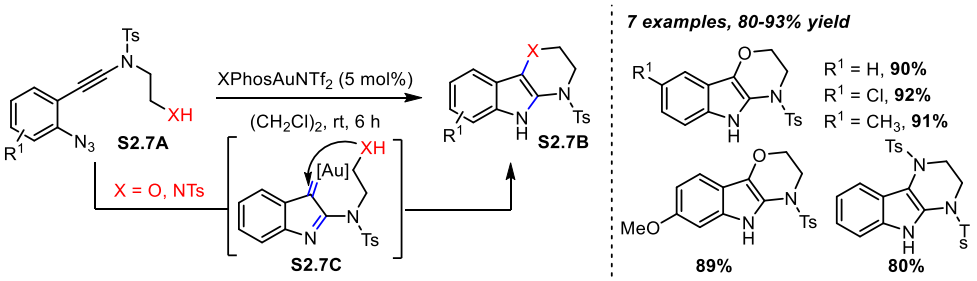

Scheme S2.7: *Gold-Catalyzed Intramolecular X−H Insertion of α-Imino Gold Carbenes*

(Shen, C.-H.; Pan, Y.; Yu, Y.-F.; Wang, Z.-S.; He, W.; Li, T.; Ye, L.-W. *J. Organomet. Chem.* **2015**, *795*, 63−67)

The same group also disclosed benzyl azides as nitrene transfer reagents for an intramolecular X−H insertion into α-imino gold carbenes to form isoquinoline derivatives (Scheme S2.8). The reaction of (azido)ynamides **S2.8A** in the presence of 5 mol % BrettPhosAuNTf$_2$ as the catalyst and 1.1 equiv of DDQ as the oxidant in $(CH_2Cl)_2$ at 80 °C afforded a wide range of valuable [1,4]oxazino[3,2-c]isoquinolines **S2.8B** in good yields. The electron-withdrawing/deficient substituents on the phenyl ring were well tolerated in this transformation.

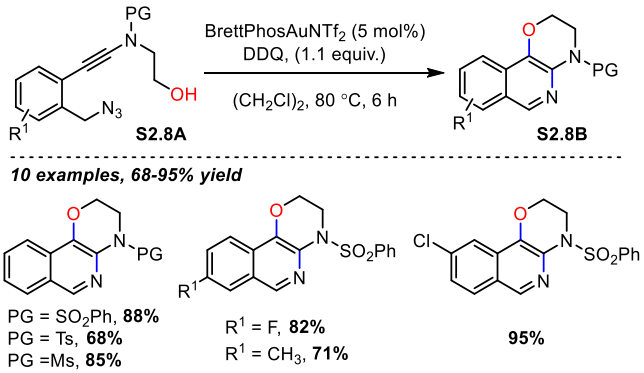

Scheme S2.8: *Gold-Catalyzed Intramolecular O−H Insertion to Benzyl Azides*

(Pan, Y.; Chen, G.-W.; Shen, C.-H.; He, W.; Ye, L.-W. *Org. Chem. Front.* **2016**, *3*, 491−495)

Employing a similar strategy, Qiu *et al.* in 2018 developed a mild and facile synthesis of fused tetracyclic indoles **S2.9B** by employing a gold-catalysed intramolecular bicyclization of 2-alkynyl arylazides **S2.9A** with a benzyl alcohol moiety attached to the pendant alkyne unit

(Scheme S2.9). This domino cyclisation showed good substrate scope and functional group tolerance. Along with oxygen nucleophile, this protocol wasalso compatible with nitrogen and carbon containing nucleophiles.[9]

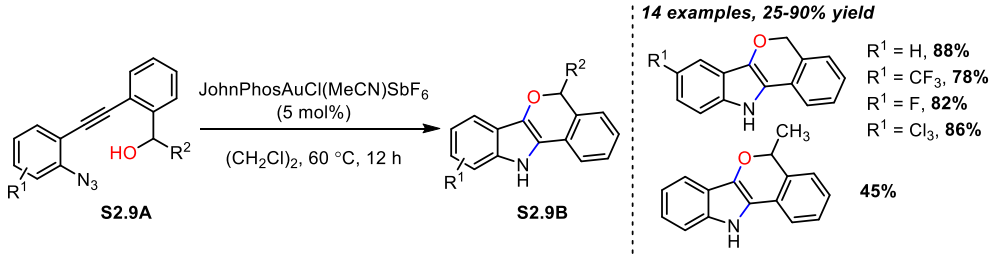

Scheme S2.9: *Gold-Catalyzed Intramolecular benzylic O−H Insertion*

(Cai, J.; Wu, B.; Rong, G.; Zhang, C.; Qiu, L.; Xu, X. *Org. Lett.* **2018**, *20*, 2733−2736)

2.0.4. Formal Annulation

In 2012, Xiao and L. Zhang reported the first gold-catalyzed formal (3 + 2) annulation of nitriles with α-imino gold carbenes for the synthesis of a wide range of bicyclic imidazoles **S2.10C**. The mechanism for this cascade proceeded through the formation of α-imino gold carbenes **S2.10E**, followed by the nucleophilic attack of nitrogen atom of the nitrile, and subsequent closure of the five-membered ring (Scheme S2.10). Different azidoalkynes **S2.10A** and nitriles **S2.10B** were compatible in this protocol affording bicyclic imidazoles **S2.10C** in moderate to good yields.

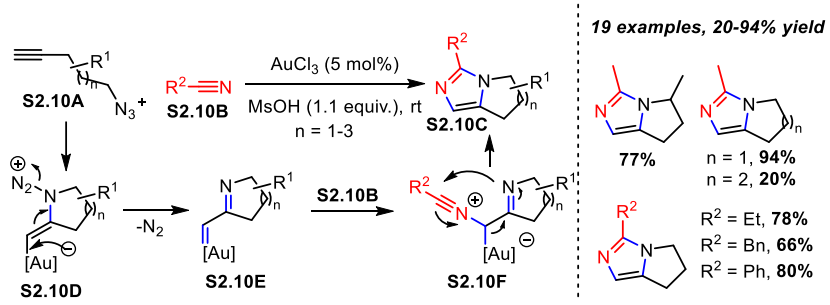

Scheme 10. *Au(III)-Catalyzed Formal (3 + 2) Annulation of Nitriles with α-Imino Gold Carbenes*

(Xiao, Y.; Zhang, L.*Org. Lett.* **2012**, *14*, 4662−4665)

Trapping of the α-imino gold carbenes generated by the *o*-azidoalkynes with various types of nucleophiles weredemonstrated well, and thus on similar lines, Zhang and group documented the gold-catalyzed formal (3 + 2) annulation of 2- alkynyl arylazides **S2.11A** with a wide range of alkynols **S2.11B** for the synthesis of pyrroloindolone derivatives **S2.11C** in moderate to good yields (Scheme S2.11). The mechanism for this annulation reaction proceeded through the generation of α-imino gold carbene intermediate **S2.11D** *via* gold-catalyzed 5-*endo dig* cyclization, followed by formal O−H insertion into the [Au] carbenes. Next, the indole moiety **S2.11E** underwent a Saucy–Marbet rearrangement, followed by a gold-catalyzed intramolecular hydroamination of allenyl intermediate **S2.11F** which afforded the pyrroloindolones **S2.11C**. It is noteworthy that, employing enantiopure (S)-3-butyn-2-ol substrates permitted the synthesis of optically active pyrroloindolones compounds with high ee.

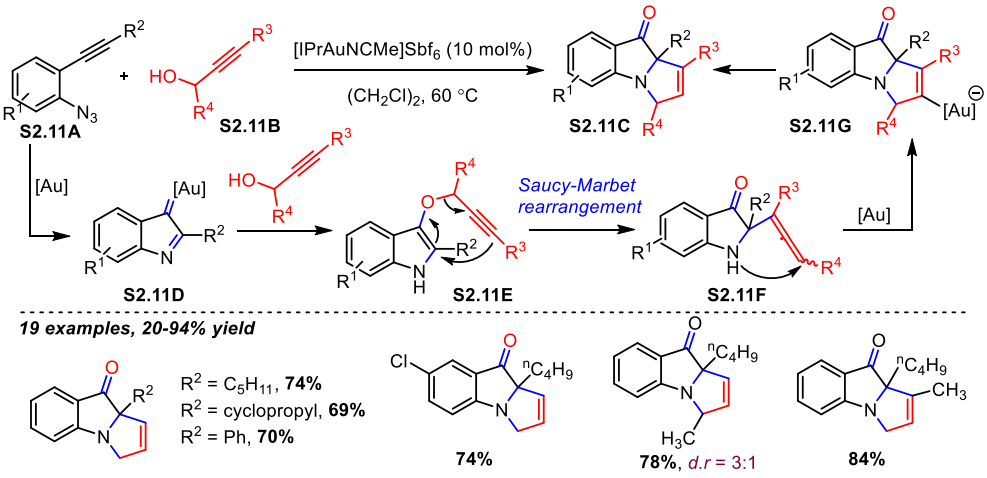

Scheme S2.11: *Au(III)-Catalyzed Formal (3 + 2) Annulation of Propargyl alcohol with α-Imino Gold Carbenes*

(Li, N.; Wang, T.-Y.; Gong, L.-Z.; Zhang, L. *Chem.- Eur. J.* **2015**, *21*, 3585−3588)

The reaction of a hydroxyl group bearing 3-(2-azidophenyl) prop-2-yn-1-ols **S2.12A** with gold catalyst along with external aldehyde **S2.12B** which provided [1,3]dioxino[5,4-b]indoles **S2.12C** was reported by Zhang and Rao in 2017. Mechanistically, the reaction procceded *via* formal [4 + 2] cycloaddition of α-imino gold carbene intermediate **S2.12D** with aldehyde **S2.12B** (Scheme S2.12, path a). Interestingly, only the presence of electron-withdrawing groups, such as 3,5-dichloro or 3-cyano, in the phenyl ring accelerated this transformation, by avoiding a

competitive initial aldehyde attack on the gold-activated alkyne that led to 1,3-dioxine scaffolds **S2.12H** (Scheme S2.12, path b).

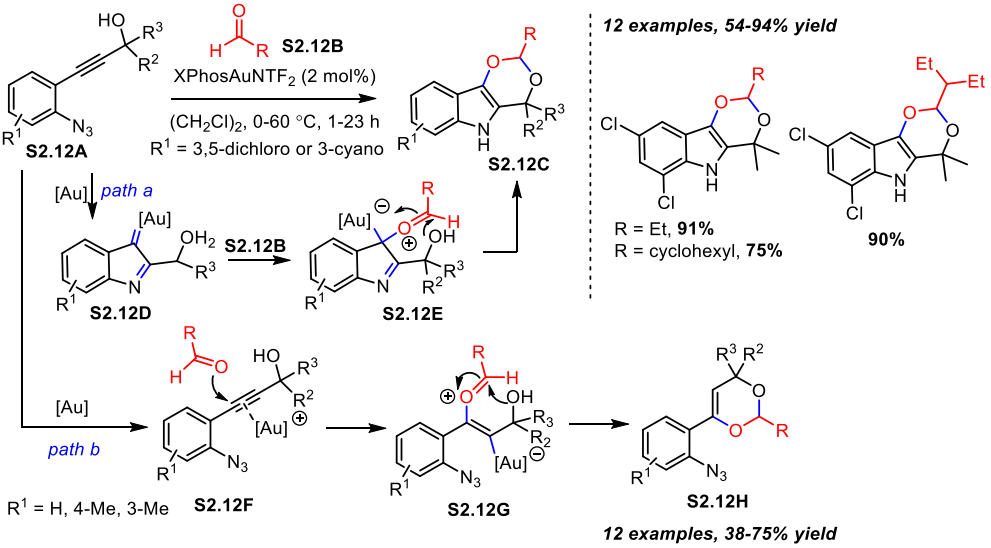

Scheme S2.12: *Gold-Catalyzed Intermolecular (3+2) Annulation of α-Imino Gold Carbenes with Aldehyde*

(Zhang, X.; Sun, X.; Fan, H.; Li, P.; Chang, L.; Rao, W. *Eur. J. Org. Chem.*, ***2016***, 4265)

During the total synthesis of Dictyodendrin B & F and the formal synthesis of Dictyodendrin C and E, in 2017, Ohno's group reported the formation of the pyrrolo[2,3-c]carbazoles **S2.13C/C'** through a gold-catalyzed formal (4 +2) annulation of azido diynes **S2.13A** with pyrroles **S2.13B** (Scheme S2.13). As illustrated, the mechanism involved the generation of α-imino gold carbene species **S2.13D** followed by arylation at the 3- or 2-position of pyrroles into the carbenes, affording the intermediates **S2.13E** and **S2.13E'**, respectively. Lastly, 6-*endo*-dig hydroarylation furnished pyrrolo[2,3-c]carbazoles **S2.13C** and pyrrolo[3,2-c]carbazoles **S2.13C'**.

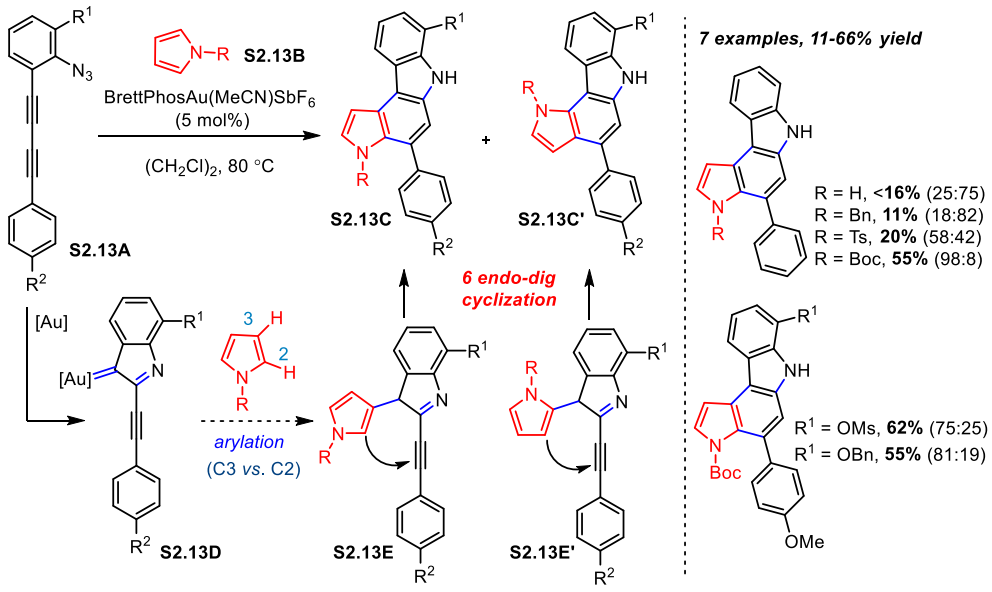

Scheme S2.13: *Gold-Catalyzed Intermolecular (4+2) Annulation with Pyrroles*

(Matsuoka, J.; Matsuda, Y.; Kawada, Y.; Oishi, S.; Ohno, H. *Angew. Chem., Int. Ed.* **2017**, *56*, 7444−7448)

In 2019, a gold(III)-catalysed annulation of azido alkynes **S2.14A** with nitriles **S2.14B** was described by Xu's group (Scheme S2.14). The reaction was catalyzed by $AuCl_3$ (5 mol %) at room temperature affording various functionalized oxazolo[4,5-c]quinolines **S2.14C** in good to excellent yields with a good substrate scope. The proposed mechanism for this formal (3 + 2) annulation proceeded through the generation of α-imino gold carbene species **S2.14D** by intramolecular 6-*endo*-dig cyclization, followed by capturing the gold carbenes with nitriles **S2.14B**, yielding the final oxazolo[4,5-c]quinoline products.

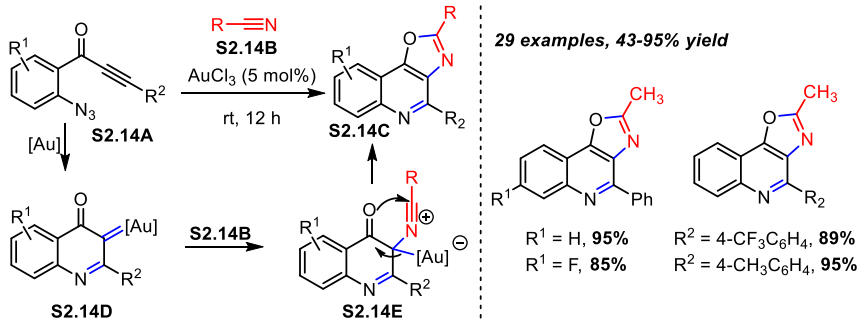

Scheme S2.14: *Gold-Catalyzed Formal (3 + 2) Annulation of Azido Alkynes with Nitriles*

(Su, H.; Bao, M.; Pei, C.; Hu, W.; Qiu, L.; Xu, X. *Org. Chem. Front.* **2019**, *6*, 2404−2409)

2.0.5. Cyclopropanation/Cyclopropenation

In 2014, Ohno and Fujii demonstrated that the alkene moiety also acts as a nucleophile to trap the α-imino gold carbene for the efficient synthesis of cyclopropane-fused indoloquinolines in good to high yields. The reaction proceeded through the gold-catalyzed tandem cyclization of (azido)ynamides **S2.15A** to generate α-imino gold carbene species **S2.15C**, which was then trapped by pendant alkene unit (Scheme S2.15). Moreover, the substrate scope studies showed that the formation of different types of indoloquinolines and indole-fused polycyclic compounds could be attained by employing other trapping agents like allylsilane and tethered nucleophiles.

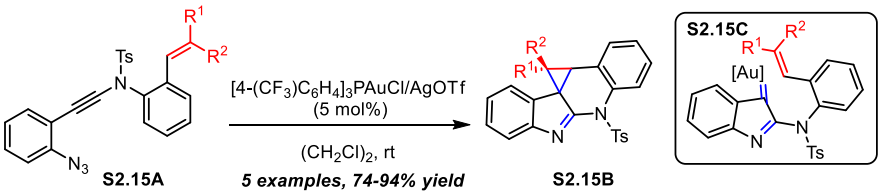

Scheme S2.15: *Gold-Catalyzed Cascade Cylopropanation of (Azido)ynamides*

(Tokimizu, Y.; Oishi, S.; Fujii, N.; Ohno, H. *Org. Lett.* **2014**, *16*, 3138−3141)

In 2016, Gong et al. reported an efficient synthetic route for arene-fused carbazole **S2.16C** from 2-alkynyl arylazides **S2.16A** and external terminal alkynes **S2.16B** (Scheme S2.16). The reaction was catalysed by $IPrAuNTf_2$ (5 mol %) along with BzOH (20 mol %) as an additive, producing a wide range of aryl-fused carbazoles **S2.16C** in moderate to good yields. Remarkably, the yield of product was improved by the addition of benzoic acid and water. The aryl ring of azido alkynes bearing electron-donating, electron-withdrawing, and bulky substituents along with different terminal alkynes were well tolerated. Intheir proposed mechanism, initially the generated α-imino gold carbene intermediates **S2.16D** underwent an intermolecular cyclopropenation with terminal alkynes **S2.16B**, and further converted into alkenyl gold carbene intermediates **S2.16F**. Finally, the product **S2.16C** was formed by an intramolecular Friedel−Crafts type reaction, followed by protonation & tautomerization.

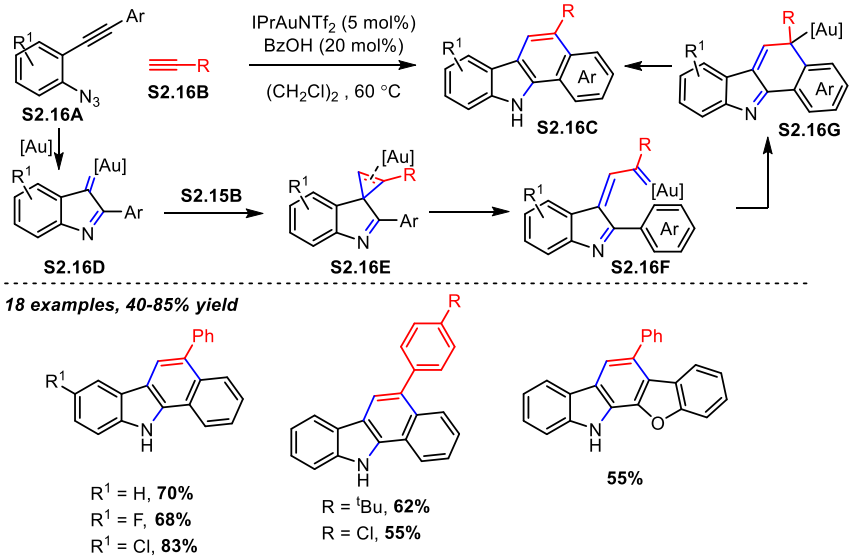

Scheme S2.16: *Gold-Catalyzed Cascade reaction of 2-Alkynyl Arylazides with Alkynes*

(Li, N.; Lian, X.-L.; Li, Y.-H.; Wang, T.-Y.; Han, Z.-Y.; Zhang, L.; Gong, L.-Z. *Org. Lett.* **2016**, *18*, 4178−4181)

2.0.6. 4π-Electrocyclization

In 2012, L. Zhang and coworkers reported anefficient synthesis of 2,3-dihydro-1H-pyrrolizines **S2.17B** having an electron-withdrawing group at the 5-position through a gold-catalyzed cascade cyclization of linear azidoenynes **S2.17A** (Scheme S2.17). This cascade cyclisation was catalyzed by BrettPhosAuNTf$_2$ (5mol %) in a toluene solvent. The reaction proceeded *via* the formation of α-imino gold carbene intermediate **S2.17C**, followed by a 4π-electrocyclization yielding the desired pyrrolizines **S2.17B** in good yields. Moreover, the reactions were compatible with various electron-withdrawing groups (EWGs) such as ester, acyl, and sulfonyl groups.

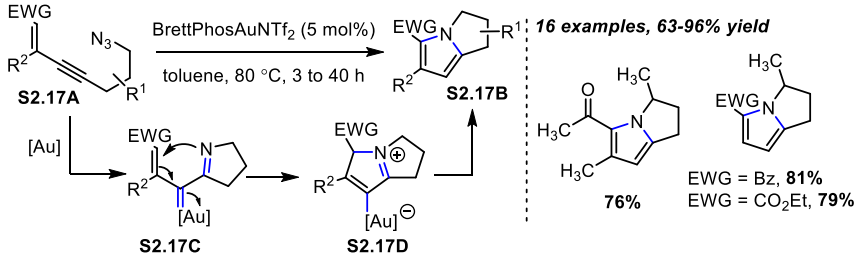

Scheme S2.17: *Gold-Catalyzed Cascade Cyclization of Linear Azidoenynes*

(Yan, Z.-Y.; Xiao, Y.; Zhang, L. *Angew. Chem., Int. Ed.* **2012**, *51*, 8624−8627)

2.0.7. Carbene Metathesis

In 2017, Ye and co-workers documented a facile strategy for divergent synthesis pyrrolo[2,3,-c]indoles **S2.18B** (Scheme S2.18). The reaction of azido-diynes **S2.18A** in presence of $Ph_3PAuNTf_2$ (2 mol %) as the catalyst in nitromethane as solvent, (or in the presence of Cu(I) as the catalyst and N-oxide as the external oxidant which produced pyrrolo[3,4-*c*]quinolin-1-ones) produced pyrrolo[2,3,-c]indoles (**S2.18B**) in moderate to high yields. According to control experiments and theoretical calculations, the author proposed the mechanism that involved generation of α-imino gold carbenes **S2.18C**, which were further trapped by pendant alkyne moiety to form enylium-cationic intermediates **S2.18D**. Next, intermediates **S2.18D** were attacked by trace amounts of water in the reaction system, followed by protodeauration, furnishing intermediates **S2.18F.** Finally, the end products were achieved by enol tautomerisation, aromatization, and oxidation steps.

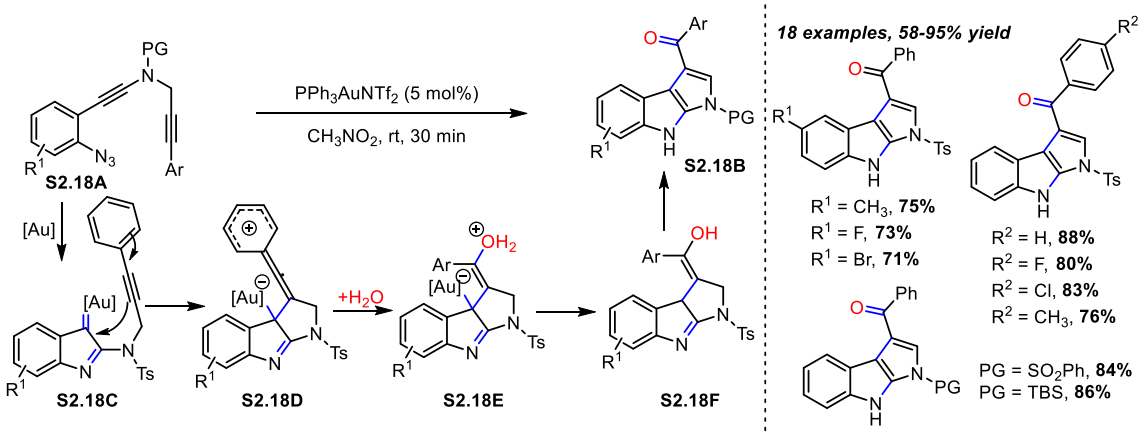

Scheme S2.18: *Gold-Catalyzed Cascade Cyclization of Azido-Diynes*

(Shen, W.-B.; Sun, Q.; Li, L.; Liu, X.; Zhou, B.; Yan, J.-Z.; Lu, X.;Ye, L.-W. *Nat. Commun.* **2017**, *8*, 1748)

2.1. Gold-Catalyzed Intermolecular Nitrene-Transfer Reactions based on Azides

In 2015, Ye and co-workers documented the synthesis of 2-aminoindoles by employing the first intermolecular nitrene-transfer reaction using external azide reagents. The reactions were catalyzed by 5 mol % $IPrAuNTf_2$, and 3-bromobenzyl azide **S2.19B** (acts as best nitrene-transfer reagent) to react with different ynamides **S2.19A**, providing a mild and efficient method for the

synthesis of wide range of 2-aminoindoles **S2.19C** (Scheme S2.19). Interestingly, other benzyl azides were also compatible nitrene-transfer reagents and could be further functionalized.

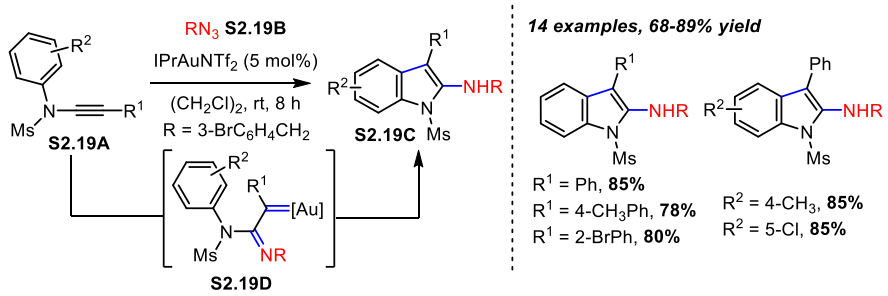

Scheme S2.19: *Gold-Catalyzed Intermolecular Reaction of external Azides with Ynamides*

(Shu, C.; Wang, Y.-H.; Zhou, B.; Li, X.-L.; Ping, Y.-F.; Lu, X.; Ye, L.-W. *J. Am. Chem. Soc.***2015**, *137*, 9567−9570)

In the same report, 2-indolomethyl azides **S2.20A** were used as nitrene-transfer reagents in gold-catalyzed reaction with ynamides substrate **S2.20B**. The reaction underwent formal (4 + 2) annulation instead of (3 + 2) annulation for the formation of 3-amino-β-carbolines **S2.20C** with wide range of substrate scope and functional group tolerance. Mechanistically, the reaction procced *via* inter-molecular nitrene insertion to α-imino gold carbene **S2.20D** followed by the heterocyclic attack due to the greater nucleophilicity of the indole ring. The 3-amino-β-carboline derivatives **S2.20C** were finally attained by C–H insertion and oxidation protocol (Scheme S2.20).

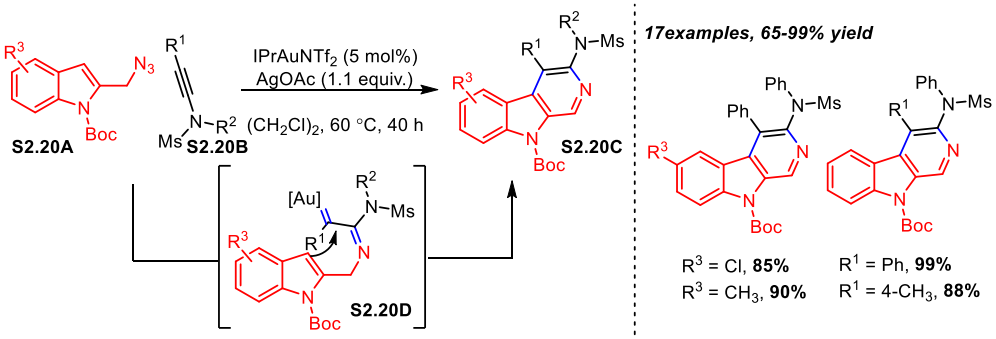

Scheme S2.20: *Gold-Catalyzed Intermolecular (4 + 2) Annulation with 2-indolomethyl Azide*

Surprisingly, when 3-indolomethyls **S2.21A** were employed in the gold-catalysed reaction with ynamides **S2.21B,** similar 3-amino-β-carbolines **S2.21C** were obtained in moderate to good yields (Scheme S2.21). The mechanism proceeded through the intramolecular reaction of α-imino gold carbene intermediate **S2.21D** with the C3-carbon of indole ring to form spiro

intermediate **S2.21E** which underwent a 1,2-alkyl group migration from C3 to C2 of the indole skeleton. Finally, protodeauration and aromatization steps furnished β-carboline derivatives **S2.21C**.

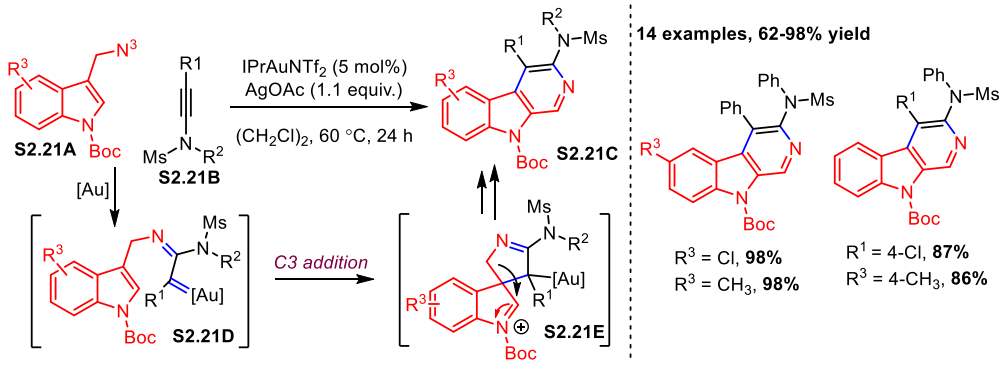

Scheme S2.21: *Gold-Catalyzed Intermolecular (4 + 2) Annulation with 3-indolomethyl Azide*

(Zhou, B.; Zhang, Y.-Q.; Liu, X.; Ye, L.-W. *Sci. Bull.* **2017**, *62*, 1201−1206)

3.0. Conclusion

The gold-catalyzed intramolecular cyclisation of azidoalkynes is one of the original reactions for invoking the existence of gold-carbene intermediates in general. This domain has been expanded with the introduction of various gold-catalyzed transformations providing powerful and effective methods for the synthesis of valuable natural or non-natural scaffolds by involving the intermediates that are generated *via* either inter or intramolecular nitrene-transfer. However, there are no studies related to understanding how the inter- and intramolecular nitrene transformations compete with each other. We have had success earlier in interrupting o-alkynylnitrobenzens with external nitrene transfer reagents. On similar lines, we were interested to study the gold-catalyzed cyclization of o-azidoalkynes in the presence of external nitrene transfer reagents like 1,2-benzisoxazoles and anthranils. The outcome of these reactions is expected to provide a fresh perspective on the interruption of the metal carbene/cyclization in the process of controlling the selectivity and expanding the scope.

4.0. Introduction

The gold-catalyzed transformations involving nitrene/oxygen transfer reactions of alkynes leading to the α-imino/α-oxo gold carbene intermediates respectively represents a significant advance in the homogeneous gold-catalysis.[10] As mentioned in introduction, Toste and co-workers first documented the possibility of generating α-imino gold carbenes employing azide as a nitrogen source (Scheme S2.1) and opened a new chapter in the gold catalysis "gold-catalyzed nitrene transfer reactions" and being expanded with the introduction of novel nitrogen transferring reagents like nitrogen ylides, isoxazoles and anthranils and providing elegant approaches for the development of complex N-containing heterocyclic scaffolds.[4]

As a part of our ongoing research on the catalytic nitroalkyne cycloisomerization[11], we examined the possibility of trapping the α-oxo gold carbene intermediates which are proposed in these cyclizations with the external N-centered nucleophiles such as anthranil and 1,2 benzo[*d*]isoxazole (Chapter 1, Section A).[12] Importantly, in these cases there exist competing alkyne functionalization (internal redox cyclisation with nitro group *vs* external nitrogen transfer) *inter-alia* competition between α-oxo- *vs* α-imino gold carbene intermediate formation. However, in both the instances, the intramolecular oxygen transfer was facile over the intermolecular nitrogen transfer. In addition, a competition experiment for carbene transfer to the anthranil and 1,2-benzisoxazole in the same-pot revealed that 1,2-benzisoxazole is more reactive (Chapter 1, Section A, Part B). This is an interesting observation and it was realized that reports on the competition for nitrogen-transfer between established nitrogen transfer reagents are scarce. Tuning such competing processes in complementary fashion is expected to deliver complex heterocyclic scaffolds via sequential C–N bond formations in one-pot. For example the intramolecular cyclization of o-alkynylaryl azides **1** is a well-established process that would generate the α-imino gold carbene intermediate **A**, which would be further captured by a variety of internal/external nucleophiles. On the other hand, anthranils **2**,[4b,13] 1,2-benzisoxazoles **3**[14] and related nitrogen transfer reagents are known to add to the alkynes, leading to the α-imino gold carbene intermediates **B**. We speculated that the reaction of o-alkynylaryl azide **1** in the presence of anthranil **2** or 1,2-benzisoxazoles **3** should lead to different products, depending on the intra *vs* intermolecular nitrogen transfer process, regioselectivity and the imino gold carbene intermediate involved. With anthranil **2**, either intra or intermolecular nitrogen transfer[15] is

expected to provide the indol-3-ylidene **4**. The same reaction in the presence of 1,2-benzisoxazoles **3** will be interesting. If the reaction proceeds *via* initial internal nitrogen transfer, the resulting carbene intermediate **A''** will be trapped by the external nitrogen nucleophile[14b] to provide a spiro indol-3-ylidene **5**. On the other hand, external nitrogen transfer leads to the gold carbene **B''**,[14a] which can lead to **5** if the 6n-cyclization of the initially formed quinomethide intermediate is facile. However, there exists another possibility of internal nitrene insertion[16] to the imine C-H that should lead to quianozoline **6** (Figure F2.2).

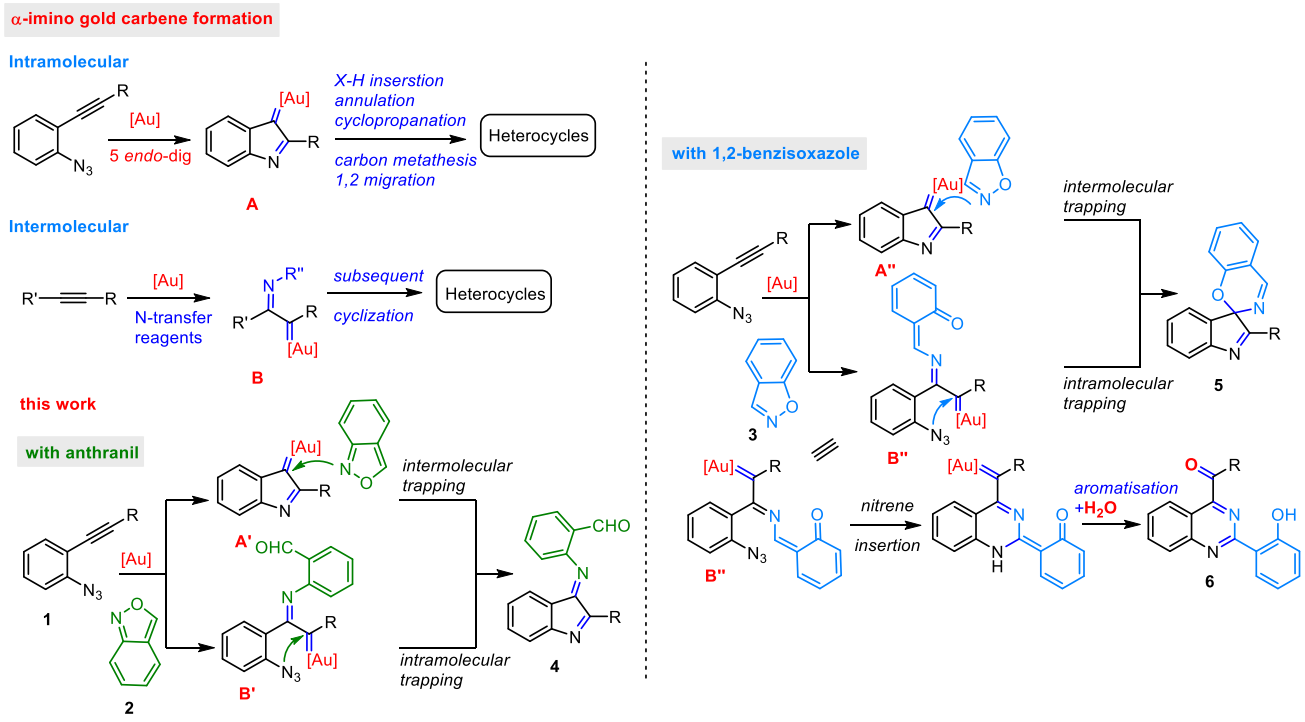

Figure F2.2: *Formation of α-Imino Gold Carbene Intermediates via Inter-/Intramolecular Nitrogen Transfer and a Working Hypothesis on Securing Product Diversity Possible via Competitive Inter Vs. Intramolecular Nitrogen Transfer/Trapping*

5.0. Present Work

The initial examination of our hypothesis commenced with a reaction of 1-azido-2-(phenylethynyl)benzene **1a** with 1,2-benzo[*d*]isoxazole **3a**, employing 5 mol % of $AuCl_3$ in 1,2-dichloroethane at room temperature. To our delight, the proposed cascade reaction indeed occurred and a new product with an expected mass corresponding to the desired quinazoline derivative **6aa** was observed in a low yield (8%; Table 1, entry 1). Heating the reaction mixture

at 80 °C, increased the yield of product **6aa** but not to greater extent (35%, entry 2). Coming to the ^{1}H NMR spectrum of compound **6aa**, the aromatic proton ortho to the OH group was seen to resonate at δ6.96 ppm (ddd, J = 8.1, 7.1, 1.2 Hz). The absence of the alkyne carbons in the ^{13}C NMR spectrum of **6aa** and the appearance of a carbonyl carbon at δ192.4 ppm indicated the modification of the alkyne unit. In addition, the presence of 8 quaternary carbons in ^{13}C NMR confirmed the proposed structure of **6aa** (in compound **5aa**, 7 quaternary carbons are present). Finally, the constitution of **6aa** has been confirmed as $C_{21}H_{15}N_2O_2$ by the HRMS ($[M+H]^+$) peak corresponding the M/Z 327.1122. This analytical structure validation revealed that it was the desired quinazoline **6aa** and, importantly, it proved the point that interrupting the intramolecular cyclization of o-alkynylphenylazides with external nitrene transfer is possible.

With this structure confirmation, we further moved to increase the yield of product by varying different catalyst. In case of AuCl/Pd-complex/$PtCl_2$, there was either decrease in the yield or complex mixture formation (entry 3-5). Next, the use of $PPh_3AuCl/AgSbF_6$ as the catalyst led to a significant improvement in the yield, with **6aa** being isolated in 50% yield within 2h at 80 °C (entry 6). Several other phosphine ligands/NHC gold carbene as well as with silver additive combination were also screened (entries 7−10). Gratifyingly, with the JohnphosAuCl and $AgSbF_6$ combination, yield of **6aa** was seen to be increased to 78% (entry 10). Finally, the survey of solvents suggested that neither nonpolar nor highly polar solvents were able to give satisfactory results (entry 11-15).

Table 1. *Optimization of Catalysts and Reaction Conditions*[a]

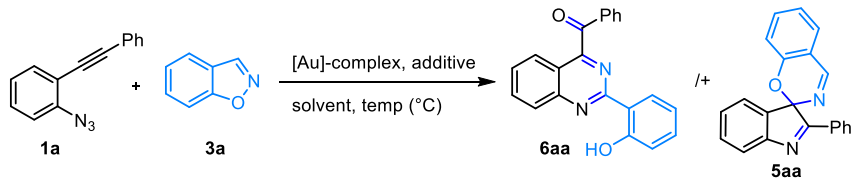

Sr no.	Catalyst	Temperature	Solvent	Yield (%)[b]
1	$AuCl_3$	rt	DCE	8 (**6aa**)
2	$AuCl_3$	80 °C	DCE	35 (**6aa**)
3	AuCl	80 °C	DCE	20 (**6aa**)
4	$Pd(OAc)_2$	80 °C	DCE	complex mixture

5	$PtCl_2$	80 °C	DCE	complex mixture
6	$Au(PPh_3)Cl/AgSbf_6$	80 °C	DCE	50 (**6aa**)
7	$IPrAuCl/AgNTf_2$	80 °C	DCE	64 (**6aa**)
8	$JohnphosAuCl/AgNTf_2$	80 °C	DCE	72 (**6aa**)
9	JohnphosAuCl/AgOTf	80 °C	DCE	75 (**6aa**)
10	**JohnphosAuCl/ $AgSbf_6$**	**80 °C**	**DCE**	**78 (6aa)**
11	JohnphosAuCl/ $AgSbf_6$	40 °C	DCM	56 (**6aa**)
12	JohnphosAuCl/ $AgSbf_6$	80 °C	Toluene	–
13	JohnphosAuCl/ $AgSbf_6$	80 °C	Acetonitrile	–
14	JohnphosAuCl/ $AgSbf_6$	80 °C	1,4 Dioxane	–
15	JohnphosAuCl/ $AgSbf_6$	80 °C	DMSO	–

[a]Unless indicated otherwise, the reaction of **1a** (0.1 mmol) and **2a** (0.11 mmol) was carried out at 80 °C in the presence of catalysts (5 mol %) and/or additive (10 mol %) in DCE (1 mL). [b]Isolated yield.

The optimized conditions were then applied to various *o*-azidoalkynes and 1,2-benzo[*d*]isoxazole to examine the substrate scope of this reaction (Scheme S2.22). The variation of substituents on the azido alkyne core was initially investigated. The reaction proved to be compatible, with the presence of several functional groups such as halogen (**1ba-1ca**), $–CF_3$ (**1da**), $–NO_2$ (**1ea**) and –CN (**1fa**) located at 4-positions (*para* to azide moiety) of the aryl group, providing the corresponding products in 58−68% yields. The structure of **4da** was clearly demonstrated by X-ray analysis (Figure F2.3, 1st one). However, 5-bromo- and 5-chloro-substituted substrates were also well-tolerated, giving the desired products with fairly good yields (**6ga** and **6ha**). An electron rich $–CH_3$ substituent at the 4–position to the alkynyl functionality led to an excellent yield (**6ia**). Subsequently, the substitution variation at the pendant alkyne terminus of azidoalkyne **1** was investigated. The phenyl group bearing electron withdrawing/bulky substituents were all well tolerated, and the desired quinazoline products **6ja-6ka** was also isolated in good yields. The cyclopropyl (**1l**) and *n*-propyl-substituted (**1m**) substrate also underwent this cascade reaction smoothly, leading to quinazoline **6la** and **6ma** in a 72% and 45% respectively. It is noteworthy that the high yield was retained, and even the reaction was carried out on gram scale (**6aa**, 76% yield, note b).

Figure F2.3: *Single Crystal X-ray Diffraction of Compound* ***4da*** *and* ***4'ad***

Thereafter, the generality for the 1,2-benzo[*d*]isoxazole substrates was examined with various azidoalkyne. The 1,2-benzisoxazoles bearing electron–withdrawing,–donating groups or halogens were seen to undergo the desired cascade reaction to afford quinazoline products. When 5–fluoro 1,2-benzo[*d*]isoxazole was used with different substituted azidoalkyne, the desired quinazoline products (**6ab**, **6cb**, **6ib**, **6lb**) was obtained in moderate to good yields. On the other hand, electron–donating group such as $–CH_3$ on 1,2-benzo[*d*]isoxazole (**3e**) were treated with different azidoalkyne and found to be well compatible providing the corresponding quinazoline derivatives in good to moderate yields. In case of 1,2-benzisoxazole substrates with the electron-withdrawing group $–NO_2$ (**3f**), –Br (**3d**)/–Cl (**3c**) and bulky substituents like *t*-butyl (**3g**), the azidoalkyne cyclization seems to be dominated. Similarly, when EWG group was present para to the azide group, the spiroindoline derivatives were obtained as a side or sole products (**5**). This is an interesting observation and reveals that if the dissociation of azide to the corresponding nitrene is facile, the intramolecular nitrogen transfer occurred over the intermolecular addition of benzisoxazole.[17] Coming to the structure of spiroindoline **5ad,** in the ^{1}H NMR spectrum, a total number of 12 aromatic proton were seen. The presence of an imine was indicated by the appearance of proton at δ8.44 ppm as a doublet with coupling constant J = 0.8 Hz confirmed the addition of 1,2-benzo[*d*]isoxazole group. The absence of alkyne carbons in the ^{13}C NMR spectrum of **5ad** indicated the modification at the alkyne functionality. Moreover, the appearance of imine carbon of oxazine ring seen to resonate at δ156.0 ppm as doublet and of indoline ring at δ175.0 ppm as a singlet. Finally, the presence of a strong peak in the HRMS spectrum at *m/z* 389.0294 ($[M+H]^+$) for $C_{21}H_{14}N_2OBr$ supported the established structure of compound **5ad.** Finally, the single crystal X–ray diffraction data analysis further confirmed the structure of **5ad** (Figure F2.3, 2nd one).

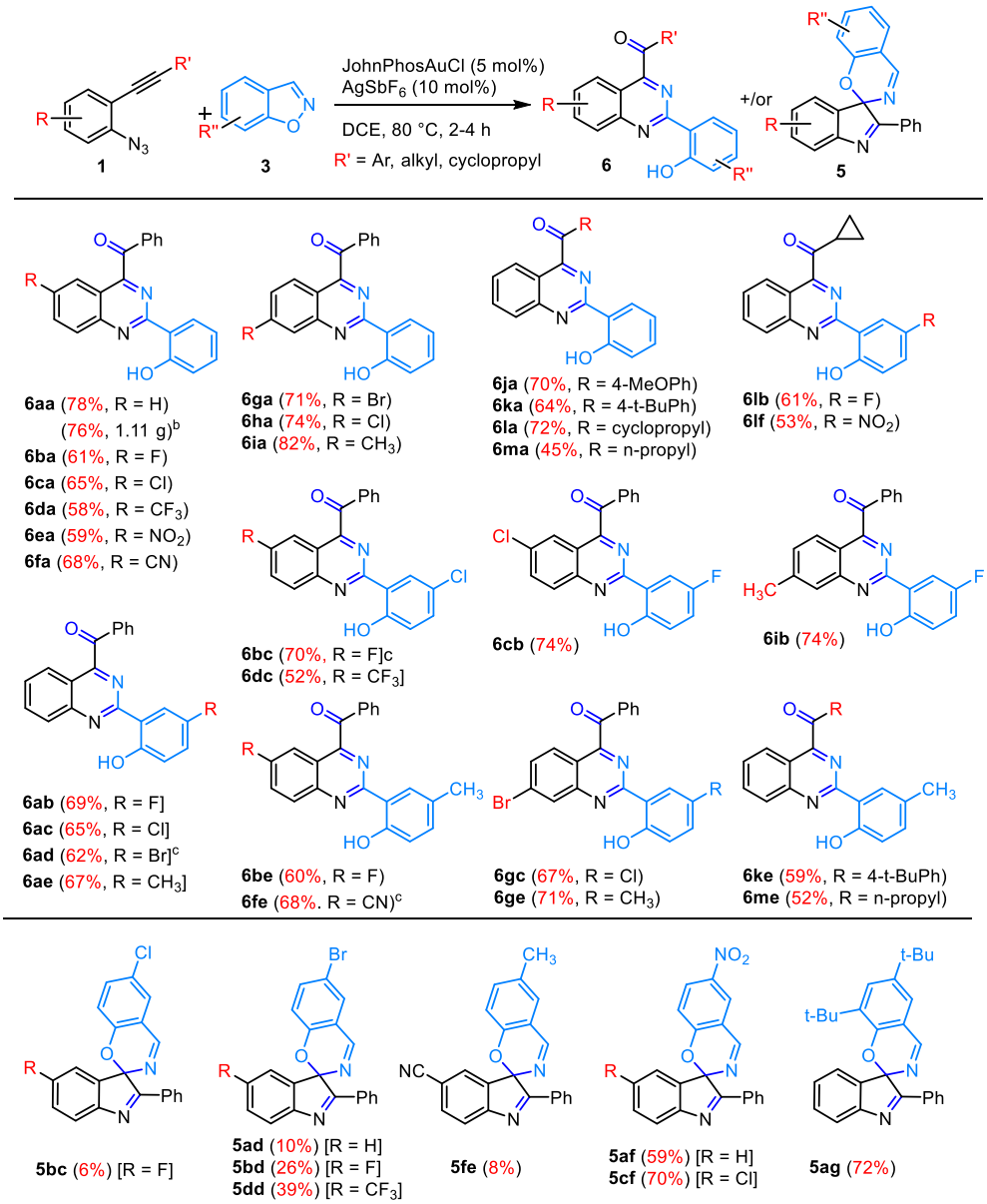

[a]The reaction of azidoalkyne **1** (0.2 mmol) and 1,2-benzoisoxazole **3** (0.22 mmol) was carried out in the presence of JohnphosAuCl (5 mol %) and $AgSbF_6$ (10 mol %) in DCE (1.0 mL) at 80 °C in a reaction vial for 2-4 h. [b]gram scale reaction, [c]side or sole product of **5.**

Scheme S2.22: *Reaction Scope with Different Azidoalkynes and 1,2-Benzo[d]isoxazole*[a]

Next, the same reaction conditions were further explored to see the reaction of azidoalkyne **1a** with the isomeric 2,1 benzo[*c*]isoxazole (anthranil) **2a**, interestingly the uncharacterised red colour product **5aa** was obtained in 72% yield. The structure of **4aa** was established with the help of spectral and analytical data. For example, in the ^{1}H NMR spectrum

of compound **4aa**, 13 aromatic protons are present along with the aldehyde proton that resonated at δ10.19 ppm thus confirming the addition of anthranil group through N-O bond cleavage. The aromatic proton ortho to the formyl group was seen to resonate at δ8.45 ppm (dd, J = 7.9, 1.6 Hz) and the aromatic proton ortho to the alkyne unit shifted to downfield (δ 7.66 ppm) when compared to (δ 7.51 ppm) that of the starting compound. The absence of alkyne carbons in the ^{13}C NMR spectrum of **4aa** and appearance of two imine carbons (at δ 165.7 and δ 166.0 ppm) and aldehyde carbon at δ 189.6 ppm further confirmed the structure of compound **4aa**. Next, the constitution of **4aa** has been confirmed as $C_{21}H_{15}N_2O$ by the HRMS peak at 311.1183 corresponding to $[M+H]^+$. Finally, single crystal X-ray crystal structural analysis of compound **4aa** revealed that it was the (*E*)-2-((2-phenyl-3*H*-indol-3-ylidene)amino)benzaldehyde. The isolation of compound **4aa** proved the point that the reaction proceeds *via* initial internal nitrogen transfer from azide group and its trapping with anthranil.

The generality of the reaction was further explored by varying different substituents on aryl unit of azidoalkyne (**1**) as well as on 2,1 benzo[*c*]isoxazole (**2**). The corresponding indol-3-ylidene products **4** were obtained in good to excellent yields. However, in case of strong electron withdrawing substituents such as $–CF_3$ (**1d**), $–NO_2$ (**1e**), –CN (**1f**) on the para-position of azide group provided the resultant indol-3-ylidene product in high yield. With alkyl azide, the reaction led to decomposition, and with cyclopropyl substituted azidoalkyne, the corresponding indol-3-ylidene **4la** was formed in 62% yield. Next, we varied the substituents on the anthranil ring. When halogen-substituted anthranils were employed as the substrates, the reactions in general resulted in the corresponding indol-3-ylidene **5ab**–**5ac, 5ae**–**5af** in moderate to good yields depending upon the position of the halogen atom. The yields are moderate when the halogen is placed para to the nitrogen. On the other hand, with electron rich $–CH_3$ group on 5- position of anthranil, the corresponding indol-3-ylidene product **4ad** was obtained in 71% yield (Scheme S2.23).

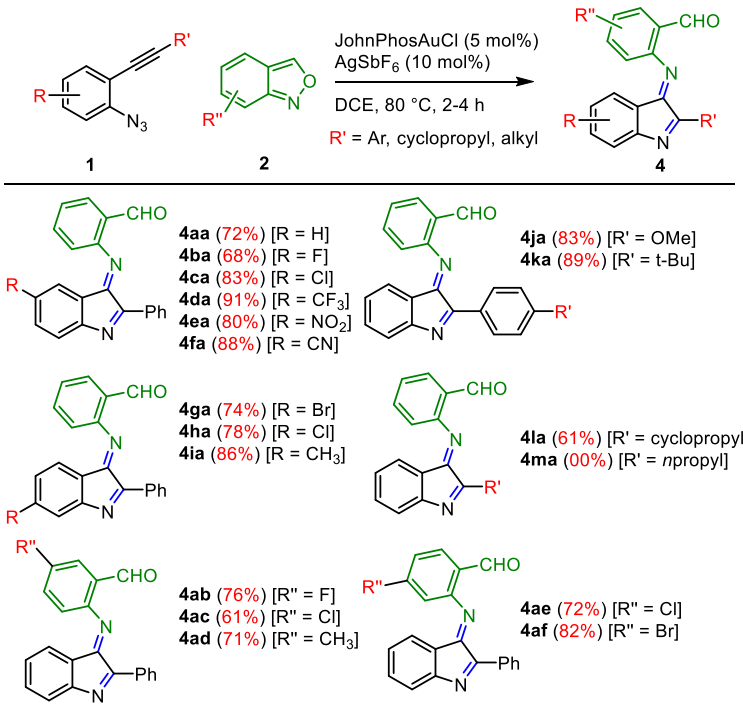

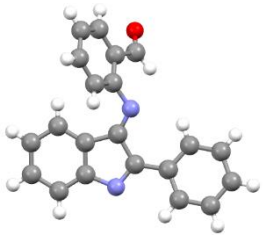

*Single crystal X-ray diffraction of compound **4aa***

[a]The reaction of azidoalkyne **1** (0.2 mmol) and anthranil **2** (0.22 mmol) was carried out in the presence of JohnphosAuCl (5 mol %) and $AgSbF_6$ (10 mol %) in DCE (1.0 mL) at 80 °C in a reaction vial for 2-4 h.

Scheme S2.23: *Reaction Scope with Different Azidoalkynes and Anthranils*[a]

6.0. Control Experiments

6.0.1 Control Experiments with 1,2-Benzo[*d*]isoxazole

Next, some control experiments have been conducted to understand the mechanistic course of these cyclizations. As shown in Scheme S2.24, when the reaction of azidoalkyne **1a** and 1,2-benzoisoxazole **3a** was carried out in the presence of $H_2{}^{18}O$, more than 60% incorporation of ^{18}O was noticed (see Experimental Section). This provided an indirect support for the competing intermolecular nitrogen transfer and the existence of corresponding α-imino gold carbene (evidenced by the HRMS of the intermediates from an experiment conducted employing the stoichiometric amount of gold-catalyst) that underwent proto deauration at the final stages. This has been further supported by the isolation of cyclopropane **7** when the reaction was carried out in the presence of excess styrene. This is an important observation that supports the protodeauration as a final event and indicates that the nitrene generation/insertion may not be

requiring the assistance from the gold-complex. Next, in order to see the reactivity of 1,2-benzisoxazole in competition with the other known nucleophiles, the reactions were carried out in the presence of excess and equimolar amount of allyl alcohol. In the former case, the reported pseudoindoxyl product **8** was obtained as a major product, along with the quinazoline **6aa** as a minor product.

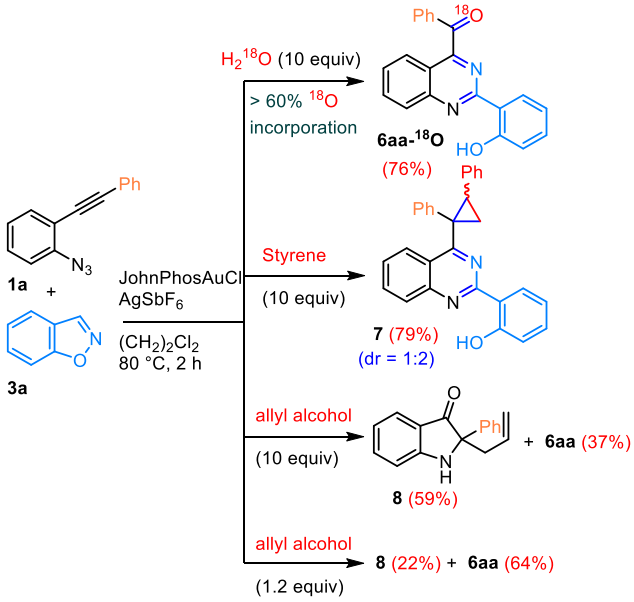

Scheme S2.24: *Control Experiments with 1,2-Benzoisoxazole.*

6.0.2 Control Experiments with Anthranil

Next, similar control experiments were carried out employing azidoalkyne **1a** and anthranil **2a**. As shown in Scheme S2.25, the reaction in the presence of $H_2{}^{18}O$ isotopic labelling showed incorporation of ^{18}O to α-imino gold carbene (its presence was detected in HRMS). However, the indolinone **4aa** was the main product. Further, in the presence of excess styrene, the cyclopropane adduct **10** could not be isolated in reasonable amounts to characterize. Nevertheless, the HRMS analysis showed its presence in the crude reaction mixture. Both these control reactions proved that the reaction proceeds *via* intramolecular α-imino gold carbene formation followed by intermolecular trapping with anthranil. Next the competition experiments between the anthranil and allylic alcohol gave results similar to what had been noticed in the case of 1,2 benzoisoxazole. Overall, these control experiments provided an indirect support for our hypothesis of competing intermolecular nucleophilic addition in case of 1,2 benzisoxazole and

intermolecular carbene transfer when it came to its isomer anthranil. However, the formation of indolin-3-one **8** in substantial amounts even when 1.2 equiv of allyl alcohol was employed (in the original report of Gagosz, 10 equiv of allylic alcohol was employed) in competition to **2a** or **3a**, though highly speculative indicates the possible addition of allylic alcohol prior to the azido alkyne cycloisomerization[18] that was proposed in general.

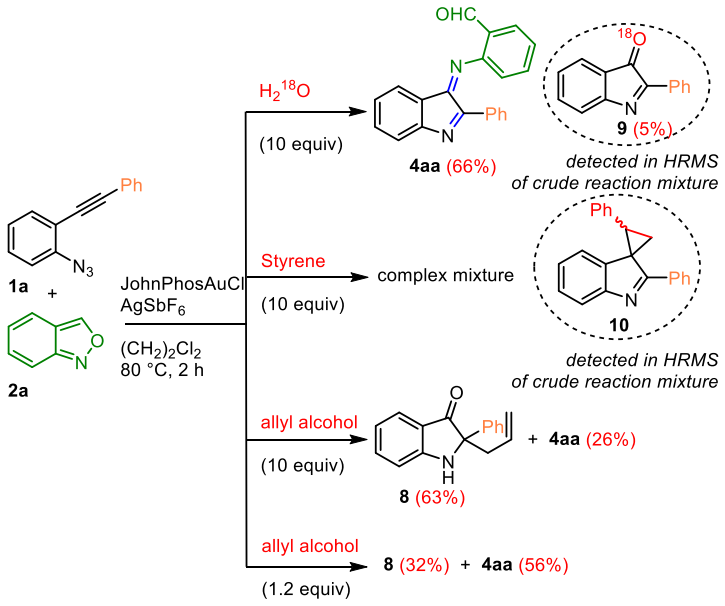

Scheme S2.25: *Control Experiments with Anthranil*

7.0. Reaction with other N-Centered Nucleophile

Having successfully studied the competing inter- *vs* intramolecular nitrogen transfer reactions employing anthranil and isobenzoxazole, next, the scope of some of the other N-centered nucleophiles has been carried out. As depicted in Scheme S2.26, when the reaction was carried out in presence of an external azide **9aa** (which was also known to participate in carbene transfer), as expected the indol-3-ylidene product **10aa** was obtained in 86% yield. However, when benzofuroxan **11a** was employed as an external nucleophile, the 2-phenyl-3*H*-indol-3-one **12aa** was obtained in 79% yield. The formation of **12aa** is expected either by simple protodemetallation after the intramolecular azidoalkyne cycloisomerization or *via* oxygen transfer to the gold carbene intermediate. The spectral data of compound **12aa** was in agreement with the data reported by Liu group.[19] In both the cases, though the possibility of intermolecular addition may not be ruled out the reaction seems to be proceeding *via* intramolecular nitrogen

transfer through 5-*endo* dig mode of cyclisation and subsequent carbene transfer to the external azide or of N-oxide.

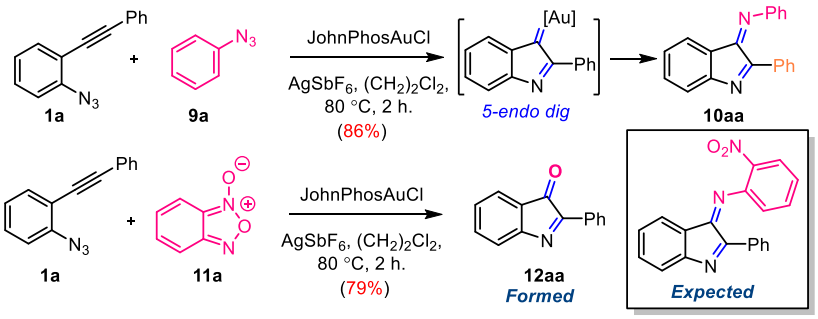

[a]The reaction of azidoalkyne **1** (0.2 mmol) and other nucleophile **9/11** (0.22 mmol) was carried out in the presence of JohnphosAuCl (5 mol %) and $AgSbF_6$ (10 mol %) in DCE (1.0 mL) at 80 °C in a reaction vial for 2-4 h.

Scheme S2.26: *Reaction with Other Nucleophile*[a]

8.0. Reactivity of Nitro over Azide Group

At the outset, the substrate **13** having both nitro as well as azide groups at *ortho* to the alkyne functionality (Scheme S2.27) has been designed/synthesized to understand the intramolecular competition between the oxygen *vs* nitrene transfer. When the reaction was carried out under optimized Au(III) and Au(I) conditions, in both instances, isatogen **14** having the intact azide group was obtained exclusively in 76% and 89% respectively. The structure of **14** was established with the help of spectral and analytical data as well as by single crystal X–ray diffraction studies**.**

Next, the same reactions were carried out in the presence of external nitrene transfer reagents 2,1-benzo[*c*]isoxazole **2a** and 1,2 benzo[*d*]isoxazole **3a**. Interestingly, in both the cases, starting **2a** and **3a** were recovered along with isatogen **14**. These experiments indicate that the internal redox cyclization is facile over the nitrene transfer. At the same, the isolation of the product with intact azide group even when the reaction was heated at 80 °C, reveals that, the generation of a nitrene during the classical azidoalkyne cyclization is facilitated by the presence of both gold-complex and the alkyne.

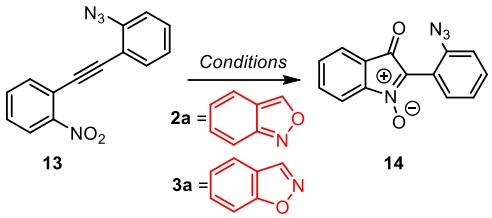

Sr no.	Conditions	Yield (14)
1	$AuCl_3$, $(CH_2)_2Cl_2$, rt, 2h	76%
2	JohnPhosAuCl $AgSbF_6$,$(CH_2)_2Cl_2$, 80 °C, 2h.	89%
3	**2a**/**3a** $AuCl_3$, $(CH_2)_2Cl_2$, rt, 2h	72%
4	**2a**/**3a** JohnPhosAuCl, $AgSbF_6$, $(CH_2)_2Cl_2$, 80 °C, 2 h.	86%

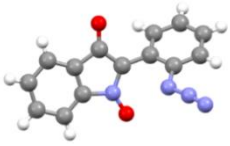

*ORTEP Diagram of Compound **14***

***Scheme S2.27**: Competition between Nitro and Azide Group*

9.0. Conclusion

To conclude, competitive formation of a-imino gold carbenes from inter *vs*. intramolecular nitrogen transfer has been examined for the first time, employing ortho alkynylazides that are known to form these gold carbenes *via* intramolecular nitrogen transfer, and isomeric anthranils and 1,2-benzisoxazoles that have been deployed as intermolecular nitrogen transfer reagents. The results are impressive, with a clear reactivity difference: intermolecular transfer is observed exclusively with 1,2-benzisoxazoles and an intramolecular nitrogen transfer from azide and subsequent carbene trapping is observed with anthranil. In addition, the substrate scope studied with 1,2-benzisoxazoles derivatives revealed how the electron withdrawing groups present on either of the substrates causes a switch in the competition. At the outset, a simple catalytic method for the synthesis of highly functionalized quinazolines has been established.

Experimental Section

Gold Carbene Complex Experiment

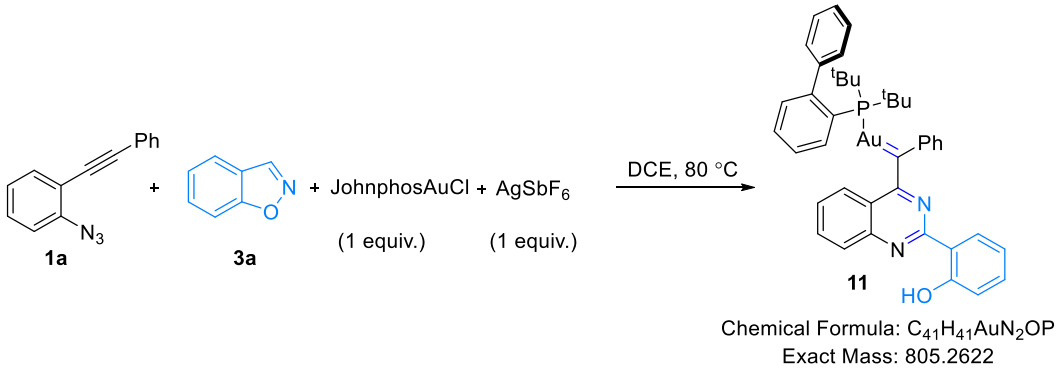

Chemical Formula: $C_{41}H_{41}AuN_2OP$
Exact Mass: 805.2622

In an oven dried reaction vial, JohnPhosAuCl (1 equiv.) and $AgSbF_6$ (1 equiv.) were added followed by addition of DCE and the reaction mixture was stirred at room temperature for 10-15 minutes. To this gold complex solution was added dropwise a DCE solution of azidoalkyne (**1**) (1 equiv), and 1,2- benzo[*d*]isoxazole (**3a**) (1.1 equiv) over 5 minutes. The resulting solution was stirred at 80 °C until the complete disappearance of the starting azidoalkyne as indicated by TLC. The crude reaction mixture was analysed by HRMS and shows (M^+) peak of gold carbene complex **11**.

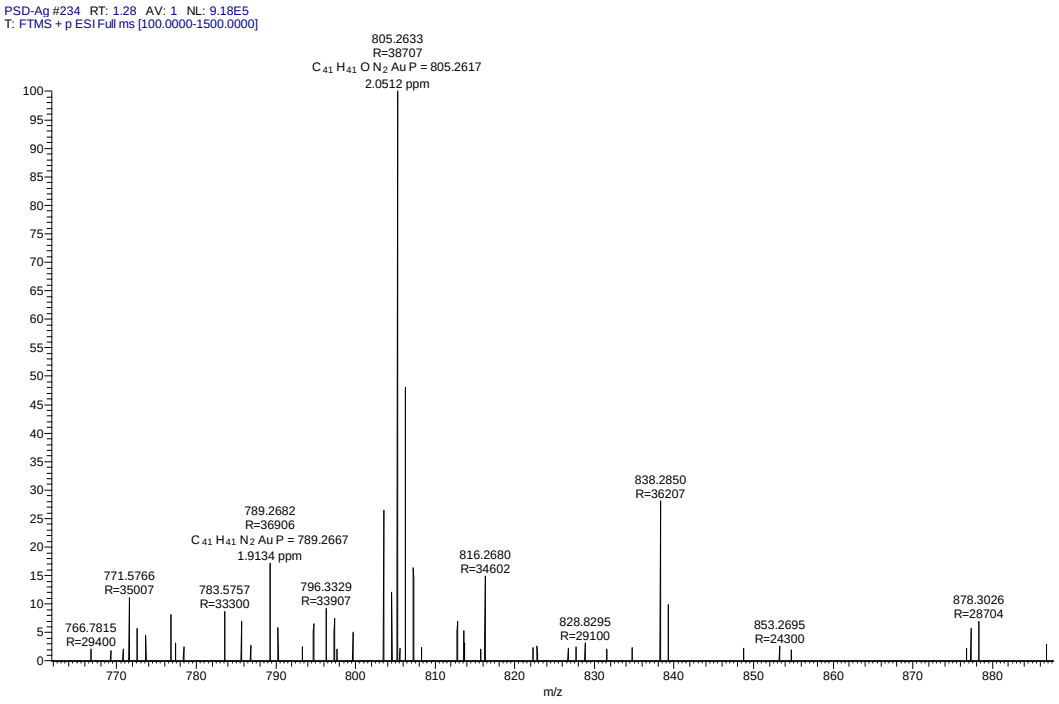

Carbene Trapping Experiments by Employing Excess $H_2{}^{18}O$

In 1,2- benzo[*d*]isoxazole case-

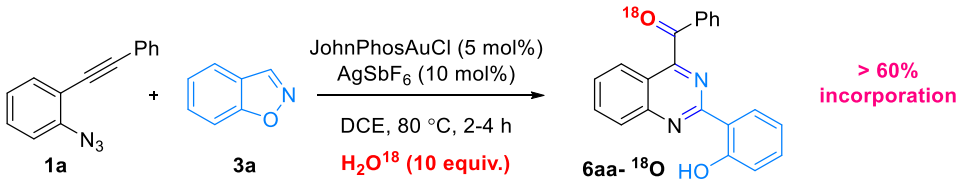

In an oven dried reaction vial, JohnPhosAuCl (5 mol %) and $AgSbF_6$ (10 mol%) were added followed by addition of DCE and the reaction mixture was stirred at room temperature for 10-15 minutes. To this gold complex solution was added dropwise a DCE solution of azidoalkyne (**1**) (1 equiv), 1,2- benzo[*d*]isoxazole (**3a**) (1.1 equiv) and H_2O^{18} (10 equiv) over 5 minutes. The resulting solution was stirred at 80 °C until the complete disappearance of the starting azidoalkyne as indicated by TLC. The reaction mixture was concentrated under reduced pressure and the resulting crude was purified by column chromatography to afford the oxygen labelled quinazoline products **6aa-^{18}O.**

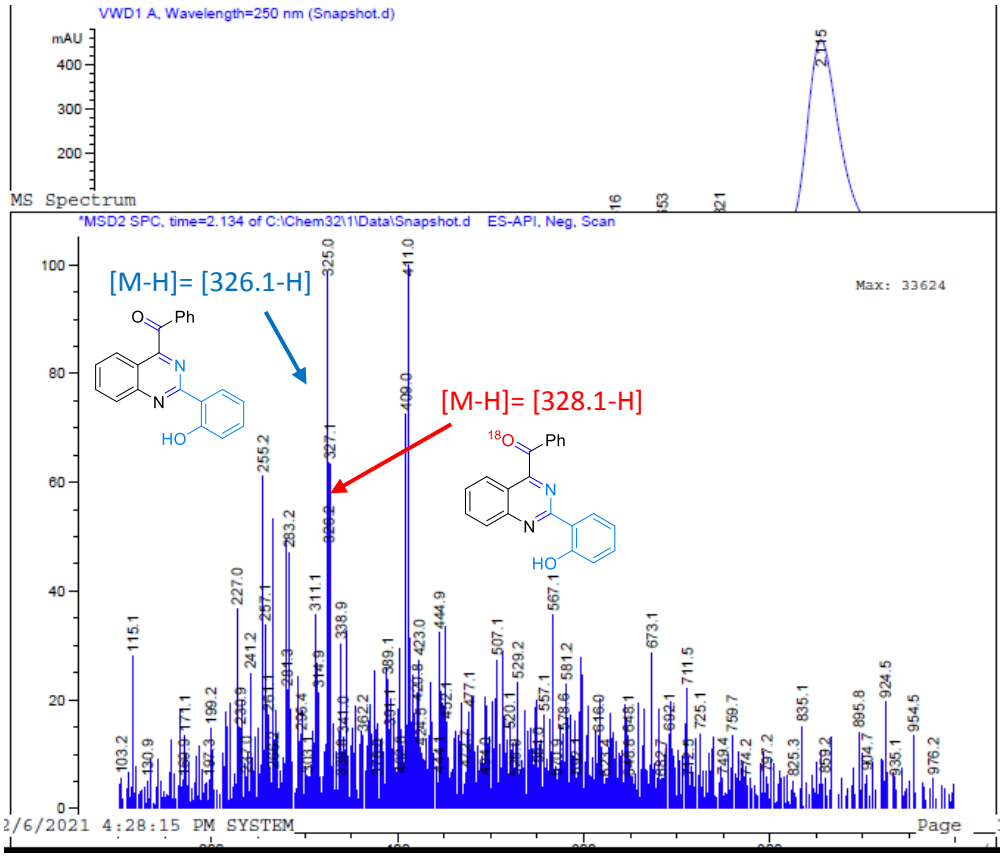

In 2,1- benzo[*c*]isoxazole case-

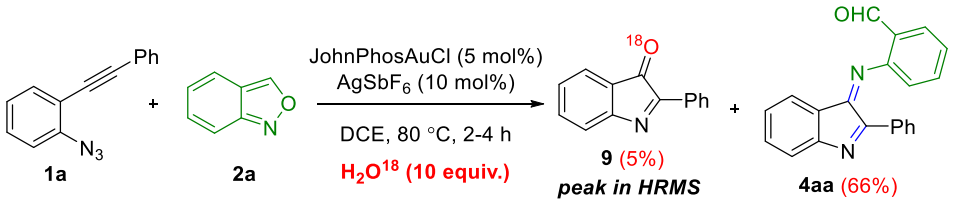

In an oven dried reaction vial, JohnPhosAuCl (5 mol %) and $AgSbF_6$ (10 mol%) were added followed by addition of DCE and the reaction mixture was stirred at room temperature for 10-15 minutes. To this gold complex solution was added dropwise a DCE solution of azidoalkyne (**1**) (1 equiv), 2,1- benzo[*c*]isoxazole (**2a**) (1.1 equiv) and H_2O^{18} (10 equiv) over 5 minutes. The resulting solution was stirred at 80 °C until the complete disappearance of the starting azidoalkyne as indicated by TLC. The crude reaction mixture was analysed by HRMS and shows peak of oxygen labelled indolinone (**7**) compound along with **4aa**. Further, the reaction mixture was concentrated under reduced pressure and the resulting crude was purified by column chromatography to afford indol-3-ylidene products **4aa** in 66% yield**.**

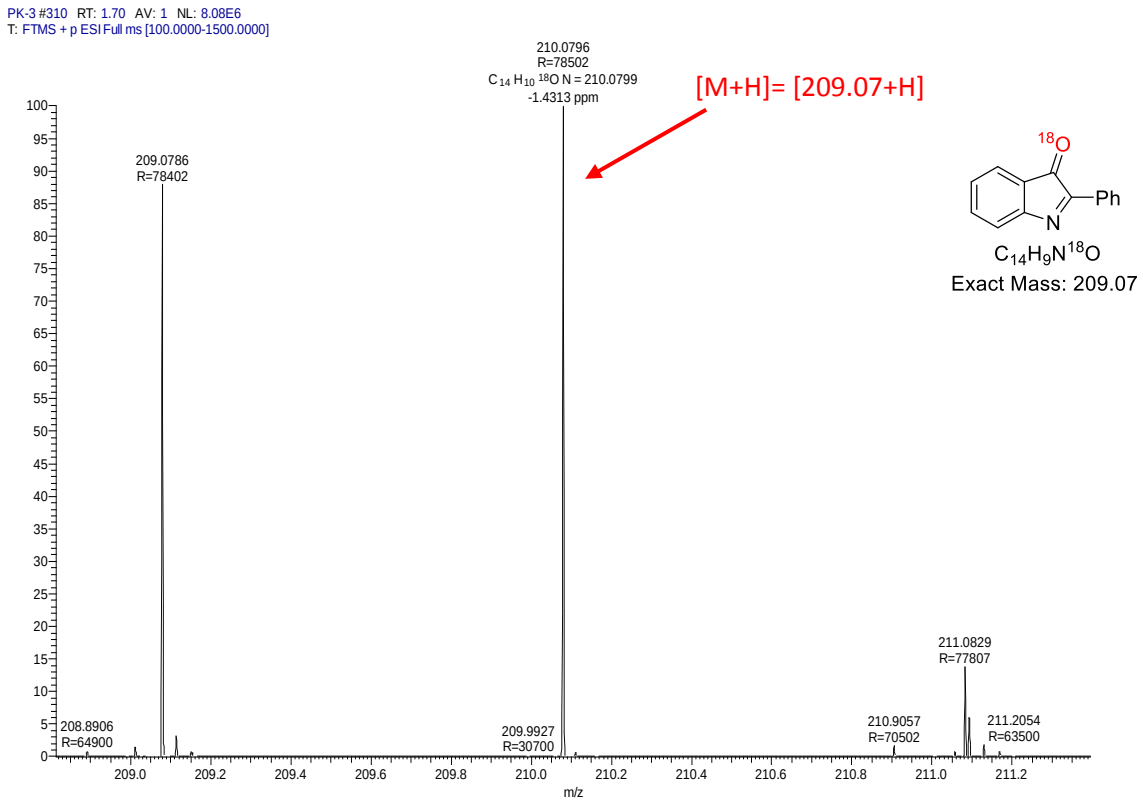

Carbene Trapping Experiment by Employing Excess Styrene

In 1,2- benzo[*d*]isoxazole case-

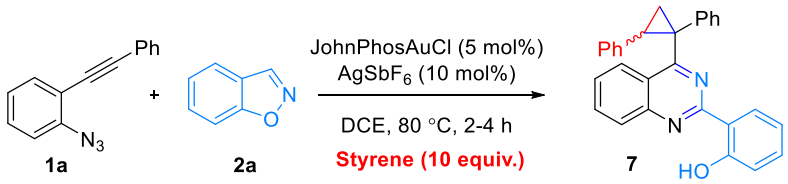

In an oven dried reaction vial, JohnPhosAuCl (5 mol %) and $AgSbF_6$ (10 mol%) were added followed by addition of DCE and the reaction mixture was stirred at room temperature for 10-15 minutes. To this gold complex solution was added dropwise a DCE solution of azidoalkyne (**1a**) (1 equiv), 1,2- benzo[*d*]isoxazole (**2a**) (1.1 equiv) and styrene (10 equiv.) over 5 minutes. The resulting solution was stirred at 80 °C until the complete disappearance of the starting azidoalkyne as indicated by TLC. The reaction mixture was concentrated under reduced pressure and the resulting crude was purified by column chromatography to afford the quinazoline cyclopropane adduct **7**.

2-(4-(1,2-diphenylcyclopropyl)quinazolin-2-yl)phenol (*2:1 dr*) (7)

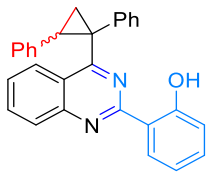

R_f = 0.4 (10% EtOAc in petroleum ether); yield: 72 mg (76%); white gummy solid; IR (neat)ν_{max} 3775, 2930, 2856, 1597, 1453, 1199, 758 cm^{-1}; ^1H NMR (400 MHz, $CDCl_3$): δ 2.36 (dd, *J* = 13.9, 5.4 Hz, 0.5H), 2.53–2.68 (m, 2H), 3.14 (dd, *J* = 13.9, 9.5 Hz, 0.5H), 5.84 (dd, *J* = 9.8, 7.4 Hz, 1H), 5.95 (dd, *J* = 9.4, 5.4 Hz, 0.5H), 6.38–6.49 (m, 2H), 6.56 (dd, *J* = 8.0, 1.6 Hz, 1H), 6.97–7.04 (m, 2H), 7.12 (td, *J* = 7.5, 1.0 Hz, 0.5H), 7.15–7.23 (m, 2H), 7.24–7.30 (m, 1H), 7.31–7.53 (m, 14.5H), 7.79 (d, *J* = 7.7 Hz, 0.5H), 7.87 (d, J=7.8 Hz, 1H), 7.90–7.96 (m, 3H), 13.70 (br. s., 1H) ppm; ^{13}C NMR (100 MHz, $CDCl_3$): δ 43.0 (d), 45.7 (d), 72.9 (d), 73.3 (d), 73.3 (s), 73.4 (s), 115.2 (s), 115.3 (s), 117.5 (d), 117.5 (d), 118.9 (d), 119.1 (d), 121.4 (d), 121.5 (d), 122.0 (d), 122.3 (d), 126.1 (d), 126.2 (d, 2C), 126.8 (d), 127.1 (d), 127.5 (d), 127.7 (d), 127.8 (d), 127.9 (d), 127.9 (d), 128.6 (d, 2C), 128.9 (d), 128.9 (d, 2C), 128.9 (d, 2C), 129.0 (d), 129.2 (d), 129.3 (d), 131.3 (d), 131.4 (d), 131.7 (s), 132.7 (s), 133.2 (d), 133.3 (d), 141.4 (s), 141.9 (s), 143.1 (s), 143.9 (s), 153.6 (s), 153.8 (s), 161.2 (s), 161.5 (s), 175.3 (s), 176.0 (s), 178.6 (s), 179.0 (s) ppm; HRMS (ESI) calcd. for $C_{29}H_{23}N_2O$: 415.1805 $[M + H]^+$; found: 415.1807.

In 2,1- benzo[*c*]isoxazole case-

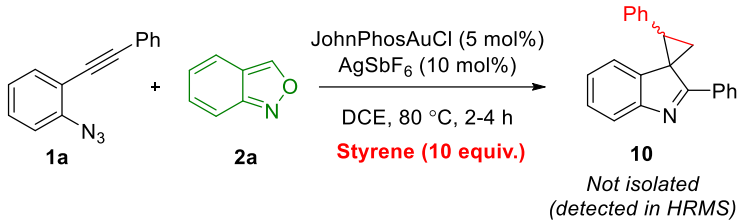

In an oven dried reaction vial, JohnPhosAuCl (5 mol %) and $AgSbF_6$ (10 mol%) were added followed by addition of DCE and the reaction mixture was stirred at room temperature for 10-15 minutes. To this gold complex solution was added dropwise a DCE solution of azidoalkyne (**1a**) (1 equiv), 2,1- benzo[*c*]isoxazole (**2a**) (1.1 equiv) and styrene (10 equiv.) over 5 minutes. The resulting solution was stirred at 80 °C until the complete disappearance of the starting azidoalkyne as indicated by TLC. The crude reaction mixture was analysed by HRMS and shows presence of cyclopropane adduct **10**.

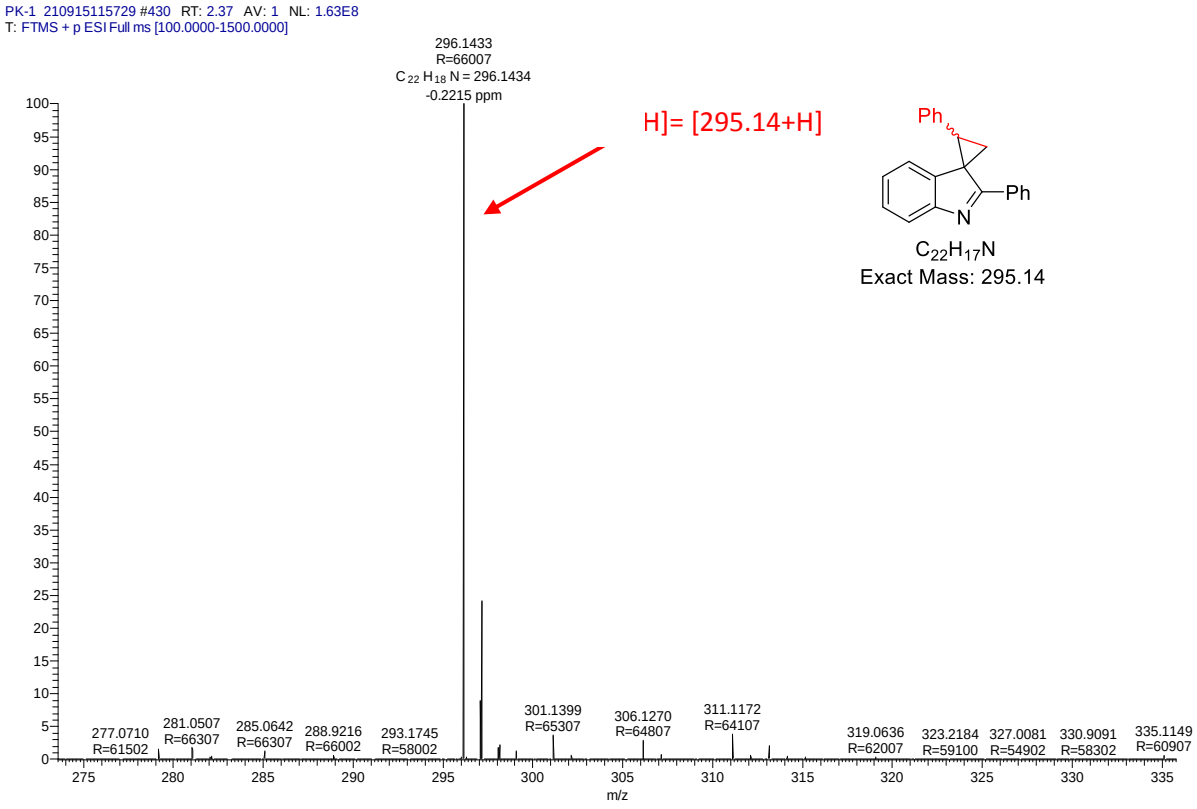

General Procedure for the Competitive Reactions with Allylic Alcohol

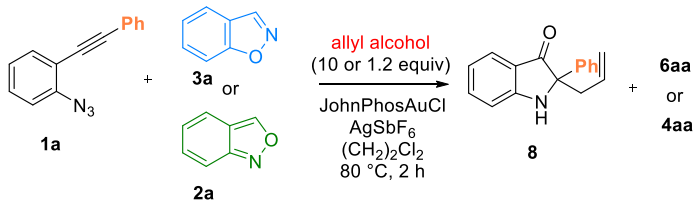

In an oven dried reaction vial, JohnPhosAuCl (5 mol %) and $AgSbF_6$ (10 mol%) were added followed by addition of DCE and the reaction mixture was stirred at room temperature for 10-15 minutes. To this gold complex solution was added dropwise a DCE solution of azidoalkyne (**1a**) (1 equiv), 1,2- benzo[*d*]isoxazole (**3a**) (1.1 equiv) or 2,1- benzo[*c*]isoxazole (**2a**) (1.1 equiv) and allyl alcohol (10 equiv. or 1.2 equivalent) over 5 minutes. The resulting solution was stirred at 80 °C until the complete disappearance of the starting azidoalkyne as indicated by TLC. The reaction mixture was concentrated under reduced pressure and the resulting crude was purified by column chromatography to afford the spiroindolin-3-one product **8** along with quinazoline **6aa** or indol-3-ylidene product **4aa**.

2-allyl-2-phenylindolin-3-one (8)

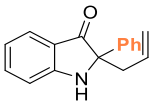

R_f = 0.5 (10% EtOAc in petroleum ether); yellow solid; ^{1}H NMR (400 MHz, $CDCl_3$): δ 2.57 (dd, J = 14.0, 8.4 Hz, 1H), 2.98 (dd, J = 14.0, 5.9 Hz, 1H), 4.96–5.03 (m, 2H), 5.06–5.13 (m, 1H), 5.44–5.57 (m, 1H), 6.72–6.79 (m, 1H), 6.89 (d, J = 8.3 Hz, 1H), 7.17–7.23 (m, 1H), 7.24–7.30 (m, 2H), 7.41 (ddd, J = 8.2, 7.2, 1.3 Hz, 1H), 7.50 (d, J = 7.8 Hz, 1H), 7.52–7.56 (m, 2H) ppm; ^{13}C NMR (100 MHz, $CDCl_3$): δ 42.8 (t), 70.7 (s), 112.3 (d), 119.3 (d), 119.6 (s), 119.7 (t), 125.4 (d), 125.9 (d, 2C), 127.6 (d), 128.6 (d, 2C), 132.6 (d), 137.4 (d), 138.5 (s), 160.2 (s), 201.1 (s) ppm; HRMS (ESI) calcd. for: $C_{17}H_{16}NO$: 250.1226 $[M+H]^+$; found: 250.1223.

General Procedure for the Synthesis of Quinazoline derivatives

In general, all reactions were carried out employing 50 mg of *o*-azidoalkyne **1**.

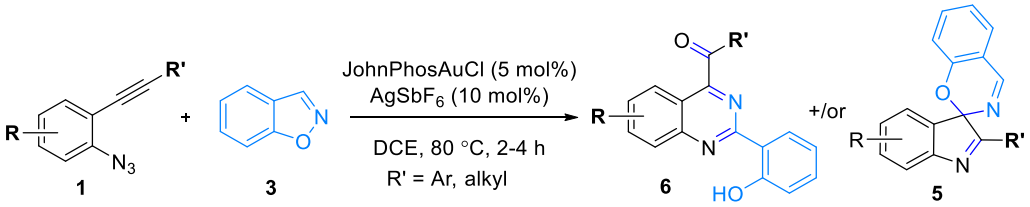

In an oven dried reaction vial, JohnPhosAuCl (5 mol %) and $AgSbF_6$ (10 mol%) were added followed by addition of DCE and the reaction mixture was stirred at room temperature for 10-15 minutes. To this gold complex solution was added a DCE solution of azidoalkyne (**1**) (1 equiv) and 1,2- Benzo[*d*]isoxazole (**3**) (1.1 equiv) dropwise over 5 minutes. The resulting solution was stirred at 80 °C until the complete disappearance of the starting azidoalkyne as indicated by TLC. The reaction mixture was concentrated under reduced pressure and the resulting crude was purified by column chromatography to afford the quinazoline products **6** and/or with the small amounts of spiro product **5**.

(2-(2-hydroxyphenyl)quinazolin-4-yl)(phenyl)methanone (6aa)

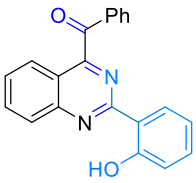

R_f = 0.4 (15% EtOAc in petroleum ether); yield: 58 mg (78%); pale yellow solid; IR (neat)ν_{max} 1672, 1584, 1544, 1478, 1230, 821 cm^{-1}; ^1H NMR (400 MHz, $CDCl_3$): δ 6.96 (ddd, J = 8.1, 7.1, 1.2 Hz, 1H), 7.10 (dd, J = 8.3, 1.0 Hz, 1H), 7.40–7.46 (m, 1H), 7.51–7.57 (m, 2H), 7.63 (ddd, J = 8.3, 7.0, 1.2 Hz, 1H), 7.68–7.74 (m, 1H), 7.99 (ddd, J = 8.5, 7.0, 1.4 Hz, 1H), 8.03–8.14 (m, 4H), 8.56 (dd, J = 8.0, 1.8 Hz, 1H), 13.49 (s, 1H) ppm; ^{13}C NMR (100 MHz, $CDCl_3$): δ 117.8 (d), 118.8 (s), 119.2 (d), 120.1 (s), 126.1 (d), 127.6 (d), 128.2 (d), 128.8 (d, 2C), 130.0 (d), 130.7 (d, 2C), 133.6 (d), 134.6 (d), 135.0 (s), 135.4 (d), 149.2 (s), 160.6 (s), 160.9 (s), 164.5 (s), 192.4 (s) ppm; HRMS (ESI) calcd. for $C_{21}H_{15}N_2O_2$: 327.1134 $[M + H]^+$; found: 327.1122.

(6-fluoro-2-(2-hydroxyphenyl)quinazolin-4-yl)(phenyl)methanone (6ba)

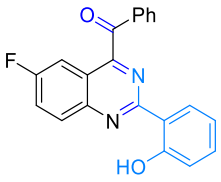

R_f = 0.4 (15% EtOAc in petroleum ether); yield: 44 mg (61%); yellow solid; IR (neat)ν_{max} 1668, 1586, 1543, 1220, 753 cm^{-1}; ^1H NMR (400 MHz, $CDCl_3$): δ 6.96 (ddd, J = 8.1, 7.1, 1.1 Hz, 1H), 7.09 (dd, J = 8.3, 0.9 Hz, 1H), 7.43

(ddd, J = 8.4, 7.0, 1.8 Hz, 1H), 7.52–7.59 (m, 2H), 7.68–7.76 (m, 1H), 7.76–7.80 (m, 2H), 8.03–8.10 (m, 2H), 8.10–8.17 (m, 1H), 8.52 (dd, J = 8.1, 1.7 Hz, 1H), 13.15 (s, 1H) ppm; ^{13}C NMR (100 MHz, $CDCl_3$): δ 109.9 (dd, $J_{C\text{-}F}$ = 23.65 Hz), 117.9 (d), 118.6 (s), 119.3 (d), 120.6 (ds, $J_{C\text{-}F}$ = 9.92 Hz), 125.7 (dd, $J_{C\text{-}F}$ = 25.94 Hz), 128.8 (d, 2C), 129.9 (d), 130.2 (dd, $J_{C\text{-}F}$ = 9.14 Hz), 130.8 (d, 2C), 133.6 (d), 134.7 (d), 134.8 (s), 146.7 (s), 159.6 (s), 160.1 (ds, $J_{C\text{-}F}$ = 3.05 Hz), 160.7 (s), 161.0 (ds, $J_{C\text{-}F}$ = 253.3 Hz), 163.2 (s), 191.9 (s) ppm; HRMS (ESI) calcd. for $C_{21}H_{14}N_2O_2F$: 345.1039 $[M + H]^+$; found: 345.1032.

(6-chloro-2-(2-hydroxyphenyl)quinazolin-4-yl)(phenyl)methanone (6ca)

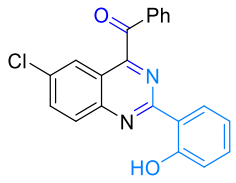

R_f = 0.4 (15% EtOAc in petroleum ether); yield: 46 mg (65%); yellow solid; IR (neat)ν_{max} 1665, 1546, 1236, 835, 755 cm^{-1}; ^{1}H NMR (400 MHz, $CDCl_3$): δ 6.95 (ddd, J = 8.1, 7.1, 1.2 Hz, 1H), 7.08 (dd, J = 8.3, 1.0 Hz, 1H), 7.43 (ddd, J = 8.4, 7.0, 1.8 Hz, 1H), 7.53–7.59 (m, 2H), 7.69–7.75 (m, 1H), 7.91 (dd, J = 9.0, 2.3 Hz, 1H), 8.03–8.06 (m, 2H), 8.10 (d, J = 2.3 Hz, 1H), 8.07 (d, J = 1.1 Hz, 1H), 8.52 (dd, J = 8.1, 1.7 Hz, 1H), 13.16 (s, 1H) ppm; ^{13}C NMR (100 MHz, $CDCl_3$): δ 117.9 (d), 118.6 (s), 119.3 (d), 120.5 (s), 125.1 (d), 128.9 (d, 2C), 129.1 (d), 130.0 (d), 130.8 (d, 2C), 133.8 (d), 134.1 (s), 134.7 (s), 134.8 (d), 136.4 (d), 147.9 (s), 160.6 (s), 160.8 (s), 163.1 (s), 191.8 (s) ppm; HRMS (ESI) calcd. for $C_{21}H_{14}N_2O_2Cl$: 361.0744 $[M + H]^+$; found: 361.0737.

(2-(2-hydroxyphenyl)-6-(trifluoromethyl)quinazolin-4-yl)(phenyl)methanone (6da)

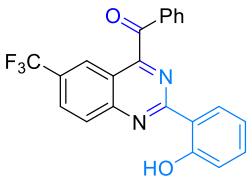

R_f = 0.4 (15% EtOAc in petroleum ether); yield: 40 mg (58%); pale yellow solid; IR (neat)ν_{max} 1670, 1582, 1549, 1311, 1120, 748 cm^{-1}; ^{1}H NMR (400 MHz, $CDCl_3$): δ 6.96 (ddd, J = 8.1, 7.1, 1.2 Hz, 1H), 7.09 (dd, J = 8.3, 0.9 Hz, 1H), 7.42–7.49 (m, 1H), 7.54–7.61 (m, 2H), 7.70–7.77 (m, 1H), 8.06–8.12 (m, 2H), 8.14 (dd, J = 8.9, 1.9 Hz, 1H), 8.21 (d, J = 8.9 Hz, 1H), 8.40–8.45 (m, 1H), 8.54 (dd, J = 8.1, 1.7 Hz, 1H), 13.13 (s, 1H) ppm; ^{13}C NMR (100 MHz, $CDCl_3$): δ 118.1 (d), 118.3 (s), 119.2 (s), 119.4 (d), 121.9 (s), 124.2 (qd, $J_{C\text{-}F}$ = 4.58 Hz), 124.6 (s), 128.9 (d), 128.9 (d, 2C), 130.3 (d), 130.9 (d, 2C), 131.0 (qd, $J_{C\text{-}F}$ = 3.05 Hz), 134.4 (d), 134.6 (s), 134.9 (d), 150.6 (s), 161.2 (s), 162.1 (s), 164.8 (s), 191.5 (s) ppm; HRMS (ESI) calcd. for $C_{22}H_{14}N_2O_2F_3$: 395.1007 $[M + H]^+$; found: 395.1003.

(2-(2-hydroxyphenyl)-6-nitroquinazolin-4-yl)(phenyl)methanone (6ea)

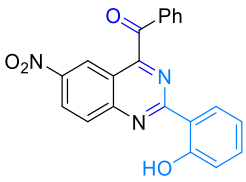

R_f = 0.4 (15% EtOAc in petroleum ether); yield: 42 mg (59%); yellow solid; IR (neat)ν_{max} 1547, 1463, 1242, 750 cm^{-1}; ^1H NMR (400 MHz, $CDCl_3$): δ 6.96 (ddd, J = 8.1, 7.1, 1.2 Hz, 1H), 7.09 (dd, J = 8.3, 1.0 Hz, 1H), 7.44 (ddd, J = 8.4, 7.0, 1.8 Hz, 1H), 7.53–7.60 (m, 2H), 7.69–7.76 (m, 1H), 7.96–8.01 (m, 1H), 8.03–8.09 (m, 3H), 8.26–8.29 (m, 1H), 8.52 (dd, J = 8.1, 1.7 Hz, 1H), 13.17 (s, 1H) ppm; ^{13}C NMR (100 MHz, $CDCl_3$): δ 118.0 (d), 118.6 (s), 119.4 (d), 121.0 (s), 122.2 (s), 128.4 (d), 128.9 (d, 2C), 129.2 (d), 130.1 (d), 130.8 (d, 2C), 133.9 (d), 134.7 (s), 134.8 (d), 138.9 (d), 148.1 (s), 160.7 (s), 160.9 (s), 163.1 (s), 191.8 (s) ppm; HRMS (ESI) calcd. for $C_{21}H_{14}N_3O_4$: 372.0979 $[M + H]^+$; found: 372.0971.

4-benzoyl-2-(2-hydroxyphenyl)quinazoline-6-carbonitrile (6fa)

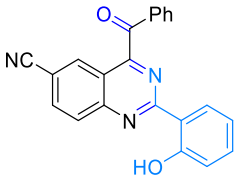

R_f = 0.4 (15% EtOAc in petroleum ether); yield: 49 mg (68%); yellow solid; IR (neat)ν_{max} 1680, 1549, 1467, 1320, 837, 751 cm^{-1}; ^1H NMR (400 MHz, $CDCl_3$): δ 6.98 (td, J = 7.6, 1.1 Hz, 1H), 7.11 (dd, J = 8.3, 1.1 Hz, 1H), 7.49 (ddd, J = 8.4, 7.0, 1.8 Hz, 1H), 7.55–7.63 (m, 2H), 7.70–7.79 (m, 1H), 8.03–8.16 (m, 3H), 8.16–8.22 (m, 1H), 8.46–8.61 (m, 2H), 13.02 (s, 1H) ppm; ^{13}C NMR (100 MHz, $CDCl_3$): δ 111.8 (s), 117.4 (s), 118.2 (d), 119.5 (d), 119.6 (s), 129.0 (d, 2C), 129.1 (d), 130.4 (d), 130.9 (d, 2C), 132.6 (d), 134.4 (s), 134.9 (d), 135.1 (d), 135.9 (d), 150.6 (s), 161.4 (s), 162.7 (s), 164.4 (s), 191.2 (s) ppm; HRMS (ESI) calcd. for $C_{22}H_{14}N_3O_2$: 352.1086 $[M + H]^+$; found: 352.1072.

(7-bromo-2-(2-hydroxyphenyl)quinazolin-4-yl)(phenyl)methanone (6ga)

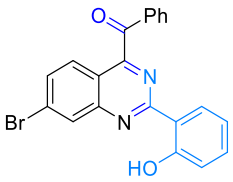

R_f = 0.4 (15% EtOAc in petroleum ether); yield: 66 mg (71%); yellow solid; IR (neat)ν_{max} 1585, 1539, 1340, 752 cm^{-1}; ^1H NMR (400 MHz, $CDCl_3$): δ 6.98 (ddd, J = 8.1, 7.1, 1.1 Hz, 1H), 7.11 (dd, J = 8.3, 1.0 Hz, 1H), 7.49 (ddd, J = 8.4, 7.0, 1.7 Hz, 1H), 7.55–7.63 (m, 2H), 7.75 (tt, J = 7.4, 1.3 Hz, 1H), 8.06–8.15 (m, 2H), 8.23 (d, J = 9.3 Hz, 1H), 8.55 (dd, J = 8.1, 1.8 Hz, 1H), 8.74 (dd, J = 9.3, 2.5 Hz, 1H), 9.00–9.12 (m, 1H), 13.00 (s, 1H) ppm; ^{13}C NMR (100 MHz, $CDCl_3$): δ 118.1 (s), 118.2 (d), 118.9 (s), 119.6 (d), 123.2 (d), 128.8 (d), 129.0 (d, 2C), 129.3 (d), 130.5 (d), 130.9 (d, 2C), 134.3 (s), 135.0 (d), 135.1 (d), 146.0 (s), 151.7 (s), 161.5 (s), 163.1 (s), 165.8 (s), 191.0 (s) ppm; HRMS (ESI) calcd. for $C_{21}H_{14}N_2O_2Br$: 405.0233 $[M + H]^+$; found: 405.0242.

(7-chloro-2-(2-hydroxyphenyl)quinazolin-4-yl)(phenyl)methanone (6ha)

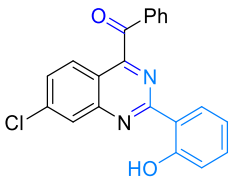

R_f = 0.4 (15% EtOAc in petroleum ether); yield: 53 mg (74%); pale yellow solid; IR (neat)ν_{max} 1666, 1595, 1549, 1467, 1308, 749 cm^{-1}; ^1H NMR (400 MHz, $CDCl_3$): δ 6.96 (ddd, J = 8.1, 7.1, 1.1 Hz, 1H), 7.09 (dd, J = 8.4, 1.0 Hz, 1H), 7.44 (ddd, J = 8.4, 7.1, 1.8 Hz, 1H), 7.52–7.61 (m, 2H), 7.68–7.76 (m, 1H), 7.91 (dd, J = 9.0, 2.3 Hz, 1H), 8.01–8.08 (m, 2H), 8.11 (d, J = 1.9 Hz, 2H), 8.53 (dd, J = 8.0, 1.8 Hz, 1H), 13.15 (s, 1H) ppm; ^{13}C NMR (100 MHz, $CDCl_3$): δ 118.0 (d), 118.5 (s), 118.5 (s), 119.3 (d), 126.7 (d), 127.6 (d), 128.1 (d, 2C), 128.9 (s), 129.3 (d), 130.1 (s), 130.8 (d, 2C), 134.0 (d), 134.8 (d), 142.0 (s), 150.0 (s), 161.0 (s), 161.5 (s), 164.1 (s), 191.9 (s) ppm; HRMS (ESI) calcd. for $C_{21}H_{14}N_2O_2Cl$: 361.0744 $[M + H]^+$; found: 361.0736.

(7-chloro-2-(2-hydroxyphenyl)quinazolin-4-yl)(phenyl)methanone (6ia)

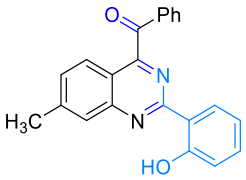

R_f = 0.4 (15% EtOAc in petroleum ether); yield: 60 mg (82%); yellow solid; IR (neat)ν_{max} 1672, 1547, 1483, 1229, 757 cm^{-1}; ^1H NMR (400 MHz, $CDCl_3$): δ 2.63 (s, 3H), 6.90–6.99 (m, 1H), 7.08 (dd, J = 8.3, 0.8 Hz, 1H), 7.38–7.47 (m, 2H), 7.50–7.59 (m, 2H), 7.65–7.73 (m, 1H), 7.88 (s, 1H), 7.95 (d, J = 8.5 Hz, 1H), 8.01–8.10 (m, 2H), 8.55 (dd, J = 8.0, 1.6 Hz, 1H), 13.57 (br. s., 1H) ppm; ^{13}C NMR (100 MHz, $CDCl_3$): δ 22.3 (q), 117.8 (d), 118.3 (s), 118.9 (s), 119.1 (d), 125.7 (d), 126.5 (d), 128.8 (d, 2C), 129.9 (d), 130.5 (d), 130.7 (d, 2C), 133.4 (d), 134.5 (d), 135.1 (s), 146.8 (s), 149.5 (s), 160.6 (s), 160.9 (s), 163.8 (s), 192.5 (s) ppm; HRMS (ESI) calcd. for $C_{22}H_{17}N_2O_2$: 391.1290 $[M + H]^+$; found: 341.1280.

(2-(2-hydroxyphenyl)quinazolin-4-yl)(4-methoxyphenyl)methanone (6ja)

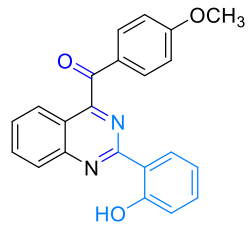

R_f = 0.4 (15% EtOAc in petroleum ether); yield: 50 mg (70%); yellow solid; IR (neat)ν_{max} 1662, 1589, 1544, 1252, 1163, 758 cm^{-1}; ^1H NMR (400 MHz, $CDCl_3$): δ 3.91 (s, 3H), 6.94–6.99 (m, 1H), 6.99–7.02 (m, 2H), 7.09 (dd, J = 8.3, 1.0 Hz, 1H), 7.40–7.46 (m, 1H), 7.62 (ddd, J = 8.3, 7.0, 1.1 Hz, 1H), 7.95–8.00 (m, 1H), 8.01–8.12 (m, 4H), 8.58 (dd, J = 8.0, 1.8 Hz, 1H), 13.53 (br. s., 1H) ppm; ^{13}C NMR (100 MHz, $CDCl_3$): δ 55.7 (q), 114.2 (d, 2C), 117.8 (d), 118.9 (s), 119.1 (d), 120.2 (s), 126.3 (d), 127.5 (d), 128.0 (d), 128.1 (d), 130.0 (d), 133.2 (d, 2C), 133.5 (d), 135.3 (d), 149.2 (s), 160.6 (s), 160.9 (s), 164.8 (s), 165.0 (s), 190.8 (s) ppm; HRMS (ESI) calcd. for $C_{22}H_{17}N_2O_3$: 357.1239 $[M + H]^+$; found: 357.1241.

(4-(tert-butyl)phenyl)(2-(2-hydroxyphenyl)quinazolin-4-yl)methanone (6ka)

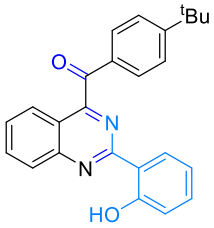

R_f = 0.4 (15% EtOAc in petroleum ether); yield: 44 mg (64%); yellow solid; IR (neat)ν_{max} 1671, 1597, 1543, 1234, 751 cm^{-1}; ^1H NMR (400 MHz, $CDCl_3$): δ 1.38 (s, 9H), 6.94–7.00 (m, 1H), 7.10 (dd, J = 8.3, 0.8 Hz, 1H), 7.40–7.47 (m, 1H), 7.53–7.57 (m, 2H), 7.58–7.65 (m, 1H), 7.94–8.06 (m, 4H), 8.10 (d, J = 8.5 Hz, 1H), 8.59 (dd, J = 8.0, 1.8 Hz, 1H), 13.54 (br. s., 1H) ppm; ^{13}C NMR (100 MHz, $CDCl_3$): δ 31.0 (q, 3C), 35.4 (s), 117.8 (d), 118.9 (s), 119.1 (d), 120.1 (s), 125.9 (d, 2C), 126.2 (d), 127.5 (d), 128.1 (d), 130.1 (d), 130.7 (d, 2C), 132.4 (s), 133.5 (d), 135.3 (d), 149.1 (s), 158.8 (s), 160.6 (s), 160.9 (s), 165.0 (s), 192.0 (s) ppm; HRMS (ESI) calcd. for $C_{25}H_{23}N_2O_2$: 383.1760 $[M + H]^+$; found: 383.1755.

cyclopropyl(2-(2-hydroxyphenyl)quinazolin-4-yl)methanone (6la)

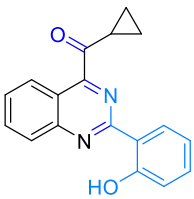

R_f = 0.4 (15% EtOAc in petroleum ether); yield: 57 mg (72%); yellow solid; IR (neat)ν_{max} 1685, 1535, 1470, 1218, 750 cm^{-1}; ^1H NMR (400 MHz, $CDCl_3$): δ 1.30 (dt, J = 7.8, 3.6 Hz, 2H), 1.40–1.52 (m, 2H), 3.35 (ddd, J = 7.9, 4.6, 3.3 Hz, 1H), 6.97–7.06 (m, 1H), 7.09 (d, J = 8.3 Hz, 1H), 7.40–7.49 (m, 1H), 7.65 (ddd, J = 8.3, 7.1, 1.0 Hz, 1H), 7.89–7.98 (m, 1H), 7.99–8.08 (m, 1H), 8.59–8.80 (m, 2H), 13.49 (s, 1H) ppm; ^{13}C NMR (100 MHz, $CDCl_3$): δ 13.7 (t, 2C), 19.3 (d), 117.9 (d), 118.8 (s), 119.0 (s), 119.1 (d), 126.9 (d), 127.2 (d), 128.7 (d), 129.7 (d), 133.4 (d), 135.0 (d), 149.9 (s), 160.3 (s), 160.6 (s), 160.8 (s), 202.4 (s) ppm; HRMS (ESI) calcd. for $C_{18}H_{15}N_2O_2$: 291.1134 $[M + H]^+$; found: 291.1129.

1-(2-(2-hydroxyphenyl)quinazolin-4-yl)butan-1-one (6ma):

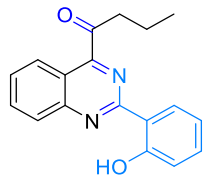

R_f = 0.5 (10% EtOAc in petroleum ether); yield: 36 mg (45%); dark yellow syrup; IR (neat) ν_{max} 1651, 1556, 1228, 744 cm^{-1}; ^1H NMR (400 MHz, $CDCl_3$): δ 1.11 (t, J = 7.4 Hz, 3H), 1.83–1.95 (m, 2H), 3.37 (t, J = 7.2 Hz, 2H), 7.04 (ddd, J = 8.1, 7.1, 1.2 Hz, 1H), 7.11 (dd, J = 8.2, 0.9 Hz, 1H), 7.46 (ddd, J = 8.4, 7.0, 1.8Hz, 1H), 7.68 (ddd, J = 8.4, 6.9, 1.2 Hz, 1H), 7.96 (ddd, J = 8.4, 6.9, 1.4 Hz, 1H), 8.05 (dq, J = 8.5, 0.6 Hz, 1H), 8.59–8.72 (m, 2H), 13.50 (s, 1H) ppm; ^{13}C NMR (100 MHz, $CDCl_3$): δ 13.8 (q), 17.3 (t), 42.1 (t), 117.9 (d), 118.8 (s), 119.0 (s), 119.2 (d), 126.7 (d),

127.3 (d), 128.8 (d), 129.6 (d), 133.5 (d), 135.0 (d), 149.9 (s), 160.3 (s), 160.7 (s), 160.9 (s), 203.5 (s) ppm; HRMS (ESI) calcd. for: $C_{18}H_{17}N_2O_2$: 293.1290 $[M+H]^+$; found: 293.1282.

(2-(5-fluoro-2-hydroxyphenyl)quinazolin-4-yl)(phenyl)methanone (6ab)

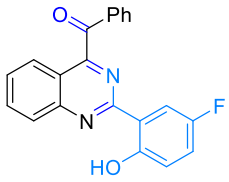

R_f = 0.4 (15% EtOAc in petroleum ether); yield: 54 mg (69%); yellow solid; IR (neat)ν_{max} 1674, 1546, 1484, 1232, 757 cm^{-1}; ^1H NMR (400 MHz, $CDCl_3$): δ 7.04 (dd, J = 9.1, 4.7 Hz, 1H), 7.11–7.18 (m, 1H), 7.52–7.59 (m, 2H), 7.64–7.75 (m, 2H), 7.98–8.06 (m, 3H), 8.12 (d, J = 8.5 Hz, 1H), 8.08 (d, J = 8.4 Hz, 1H), 8.23 (dd, J = 9.9, 3.1 Hz, 1H), 13.22 (br. s., 1H) ppm; ^{13}C NMR (100 MHz, $CDCl_3$): δ 115.0 (dd, $J_{C\text{-}F}$ = 25.18 Hz), 118.8 (dd, $J_{C\text{-}F}$ = 7.63 Hz), 120.3 (s), 120.6 (dd, $J_{C\text{-}F}$ = 23.65 Hz), 120.8 (s), 126.2 (d), 127.7 (d), 128.6 (d), 128.9 (d, 2C), 130.7 (d, 2C), 134.8 (d), 134.9 (s), 135.6 (d), 149.2 (s), 154.6 (s), 157.0 (s), 159.6 (ds, $J_{C\text{-}F}$ = 3.05 Hz), 164.7 (s), 192.2 (s) ppm; HRMS (ESI) calcd. for $C_{21}H_{14}N_2O_2F$: 345.1039 $[M + H]^+$; found: 345.1030.

(6-chloro-2-(5-fluoro-2-hydroxyphenyl)quinazolin-4-yl)(phenyl)methanone (6cb)

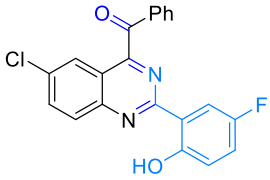

R_f = 0.4 (15% EtOAc in petroleum ether); yield: 55 mg (74%); yellow solid; IR (neat)ν_{max} 1654, 1545, 1455, 1220, 752 cm^{-1}; ^1H NMR (400 MHz, $CDCl_3$): δ 7.03 (dd, J = 9.0, 4.6 Hz, 1H), 7.15 (ddd, J = 9.0, 7.6, 3.3 Hz, 1H), 7.53–7.61 (m, 2H), 7.73 (tt, J = 7.5, 1.3 Hz, 1H), 7.94 (dd, J = 9.0, 2.3 Hz, 1H), 8.02–8.09 (m, 3 H), 8.10 –8.14 (m, 1H), 8.19 (dd, J = 9.8, 3.2 Hz, 1H), 12.89 (br. s., 1H) ppm; ^{13}C NMR (100 MHz, $CDCl_3$): δ 115.0 (dd, $J_{C\text{-}F}$ = 25.18 Hz), 119.0 (dd, $J_{C\text{-}F}$ = 7.63 Hz), 120.7 (s), 120.9 (dd, $J_{C\text{-}F}$ = 23.65 Hz), 125.2 (d), 128.9 (d, 2C), 129.2 (d), 130.8 (d, 2C), 134.6 (ds, $J_{C\text{-}F}$ = 2.29 Hz), 135.0 (d), 136.6 (d), 147.9 (s), 154.7 (s), 156.9 (s), 157.0 (ds, $J_{C\text{-}F}$ = 267.03 Hz), 159.7 (s), 163.3 (s), 191.6 (s) ppm; HRMS (ESI) calcd. for $C_{21}H_{13}N_2O_2FCl$: 379.0650 $[M + H]^+$; found: 379.0631.

(2-(5-fluoro-2-hydroxyphenyl)-7-methylquinazolin-4-yl)(phenyl)methanone (6ib)

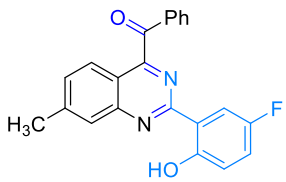

R_f = 0.4 (15% EtOAc in petroleum ether); yield: 57 mg (74%); yellow solid; IR (neat)ν_{max} 1547, 1483, 1234, 885, 805 cm^{-1}; ^1H NMR (400 MHz, $CDCl_3$): δ 2.64 (s, 3H), 6.95–7.07 (m, 1H), 7.13 (ddd, J = 9.0, 7.7, 3.3 Hz, 1H), 7.48 (dd, J = 8.6, 1.6 Hz, 1H), 7.51–7.58 (m, 2H), 7.70 (tt, J = 7.4, 1.3 Hz, 1H), 7.89 (s, 1H), 7.96 (d, J = 8.5 Hz, 1H), 8.00–8.08 (m, 2H), 8.22 (dd, J =

9.9, 3.2 Hz, 1H), 13.29 (br. s., 1H) ppm; ^{13}C NMR (100 MHz, $CDCl_3$): δ 22.4 (q), 115.0 (dd, $J_{C\text{-}F}$ = 25.18 Hz), 118.5 (s), 118.8 (dd, $J_{C\text{-}F}$ = 7.63 Hz), 119.2 (ds, $J_{C\text{-}F}$ = 7.63 Hz), 120.3 (dd, $J_{C\text{-}F}$ = 24.41 Hz), 125.8 (d), 126.6 (d), 128.8 (d, 2C), 130.7 (d, 2C), 130.9 (d), 134.6 (d), 135.0 (s), 147.1 (s), 149.5 (s), 154.6 (s), 157.0 (ds, $J_{C\text{-}F}$ = 1.52 Hz), 159.7 (ds, $J_{C\text{-}F}$ = 3.05 Hz), 164.0 (s), 192.4 (s) ppm; HRMS (ESI) calcd. for $C_{22}H_{16}N_2O_2F$: 359.1196 $[M + H]^+$; found: 359.1195.

cyclopropyl(2-(5-fluoro-2-hydroxyphenyl)quinazolin-4-yl)methanone (6lb)

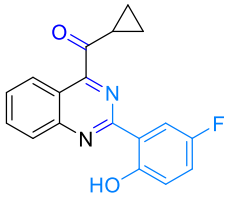

R_f = 0.4 (15% EtOAc in petroleum ether); yield: 51 mg (61%); yellow solid; IR (neat)ν_{max} 1684, 1534, 1469, 1233, 1214, 763 cm^{-1}; ^{1}H NMR (400 MHz, $CDCl_3$): δ 1.30–1.35 (m, 2H), 1.43–1.50 (m, 2H), 3.32 (tt, J = 7.9, 4.6 Hz, 1H), 7.03 (dd, J = 9.0, 4.8 Hz, 1H), 7.15 (ddd, J = 9.0, 7.7, 3.3 Hz, 1H), 7.68 (ddd, J = 8.4, 6.9, 1.3 Hz, 1H), 7.92–8.01 (m, 1H), 8.02–8.09 (m, 1H), 8.35 (dd, J = 9.9, 3.3 Hz, 1H), 8.61–8.73 (m, 1H), 13.22 (s, 1H) ppm; ^{13}C NMR (100 MHz, $CDCl_3$): δ 13.8 (t, 2C), 19.4 (d), 114.7 (dd, $J_{C\text{-}F}$ = 25.18 Hz), 118.9 (dd, $J_{C\text{-}F}$ = 7.63 Hz), 119.1 (ds, $J_{C\text{-}F}$ = 7.63 Hz), 120.4 (dd, $J_{C\text{-}F}$ = 23.65 Hz), 127.0 (d), 127.3 (d), 129.1 (d), 135.2 (d), 149.9 (s), 154.6 (s), 156.9 (s), 157.0 (ds, $J_{C\text{-}F}$ = 275.4 Hz), 159.7 (s), 160.5 (s), 202.2 (s) ppm; HRMS (ESI) calcd. for $C_{18}H_{14}N_2O_2F$: 309.1039 $[M + H]^+$; found: 309.1035.

(2-(5-chloro-2-hydroxyphenyl)quinazolin-4-yl)(phenyl)methanone (6ac)

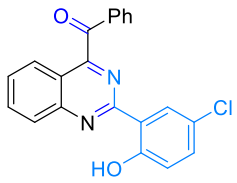

R_f = 0.4 (15% EtOAc in petroleum ether); yield: 53 mg (65%); yellow solid; IR (neat)ν_{max} 1680, 1547, 1463, 1222, 747, 661 cm^{-1}; ^{1}H NMR (400 MHz, $CDCl_3$): δ 7.03 (d, J = 8.8 Hz, 1H), 7.36 (dd, J = 8.8, 2.8 Hz, 1H), 7.53–7.61 (m, 2H), 7.66 (ddd, J = 8.3, 7.0, 1.1 Hz, 1H), 7.72 (tt, J = 7.4, 1.3 Hz, 1H), 7.98–8.08 (m, 4H), 8.09–8.15 (m, 1H), 8.52 (d, J = 2.8 Hz, 1H), 13.44 (br. s., 1H) ppm; ^{13}C NMR (100 MHz, $CDCl_3$): δ 119.4 (d), 119.8 (s), 120.3 (s), 124.0 (s), 126.2 (d), 127.6 (d), 128.6 (d), 128.9 (d, 2C), 129.1 (d), 130.7 (d, 2C), 133.3 (d), 134.8 (d), 134.8 (s), 135.6 (d), 149.1 (s), 159.4 (s), 159.5 (s), 164.9 (s), 192.2 (s) ppm; HRMS (ESI) calcd. for $C_{21}H_{14}N_2O_2Cl$: 361.0744 $[M + H]^+$; found: 361.0740.

(2-(5-chloro-2-hydroxyphenyl)-6-fluoroquinazolin-4-yl)(phenyl)methanone (6bc)

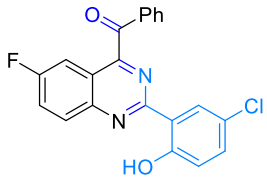

R_f = 0.4 (15% EtOAc in petroleum ether); yield: 56 mg (70%); yellow solid; IR (neat)ν_{max} 1674, 1543, 1474, 1218, 1163, 756, 694 cm^{-1}; ^1H NMR (400 MHz, $CDCl_3$): δ 7.04 (d, J = 8.9 Hz, 1H), 7.37 (dd, J = 8.8, 2.8 Hz, 1H), 7.54–7.61 (m, 2H), 7.71–7.83 (m, 3H), 8.01–8.07 (m, 2H), 8.12–8.19 (m, 1H), 8.49 (d, J = 2.6 Hz, 1H), 13.11 (br. s., 1H) ppm; ^{13}C NMR (100 MHz, $CDCl_3$): δ 110.0 (dd, $J_{C\text{-}F}$ = 23.65 Hz), 119.4 (d), 119.6 (s), 120.9 (s), 124.2 (s), 126.0 (dd, $J_{C\text{-}F}$ = 25.94 Hz), 129.0 (d, 2C), 129.0 (d), 130.3 (s), 130.4 (s), 130.8 (d, 2C), 133.4 (d), 134.6 (s), 134.9 (d), 150.6 (s), 159.2 (s), 162.4 (s), 163.7 (s), 191.7 (s) ppm; HRMS (ESI) calcd. for $C_{21}H_{13}N_2O_2ClF$: 379.0644 $[M + H]^+$; found: 379.0647.

(2-(5-chloro-2-hydroxyphenyl)-6-(trifluoromethyl)quinazolin-4-yl)(phenyl)methanone (6dc)

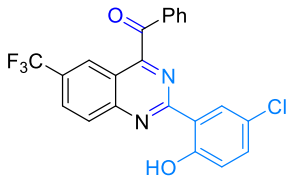

R_f = 0.4 (15% EtOAc in petroleum ether); yield: 39 mg (52%); yellow solid; IR (neat)ν_{max} 1670, 1588, 1548, 1317, 1216, 1130, 840 cm^{-1}; ^1H NMR (400 MHz, $CDCl_3$): δ 7.05 (d, J = 8.9 Hz, 1H), 7.40 (dd, J = 8.8, 2.8 Hz, 1H), 7.56–7.62 (m, 2H), 7.72–7.79 (m, 1H), 8.03–8.10 (m, 2H), 8.17 (dd, J = 8.9, 1.9 Hz, 1H), 8.24 (d, J = 8.9 Hz, 1H), 8.38–8.43 (m, 1H), 8.51 (d, J = 2.8 Hz, 1H), 13.09 (br. s., 1H) ppm; ^{13}C NMR (100 MHz, $CDCl_3$): δ 119.3 (s), 119.4 (s), 119.7 (d), 121.8 (s), 124.4 (qd, $J_{C\text{-}F}$ = 4.58 Hz), 129.0 (d), 129.0 (d, 2C), 129.4 (d), 130.2 (s), 130.8 (d, 2C) 131.3 (qd, $J_{C\text{-}F}$ = 3.05 Hz), 134.2 (d), 134.4 (s), 135.2 (d), 150.5 (s), 159.7 (s), 161.1 (s), 165.3 (s), 191.3 (s) ppm; HRMS (ESI) calcd. for $C_{22}H_{13}N_2O_2ClF_3$: 429.0618 $[M + H]^+$; found: 429.0611.

(7-bromo-2-(5-chloro-2-hydroxyphenyl)quinazolin-4-yl)(phenyl)methanone (6gc)

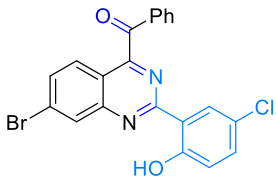

R_f = 0.4 (15% EtOAc in petroleum ether); yield: 49 mg (67%); yellow solid; IR (neat)ν_{max} 2928, 1656, 1543, 1466, 1221, 830, 756, 684 cm^{-1}; ^1H NMR (400 MHz, $CDCl_3$): δ 7.03 (d, J = 8.9 Hz, 1H), 7.37 (dd, J = 8.8, 2.7 Hz, 1H), 7.55–7.60 (m, 2H), 7.71–7.76 (m, 1H), 7.98–8.01 (m, 1H), 8.02–8.05 (m, 2H), 8.06–8.10 (m, 1H), 8.26 (dd, J = 2.1, 0.4 Hz, 1H), 8.49 (d, J = 2.8 Hz, 1H), 13.11 (br. s., 1H) ppm; ^{13}C NMR (100 MHz, $CDCl_3$): δ 119.5 (d), 119.6 (s), 121.1 (s), 122.7 (s), 124.2 (s), 128.5 (d), 129.0 (d, 2C), 129.2 (d), 129.2 (d), 130.8 (d, 2C), 133.7 (d), 134.6

(s), 135.0 (d), 139.2 (d), 148.0 (s), 159.4 (s), 159.6 (s), 163.5 (s), 191.6 (s) ppm; HRMS (ESI) calcd. for $C_{21}H_{13}N_2O_2ClBr$: 438.9843 $[M + H]^+$; found: 438.9844.

(2-(5-bromo-2-hydroxyphenyl)quinazolin-4-yl)(phenyl)methanone (6ad)

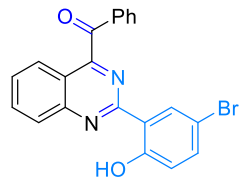

R_f = 0.4 (15% EtOAc in petroleum ether); yield: 57 mg (62%); yellow solid; IR (neat)ν_{max} 1683, 1541, 1466, 1224, 880, 752 cm^{-1}; ^1H NMR (400 MHz, $CDCl_3$): δ 6.99 (d, J = 8.8 Hz, 1H), 7.49 (dd, J = 8.8, 2.6 Hz, 1H), 7.53–7.60 (m, 2 H), 7.66 (ddd, J = 8.3, 7.0, 1.1 Hz, 1H), 7.72 (tt, J = 7.4, 1.3 Hz, 1H), 7.98–8.07 (m, 4H), 8.10–8.14 (m, 1H), 8.67 (d, J = 2.6 Hz, 1H), 13.47 (br. s., 1H) ppm; ^{13}C NMR (100 MHz, $CDCl_3$): δ 111.1 (s), 119.8 (d), 120.3 (s), 120.4 (s), 126.2 (d), 127.6 (d), 128.6 (d), 128.9 (d, 2C), 130.7 (d, 2C), 132.1 (d), 134.8 (d), 135.6 (d), 136.1 (d), 149.1 (s), 159.4 (s), 159.9 (s, 2C), 164.9 (s), 192.2 (s) ppm; HRMS (ESI) calcd. for $C_{21}H_{14}N_2O_2Br$: 405.0239 $[M + H]^+$; found: 405.0233.

(2-(2-hydroxy-5-methylphenyl)quinazolin-4-yl)(phenyl)methanone (6ae)

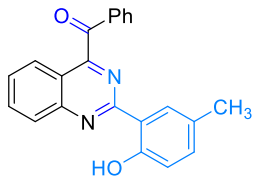

R_f = 0.4 (15% EtOAc in petroleum ether); yield: 52 mg (67%); yellow solid; IR (neat)ν_{max} 1674, 1545, 1452, 1228, 746, 693 cm^{-1}; ^1H NMR (400 MHz, $CDCl_3$): δ 2.32 (s, 3H), 7.00 (d, J = 8.4 Hz, 1H), 7.22–7.26 (m, 1H), 7.52–7.58 (m, 2H), 7.61 (ddd, J = 8.3, 7.0, 1.2 Hz, 1H), 7.67–7.73 (m, 1H), 7.95–8.01 (m, 1H), 8.01–8.07 (m, 3H), 8.08–8.12 (m, 1H), 8.35 (d, J = 1.9 Hz, 1H), 13.27 (br. s., 1H) ppm; ^{13}C NMR (100 MHz, $CDCl_3$): δ 20.6 (q), 117.7 (d), 118.4 (s), 120.0 (s), 126.1 (d), 127.6 (d), 128.1 (d), 128.2 (s), 128.8 (d, 2C), 129.7 (d), 130.7 (d, 2C), 134.5 (d), 134.6 (d), 135.0 (s), 135.3 (d), 149.3 (s), 158.8 (s), 160.7 (s), 164.6 (s), 192.4 (s) ppm; HRMS (ESI) calcd. for $C_{22}H_{17}N_2O_2F$: 341.1290 $[M + H]^+$; found: 341.1281.

(6-fluoro-2-(2-hydroxy-5-methylphenyl)quinazolin-4-yl)(phenyl)methanone (6be)

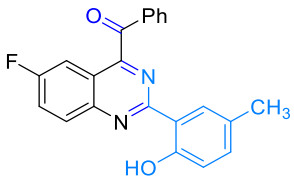

R_f = 0.4 (15% EtOAc in petroleum ether); yield: 45 mg (60%); yellow solid; IR (neat)ν_{max} 1666, 1546, 1493, 1211, 800, 640 cm^{-1}; ^1H NMR (400 MHz, $CDCl_3$): δ 2.32 (s, 3H), 6.99 (d, J = 8.4 Hz, 1H), 7.24 (dd, J = 8.3, 2.3 Hz, 1H), 7.52–7.60 (m, 2H), 7.69–7.80 (m, 3H), 8.04–8.09 (m, 2H), 8.09–8.16 (m, 1H), 8.31 (d, J = 2.0 Hz, 1H), 12.94 (s, 1H) ppm; ^{13}C NMR (100 MHz, $CDCl_3$): δ 20.6 (q), 109.8 (dd, $J_{C\text{-}F}$ = 23.65 Hz), 117.7 (d), 118.1 (s), 120.4 (ds, $J_{C\text{-}F}$ = 9.92 Hz),

125.7 (dd, $J_{C\text{-}F}$ = 25.94 Hz), 128.4 (s), 128.9 (d, 2C), 129.6 (s), 130.2 (dd, $J_{C\text{-}F}$ = 9.16 Hz), 130.8 (d, 2C), 134.6 (dd, $J_{C\text{-}F}$ = 14.50 Hz), 134.8 (s), 146.7 (s), 158.5 (s), 159.6 (ds, $J_{C\text{-}F}$ = 253.30 Hz), 160.2 (s), 160.2 (s), 163.3 (ds, $J_{C\text{-}F}$ = 5.34 Hz), 192.0 (s) ppm; HRMS (ESI) calcd. for $C_{22}H_{16}N_2O_2F$: 359.1196 $[M + H]^+$; found: 359.1190.

4-benzoyl-2-(2-hydroxy-5-methylphenyl)quinazoline-6-carbonitrile (6fe)

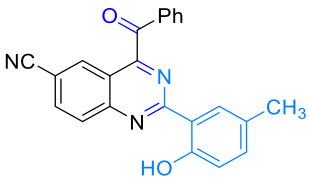

R_f = 0.4 (15% EtOAc in petroleum ether); yield: 51 mg (68%); yellow solid; IR (neat)ν_{max} 2856, 1675, 1597, 1455, 1320, 758 cm^{-1}; ^1H NMR (400 MHz, $CDCl_3$): δ 2.32 (s, 3H), 7.01 (d, J = 8.4 Hz, 1H), 7.30 (dd, J = 8.4, 2.3 Hz, 1H), 7.56–7.61 (m, 2H), 7.72–7.78 (m, 1H), 8.05–8.11 (m, 3H), 8.15–8.20 (m, 1H), 8.32 (d, J = 1.9 Hz, 1H), 8.48 (dd, J = 1.8, 0.8 Hz, 1H), 12.82 (s, 1H) ppm; ^{13}C NMR (100 MHz, $CDCl_3$): δ 20.6 (q),111.7 (s), 117.4 (s), 117.7 (s), 118.0 (d), 119.4 (s), 128.7 (s), 129.0 (d, 2C), 129.1 (d), 130.1 (d), 130.9 (d, 2C), 132.5 (d), 134.4 (s), 135.1 (d), 135.8 (d), 135.9 (d), 150.7 (s), 159.4 (s), 162.8 (s), 164.5 (s), 191.3 (s) ppm; HRMS (ESI) calcd. for $C_{23}H_{16}N_3O_2$: 366.1237 $[M + H]^+$; found: 366.1234.

(7-bromo-2-(2-hydroxy-5-methylphenyl)quinazolin-4-yl)(phenyl)methanone (6ge)

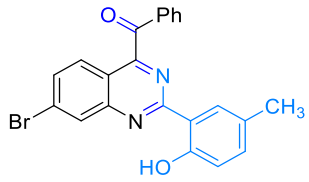

R_f = 0.4 (15% EtOAc in petroleum ether); yield: 64 mg (71%); yellow solid; IR (neat)ν_{max} 2358, 1656, 1550, 1492, 1227, 836, 750, 673 cm^{-1}; ^1H NMR (400 MHz, $CDCl_3$): δ 2.32 (s, 3H), 6.99 (d, J = 8.3 Hz, 1H), 7.25 (dd, J = 8.6, 2.1 Hz, 1H), 7.53–7.59 (m, 2H), 7.70–7.75 (m, 1H), 7.95–7.99 (m, 1H), 8.05 (ddd, J = 8.8, 7.3, 1.7 Hz, 3H), 8.23 (dd, J = 2.1, 0.5 Hz, 1H), 8.31 (d, J = 2.0 Hz, 1H), 12.95 (s, 1H) ppm; ^{13}C NMR (100 MHz, $CDCl_3$): δ 20.6 (t), 117.8 (d), 118.1 (s), 120.9 (s), 122.0 (s), 128.3 (d), 128.4 (s), 128.9 (d, 2C), 129.2 (d), 129.7 (d), 130.8 (d, 2C), 134.7 (s), 134.8 (d), 134.9 (d), 138.9 (d), 148.2 (s), 158.8 (s), 160.8 (s), 163.1 (s), 191.8 (s) ppm; HRMS (ESI) calcd. for $C_{22}H_{16}N_2O_2Br$: 419.0390 $[M + H]^+$; found: 419.0391.

(4-(tert-butyl)phenyl)(2-(2-hydroxy-5-methylphenyl)quinazolin-4-yl)methanone (6ke)

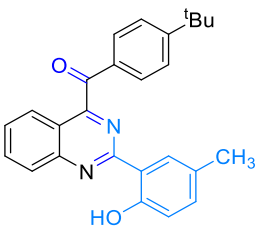

R_f = 0.4 (15% EtOAc in petroleum ether); yield: 43 mg (59%); yellow solid; IR (neat)ν_{max} 1669, 1605, 1548, 1491, 1224, 744 cm^{-1}; ^1H NMR (400 MHz, $CDCl_3$): δ 1.38 (s, 9H), 2.33 (s, 3H), 7.00 (d, J = 8.3 Hz, 1H), 7.22–7.26 (m, 1H), 7.53–7.57 (m, 2H), 7.60 (ddd, J = 8.3, 7.1, 1.1 Hz,

1H), 7.95–8.02 (m, 4H), 8.09 (d, J = 8.4 Hz, 1H), 8.38 (d, J = 1.1 Hz, 1H), 13.33 (s) ppm; ^{13}C NMR (100 MHz, $CDCl_3$): δ 20.6 (q), 31.0 (q, 3C), 35.4 (s), 117.6 (d), 118.4 (s), 120.0 (s), 125.9 (d, 2C), 126.1 (d), 127.5 (d), 128.0 (d), 128.2 (s), 129.8 (d), 130.7 (d, 2C), 132.4 (s), 134.5 (d), 135.3 (d), 149.2 (s), 158.8 (s), 158.8 (s), 160.7 (s), 165.1 (s), 192.1 (s) ppm; HRMS (ESI) calcd. for $C_{26}H_{25}N_2O_2$: 397.1916 $[M + H]^+$; found: 397.1911.

1-(2-(2-hydroxy-5-methylphenyl)quinazolin-4-yl)butan-1-one (6me)

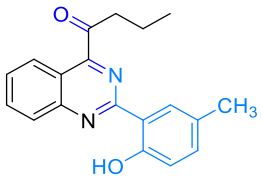

R_f = 0.5 (10% EtOAc in petroleum ether); yield: 43 mg (52%); dark yellow gum; IR (neat) ν_{max} 1654, 1551, 1444, 1225, 1131, 798, 751 cm^{-1}; ^{1}H NMR (400 MHz, $CDCl_3$): δ 1.12 (t, J = 7.4 Hz, 3H), 1.84–1.95 (m, 2H), 2.42 (s, 3H), 3.37 (t, J = 7.2 Hz, 2H), 7.01 (d, J = 8.3 Hz, 1H), 7.27 (dd, J = 8.3, 2.3 Hz, 1H), 7.64–7.70 (m, 1H), 7.93–7.98 (m, 1H), 8.04 (d, J = 8.1 Hz, 1H), 8.43 (d, J = 1.9 Hz, 1H), 8.62–8.67 (m, 1H), 13.30 (s, 1H) ppm; ^{13}C NMR (100 MHz, $CDCl_3$): δ13.8 (q), 17.3 (t), 20.8 (q), 42.2 (t), 117.8 (d), 118.3 (s), 118.9 (s), 126.6 (d), 127.4 (d), 128.2 (s), 128.7 (d), 129.4 (d), 134.5 (d), 135.0 (d), 150.0 (s), 158.7 (s), 160.4 (s), 160.8 (s), 203.6 (s) ppm; HRMS (ESI) calcd. for: $C_{19}H_{19}N_2O_2$: 307.1447 $[M+H]^+$; found: 307.1451.

cyclopropyl(2-(2-hydroxy-5-nitrophenyl)quinazolin-4-yl)methanone (6lf)

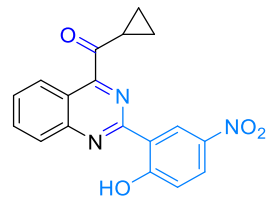

R_f = 0.4 (15% EtOAc in petroleum ether); yield: 49 mg (53%); yellow solid; IR (neat)ν_{max} 1685, 1585, 1471, 1340, 1092, 759 cm^{-1}; ^{1}H NMR (400 MHz, $CDCl_3$): δ 1.34–1.41 (m, 2H), 1.47–1.54 (m, 2H), 3.25–3.42 (m, 1H), 7.15 (d, J = 9.0 Hz, 1H), 7.75 (ddd, J = 8.4, 6.8, 1.4 Hz, 1H), 7.97–8.12 (m, 2H), 8.29 (dd, J = 9.1, 2.9 Hz, 1H), 8.63–8.72 (m, 1H), 9.57 (d, J = 2.9 Hz, 1H), 14.43 (br. s., 1H) ppm; ^{13}C NMR (100 MHz, $CDCl_3$): δ14.1 (t, 2C), 19.6 (d), 118.5 (s), 118.7 (d), 119.5 (s), 126.2 (d), 127.1 (d), 127.2 (d), 128.4 (d), 129.7 (d), 135.7 (d), 140.3 (s), 149.4 (s) 158.8 (s), 161.1 (s), 165.9 (s), 201.9 (s) ppm; HRMS (ESI) calcd. for $C_{18}H_{14}N_3O_4$: 336.0984 $[M + H]^+$; found: 336.0975.

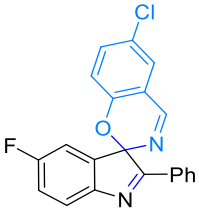

6-chloro-5'-fluoro-2'-phenylspiro[benzo[e][1,3]oxazine-2,3'-indole] (5bc)

R_f = 0.3 (10% EtOAc in petroleum ether); yield: 5 mg (6%); dark yellow syrup; ^{1}H NMR (400 MHz, $CDCl_3$): δ6.82–6.88 (m, 2H), 7.08–7.16 (m, 1H), 7.38–7.52 (m, 5H), 7.57 (dd, J = 8.4, 4.4 Hz, 1H), 8.09–8.18 (m, 2H),

8.45 (d, J = 0.6 Hz, 1H) ppm; ^{13}C NMR (100 MHz, $CDCl_3$): δ 99.6 (s), 109.9 (dd, $J_{C\text{-}F}$ = 25.95 Hz), 117.3 (s), 117.9 (dd, $J_{C\text{-}F}$ = 23.65 Hz), 118.7 (d), 122.6 (dd, $J_{C\text{-}F}$ = 8.39 Hz), 127.3 (d), 127.8 (s), 128.6 (d, 2C), 128.6 (d, 2C), 130.9 (s), 131.6 (d), 134.6 (d), 138.3 (ds, $J_{C\text{-}F}$ = 8.39 Hz), 147.9 (ds, $J_{C\text{-}F}$ = 3.05 Hz), 152.1 (s), 156.5 (d), 160.1 (ds, $J_{C\text{-}F}$ = 247.95 Hz), 175.2 (ds, $J_{C\text{-}F}$ = 4.58 Hz) ppm; HRMS (ESI) calcd. for: $C_{21}H_{13}N_2OClF$: 363.0695 $[M+H]^+$; found: 363.0686.

6-bromo-2'-phenylspiro[benzo[e][1,3]oxazine-2,3'-indole] (5ad)

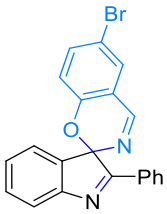

R_f = 0.3 (10% EtOAc in petroleum ether); yield: 9 mg (10%); dark yellow syrup; ^{1}H NMR (400 MHz, $CDCl_3$): δ 6.75–6.79 (m, 1H), 7.09 (td, J = 7.4, 1.0 Hz, 1H), 7.14–7.19 (m, 1H), 7.40–7.47 (m, 3H), 7.47–7.56 (m, 3H), 7.63 (d, J = 7.6 Hz, 1H), 8.14–8.20 (m, 2H), 8.44 (d, J = 0.8 Hz, 1H) ppm; ^{13}C NMR (100 MHz, $CDCl_3$): δ 99.7 (s), 114.5 (s), 118.1 (s), 119.1 (d), 121.7 (d), 121.8 (d), 126.7 (d), 128.6 (d, 2C), 128.8 (d, 2C), 130.1 (d), 131.1 (s), 131.6 (d), 131.7 (d), 136.8 (s), 137.2 (d), 151.9 (s), 153.0 (s), 156.0 (d), 175.0 (s) ppm; HRMS (ESI) calcd. for: $C_{21}H_{14}N_2OBr$: 389.0289 $[M+H]^+$; found: 389.0294.

6-bromo-5'-fluoro-2'-phenylspiro[benzo[e][1,3]oxazine-2,3'-indole] (5bd)

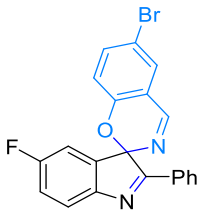

R_f = 0.3 (10% EtOAc in petroleum ether); yield: 22 mg (26%); dark yellow syrup; ^{1}H NMR (400 MHz, $CDCl_3$): δ 6.76–6.82 (m, 1H), 6.86 (dd, J = 7.3, 2.5 Hz, 1H), 7.08–7.15 (m, 1H), 7.41–7.50 (m, 3H), 7.52–7.60 (m, 3H), 8.10–8.16 (m, 2H), 8.44 (d, J = 0.6 Hz, 1H) ppm; ^{13}C NMR (100 MHz, $CDCl_3$): δ 99.5 (s), 109.9 (dd, $J_{C\text{-}F}$ = 25.18 Hz), 114.8 (s), 117.8 (s), 117.9 (dd, $J_{C\text{-}F}$ = 22.89 Hz), 119.0 (d), 122.6 (dd, $J_{C\text{-}F}$ = 8.39 Hz), 128.6 (d, 2C), 128.6 (d, 2C), 130.3 (d), 130.9 (s), 131.6 (d), 137.5 (d), 138.3 (ds, $J_{C\text{-}F}$ = 7.63 Hz), 147.9 (ds, $J_{C\text{-}F}$ = 2.29 Hz), 152.6 (s), 156.3 (d), 160.1 (ds, $J_{C\text{-}F}$ = 247.95 Hz), 175.1 (ds, $J_{C\text{-}F}$ = 3.81 Hz) ppm; HRMS (ESI) calcd. for: $C_{21}H_{13}N_2OBrF$: 407.0195 $[M+H]^+$; found: 407.0182.

6-bromo-5'-((difluoro-l3-methyl)-l2-fluoraneyl)-2'-phenylspiro[benzo[e][1,3]oxazine-2,3'-indole] (5dd)

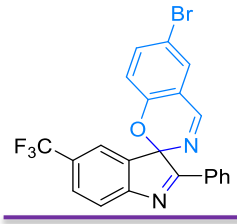

R_f = 0.3 (10% EtOAc in petroleum ether); yield: 31 mg (39%); dark yellow syrup; ^{1}H NMR (400 MHz, $CDCl_3$): δ 6.77–6.80 (m, 1H), 7.46–7.47 (m,

1H), 7.47–7.52 (m, 2H), 7.57–7.60 (m, 3H), 7.72–7.80 (m, 2H), 8.16–8.20 (m, 2H), 8.45 (d, J = 0.8 Hz, 1H) ppm; ^{13}C NMR (100 MHz, $CDCl_3$): δ 99.6 (s), 114.9 (s), 117.3 (s), 118.8 (qd, $J_{C\text{-}F}$ = 3.81 Hz), 119.0 (d), 121.8 (d), 125.1 (s), 128.5 (s), 128.7 (d, 2C), 128.9 (s), 129.1 (d, 2C), 129.1 (qd, $J_{C\text{-}F}$ = 3.82 Hz), 130.5 (d), 130.6 (s), 132.2 (d), 137.7 (d), 152.4 (s), 154.8 (ds, $J_{C\text{-}F}$ = 1.53 Hz), 156.4 (d), 177.3 (s) ppm; HRMS (ESI) calcd. for: $C_{22}H_{13}N_2OF_3Br$: 457.0163 $[M+H]^+$; found: 457.0166.

6-methyl-2'-phenylspiro[benzo[e][1,3]oxazine-2,3'-indole]-5'-carbonitrile (5fe)

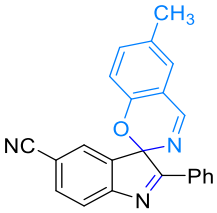

R_f = 0.3 (10% EtOAc in petroleum ether); yield: 5 mg (8%); dark yellow syrup; ^{1}H NMR (400 MHz, $CDCl_3$): δ 2.42 (s, 3H), 6.79 (d, J = 8.3 Hz, 1H), 7.22–7.26 (m, 1H), 7.27–7.32 (m, 1H), 7.37 (dd, J = 1.6, 0.6 Hz, 1H), 7.42–7.52 (m, 2H), 7.53 (d, J = 7.4 Hz, 1H), 7.66–7.76 (m, 2H), 8.19–8.29 (m, 2H), 8.48 (d, J = 0.6 Hz, 1H) ppm; ^{13}C NMR (100 MHz, $CDCl_3$): δ 20.6 (q), 99.0 (s), 109.6 (s), 116.5 (s), 116.9 (d), 118.6 (s), 122.2 (d), 125.4 (d), 128.1 (d), 128.7 (d, 2C), 129.4 (d, 2C), 130.5 (s), 132.5 (d), 133.0 (s), 135.8 (d), 136.1 (d), 137.9 (s), 151.1 (s), 155.7 (s), 158.5 (d), 178.5 (s) ppm; HRMS (ESI) calcd. for: $C_{23}H_{16}N_3O$: 350.1295 $[M+H]^+$; found: 350.1287.

6-nitro-2'-phenylspiro[benzo[e][1,3]oxazine-2,3'-indole] (5af)

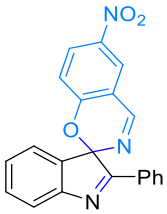

R_f = 0.3 (10% EtOAc in petroleum ether); yield: 41 mg (59%); dark yellow syrup; ^{1}H NMR (400 MHz, $CDCl_3$): δ 6.98 (d, J = 8.6 Hz, 1H), 7.10–7.21 (m, 2H), 7.42–7.56 (m, 4H), 7.65 (d, J = 7.8 Hz, 1H), 8.09–8.16 (m, 2H), 8.29–8.38 (m, 2H), 8.54–8.61 (m, 1H) ppm; ^{13}C NMR (100 MHz, $CDCl_3$): δ 99.6 (s), 114.5 (s), 117.0 (d), 120.7 (d), 120.9 (d), 122.5 (d), 126.0 (d), 127.6 (d, 2C), 127.7 (d, 2C), 128.9 (d), 129.9 (s), 130.8 (d), 131.1 (d), 135.7 (s), 141.5 (s), 150.8 (s), 154.3 (d), 158.0 (s), 173.4 (s) ppm; HRMS (ESI) calcd. for: $C_{21}H_{14}N_3O_3$: 363.0695 $[M+H]^+$; found: 363.0686.

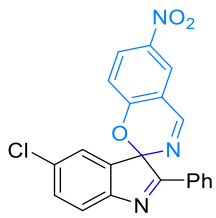

5'-chloro-6-nitro-2'-phenylspiro[benzo[e][1,3]oxazine-2,3'-indole] (5cf)

R_f = 0.3 (10% EtOAc in petroleum ether); yield: 54 mg (70%); dark yellow syrup; ^{1}H NMR (400 MHz, $CDCl_3$): δ 7.00 (d, J = 9.9 Hz, 1H), 7.13 (d, J = 2.0 Hz, 1H), 7.41–7.48 (m, 3H), 7.49–7.55 (m, 1H), 7.57 (d, J = 8.3 Hz, 1H),

8.05–8.11 (m, 2H), 8.32–8.38 (m, 2H), 8.57 (d, J = 0.6 Hz, 1H) ppm; ^{13}C NMR (100 MHz, $CDCl_3$): δ 100.4 (s), 115.1 (s), 118.0 (d), 122.4 (d), 122.8 (d), 123.8 (d), 128.6 (d, 2C), 128.8 (d, 2C), 130.1 (d), 130.6 (s), 132.0 (d), 132.0 (s), 132.4 (s), 138.3 (s), 142.7 (s), 150.4 (s), 155.6 (d), 158.5 (s), 174.7 (s) ppm; HRMS (ESI) calcd. for: $C_{21}H_{13}N_3O_3Cl$: 390.0640 $[M+H]^+$; found: 390.0636.

6,8-di-tert-butyl-2'-phenylspiro[benzo[e][1,3]oxazine-2,3'-indole] (5ag)

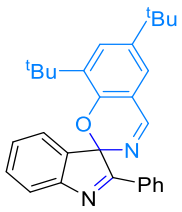

R_f = 0.3 (10% EtOAc in petroleum ether); yield: 69 mg (72%); dark yellow syrup; ^{1}H NMR (400 MHz, $CDCl_3$): δ 1.12 (s, 9H), 1.39 (s, 9H), 6.99–7.05 (m, 1H), 7.06–7.10 (m, 1H), 7.24 (d, J = 2.4 Hz, 1H), 7.37–7.41 (m, 1H), 7.41–7.50 (m, 4H), 7.59–7.65 (m, 1H), 8.24–8.31 (m, 2H), 8.46 (s, 1H) ppm; ^{13}C NMR (100 MHz, $CDCl_3$): δ 29.4 (q, 3C), 31.4 (q, 3C), 34.5 (s, 2C), 99.2 (s), 117.1 (s), 121.5 (d), 121.9 (d), 122.3 (d), 126.4 (d), 128.4 (d, 2C), 128.9 (d), 128.9 (d, 2C), 131.2 (d), 131.3 (d), 131.4 (s), 136.6 (s), 138.2 (s), 144.8 (s), 150.0 (s), 151.9 (s), 158.8 (d), 175.8 (s) ppm; HRMS (ESI) calcd. for: $C_{29}H_{31}N_2O$: 243.2431 $[M+H]^+$; found: 243.2426.

General Procedure for the Synthesis of indol-3-ylidene derivatives

In general, all reactions were carried out employing 50 mg of *o*-azidoalkyne **1**.

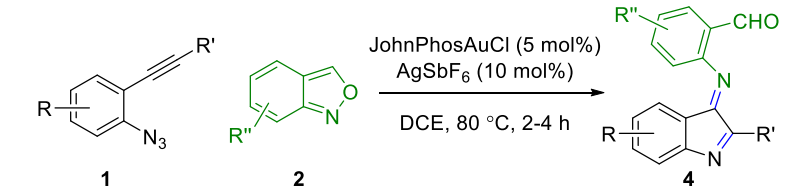

1 **2** **4**

R' = Ar, cyclopropyl,alkyl

In an oven dried reaction vial, JohnPhosAuCl (5 mol %) and $AgSbF_6$ (10 mol%) were added followed by addition of DCE and the reaction mixture was stirred at room temperature for 10-15 minutes. To this gold complex solution was added dropwise a DCE solution of azidoalkyne (**1**) (1 equiv) and 2,1- Benzo[*c*]isoxazole (**2**) (1.1 equiv) over 5 minutes. The resulting solution was stirred at 80 °C until the complete disappearance of the starting azidoalkyne as indicated by TLC. The reaction mixture was concentrated under reduced pressure and the resulting crude was purified by column chromatography to afford the indol-3-ylidene products **4.**

(E)-2-((2-phenyl-3H-indol-3-ylidene)amino)benzaldehyde (4aa)

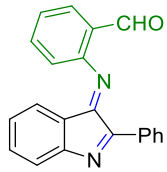

R_f = 0.3 (10% EtOAc in petroleum ether); yield: 51 mg (79%); dark red solid; IR (neat)ν_{max} 2924, 1695, 1599, 1454, 1207, 751, 692 cm^{-1}; ^1H NMR (400 MHz, $CDCl_3$): δ 6.43 (d, J = 7.4 Hz, 1H), 6.91 (td, J = 7.5, 0.9 Hz, 1H), 6.98–7.04 (m, 1H), 7.36–7.46 (m, 2H), 7.48–7.58 (m, 4H), 7.66 (td, J = 7.7, 1.4 Hz, 1H), 8.03 (dd, J = 7.8, 1.3 Hz, 1H), 8.45 (dd, J = 7.9, 1.6 Hz, 2H), 10.19 (s, 1H) ppm; ^{13}C NMR (100 MHz, $CDCl_3$): δ 118.1 (d), 121.5 (s), 121.9 (d), 124.3 (s), 125.6 (d), 125.7 (d), 127.0 (d), 128.5 (d, 2C), 129.4 (d), 130.0 (d, 2C), 131.3 (d), 131.7 (s), 134.0 (d), 135.2 (d), 152.3 (s), 158.1 (s), 165.7 (s), 166.0 (s), 189.6 (d) ppm; HRMS (ESI) calcd. for: $C_{21}H_{15}N_2O$: 311.1179 $[M+H]^+$; found: 311.1183.

(E)-2-((5-fluoro-2-phenyl-3H-indol-3-ylidene)amino)benzaldehyde (4ab)

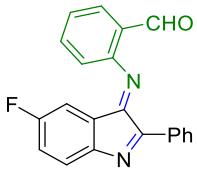

R_f = 0.4 (10% EtOAc in petroleum ether); yield: 47 mg (68%); dark red solid; IR (neat)ν_{max} 2358, 1696, 1458, 1263, 1191, 801, 757, 686 cm^{-1}; ^1H NMR (400 MHz, $CDCl_3$): δ6.11 (dd, J = 7.7, 2.4 Hz, 1H), 6.95–7.01 (m, 1H), 7.07 (td, J = 8.6, 2.6 Hz, 1H), 7.42–7.57 (m, 5H), 7.64–7.72 (m, 1H), 8.03 (dd, J = 7.8, 1.3 Hz, 1H), 8.43 (dd, J = 7.9, 1.4 Hz, 2H), 10.18 (s, 1H) ppm; ^{13}C NMR (100 MHz, $CDCl_3$): δ113.2 (dd, $J_{C\text{-}F}$ = 25.94 Hz), 117.7 (d), 119.6 (dd, $J_{C\text{-}F}$ = 23.65 Hz), 122.6 (dd, $J_{C\text{-}F}$ = 8.39 Hz), 124.2 (s), 126.0 (d), 128.5 (d, 2C), 129.8 (d, 2C), 130.1 (d), 131.4 (d), 131.5 (s), 135.2 (d), 151.2 (s), 154.0 (ds, $J_{C\text{-}F}$ = 3.05 Hz), 159.9 (s), 162.4 (ds, $J_{C\text{-}F}$ = 227.3 Hz), 164.7 (s), 166.0 (ds, $J_{C\text{-}F}$ = 3.81 Hz), 189.5 (d) ppm; HRMS (ESI) calcd. for: $C_{21}H_{14}N_2OF$: 329.1085 $[M+H]^+$; found: 329.1083.

(E)-2-((5-chloro-2-phenyl-3H-indol-3-ylidene)amino)benzaldehyde (4ca)

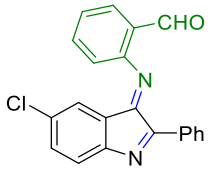

R_f = 0.4 (10% EtOAc in petroleum ether); yield: 56 mg (83%); red solid; IR (neat) ν_{max} 2113, 1692, 1444, 1265, 828, 751, 690 cm^{-1}; ^1H NMR (400 MHz, $CDCl_3$): δ6.36 (d, J = 1.9 Hz, 1H), 6.98 (d, J = 7.9 Hz, 1H), 7.34–7.38 (m, 1H), 7.42–7.57 (m, 5H), 7.68 (td, J = 7.7, 1.4 Hz, 1H), 8.04 (dd, J = 7.8, 1.3 Hz, 1H), 8.38–8.51 (m, 2H), 10.18 (s, 1H) ppm; ^{13}C NMR (100 MHz, $CDCl_3$): δ117.7 (d), 122.6 (d), 122.6 (s), 124.3 (s), 125.7 (d), 126.1 (d), 128.5 (d, 2C), 130.0 (d, 2C), 130.2 (d), 131.4 (d),

131.5 (s), 132.3 (s), 133.4 (d), 135.2 (d), 151.2 (s), 156.4 (s), 164.5 (s), 166.1 (s), 189.6 (d) ppm; HRMS (ESI) calcd. for: $C_{21}H_{14}N_2OCl$: 345.0789 $[M+H]^+$; found: 345.0789.

(E)-2-((2-phenyl-3H-indol-3-ylidene)amino)benzaldehyde (4da)

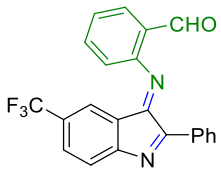

R_f = 0.3 (10% EtOAc in petroleum ether); yield: 60 mg (91%); red solid; IR (neat) ν_{max} 2357, 1693, 1595, 1446, 1065, 912, 752, 683 cm^{-1}; ^1H NMR (400 MHz, $CDCl_3$): δ6.62 (s, 1H), 6.97–7.03 (m, 1H), 7.46–7.60 (m, 4H), 7.60–7.64 (m, 1H), 7.66–7.72 (m, 2H), 8.05 (dd, J = 7.9, 1.3 Hz, 1H), 8.45–8.57 (m, 2H), 10.20 (s, 1H) ppm; ^{13}C NMR (100 MHz, $CDCl_3$): δ117.6 (d), 121.6 (s), 121.9 (d), 122.1 (qd, J_{C-F} = 3.82 Hz), 124.5 (s), 126.3 (d), 128.6 (d, 2C), 128.9 (s), 129.2 (s), 130.3 (d, 2C), 130.6 (d), 131.1 (qd, J_{C-F} = 3.82 Hz), 131.2 (s), 132.0 (d), 135.1 (d), 151.0 (s), 160.6 (s), 164.2 (s), 167.9 (s), 189.6 (s) ppm; HRMS (ESI) calcd. for: $C_{22}H_{14}N_2OF_3$: 379.1053 $[M+H]^+$; found: 379.1050.

(E)-2-((5-nitro-2-phenyl-3H-indol-3-ylidene)amino)benzaldehyde (4ea)

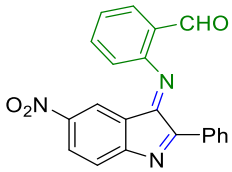

R_f = 0.5 (15% EtOAc in petroleum ether); yield: 54 mg (80%); dark red solid; IR (neat)ν_{max} 1692, 1441, 1265, 828, 752, 663 cm^{-1}; ^1H NMR (400 MHz, $CDCl_3$): δ6.42 (d, J = 1.6 Hz, 1H), 6.90 (d, J = 7.5 Hz, 1H), 7.31 (d, J = 8.1 Hz, 1H), 7.37–7.50 (m, 5H), 7.61 (td, J = 7.7, 1.4 Hz, 1H), 7.96 (dd, J = 7.8, 1.3 Hz, 1H), 8.26–8.47 (m, 2H), 10.19 (s, 1H) ppm; ^{13}C NMR (100 MHz, $CDCl_3$): δ 117.7 (d), 120.1 (s), 122.9 (s), 123.1 (d), 124.4 (s), 126.2 (d), 128.5 (d), 128.6 (d, 2C), 130.0 (d, 2C), 130.2 (d), 131.4 (s), 131.6 (d), 135.2 (d), 136.4 (d), 151.3 (s), 156.9 (s), 164.5 (s), 166.0 (s), 189.6 (d) ppm; HRMS (ESI) calcd. for: $C_{21}H_{14}N_3O_3$: 356.1030 $[M+H]^+$; found: 356.1020.

(E)-2-((6-methyl-2-phenyl-3H-indol-3-ylidene)amino)benzaldehyde (4fa)

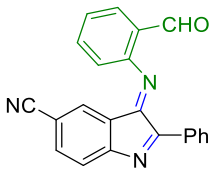

R_f = 0.3 (10% EtOAc in petroleum ether); yield: 61 mg (88%); red solid; IR (neat)ν_{max} 2357, 2227, 1692, 1454, 1192, 844, 754, 679 cm^{-1}; ^1H NMR (400 MHz, $CDCl_3$): δ6.68 (s, 1H), 6.96 (d, J = 7.9 Hz, 1H), 7.47–7.56 (m, 3H), 7.56–7.63 (m, 2H), 7.67–7.77 (m, 2H), 8.05 (dd, J = 7.8, 1.1 Hz, 1H), 8.50 (d, J = 7.4 Hz, 2H), 10.17 (s, 1H) ppm; ^{13}C NMR (100 MHz, $CDCl_3$): δ 110.3 (s), 117.3 (d), 118.0 (s), 121.9 (s), 122.4 (d), 124.2 (s), 126.6 (d), 128.4 (d), 128.7 (d, 2C), 130.5 (d, 2C), 131.0 (s),

131.2 (d), 132.3 (d), 135.3 (d), 138.1 (d), 150.4 (s), 161.1 (s), 163.3 (s), 168.5 (s), 189.6 (d) ppm; HRMS (ESI) calcd. for: $C_{22}H_{14}N_3O$: 336.1131 $[M+H]^+$; found: 336.1128.

(E)-2-((6-bromo-2-phenyl-3H-indol-3-ylidene)amino)benzaldehyde (4ga)

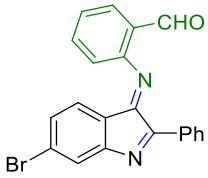

R_f = 0.5 (15% EtOAc in petroleum ether); yield: 48 mg (74%); red solid; IR (neat)ν_{max} 2359, 1696, 1605, 1525, 1333, 751, 685 cm^{-1}; ^1H NMR (400 MHz, $CDCl_3$): δ6.98–7.03 (m, 1H), 7.26 (d, J = 2.3 Hz, 1H), 7.52–7.62 (m, 4H), 7.63–7.67 (m, 1H), 7.74 (td, J = 7.7, 1.4 Hz, 1H), 8.08 (dd, J = 7.8, 1.3 Hz, 1H), 8.34 (dd, J = 8.4, 2.2 Hz, 1H), 8.51–8.57 (m, 2H), 10.20 (s, 1H) ppm; ^{13}C NMR (100 MHz, $CDCl_3$): δ 117.5 (d), 120.7 (d), 121.7 (s), 121.9 (d), 124.5 (s), 126.8 (d), 128.8 (d, 2C), 129.6 (d), 130.6 (d, 2C), 131.1 (d), 131.4 (s), 132.5 (d), 135.3 (d), 146.4 (s), 150.3 (s), 162.6 (s), 163.4 (s), 169.8 (s), 189.7 (d) ppm; HRMS (ESI) calcd. for: $C_{21}H_{14}N_2OBr$: 389.0290 $[M+H]^+$; found: 389.0293.

(E)-2-((6-chloro-2-phenyl-3H-indol-3-ylidene)amino)benzaldehyde (4ha)

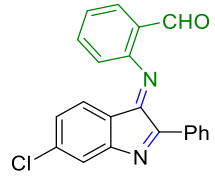

R_f = 0.4 (10% EtOAc in petroleum ether); yield: 53 mg (78%); red solid; IR (neat) ν_{max} 2357, 1697, 1324, 1268, 1120, 845, 757 cm^{-1}; ^1H NMR (400 MHz, $CDCl_3$): δ6.34 (d, J = 8.0 Hz, 1H), 6.88 (dd, J = 8.0, 1.9 Hz, 1H), 6.95–7.00 (m, 1H), 7.43 (t, J = 7.6 Hz, 1H), 7.47–7.58 (m, 4H), 7.65 (td, J = 7.7, 1.4 Hz, 1H), 8.02 (dd, J = 7.8, 1.3 Hz, 1H), 8.46 (dd, J = 8.3, 1.4 Hz, 2H), 10.17 (s, 1H) ppm; ^{13}C NMR (100 MHz, $CDCl_3$): δ117.9 (d), 119.7 (s), 122.4 (d), 124.3 (s), 125.8 (d), 126.0 (d), 126.7 (d), 128.5 (d, 2C), 129.8 (d), 130.1 (d, 2C), 131.4 (s), 131.7 (d), 135.1 (d), 139.8 (s), 151.7 (s), 159.4 (s), 164.4 (s), 167.2 (s), 189.5 (d) ppm; HRMS (ESI) calcd. for: $C_{21}H_{14}N_2OCl$: 345.0789 $[M+H]^+$; found: 345.0786.

(E)-2-((6-methyl-2-phenyl-3H-indol-3-ylidene)amino)benzaldehyde (4ia)

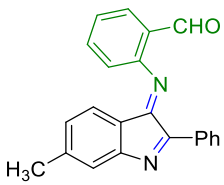

R_f = 0.5 (10% EtOAc in petroleum ether); yield: 60 mg (86%); red solid; IR (neat)ν_{max} 2357, 1691, 1604, 1458, 1271, 758, 688 cm^{-1}; ^1H NMR (400 MHz, $CDCl_3$): δ2.36 (s, 3H), 6.30 (d, J = 7.6 Hz, 1H), 6.67–6.73 (m, 1H), 6.98–7.02 (m, 1H), 7.30–7.34 (m, 1H), 7.40 (t, J = 7.6 Hz, 1H), 7.48–7.56 (m, 3H), 7.64 (td, J = 7.7, 1.4 Hz, 1H), 8.02 (dd, J = 7.8, 1.4 Hz, 1H), 8.45 (dd, J = 7.9, 1.7 Hz, 2H), 10.18 (d, J = 0.6 Hz, 1H) ppm; ^{13}C NMR (100 MHz, $CDCl_3$): δ 22.0 (q), 118.2 (d), 119.0 (s),

122.8 (d), 124.4 (s), 125.5 (d), 125.5 (d), 127.4 (d), 128.5 (d, 2C), 129.2 (d), 129.9 (d, 2C), 131.2 (d), 131.8 (s), 135.2 (d), 145.3 (s), 152.6 (s), 158.5 (s), 165.5 (s), 166.4 (s), 189.7 (d) ppm; HRMS (ESI) calcd. for: $C_{22}H_{17}N_2O$: 325.1341 $[M+H]^+$; found: 325.1344.

(E)-2-((2-(4-methoxyphenyl)-3H-indol-3-ylidene)amino)benzaldehyde (4ja)

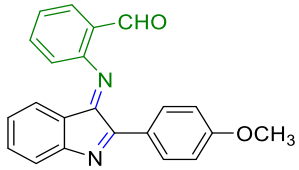

R_f = 0.5 (15% EtOAc in petroleum ether); yield: 57 mg (83%); red solid; IR (neat)ν_{max} 2925, 1696, 1256, 1169, 750 cm^{-1}; ^1H NMR (400 MHz, $CDCl_3$): δ 3.89 (s, 3H), 6.39 (d, J = 7.5 Hz, 1H), 6.85 (td, J = 7.5, 1.1 Hz, 1H), 6.97–7.04 (m, 3H), 7.29–7.52 (m, 3H), 7.61–7.69 (m, 1H), 8.02 (dd, J = 7.9, 1.3 Hz, 1H), 8.44–8.54 (m, 2H), 10.19 (s, 1H) ppm; ^{13}C NMR (100 MHz, $CDCl_3$): δ 55.4 (q), 114.0 (d, 2C), 118.1 (d), 121.4 (d), 121.5 (s), 124.3 (s), 124.4 (s), 125.5 (d), 125.6 (d), 126.5 (d), 129.3 (d), 131.8 (d, 2C), 134.0 (d), 135.2 (d), 152.4 (s), 158.5 (s), 162.4 (s), 165.1 (s), 166.2 (s), 189.6 (d) ppm; HRMS (ESI) calcd. for: $C_{22}H_{17}N_2O_2$: 341.1290 $[M+H]^+$; found: 341.1298.

(E)-2-((2-(4-(tert-butyl)phenyl)-3H-indol-3-ylidene)amino)benzaldehyde (4ka)

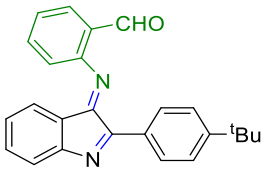

R_f = 0.5 (15% EtOAc in petroleum ether); yield: 59 mg (89%); red solid; IR (neat)ν_{max} 2959, 1693, 1597, 1453, 1267, 750, 662 cm^{-1}; ^1H NMR (400 MHz, $CDCl_3$): δ 1.38 (s, 9H), 6.41 (d, J = 7.3 Hz, 1H), 6.86–6.92 (m, 1H), 6.97–7.02 (m, 1H), 7.36–7.40 (m, 1H), 7.41–7.45 (m, 1H), 7.48–7.59 (m, 3H), 7.61–7.73 (m, 1H), 8.03 (dd, J = 7.9, 1.3 Hz, 1H), 8.36–8.44 (m, 2H), 10.20 (d, J = 0.6 Hz, 1H) ppm; ^{13}C NMR (100 MHz, $CDCl_3$): δ 31.1 (q, 3C), 35.0 (s), 118.1 (d), 121.5 (s), 121.7 (d), 124.3 (s), 125.6 (d, 2C), 125.6 (s), 125.6 (d), 126.8 (d), 128.9 (s), 129.3 (d), 129.8 (d, 2C), 134.0 (d), 135.2 (d), 152.4 (s), 154.9 (s), 158.3 (s), 165.8 (s), 165.9 (s), 189.6 (d) ppm; HRMS (ESI) calcd. for: $C_{25}H_{23}N_2O$: 367.1810 $[M+H]^+$; found: 367.1820.

(E)-2-((2-cyclopropyl-3H-indol-3-ylidene)amino)benzaldehyde (4la)

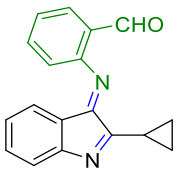

R_f = 0.5 (10% EtOAc in petroleum ether); yield: 46 mg (61%); red solid; IR (neat)ν_{max} 2358, 1693, 1655, 1571, 1453, 950, 762 cm^{-1}; ^1H NMR (400 MHz, $CDCl_3$): δ 1.23–1.28 (m, 2H), 1.35–1.47 (m, 2H), 2.40–2.53 (m, 1H), 6.41 (d, J = 7.5 Hz, 1H), 6.81 (ddd, J = 7.5, 5.4, 3.3 Hz, 1H), 7.01 (dd, J = 7.9, 0.6 Hz, 1H), 7.27–7.34 (m, 2H), 7.40 (t, J = 7.6 Hz, 1H), 7.65 (td, J = 7.7, 1.4 Hz, 1H), 8.01 (dd, J = 7.9,

1.3 Hz, 1H), 10.18 (d, J = 0.6 Hz, 1H) ppm; ^{13}C NMR (100 MHz, $CDCl_3$): δ 9.3 (d), 12.1 (t, 2C), 118.4 (d), 120.7 (d), 121.5 (s), 124.8 (s), 125.5 (d), 125.7 (d), 125.8 (d), 128.9 (d), 134.0 (d), 135.1 (d), 152.5 (s), 159.1 (s), 165.1 (s), 176.0 (s), 189.7 (d) ppm; HRMS (ESI) calcd. for: $C_{18}H_{15}N_2O$: 274.1106 $[M]^+$; found: 274.1108.

(E)-5-fluoro-2-((2-phenyl-3H-indol-3-ylidene)amino)benzaldehyde (4ab)

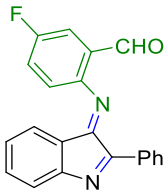

R_f = 0.5 (15% EtOAc in petroleum ether); yield: 57 mg (76%); dark red solid; IR (neat)ν_{max} 2356, 1690, 1478, 1261, 1145, 891, 752, 685 cm^{-1}; ^{1}H NMR (400 MHz, $CDCl_3$): δ 6.51 (d, J = 7.4 Hz, 1H), 6.95 (td, J = 7.6, 1.0 Hz, 1H), 7.03 (dd, J = 8.7, 4.6 Hz, 1H), 7.35–7.41 (m, 1H), 7.41–7.45 (m, 1H), 7.48–7.57 (m, 4H), 7.72 (dd, J = 8.4, 2.9 Hz, 1H), 8.36–8.47 (m, 2H), 10.15 (d, J = 2.8 Hz, 1H) ppm; ^{13}C NMR (100 MHz, $CDCl_3$): δ 114.6 (dd, $J_{C\text{-}F}$ = 22.89 Hz), 120.2 (dd, $J_{C\text{-}F}$ = 6.89 Hz), 121.3 (s), 122.1 (s), 122.4 (dd, $J_{C\text{-}F}$ = 23.65 Hz), 125.5 (d), 125.7 (ds, $J_{C\text{-}F}$ = 6.10 Hz), 127.1 (d), 128.5 (d, 2C), 129.9 (d, 2C), 131.4 (d), 131.6 (s), 134.3 (d), 148.5 (ds, $J_{C\text{-}F}$ = 3.08 Hz), 158.2 (s), 159.3 (ds, $J_{C\text{-}F}$ = 247.96 Hz), 165.9 (s), 166.6 (s), 188.3 (dd, $J_{C\text{-}F}$ = 1.53 Hz) ppm; HRMS (ESI) calcd. for: $C_{21}H_{14}N_2OF$: 329.1090 $[M+H]^+$; found: 329.1097.

(E)-5-chloro-2-((2-phenyl-3H-indol-3-ylidene)amino)benzaldehyde (4ac)

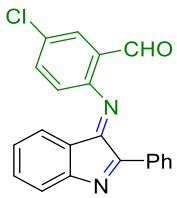

R_f = 0.5 (15% EtOAc in petroleum ether); yield: 48 mg (61%); dark red solid; IR (neat)ν_{max} 2358, 1690, 1454, 1175, 895, 746, 676 cm^{-1}; ^{1}H NMR (400 MHz, $CDCl_3$): δ 6.53 (d, J = 7.4 Hz, 1H), 6.93–7.01 (m, 2H), 7.39–7.45 (m, 1H), 7.48–7.58 (m, 4H), 7.61 (dd, J = 8.4, 2.4 Hz, 1H), 8.00 (d, J = 2.4 Hz, 1H), 8.42 (dd, J = 8.1, 1.4 Hz, 2H), 10.13 (s, 1H) ppm; ^{13}C NMR (100 MHz, $CDCl_3$): δ 119.9 (d), 121.3 (s), 122.1 (d), 125.4 (s), 125.6 (d), 127.2 (d), 128.5 (d, 2C), 128.9 (d), 129.9 (d, 2C), 131.4 (d), 131.5 (s), 131.6 (s), 134.4 (d), 135.1 (d), 150.4 (s), 158.2 (s), 165.8 (s), 166.2 (s), 188.2 (d) ppm; HRMS (ESI) calcd. for: $C_{21}H_{14}N_2OCl$: 345.0794 $[M+H]^+$; found: 345.0800.

(E)-4-chloro-2-((2-phenyl-3H-indol-3-ylidene)amino)benzaldehyde (4ad)

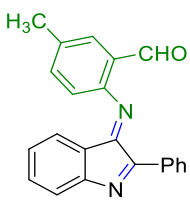

R_f = 0.3 (10% EtOAc in petroleum ether); yield: 53 mg (71%); dark red solid; IR (neat)ν_{max} 2357, 1698, 1525, 752, 673 cm^{-1}; ^{1}H NMR (400 MHz, $CDCl_3$): δ 2.49 (s, 3H), 6.52 (d, J = 7.1 Hz, 1H), 6.89–6.95 (m, 2H), 7.39 (td, J = 7.6,

1.1 Hz, 1H), 7.44–7.57 (m, 5H), 7.82–7.85 (m, 1H), 8.44 (dd, *J* = 8.0, 1.8 Hz, 2H), 10.18 (s, 1H) ppm; ^{13}C NMR (100 MHz, $CDCl_3$): δ 20.8 (q), 118.1 (d), 121.5 (s), 121.8 (d), 124.3 (s), 125.6 (d), 127.0 (d), 128.5 (d, 2C), 129.3 (d), 130.0 (d, 2C), 131.3 (d), 131.8 (s), 133.9 (d), 135.7 (s), 136.0 (d), 150.0 (s), 158.1 (s), 165.7 (s), 166.0 (s), 189.8 (d) ppm; HRMS (ESI) calcd. for: $C_{22}H_{17}N_2O$: 325.1341 $[M+H]^+$; found: 325.1346.

(E)-4-chloro-2-((2-phenyl-3H-indol-3-ylidene)amino)benzaldehyde (4ae)

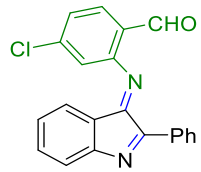

R_f = 0.5 (10% EtOAc in petroleum ether); yield: 57 mg (72%); dark red solid; IR (neat)ν_{max} 2357, 1689, 1542, 1080, 806, 751, 678 cm^{-1}; ^{1}H NMR (400 MHz, $CDCl_3$): δ6.49 (d, *J* = 7.4 Hz, 1H), 6.96 (td, *J* = 7.5, 1.0 Hz, 1H), 7.04 (d, *J* = 1.9 Hz, 1H), 7.36–7.46 (m, 2H), 7.46–7.59 (m, 4H), 7.97 (d, *J* = 8.4 Hz, 1H), 8.42 (dd, *J* = 8.1, 1.4 Hz, 2H), 10.10 (s, 1H) ppm; ^{13}C NMR (100 MHz, $CDCl_3$): δ 118.1 (d), 121.3 (s), 122.1 (d), 122.6 (s), 125.7 (d), 125.8 (d), 127.3 (d), 128.5 (d, 2C), 129.9 (d, 2C), 130.8 (d), 131.5 (d), 134.4 (d), 141.4 (s), 152.9 (s), 158.2 (s), 165.8 (s), 166.2 (d), 188.3 (d) ppm; HRMS (ESI) calcd. for: $C_{21}H_{14}N_2OCl$: 345.0789 $[M+H]^+$; found: 345.0791.

(E)-4-bromo-2-((2-phenyl-3H-indol-3-ylidene)amino)benzaldehyde (4af)

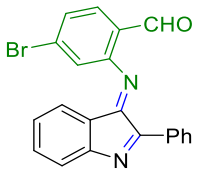

R_f = 0.5 (15% EtOAc in petroleum ether); yield: 74 mg (82%); red solid; IR (neat)ν_{max} 2558, 1690, 1578, 1452, 895, 753, 684 cm^{-1}; ^{1}H NMR (400 MHz, $CDCl_3$): δ6.50 (d, *J* = 7.4 Hz, 1H), 6.97 (td, *J* = 7.5, 1.0 Hz, 1H), 7.22 (d, *J* = 1.8 Hz, 1H), 7.43 (td, *J* = 7.6, 1.1 Hz, 1H), 7.47–7.60 (m, 5H), 7.88 (d, *J* = 8.4 Hz, 1H), 8.42 (dd, *J* = 8.0, 1.4 Hz, 2H), 10.10 (d, *J* = 0.5 Hz, 1H) ppm; ^{13}C NMR (100 MHz, $CDCl_3$): δ 121.0 (d), 121.3 (s), 122.1 (d), 123.0 (s), 125.7 (d), 127.3 (d), 128.5 (d, 2C), 128.7 (d), 129.9 (d, 2C), 129.9 (s), 130.7 (d), 131.5 (d), 134.4 (d), 152.8 (s), 158.2 (s), 165.8 (s), 166.2 (s), 188.5 (d) ppm; HRMS (ESI) calcd. for: $C_{21}H_{14}N_2OBr$: 389.0289 $[M+H]^+$; found: 389.0294.

General Procedure for the Reaction with Other Nucleophile:

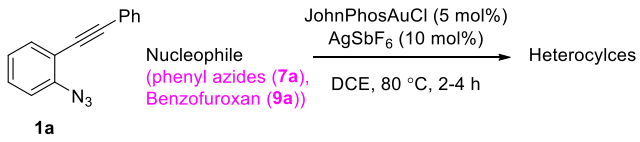

In an oven dried reaction vial, JohnPhosAuCl (5 mol %) and $AgSbF_6$ (10 mol%) were added followed by addition of DCE and the reaction mixture was stirred at room temperature for 10-15

minutes. To this gold complex solution was added dropwise a DCE solution of azidoalkyne (**1a**) (1 equiv) and phenyl azide(**9a**)/benzofuroxan(**11a**) (1.1 equiv) over 5 minutes. The resulting solution was stirred at 80 °C until the complete disappearance of the starting azidoalkyne as indicated by TLC. The reaction mixture was concentrated under reduced pressure and the resulting crude was purified by column chromatography to afford the indoline products**.**

(E)-N-(2-phenyl-3H-indol-3-ylidene)aniline (10aa)

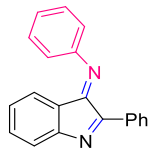

R_f = 0.5 (10% EtOAc in petroleum ether); yield: 55 mg (86%); red solid; IR (neat)ν_{max} 2358, 1701, 1525, 1075, 757, 674 cm^{-1}; ^1H NMR (400 MHz, $CDCl_3$): δ 6.44–6.54 (m, 1H), 6.82 (td, J = 7.5, 1.0 Hz, 1H), 6.89–6.95 (m, 2H), 7.16–7.21 (m, 1H), 7.28 (td, J = 7.6, 1.1 Hz, 1H), 7.34–7.45 (m, 6H), 8.32–8.41 (m, 2H) ppm; ^{13}C NMR (100 MHz, $CDCl_3$): δ117.6 (d, 2C), 121.5 (d), 121.6 (s), 125.2 (d), 125.8 (d), 126.9 (d), 128.4 (d, 2C), 129.4 (d, 2C), 130.1 (d, 2C), 131.1 (d), 132.1 (s), 133.2 (d), 150.3 (s), 157.9 (s), 164.2 (s), 166.5 (s) ppm; HRMS (ESI) calcd. for: $C_{20}H_{15}N_2$: 283.1235 $[M+H]^+$; found: 283.1237.

2-phenyl-3H-indol-3-one (12aa)

R_f = 0.5 (10% EtOAc in petroleum ether); yield: 38 mg (79%); red solid; IR (neat)ν_{max} 2360, 1698, 1617, 1538, 736, 624 cm^{-1}; ^1H NMR (400 MHz, $CDCl_3$): δ 7.15–7.22 (m, 2H), 7.35 (s, 1H), 7.38–7.51 (m, 5H), 8.30 (dd, J = 8.4, 1.4 Hz, 1H) ppm; ^{13}C NMR (100 MHz, $CDCl_3$): δ122.0 (d), 123.1 (s), 124.7 (d), 128.3 (d), 128.8 (d, 2C), 129.2 (d, 2C), 130.0 (s), 132.1 (d), 136.8 (d), 159.7 (s), 161.1 (s), 193.5 (s) ppm; HRMS (ESI) calcd. for: $C_{14}H_{10}NO$: 208.0762 $[M+H]^+$; found: 208.0764.

Intramolecular study-

2-(2-azidophenyl)-3-oxo-3H-indole 1-oxide (14)

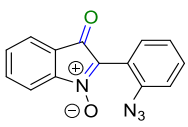

R_f = 0.5 (10% EtOAc in petroleum ether); yield: 38 mg (79%); dark yellow syrup; IR (neat)ν_{max} 2360, 1698, 1617, 1538, 736, 624 cm^{-1}; ^1H NMR (400 MHz, $CDCl_3$): δ 7.18–7.22 (m, 1H), 7.24 (dt, J = 8.8, 0.8 Hz, 1H), 7.40–7.48 (m, 2H), 7.48–7.55 (m, 1H), 7.59–7.62 (m, 1H), 7.62–7.68 (m, 2H) ppm; ^{13}C NMR (100 MHz, $CDCl_3$): δ114.4 (d), 115.9 (s), 119.2 (d), 121.8 (d), 123.2 (s), 124.8 (d), 131.5 (d), 131.7 (d), 131.8 (d), 134.6 (d), 140.2 (s), 147.4 (s), 185.2 (s) ppm; HRMS (ESI) calcd. for: $C_{14}H_9N_4O_2$: 265.0720 $[M+H]^+$; found: 265.077.

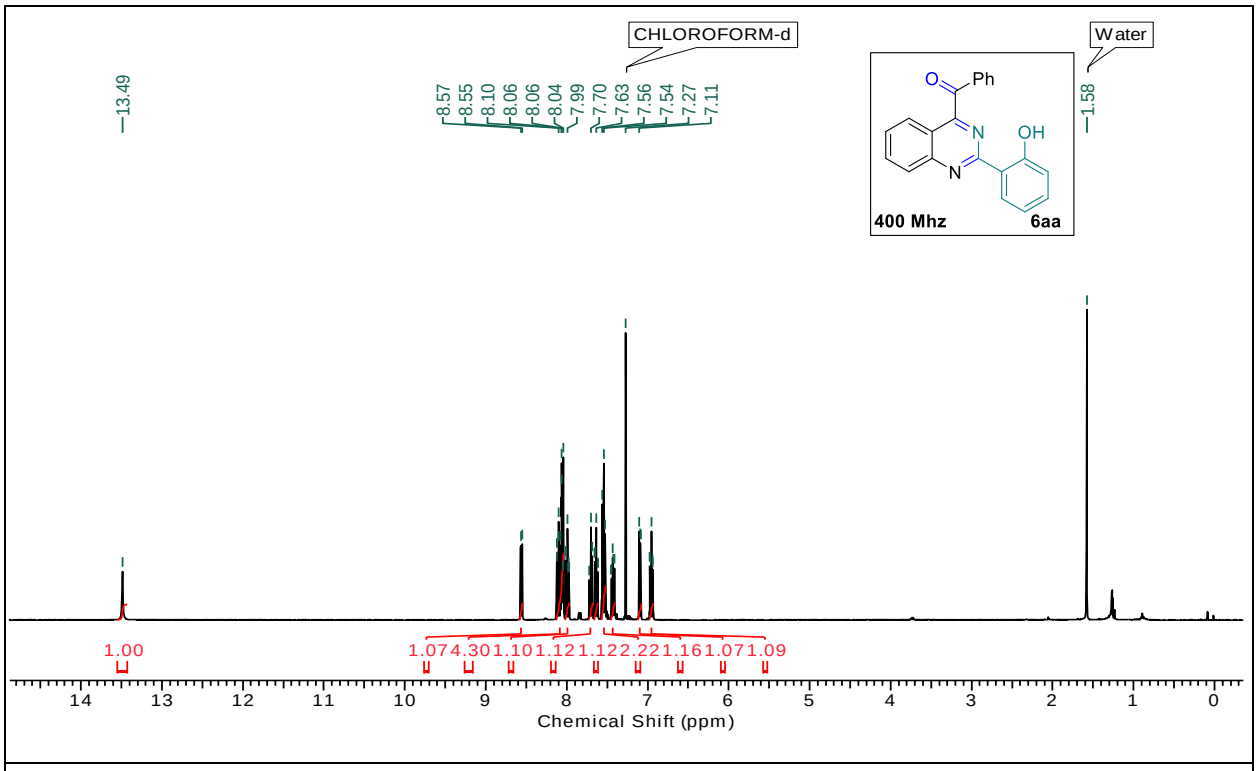

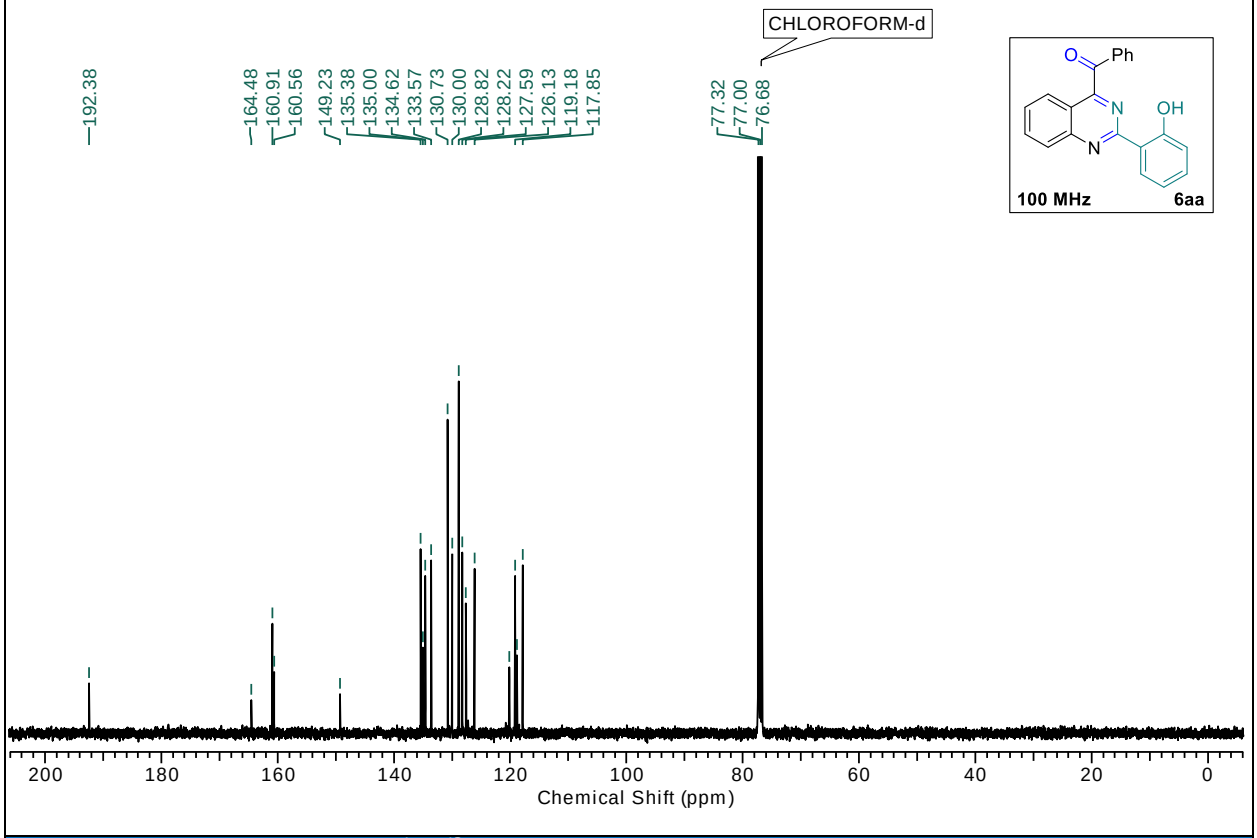

^{1}H /^{13}C NMR Spectrum of 6aa in $CDCl_3$

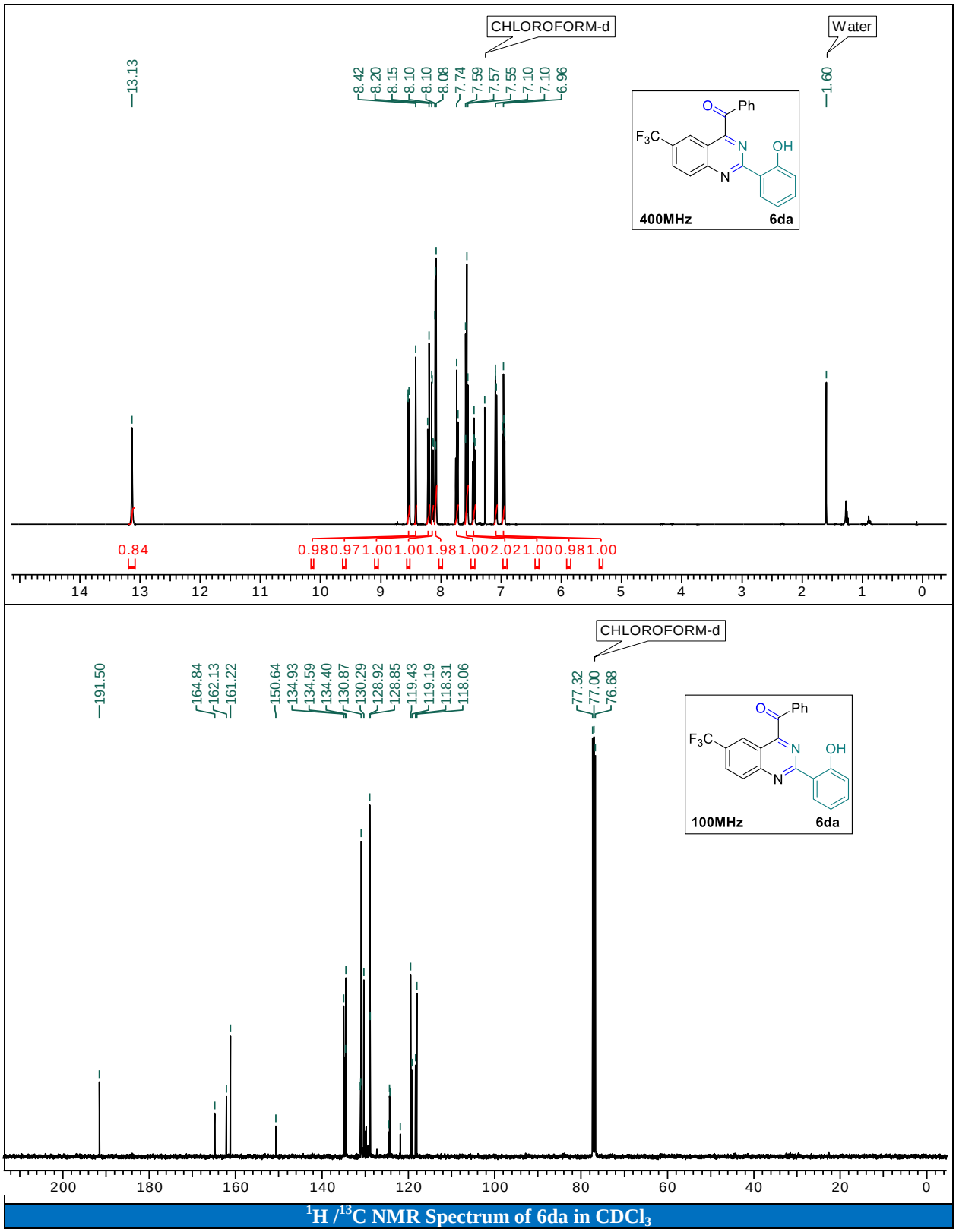

^{1}H /^{13}C NMR Spectrum of 6da in $CDCl_3$

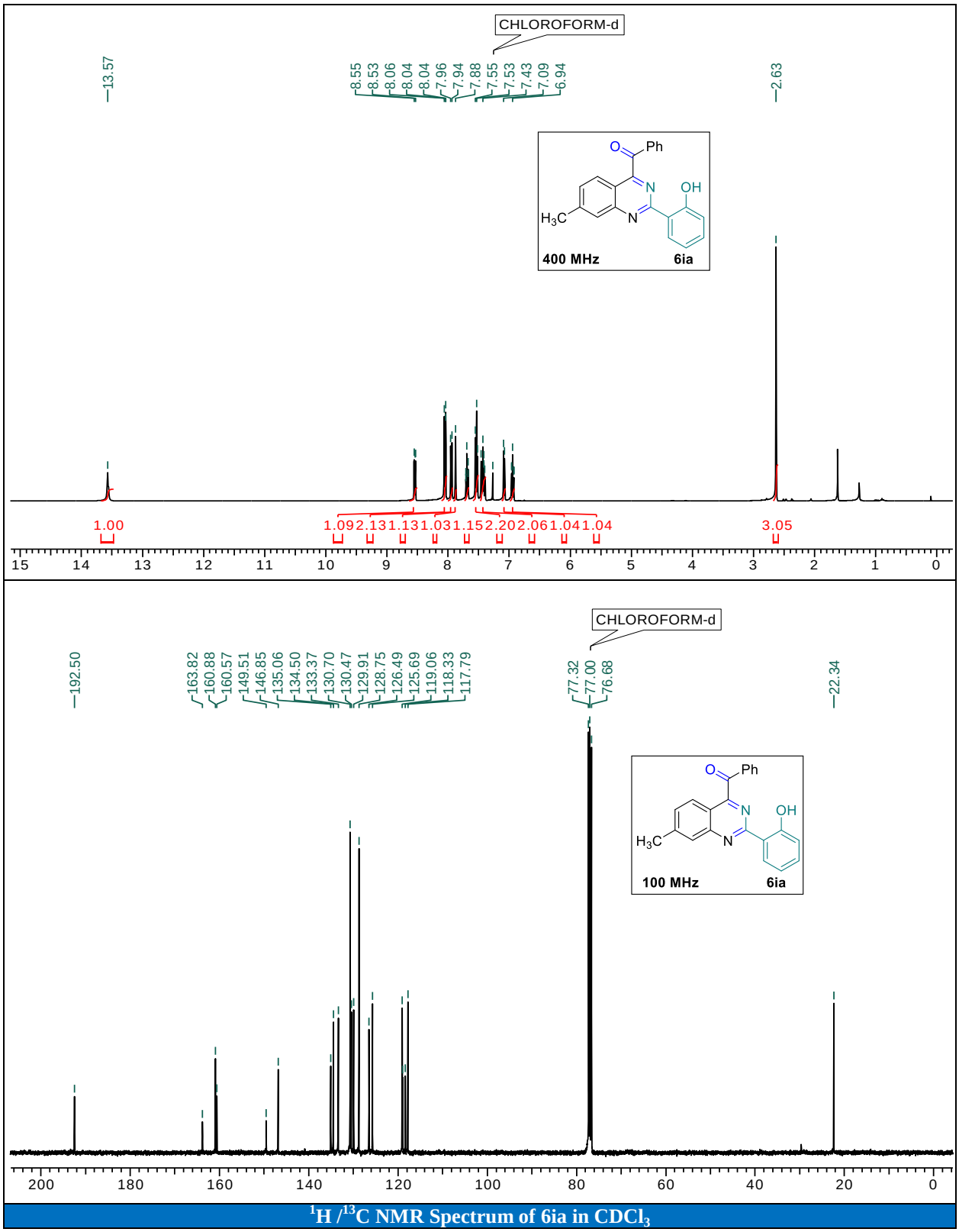

^{1}H /^{13}C NMR Spectrum of 6ia in $CDCl_3$

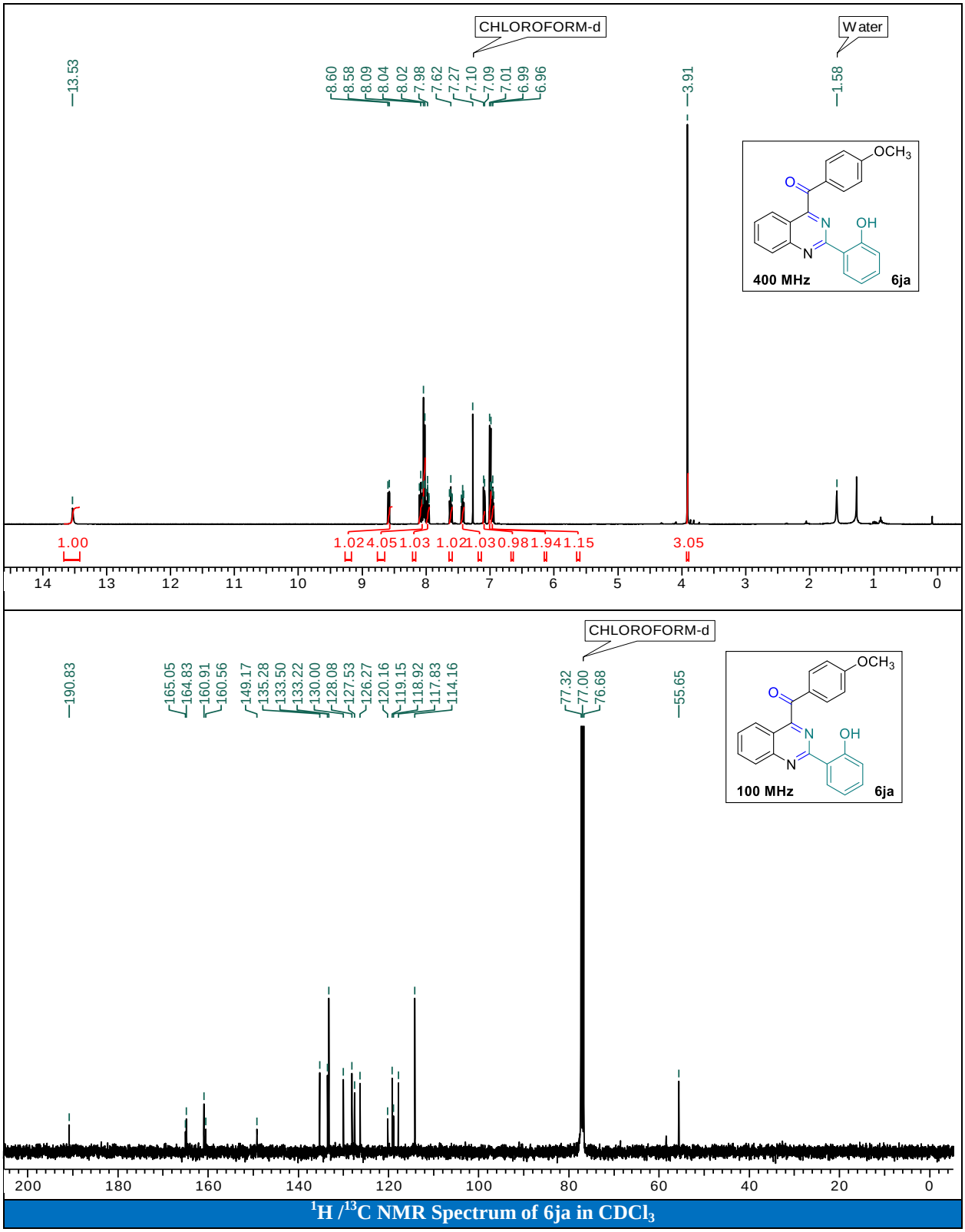

^{1}H /^{13}C NMR Spectrum of 6ja in $CDCl_3$

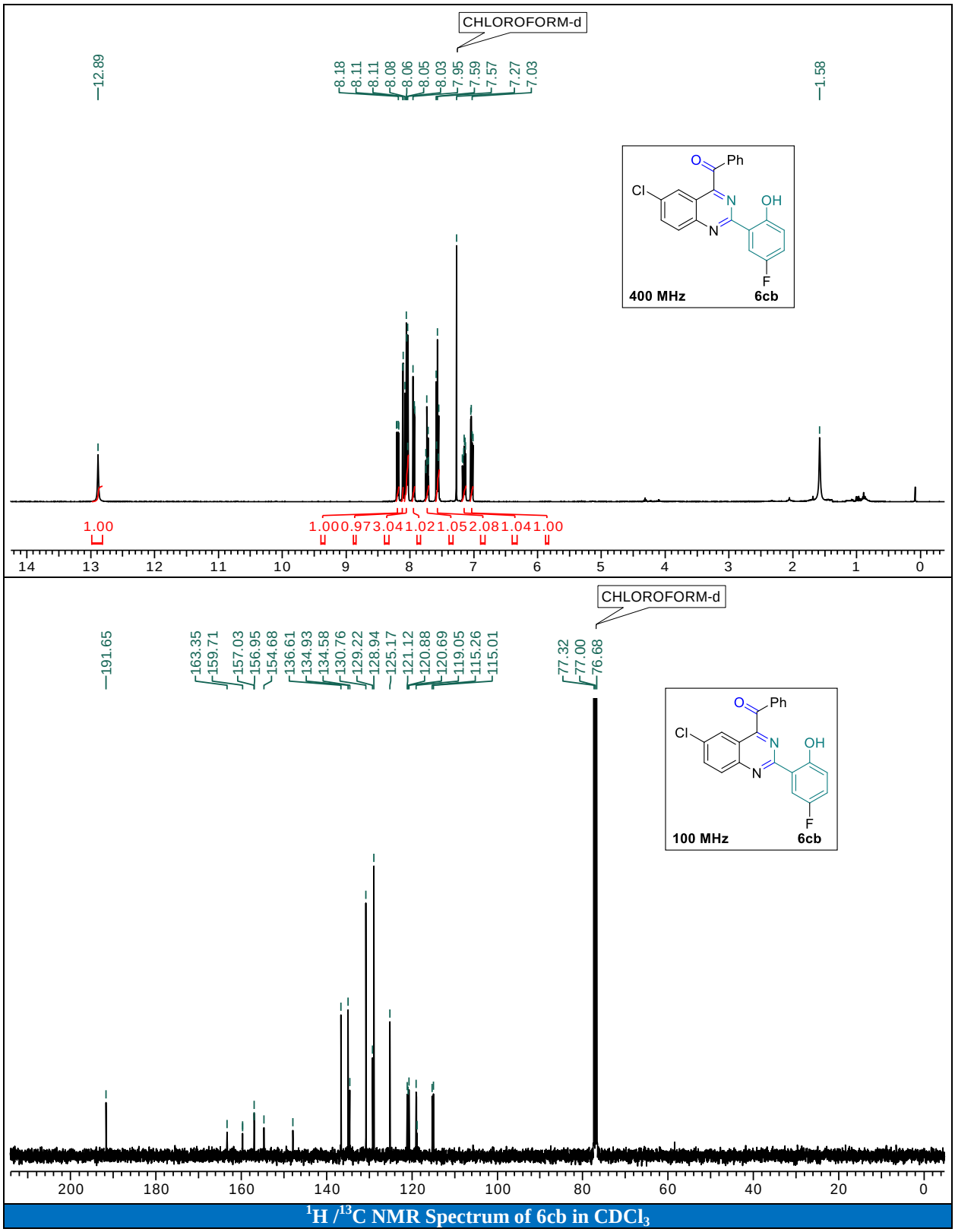

^{1}H /^{13}C NMR Spectrum of 6cb in $CDCl_3$

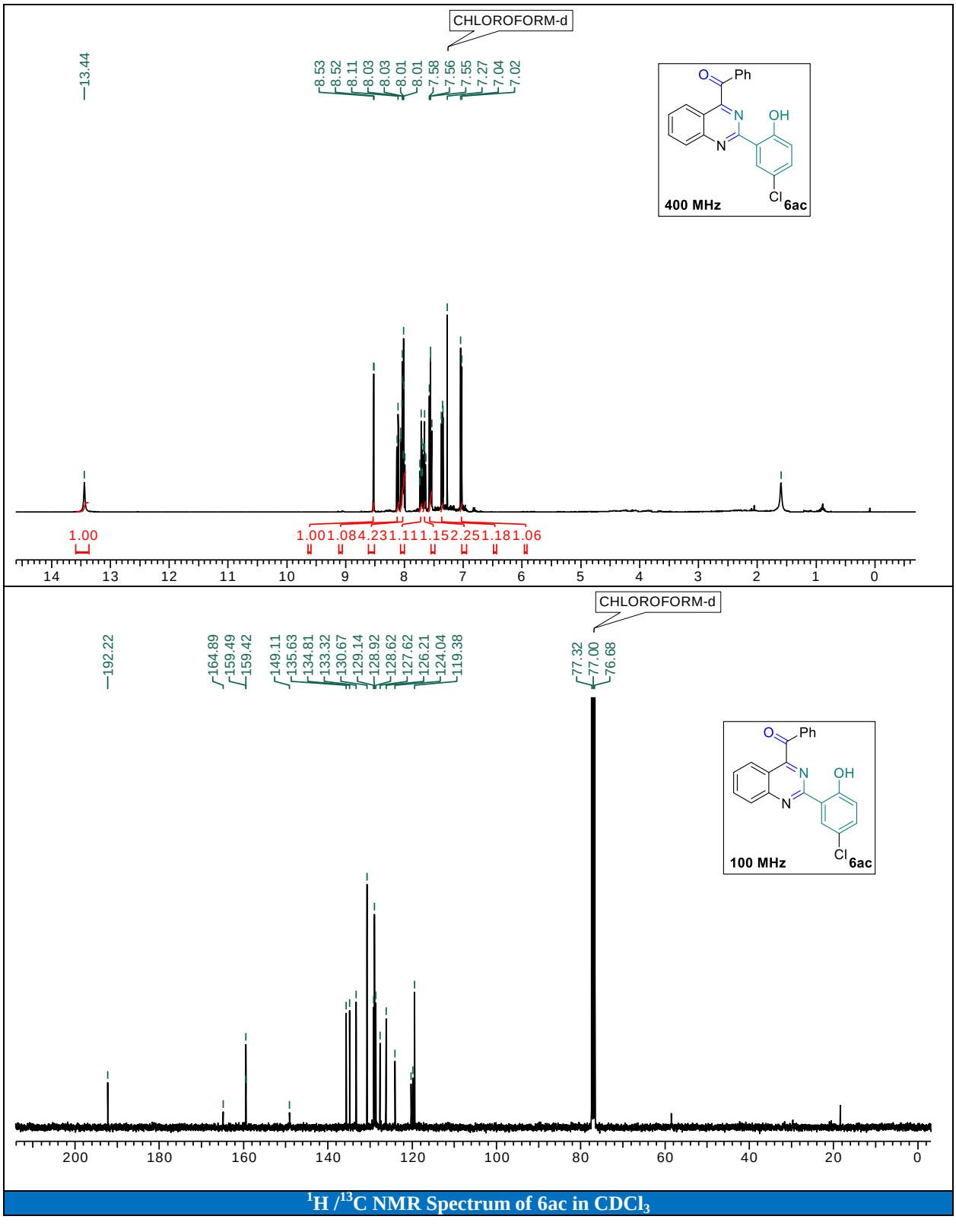

^{1}H /^{13}C NMR Spectrum of 6ac in $CDCl_3$

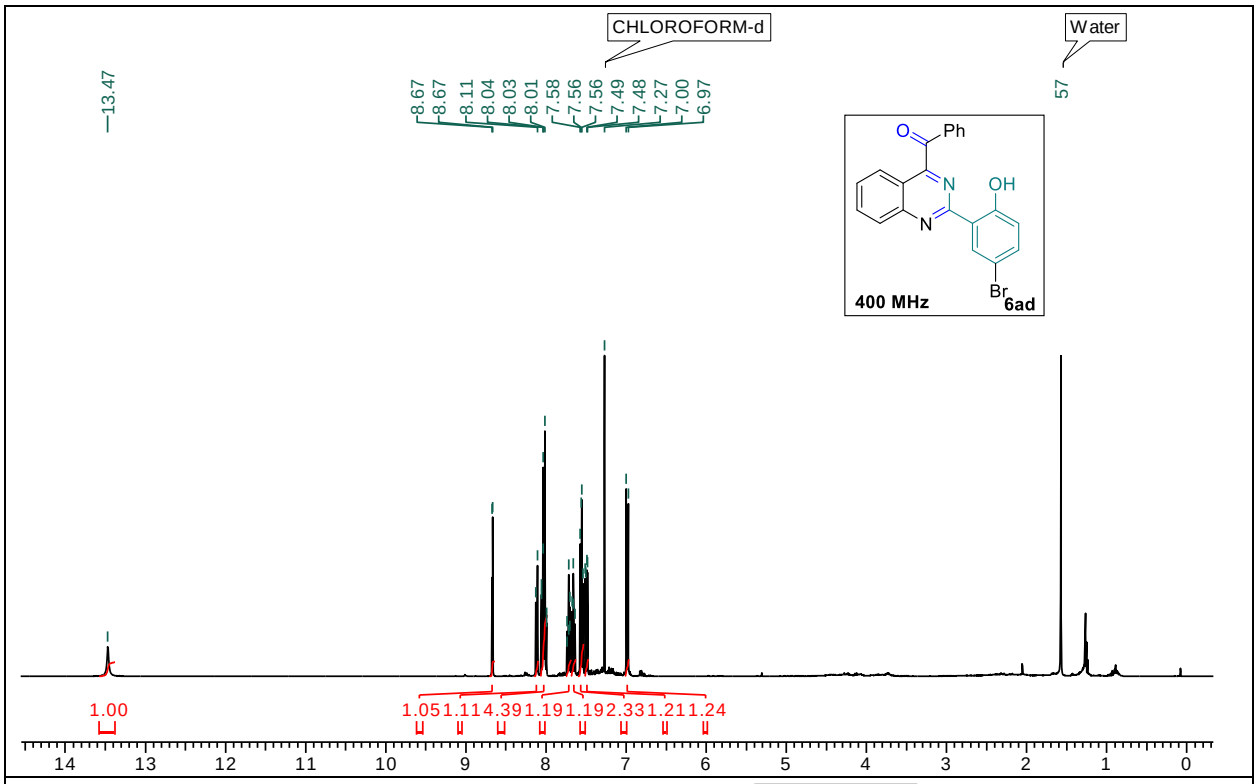

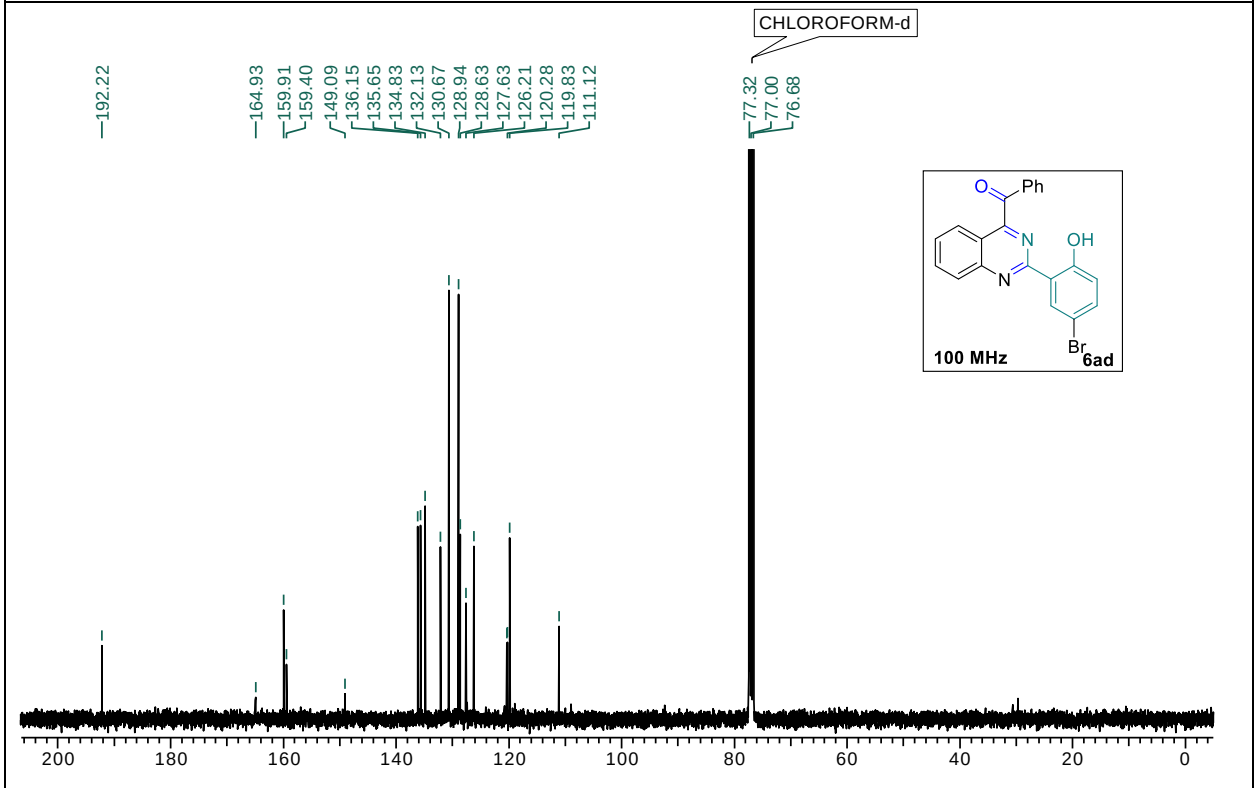

^{1}H /^{13}C NMR Spectrum of 6ad in $CDCl_3$

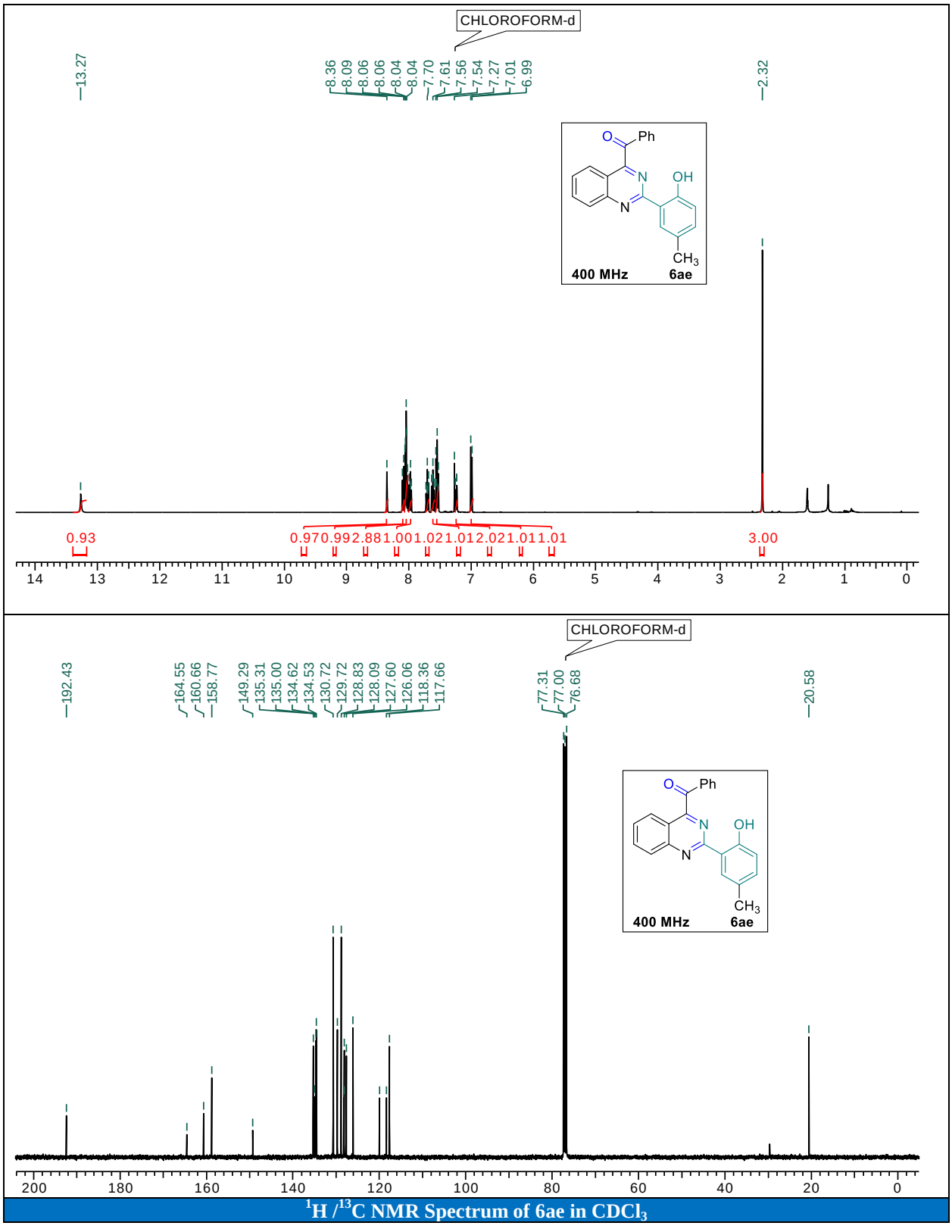

^{1}H /^{13}C NMR Spectrum of 6ae in $CDCl_3$

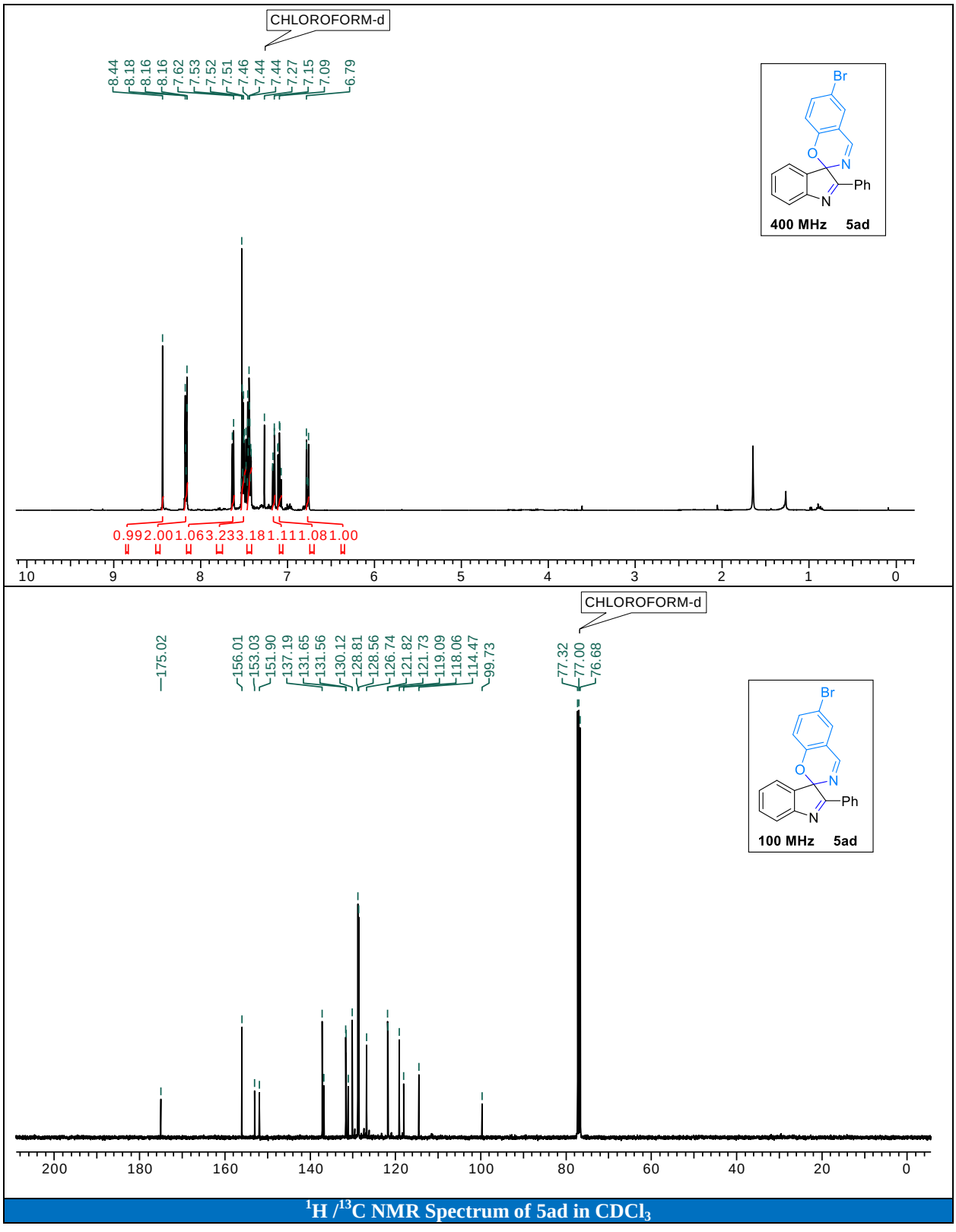

^{1}H /^{13}C NMR Spectrum of 5ad in $CDCl_3$

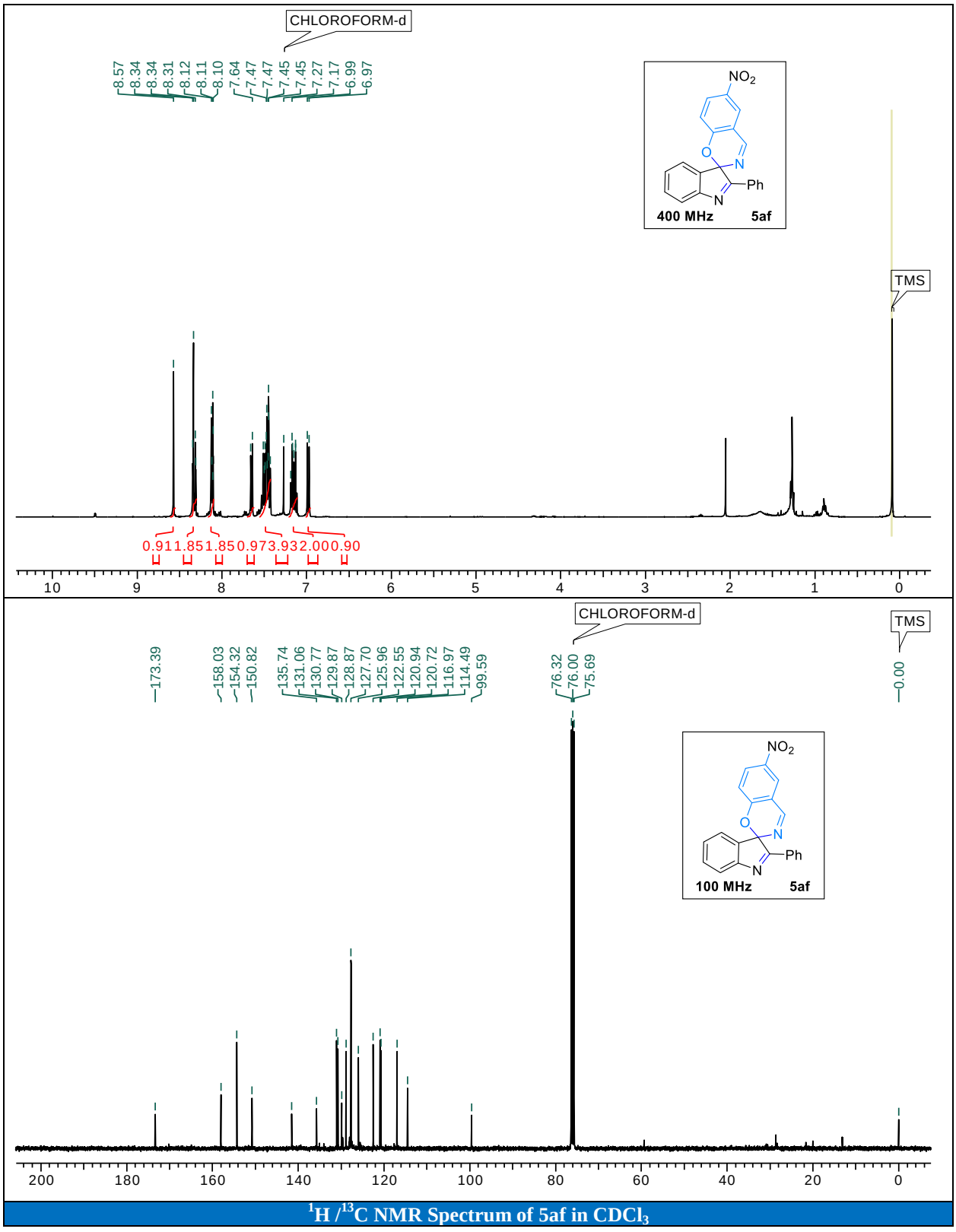

^{1}H /^{13}C NMR Spectrum of 5af in $CDCl_3$

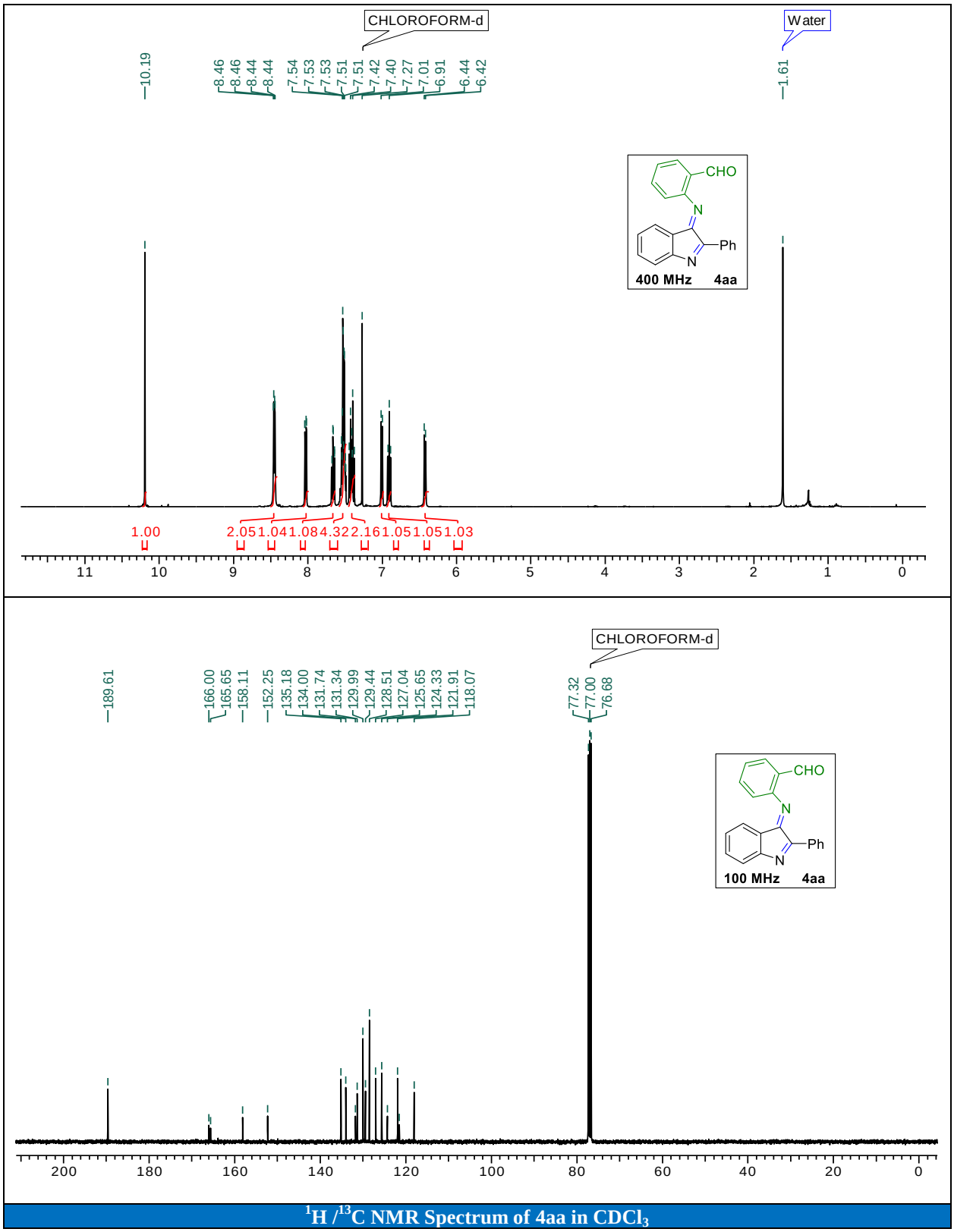

^{1}H /^{13}C NMR Spectrum of 4aa in $CDCl_3$

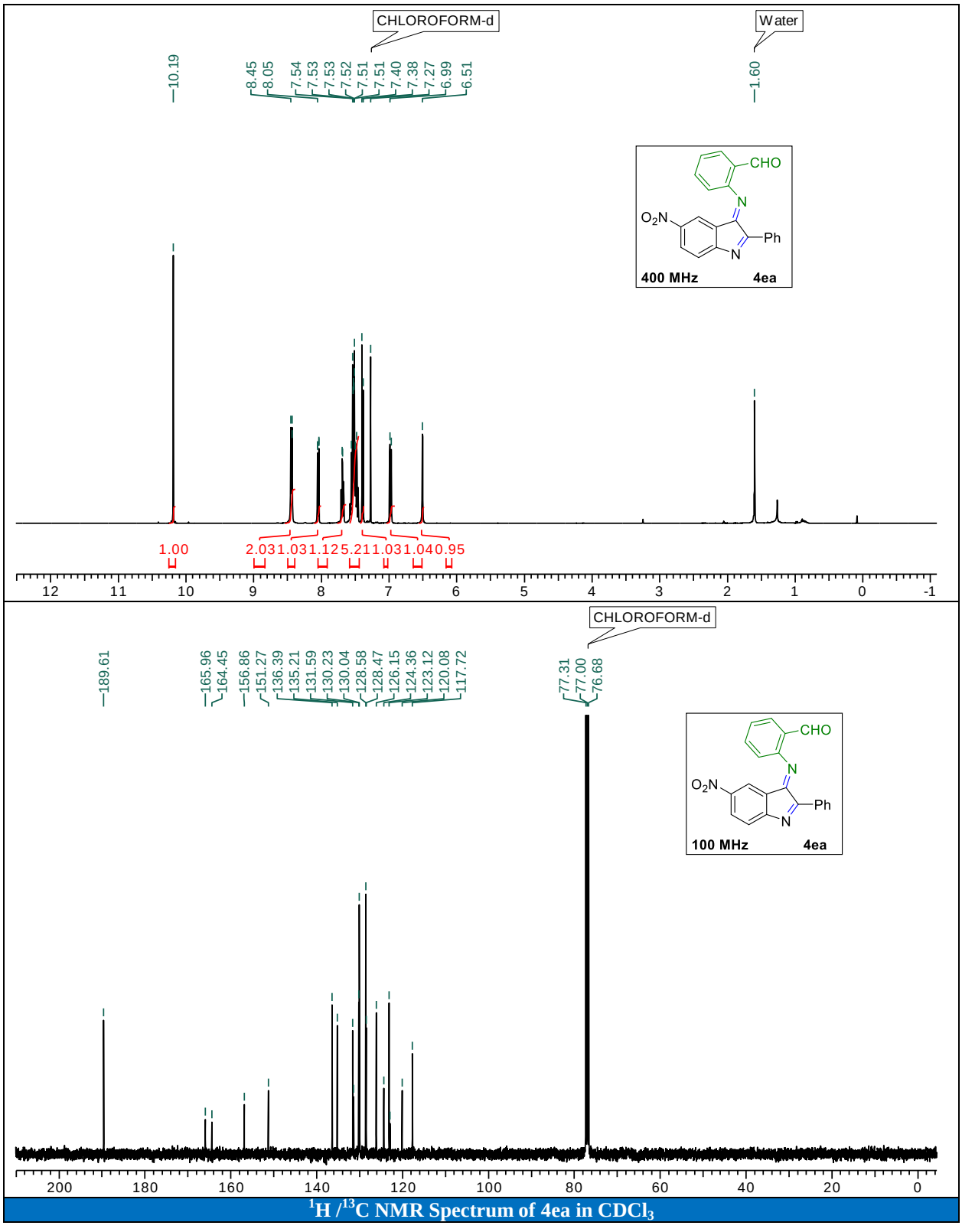

^{1}H /^{13}C NMR Spectrum of 4ea in $CDCl_3$

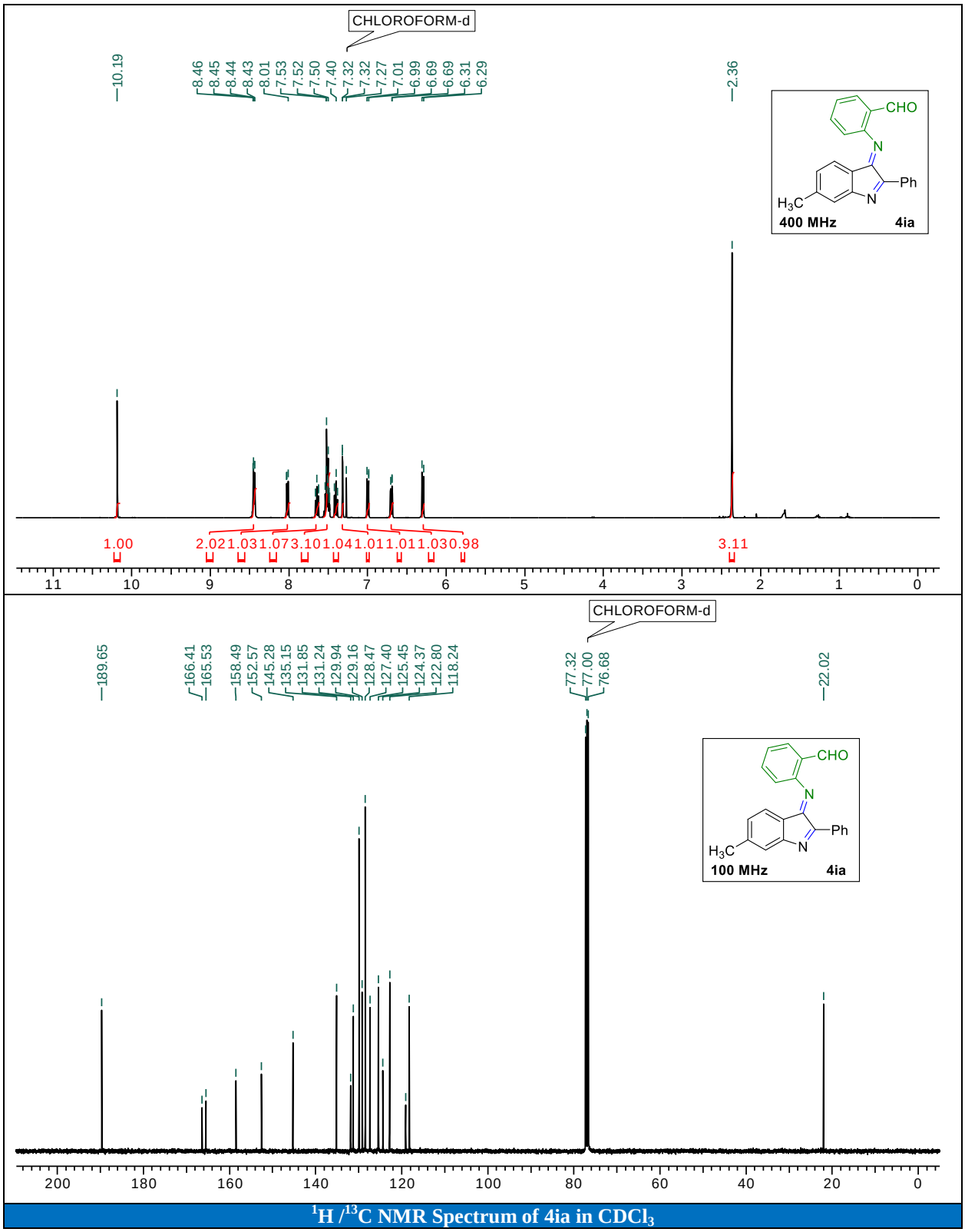

^{1}H /^{13}C NMR Spectrum of 4ia in $CDCl_3$

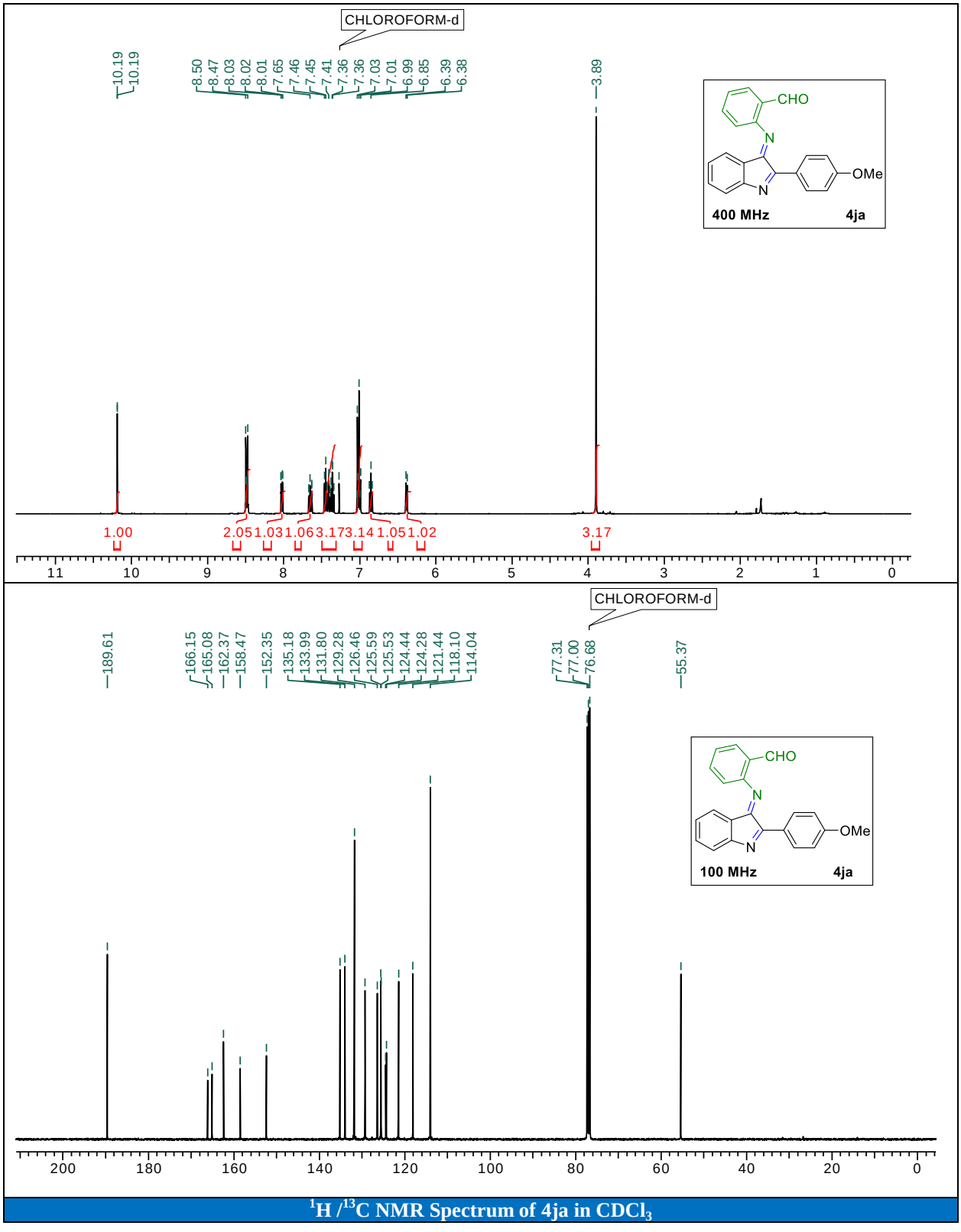

^{1}H /^{13}C NMR Spectrum of 4ja in $CDCl_3$

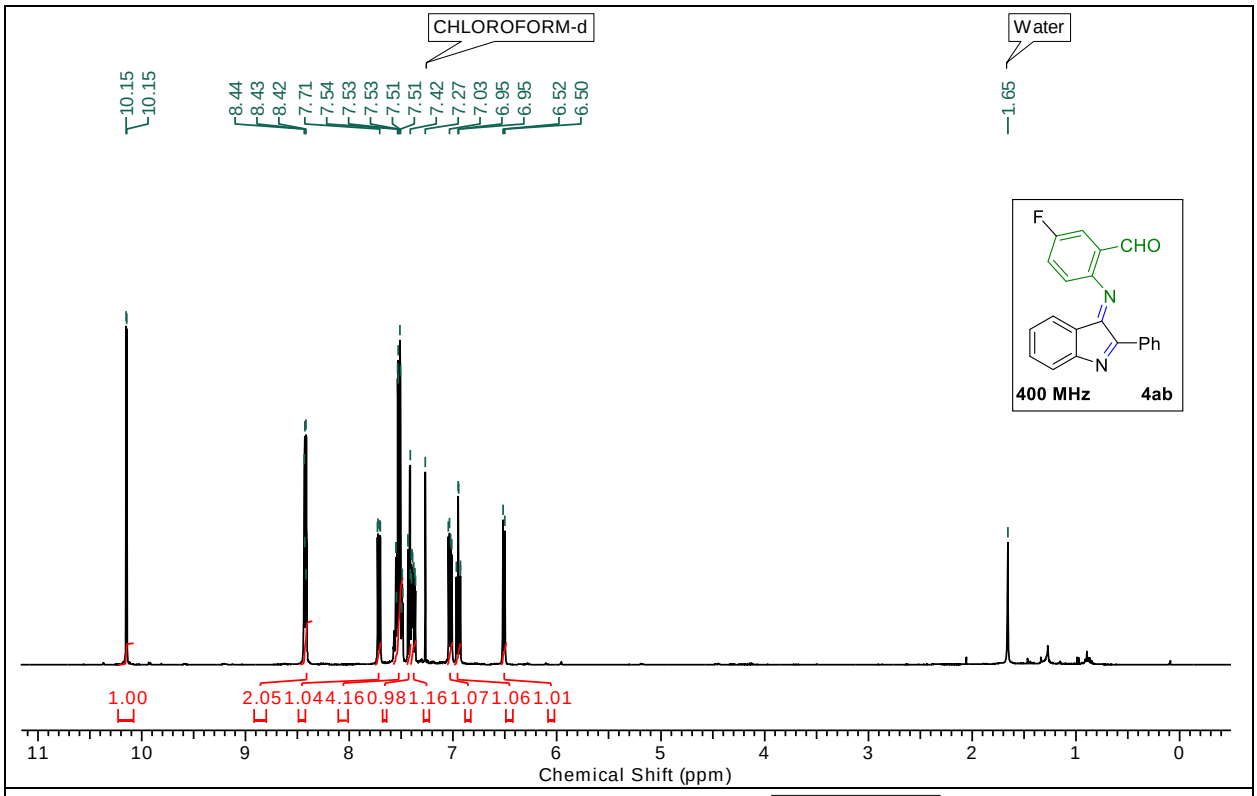

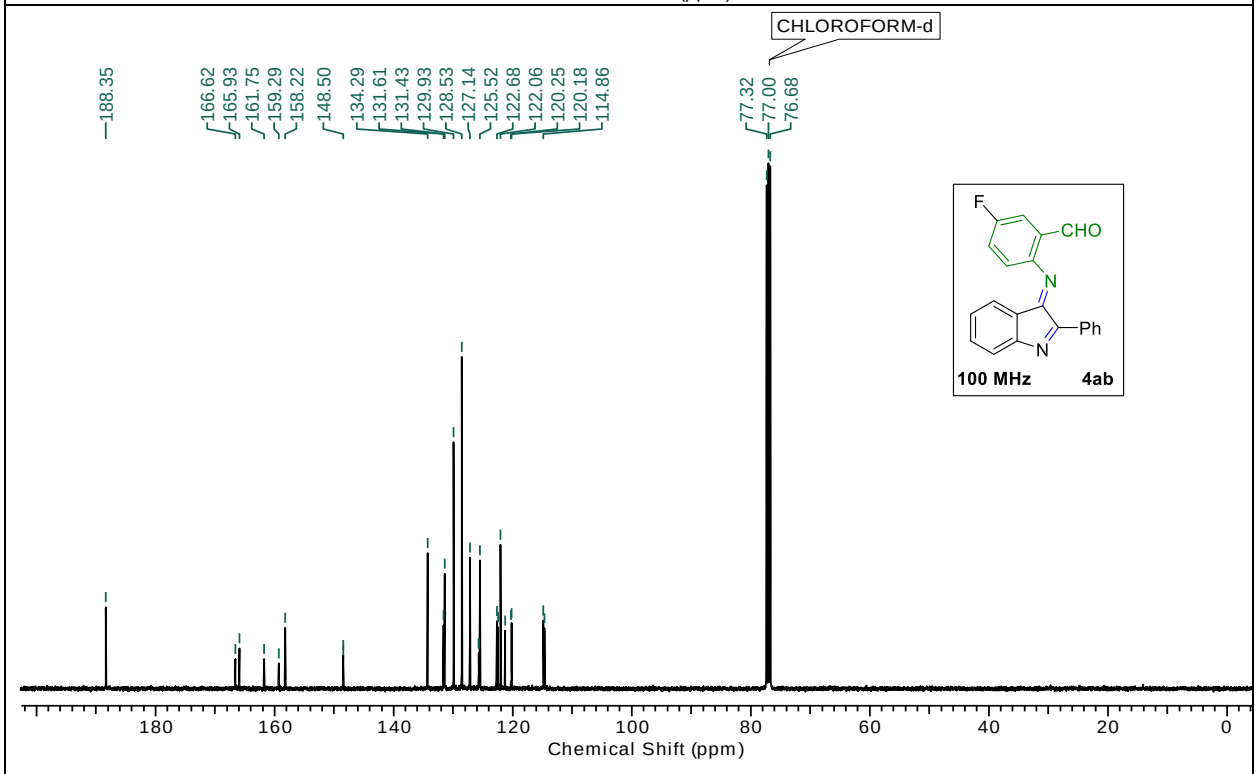

^{1}H /^{13}C NMR Spectrum of 4ab in $CDCl_3$

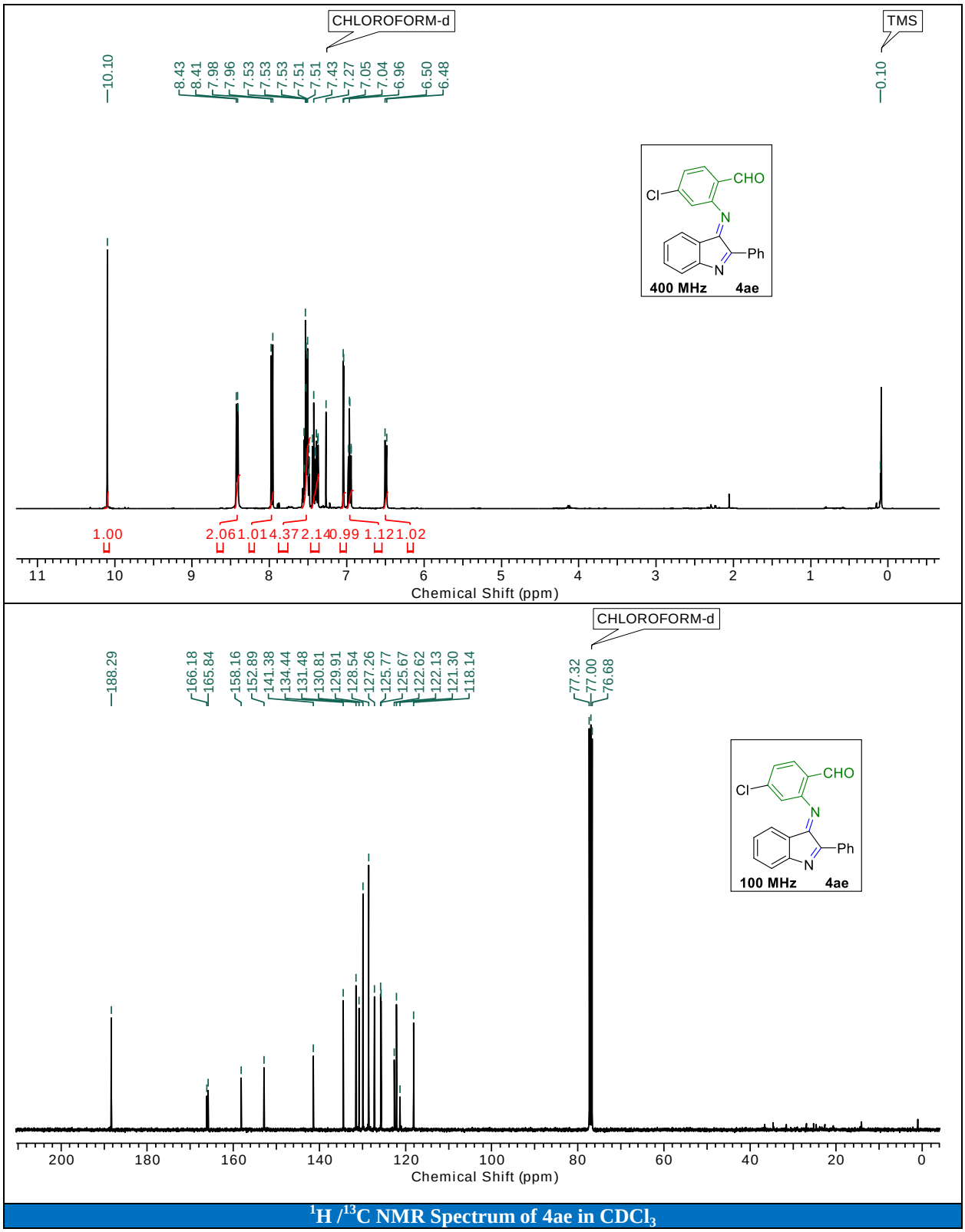

^{1}H /^{13}C NMR Spectrum of 4ae in $CDCl_3$

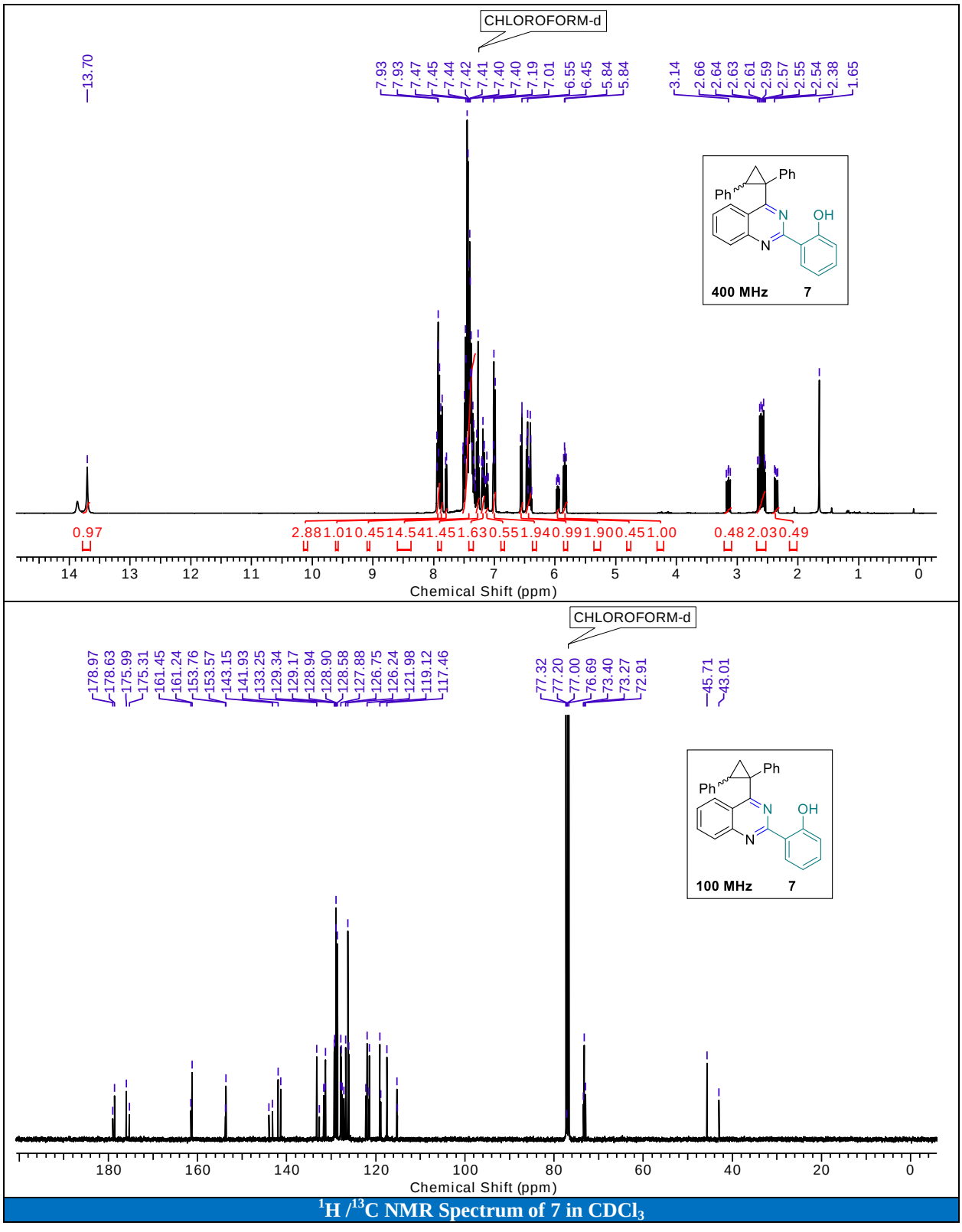

^{1}H /^{13}C NMR Spectrum of 7 in $CDCl_3$

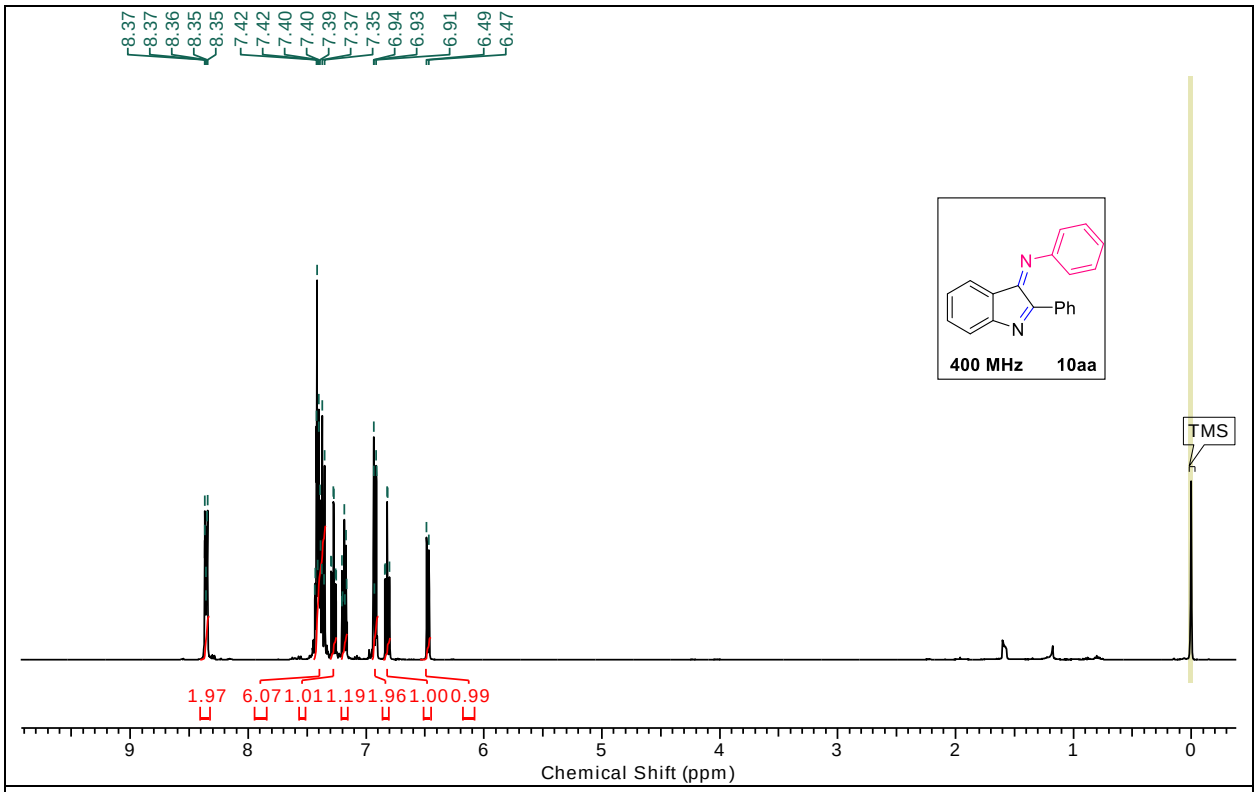

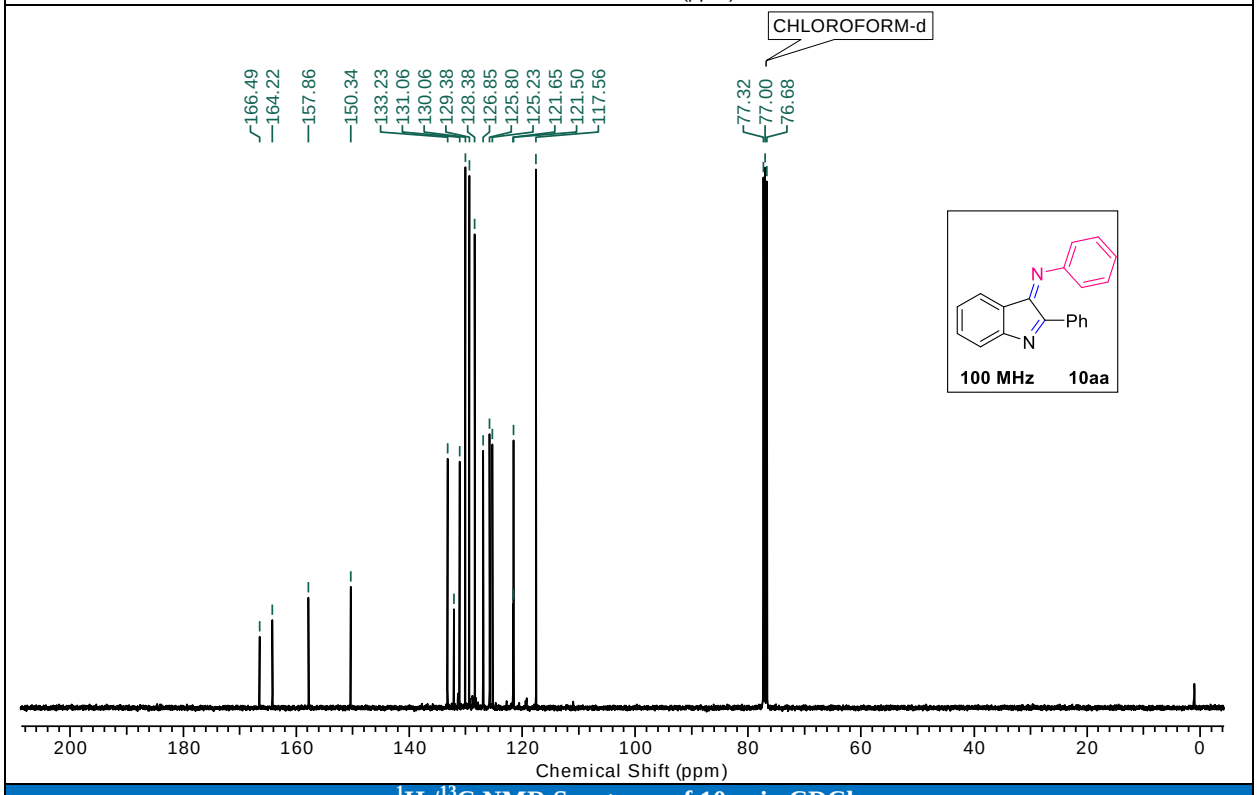

^{1}H /^{13}C NMR Spectrum of 10aa in $CDCl_3$

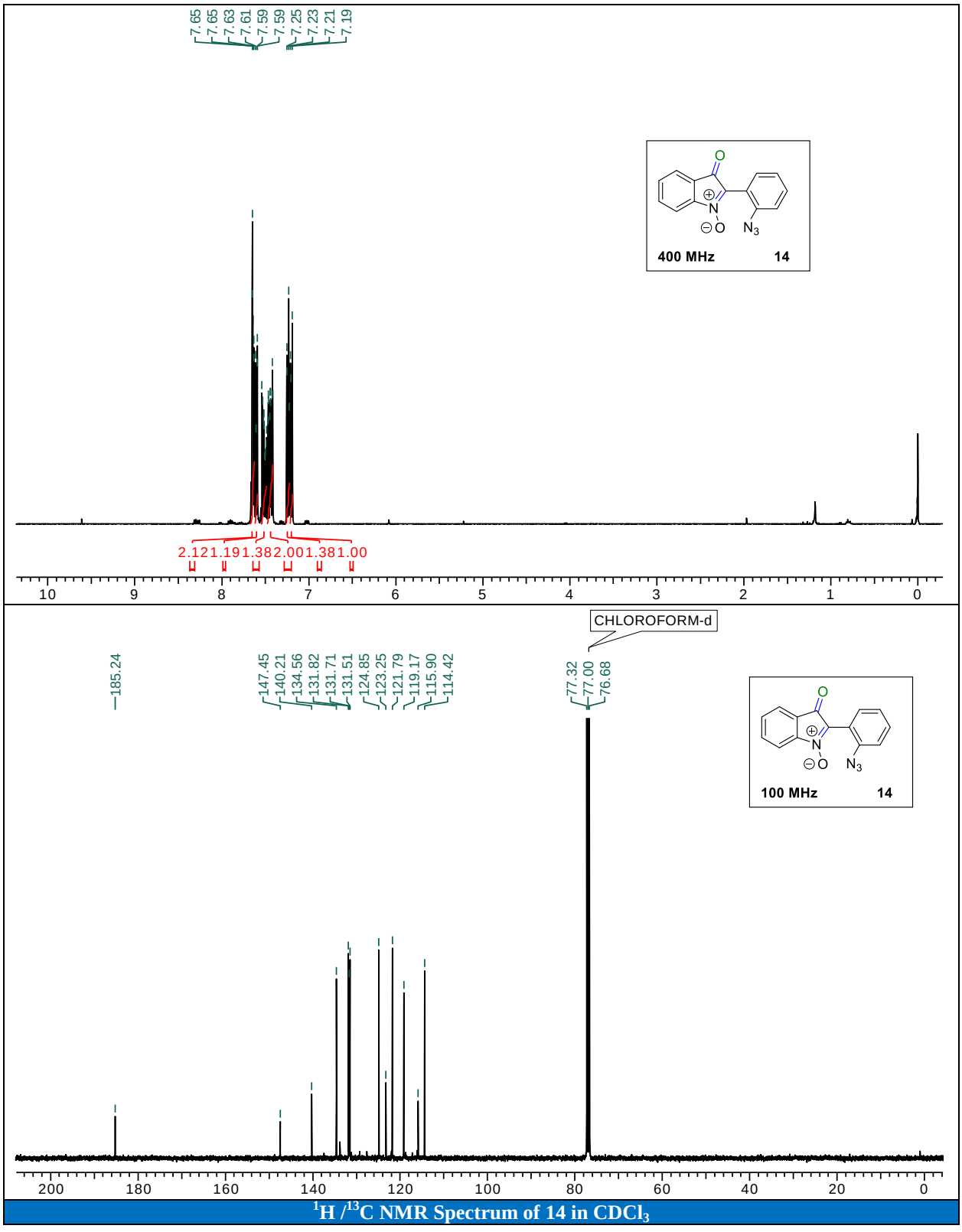

^{1}H /^{13}C NMR Spectrum of 14 in $CDCl_3$

1) Pflästerera, D.; Hashmi, S. *Chem. Soc. Rev*., **2016**, *45*, 1331.

2) a) Gorin, D. J.; Sherry, B. D.; Toste, F. D. *Chem. Rev.* **2008**, *108*, 3351. b) Hashmi, A. S. K. *Angew. Chem. Int. Ed.* **2010**, *49*, 5232.

3) Yeom, H.; Shin, S. *Acc. Chem. Res*. **2014**, *47*, 966.

4) a) Sahani, R. L.; Ye, L.-W.; Liu, R.-S. *Adv. Organomet. Chem.* **2020**, *73*, 195. b) Aguilar, E.; Santamaría, J. *Org. Chem. Front.* **2019**, *6*, 1513. c) Davies, P. W.; Garzon, M. *Asian J. Org. Chem.* **2015**, *4*, 694. d) Ye, L.-W.; Zhu, X.-Q.; Sahani, R. L.; Xu, Y.; Qian, P.-C.; Liu, R.-S. *Chem. Rev.* **2021**, *121*, 9039.

5) a) Zheng, Z.; Wang, Z.; Wang, Y.; Zhang, L. *Chem. Soc. Rev*. **2016**, *45*, 4448. b) Zhang, L. *Acc. Chem. Res.* **2014**, *47*, 877. c) Xiao, J.; Li, X. *Angew. Chem., Int. Ed.* **2011**, *50*, 7226.

6) a) Pflasterer, D.; Hashmi, A. S. K. *Chem. Soc. Rev.* **2016**, *45*, 1331. b) Rudolph, M.; Hashmi, A. S. K. *Chem. Soc. Rev.* **2012**, *41*, 2448. c) Hashmi, A. S. K.; Rudolph, M. *Chem. Soc. Rev.* **2008**, *37*, 1766.

7) a) Fabian, W. M. F.; Bakulev, V. A.; Kappe, C. O. *J. Org. Chem.* **1998**, *63*, 5801. b) Harmon, R. E.; Stanley, F.; Gupta, S. K.; Johnson, J. *J. Org. Chem.* **1970**, *35*, 3444.

8) Zhang, X.; Sun, X.; Cui, X.; Zhang, H. *Youji Huaxue* **2015**, *35*, 1700.

9) Cai, J.; Wu, B.; Rong, G.; Zhang, C.; Qiu, L.; Xu, X. *Org. Lett.* **2018**, *20*, 2733.

10) a) Zi, W.; Toste, F. D. *Chem. Soc. Rev.* **2016**, *45*, 4567. b) Harris, R. J.; Widenhoefer, R. A. *Chem. Soc. Rev.* **2016**, *45*, 4533. c) Asiri, A. M.; Hashmi, A. S. K. *Chem. Soc. Rev.* **2016**, *45*, 4471. d) Liu, L.; Zhang, J. *Chem. Soc. Rev.* **2016**, *45*, 506. e) Jia, M.; Ma, S. *Angew. Chem., Int. Ed.* **2016**, *55*, 9134. f) Dorel, R.; Echavarren, A. M. *Chem. Rev.* **2015**, *115*, 9028. g) Wang, Y.; Muratore, M. E.; Echavarren, A. M. *Chem. - Eur. J.* **2015**, *21*, 7332. h) Qian, D.; Zhang, J. *Chem. Soc. Rev.* **2015**, *44*, 677. i) Wei, F.; Song, C.; Ma, Y.; Zhou, L.; Tung, C.-H.; Xu, Z. *Sci. Bull.* **2015**, *60*, 1479. j) Fensterbank, L.; Malacria, M. *Acc. Chem. Res.* **2014**, *47*, 953. k) Obradors, C.; Echavarren, A. M. *Acc. Chem. Res.* **2014**, *47*, 902. l) Wang, Y.-M.; Lackner, A. D.; Toste, F. D. *Acc. Chem. Res.* **2014**, *47*, 889. m) Hashmi, A. S. K. *Acc. Chem. Res.* **2014**, 47, 864.

11) a) Ramana, C. V.; Patel, P.; Vanka, K.; Miao, B. C.; Degterev, A. *Eur. J. Org. Chem.* **2010**, 5955. b) Patel, P.; Ramana, C. V. *Org. Biomol. Chem.* **2011**, *9*, 7327. c) Patel, P.; Ramana, C. V. *J. Org. Chem.* **2012**, *77*, 10509. d) Reddy, B. N.; Ramana, C. V. *Chem. Commun.* **2013**, *49*, 9767. e) Patel, P.; Reddy, B. N.; Ramana, C. V. *Tetrahedron* **2014**, *70*, 510. f)

Kumar, C. V. S.; Ramana, C. V. *Org. Lett.* **2014**, *16*, 4766. g) Dhote, P. S.; Ramana, C. V. *Org. Lett.* **2019**, *21*, 6221.

12) a) Dhote, P. S.; Ramana, C. V. *Org. Lett.* **2021**, *23*, 2632. b) Dhote, P. S.; Pund, K.; Ramana, C. V. *J. Org. Chem.* **2021**, *86*, 10874.
13) Gao, Y.; Nie, J.; Huo, Y.; Hu, X. Q. *Org. Chem. Front.* **2020**, *7*, 1177.
14) a) Jadhav, P. D.; Lu, X.; Liu, R.-S. *ACS Catal.* **2018**, *8*, 9697. b) Xu, W.; Zhao, J.; Li, X.; Liu, X. *J. Org. Chem.* **2018**, *83*, 15470.
15) a) Mokar, B. D.; Jadhav, P. D.; Pandit, Y. B.; Liu, R. S. *Chem. Sci*. **2018**, *9*, 4488. b) Kumar, R.; Singh, R.; Skaria, M.; Chen, L.; Cheng, M. J.; Liu, R. S. *Chem. Sci*. **2019**, *10*, 1201.
16) a) Egger, J.; Carreira, E. M. *Nat. Prod. Rep.*, **2014**, *31*, 449. b) Kong, C.; Jana, N.; Jones, C.; Driver, T. G. *J. Am. Chem. Soc.* **2016**, *138*, 13271. c) Fauché, K.; Nauton, L.; Jouffret, L.; Cisnetti, F.; Gautier, A. *Chem. Commun.* **2017**, *53*, 2402.
17) a) Horner, L.; Christmann, A. *Angew. Chem., Int. Ed.* **1963**, *2*, 599. b) S.; Patai, Y.; Gotshal, *J. Chem. Soc. B* **1966**, 489. c) Labbe, G. *Chem. Rev.* **1969**, 69, 345. d) Smith, P. A. S. *Azides and Nitrenes, Reactivity and Utility;* Ed.-Scriven, E. F. V.; Academic Press, **1984**, 95. e) Goriya, Y.; Ramana, C. V. *Tetrahedron* **2010**, 66, 7642.
18) Zhang, X.; Sun, X.; Fan, H.; Li, P.; Lyu, C.; Rao, W. *Eur. J. Org. Chem*. **2016**, 4265.
19) Liu, Q.; Chen, P.; Liu, G. *ACS Catal.* **2013**, *3*, 178.

Chapter III

Metal Free McMurry Type Coupling: Synthesis of 2H-indazole π-Conjugated Scaffolds

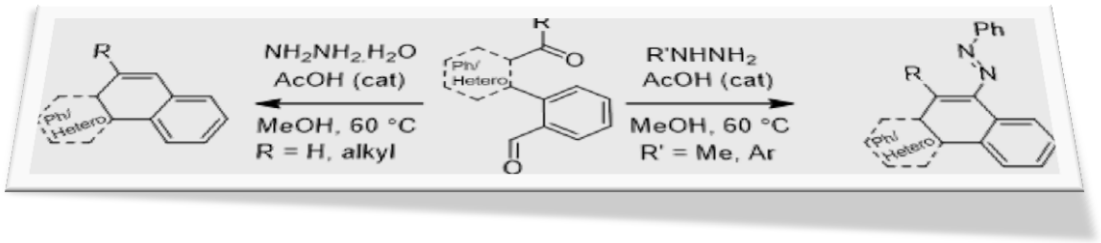

1.0. Introduction

Construction of polysubstituted alkenes has been a long-lasting task in organic synthesis, because of the problems with controlling the regio-, chemo-, and stereoselectivity.[1] Many powerful synthetic methods have been developed, such as Wittig, cross coupling and olefin metathesis, and their importance has also been recognized by the Nobel board. Apart from these classical olefination methods, the coupling of two carbonyl compounds, usually in the presence of a stoichiometric amount of a titanium reagent (the so-called McMurry reaction, Scheme S3.1)[2] has gained much attention for the synthesis of biologically active natural products, macrocyclic compounds, the synthesis of sterically hindered or strained alkenes, medium or large rings, etc.[3]

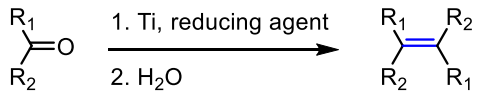

Scheme S3.1: *General McMurry Reaction*

1.1. History of McMurry Reaction

In 1970, Schreibmann and group found an unexpected result during the pinacol coupling of carbonyl compounds using amalgamated aluminum: olefins were obtained as side products.[4] Next, Sharpless and coworkers reported the deoxygenative coupling of aliphatic and aromatic carbonyl compounds using a low-valent tungsten species, generated by the reduction of WCl_6 with BuLi.[5] Inspired by these results, in 1973, the Mukaiyama group (Scheme S3.2, eq. 1)[6] and the Tyrlik group (Scheme S3.2, eq. 2)[7] reported the first titanium mediated reactions using $TiCl_4$/Zn and $TiCl_3$/Mg reagents, respectively. At the same time, McMurry made a serendipitous discovery: in attempts to selectively deoxygenate the α,β-unsaturated ketone, he found that the $TiCl_3/LiAlH_4$ reagent reductively dimerized an α,β-unsaturated ketone to a triene (Scheme S3.2, eq. 3).[8a] However, the previous known methods were found to be incompatible for the coupling of aliphatic ketones. Later, in 1974, he documented the $TiCl_3/LiAlH_4$ assisted deoxygenative coupling of both aromatic and aliphatic carbonyl compounds. During these studies, McMurry and team systematically studied the limitations and generality of the reaction, and they also developed more effective and reproducible deoxygenative reagents such as $TiCl_3$/K,[8b,8c] $TiCl_3$(DME)1.5/Zn-Cu [2,8c,8d] and $TiCl_3$/Li.[8c] Because of his efforts to promote this protocol and

make it synthetically applicable, these reactions came to be recognized as the McMurry coupling reactions.

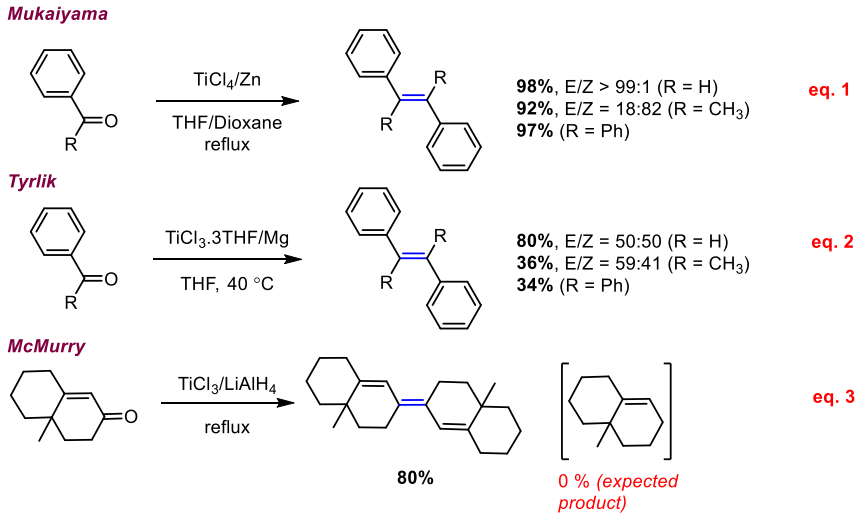

Scheme S3.2: *Early Examples of the Titanium-Mediated Deoxygenative Coupling of Carbonyl Compounds*

Pioneering efforts from various groups have revealed that this reactions works well in intramolecular dicarbonyl coupling reactions and is extremely useful in the synthesis of strained, unusual molecules of different ring sizes, for π-conjugated polyaromatic and for macrocyclic systems where traditional coupling reactions have seen a limited scope. However, there are certain limitations for the McMurray coupling. These include the generation of stoichiometric quantities of metal waste and poor chemo-selectivity/functional group tolerance, in general. In particular, reproducibility is a common issue and it was not seen to be compatible for intermolecular reactions, especially for cross-couplings.

1.2. Literature Reports on Dicarbonyl Coupling

However, in the context of some of the unexpected (?) results (see the next section), a vigorous SciFinder search has been carried out, which revealed some interesting older reports documenting McMurray like coupling reactions under classical metal-mediated reductions such as Wolff-Kishner and Clemmensen Reductions and even under simple acidic/basic conditions. They were, however, limited mainly to the biary-2,2'-dicarbonyl compounds. These reports are much older than the original (?) report of the 1970s by Schreibmann, who documented olefins as

the side product during the pinacol coupling with the aluminum amalgam. Interestingly, these reports have mostly gone unnoticed, even in some of the recent reports where a similar transformation was conducted in a more complicated fashion. These reactions will be discussed in detail in a chronological fashion.

1.2.1 Formation of Anomalous Olefins under Wolff-Kishner/Clemmensen Reduction of 1,6-dicarbonyls

Perkin and Robinson documented the first coupling of a dicarbonyl to an olefin under Wolff-Kishner reduction conditions (Scheme S3.3). In dealing with the structure elucidation of the natural product Brazilin, the reduction of trimethylbrazilone **S3.3A** (derived from the oxidation of trimethylbrazilin) has been attempted under Wolff-Kishner reduction conditions employing phenylhydrazine in EtOH. This was not seen to proceed satisfactorily, but in refluxing acetic acid gave deoxytrimethylbrazilone **S3.3B**. However, the correct structure of the product has been proposed by Richards and Tomlinson later.

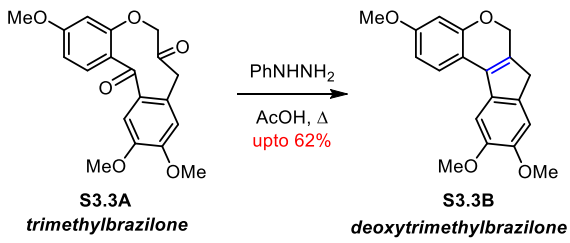

S3.3A
trimethylbrazilone

S3.3B
deoxytrimethylbrazilone

Scheme S3.3: *Perkin's Dicarbonyl Coupling Using Wolff-Kishner Reduction Conditions*

(Gilbody, A. W.; Perkin, W. H. *J. Chem. Soc*., *Transactions* **1902**, *81*, 1040–1056; Perkin, W. H.; Robinson, R. *J. Chem. Soc*., **1908**, 489–4xy; Perkin, W. H.; Ray, J. N.; Robinson, R. *J. Chem. Soc*., **1928**, 1504–1513; Richards, R. E.; Tomlinson, M. L. *Nature*, **1948**, *162*, 693–694)

Along similar lines, in 1937, as a part of exploring the chemistry of pyrene, Langbein and co-workers carried out the reduction of 5-formylphenanthrene-4-carboxylic acid **S3.4A** with phenyl hydrazine and hydrazine hydrate in refluxing AcOH. In case of hydrazine, 4-hydroxypyrene **S3.4C** was obtained in 74.0% yield. On the other hand, when the reduction was conducted with phenylhydrazine, it gave 4-hydroxy-5-phenylazopyrene **S3.4B** in 70.0% yield (Scheme S3.4).

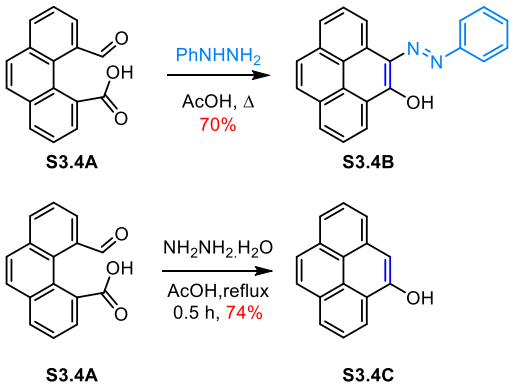

Scheme S3.4: Langbein*'s Pyrene Synthesis Using Dicarbonyl Coupling*

(Vollmann, H.; Becker, H.; Corell, M.; Streeck, H.; Langbein, G. *Justus Liebigs Annalen der Chemie* **1937**, *531*, 1–159)

A year later, Suszko and Schillak reported a similar condensation of a dicarbonyl under Clemmensen reduction conditions. The attempted reduction of the tetrabenzocyclodecatetraene-1:6-dione with Zn-Hg and HCl in EtOH at reflux gave tetrabenzonaphthalene in quantitative yields (Scheme S3.5).

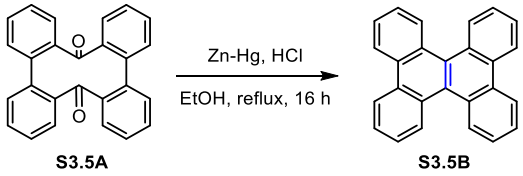

Scheme S3.5: Suszko*'s Dicarbonyl Coupling Using Clemmensen Reduction Conditions*

(Suszko, J.; Schillak, R. *Roczniki Chemii*, **1934**, *14*, 1216–1225)

In the context of synthesizing 2,2'-diethylbiphenyl, the Clemmensen reduction of diphenyl 2,2'-diacetyl (**S3.6A**) has been attempted by Turner and co-workers. The employed conditions involved the refluxing of **S3.6A** in the presence of zing amalgam in concentrated hydrochloric acid. Interestingly, the 9,10-dimethylphenanthrene **S3.6B** was obtained in quantitative yields (Scheme S3.6). Though this reaction was quite interesting, Turner's group focused more on synthesizing the original target 2,2'-diethylbiphenyl and did not pay as much attention on this reaction as the formation of olefins (however, not *via* the condensation resulting from the dehydration of the intermediate alcohols obtained from the ketone reduction) in the Clemmensen reduction, especially when conducted under mild acidic conditions. To overcome

this bottleneck, the reduction of the diketone **S3.6A** was attempted with hydrazine in aqueous NaOH at reflux. Under these conditions, the 7-methyl-5H-dibenzo[a,c][7]annulene (**S3.6C**) was obtained in 55.0% yield along with the phenanthrene **S3.6B** as a minor product. An interesting mechanism that comprises of the initial formation of diazocine **S3.6D** and subsequent chelotropic nitrogen elimination has been extended for the formation of phenanthrene **S3.6B**.

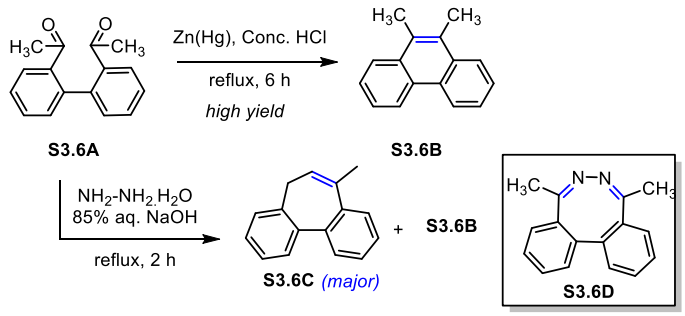

Scheme S3.6: *Turner's Dicarbonyl Coupling Using Zn(Hg) and conc. HCl*

(Hall, D; Ladbury, J.; Lessliea, M.; Turner, E. *J. Chem. Soc*., **1956**, 3475–3482)

In the same year, Bacon and coworkers reported the hydrazine mediated intramolecular dicarbonyl coupling of **S3.7A** to form diazocine derivatives **S3.7C** in major amount, along with phenanthrene **S3.7B** as the minor product. The reaction involves high temperature heating, as well as long reaction time (Scheme S3.7, eq. 1). On the other hand, the reaction of biphenyl 2,2'-dicarbaldehyde substrates **S3.7D** with hydrazine in acetic acid or in the presence of base in protic solvents produced the phenanthrene compound **S3.7E** as the sole product (Scheme S3.7, eq. 2). The reaction of 4,5-disubstituted methyl groups on dicarbaldehyde failed to give the corresponding cyclized product. This may be due to steric hindrance. The reaction with 2,2',6,6'-tetra-aldehyde, on the other hands, afforded pyrene in 66.0% yield.

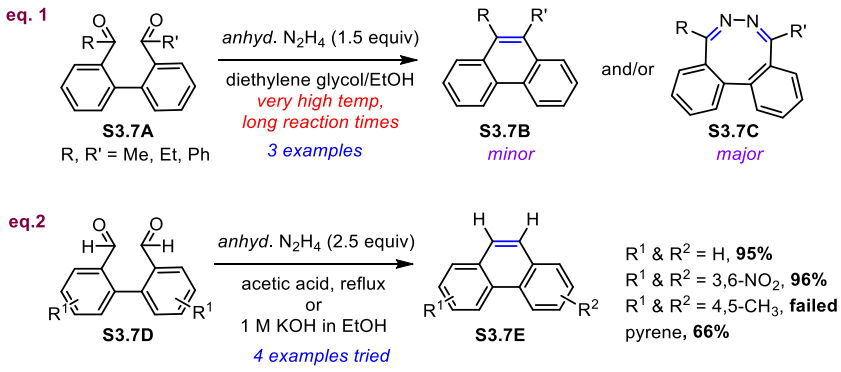

Scheme S3.7: *Bacon's Dicarbonyl Coupling with Hydrazine*

(Bacon, R. G. R.; Lindsay, W. S, *Chem. and Ind.*, **1956**,1479; Bacon, R. G. R.; Lindsay, W. S. *J. Chem. Soc*., **1958**, 1375; Bacon, R. G. R.; Lindsay, W. S. *J. Chem. Soc*., **1958**, 1382)

In an extension of earlier work, the same group documented the intramolecular dialdehyde coupling with phenylhydrazine for the synthesis of 9-arylazophenanthrene **S3.8B** (Scheme S3.8). Mechanistically, the reaction involves the formation of a hydrazone intermediate **S3.8C**, which upon umpolong addition to the other carbonyl group *via* the delocalization by the secondary nitrogen atom of hydrazine, and subsequent hydrolysis of **S3.8D** produced the azo-substituted olefin compound. The reactions are compatible with different substituted aryl hydrazines. However, with methyl hydrazine, the *trans*-9,l0-dihydro-10-methylazophenanthren-9-ol was obtained in 60.0% yield after 2h.

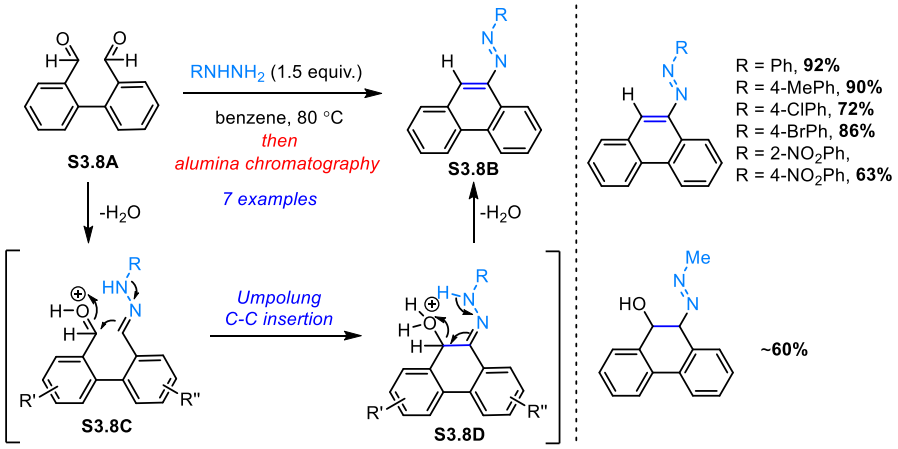

Scheme S3.8: *Bacon's Dicarbonyl Coupling with Phenyl Hydrazine*

(Auret, B.; Bacon, R. G. R.; Bankhead, R.; Bigg, D. C. H.; Ramsey, J. *J. Chem. Soc., Perkin Trans. 1* **1974**, 2153; Bacon, R. G. R.; Bigg, D. C. H. *J. Chem. Soc., Perkin Trans. 1* **1974**, 2156)

The reaction between diazo compounds **S3.9B** and thiocarbonyl compounds **S3.9D** (generated from the corresponding carbonyl compounds) for the synthesis of olefins **S3.9F** was reported in 1970, and is known as the Barton-Kellogg olefination reaction.[9] Mechanistically, the reaction procced through an episulphide intermediate **S3.9E** *via* 1,3-dipolar cycloaddition and dinitrogen elimination, which on desulphuration by PPh_3 afforded an alkene product in good yield (Scheme S.3.9).

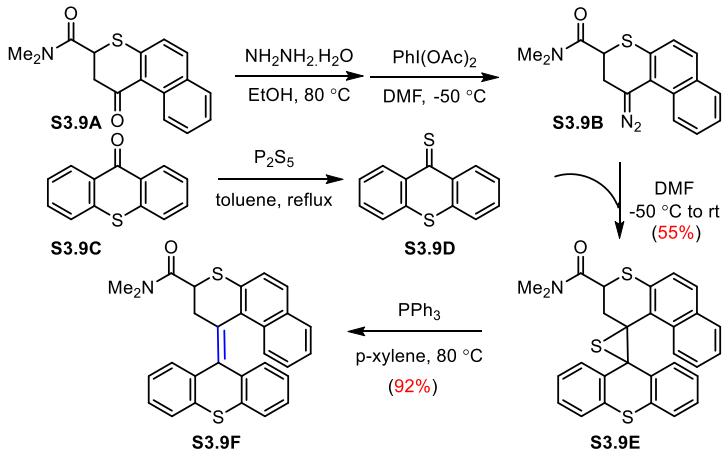

Scheme S3.9: *The Barton-Kellogg Olefination Reaction*

(Barton, D. H. R.; Willis, B. J. *J. Chem. Soc. D* **1970**, 1225.; Kellogg, R. M.; Wassenaar, S. *Tetrahedron Lett.* **1970**, *11*, 1987)

As depicted in Scheme S3.10, Jung and Hagiwara developed an improved method for the synthesis of more sterically encumbered phenanthrene derivatives **S3.10B** that comprise of heating the bis-tosylhydrazones in the presence of base (*Method A*) or heating the dianions of the corresponding bis-tosylhydrazones in the presence of CuI.P(OEt)$_3$ (*Method B*).

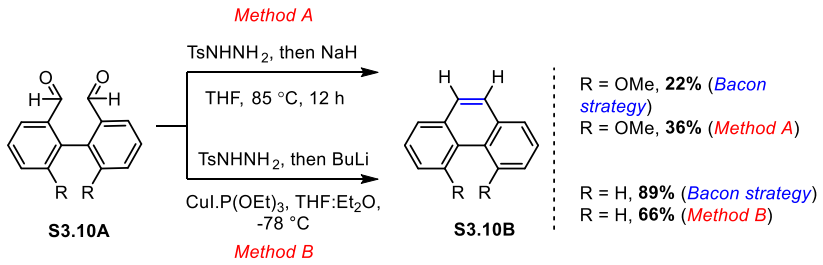

Scheme S3.10: *Jung's and Hagiwara's Dialdehyde Coupling via Tosylhydrazone Intermediate*

(Jung, M.; Hagiwara, A. *Tetrahedron Lett.* **1991**, *32*, 3025–3028)

Recently, Wang and co-workers documented a Rhodium(II)-catalyzed intramolecular cyclization of bis(*N*-tosylhydrazone)s **S3.11B** for converting the dicarbonyl functionality into C=C bonds through carbene transfer. This strategy was employed for the synthesis of the polycyclic aromatic hydrocarbon **S3.11C** (Scheme S3.11) with good substrates scope and functional group compatibility and in excellent yields. Similar, the carbene transfer protocol

were employed by the Sun group for the synthesis of polyaromatic compounds by employing a gold catalyst.[10]

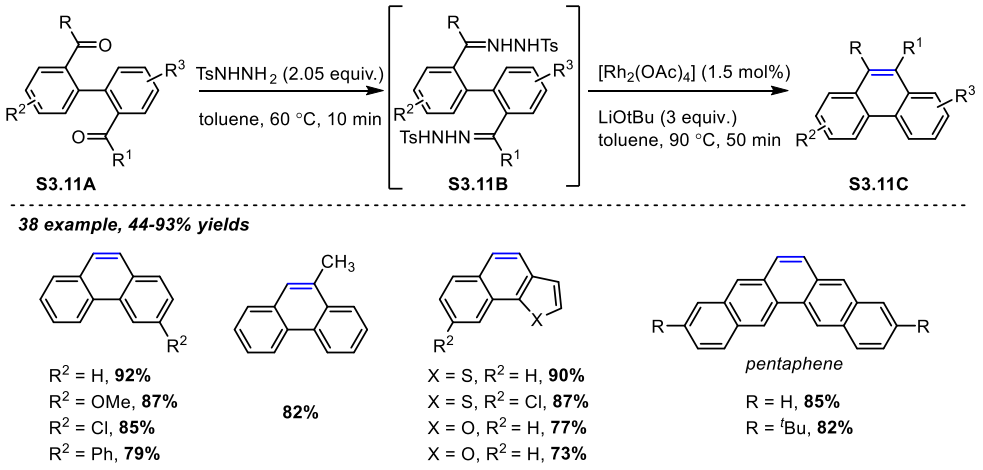

Scheme S3.11: *Wang's Intramolecular Carbene Transfer Using Rhodium Complex*

(Xia, Y.; Liu, Z.; Xiao, Q.; Qu, P.; Ge, R.; Zhang, Y.; Wang J. *Angew. Chem. Int. Ed.* **2012**, *51*, 1–5)

Next year, the same group reported the base mediated intramolecular formal diazo carbon insertion of N-tosylhydrazones (compounds **S3.12B**) into keto C-C bonds for the synthesis of phenanthrols, and the naphthols analogue **S3.12C** (Scheme S3.12). Mechanistically, the reaction proceeds through the resonance structure of N-tosylhydrazone **S3.12D,** followed by base catalysed nucleophilic attack on the keto carbonyl group to form **S3.12E**. This intermediate undergoes N_2 elimination *via* 1,2-alkyl/aryl shift, affording the carbonyl intermediate **S3.12F**, which upon keto-enol tautomerization, leads to the product **S3.12C**. Both electron donating, as well as withdrawing substituents on the aryl unit are well tolerated, affording the products in good to excellent yields.

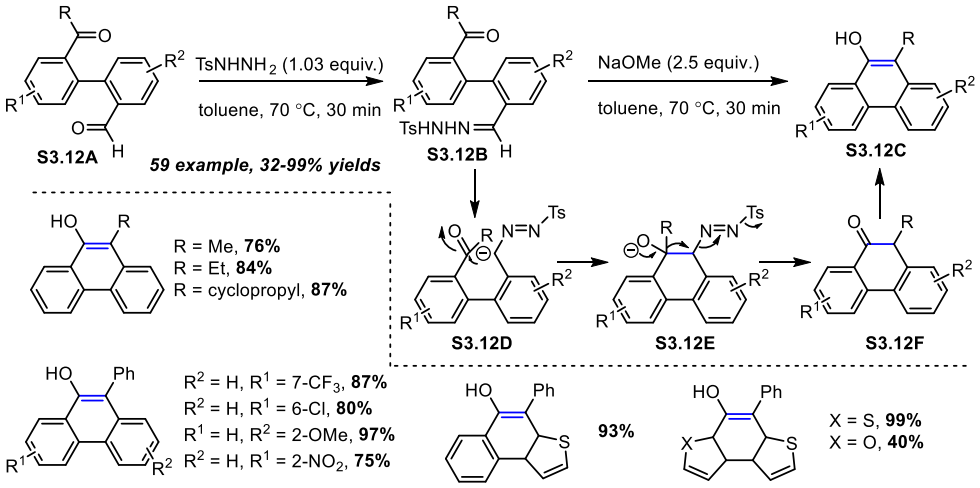

Scheme S3.12: *Wang's Intramolecular Diazo Carbon Insertion Using NaOMe.*

(Xia, Y.; Qu, P.; Liu, Z.; Ge, R.; Xiao, Q.; Zhang, Y.; Jianbo W. *Angew. Chem. Int. Ed.* **2013**, *52*, 2543 –2546)

1.2.2. Reaction with Thio-Intermediate

In 1992, Steliou and co-workers reported the intramolecular reaction of 2,2'-dibenzoylbiphenyl compounds **S3.13A**, producing the dithiocarbonyl intermediate first (**S3.13B)**, which on heating afforded the phenanthrene scaffold **S3.13C** with releasing of S_2 (Scheme S3.13). The scope of the reaction has been studied by placing different substituents on the carbonyl group, affording the corresponding products in moderate to good yields.

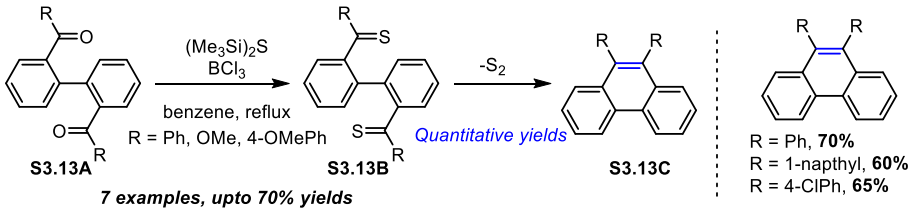

Scheme S3.13: *Steliou's Deoxygenative Intramolecular Dicarbonyl Coupling.*

(Steliou, K. Salama, P. Brodeur, D. Gareau, Y. *J. Am.Chem. Soc.* **1987**, *109*, 926; Steliou, K. Salama, P. Yu, X. *J. Am. Chem. Soc.* **1992**, *114*, 1456)

Mlostoń and coworkers described the intermolecular reductive homo-dimerization of the thiocarbonyl compound **S3.14B** in a transition-metal-free protocol by the consecutive treatment of carbonyl-derived thiocarbonyls with trimethylsilyldiazomethane and desulphurisation by tetrabutylammonium fluoride, affording the alkene scaffold **S3.14D** (Scheme S3.14).

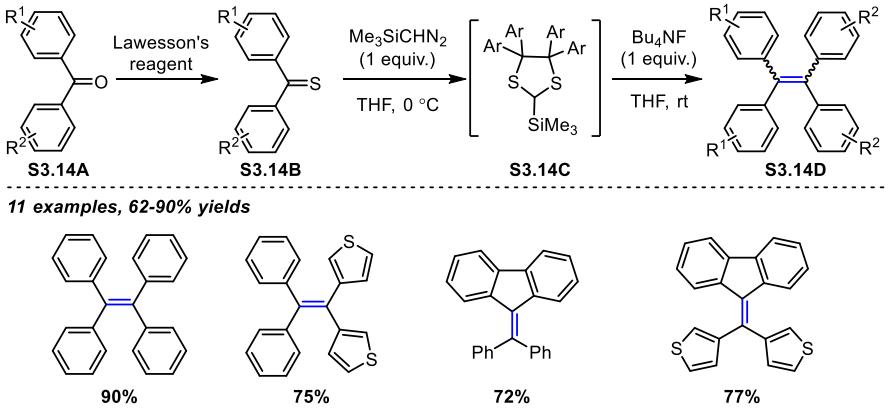

Scheme S3.14: *Mlostoń's Deoxygenative Intermolecular Dicarbonyl Coupling.*

(Mlostoń, G.; Pipiak, P.; Hamera-Fałdyga, R.; Heimgartner, H. *Beilstein J. Org. Chem.* **2017**, *13*, 1900)

1.2.3. Reaction with Phosphite or Silane

In 2000, Fourmigue and group reported $P(OMe)_3$ facilitated reductive homo-dimerization of the 1,3-dithiol-2-one scaffold **S3.15A** to the tetrathiafulvalene scaffold **S3.15B** with a new C=C bond formation (Scheme S3.15, eq. 1). A similar strategy was employed by Nielsen's group, where a dialkynylterephthalaldehyde compound **S3.13C** underwent the reductive carbonyl coupling in the presence of $P(OEt)_3$, which acted as a reductant (Scheme S3.15, eq. 2). The mechanism proceeds *via* the formation of a dioxaphospholane intermediate **S3.13D** from the two starting aldehydes and $P(OEt)_3$, which, on further heating along with the 1,3-dithiol-2-thione **S3.15E** and in the presence of $P(OEt)_3$, altered the terminal formyl groups into dithiafulvene groups, whereas the deoxygenative decomposition of the dioxaphospholane group afforded the stilbene product **S3.15F**.

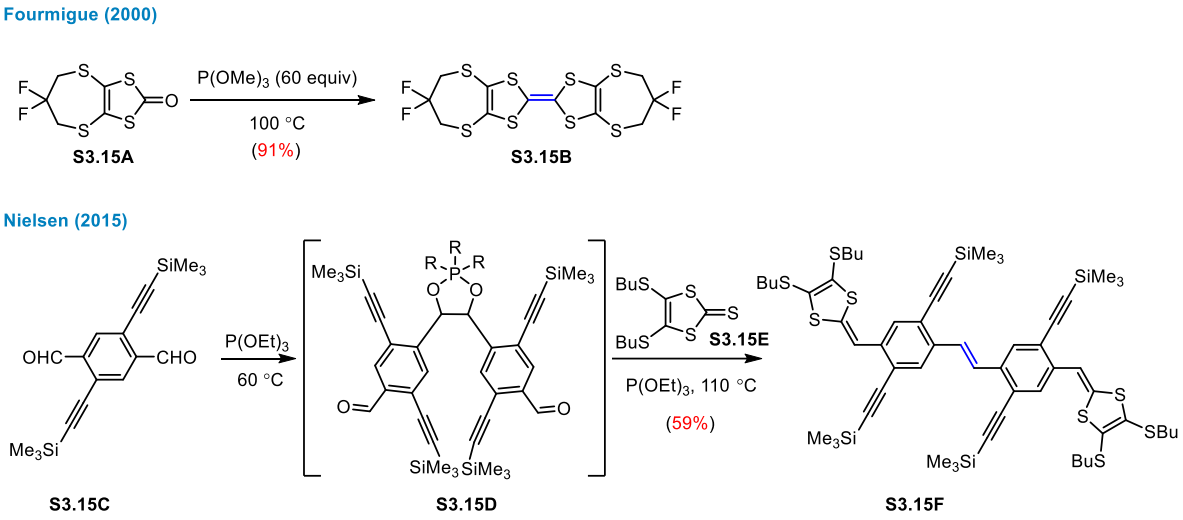

Scheme S3.15: *Deoxygenative Reductive Homocoupling using P(OR)$_3$*

(Dautel, O. J.; Fourmigué, M. *J. Org. Chem.* **2000**, *65*, 6479; Schou, S. S.; Parker, C. R.; Lincke, K.; Jennum, K.; Vibenholt, J.; Kadziola, A.; Nielsen, M. B. *Synlett* **2013**, *24*, 231; Petersen, J. F.; Tortzen, C. G.; Jørgensen, F. P.; Parker, C. R.; Nielsen, M. B. *Tetrahedron Lett.* **2015**, *56*, 1894)

In 2016, Wagner and coworkers reported the deoxygenative dimerization of benzophenone derivatives **S3.16A** in the presence of Si_2Cl_6 as a reductant. The reaction proceeds *via* the formation of the Cl_2Si–benzophenone adduct **S3.16D** as a key intermediate. The coordination of a second benzophenone substrate formed a five membered dioxasilolane intermediate that further underwent deoxygenation affording the benzopinacolone derivative **S3.16E**. Next, the tetraaryl-olefin product **S3.16B** was formed by the second deoxygenation/1,2-aryl migration sequence initiated by another molecule of Si_2Cl_6 (Scheme S3.16).

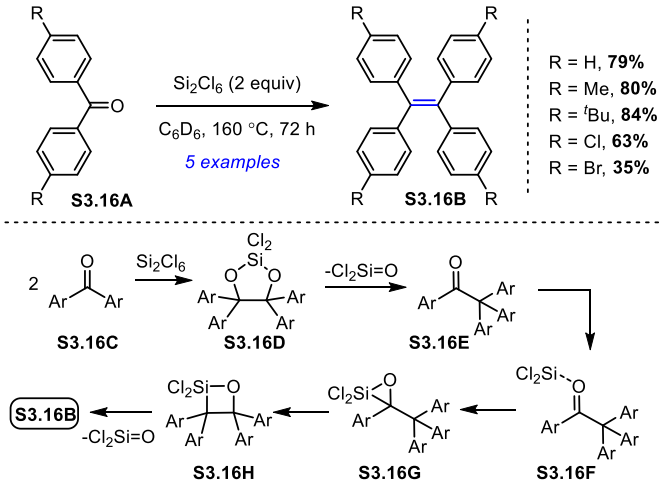

Scheme S3.16: *Deoxygenative Homocoupling by using Si_2Cl_6.*

(Moxter, M.; Tillmann, J.; Füser, M.; Bolte, M.; Lerner, H.-W.; Wagner, M. *Chem. Eur. J.* **2016**, *22*, 16028)

2.0. Conclusion

We have compiled all the documented reports on the reductive coupling of biaryl-2,2'-dicarbonyl compounds, mainly to show that the original reports are primarily restricted to the anomalous formation of olefins during the Wolf-Kishner and Clemmensen reductions. However, in the majority of the cases, the employed conditions are harsh – requiring strong acids/bases and heating at elevated temperatures. In order to address this, the corresponding N-tosyl hydrazones have been employed as substrates to conduct these couplings under milder conditions and with more functional group tolerance. In addition, some sulfur and phophite based methods have been also documented. However, as one can observe, there are not many applications for most of these methods, except the Bacon Reaction that had been employed in the synthesis of polyaromatic hydrocarbons in a couple of cases. In the next part, we will deal with how endeavours in this domain have started with reinventing the Bacon's reaction in the guise of synthesizing some cyclic azepines, and identifying much milder conditions in order to bring about this transformation.

3.0. Initial Hypothesis and Present Work

As described in the first section of Chapter 1, simple method has been developed for the synthesis of diversely substituted 2-(3-alkanoyl-2*H*-indazol-2-yl)benzaldehydes and the corresponding acetophenones. These compounds possess suitably positioned pendant carbonyl groups on the adjacent rings for further ring annulation. Aiming at constructing the azepine or diazocine rings, the reaction of the dicarbonyl derivative **1a** with ammonia and hydrazine was examined in refluxing methanol in the presence of 10 mol% of acetic acid. As expected, with ammonia, the azepine cyclic aminal compound **2a** (5-methoxy-7-propyl-5H-benzo[6,7][1,4]diazepino[1,2-b]indazole) was obtained in excellent yields (Scheme S3.17, eq. 1). The compound was characterized with the help of spectral and analytical data. For example, in the ^{1}H NMR of product **2a**, the loss of the aldehyde proton, as well as the presence of methoxy and benzylic protons (singlet) at 3.61 ppm and 5.02 ppm respectively indicated the aminal formation. The ^{13}C NMR clearly shows the disappearance of two carbonyl peaks and the presence of imine carbon at 159.1 ppm, as well as a benzylic carbon that appeared as doublet at 89.5 ppm, confirming the structure of the cyclic product. Then, the constitution of **2a** has been established as $C_{19}H_{20}N_3O$ by the presence of a peak corresponding to $[M+H]^+$ at 306.1609 in the HRMS.

Next, under similar conditions, we conducted the reaction of the dicarbonyl derivative **1a** with hydrazine monohydrate. The reaction was facile and provided exclusively a non-polar fluorescent compound **3a** in 90.0% yield (Scheme S3.17, eq. 2). The structure of this compound as 6-propylindazolo[2,3-a]quinoline has been established with the help of spectral and analytical data. In the ^{1}H NMR of product **3a**, the loss of the aldehydic proton and the presence of olefinic proton at 7.43 ppm appearing as a singlet indicated the deoxygenative coupling. In the ^{13}C NMR spectrum of product **3a**, there are no carbonyl peaks present and the presence of two new aromatic carbons, one as a doublet and the other as a singlet (multiplicity confirmed from DEPT-135 spectra) has been noticed. Moreover, the upfield shift of the methylene group (adjacent to keto) from 44.2 to 35.1 ppm indicated that it was positioned on an aromatic ring. Next, the observed peak 261.1402 in HRMS corresponding to the $[M+H]^+$ indicated the constitution of **3a** as $C_{18}H_{17}N_2$. This was initially a surprise for us, as examination of the recent reports revealed that such a ring closure has been executed employing the corresponding bis-tosylhydrazones in

the presence of [Rh]- or [Au]-catalyst and/or a base (as shown in the Introduction section). However, further search in the literature revealed even more interesting reports of Bacon and co-workers, which have not been highlighted in recent works. Though the employed conditions in our case are more convenient and with good yields, considering the fact that the same reaction has also been explored for the synthesis of even higher polycyclic scaffolds, we have restricted the scope of the reaction by employing a couple of indazole substrates and also examined the compatibility of simple 2,2'biaryldicarbonyl compounds.

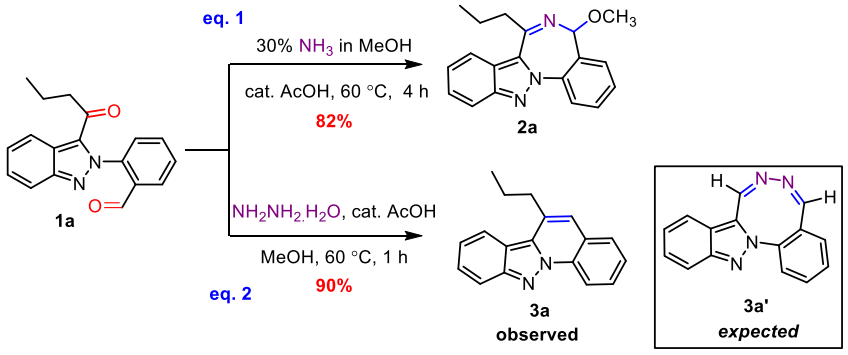

Scheme S3.17: *Reaction with Ammonia and Hydrazine Monohydrate.*

As shown in Scheme S3.18, indazole substrates having electron withdrawing/donating groups such as –CN, –F, –Me on the aryl unit of the indazole moiety have been employed. Interestingly, with the substrate having –CN, the best reaction outcome was observed. Similarly, the reaction with different alkyl substituents/units at the ketone moiety of diaryl compounds showed minimal influence on the reaction outcome and provided the corresponding phenanthrene scaffolds in good to excellent yields. Then, the substituents on the aryl unit of the aldehyde moiety or the thiophene ring (**1l**) were explored and it was found that the substrate having either halogen –F (**1j**) or electron rich –OMe (**1i**) substituents afforded the products in decent yield. However, diacetyl substrates such as (**1m**) and (**1n**) and diphenyl ether (**1o**) failed to provide the cyclised products.

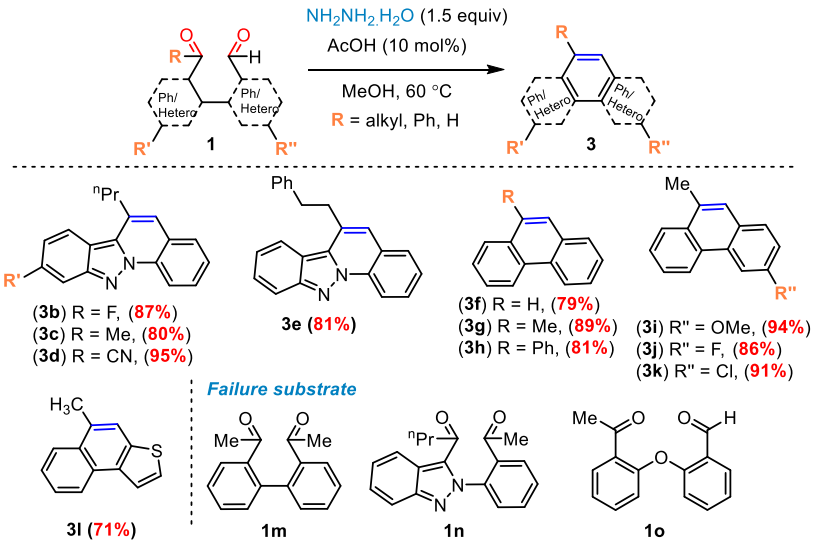

***Scheme S3.18**: Substrate Scope with Hydrazine Monohydrate.*

Given the significance of azo compounds as dyes and in medicinal chemistry with broad-spectrum applications,[11] we were further interested to examine the reaction with phenyl hydrazine, which was expected to provide the cyclized products having the phenylazo group placed at the aldehyde carbon. Initially, the reaction of 2-(3-butyryl-2H-indazol-2-yl)benzaldehyde (**1a**) and phenyl hydrazine was carried out using Bacon's two step protocol. The product (E)-5-(phenyldiazenyl)-6-propylindazolo[2,3-a]quinoline (**4aa**) was obtained in 73.0% yield as a red coloured dye. On the other hand, under the present reaction conditions, the azo product **4aa** was obtained in 86.0% yield. Coming to the ^{1}H NMR of product **4aa**, the loss of the aldehyde proton and the presence of 5 extra aromatic protons indicated the addition of the phenyl hydrazine moiety. In ^{13}C NMR, the disappearance of two carbonyl peaks indicated the intramolecular dicarbonyl coupling. Next, the constitution of product **4aa** was confirmed as $C_{24}H_{21}N_4$ by $[M+H]^+$, found as 365.1763 in the HRMS. The assigned structure of compound **4aa** was further established with the help of single crystal X-ray diffraction analysis.

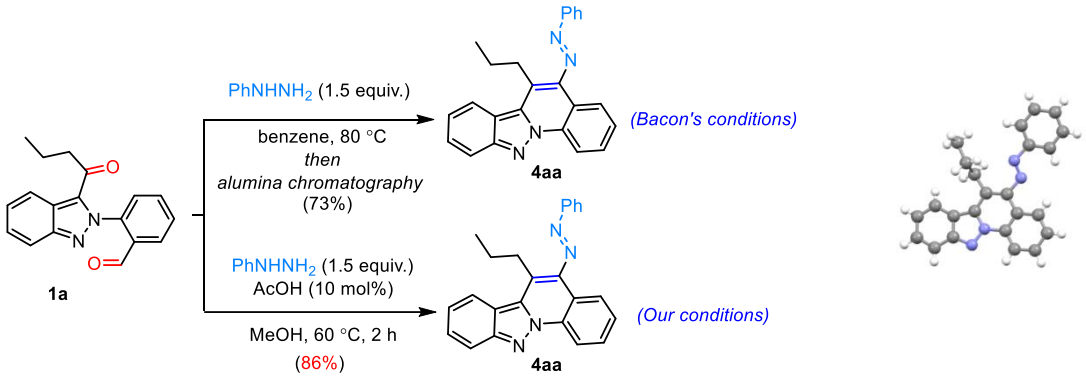

Scheme S3.19: *Phenyl Hydrazine Mediated Dicarbonyl Coupling and Single Crystal XRD.*

Next, we examined the reaction scope by varying the substituents on both indazole and phenyl hydrazine units (Scheme S3.20). Initially, the scope of the reaction was explored by varying the length and the nature of the pendant group of the ketone moiety. The reactions proceeded well and the corresponding azo-compounds were obtained in good yields. Interestingly, the –OAc, and –OTBS groups on the alkyl unit of the ketone moiety were well tolerated and provided the corresponding products **7da** and **7ea** in good yields.

Next, the substituents on the aryl unit of the indazole moiety were examined. Substrates having either halogen –F (**5f**), electron rich –Me (**5g**) or electron withdrawing groups such as –CO_2Me (**5h**) and –CN (**5i**), all afforded the corresponding cyclized products in decent yields. However, the substrates having electron rich substituents provided the azo product (**7ga**) in relatively high yields.

Next, the substrate scope was examined by varying the substituents on the pendant aryl ring bearing the aldehyde moiety. As shown in Scheme S3.20, in all cases, the corresponding products were obtained in good to excellent yields (**7ja-7na**). Finally, the scope of the different phenyl hydrazine substrates has been examined under the current reaction conditions. The phenyl groups bearing electron rich substituents or halogen at the position *para* to hydrazine, provided the corresponding azo-products (**7ab-7ac**), albeit in slightly lower yields, along with the corresponding cyclized product **3a** in minor quantity. On the other hand, the substrates having electron donating groups, like –ethyl at the *ortho* position, afforded the product **7ae** in good yield, with trace amount of the cyclized side product. The dichloro- substituents at *ortho* and/or *meta* were found to be well tolerated and the corresponding cyclized azo-products were obtained

in relatively low yields (**7af-7ag**), along with the simple dicarbonyl coupling compound **3a** as minor products. In the majority of the cases, there was no requirement of column chromatography and a simple recrystallization was sufficient to get analytically pure compounds.

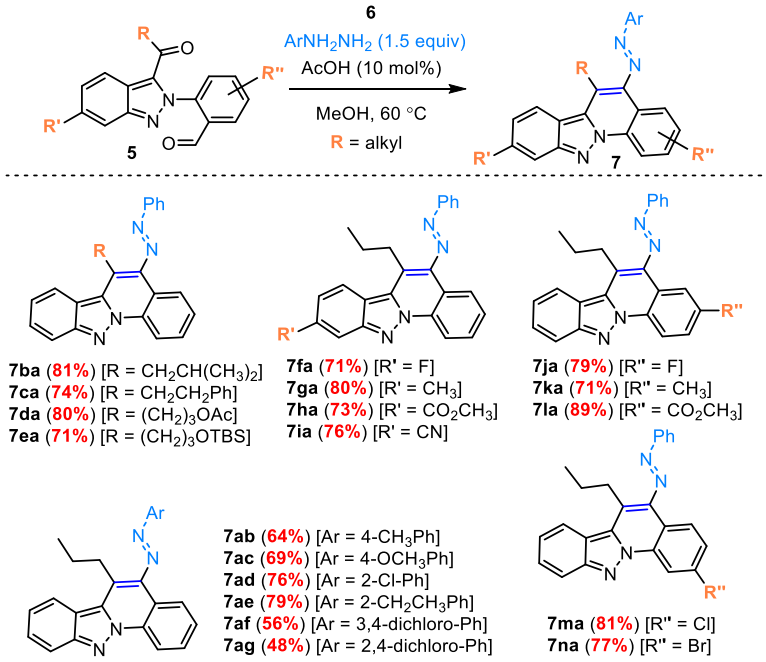

***Scheme S3.20**: Substrate Scope with Indazoles Dicarbonyl Substrates.*

Next, considering the fact that the even with diaryl 2,2'-dicarbonyl, the scope of the phyenylhydrazine reaction is limited mainly to a couple of substrates, and given the one-step synthesis/simplicity of our conditions, we explored the substrate scope by employing a broad-set of diaryl 2,2'-dicarbonyl compounds. As shown in Scheme S3.21, initially, the substrate scope was examined by employing the dialdehyde **8a** and the ketones **8b** and **8c**, where one of the aldehyde units was replaced with acetyl or benzoyl groups respectively. In all the cases, the reactions proceeded smoothly and provided the corresponding azo-compounds in excellent yields. Then, the substituents on the aryl unit of the aldehyde moiety were explored and it was found that substrates having either halogen –F (**8d**) or electron rich –OMe (**8e**) substituents, all afforded the corresponding azo products in decent yields.

Next, the different scope of the various arylhydrazines **9b-9h** was examined. Despite the nature of the substitute present on the phenyl ring of the arylhydrazine, the reactions proceeded smoothly and provided the corresponding azo-products. Next, the reaction with dialdehyde

substrates (**8a**) was examined with different phenyl hydrazine derivatives and to our delight, these substrates were also well tolerated, furnishing the desired products (**10ab**, **10ac**, **10af**, **10ai**) in good to excellent yields. However, the corresponding simple condensation product **3g** (resulting in the reaction of **1g** with hydrazine. monohydrate) was also obtained in small amounts (~5 – 9%). Even in case of the arylhydrazine **8f-8h** having the substituents at the *ortho* or *meta* position to hydrazine as well, the reactions proceeded smoothly and the corresponding products **10bf-10bh** were secured in good yields.

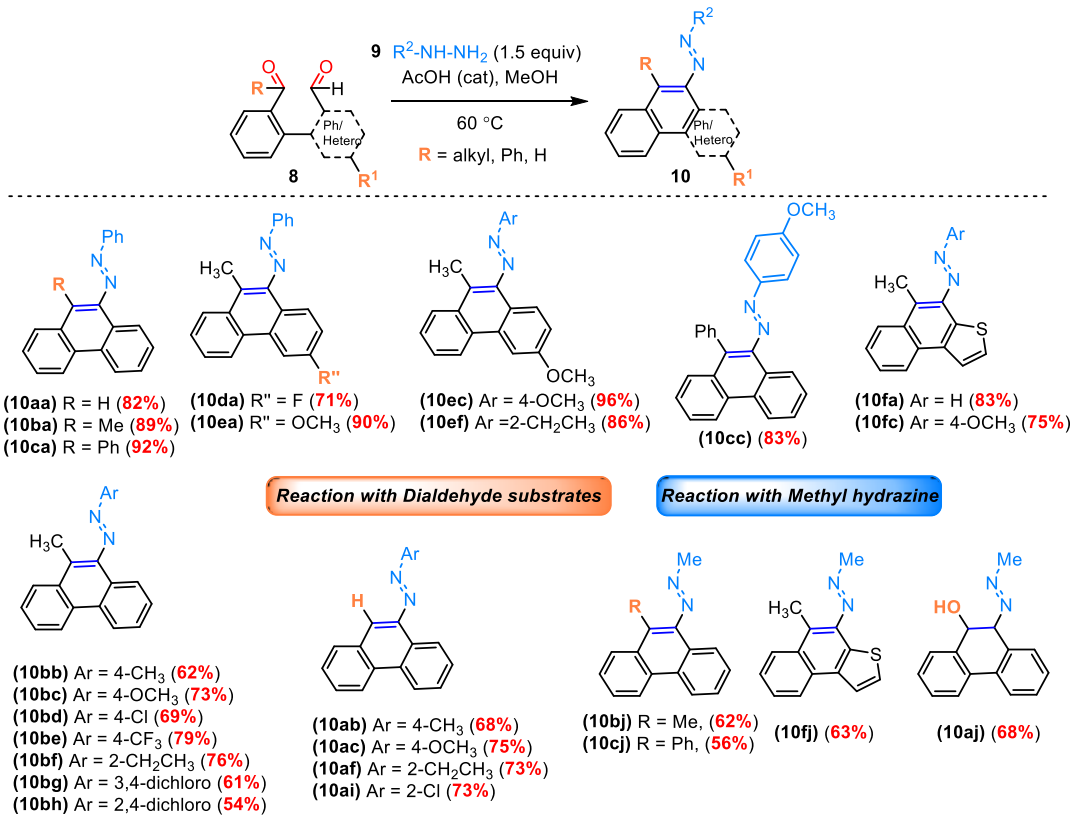

Scheme S3.21: *Substrate Scope with Diaryl 2,2'-Dicarbonyl Substrates.*

Next, the scope of this reaction has been further expanded by examining the compatibility of both arylhydrazines and dicarbonyl compounds. Furthermore, the reactions with the substrate **1f** having a benzothiophene unit with aryl hydrazines **9a** and **9c** proceeded smoothly and afforded the corresponding azo products **10fa** and **10fc** respectively in good yields. In addition, this methodology was further explored by using methyl hydrazine (**9j**) as substrate. The reaction proceeded well with phenyl as well as heteroaryl -dicarbonyl compounds, giving the azo cyclized

product in 56-63% yield (**10bj, 10cj, 10fj**). In case of the dialdehyde substrate (**8a**), the anticipated C-C bond insertion *via* Umpolung fashion occurs smoothly, while the subsequent dehydration does not occur (**10aj**).

To further demonstrate the practicability of this protocol, a 500 mg scale reaction was carried out. Interestingly, for the reaction of **1a** with phenyl hydrazine, two spots were seen in the TLC after heating for 2 h. Even after heating for a longer time, the conversion was not complete. Initially, we separated both the spots through column chromatography. However, it was noticed that in $CDCl_3$, the compound corresponding to the 2nd spot converted completely to the azo product **4a**. This was an interesting result, which encouraged us to examine the structure of this intermediate. The initial crystallization of the crude reaction mixture provided exclusively the azo compound. Next, when the mother liquor was further allowed to slowly evaporate, crystals of the intermediate corresponding to the 2nd spot were obtained. The X-ray analysis of this compound showed that it was the intermediate azo-alcohol, the dehydration of which provided the final azo compound. For full conversion, when the reaction was carried out on large scales, the reaction mixture was subjected to heat for 2 h, then usual workup and concentrated and finally one mL $CDCl_3$ was added and the stirring was continued at room temperature for an additional 2 h.

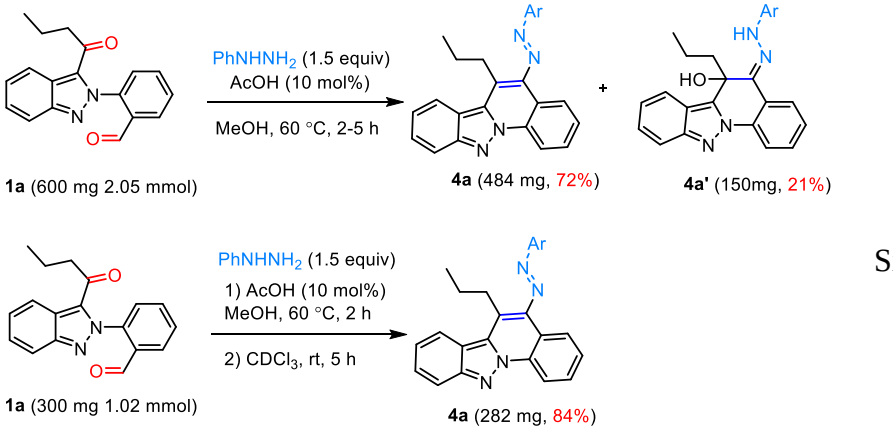

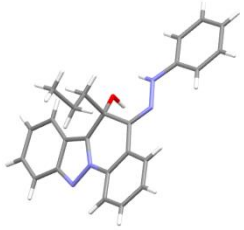

Single Crystal XRD of **4a'**

Scheme S3.22: *Gram scale Reactions and Intermediate Isolation.*

4.0. Mechanical properties of the Compound 4a Crystal

During purification of compounds, compound **4a** was recrystallized in acetonitrile solvent, which resulted in the formation of a red needle crystal that could be observed by the naked eye. Afterwards, these crystals were analyzed under a polarizing microscope, which showed a long needle like morphology. In literature, it has been documented that crystals of some organic compounds show elasticity.[12] Just to check this hypothesis; we have employed forceps and needles to see the mechanical behavior of these long needle types of crystals. Interestingly, these crystals showed elastic bending. Next, single crystal data was collected and interactions between molecules were analyzed, which showed that the molecules are crystallized in the $P2_1/n$ space group of the monoclinic crystal system. As seen in the single crystal unit cell, there is only one molecule in the asymmetric unit and molecules are connected *via* C-H…N dimers (D =3.541 Å, d=2.647 Å and θ=157°) and C-H…π (D = 3.637 Å, d=2.855 Å and θ=140°) and C-H…N D =3.554 Å, d=2.619Å and θ=168°, interactions. The crystal packing arrangement of molecules along a-axis can be seen in Figure F3.1. Currently, investigation of the mechanical behavior of crystals obtained from the other compounds as well as their single crystal diffraction studies are currently under progress in our lab.

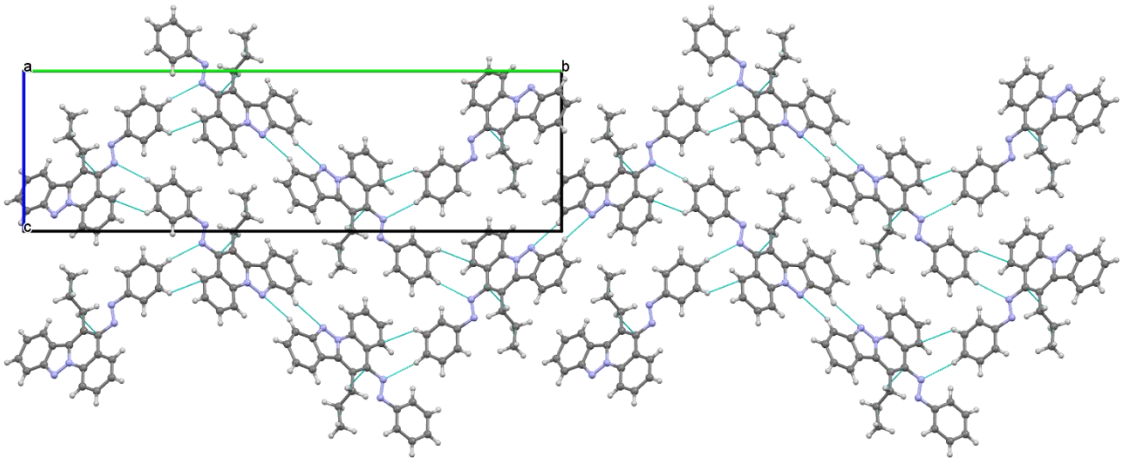

Figure F3.1*: Crystal Packing Diagram, which shows C–H···N and C–H···π Interactions.*

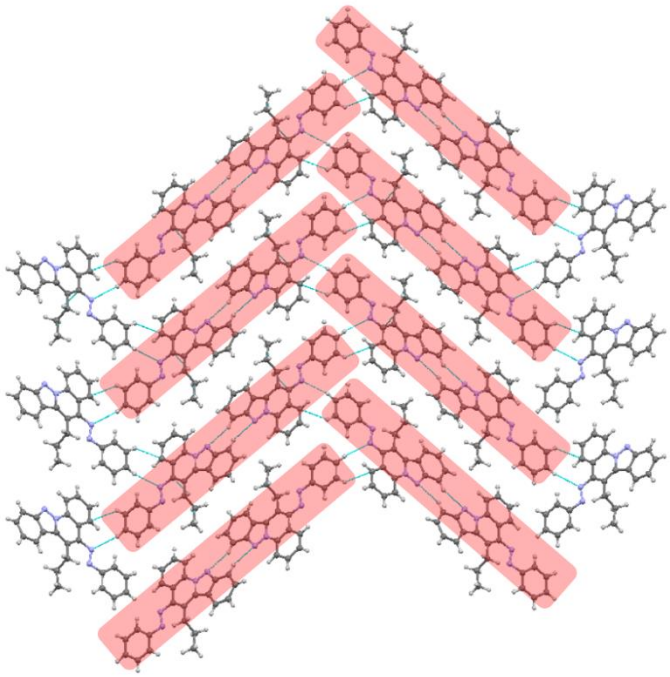

***Figure F3.2**: Two consecutive molecules are connected via C–H···N dimers (highlighted in faded red color), C–H···π and C–H···N. C–H···N dimers are arranged in zig-zag manner in crystal packing. Arrangement of strong and weak intermolecular interactions around 90° orientation is responsible for elastic bending*

5.0. Conclusion

To conclude, in the guise of synthesizing the diazocene compounds, we have come across the hydrazine mediated apparent McMurray like dicarbonyl coupling reaction and a similar dicarbonyl coupling, along with the installation of a phenyazo group when hydrazine was replaced with either aryl-/alkylhydrazine. These two interesting methods have been suitably applied for extending the synthetic utility of the dicarbonyl indazoles prepared as a part our initial experiments on the gold-oxo carbenes. Considering the fact that the current conditions are mild and/or step-economic, we have also expanded the scope of these reactions with the simple diaryl-2,2'-dicarbonyl compounds. In addition, the crystals of the parent phenyazo-compound **4a** were seen to have interesting mechanical properties, which were established with the help of physical-/X-ray diffraction studies. How these mechanical properties *inter alia* the crystal packing will be influenced by the substituents present on either of the three aryl rings is an interesting question and work in this direction is currently in progress.

Experimental Section

General Procedure for the Azepine Compound 2a

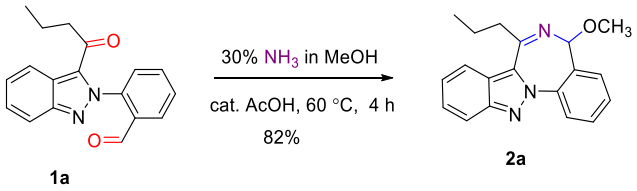

To a flame-dried 5 ml vial equipped with a magnetic stirrer were added a dicarbonyl compound **1a** (1 equiv), 30% NH_3 solution (5 equiv), MeOH (1 ml) and lastly AcOH (10 mol%). After stirring at 60 °C for 4 h, the mixture was transferred to 25 ml round bottom flask and DCM (10 ml) and H_2O (10 ml) were added. The mixture was separated and organic layer was washed with H_2O (three times), dried over Na_2SO_4, filtered, concentrated and purified by column chromatography on silica gel to afford the azepine cyclic aminal compound **2a**.

5-Methoxy-7-propyl-5H-benzo[6,7][1,4]diazepino[1,2-b]indazole (2a)

R_f = 0.4 (10% EtOAc in petroleum ether); yield: 26 mg (82%); colorless gum; ^{1}H NMR (400 MHz, $CDCl_3$): δ 0.81 (t, J = 7.4 Hz, 3H), 1.59–1.65 (m, 2H), 2.87–3.05 (m, 2H), 3.61 (s, 3H), 5.02 (s, 1H), 7.29–7.35 (m, 1H), 7.43–7.48 (m, 1H), 7.51–7.56 (m, 2H), 7.87–7.93 (m, 3H), 7.99– 8.04 (m, 1H) ppm; ^{13}C NMR (100 MHz, $CDCl_3$): δ 13.5 (q), 20.3 (t), 40.5 (t), 55.9 (q), 89.5 (d), 118.4 (d), 120.4 (d), 120.6 (s), 123.8 (d), 124.2 (d), 124.2 (d), 127.4 (d), 128.9 (d), 129.0 (d), 131.9 (s), 134.4 (s), 136.2 (s), 148.0 (s), 159.1 (s) ppm; HRMS (ESI) calcd. for $C_{19}H_{20}N_3O$: 306.1606 $[M + H]^+$; found: 306.1609.

General Procedure for Dicarbonyl Coupling

In general, all reactions were carried out employing 30 mg of dicarbonyl compound **1/5/8**.

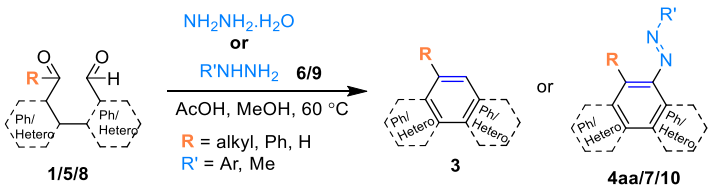

To a flame-dried 5 ml vial equipped with a magnetic stirrer were added a dicarbonyl compound **1/5/8** (1 equiv), hydrazine hydrate/phenyl/methyl hydrazine/hydrazine hydrochloride **6/9** (1.2

equiv), MeOH (1 ml) and AcOH (10 mol%). After stirring at 60 °C for 2-3 h, the mixture was transferred to 25 ml round bottom flask and DCM (10 ml) and H_2O (10 ml) were added. The mixture was separated and organic layer was washed with H_2O (three times), dried over Na_2SO_4, filtered, concentrated and purified by column chromatography on silica gel to afford the products **3/4aa/7/10**.

6-Propylindazolo[2,3-a]quinoline (3a)

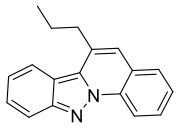

R_f = 0.4 (5% EtOAc in petroleum ether); yield: 24 mg (90%); cream white solid; IR (neat)ν_{max} 2920, 2860, 1617, 1347, 737 cm^{-1}; ^1H NMR (400 MHz, $CDCl_3$): δ 1.16 (t, J = 7.4 Hz, 3H), 1.91–2.05 (m, 2H), 3.21–3.31 (m, 2H), 7.24–7.35 (m, 1H), 7.43 (s, 1H), 7.53–7.63 (m, 2H), 7.75 (ddd, J = 8.4, 7.1, 1.3 Hz, 1H), 7.84–7.92 (m, 1H), 8.00 (d, J = 8.6 Hz, 1H), 8.13 (d, J = 8.5 Hz, 1H), 8.94 (d, J = 8.5 Hz, 1H) ppm; ^{13}C NMR (100 MHz, $CDCl_3$): δ 14.0 (q), 22.0 (t), 35.1 (t), 116.5 (s), 116.8 (d), 117.2 (d), 120.9 (d), 121.6 (d), 121.6 (d), 125.1 (s), 126.1 (d), 127.4 (d), 127.7 (d), 128.5 (d), 132.2 (s), 132.4 (s), 133.0 (s), 149.3 (s) ppm; HRMS (ESI) calcd. for $C_{18}H_{17}N_2$: 261.1401 $[M + H]^+$; found: 261.1402.

9-Fluoro-6-propylindazolo[2,3-a]quinoline (3b)

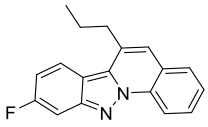

R_f = 0.4 (5% EtOAc in petroleum ether); yield: 23.5 mg (87%); white solid; IR (neat)ν_{max} 2921, 2363, 1722, 1617, 1540, 1455, 1082, 740 cm^{-1}; ^1H NMR (400 MHz, $CDCl_3$): δ 1.16 (t, J = 7.3 Hz, 3H), 1.88–1.98 (m, 2H), 3.22 (t, J = 7.6 Hz, 2H), 7.06 (td, J = 9.1, 1.9 Hz, 1H), 7.46 (s, 1H), 7.51–7.65 (m, 2H), 7.76 (t, J = 7.6 Hz, 1H), 7.87 (d, J = 7.9 Hz, 1H), 8.07 (dd, J = 9.1, 5.3 Hz, 1H), 8.89 (d, J = 8.5 Hz, 1H) ppm; ^{13}C NMR (100 MHz, $CDCl_3$): δ 14.0 (q), 21.8 (t), 35.0 (t), 100.2 (dd, $J_{C\text{-}F}$ = 23.65 Hz), 111.7 (dd, $J_{C\text{-}F}$ = 27.47 Hz), 113.6 (s), 117.1 (d), 122.4 (d), 123.2 (dd, $J_{C\text{-}F}$ = 11.44 Hz), 124.8 (s), 126.1 (d), 127.7 (d), 128.7 (d), 131.9 (s), 132.4 (s), 132.9 (s), 149.6 (ds, $J_{C\text{-}F}$ = 13.73 Hz), 161.3 (ds, $J_{C\text{-}F}$ = 244.90 Hz) ppm; HRMS (ESI) calcd. for $C_{18}H_{16}N_2F$: 279.1292 $[M + H]^+$; found: 279.1293.

9-Methyl-6-propylindazolo[2,3-a]quinoline (3c)

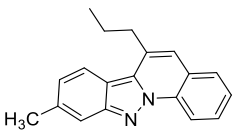

R_f = 0.4 (5% EtOAc in petroleum ether); yield: 21.5 mg (80%); white solid; IR (neat)ν_{max} 2925, 1718, 1633, 1454, 1086, 798, 751 cm^{-1}; ^1H NMR (400 MHz, $CDCl_3$): δ 1.16 (t, J = 7.4 Hz, 3H), 1.90–2.04 (m, 2H),

2.59 (s, 3H), 3.24 (t, *J* = 7.6 Hz, 2H), 7.12 (d, *J* = 8.1 Hz, 1H), 7.41 (s, 1H), 7.57 (t, *J* = 7.5 Hz, 1H), 7.70–7.79 (m, 2H), 7.86 (d, *J* = 7.6 Hz, 1H), 8.01 (d, *J* = 8.5 Hz, 1H), 8.91 (d, *J* = 8.4 Hz, 1H) ppm; ^{13}C NMR (100 MHz, $CDCl_3$): δ 14.0 (q), 22.0 (t), 22.3 (q), 35.1 (t), 114.7 (s), 115.5 (d), 117.1 (d), 121.0 (d), 121.5 (d), 123.6 (d), 125.0 (s), 125.8 (d), 127.6 (d), 128.4 (d), 132.1 (s), 132.3 (s), 133.1 (s), 137.5 (s), 150.0 (s) ppm; HRMS (ESI) calcd. for $C_{19}H_{19}N_3$: 275.1543 $[M + H]^+$; found: 275.1544.

6-Propylindazolo[2,3-a]quinoline-9-carbonitrile (3d)

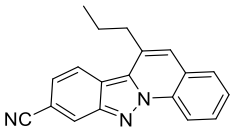

R_f = 0.4 (5% EtOAc in petroleum ether); yield: 24 mg (95%); white solid; IR (neat)ν_{max} 2922, 2212, 1446, 1350, 1090, 750 cm^{-1}; ^{1}H NMR (400 MHz, $CDCl_3$): δ 1.17 (t, *J* = 7.3 Hz, 3H), 1.88–2.01 (m, 2H), 3.24 (t, *J* = 7.6 Hz, 2H), 7.39 (dd, *J* = 8.6, 1.3 Hz, 1H), 7.53 (s, 1H), 7.62–7.71 (m, 1H), 7.76–7.85 (m, 1H), 7.91 (d, *J* = 7.9 Hz, 1H), 8.19 (d, *J* = 8.6 Hz, 1H), 8.36 (s, 1H), 8.93 (d, *J* = 8.5 Hz, 1H) ppm; ^{13}C NMR (100 MHz, $CDCl_3$): δ 13.9 (q), 21.8 (t), 34.9 (t), 110.5 (s), 117.4 (d), 118.1 (s), 119.7 (s), 121.4 (d), 122.9 (d), 123.1 (d), 123.4 (d), 125.4 (s), 127.1 (d), 127.9 (d), 129.1 (d), 132.3 (s), 132.4 (s), 132.8 (s), 147.5 (s) ppm; HRMS (ESI) calcd. for $C_{19}H_{16}N_3$: 286.1339 $[M + H]^+$; found: 286.1336.

6-Phenethylindazolo[2,3-a]quinoline (3e)

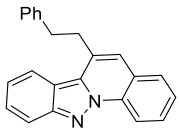

R_f = 0.4 (5% EtOAc in petroleum ether); yield: 22 mg (81%); white solid; IR (neat)ν_{max} 2922, 1715, 1619, 1451, 1359, 1023, 744 cm^{-1}; ^{1}H NMR (400 MHz, $CDCl_3$): δ 3.20–3.32 (m, 2H), 3.57–3.69 (m, 2H), 7.29–7.43 (m, 7H), 7.55–7.64 (m, 2H), 7.77 (t, *J* = 7.8 Hz, 1H), 7.85 (d, *J* = 7.9 Hz, 1H), 8.03 (d, *J* = 8.6 Hz, 1H), 8.22 (d, *J* = 8.4 Hz, 1H), 8.96 (d, *J* = 8.5 Hz, 1H) ppm; ^{13}C NMR (100 MHz, $CDCl_3$): δ 34.7 (t), 35.1 (t), 116.5 (s), 117.0 (d), 117.2 (d), 121.1 (d), 121.5 (d), 121.8 (d), 125.0 (s), 126.2 (d), 126.4 (d), 127.5 (d), 127.8 (d), 128.5 (d, 2C), 128.6 (d, 2C), 128.7 (d), 129.3 (s), 131.6 (s), 131.9 (s), 133.1 (s), 140.9 (s), 149.4 (s) ppm; HRMS (ESI) calcd. for $C_{23}H_{19}N_2$: 323.1543 $[M + H]^+$; found: 323.1543.

Phenanthrene (3f)

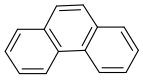

R_f = 0.4 (5% EtOAc in petroleum ether); yield: 21 mg (79%); white solid; ^{1}H NMR (400 MHz, $CDCl_3$): δ 7.58–7.65 (m, 2 H), 7.65–7.71 (m, 2 H), 7.76 (s, 2

H), 7.89–7.95 (m, 2 H), 8.71 (d, *J* = 7.9 Hz, 2 H) ppm; ^{13}C NMR (100 MHz, $CDCl_3$): δ 122.6 (d, 2C), 126.5 (d, 3C), 126.9 (d, 2C), 128.5 (d, 3C), 130.3 (s, 2C), 132.0 (s, 2C) ppm. The analytical data match those reported in the literature. (Y. Xia, Z. Liu, Q. Xiao, P. Qu, R. Ge, Y. Zhang, J. Wang, *Angew. Chem. Int. Ed.*, **2012**, *51*, 5714–5717)

9-Methylphenanthrene (3g)

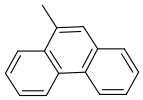

R_f = 0.4 (5% EtOAc in petroleum ether); yield: 23 mg (89%); white solid; ^{1}H NMR (400 MHz, $CDCl_3$): δ 2.74–2.81 (m, 3H), 7.55–7.65 (m, 3H), 7.65–7.71 (m, 2H), 7.79–7.85 (m, 1H), 8.05–8.12 (m, 1H), 8.67 (d, *J* = 7.6 Hz, 1H), 8.71–8.79 (m, 1H) ppm; ^{13}C NMR (100 MHz, $CDCl_3$): δ 20.0 (q), 122.4 (d), 123.0 (d), 124.7 (d), 125.8 (d), 126.2 (d), 126.5 (d), 126.6 (d), 126.7 (d), 127.8 (d), 129.7 (s), 130.4 (s), 132.0 (s), 132.1 (s), 132.5 (s) ppm. The analytical data match those reported in the literature. (Y. Xia, Z. Liu, Q. Xiao, P. Qu, R. Ge, Y. Zhang, J. Wang, *Angew. Chem. Int. Ed.*, **2012**, *51*, 5714–5717).

9-Phenylphenanthrene (3h)

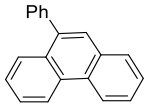

R_f = 0.4 (5% EtOAc in petroleum ether); yield: 22 mg (81%); white solid; ^{1}H NMR (400 MHz, $CDCl_3$): δ 7.46–7.59 (m, 6H), 7.59–7.64 (m, 1H), 7.64–7.68 (m, 1H), 7.68–7.73 (m, 2H), 7.87–7.97 (m, 2H), 8.69–8.84 (m, 2H) ppm; ^{13}C NMR (100 MHz, $CDCl_3$): δ 122.5 (d), 122.9 (d), 126.4 (d), 126.5 (d), 126.6 (d), 126.8 (d), 126.9 (d), 127.4 (d), 127.5 (d), 128.3 (d, 2C), 128.6 (d), 129.9 (s), 130.0 (d, 2C), 130.6 (s), 131.1 (s), 131.5 (s), 138.8 (s), 140.8 (s) ppm. The analytical data match those reported in the literature. (C. C. McAtee, P. S. Riehl, C. S. Schindler, *J. Am. Chem. Soc.* **2017**, *139*, 2960–2963)

3-Methoxy-9-methylphenanthrene (3i)

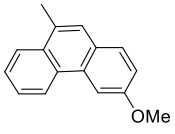

R_f = 0.4 (5% EtOAc in petroleum ether); yield: 25 mg (94%); white solid; ^{1}H NMR (400 MHz, $CDCl_3$): δ 2.74 (s, 3H), 3.97 (s, 3H), 7.20 (d, *J* = 2.6 Hz, 1H), 7.22–7.28 (m, 1H), 7.54 (s, 1H), 7.57–7.68 (m, 2H), 8.02–8.07 (m, 1H), 8.56 (d, *J* = 9.0 Hz, 1H), 8.63 (d, *J* = 8.0 Hz, 1H) ppm; ^{13}C NMR (100 MHz, $CDCl_3$): δ 20.0 (q), 55.4 (q), 108.0 (d), 116.2 (d), 122.5 (d), 124.0 (s), 124.1 (d), 124.6 (d), 125.5 (d), 126.3 (d), 126.4 (d), 130.5 (s), 131.0 (s), 133.2 (s), 133.4 (s), 158.3 (s)ppm. The analytical data match those reported in the literature. (Shu, C.; Li, L.; Chen, C.-B.; Shen, H.-C.; Ye, L.-W. *Chem.-Asian J.* **2014**, *9*, 1525−1529)

3-Fluoro-9-methylphenanthrene (3j)

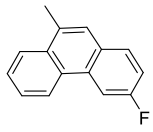

R_f = 0.4 (5% EtOAc in petroleum ether); yield: 22 mg (86%); white solid; ^{1}H NMR (400 MHz, $CDCl_3$): δ 2.75 (d, J = 1.0 Hz, 3H), 7.34 (td, J = 8.8, 2.8 Hz, 1H), 7.44 (dd, J = 9.5, 2.6 Hz, 1H), 7.53 (s, 1H), 7.62–7.71 (m, 2H), 8.04–8.10 (m, 1H), 8.59–8.67 (m, 2H) ppm; ^{13}C NMR (100 MHz, $CDCl_3$): δ 20.0 (d), 111.7 (dd, $J_{C\text{-}F}$ = 19.84 Hz), 114.5 (dd, $J_{C\text{-}F}$ = 23.65 Hz), 122.8 (d), 124.7 (d), 124.8 (d), 124.8 (d), 126.0 (dd, $J_{C\text{-}F}$ = 3.81 Hz), 126.3 (d), 126.6 (d), 130.1 (s), 131.5 (ds, $J_{C\text{-}F}$ = 1.45 Hz, 133.3 (ds, $J_{C\text{-}F}$ = 8.72 Hz), 134.0 (s), 160.2 (ds, $J_{C\text{-}F}$ = 245.59 Hz) ppm. The analytical data match those reported in the literature. (Shu, C.; Li, L.; Chen, C.-B.; Shen, H.-C.; Ye, L.-W. *Chem.-Asian J.* **2014**, *9*, 1525−1529).

3-Chloro-9-methylphenanthrene (3k)

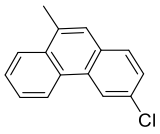

R_f = 0.4 (5% EtOAc in petroleum ether); yield: 24 mg (91%); white solid; ^{1}H NMR (400 MHz, $CDCl_3$): δ 2.74 (d, J = 1.0 Hz, 3H), 7.49–7.59 (m, 2H), 7.66–7.72 (m, 2H), 7.74 (d, J = 8.5 Hz, 1H), 8.01–8.13 (m, 1H), 8.59–8.68 (m, 2H) ppm; ^{13}C NMR (100 MHz, $CDCl_3$): δ 20.0 (q), 122.2 (d), 123.0 (d), 124.7 (d), 126.0 (d), 126.5 (d), 127.0 (d), 127.1 (d), 129.2 (d), 129.4 (s), 130.2 (s), 130.7 (s), 131.7 (s), 132.3 (s), 132.9 (s) ppm. The analytical data match those reported in the literature. (C. C. McAtee, P. S. Riehl, C. S. Schindler, *J. Am. Chem. Soc.* **2017**, *139*, 2960–2963).

5-Methylnaphtho[2,1-b]thiophene (3l)

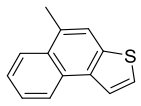

R_f = 0.4 (5% EtOAc in petroleum ether); yield: 18 mg (70%); white solid; ^{1}H NMR (400 MHz, $CDCl_3$): δ 2.78 (s, 3H), 7.51 (d, J = 5.4 Hz, 1H), 7.55–7.69 (m, 2H), 7.76 (s, 1H), 7.97 (d, J = 5.4 Hz, 1H), 8.06–8.13 (m, 1H), 8.33–8.40 (m, 1H) ppm; ^{13}C NMR (100 MHz, $CDCl_3$): δ 29.7 (q), 120.8 (d), 122.0 (d), 124.1 (d), 124.5 (d), 124.9 (d), 125.1 (d), 126.1 (d), 129.4 (s), 130.5 (s), 131.2 (s), 134.8 (s), 137.3 (s) ppm. The analytical data match those reported in the literature. (Wang, R.; Chen, Y.; Shu, M.; Zhao, W.; Tao, M.; Du, C.; Fu, X.; Li, A.; Lin, Z. *Chem. Eur. J.* **2020**, *26*, 1941–1946)

(E)-5-(Phenyldiazenyl)-6-propylindazolo[2,3-a]quinoline (4aa)

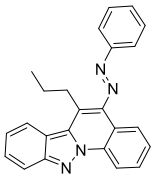

R_f = 0.4 (5% EtOAc in petroleum ether); yield: 32 mg (86%); red solid; IR (neat)ν_{max} 2958, 2352, 1454, 1359, 1226, 747 cm^{-1}; ^1H NMR (400 MHz, $CDCl_3$): δ 1.15 (t, J = 7.4 Hz, 3H), 1.89–2.02 (m, 2H), 3.49–3.61 (m, 2H), 7.30–7.40 (m, 1H), 7.52–7.67 (m, 5H), 7.79 (ddd, J = 8.4, 7.1, 1.3 Hz, 1H), 8.00–8.09 (m, 3H), 8.18 (d, J = 8.5 Hz, 1H), 8.64 (dd, J = 8.4, 1.0 Hz, 1H), 9.03 (dd, J = 8.4, 0.8 Hz, 1H) ppm; ^{13}C NMR (100 MHz, $CDCl_3$): δ 14.3 (q), 23.5 (t), 29.8 (t), 117.3 (d), 117.5 (d), 118.4 (s), 119.5 (s), 121.7 (d), 121.9 (d), 122.8 (d, 2C), 125.6 (d), 126.7 (d), 127.7 (d), 128.5 (s), 129.0 (d), 129.3 (d, 2C), 131.5 (d), 131.8 (s), 133.3 (s), 140.9 (s), 149.7 (s), 153.2 (s) ppm; HRMS (ESI) calcd. for $C_{24}H_{21}N_4$: 365.1761 $[M + H]^+$; found: 365.1763.

(E)-6-Isobutyl-5-(phenyldiazenyl)indazolo[2,3-a]quinoline (7ba)

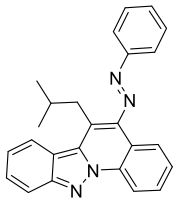

R_f = 0.4 (5% EtOAc in petroleum ether); yield: 30 mg (81%); red solid; IR (neat)ν_{max} 2957, 2356, 1688, 1461, 752, 687 cm^{-1}; ^1H NMR (400 MHz, $CDCl_3$): δ 1.03 (s, 3H), 1.05 (s, 3H), 2.28–2.33 (m, 1H), 3.59 (d, J = 7.4 Hz, 2H), 7.34–7.38 (m, 1H), 7.54–7.67 (m, 5H), 7.80 (ddd, J = 8.4, 7.1, 1.3 Hz, 1H), 8.02–8.09 (m, 3H), 8.19 (d, J = 8.5 Hz, 1H), 8.64 (dd, J = 8.5, 1.1 Hz, 1H), 9.06 (dd, J = 8.5, 1.0 Hz, 1H) ppm; ^{13}C NMR (100 MHz, $CDCl_3$): δ 22.7 (q, 2C), 29.2 (d), 35.7 (t), 117.4 (d), 118.3 (s), 118.4 (s), 121.8 (d), 121.9 (d), 122.8 (d, 2C), 125.8 (d), 126.9 (d), 127.8 (d), 129.1 (d), 129.4 (d, 3C), 129.6 (s), 131.5 (d), 132.0 (s), 133.4 (s), 141.6 (s), 149.5 (s), 153.1 (s) ppm; HRMS (ESI) calcd. for $C_{25}H_{23}N_4$: 379.1917 $[M + H]^+$; found: 379.1914.

(E)-6-Phenethyl-5-(phenyldiazenyl)indazolo[2,3-a]quinoline (7ca)

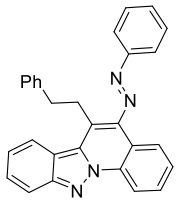

R_f = 0.4 (5% EtOAc in petroleum ether); yield: 26 mg (74%); red solid; IR (neat)ν_{max} 2925, 2353, 1689, 1461, 1224, 747, 690 cm^{-1}; ^1H NMR (400 MHz, $CDCl_3$): δ 3.16–3.31 (m, 2H), 3.85–3.94 (m, 2H), 7.20–7.26 (m, 1H), 7.31 (d, J = 4.4 Hz, 4H), 7.35–7.42 (m, 1H), 7.56–7.68 (m, 5H), 7.82 (ddd, J = 8.5, 7.1, 1.3 Hz, 1H), 8.00–8.11 (m, 3H), 8.31 (d, J = 8.5 Hz, 1H), 8.66 (dd, J = 8.4, 1.0 Hz, 1H), 9.06 (dd, J = 8.4, 0.8 Hz, 1H) ppm; ^{13}C NMR (100 MHz, $CDCl_3$): δ 29.8 (t), 36.2 (t), 117.3 (d), 117.6 (d), 118.3 (s), 119.7 (s), 121.6 (d), 122.1 (d), 122.9 (d, 2C), 125.7 (d), 126.3 (d), 126.8 (d), 127.0 (s), 127.8 (d), 128.3 (d, 2C), 128.6 (d, 2C), 129.2 (d), 129.3 (d, 2C), 131.6 (d), 133.4 (s), 140.9

(s), 141.2 (s, 2C), 149.7 (s), 153.1 (s) ppm; HRMS (ESI) calcd. for $C_{29}H_{23}N_4$: 427.1917 $[M + H]^+$; found: 427.1921.

(E)-3-(5-(Phenyldiazenyl)indazolo[2,3-a]quinolin-6-yl)propyl acetate (7da)

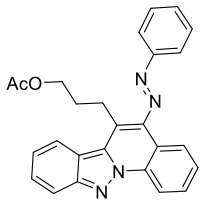

R_f = 0.4 (5% EtOAc in petroleum ether); yield: 29 mg (80%); red gummy solid; IR (neat)ν_{max} 2931, 2348, 1736, 1527, 1237, 753 cm^{-1}; ^1H NMR (400 MHz, $CDCl_3$): δ 2.04 (s, 3H), 2.24–2.35 (m, 2H), 3.60–3.71 (m, 2H), 4.30 (t, J = 6.1 Hz, 2H), 7.36 (ddd, J = 8.5, 6.7, 0.9 Hz, 1H), 7.56–7.68 (m, 5H), 7.82 (ddd, J = 8.5, 7.1, 1.3 Hz, 1H), 8.04–8.10 (m, 3H), 8.29 (d, J = 8.5 Hz, 1H), 8.64 (dd, J = 8.4, 0.9 Hz, 1H), 9.05 (dd, J = 8.5, 0.8 Hz, 1H) ppm; ^{13}C NMR (100 MHz, $CDCl_3$): δ 20.8 (q), 24.9 (t), 29.1 (t), 64.2 (t), 117.3 (d), 117.6 (d), 118.2 (s), 119.7 (s), 121.5 (d), 122.1 (d), 122.9 (d, 2C), 125.7 (d), 126.5 (s), 126.9 (d), 127.8 (d), 129.3 (d), 129.4 (d, 2C), 131.5 (s), 131.7 (d), 133.4 (s), 141.1 (s), 149.7 (s), 153.1 (s), 171.1 (s) ppm; HRMS (ESI) calcd. for $C_{26}H_{23}N_4O_2$: 423.1816 $[M + H]^+$; found: 423.1811.

(E)-6-(3-((Tert-butyldimethylsilyl)oxy)propyl)-5-(phenyldiazenyl)indazolo[2,3-a]quinoline (7ea)

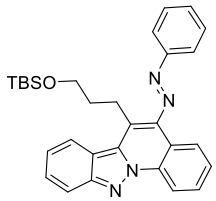

R_f = 0.6 (5% EtOAc in petroleum ether); yield: 25 mg (71%); red gummy solid; IR (neat)ν_{max} 2940, 2863, 2336, 1463, 1243, 1097, 836, 757 cm^{-1}; ^1H NMR (400 MHz, $CDCl_3$): δ 0.13 (s, 6H), 0.97 (s, 9H), 2.14 (dd, J = 11.2, 5.8 Hz, 2H), 3.59–3.72 (m, 2H), 3.89 (t, J = 5.7 Hz, 2H), 7.31–7.36 (m, 1H), 7.55–7.68 (m, 5H), 7.78–7.85 (m, 1H), 8.01–8.10 (m, 3H), 8.50 (d, J = 8.5 Hz, 1H), 8.63 (dd, J = 8.4, 0.9 Hz, 1H), 9.01–9.09 (m, 1H) ppm; ^{13}C NMR (100 MHz, $CDCl_3$): δ -5.3 (q, 2C), 18.4 (s), 25.3 (t), 26.0 (q, 3C), 33.2 (t), 63.2 (t), 117.2 (d), 117.3 (d), 118.4 (s), 119.7 (s), 122.0 (d), 122.4 (d), 122.8 (d, 2C), 125.6 (d), 126.8 (d), 127.8 (d), 128.1 (s), 129.1 (d), 129.3 (d, 2C), 131.5 (d), 131.9 (s), 133.2 (s), 141.0 (s), 149.6 (s), 153.2 (s) ppm; HRMS (ESI) calcd. for $C_{30}H_{35}N_4OSi$: 495.2575 $[M + H]^+$; found: 495.2576.

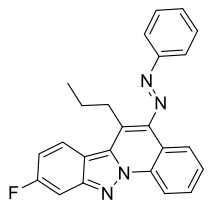

(E)-9-Fluoro-5-(phenyldiazenyl)-6-propylindazolo[2,3-a]quinoline (7fa)

R_f = 0.4 (5% EtOAc in petroleum ether); yield: 26 mg (71%); red solid; IR (neat)ν_{max} 2950, 2354, 1629, 1228, 1135, 756 cm^{-1}; ^1H NMR (400 MHz, $CDCl_3$): δ 1.12 (t, J = 7.4 Hz, 3H), 1.86–1.96 (m, 3H), 3.40–3.49 (m, 2H),

7.11 (td, *J* = 9.1, 2.3 Hz, 1H), 7.57–7.67 (m, 5H), 7.80 (ddd, *J* = 8.5, 7.1, 1.3 Hz, 1H), 8.02–8.07 (m, 2H), 8.10 (dd, *J* = 9.1, 5.1 Hz, 1H), 8.53 (dd, *J* = 8.4, 0.9 Hz, 1H), 8.99 (dd, *J* = 8.5, 0.8 Hz, 1H) ppm; ^{13}C NMR (100 MHz, $CDCl_3$): δ 14.3 (q), 23.3 (t), 29.7 (t), 100.7 (dd, $J_{C\text{-}F}$ = 23.65 Hz), 112.6 (dd, $J_{C\text{-}F}$ = 27.47 Hz), 115.2 (s), 117.3 (d), 119.3 (s), 122.9 (d, 2C), 123.4 (dd, $J_{C\text{-}F}$ = 10.68 Hz), 125.5 (d), 126.8 (d), 129.4 (d), 129.4 (d, 2C), 131.8 (d), 132.2 (s), 133.0 (s), 142.0 (s), 149.8 (ds, $J_{C\text{-}F}$ = 25.18 Hz), 153.0 (s), 161.4 (s), 163.9 (s) ppm; HRMS (ESI) calcd. for $C_{24}H_{20}N_4F$: 383.1667 $[M + H]^+$; found: 383.1668.

(E)-9-Methyl-5-(phenyldiazenyl)-6-propylindazolo[2,3-a]quinoline (7ga)

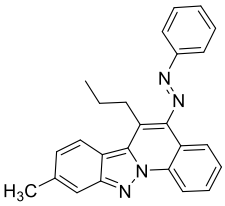

R_f = 0.4 (5% EtOAc in petroleum ether); yield: 30 mg (80%); red solid; IR (neat)ν_{max} 2933, 2353, 1685, 1459, 758 cm^{-1}; ^{1}H NMR (400 MHz, $CDCl_3$): δ 1.14 (t, *J* = 7.4 Hz, 3H), 1.87–2.00 (m, 2H), 2.57–2.62 (m, 3H), 3.49–3.59 (m, 2H), 7.19 (dd, *J* = 8.6, 1.3 Hz, 1H), 7.55–7.67 (m, 4H), 7.75–7.83 (m, 2H), 8.01–8.10 (m, 3H), 8.65 (dd, *J* = 8.4, 0.9 Hz, 1H), 9.00 (dd, *J* = 8.5, 0.9 Hz, 1H) ppm; ^{13}C NMR (100 MHz, $CDCl_3$): δ 14.3 (q), 22.3 (q), 23.5 (t), 29.8 (t), 116.2 (d), 116.6 (s), 117.2 (d), 119.3 (s), 121.2 (d), 122.8 (d, 2C), 124.7 (d), 125.6 (d), 126.5 (d), 128.4 (s), 128.9 (d), 129.3 (d, 2C), 131.4 (d), 131.8 (s), 133.4 (s), 137.8 (s), 140.8 (s), 150.4 (s), 153.2 (s) ppm; HRMS (ESI) calcd. for $C_{25}H_{23}N_4$: 379.1917 $[M + H]^+$; found: 379.1922.

(E)-5-(Phenyldiazenyl)-6-propylindazolo[2,3-a]quinolin-9-yl acetate (7ha)

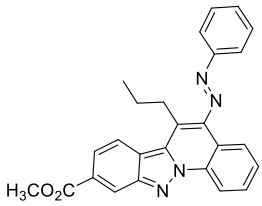

R_f = 0.5 (7% EtOAc in petroleum ether); yield: 27 mg (76%); red solid; IR (neat)ν_{max} 2932, 2357, 1718, 1545, 1230, 757 cm^{-1}; ^{1}H NMR (400 MHz, $CDCl_3$): δ 1.15 (t, *J* = 7.4 Hz, 3H), 1.87–2.01 (m, 2H), 3.46–3.58 (m, 2H), 4.03 (s, 3H), 7.59–7.69 (m, 4H), 7.78–7.88 (m, 1H), 7.96 (dd, *J* = 8.8, 1.4 Hz, 1H), 8.04–8.12 (m, 2H), 8.20 (d, *J* = 8.9 Hz, 1H), 8.60 (dd, *J* = 8.4, 1.0 Hz, 1H), 8.80 (s, 1H), 9.06 (dd, *J* = 8.5, 0.9 Hz, 1H) ppm; ^{13}C NMR (100 MHz, $CDCl_3$): δ 14.3 (q), 23.5 (t), 29.7 (t), 52.3 (q), 117.5 (d), 119.9 (s), 120.5 (s), 120.8 (d), 121.5 (d), 121.7 (d), 122.9 (d, 2C), 125.6 (d), 127.3 (d), 127.9 (s), 129.3 (d), 129.3 (s), 129.4 (d, 2C), 131.7 (d), 131.9 (s), 133.2 (s), 141.4 (s), 148.9 (s), 153.1 (s), 167.3 (s) ppm; HRMS (ESI) calcd. for $C_{26}H_{23}N_4O_2$: 423.1816 $[M + H]^+$; found: 423.1815.

(E)-5-(Phenyldiazenyl)-6-propylindazolo[2,3-a]quinoline-9-carbonitrile (7ia)

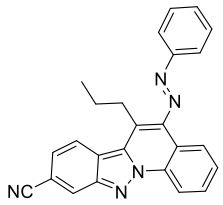

R_f = 0.4 (5% EtOAc in petroleum ether); yield: 26 mg (71%); red solid; IR (neat)ν_{max} 2923, 2348, 1550, 1497, 1249, 755, 698 cm^{-1}; ^1H NMR (400 MHz, $CDCl_3$): δ 1.14 (t, J = 7.3 Hz, 3H), 1.87–1.99 (m, 2H), 3.41–3.50 (m, 2H), 7.46 (dd, J = 8.6, 1.4 Hz, 1H), 7.61–7.71 (m, 4H), 7.85 (ddd, J = 8.4, 7.1, 1.4 Hz, 1H), 8.05–8.09 (m, 2H), 8.23 (dd, J = 8.8, 0.8 Hz, 1H), 8.40–8.44 (m, 1H), 8.52 (dd, J = 8.4, 0.9 Hz, 1H), 9.03 (dd, J = 8.5, 0.8 Hz, 1H) ppm; ^{13}C NMR (100 MHz, $CDCl_3$): δ 14.3 (q), 23.4 (t), 29.6 (t), 110.8 (s), 117.6 (d), 119.5 (s), 119.7 (s), 120.1 (s), 122.2 (d), 123.0 (d, 2C), 123.2 (d), 123.9 (d), 125.6 (d), 126.7 (s), 127.7 (d), 129.5 (d, 2C), 129.6 (d), 132.0 (d), 132.2 (s), 133.1 (s), 142.3 (s), 147.9 (s), 153.0 (s) ppm; HRMS (ESI) calcd. for $C_{25}H_{20}N_5$: 390.1713 $[M + H]^+$; found: 390.1712.

(E)-3-Fluoro-5-(phenyldiazenyl)-6-propylindazolo[2,3-a]quinoline (7ja)

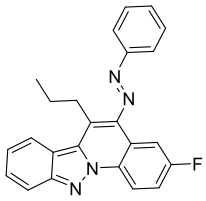

R_f = 0.4 (5% EtOAc in petroleum ether); yield: 29 mg (79%); red solid; IR (neat)ν_{max} 2927, 2863, 2532, 1457, 1245, 756 cm^{-1}; ^1H NMR (400 MHz, $CDCl_3$): δ 1.16 (t, J = 7.3 Hz, 3H), 1.92–2.03 (m, 2H), 3.53–3.69 (m, 2H), 7.33–7.40 (m, 1H), 7.48–7.55 (m, 1H), 7.55–7.68 (m, 4H), 7.97–8.08 (m, 3H), 8.18 (d, J = 8.4 Hz, 1H), 8.55 (dd, J = 11.1, 2.8 Hz, 1H), 9.02 (dd, J = 9.3, 5.4 Hz, 1H) ppm; ^{13}C NMR (100 MHz, $CDCl_3$): δ 14.3 (q), 23.5 (t), 29.8 (t), 111.0 (dd, $J_{C\text{-}F}$ = 26.70 Hz), 117.4 (dd, $J_{C\text{-}F}$ = 25.18 Hz), 117.5 (d), 118.6 (s), 119.4 (dd, $J_{C\text{-}F}$ = 8.39 Hz), 120.6 (ds, $J_{C\text{-}F}$ = 9.92 Hz), 121.6 (d), 122.3 (d), 122.8 (d, 2C), 127.8 (d), 129.4 (d, 2C), 130.0 (s), 131.5 (s), 131.6 (d), 139.4 (s), 149.6 (s), 153.2 (s), 160.1 (s), 162.5 (s) ppm; HRMS (ESI) calcd. for $C_{24}H_{20}N_4F$: 383.1667 $[M + H]^+$; found: 383.1672.

(E)-3-Methyl-5-(phenyldiazenyl)-6-propylindazolo[2,3-a]quinoline (7ka)

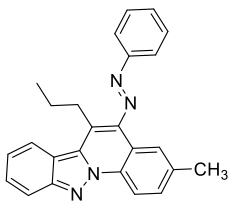

R_f = 0.4 (5% EtOAc in petroleum ether); yield: 26 mg (71%); red solid; IR (neat)ν_{max} 2956, 2869, 2354, 1455, 1359, 1226, 748, 686 cm^{-1}; ^1H NMR (400 MHz, $CDCl_3$): δ 1.13 (t, J = 7.4 Hz, 3H), 1.86–2.01 (m, 3H), 2.55 (s, 3H), 3.42–3.55 (m, 2H), 7.30–7.35 (m, 1H), 7.57–7.66 (m, 5H), 7.97–8.07 (m, 3H), 8.15 (d, J = 8.4 Hz, 1H), 8.36 (s, 1H), 8.89 (d, J = 8.5 Hz, 1H) ppm; ^{13}C NMR (100 MHz, $CDCl_3$): δ 14.3 (q), 21.8 (q), 23.5 (t), 29.8 (t), 117.1 (d), 117.3 (d), 118.3 (s), 119.6 (s), 121.6 (d), 121.7 (d), 122.8 (d, 2C), 124.9 (d), 127.5 (d), 127.8 (s), 129.3 (d, 2C), 130.5 (d), 131.4

(d), 131.5 (s), 136.7 (s, 2C), 140.9 (s), 149.5 (s), 153.1 (s) ppm; HRMS (ESI) calcd. for $C_{25}H_{23}N_4$: 379.1917 $[M + H]^+$; found: 379.1918.

(E)-2-Chloro-5-(phenyldiazenyl)-6-propylindazolo[2,3-a]quinoline (7ma)

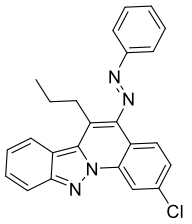

R_f = 0.4 (15% EtOAc in petroleum ether); yield: 30 mg (81%); red solid; IR (neat)ν_{max} 2959, 2352, 1603, 1460, 1226, 751 cm^{-1}; ^1H NMR (400 MHz, $CDCl_3$): δ 1.14 (t, J = 7.3 Hz, 3H), 1.88–2.00 (m, 2H), 3.49–3.59 (m, 2H), 7.36 (ddd, J = 8.5, 6.8, 0.9 Hz, 1H), 7.51–7.67 (m, 5H), 8.00–8.06 (m, 3H), 8.15 (d, J = 8.5 Hz, 1H), 8.64 (d, J = 9.0 Hz, 1H), 9.03 (d, J = 2.0 Hz, 1H) ppm; ^{13}C NMR (100 MHz, $CDCl_3$): δ 14.3 (q), 23.4 (t), 29.7 (t), 117.1 (d), 117.6 (d), 117.8 (s), 118.4 (s), 121.6 (d), 122.3 (d), 122.8 (d, 2C), 127.3 (d), 127.3 (d), 128.1 (d), 129.4 (d, 2C), 129.5 (s), 131.6 (d), 132.2 (s), 133.7 (s), 135.2 (s), 140.1 (s), 149.8 (s), 153.1 (s) ppm; HRMS (ESI) calcd. for $C_{24}H_{20}N_4Cl$: 399.1371 $[M + H]^+$; found: 399.1373.

(E)-2-Bromo-5-(phenyldiazenyl)-6-propylindazolo[2,3-a]quinoline (7na)

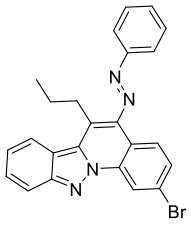

R_f = 0.4 (5% EtOAc in petroleum ether); yield: 27 mg (77%); red solid; IR (neat)ν_{max} 2925, 2353, 1689, 1597, 1460, 752 cm^{-1}; ^1H NMR (400 MHz, $CDCl_3$): δ 1.14 (t, J = 7.4 Hz, 3H), 1.89–2.02 (m, 2H), 3.50–3.58 (m, 2H), 7.32–7.41 (m, 1H), 7.56–7.65 (m, 4H), 7.70 (dd, J = 8.9, 2.1 Hz, 1H), 7.98–8.09 (m, 3H), 8.16 (d, J = 8.6 Hz, 1H), 8.58 (d, J = 9.0 Hz, 1H), 9.21 (d, J = 2.0 Hz, 1H) ppm; ^{13}C NMR (100 MHz, $CDCl_3$): δ 14.3 (q), 23.4 (t), 29.8 (t), 117.6 (d), 118.1 (s), 118.5 (s), 120.1 (d), 121.7 (d), 122.4 (d), 122.8 (d, 2C), 123.2 (s), 127.4 (d), 128.1 (d), 129.4 (d, 2C), 129.7 (s), 130.0 (d), 131.6 (d), 132.2 (s), 133.8 (s), 140.2 (s), 149.8 (s), 153.1 (s) ppm; HRMS (ESI) calcd. for $C_{24}H_{20}N_4Br$: 443.0866 $[M + H]^+$; found: 443.0862.

(E)-6-Propyl-5-(p-tolyldiazenyl)indazolo[2,3-a]quinoline (7ab)

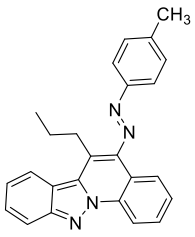

R_f = 0.5 (5% EtOAc in petroleum ether); yield: 25 mg (64%); red solid; IR (neat)ν_{max} 2946, 2353, 1543, 1363, 1230, 748 cm^{-1}; ^1H NMR (400 MHz, $CDCl_3$): δ 1.14 (t, J = 7.4 Hz, 3H), 1.89–2.02 (m, 2H), 2.51 (s, 3H), 3.45–3.57 (m, 2H), 7.34 (ddd, J = 8.4, 6.8, 0.9 Hz, 1H), 7.42 (m, J = 8.0 Hz, 2H), 7.56–7.65 (m, 2H), 7.79 (ddd, J = 8.5, 7.1, 1.3 Hz, 1H), 7.97 (m, J = 8.3 Hz, 2H), 8.04 (d, J = 8.8 Hz, 1H), 8.18 (d, J = 8.5 Hz, 1H), 8.59 (dd, J = 8.4, 0.9 Hz, 1H), 9.03 (dd, J =

8.4, 0.8 Hz, 1H) ppm; ^{13}C NMR (100 MHz, $CDCl_3$): δ 14.3 (t), 21.6 (t), 23.4 (d), 29.7 (d), 117.3 (d), 117.4 (d), 118.3 (s), 119.6 (s), 121.7 (d), 121.7 (d), 122.8 (d, 2C), 125.6 (d), 126.7 (d), 127.7 (d), 127.7 (d), 129.0 (d), 130.0 (d, 2C), 131.9 (s), 133.3 (s), 141.2 (s), 142.3 (s), 149.7 (s), 151.4 (s) ppm; HRMS (ESI) calcd. for $C_{25}H_{23}N_4$: 379.1917 $[M + H]^+$; found: 379.1924.

(E)-5-((4-Methoxyphenyl)diazenyl)-6-propylindazolo[2,3-a]quinoline (7ac)

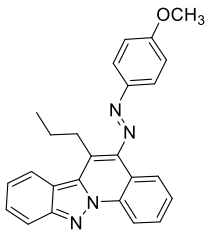

R_f = 0.4 (7% EtOAc in petroleum ether); yield: 28 mg (69%); red solid; IR (neat)ν_{max} 2929, 2354, 1596, 1500, 1248, 1144, 749 cm^{-1}; ^{1}H NMR (400 MHz, $CDCl_3$): δ 1.14 (t, J = 7.3 Hz, 3H), 1.89–2.03 (m, 2H), 3.43–3.57 (m, 2H), 3.96 (s, 3H), 7.05–7.17 (m, 2H), 7.33 (ddd, J = 8.4, 6.7, 0.9 Hz, 1H), 7.55–7.68 (m, 2H), 7.79 (ddd, J = 8.4, 7.1, 1.4 Hz, 1H), 8.00–8.10 (m, 3H), 8.18 (d, J = 8.5 Hz, 1H), 8.55 (dd, J = 8.4, 1.1 Hz, 1H), 9.03 (dd, J = 8.5, 1.0 Hz, 1H) ppm; ^{13}C NMR (100 MHz, $CDCl_3$): δ 14.3 (t), 21.6 (t), 23.4 (d), 29.7 (d), 117.3 (d), 117.4 (d), 118.3 (s), 119.6 (s), 121.7 (d), 121.7 (d), 122.8 (d, 2C), 125.6 (d), 126.7 (d), 127.7 (d), 127.7 (d), 129.0 (d), 130.0 (d, 2C), 131.9 (s), 133.3 (s), 141.2 (s), 142.3 (s), 149.7 (s), 151.4 (s) ppm; HRMS (ESI) calcd. for $C_{25}H_{23}N_4O$: 395.1866 $[M + H]^+$; found: 395.1877.

(E)-5-((2-Chlorophenyl)diazenyl)-6-propylindazolo[2,3-a]quinoline (7ad)

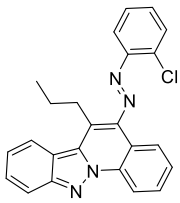

R_f = 0.5 (5% EtOAc in petroleum ether); yield: 31 mg (76%); red solid; IR (neat)ν_{max} 2923, 2354, 1591, 1508, 1455, 743 cm^{-1}; ^{1}H NMR (400 MHz, $CDCl_3$): δ 1.19 (t, J = 7.4 Hz, 3H), 1.99 (dq, J = 15.4, 7.5 Hz, 2H), 3.64–3.74 (m, 2H), 7.38 (ddd, J = 8.4, 6.8, 0.9 Hz, 1H), 7.42–7.50 (m, 2H), 7.61 (ddd, J = 8.6, 6.8, 1.0 Hz, 1H), 7.65–7.70 (m, 2H), 7.76–7.81 (m, 1H), 7.81–7.85 (m, 1H), 8.04–8.08 (m, 1H), 8.19 (d, J = 8.5 Hz, 1H), 9.06 (dd, J = 8.5, 1.0 Hz, 1H), 9.03 (dd, J = 8.5, 1.0 Hz, 1H) ppm; ^{13}C NMR (100 MHz, $CDCl_3$): δ 14.4 (q), 23.6 (t), 30.0 (t), 116.9 (d), 117.2 (d), 117.7 (d), 118.8 (s), 119.1 (s), 121.7 (d), 122.4 (d), 126.4 (d), 127.3 (d), 127.4 (d), 127.8 (d), 129.1 (d), 130.9 (d), 131.7 (d), 131.9 (s), 132.0 (s), 133.3 (s), 135.9 (s), 139.9 (s), 149.6 (s), 149.7 (s) ppm; HRMS (ESI) calcd. for $C_{24}H_{20}N_4Cl$: 399.1371 $[M + H]^+$; found: 399.1375.

(E)-5-((2-Ethylphenyl)diazenyl)-6-propylindazolo[2,3-a]quinoline (7ae)

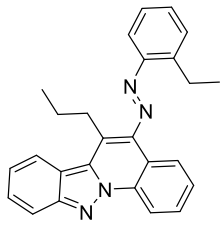

R_f = 0.4 (5% EtOAc in petroleum ether); yield: 32 mg (79%); dark red solid; IR (neat)ν_{max} 2947, 2868, 2352, 1462, 1230, 751 cm^{-1}; ^1H NMR (400 MHz, $CDCl_3$): δ 1.16 (t, J = 7.3 Hz, 3H), 1.38 (t, J = 7.6 Hz, 3H), 1.91–2.02 (m, 2H), 3.25 (q, J = 7.6 Hz, 2H), 3.55–3.63 (m, 2H), 7.33–7.41 (m, 2H), 7.46–7.54 (m, 2H), 7.57–7.65 (m, 2H), 7.76–7.85 (m, 2H), 8.05 (d, J = 8.8 Hz, 1H), 8.19 (d, J = 8.4 Hz, 1H), 8.66 (dd, J = 8.4, 0.8 Hz, 1H), 9.01–9.09 (m, 1H) ppm; ^{13}C NMR (100 MHz, $CDCl_3$): δ 14.3 (q), 16.4 (q), 23.5 (t), 24.7 (t), 29.6 (t), 114.9 (d), 117.3 (d), 117.4 (d), 118.3 (s), 119.7 (s, 2C), 121.7 (d), 122.0 (d), 125.7 (d), 126.6 (d), 126.8 (d), 128.0 (d), 129.2 (d), 129.2 (s), 130.1 (d), 131.8 (d), 132.1 (s), 133.1 (s), 144.8 (s), 149.2 (s), 150.9 (s) ppm; HRMS (ESI) calcd. for $C_{26}H_{25}N_4$: 393.2074 $[M + H]^+$; found: 393.2074.

(E)-5-((3,4-Dichlorophenyl)diazenyl)-6-propylindazolo[2,3-a]quinoline (7af)

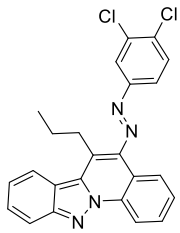

R_f = 0.5 (5% EtOAc in petroleum ether); yield: 25 mg (56%); red solid; IR (neat)ν_{max} 2938, 2350, 1453, 1366, 1113, 750 cm^{-1}; ^1H NMR (400 MHz, $CDCl_3$): δ 1.15 (t, J = 7.3 Hz, 3H), 1.89–1.99 (m, 2H), 3.55–3.65 (m, 2H), 7.36–7.42 (m, 1H), 7.59–7.67 (m, 2H), 7.70 (d, J = 8.6 Hz, 1H), 7.78–7.85 (m, 1H), 7.91 (dd, J = 8.5, 2.3 Hz, 1H), 8.06 (d, J = 8.6 Hz, 1H), 8.12 (d, J = 2.3 Hz, 1H), 8.19 (d, J = 8.5 Hz, 1H), 8.78 (dd, J = 8.4, 1.1 Hz, 1H), 9.04 (dd, J = 8.5, 1.0 Hz, 1H) ppm; ^{13}C NMR (100 MHz, $CDCl_3$): δ 14.4 (q), 23.6 (t), 30.0 (t), 117.4 (d), 117.8 (d), 118.8 (s), 119.1 (s), 121.6 (d), 122.4 (d), 122.5 (d), 123.8 (d), 125.8 (d), 127.1 (d), 127.8 (d), 129.2 (d), 131.1 (d), 131.3 (s), 131.6 (s), 133.3 (s), 133.8 (s), 135.2 (s), 139.9 (s), 149.7 (s), 152.2 (s) ppm; HRMS (ESI) calcd. for $C_{24}H_{19}N_4Cl_2$: 433.0981 $[M + H]^+$; found: 433.0985.

(E)-5-((2,4-Dichlorophenyl)diazenyl)-6-propylindazolo[2,3-a]quinoline (7ag)

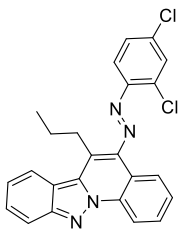

R_f = 0.4 (5% EtOAc in petroleum ether); yield: 21 mg (48%); dark red solid; mp: 134–136 °C; IR (neat)ν_{max} 2927, 2353, 1686, 1555, 1455, 1365, 748 cm^{-1}; ^1H NMR (400 MHz, $CDCl_3$): δ 1.17 (t, J = 7.3 Hz, 3H), 1.91–2.06 (m, 2H), 3.63–3.73 (m, 2H), 7.36–7.44 (m, 2H), 7.61 (ddd, J = 8.1, 7.3, 0.8 Hz, 1H), 7.65–7.70 (m, 2H), 7.76–7.84 (m, 2H), 8.06 (d, J = 8.6 Hz, 1H), 8.18 (d, J = 8.5 Hz, 1H), 9.03 (dd, J = 8.5, 0.9 Hz, 1H), 9.09 (dd, J = 8.5, 0.9 Hz, 1H) ppm; ^{13}C NMR (100 MHz, $CDCl_3$): δ 14.4 (q), 23.6 (t), 30.1 (t), 117.2 (d), 117.6 (d), 117.8 (s), 118.9 (s), 119.0 (s), 121.6

(d), 122.6 (d), 126.4 (d), 127.4 (d), 127.8 (d), 127.9 (d), 129.2 (d), 130.6 (d), 131.6 (s), 133.0 (s), 133.3 (s), 136.6 (s), 137.3 (s), 139.5 (s), 148.2 (s), 149.7 (s) ppm; HRMS (ESI) calcd. for $C_{24}H_{19}N_4Cl_2$: 433.0981 $[M + H]^+$; found: 433.0989.

(E)-1-(Phenanthren-9-yl)-2-phenyldiazene (10aa)

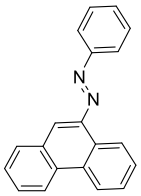

R_f = 0.4 (5% EtOAc in petroleum ether); yield: 33 mg (82%); red solid; IR (neat)ν_{max} 2353, 1699, 1532, 756 cm^{-1}; ^1H NMR (400 MHz, $CDCl_3$): δ 7.52–7.58 (m, 1H), 7.58–7.68 (m, 3H), 7.70–7.76 (m, 1H), 7.76–7.83 (m, 2H), 8.01 (s, 1H), 8.07 (d, J = 7.8 Hz, 1H), 8.09–8.15 (m, 2H), 8.74 (d, J = 8.3 Hz, 1H), 8.77–8.82 (m, 1H), 8.95–9.02 (m, 1H) ppm; ^{13}C NMR (100 MHz, $CDCl_3$): δ 111.8 (d), 122.7 (d), 122.8 (d), 123.3 (d, 2C), 124.2 (d), 127.0 (d), 127.1 (d), 127.2 (d), 127.7 (d), 129.2 (d, 2C), 130.0 (d), 131.0 (s), 131.0 (s), 131.2 (d), 131.3 (s), 131.7 (s), 146.6 (s), 153.2 (s) ppm; HRMS (ESI) calcd. for $C_{20}H_{15}N_2$: 283.1230 $[M + H]^+$; found: 283.1230.

(E)-1-(10-Methylphenanthren-9-yl)-2-phenyldiazene (10ba)

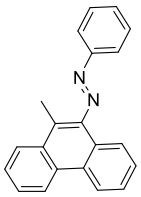

R_f = 0.4 (5% EtOAc in petroleum ether); yield: 35 mg (89%); red solid; IR (neat)ν_{max} 2352, 1508, 1447, 817, 746 cm^{-1}; ^1H NMR (400 MHz, $CDCl_3$): δ 2.69 (s, 3H), 7.54–7.68 (m, 5H), 7.68–7.74 (m, 2H), 8.04–8.07 (m, 1H), 8.08–8.12 (m, 2H), 8.19–8.26 (m, 1H), 8.70–8.82 (m, 2H) ppm; ^{13}C NMR (100 MHz, $CDCl_3$): δ 13.9 (q), 122.4 (s), 122.6 (d), 122.8 (d, 2C), 122.9 (s), 124.1 (d), 125.6 (d), 126.4 (d), 126.5 (s), 126.7 (d), 126.9 (d), 127.0 (d), 129.3 (d, 2C), 130.0 (s), 130.1 (s), 131.5 (d), 132.2 (s), 147.1 (s), 152.8 (s) ppm; HRMS (ESI) calcd. for $C_{21}H_{17}N_2$: 297.1386 $[M + H]^+$; found: 297.1392.

(E)-1-Phenyl-2-(10-phenylphenanthren-9-yl)diazene (10ca)

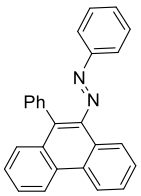

R_f = 0.4 (5% EtOAc in petroleum ether); yield: 34 mg (92%); red solid; IR (neat)ν_{max} 2930, 2353, 1532, 1453, 756, 697 cm^{-1}; ^1H NMR (400 MHz, $CDCl_3$): δ 7.34–7.39 (m, 3H), 7.41 (d, J = 6.8 Hz, 2H), 7.44–7.48 (m, 3H), 7.51–7.57 (m, 1H), 7.62–7.67 (m, 3H), 7.69–7.78 (m, 3H), 8.20 (d, J = 8.3 Hz, 1H), 8.78–8.86 (m, 2H) ppm; ^{13}C NMR (100 MHz, $CDCl_3$): δ 122.4 (d, 2C), 122.6 (d), 122.8 (d), 124.7 (d), 125.9 (s), 126.8 (d), 126.9 (d), 126.9 (s), 127.1 (d), 127.2 (d), 127.7 (d, 2C), 128.3 (d), 128.6 (s), 129.0 (d, 2C), 130.2 (s), 130.7 (s), 131.1 (d), 131.6 (d, 2C), 132.0 (s), 136.9 (s), 146.3 (s), 152.9 (s) ppm; HRMS (ESI) calcd. for $C_{26}H_{19}N_2$: 359.1548 $[M + H]^+$; found: 359.1548.

(E)-1-(6-Fluoro-10-methylphenanthren-9-yl)-2-phenyldiazene (10da)

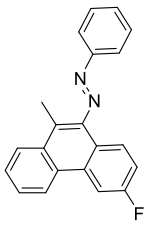

R_f = 0.4 (5% EtOAc in petroleum ether); yield: 27 mg (71%); red solid; IR (neat)ν_{max} 2223, 1684, 1494, 1449, 873, 750 cm^{-1}; ^1H NMR (400 MHz, $CDCl_3$): δ 2.72 (s, 3H), 7.39 (ddd, J = 9.1, 7.8, 2.7 Hz, 1H), 7.57–7.65 (m, 3H), 7.66–7.74 (m, 2H), 7.81 (dd, J = 11.3, 2.8 Hz, 1H), 8.06–8.10 (m, 2H), 8.20–8.24 (m, 1H), 8.66 (d, J = 8.4 Hz, 1H), 8.70 (dd, J = 9.1, 5.6 Hz, 1H) ppm; ^{13}C NMR (100 MHz, $CDCl_3$): δ 14.0 (q), 109.0 (dd, $J_{C\text{-}F}$ = 23.65 Hz), 115.1 (dd, $J_{C\text{-}F}$ = 23.65 Hz), 122.8 (d), 122.9 (d, 2C), 124.9 (dd, $J_{C\text{-}F}$ = 8.39 Hz), 125.8 (d), 126.6 (s), 126.6 (s), 126.9 (d), 127.2 (d), 127.8 (ds, $J_{C\text{-}F}$ = 9.16 Hz), 129.3 (d, 2C), 129.9 (s), 131.7 (s), 131.7 (d), 146.0 (ds, $J_{C\text{-}F}$ = 3.82 Hz), 152.7 (s), 160.3 (ds, $J_{C\text{-}F}$ = 245.67 Hz) ppm; HRMS (ESI) calcd. for $C_{21}H_{16}N_2F$: 315.1292 $[M + H]^+$; found: 315.1287.

(E)-1-(6-Methoxy-10-methylphenanthren-9-yl)-2-phenyldiazene (10ea)

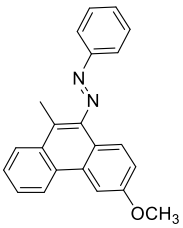

R_f = 0.4 (5% EtOAc in petroleum ether); yield: 35 mg (90%); red solid; IR (neat)ν_{max} 2354, 1615, 1534, 1459, 1219, 747 cm^{-1}; ^1H NMR (400 MHz, $CDCl_3$): δ 2.72 (s, 3H), 3.89 (s, 3H), 7.30 (dd, J = 9.1, 2.8 Hz, 1H), 7.58–7.60 (m, 1H), 7.60–7.64 (m, 3H), 7.64–7.71 (m, 2 H), 8.09 (dd, J = 8.1, 1.3 Hz, 2H), 8.20 (dd, J = 8.2, 1.2 Hz, 1H), 8.64 (d, J = 9.1 Hz, 2H) ppm; ^{13}C NMR (100 MHz, $CDCl_3$): δ 14.0 (q), 55.3 (q), 105.2 (d), 116.3 (d), 122.4 (d), 122.7 (d, 2C), 124.2 (s), 124.2 (d), 124.4 (s), 125.7 (d), 126.0 (d), 126.9 (d), 127.7 (s), 129.3 (d, 2C), 130.3 (s), 131.1 (s), 131.4 (d), 146.3 (s), 152.8 (s), 158.4 (s) ppm; HRMS (ESI) calcd. for $C_{22}H_{19}N_2O$: 327.1492 $[M + H]^+$; found: 327.1494.

(E)-1-(5-Methylnaphtho[2,1-b]thiophen-4-yl)-2-phenyldiazene (10fa)

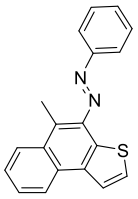

R_f = 0.4 (5% EtOAc in petroleum ether); yield: 34 mg (83%); orange solid; IR (neat)ν_{max} 2357, 1695, 1412, 757, 691 cm^{-1}; ^1H NMR (400 MHz, $CDCl_3$): δ 3.35 (s, 3H), 7.48–7.54 (m, 1H), 7.56–7.60 (m, 2H), 7.60 –7.65 (m, 1H), 7.65–7.69 (m, 1H), 7.73 (td, J = 7.5, 1.2 Hz, 1H), 8.01 (d, J = 5.5 Hz, 1H), 8.11–8.18 (m, 2H), 8.35–8.40 (m, 1H), 8.42 (d, J = 7.6 Hz, 1H) ppm; ^{13}C NMR (100 MHz, $CDCl_3$): δ 13.4 (q), 120.5 (d), 122.8 (d, 2C), 124.2 (d), 125.5 (s), 125.7 (d), 126.1 (d), 128.3 (d), 129.2 (d, 2C), 129.5 (d), 130.7 (s), 130.8 (d), 131.6 (s), 136.4 (s), 137.7 (s), 142.8 (s), 152.5 (s) ppm; HRMS (ESI) calcd. for $C_{19}H_{15}N_2S$: 303.0956 $[M + H]^+$; found: 303.0954.

(E)-1-(10-Methylphenanthren-9-yl)-2-(p-tolyl)diazene (10bb)

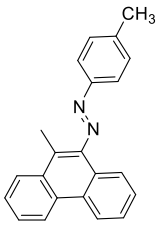

R_f = 0.4 (5% EtOAc in petroleum ether); yield: 26 mg (62%); red solid; IR (neat)ν_{max} 2352, 1508, 1447, 817, 750 cm^{-1}; ^1H NMR (400 MHz, $CDCl_3$): δ 2.52 (s, 3H), 2.67 (s, 3H), 7.43 (d, 2H), 7.53–7.60 (m, 1H), 7.63–7.67 (m, 1H), 7.67–7.75 (m, 2H), 7.98–8.05 (m, 3H), 8.18–8.25 (m, 1H), 8.71–8.80 (m, 2H) ppm; ^{13}C NMR (100 MHz, $CDCl_3$): δ 13.8 (q), 21.6 (q), 121.9 (s), 122.6 (d), 122.8 (d, 2C), 122.9 (d), 124.1 (d), 125.5 (d), 126.4 (d), 126.5 (d), 126.5 (s), 126.6 (s), 126.8 (d), 127.0 (d), 129.9 (d, 2C), 129.9 (s), 132.3 (s), 142.2 (s), 147.2 (s), 150.9 (s) ppm; HRMS (ESI) calcd. for $C_{22}H_{19}N_2$: 311.1543 $[M + H]^+$; found: 311.1547.

(E)-1-(4-Methoxyphenyl)-2-(10-methylphenanthren-9-yl)diazene (10bc)

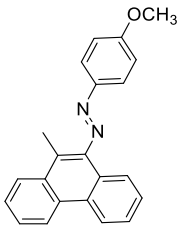

R_f = 0.4 (5% EtOAc in petroleum ether); yield: 32 mg (73%); red solid; IR (neat)ν_{max} 2351, 1594, 1504, 1454, 1251, 1141, 757 cm^{-1}; ^1H NMR (400 MHz, $CDCl_3$): δ 2.66 (s, 3H), 3.95 (s, 3H), 7.03–7.16 (m, 2H), 7.52–7.61 (m, 1H), 7.62–7.74 (m, 3H), 7.96–8.03 (m, 1H), 8.06–8.15 (m, 2H), 8.16–8.25 (m, 1H), 8.69–8.80 (m, 2H) ppm; ^{13}C NMR (100 MHz, $CDCl_3$): δ 13.8 (q), 55.7 (q), 114.3 (d, 2C), 121.6 (s), 122.6 (d), 122.9 (d), 124.1 (d), 124.7 (d, 2C), 125.5 (d), 126.3 (d), 126.4 (d), 126.7 (d), 126.9 (d), 129.8 (s), 129.9 (s), 132.3 (s, 2C), 147.2 (s, 2C), 162.5 (s) ppm; HRMS (ESI) calcd. for $C_{22}H_{19}N_2O$: 327.1492 $[M + H]^+$; found: 327.1494.

(E)-1-(4-Chlorophenyl)-2-(10-methylphenanthren-9-yl)diazene (10bd)

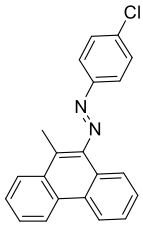

R_f = 0.5 (5% EtOAc in petroleum ether); yield: 31 mg (69%); red solid; IR (neat)ν_{max} 2353, 1534, 1464, 1230, 752 cm^{-1}; ^1H NMR (400 MHz, $CDCl_3$): δ 2.70 (s, 3H), 7.56–7.62 (m, 3H), 7.64–7.68 (m, 1H), 7.68–7.76 (m, 2H), 8.00–8.05 (m, 2H), 8.07 (d, J = 7.9 Hz, 1H), 8.17–8.27 (m, 1H), 8.69–8.81 (m, 2H) ppm; ^{13}C NMR (100 MHz, $CDCl_3$): δ 13.9 (q), 122.6 (d), 123.0 (d), 123.2 (s), 124.1 (d, 2C), 124.1 (d), 125.7 (d), 126.3 (s), 126.5 (d), 126.9 (d), 126.9 (d), 127.1 (d), 129.5 (d, 2C), 130.0 (s), 130.2 (s), 132.1 (s), 137.5 (s), 146.7 (s), 151.1 (s) ppm; HRMS (ESI) calcd. for $C_{21}H_{16}N_2Cl$: 331.0997 $[M + H]^+$; found: 331.0991.

(E)-1-(10-Methylphenanthren-9-yl)-2-(4-(trifluoromethyl)phenyl)diazene (10be)

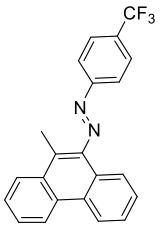

R_f = 0.4 (5% EtOAc in petroleum ether); yield: 39 mg (79%); red solid; IR (neat)ν_{max} 2347, 1320, 1122, 1063, 749 cm^{-1}; ^1H NMR (400 MHz, $CDCl_3$): δ 2.74 (s, 3H), 7.59 (ddd, J = 8.3, 7.0, 1.3 Hz, 1H), 7.65–7.69 (m, 1H), 7.69–7.74 (m, 2H), 7.89 (d, J = 8.3 Hz, 2H), 8.10–8.19 (m, 3H), 8.21–8.28 (m, 1H), 8.72–8.81 (m, 2H) ppm; ^{13}C NMR (100 MHz, $CDCl_3$): δ 14.0 (q), 119.4 (s), 122.7 (d), 123.0 (d, 2C), 123.0 (d), 124.1 (d), 124.4 (s), 125.9 (d), 126.1 (qd, $J_{C\text{-}F}$ = 3.82 Hz, 2C), 126.6 (d), 127.1 (d), 127.2 (d), 127.2 (d), 130.0 (s), 130.4 (s), 132.0 (s), 132.5 (s), 132.9 (s), 146.6 (s), 154.5 (s) ppm; HRMS (ESI) calcd. for $C_{22}H_{16}N_2F_3$: 365.1260 $[M + H]^+$; found: 365.1257.

(E)-1-(2-Ethylphenyl)-2-(10-methylphenanthren-9-yl)diazene (10bf)

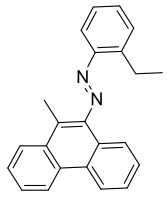

R_f = 0.4 (5% EtOAc in petroleum ether); yield: 33 mg (76%); red solid; IR (neat)ν_{max} 2933, 2353, 1700, 1543, 770 cm^{-1}; ^1H NMR (400 MHz, $CDCl_3$): δ 1.33 (t, J = 7.5 Hz, 3H), 2.69 (s, 3H), 3.19 (q, J = 7.5 Hz, 2H), 7.36–7.43 (m, 1H), 7.44–7.53 (m, 2H), 7.55–7.61 (m, 1H), 7.67–7.73 (m, 3H), 7.84 (d, J = 7.9 Hz, 1H), 8.10 (d, J = 8.1 Hz, 1H), 8.19–8.27 (m, 1H), 8.72–8.81 (m, 2H) ppm; ^{13}C NMR (100 MHz, $CDCl_3$): δ 16.5 (q), 24.8 (t), 112.0 (d), 115.9 (d), 122.7 (d, 2C), 124.3 (d), 126.5 (d), 127.0 (d), 127.0 (d), 127.1 (d), 127.6 (d), 129.9 (d), 130.1 (d), 131.0 (s), 131.0 (s), 131.4 (d), 131.6 (s), 144.5 (s), 146.9 (s), 150.8 (s) ppm; HRMS (ESI) calcd. for $C_{22}H_{19}N_2$: 311.1543 $[M + H]^+$; found: 311.1543.

(E)-1-(3,4-Dichlorophenyl)-2-(10-methylphenanthren-9-yl)diazene (10bg)

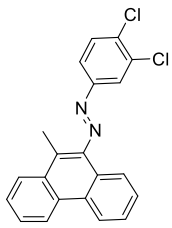

R_f = 0.4 (5% EtOAc in petroleum ether); yield: 30 mg (61%); red solid; IR (neat)ν_{max} 2354, 1594, 1453, 1086, 754 cm^{-1}; ^1H NMR (400 MHz, $CDCl_3$): δ 2.72 (s, 3H), 7.55–7.62 (m, 1H), 7.64–7.77 (m, 4H), 7.93 (dd, J = 8.5, 2.3 Hz, 1H), 8.09–8.13 (m, 1H), 8.16 (d, J = 2.3 Hz, 1H), 8.21–8.26 (m, 1H), 8.71–8.79 (m, 2H) ppm; ^{13}C NMR (100 MHz, $CDCl_3$): δ 14.1 (q), 122.7 (d), 122.7 (d), 123.0 (s), 123.8 (d), 124.1 (d), 124.4 (s), 125.9 (d), 126.1 (d), 126.6 (s), 127.1 (d), 127.2 (d), 127.2 (d), 130.0 (s), 130.4 (s), 131.1 (d), 132.0 (s), 133.7 (s), 135.4 (s), 146.3 (s), 151.6 (s) ppm; HRMS (ESI) calcd. for $C_{21}H_{15}N_2Cl_2$: 365.0607 $[M + H]^+$; found: 365.0606.

(E)-1-(2,4-Dichlorophenyl)-2-(10-methylphenanthren-9-yl)diazene (10bh)

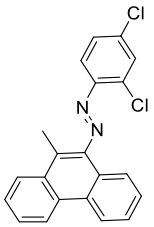

R_f = 0.4 (5% EtOAc in petroleum ether); yield: 26 mg (54%); red solid; IR (neat)ν_{max} 2353, 1589, 1453, 1086, 754 cm^{-1}; ^1H NMR (400 MHz, $CDCl_3$): δ 2.85 (s, 3H), 7.44 (dd, J = 8.5, 2.5 Hz, 1H), 7.58 (d, J = 8.5 Hz, 1H), 7.62–7.69 (m, 2H), 7.72 (ddd, J = 9.3, 7.8, 1.3 Hz, 2H), 7.84 (d, J = 2.4 Hz, 1H), 8.27 (dd, J = 8.0, 1.3 Hz, 1H), 8.41–8.51 (m, 1H), 8.68–8.80 (m, 2H) ppm; ^{13}C NMR (100 MHz, $CDCl_3$): δ 14.4 (q), 117.5 (d), 122.6 (d), 123.0 (d), 124.5 (d), 126.1 (s), 126.2 (d), 126.7 (d), 127.1 (d), 127.2 (s), 127.4 (d), 127.6 (d), 130.0 (s), 130.9 (s), 131.4 (d), 131.7 (d), 132.0 (s), 133.6 (s), 133.8 (s), 145.9 (s), 149.6 (s) ppm; HRMS (ESI) calcd. for $C_{21}H_{15}N_2Cl_2$: 365.0607 $[M + H]^+$; found: 365.0607.

(E)-1-(4-Methoxyphenyl)-2-(10-phenylphenanthren-9-yl)diazene (10cc)

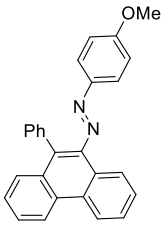

R_f = 0.4 (7% EtOAc in petroleum ether); yield: 34 mg (83%); red solid; IR (neat)ν_{max} 2932, 2352, 1596, 1501, 1252, 759 cm^{-1}; ^1H NMR (400 MHz, $CDCl_3$): δ 3.88 (s, 3H), 6.94–6.98 (m, 2H), 7.32–7.37 (m, 3H), 7.37–7.41 (m, 2H), 7.53 (dd, J = 8.2, 1.1 Hz, 1H), 7.60–7.69 (m, 4H), 7.69–7.75 (m, 2H), 8.17 (d, J = 8.3 Hz, 1H), 8.81 (t, J = 9.3 Hz, 2H) ppm; ^{13}C NMR (100 MHz, $CDCl_3$): δ 55.5 (q), 114.1 (d, 2C), 122.6 (d), 122.7 (d), 124.4 (d, 2C), 124.7 (d), 126.2 (s), 126.6 (d), 126.8 (d), 126.8 (d), 127.0 (d), 127.0 (d), 127.6 (d, 2C), 128.1 (d), 128.3 (s), 130.0 (s), 130.7 (s), 131.6 (d, 2C), 132.1 (s), 137.1 (s), 146.4 (s), 147.3 (s), 162.2 (s) ppm; HRMS (ESI) calcd. for $C_{27}H_{21}N_2O$: 389.1654 $[M + H]^+$; found: 389.1654.

(E)-1-(6-Methoxy-10-methylphenanthren-9-yl)-2-(4-methoxyphenyl)diazene (10ec)

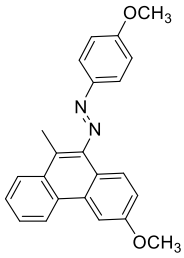

R_f = 0.3 (5% EtOAc in petroleum ether); yield: 40 mg (96%); red solid; IR (neat)ν_{max} 2352, 1607, 1501, 1249, 831, 756 cm^{-1}; ^1H NMR (400 MHz, $CDCl_3$): δ 2.68 (s, 3H), 3.88 (s, 3H), 3.94 (s, 3H), 7.09–7.15 (m, 2H), 7.25–7.32 (m, 1H), 7.51 (d, J = 2.8 Hz, 1H), 7.57–7.72 (m, 2H), 8.04–8.12 (m, 2H), 8.18 (dd, J = 8.2, 1.3 Hz, 1H), 8.63 (d, J = 9.0 Hz, 2H) ppm; ^{13}C NMR (100 MHz, $CDCl_3$): δ 13.9 (q), 55.2 (q), 55.6 (q), 105.2 (d), 114.4 (d), 116.2 (d), 122.4 (d), 123.1 (s), 124.2 (d), 124.4 (s), 124.6 (d), 125.6 (d), 125.9 (d), 126.6 (d), 128.0 (s), 130.1 (s), 131.3 (s), 146.5 (s), 147.3 (s), 158.3 (s), 162.4 (s) ppm; HRMS (ESI) calcd. for $C_{23}H_{21}N_2O_2$: 357.1603 $[M + H]^+$; found: 357.1603.

(E)-1-(2-Ethylphenyl)-2-(6-methoxy-10-methylphenanthren-9-yl)diazene (10ef)

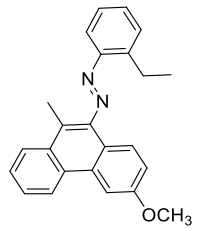

R_f = 0.3 (5% EtOAc in petroleum ether); yield: 36 mg (86%); red solid; IR (neat)ν_{max} 2932, 2356, 1612, 1457, 1216, 1039, 749 cm^{-1}; ^1H NMR (400 MHz, $CDCl_3$): δ 1.34 (t, J = 7.5 Hz, 3H), 2.70 (s, 3H), 3.21 (q, J = 7.5 Hz, 2H), 3.89 (s, 3H), 7.30 (dd, J = 9.1, 2.7 Hz, 1H), 7.39 (td, J = 7.4, 1.8 Hz, 1H), 7.46–7.55 (m, 2H), 7.60 (d, J = 2.8 Hz, 1H), 7.61–7.71 (m, 2H), 7.83 (dd, J = 8.0, 1.0 Hz, 1H), 8.20 (dd, J = 8.1, 1.3 Hz, 1H), 8.65 (d, J = 9.3 Hz, 2H) ppm; ^{13}C NMR (100 MHz, $CDCl_3$): δ 14.1 (q), 16.5 (q), 24.5 (t), 55.3 (q), 105.1 (d), 115.1 (d), 116.4 (s), 122.4 (d), 123.4 (s), 124.2 (d), 124.3 (s), 125.8 (d), 126.0 (d), 126.6 (d), 126.8 (d), 128.2 (s), 130.0 (d), 130.3 (s), 131.2 (d), 131.6 (s), 144.5 (s), 146.8 (s), 150.6 (s), 158.4 (s) ppm; HRMS (ESI) calcd. for $C_{24}H_{23}N_2O$: 355.1810 $[M + H]^+$; found: 355.1803.

(E)-1-(4-Methoxyphenyl)-2-(5-methylnaphtho[2,1-b]thiophen-4-yl)diazene (10fc)

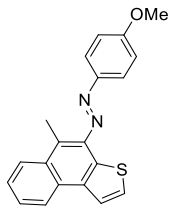

R_f = 0.4 (5% EtOAc in petroleum ether); yield: 33 mg (75%); dark orange solid; IR (neat)ν_{max} 2351, 1592, 1499, 1249, 1146, 720 cm^{-1}; ^1H NMR (400 MHz, $CDCl_3$): δ 3.31 (s, 3H), 3.92 (s, 3H), 7.04–7.10 (m, 2H), 7.59–7.67 (m, 2H), 7.67–7.73 (m, 1H), 8.00 (d, J = 5.6 Hz, 1H), 8.10–8.16 (m, 2H), 8.32–8.37 (m, 1H), 8.38–8.44 (m, 1H) ppm; ^{13}C NMR (100 MHz, $CDCl_3$): δ 13.4 (s), 55.6 (s), 114.3 (d, 2C), 120.4 (d), 124.1 (d), 124.6 (d, 2C), 125.6 (d), 125.6 (s megered), 125.9 (d), 127.9 (d), 129.4 (d), 130.4 (s), 131.7 (s), 136.3 (s), 136.3 (s), 142.8 (s), 146.9 (s), 161.9 (s) ppm; HRMS (ESI) calcd. for $C_{20}H_{17}N_2OS$: 333.1061 $[M + H]^+$; found: 333.1063.

(E)-1-(Phenanthren-9-yl)-2-(p-tolyl)diazene (10ab)

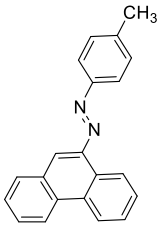

R_f = 0.5 (5% EtOAc in petroleum ether); yield: 29 mg (68%); red solid; IR (neat)ν_{max} 2354, 1510, 1455, 816, 745 cm^{-1}; ^1H NMR (400 MHz, $CDCl_3$): δ 2.50 (s, 3H), 7.40 (d, J = 8.0 Hz, 2H), 7.60–7.66 (m, 1H), 7.72 (ddd, J = 8.3, 7.0, 1.4 Hz, 1H), 7.75–7.81 (m, 2H), 7.98–8.04 (m, 3H), 8.04–8.09 (m, 1H), 8.73 (d, J = 8.3 Hz, 1H), 8.76–8.81 (m, 1H), 8.94–9.04 (m, 1H) ppm; ^{13}C NMR (100 MHz, $CDCl_3$): δ 21.6 (q), 111.7 (d), 122.7 (d), 122.7 (d), 123.3 (d, 2C), 124.2 (d), 126.9 (d), 127.0 (d), 127.1 (d), 127.6 (d), 129.9 (d, 2C), 130.0 (s), 130.9 (d), 131.0 (s), 131.4 (s), 131.5 (s), 141.8 (s), 146.7 (s), 151.4 (s) ppm; HRMS (ESI) calcd. for $C_{21}H_{17}N_2$: 297.1386 $[M + H]^+$; found: 297.1387.

(E)-1-(4-Methoxyphenyl)-2-(phenanthren-9-yl)diazene (10ac)

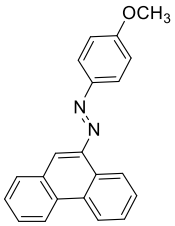

R_f = 0.3 (5% EtOAc in petroleum ether); yield: 33 mg (75%); red solid; IR (neat)ν_{max} 2353, 1596, 1506, 1250, 749, 678 cm^{-1}; ^1H NMR (400 MHz, $CDCl_3$): δ 3.94 (s, 3H), 7.07–7.13 (m, 2H), 7.60–7.67 (m, 1H), 7.67–7.74 (m, 1H), 7.74–7.80 (m, 2H), 7.98 (s, 1H), 8.03–8.08 (m, 1H), 8.08–8.16 (m, 2H), 8.68–8.82 (m, 2H), 8.94–9.02 (m, 1H) ppm; ^{13}C NMR (100 MHz, $CDCl_3$): δ 55.6 (s), 111.5 (d), 114.3 (d, 2C), 122.7 (d), 122.7 (d), 124.2 (d), 125.2 (d, 2C), 126.9 (d), 127.0 (d), 127.0 (s), 127.4 (d), 130.0 (s), 130.8 (d), 131.0 (s), 131.4 (s), 131.5 (s), 146.7 (s), 147.8 (s), 162.2 (s) ppm; HRMS (ESI) calcd. for $C_{21}H_{17}N_2O$: 313.1335 $[M + H]^+$; found: 313.1334.

(E)-1-(2-Chlorophenyl)-2-(phenanthren-9-yl)diazene (10ai)

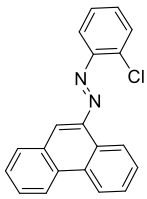

R_f = 0.5 (5% EtOAc in petroleum ether); yield: 33 mg (73%); red solid; IR (neat)ν_{max} 2355, 1542, 1509, 748 cm^{-1}; ^1H NMR (400 MHz, $CDCl_3$): δ 7.39–7.49 (m, 2H), 7.61–7.69 (m, 2H), 7.70–7.75 (m, 1H), 7.75–7.83 (m, 2H), 7.87–7.92 (m, 1H), 8.10 (t, J = 3.8 Hz, 2H), 8.73 (d, J = 8.4 Hz, 1H), 8.76–8.83 (m, 1H), 8.98–9.04 (m, 1H) ppm; ^{13}C NMR (100 MHz, $CDCl_3$): δ 113.2 (d), 118.1 (d), 122.7 (d), 122.8 (d), 124.2 (d), 127.1 (d), 127.1 (d), 127.2 (d), 127.3 (d), 128.1 (d), 129.9 (s), 130.8 (d), 131.1 (d), 131.2 (d), 131.3 (s), 131.8 (s), 131.9 (s), 135.5 (s), 146.5 (s), 149.3 (s) ppm; HRMS (ESI) calcd. for $C_{20}H_{14}N_2Cl$: 317.0835 $[M + H]^+$; found: 317.0840.

(E)-1-(2-Ethylphenyl)-2-(phenanthren-9-yl)diazene (10af)

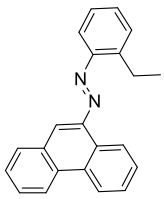

R_f = 0.4 (5% EtOAc in petroleum ether); yield: 32 mg (73%); red solid; IR (neat)ν_{max} 2932, 2355, 1524, 1453, 753 cm^{-1}; ^1H NMR (400 MHz, $CDCl_3$): δ 1.41 (t, J = 7.6 Hz, 3H), 3.33 (q, J = 7.5 Hz, 2H), 7.38 (dd, J = 8.1, 2.2 Hz, 1H), 7.43–7.51 (m, 2H), 7.62–7.67 (m, 1H), 7.70–7.76 (m, 1H), 7.76–7.82 (m, 2H), 7.83–7.88 (m, 1H), 7.96 (s, 1H), 8.05–8.10 (m, 1H), 8.71–8.76 (m, 1H), 8.79 (d, J = 9.5 Hz, 1H), 8.99–9.09 (m, 1H) ppm; ^{13}C NMR (100 MHz, $CDCl_3$): δ 16.5 (q), 24.8 (t), 112.0 (d), 115.9 (d), 122.7 (d, 2C), 124.3 (d), 126.5 (d), 127.0 (d), 127.0 (d), 127.1 (d), 127.6 (d), 129.9 (d), 130.1 (d), 131.0 (s), 131.0 (s), 131.4 (d), 131.6 (s), 144.5 (s), 146.9 (s), 150.8 (s) ppm; HRMS (ESI) calcd. for $C_{22}H_{19}N_2$: 311.1543 $[M + H]^+$; found: 311.1543.

(E)-10-(Methyldiazenyl)-9,10-dihydrophenanthren-9-ol (10aj)

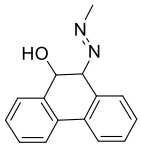

R_f = 0.5 (10% EtOAc in petroleum ether); yield: 23 mg (68%); red gummy solid; IR (neat)ν_{max} 2960, 1640, 1442, 1216, 1038, 740 cm^{-1}; ^1H NMR (400 MHz, $CDCl_3$): δ 2.30 (br. s., 1H), 3.91 (s, 3H), 4.76 (d, *J* = 8.1 Hz, 1H), 5.25 (d, *J* = 8.1 Hz, 1H), 7.16 (d, *J* = 7.5 Hz, 1H), 7.32 (td, *J* = 7.5, 1.1 Hz, 1H), 7.39 (td, J = 7.4, 1.3 Hz, 1H), 7.42–7.47 (m, 2H), 7.65 (d, *J* = 7.4 Hz, 1H), 7.81–7.86 (m, 1H), 7.88 (d, *J* = 7.9 Hz, 1H) ppm; ^{13}C NMR (100 MHz, $CDCl_3$): δ 57.3 (q), 70.0 (d), 80.8 (d), 123.7 (d), 123.9 (d), 126.6 (d), 128.1 (d), 128.2 (d), 128.4 (d), 128.7 (d), 128.8 (d), 131.8 (s), 132.5 (s), 133.0 (s), 136.0 (s) ppm; HRMS (ESI) calcd. for $C_{15}H_{15}N_2O$: 239.1184 $[M + H]^+$; found: 239.1188.

(E)-1-Methyl-2-(10-methylphenanthren-9-yl)diazene (10bj)

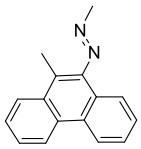

R_f = 0.4 (7% EtOAc in petroleum ether); yield: 19 mg (62%); red gummy solid; IR (neat)ν_{max} 2916, 1676, 1422, 1219, 748 cm^{-1}; ^1H NMR (400 MHz, $CDCl_3$): δ 2.52 (s, 3H), 4.35 (s, 3H), 7.53–7.60 (m, 1H), 7.62–7.66 (m, 1H), 7.66–7.70 (m, 2H), 7.76 (dd, *J* = 8.3, 1.1 Hz, 1H), 8.13–8.19 (m, 1H), 8.70–8.76 (m, 2H) ppm; ^{13}C NMR (100 MHz, $CDCl_3$): δ 13.3 (d), 58.5 (d), 120.2 (s), 122.6 (d), 122.9 (d), 123.5 (d), 125.3 (d), 126.2 (s), 126.3 (d, 2C), 126.7 (d), 127.0 (d), 129.7 (s), 129.8 (s), 132.1 (s), 146.9 (s) ppm; HRMS (ESI) calcd. for $C_{16}H_{15}N_2$: 235.1235 $[M + H]^+$; found: 235.1232.

(E)-1-Methyl-2-(10-phenylphenanthren-9-yl)diazene (10cj)

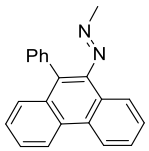

R_f = 0.4 (5% EtOAc in petroleum ether); yield: 17 mg (56%); red gummy solid; IR (neat)ν_{max} 2932, 1655, 1447, 1280, 935, 745 cm^{-1}; ^1H NMR (400 MHz, $CDCl_3$): δ 3.16 (s, 3H), 7.35–7.41 (m, 3H), 7.42–7.46 (m, 2H), 7.46–7.52 (m, 2H), 7.62–7.67 (m, 2H), 7.71 (dd, *J* = 7.8, 1.4 Hz, 1H), 8.03–8.07 (m, 2H), 8.31 (dd, *J* = 7.8, 1.4 Hz, 1H) ppm; ^{13}C NMR (100 MHz, $CDCl_3$): δ 38.5 (q), 122.6 (d), 122.7 (d), 124.4 (d, 2C), 124.7 (d), 127.4 (d), 128.0 (d), 128.0 (d), 128.0 (s mergered), 128.1 (d), 128.2 (d), 128.3 (d), 128.4 (d, 2C), 130.1 (s), 130.3 (s), 131.8 (s), 139.5 (s), 141.2 (s), 143.9 (s) ppm; HRMS (ESI) calcd. for $C_{21}H_{17}N_2$: 297.1391 $[M + H]^+$; found: 297.1392.

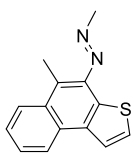

(E)-1-Methyl-2-(5-methylnaphtho[2,1-b]thiophen-4-yl)diazene (10fj)

R_f = 0.4 (5% EtOAc in petroleum ether); yield: 20 mg (63%); red gummy solid; ^1H NMR (400 MHz, $CDCl_3$): δ 3.26 (s, 3H), 4.26 (s, 3H), 7.60 (d, *J* = 5.5 Hz, 1H),

7.61–7.67 (m, 1H), 7.68–7.74 (m, 1H), 7.99 (d, J = 5.5 Hz, 1H), 8.36 (d, J = 8.3 Hz, 1H), 8.42 (d, J = 7.8 Hz, 1H) ppm; ^{13}C NMR (100 MHz, $CDCl_3$): δ 13.1 (q), 56.1 (q), 120.5 (d), 124.2 (d), 125.5 (s), 125.7 (d), 126.0 (d), 127.9 (d), 129.2 (d), 130.3 (s), 131.6 (s), 135.3 (s), 136.3 (s), 141.7 (s) ppm; HRMS (ESI) calcd. for $C_{14}H_{13}N_2S$: 241.0799 $[M + H]^+$; found: 241.0785.

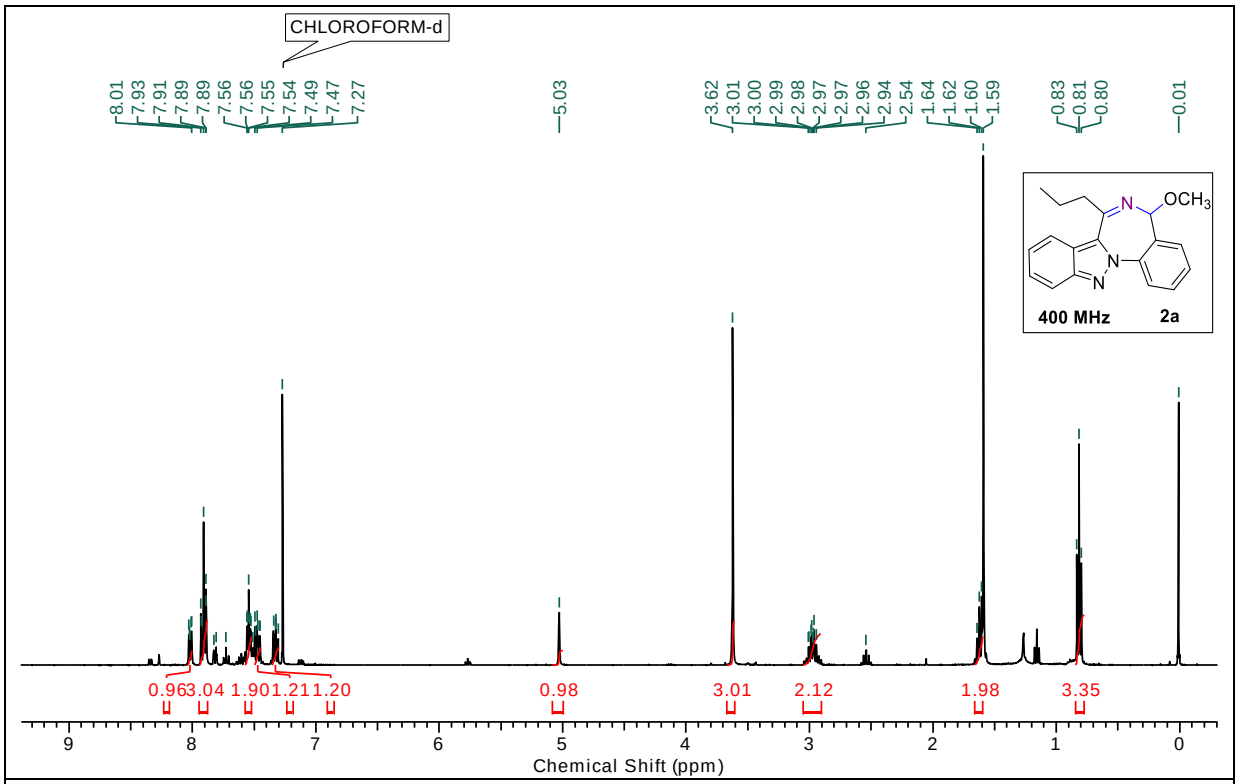

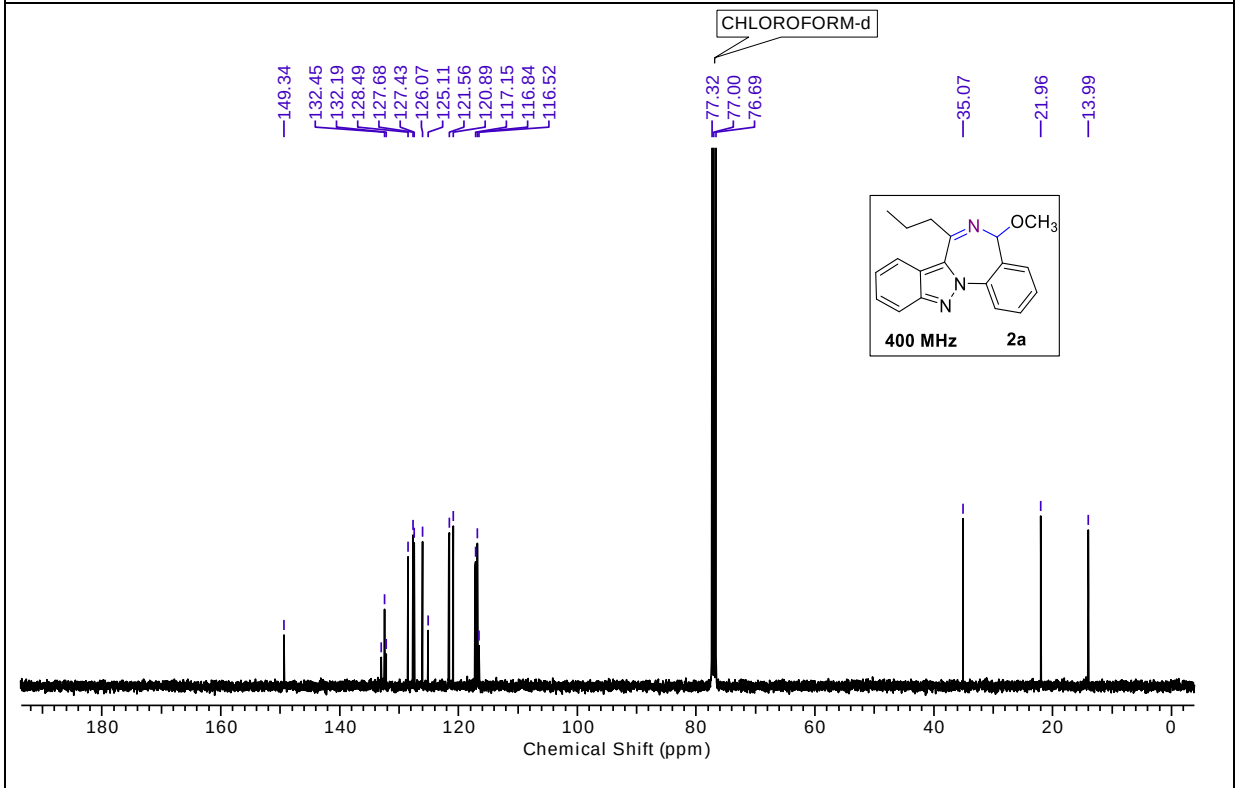

^{1}H /^{13}C NMR Spectrum of 2a in $CDCl_3$

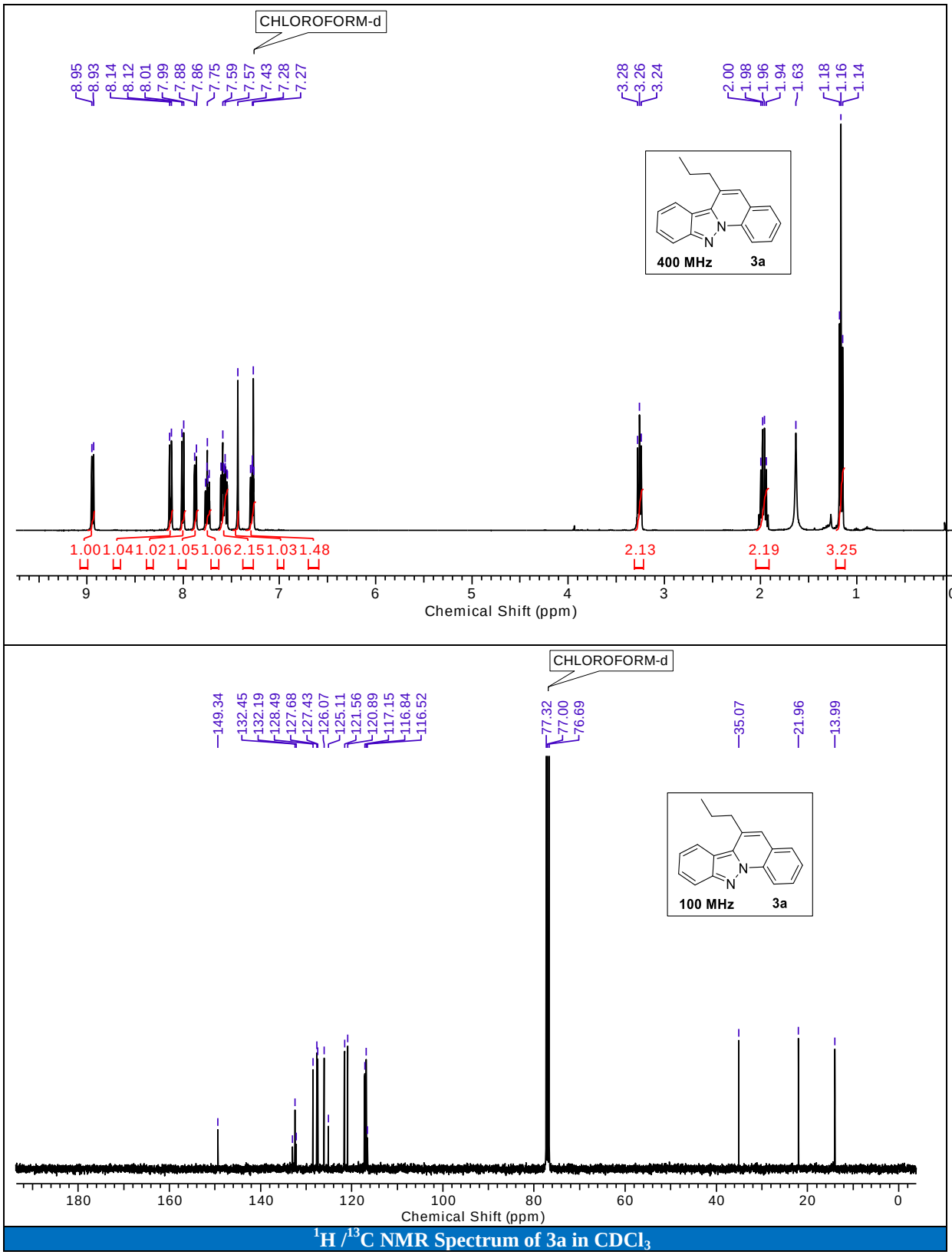

^{1}H /^{13}C NMR Spectrum of 3a in $CDCl_3$

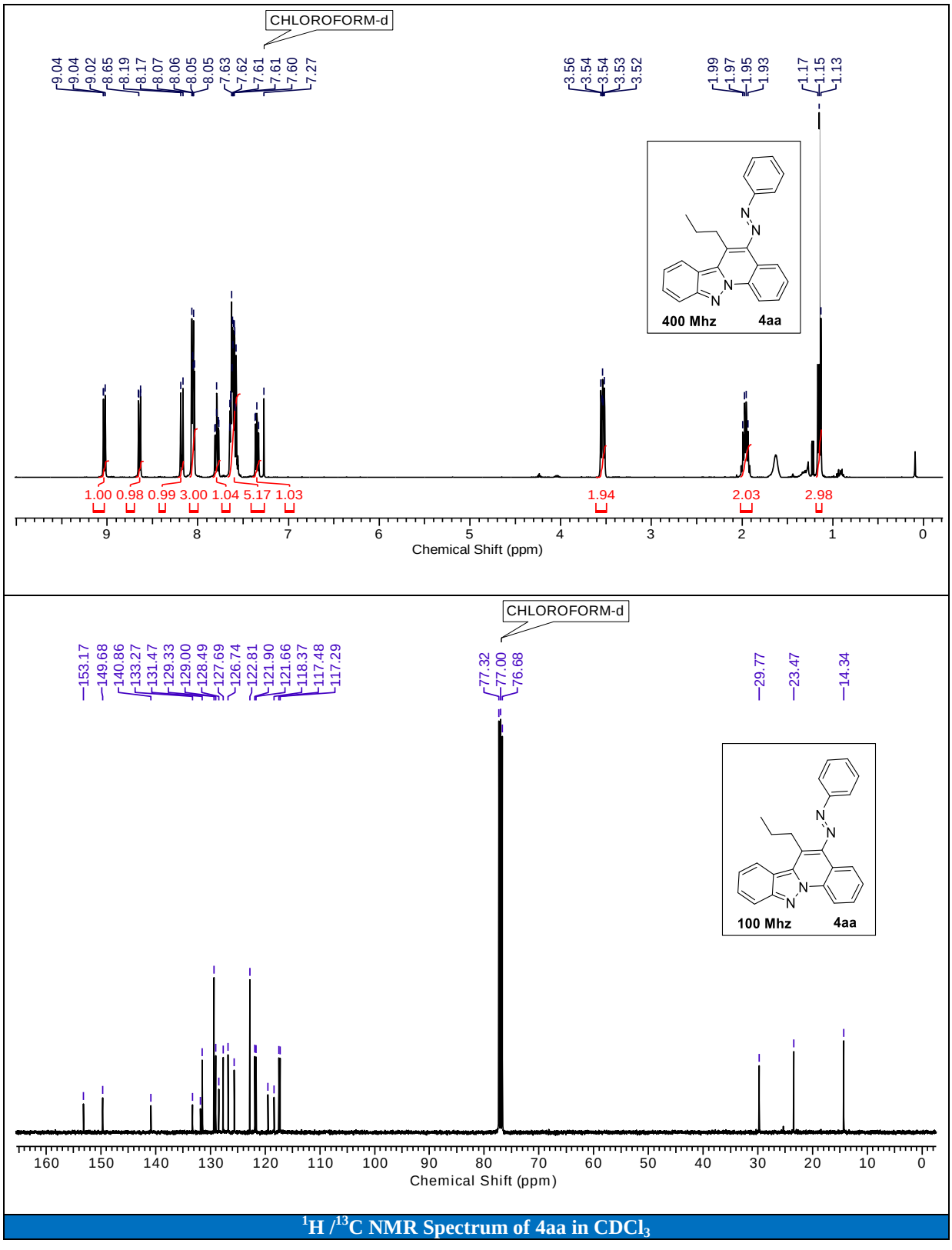

^{1}H /^{13}C NMR Spectrum of 4aa in $CDCl_3$

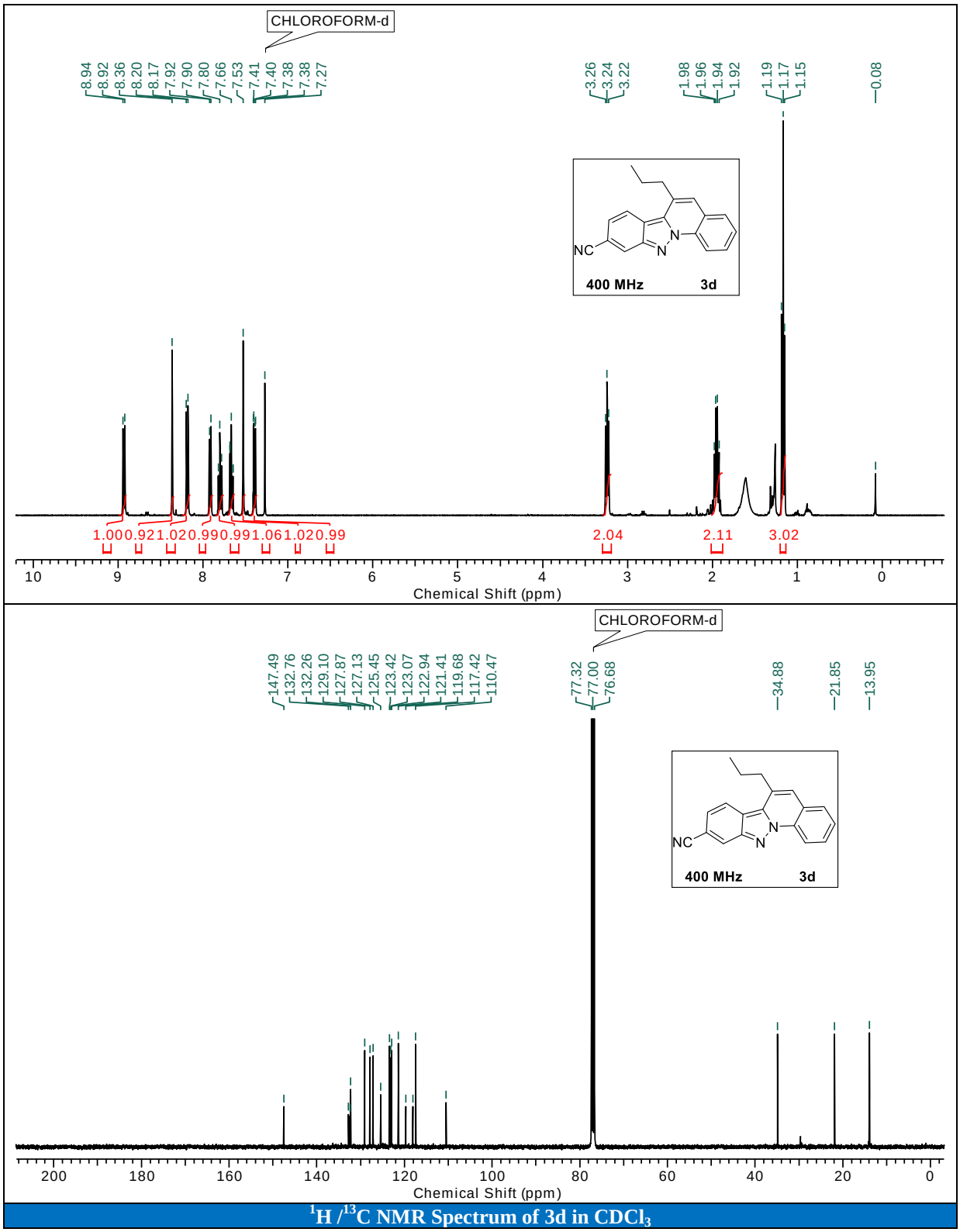

^{1}H /^{13}C NMR Spectrum of 3d in $CDCl_3$

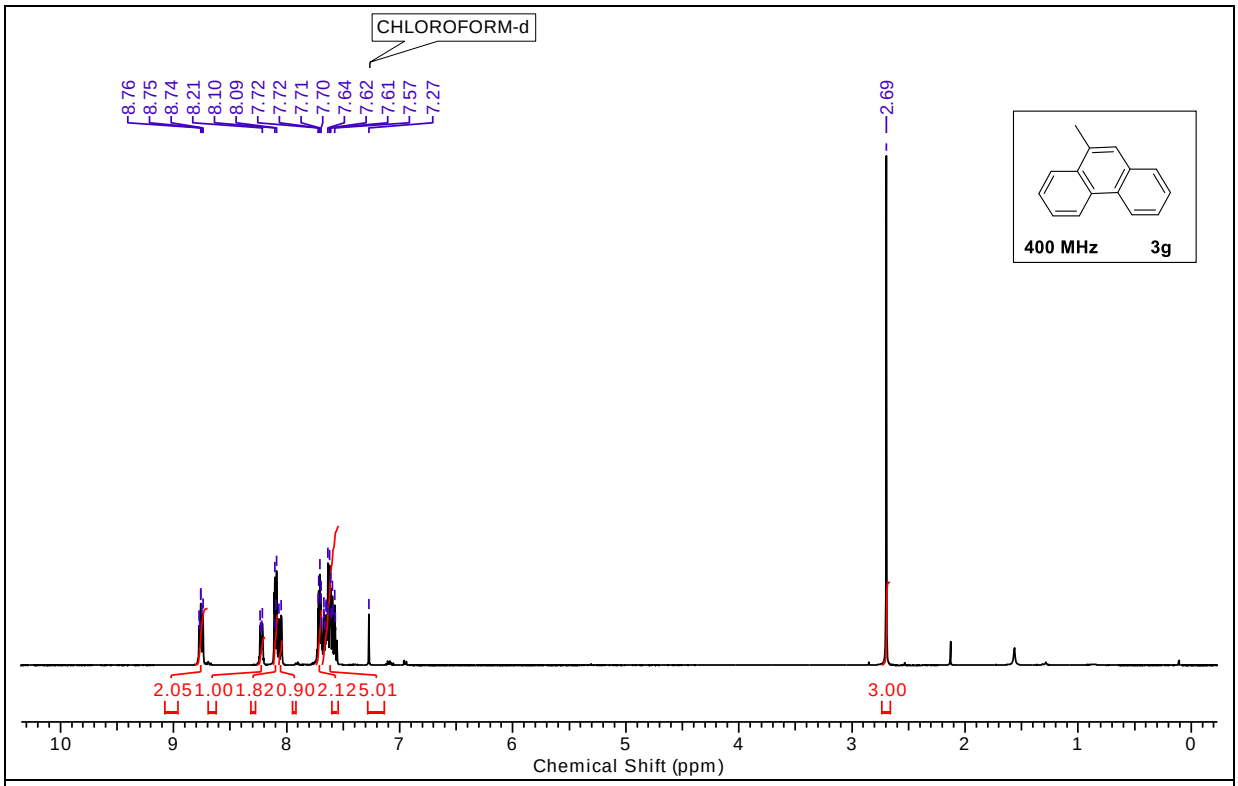

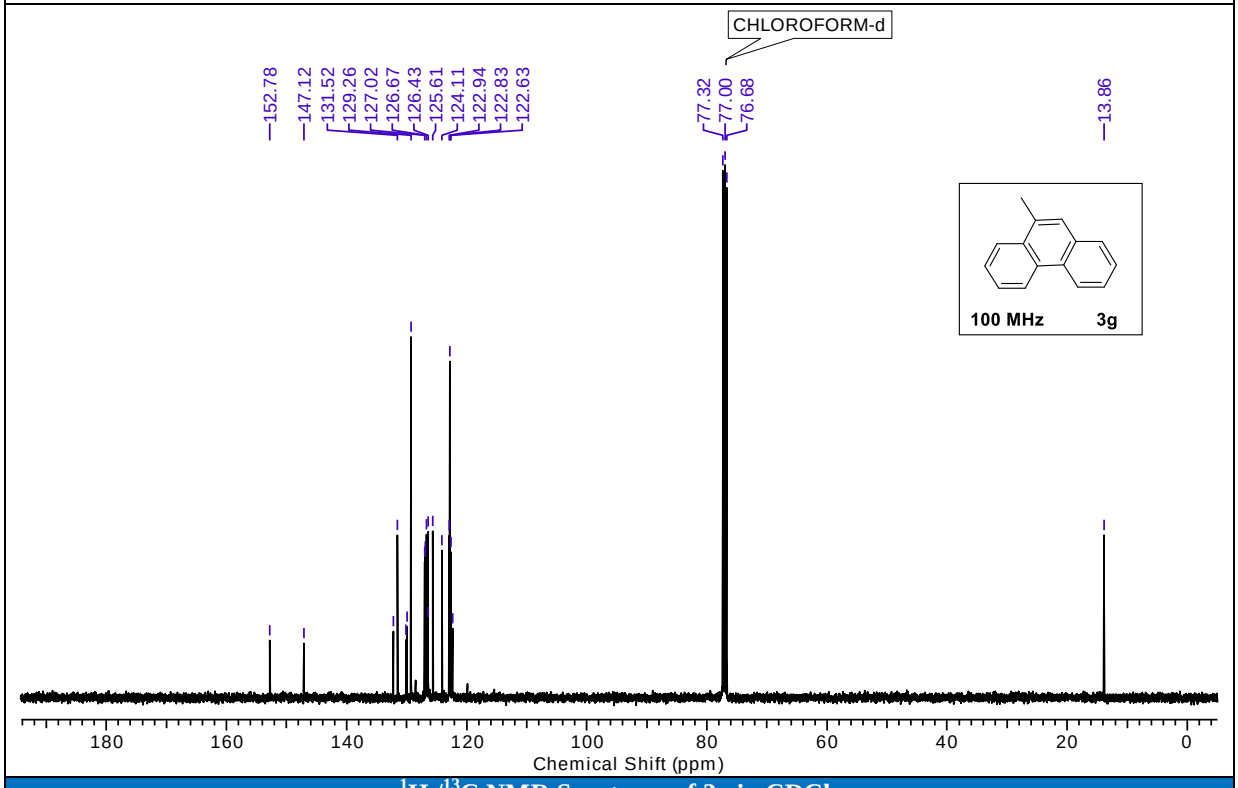

^{1}H /^{13}C NMR Spectrum of 3g in $CDCl_3$

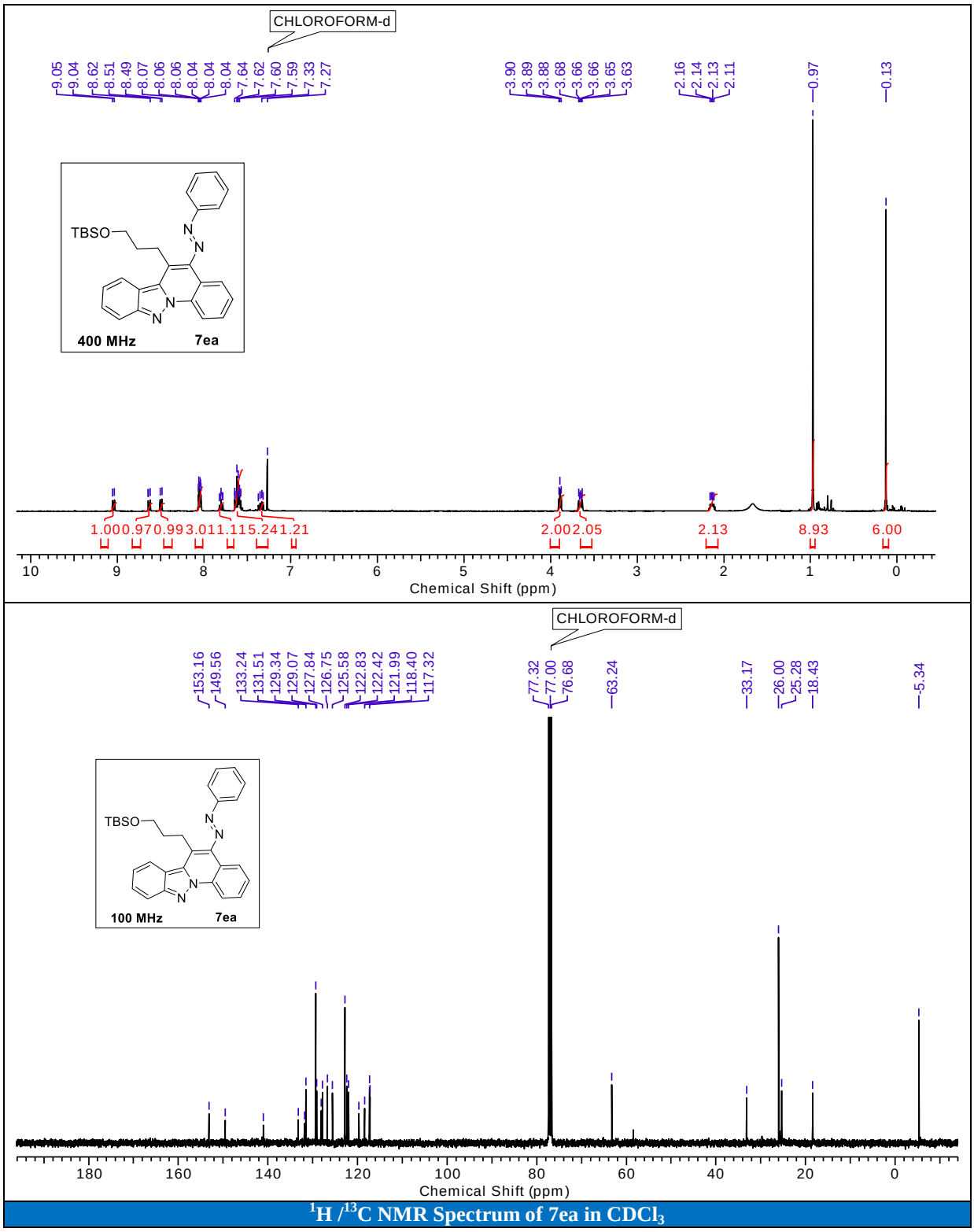

^{1}H /^{13}C NMR Spectrum of 7ea in $CDCl_3$

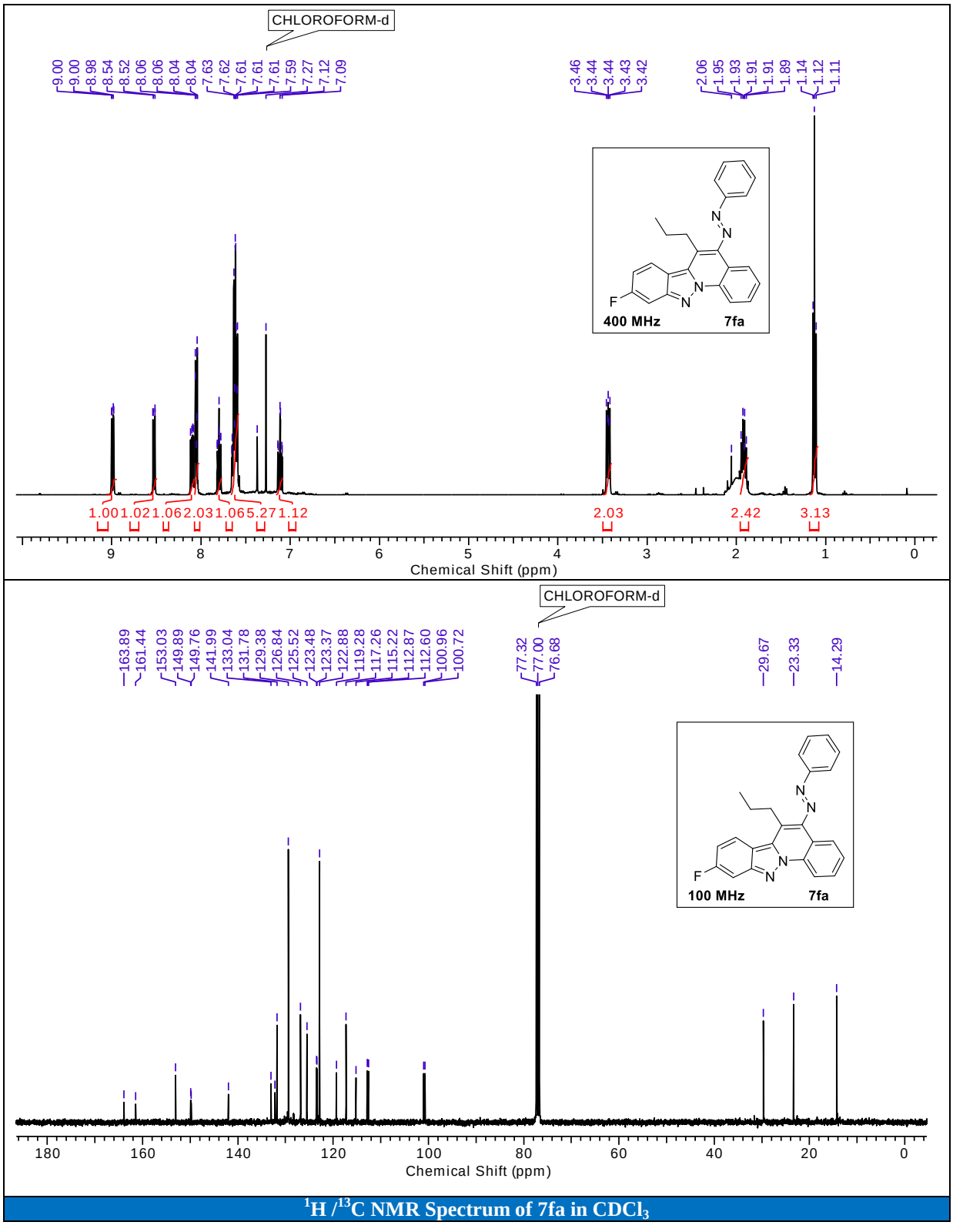

^{1}H /^{13}C NMR Spectrum of 7fa in $CDCl_3$

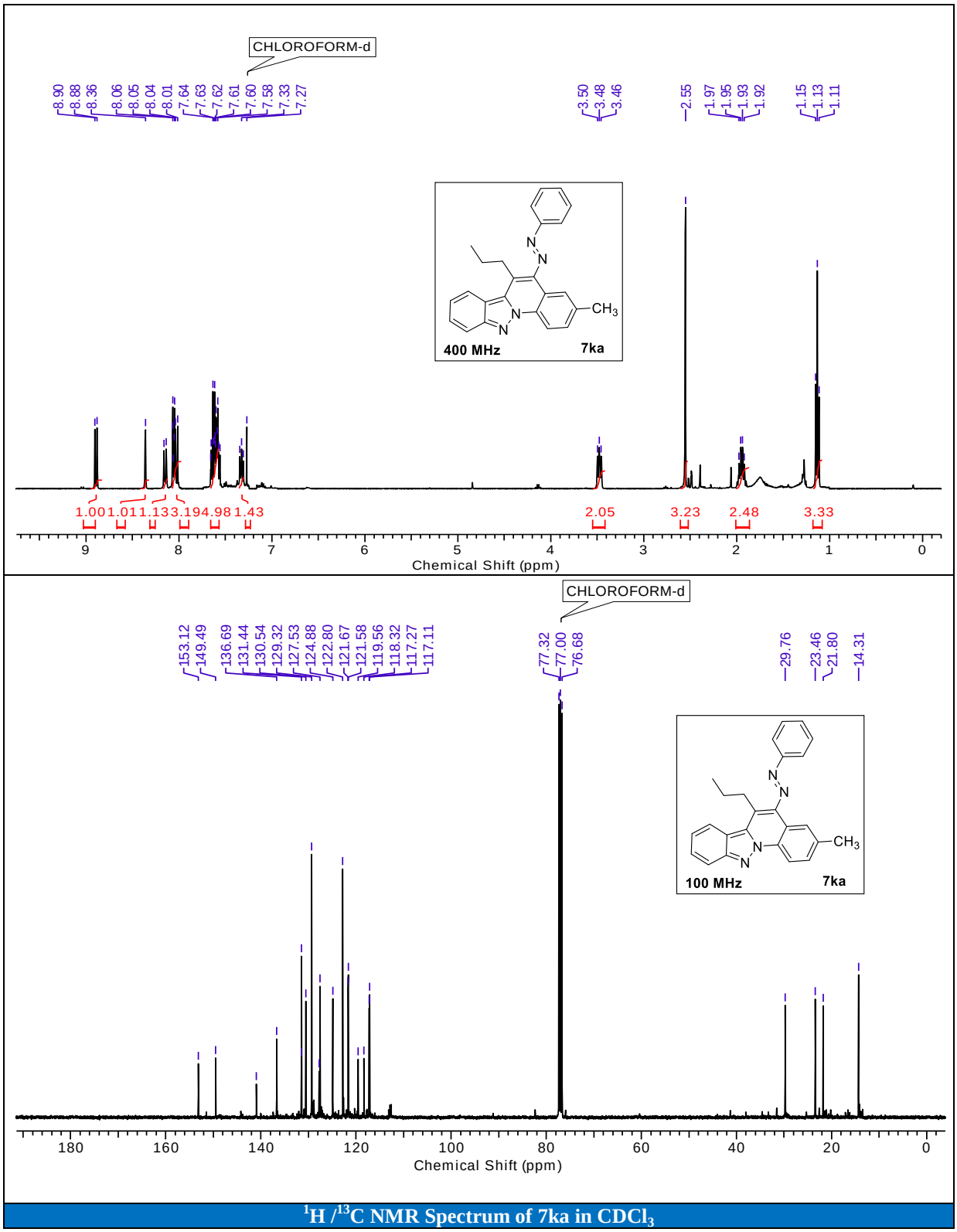

^{1}H /^{13}C NMR Spectrum of 7ka in $CDCl_3$

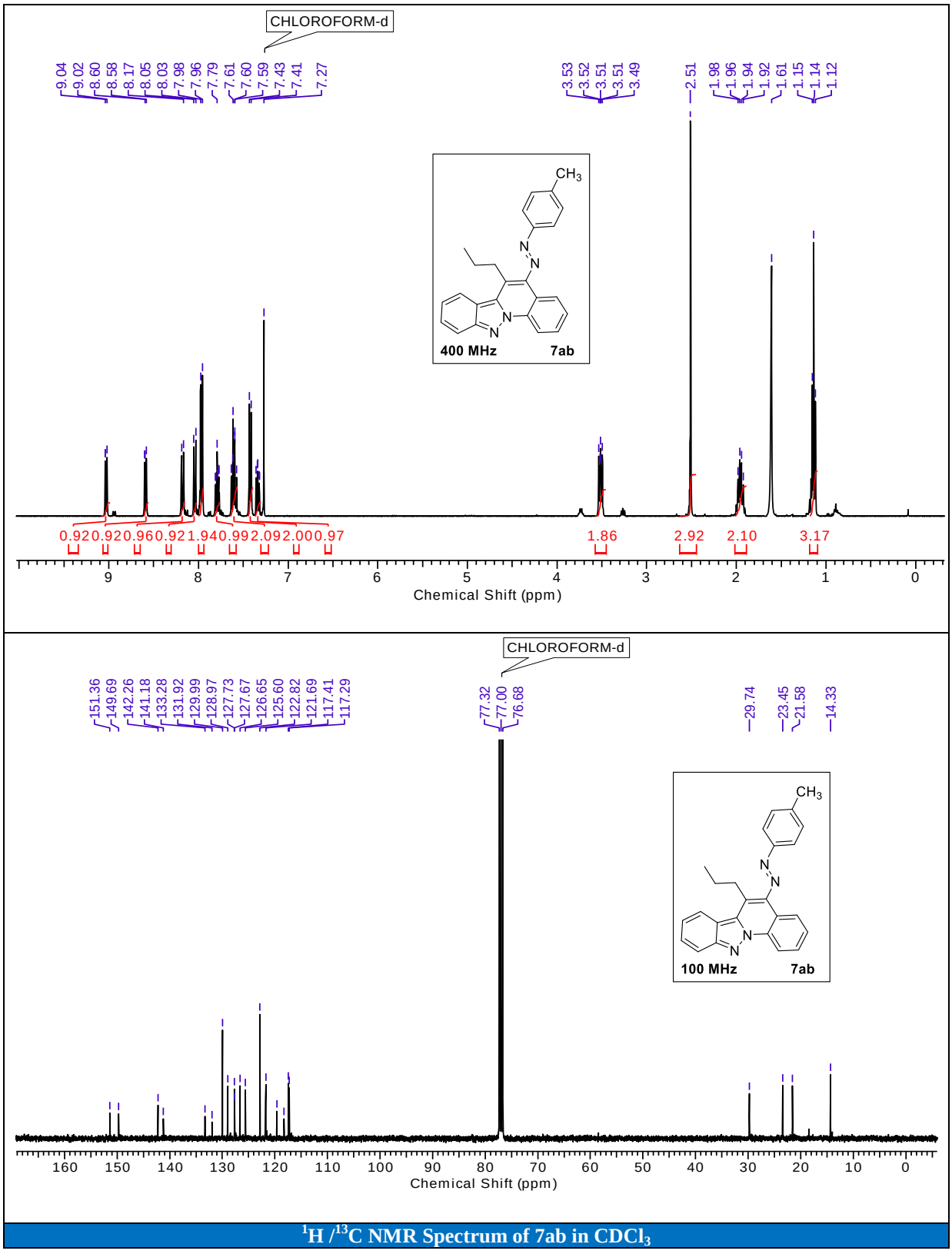

^{1}H /^{13}C NMR Spectrum of 7ab in $CDCl_3$

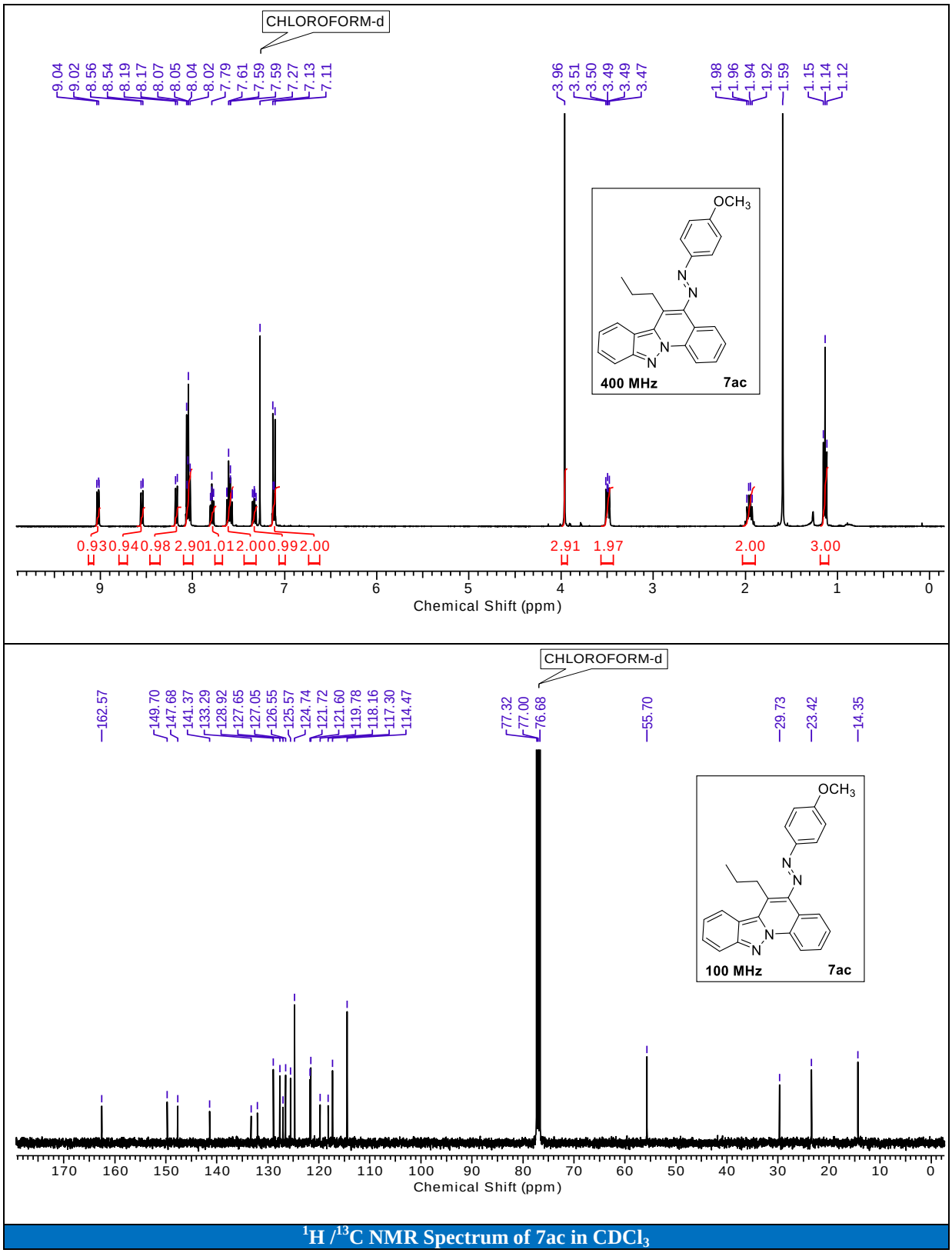

^{1}H /^{13}C NMR Spectrum of 7ac in $CDCl_3$

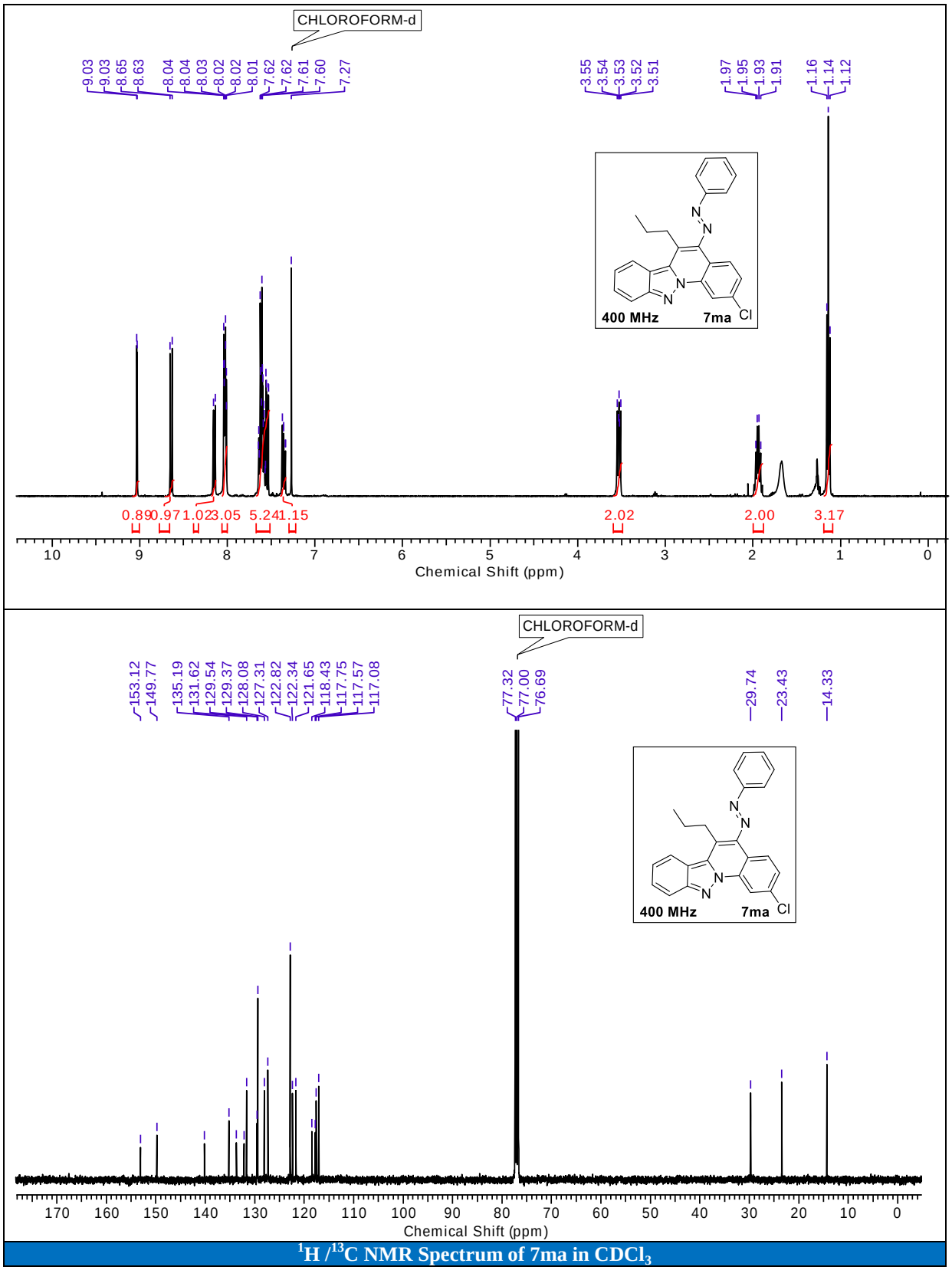

^{1}H /^{13}C NMR Spectrum of 7ma in $CDCl_3$

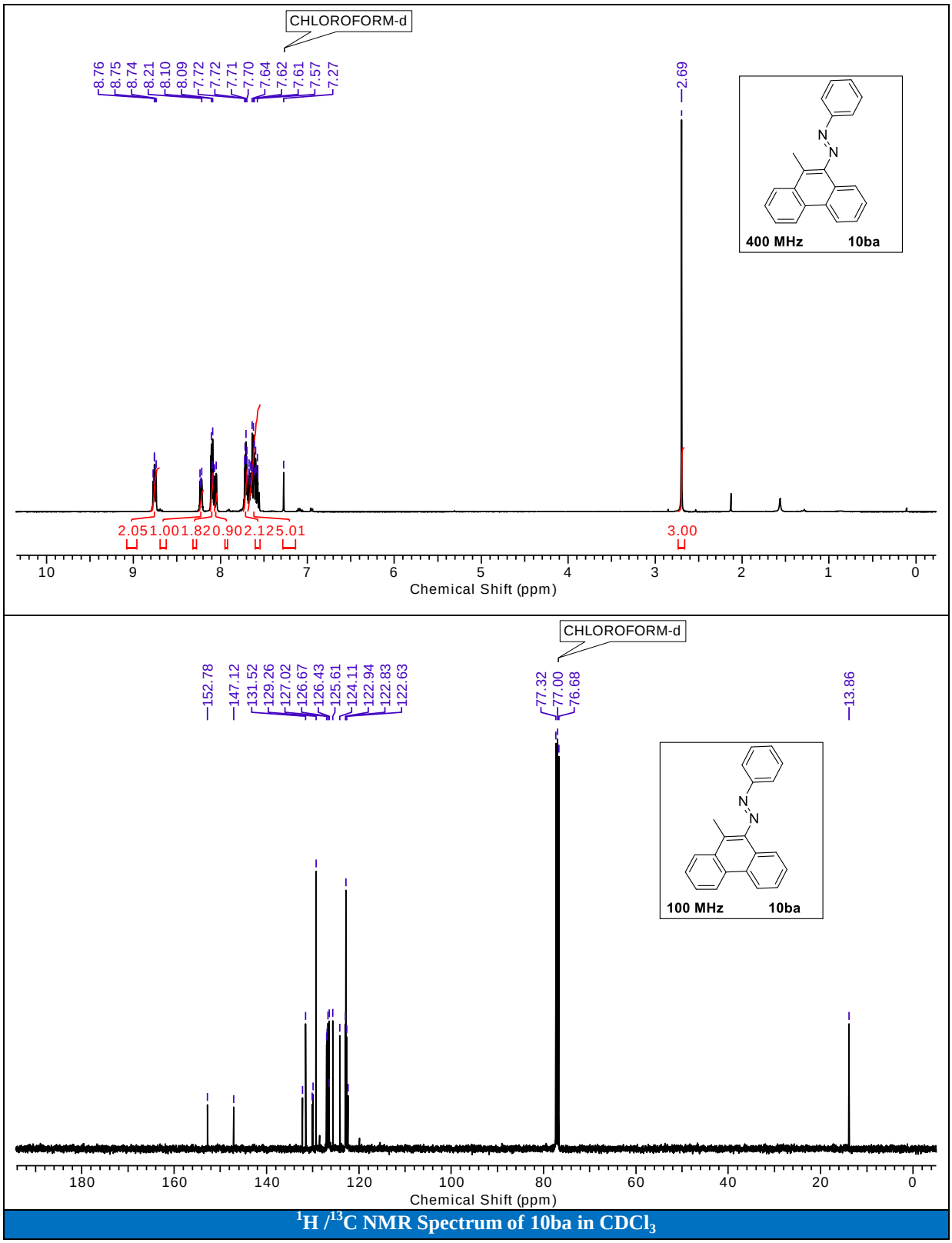

^{1}H /^{13}C NMR Spectrum of 10ba in $CDCl_3$

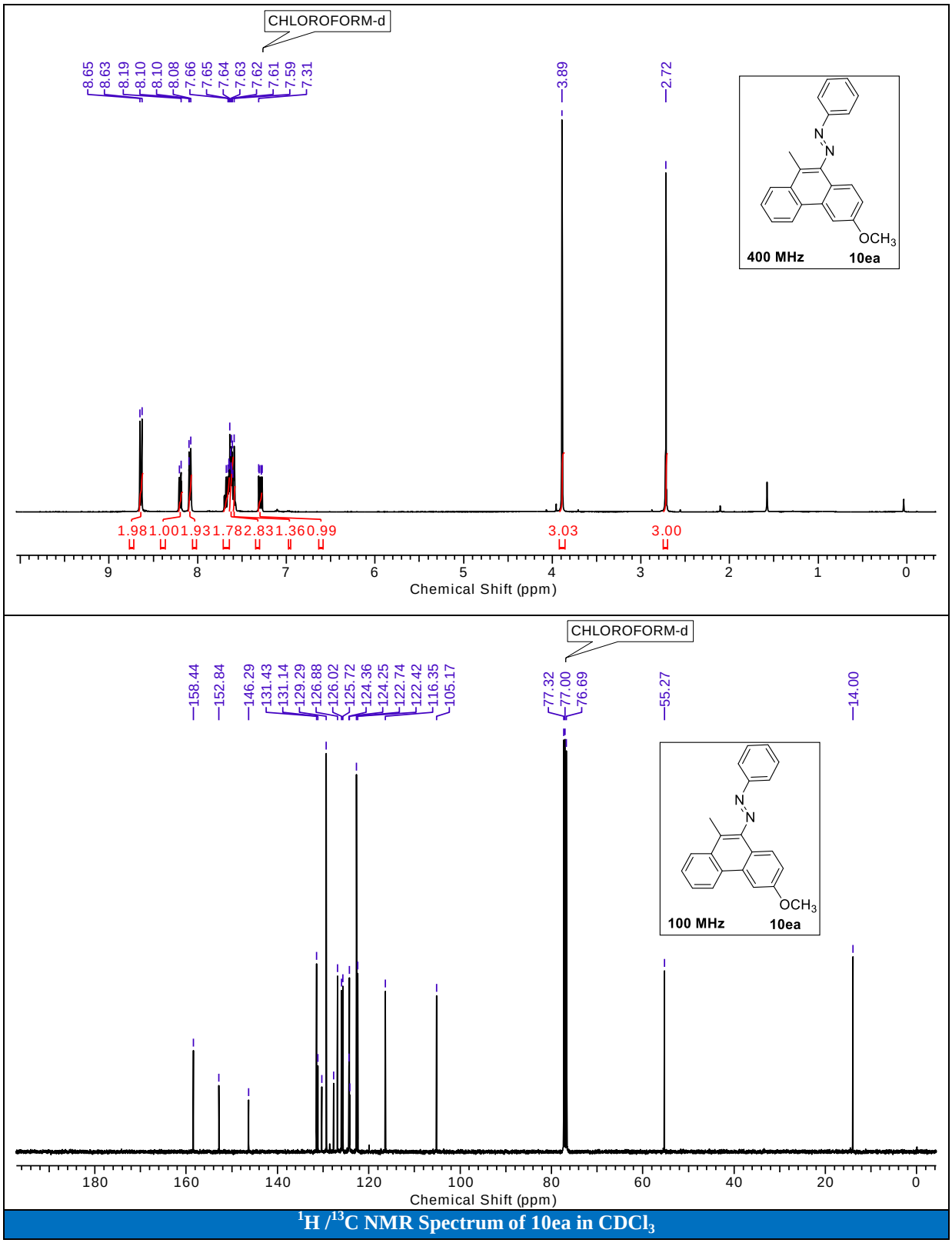

^{1}H /^{13}C NMR Spectrum of 10ea in $CDCl_3$

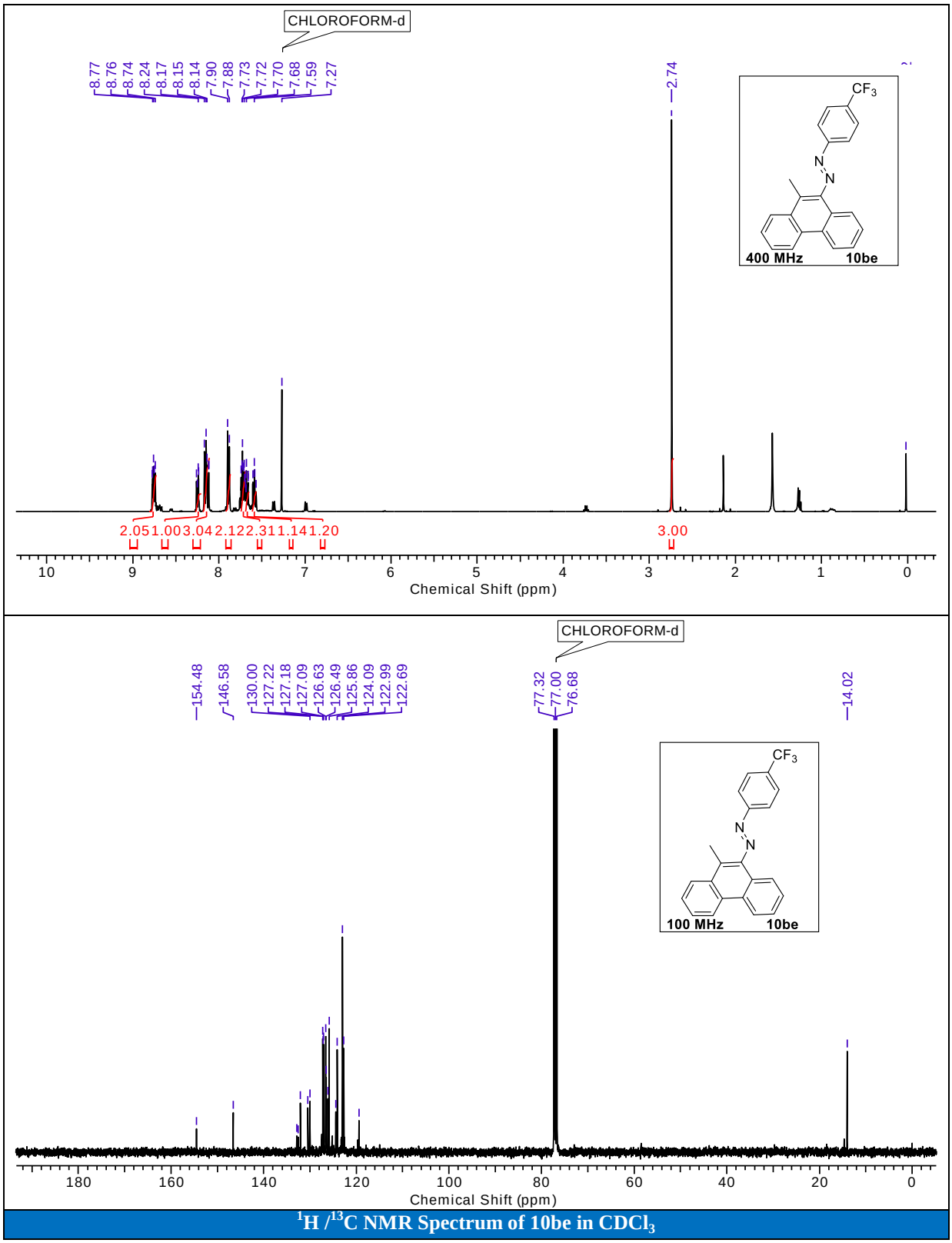

^{1}H /^{13}C NMR Spectrum of 10be in $CDCl_3$

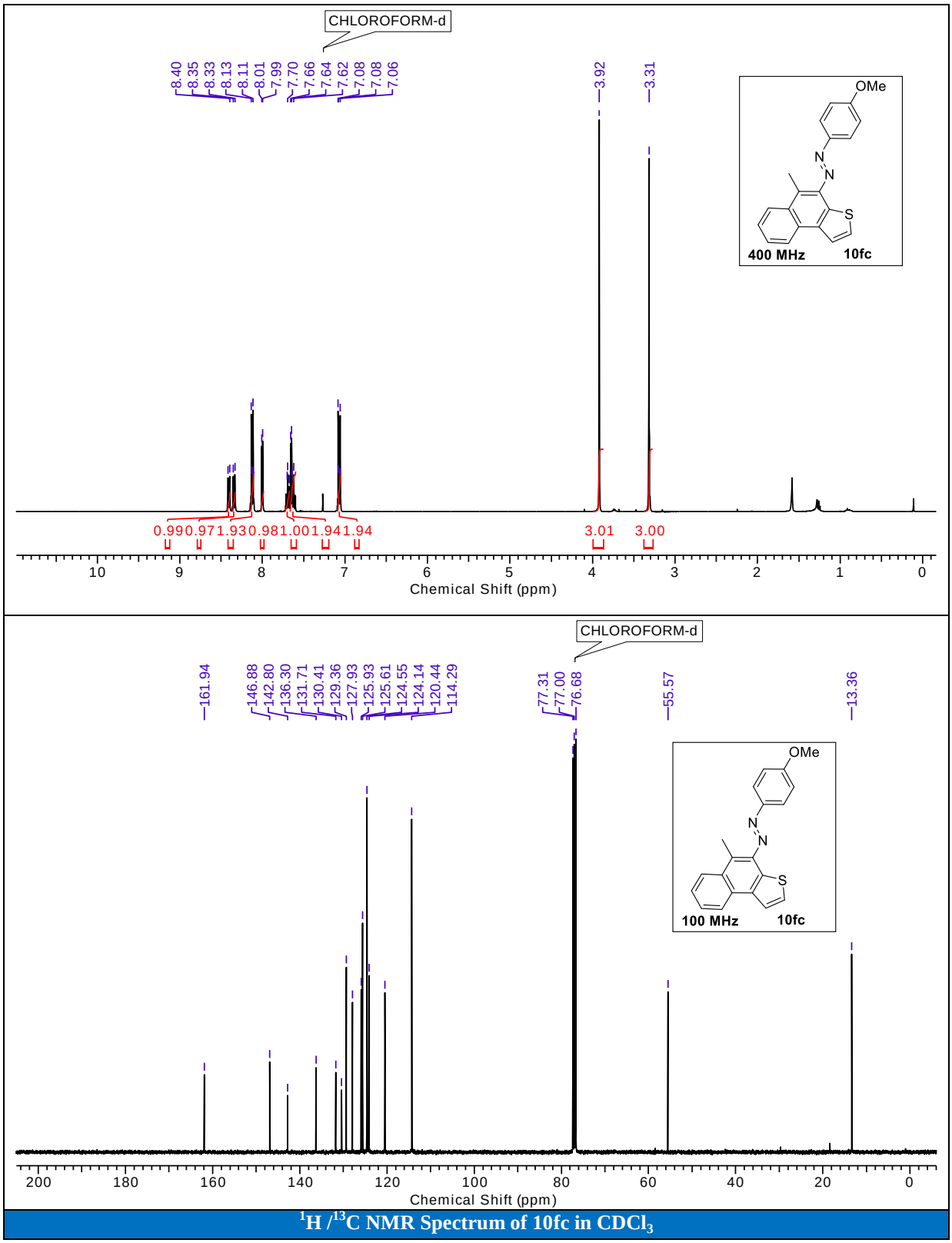

^{1}H /^{13}C NMR Spectrum of 10fc in $CDCl_3$

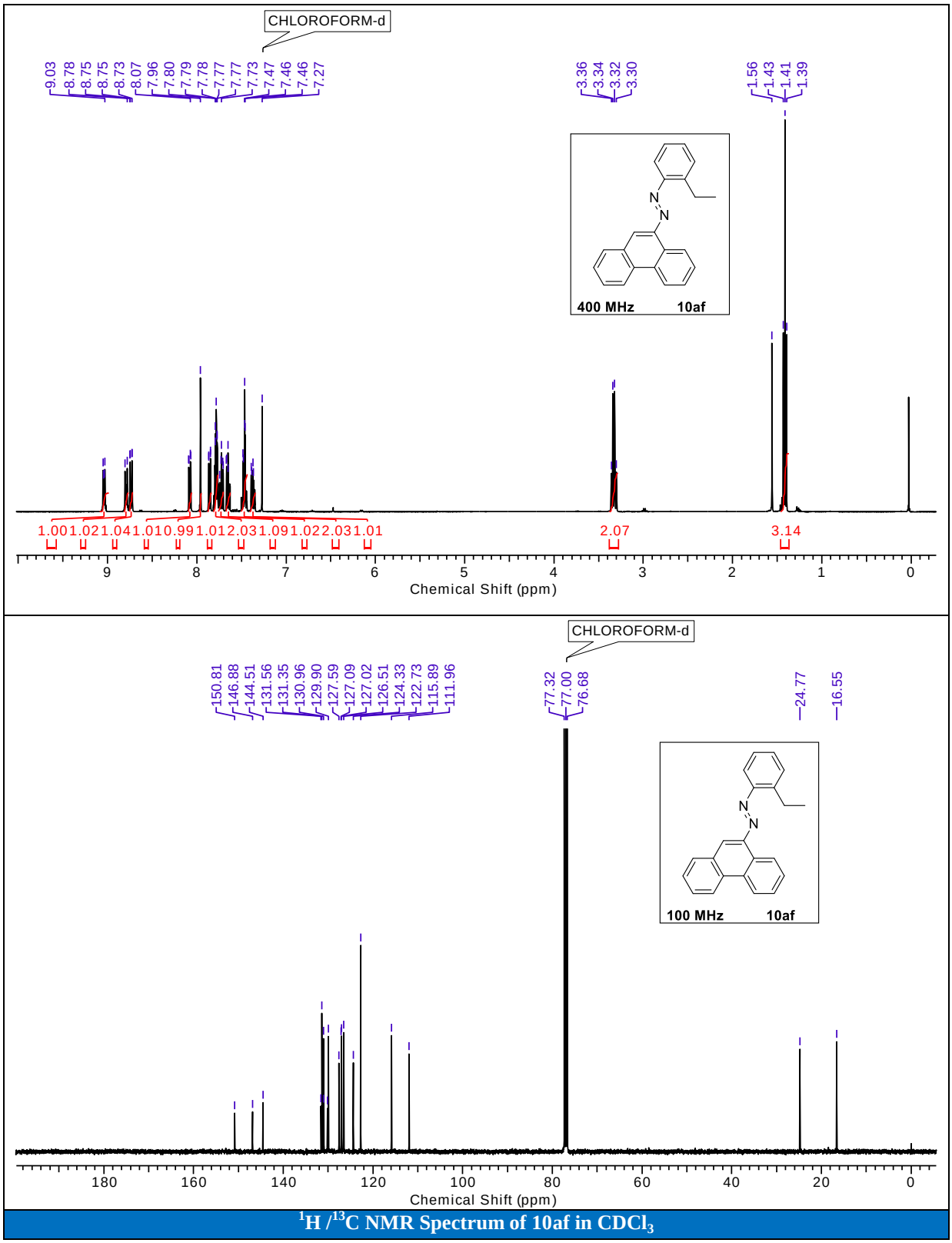

^{1}H /^{13}C NMR Spectrum of 10af in $CDCl_3$

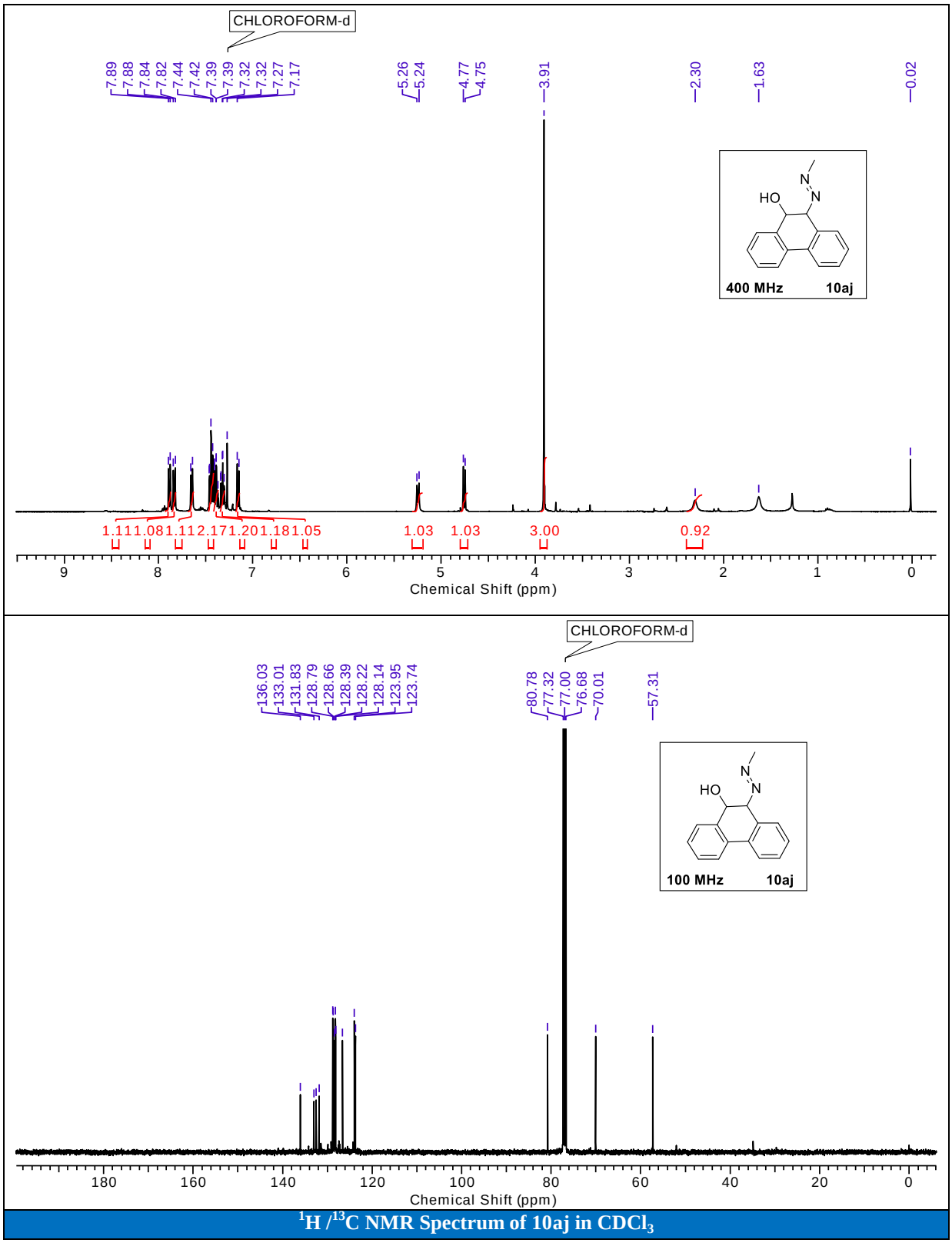

^{1}H /^{13}C NMR Spectrum of 10aj in $CDCl_3$

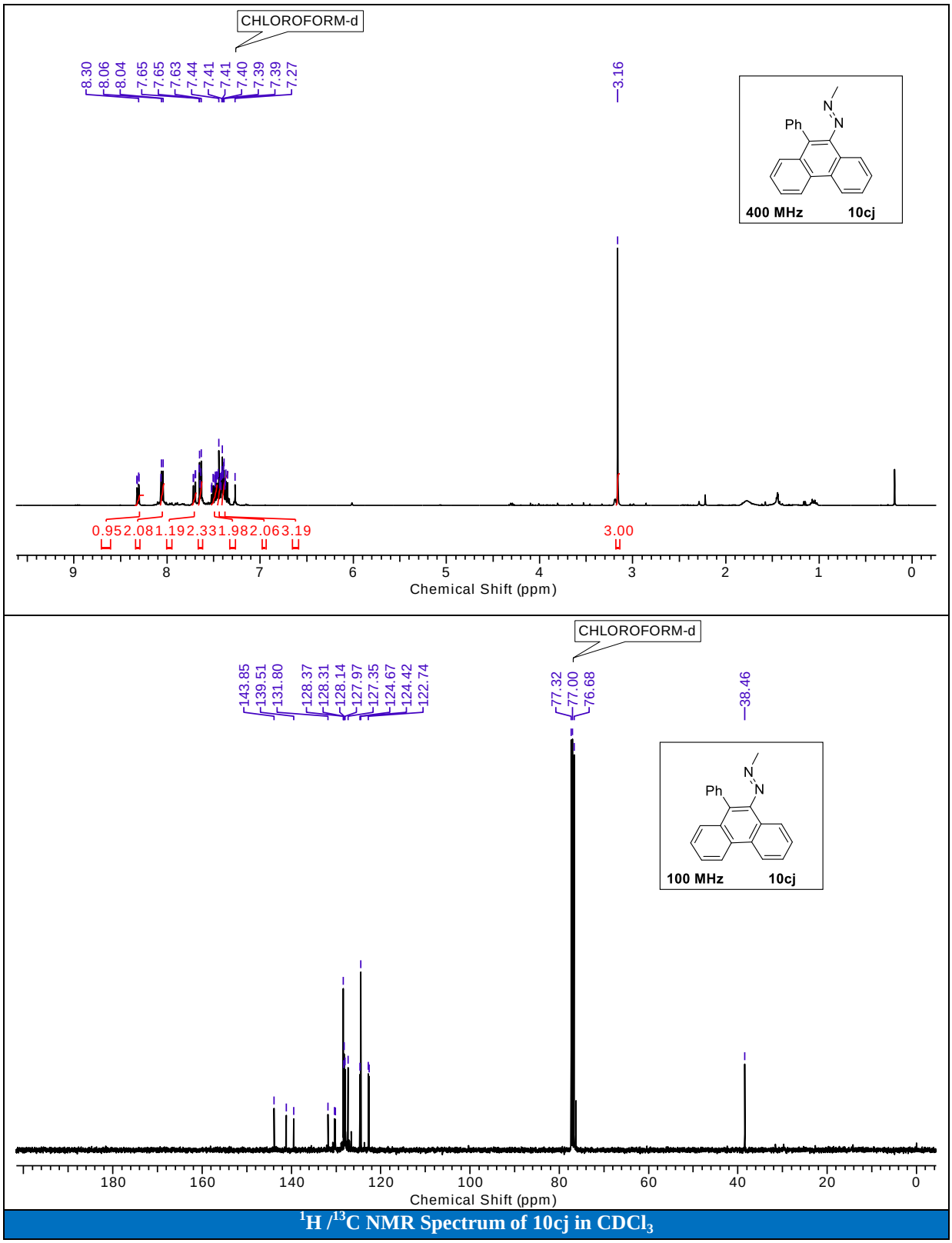

^{1}H /^{13}C NMR Spectrum of 10cj in $CDCl_3$

1) a) Flynn, A. B.; Ogilvie, W. W. *Chem. Rev.* **2007**, *107*, 4698. b) de Meijere, A. *Sci. Synth.* **2010**, *47*, 1. c) Stereoselective Alkene Synthesis, ed. by J. Wang, Topics in Current Chemistry, *327*, Springer, **2012**. d) Synthesis of Alkenes: How to Control the Stereochemistry of Alkenes, ed. by K. Ando, Essentials in Chemistry, *27*, Kyoritsu Shuppan, **2018**.

2) a) McMurry, J. E. *Acc. Chem. Res.* **1983**, *16*, 405. b) Kahn, B. E.; Rieke, R. D. *Chem. Rev.* **1988**, *88*, 733. c) McMurry, J. E. *Chem. Rev.* **1989**, *89*, 1513. d) Fürstner, A. Bogdanović, B. *Angew. Chem., Int. Ed.* **1996**, *35*, 2442. e) Modern Carbonyl Olefination: Methods and Applications, ed. by T. Takeda, Wiley-VCH: Weinheim, **2004**. f) Strategic Applications of Named Reactions in Organic Synthesis, ed.by L. Kurti, B. Czako, Academic Press, 2005. g) T. Takeda, A. Tsubouchi, *Org. React.* **2013**, *82*, 1.

3) Selected papers and review- a) Williams, D.R.; Heidebrecht, R.W.Jr., *J. Am. Chem. Soc.* **2003**, *125*, 1843. b) Shirani, H.; Bergman, J.; Janosik, T., *Tetrahedron* **2009**, *65*, 8350. c) Honda, T.; Namiki, H.; Nagase, H.; Mizutani, H., *Tetrahedron Lett*. **2003**, *44*, 3035. d) Shirani, H.; Janosik, T., *Organometallics* **2008**, *27*, 3960. e) Krayushkin1, M. M.; Yarovenko, V. N.; Semenov, S.L.; Zavarzin, I.V.; Martynkin, A. Yu.; Uzhinov, B. M., *Russian J. Org. Chem*. **2003**, *39*, 1356. f) Shirani, H.; Janosik, T., *J. Org. Chem.* **2007**, *72*, 8984. g) Sasaki, S.; Sasaki, K.;Yoshifuji, M., *J. Organomet. Chem*. **2011**, *696*, 3307.

4) Schreibmann, A. A. P. *Tetrahedron Lett.* **1970**, *11*, 4271.

5) Sharpless, K. B.; Umbreit, M. A.; Nieh, M. T.; Flood, T. C. *J. Am. Chem. Soc.* **1972**, *94*, 6538.

6) Mukaiyama, T.; Sato, T.; Hanna, J. *Chem. Lett.* **1973**, 1041.

7) Tyrlik, S.; Wolochowicz, I. *Bull. Soc. Chim. Fr.* **1973**, 2147.

8) a) McMurry, J. E.; Krepski, L. R. *J. Org. Chem.* **1976**, *41*, 3929. b) Baumstark, A. L.; McCloskey, C. J.; Witt, K. E. *J. Org. Chem.* **1978**, *43*, 3609. c) Hopf, H. Mlynek, C. *J. Org. Chem.* **1990**, *55*, 1361. d). McMurry, J. E.; Haley, G. J.; Matz, J. R.; Clardy, J. C.; Mitchell, J. *J. Am. Chem. Soc.* **1986**, *108*, 515. e) Memminger, K.; Oeser, T.; Müller, T. J. J. *Org. Lett*. **2008**, *10*, 2797. f) Eguchi, T.; Kano, H.; Arakawa, K.; Kakinuma, K. *Bull. Chem. Soc. Jpn.* **1997**, *70*, 2545. g) Eguchi, T.; Ibaragi, K.; Kakinuma, K. *J. Org. Chem.* **1998**, *63*, 2689.

9) Barton-Kellogg olefination, in Comprehensive Organic Name Reactions and Reagents, ed. by Z. Wang., Wiley: Weinheim, 2010.

10) Zhu, C.; Qiu, L.; Xu, G.; Li, J.; Sun. J. *Chem. Eur. J.* **2015**, *21*, 12871.

11) Selected papers on azo compound importance- a) Dakiky M.; Nemcova, I. *Dyes and Pigments*, **2000**, *44*, 181. b) A. Navarro and F. Sanz, *Dyes and Pigments*, **1999**, *40*, 131. c) Ali, Y.; Hamid, S.; Rashid, U. "Biomedical Applications of Aromatic Azo Compounds", *Mini-Reviews in Medicinal Chemistry* **2018**; 18(18). https://doi.org/10.2174/1389557518666180524113111.

12) a) Reddy, C. M.; Padmanabhan, K. A.; Desiraju, G. R. *Cryst. Growth Des.* **2006**, *6*, 2720; b) Ghosh, S.; Mishra, M. *Cryst. Growth Des.* **2021**, *21*, 2566.

ABSTRACT

Name of the Student: Pawan S. Dhote

Registration No. : 10CC17A26015

Faculty of Study: Chemical Science

Year of Submission: 2021

AcSIR academic centre/CSIR Lab:

CSIR-National Chemical Laboratory, Pune

Name of the Supervisor(s): Dr. C. V. Ramana

Title of the thesis: Internal Nitro-/Azidoalkyne Redox Processes in Heterocycle Synthesis and Metal free McMurry type Coupling

---

Gold catalyzed reactions are increasingly emerging in the literature since the past two decades. An interesting class of gold-catalyzed reactions that needs a mention here are the involvement of gold-carbenes in these processes. The transfer of an oxygen (*nucleophilic oxygen atom donors such as nitro, amine-/pyridine N-oxides, nitrone, sulfoxides, and epoxides*) or a nitrogen atom (*azides, nitrogen ylides, (benz)isoxazoles and anthranils*) to alkynes catalysed by gold-complexes proceeds *via* an addition−elimination process leading to α-oxo/α-imino gold carbenes respectively. What we tried to address in this thesis is: competitive inter- and intramolecular O- and or N-transfer to alkynes and subsequent trapping of the resulting gold carbenes, which led to complementary processes resulting in different heterocyclic cores.

Chapter 1 includes two sections, Section A deals with the interruption of the [Au]-catalyzed cycloisomerization of 2-alkynylnitrobenzenes leading to anthranils by the possible trapping of the postulated α-oxo gold carbene intermediates with an external N-centered nucleophile such as 2,1-benzo[*c*]isoxazole (anthranil) and 1,2-benzo[*d*]isoxazole for the synthesis of highly functionalized 3-acyl-(2-formylphenyl)-2H-indazoles with sequential C−O, C−N, and N−N bond formations and quinazoline N-oxides with sequential one C−O and two C−N bond formations respectively. Section B is focused on the synthesis of a tricyclic pseudoindoxyl scaffold that comprises of cycloisomerizarion of 2-nitroalkynylbenzenes and subsequent [3+3] cycloaddition of resulting isatogens with donor–acceptor (DA)-cyclopropanes in a one-pot protocol. Chapter 2 covers the possible interruption of the azidoalkyne cycloisomerization by employing anthranil and 1,2-benzo[*d*]isoxazole. In case of 1,2-benzo[*d*]isoxazole, the intermolecular nitrene transfer was more facile and provided quinazoline. However, when anthranil was employed, it seems that the intramolecular nitrene transfer was exclusive and provided the 3-iminoindoline derivatives exclusively. As a part of showing the synthetic utility of the dicarbonyl compounds obtained from the nitroalkynes cycloisomerization, the attempted selective monohydrazone synthesis led to us restablish an old reaction - Bacon's dicarbonyl coupling, which ended up with the synthesis of indazolo[2,3-*a*]quinoline and 5-(aryl/alky diazenyl)indazolo[2,3-*a*]quinoline derivatives (single crystal X-ray diffraction studies shows promising flexible π-conjugated materials) which is enclosed in Chapter 3.

LIST OF PUBLICATIONS

List of Publications Emanating from the Thesis work

1. **Dhote, P. S.**; Ramana, C. V. One-Pot Au[III]-/Lewis Acid Catalyzed Cycloisomerization of Nitroalkynes and [3 + 3] Cycloaddition with Donor–Acceptor Cyclopropanes. *Org. Lett.* **2019**, *16*, 6221–6224.
2. **Dhote, P. S.**; Ramana, C. V. Interrupting the [Au]-Catalyzed Nitroalkyne Cycloisomerization: Trapping the Putative α-Oxo Gold Carbene with Benzo[*c*]isoxazole. *Org. Lett.* **2021**, *23*, 2632–2637.
3. **Dhote, P. S.**; Pund, K.; Ramana, C. V. Intermolecular Interception of α-Oxo Gold Carbenes of Nitroalkyne Cycloisomerization with 1,2-Benzo[*d*]isoxazole: Synthesis of Functionalized Quinazoline 1-Oxides. *J. Org. Chem.* **2021**, 86, 10874–10882.
4. **Dhote, P. S.**; Halnor, S. V.; Ramana, C. V. Gold-Catalysed Nitroalkyne Cycloisomerization – Synthetic Utility. *Chem. Rec.* **2021** (doi.org/10.1002/tcr.202100111).
5. Raj, K. V.; **Dhote, P. S.**; Vanka, K.; Ramana, C. V. Gold-Catalyzed Complementary Nitroalkyne Internal Redox Process: A DFT Study. *Front. Chem.* **2021** (doi:10.3389/fchem.2021.689780).
6. **Dhote, P. S.**; Patel, P.; Vanka, V.; Ramana, C. V. Total synthesis of the pseudoindoxyl class of natural products. *Org. Biomol. Chem.* **2021**, (doi:10.1039/d1ob01285a)
7. **Dhote, P. S.**; Ramana, C. V. Competing Intra- *vs* Intermolecular Nitrene Transfer in the [Au]-Catalysed Reaction of 2-Alkynylphenylazides. *Chem. Sci.* (Submitted).
8. **Dhote, P. S.**; Ramana, C. V. Phenyl Hyrdrazine Enabled Umpolung Cyclization of 2,2'-dicarbonylbiaryls for the Construction of Poly (hetero)aromatic compounds. (Manuscript under Submission)

List of Publications Non-Emanating from the Thesis Work

1. **Dhote, P. S.**; Ramana, C. V.; Tothadi, S. Design and Synthesis of Elastic Crystals of 2H-indazole π-conjugated molecules (Manuscript under submission)

Patents- *Nil*

List of Posters presented with details

1. 13th CRSI-RSC Joint Symposium (CRSI-NSC-24) at IIT Madras. (7th Feb **2019**)

and

24th CRSI National Symposium in Chemistry at CSIR-CLRI, Chennai. (8-10th Feb, **2019**)

Title: Gold/Lewis Acid Catalysed Cycloisomerisation and [3+3] Cycloaddition of Nitroalkynes with Donor-Acceptor Cyclopropane

Abstract: The 2,2-disubstitutedpseudoindoxyl skeleton is one of the rarely found substructural unit in bis-indole class of natural products. Natural products like Austamide, Hunteracine pseudoindoxyl, Isatisine A, Rauniticine pseudoindoxyl are some of the representative members of this class having interesting biological activities. In this poster, we provide the details of a simple one-pot protocol for the synthesis of tricyclic pseudoindoxyl scaffold from simple 2-nitroalkynylbenzenes comprising of a gold(III) catalysed nitroalkyne cycloisomerisation leading to isatogen2 and then its [3+3] cycloddition with DA cyclopropanes mediated by a suitable Lewis acid.

2. National Science Day Celebration held at CSIR-NCL, Pune, India. (24–25 Feb **2020**)

Title: One-Pot Au[III]-/Lewis Acid Catalyzed Cycloisomerization of Nitroalkynes and [3 + 3]Cycloaddition with Donor–Acceptor Cyclopropanes.

Abstract: A one-pot protocol for the synthesis of a tricyclic pseudoindoxyl scaffold from 2-nitroalkynylbenzenes, comprising of an Au(III)-catalyzed nitroalkyne cycloisomerization leading to isatogen and its [3 + 3]-cycloaddition with donor–acceptor cyclopropanes mediated by a suitable Lewis acid, has been developed.

List of Conference Attended with Details

1. 1st Virtual International Symposium on C–H Activation organized by University of Goettingen, Germany on 29th July, 2020
2. First Virtual JNOST Conference organised by IISC-Bangalore on 31st Oct-1st Nov 2020.
3. Recent Trends in Chemical Sciences – Organic Bio-Chemistry 2020 (RTCS-OBC 2020) organised by IISER Kolkata on 26th -29th Dec 2020.
4. Virtual Photo-Cat Symposium 2021 organised by Royal Flemish Chemical Society (KVCV) and University of Antwerp, Belgium on 20th -22th Sept, 2021

OL | Organic Letters

Letter

Cite This: Org. Lett. 2019, 21, 6221−6224

pubs.acs.org/OrgLett

One-Pot Au[III]-/Lewis Acid Catalyzed Cycloisomerization of Nitroalkynes and [3 + 3]Cycloaddition with Donor−Acceptor Cyclopropanes

Pawan S. Dhote[†,‡] and Chepuri V. Ramana*[,†,‡]

[†]Division of Organic Chemistry, CSIR-National Chemical Laboratory, Dr. Homi Bhabha Road, Pune 411 008, India

[‡]Academy of Scientific and Innovative Research (AcSIR), Anusandhan Bhawan, 2 Rafi Marg, New Delhi 110002, India

Supporting Information

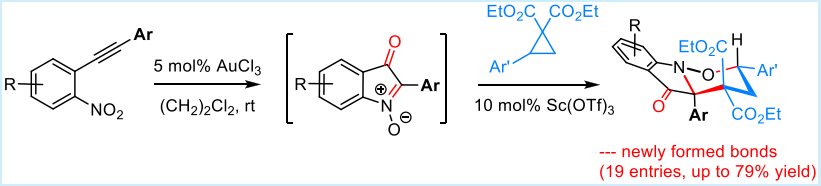

ABSTRACT: A one-pot protocol for the synthesis of a tricyclic pseudoindoxyl scaffold from 2-nitroalkynylbenzenes, comprising of an Au(III)-catalyzed nitroalkyne cycloisomerization leading to isatogen and its [3 + 3]-cycloaddition with donor−acceptor cyclopropanes mediated by a suitable Lewis acid, has been developed.

Pseudoindoxyl natural products occupy a special place in the indole alkaloids family because of their fascinating molecular structures and promising biological activities (see Figure 1).[1] In general, the biosynthesis of these pseudoindoxyl

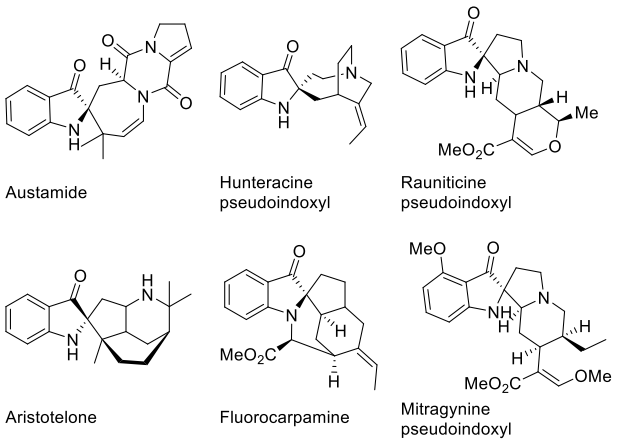

Figure 1. Representative pseudoindoxyl natural products.

natural products comprises of an oxidative rearrangement of the corresponding indole alkaloids.[2] Indeed, this is one of the key approaches employed in the synthesis of the pseudoindoxyl core.[3] However, the competing formation of 2-oxindole derivatives during the rearrangement and control over the stereochemistry of the newly generated quaternary carbon center are the major concerns.[4] In this regard, alternative approaches for constructing the pseudoindoxyl (2,2-disubstituted 1,2-dihydro-3*H*-indol-3-one) core have been explored.[5] Among these, the metal catalyzed cycloisomerization of *o*-nitrotolans[6] and *o*-azidotolans[7] and subsequent inter- and intramolecular transformations have emerged as simple and effective tools to create pseudoindoxyl cores. In this manuscript, we document a one-pot gold(III)-catalyzed nitroalkyne cycloisomerization of 2-nitrotolans and a Lewis acid catalyzed [3 + 3]-cycloaddition of the intermediate isatogen with donor−acceptor (DA) cyclopropanes leading to 2,2-spiro pseudoindoxyl derivatives. The cycloaddition reaction of DA-cyclopropanes is one of the important reactions unveiled during the past decade.[8] The (homo) cycloaddition reactions of DA-cyclopropanes with various dipolarophiles, in general,[9] and with nitrones,[10] in particular, have been well explored in natural products synthesis.[11] However, the same with isatogens has not yet been examined. Given the fact that the preparation of isatogens from nitroalkynes and the [3 + 3]-cycloaddition reaction of DA-cyclopropanes require Lewis acids, it was assumed that there is a chance of combining both the reactions in one-pot, which would lead to fused tricyclic pseudoindoxyl derivatives.[12]

With this intent, in order to identify the suitable Lewis acid for the [3 + 3]-cycloaddition, 2-phenyl- and 2-*n*pentyl isatogens **1a** and **1b**, respectively, as well as commonly employed DA-cyclopropane diethyl 2-phenylcyclopropane-1,1-dicarboxylate (**2a**) have been selected as the suitable partners and screened with the commonly employed $Sc(OTf)_3$ and $Yb(OTf)_3$ for the projected [3 + 3]-cycloaddition.[10] With both Lewis acids, the cycloaddition reaction of **2a** with **1a** and **1b** was facile at rt and provided the corresponding cycloaddition products **3aa** and **3ba** with complete diastereoselectivity. The yields in general were also good and that with $Sc(OTf)_3$ were best. The relative

Received: June 13, 2019
Published: August 5, 2019

DOI: 10.1021/acs.orglett.9b02035
Org. Lett. 2019, 21, 6221−6224

stereochemistry of the newly formed 1,2-oxazine ring has been proposed by considering the previous reports on the cycloaddition with cyclic nitrones where both experimental and theoretical calculations favored a single diastereomer having cis-orientation of the 1,4-phenyl substituents (see Figure S1, SI for the NOESY spectra of cycloaddition product **3eb** synthesized later and the representative nOes observed that support the assigned configuration/conformation).[10a,e,f] Nonetheless, this early success with the cycloaddition of isatogens with DA-cyclopropanes prompted us to proceed for the examination of the possibility of carrying out nitroalkyne cycloisomerization and cycloaddition in one-pot.

The nitroalkyne cycloisomerization leading to isatogens has been explored with [Au]- and [Pd]-complexes, though the former has a limitation of requirement of aryl substituent on the other side of alkyne (with simple alkyl substituents, it leads to isomeric anthranil derivatives).[6a] [Pd]-complexes generally lead to the isatogens.[6b] Keeping this in mind, the initial studies have been carried out by employing the nitroalkynes **4a**/**4b** and DA-cyclopropane **2a**. Initial experiments employing $PdCl_2[CH_3CN]_2$ for cycloisomerization and $Sc(OTf)_3$ for cycloaddition have been carried out in acetonitrile at rt. The procedure followed involved the stirring of a solution of nitroalkynes **4a**/**4b** along with 1.5 equiv of **2a** in the presence of 10 mol % [Pd]-complex in acetonitrile at rt (for 4−10 h), subsequent addition of 10 mol % of $Sc(OTf)_3$, and continued stirring for an additional 12−24 h. As shown in Scheme 1 (eq 2), in both cases, only corresponding isatogens were isolated. Changing the solvent to dichloromethane hampered the initial cycloisomerization itself. This led us to look at the [Au]-complexes, however, with due consideration of employing only aryl substituted derivatives such as **4a**.

Scheme 1. [3 + 3]-Cycloaddition of 2-Phenyl/*n*-Pentyl Isatogens 1a/1b with DA-Cyclopropane 2a

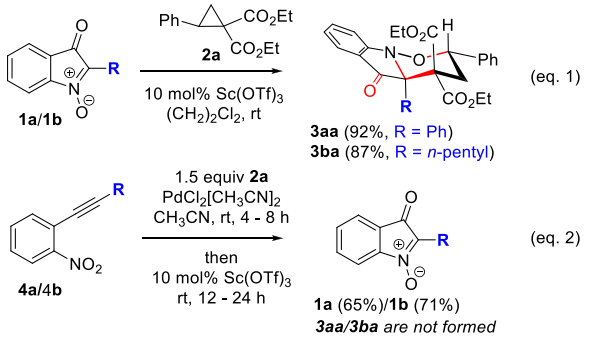

At the outset, $AuCl_3$ has been selected as a catalyst for the nitroalkynes cycloisomerization, given its superior selectivity to provide isatogens[12] over the initially discovered $AuBr_3$ by Yamamoto. Following the prescribed conditions, the cycloisomerization of **4a** has been carried out employing 5 mol % of $AuCl_3$ as a catalyst in CH_2Cl_2 as a solvent at rt. To our delight, we observed that both nitroalkyne **4a** and cyclopropane **2a** were getting consumed slowly and that the formation of product **3aa** along with the isatogen **1a** took place. The reaction was incomplete even after stirring for 24 h. The product **3aa** was isolated in 48% yield (Table 1, entry 1). Encouraged by this result, initially we looked at the possibility of bringing both cycloisomerization and cycloaddition with $AuCl_3$ alone as catalyst. In this regard, we screened different solvents, different [Au]-complexes, and some of the prescribed additives, changing the catalyst from gold to platinum and increasing the temperature to 60 °C. As shown in Table 1, the results are not encouraging (see Table S1, SI). Only when the solvent was switched from dichloromethane to dichloroethane, was the yield improved to 54% with $AuCl_3$, and there was no improvement when the solution was heated to 60 °C in the same solvent. To this end, considering the excellent cycloaddition yields of isatogen **1a** with **2a** that we had initially noticed, we looked at the possibility of carrying the [Au]-catalyzed cycloisomerization first and then adding cyclopropane **2a** and $Sc(OTf)_3$ to proceed for the cycloaddition. The results are promising, and we obtained the desired **3aa** in 65% yield. Increasing the temperature of the reaction did not improve the yield. The yield of **3aa** was improved to 71% when the reaction was carried out in the presence of 4 Å molecular sieves, at room temperature (Table 1).

Table 1. Optimization of the One-Pot Nitroalkynes Cycloisomerization/[3 + 3]-Cycloaddition Reaction[a]

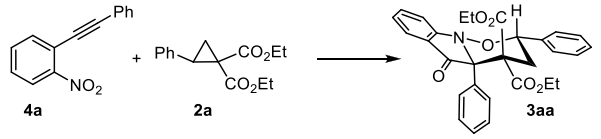

entry	cat.1	additive or cat.2	solvent	*T* (°C)	yield[b]
1	$AuCl_3$		DCM	rt	48%[c]
2	$AuCl_3$		1,2-DCE	rt	54%[c]
3	AuCl		1,2-DCE	rt	50%[c]
4	$PtCl_2$		1,2-DCE	rt	23%[c]
5	$PtCl_4$		1,2-DCE	rt	43%[c]
6	$AuCl_3$		1,2-DCE	60	55%
7	$AuCl_3$	$AgSbF_6$	1,2-DCE	60	no reaction
8	$AuCl_3$	AgOAc	1,2-DCE	60	42%[c]
9[d]	$AuCl_3$	$Sc(OTf)_3$	1,2-DCE	rt	65%
10[d]	$AuCl_3$	$Sc(OTf)_3$	1,2-DCE	60	68%
11[d,e]	$AuCl_3$	$Sc(OTf)_3$	1,2-DCE	rt	71%

[a]*Reaction conditions*: **4a** (0.1 mmol), **2a** (0.15 mmol), catalyst (5 mol %), and additive (10 mol %) in 1.0 mL of distilled solvent for 16 h. [b]Isolated yield after column chromatography. [c]10−35% isatogen recovered. [d]Stepwise addition of DAC and additive or *cat* 2. [e]In presence of 4 Å molecular sieves.

Having optimal conditions in hand, the substrate scope of this one-pot cycloisomerization/cycloaddition protocol has been examined by employing different nitroalkynes and DA-cyclopropanes with varying substituents on the aryl rings (Scheme 2). The reactions with substrates having electron-donating groups like -Me and -OMe *meta* to the nitro group are smooth, giving the corresponding cycloaddition products **3ca** and **3da** in moderate yields 56% and 74%, respectively. Even when there is an electron withdrawing group $-CO_2Me$, the reaction was facile and provided **3ea** in 75% yield. Next, the nitrotolans having -OMe and -^{t}Bu substituents *para* to the alkyne of pendant aryl ring have been subjected for this one-pot protocol and obtained the corresponding products **3fa** and **3ga** in moderate yields. Later, the scope of DA-cyclopropanes has been explored by employing DA-cyclopropanes **2b**−**2d** that bear different *para*-substituents and the dimethyl 2-(naphthalen-2-yl)cyclopropane-1,1-dicarboxylate (**2e**). In general, the reactions with these four cyclopropanes are smooth and provided the corresponding cycloaddition products in moderate to good yields. In addition, the cycloaddition reactions of 2-^{n}pentylisatogen **1b** have been carried with DA-

DOI: 10.1021/acs.orglett.9b02035
Org. Lett. 2019, 21, 6221−6224

Scheme 2. Scope for Nitroalkynes and DA-Cyclopropane in the One-Pot Cycloisomerization/Cycloaddition Reaction[a]

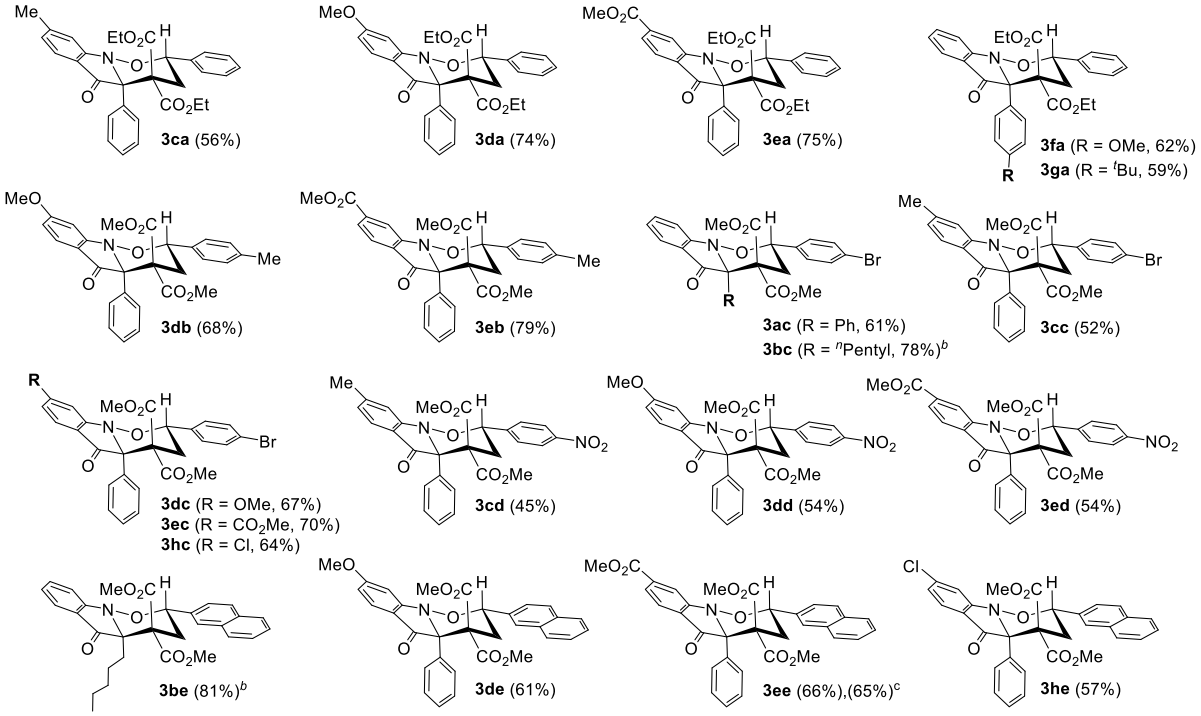

[a]*Reaction conditions*: **4** (1 equiv), **2** (1.5 equiv), $AuCl_3$ (5 mol %), and $Sc(OTf)_3$ (10 mol %). [b]Isatogen **2b** was used as the substrate. [c]2 mmol scale, employed 15 mol % $Sc(OTf)_3$.

cyclopropanes **2c** and **2e** to obtain the corresponding cycloaddition products **3bc** and **3be** in 78% and 81% yields.

As part of expanding the scope of this one-pot protocol, the compatibility of isatogens **1c**−**1e** having functional groups at the propargylic position has been examined (Scheme 3). All

Scheme 3. Limitation of Substituents at C2 and Competition between DA-Cyclopropane and Olefins

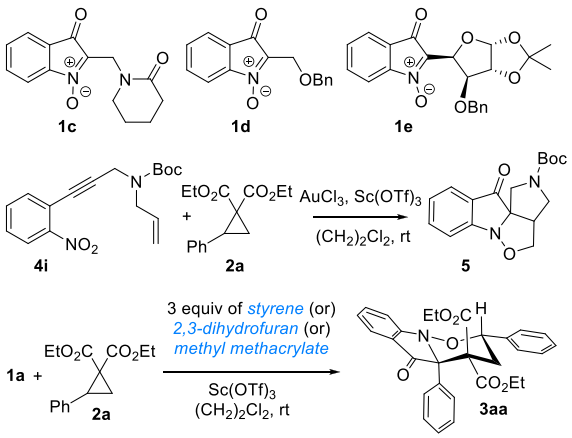

three substrates failed to undergo cycloaddition with DA-cyclopropane **2a** under established conditions. The lack of reactivity of substrates **1c**−**1e** may probably be due to the bulky C2-substituent that hinders the approaching dipolarophile. Interestingly, when the *N*-allyl propargylamide derived nitroakyne **4i** was treated with a gold complex along with the **2a**, it was found that after the cycloisomerization, the intermediate isatogen underwent an intramolecular [3 + 2]-cycloaddition with the pendant allyl group over the intermolecular [3 + 3]-cycloaddition. On the other hand, when the intermolecular completion experiments were conducted employing equal amounts of electron rich/electron deficient olefins along with DA-cyclopropane **2a**, the [3 + 3]-cycloaddition dominated the classical [3 + 2]-cycloaddition of isatogens.

In conclusion, the [3 + 3]-cycloaddition of DA-cyclopropanes with isatogens has been examined. In general, the cycloaddition reaction is highly diastereoselective and facile with 2-arylisatogens and also with 2-alkylisatogens. In the case of 2-arylisatogens, the preceding Au(III)-catalyzed nitroalkyne cycloisomerization has been successfully combined with the cycloaddition step in one-pot. On the other hand, with 2-alkylisatogens these steps have to be separately conducted, and also the cycloaddition is not facile. The functionalized alkyl groups are present at the C2 position of isatogen. Currently, work in the direction of employing this protocol in the synthesis of pseudoindoxyl natural products is in progress.

■ ASSOCIATED CONTENT

Supporting Information

The Supporting Information is available free of charge on the ACS Publications Web site. The Supporting Information is available free of charge on the ACS Publications website at DOI: 10.1021/acs.orglett.9b02035.

Characterization data, ^1H, ^{13}C NMR/DEPT, and HRMS spectra of all new compounds (PDF)

■ AUTHOR INFORMATION

Corresponding Author

*E-mail: vr.chepuri@ncl.res.in.

DOI: 10.1021/acs.orglett.9b02035
Org. Lett. 2019, 21, 6221−6224

ORCID

Chepuri V. Ramana: 0000-0001-5801-311X

Notes

The authors declare no competing financial interest.

■ ACKNOWLEDGMENTS

The authors acknowledge CSIR (India) for funding this project and DST-INSPIRE for a research fellowship to P.S.D.

■ REFERENCES

(1) (a) Steyn, P. S. *Tetrahedron Lett.* **1971**, *12*, 3331−3334. (b) Burnell, R. H.; Chapelle, A.; Khalil, M. F. *Can. J. Chem.* **1974**, *52*, 2327−2330. (c) Phillipson, J. D.; Supavita, N. *Phytochemistry* **1983**, *22*, 1809−1813. (d) Bhakuni, D. S.; Silva, M.; Matlin, S. A.; Sammes, P. G. *Phytochemistry* **1976**, *15*, 574−575. (e) Birch, J.; Wright, J. J. *J. Chem. Soc. D* **1969**, 644b.

(2) (a) Witkop, B.; Patrick, J. B. *J. Am. Chem. Soc.* **1951**, *73*, 2188−2195. (b) Dolby, L. J.; Rodia, R. M. *J. Org. Chem.* **1970**, *35*, 1493−1496. (c) Saito, I.; Imuta, M.; Matsuura, T. *Chem. Lett.* **1972**, *1*, 1173−1176. (d) Berti, C.; Greci, L.; Andruzzi, R.; Trazza, A. *J. Org. Chem.* **1982**, *47*, 4895−4899. (e) Movassaghi, M.; Schmidt, M. A.; Ashenhurst, J. A. *Org. Lett.* **2008**, *10*, 4009−4012.

(3) (a) Finch, N.; Taylor, W. I. *J. Am. Chem. Soc.* **1962**, *84*, 3871−3877. (b) Hutchison, A. J.; Kishi, Y. *J. Am. Chem. Soc.* **1979**, *101*, 6786−6788. (c) Stoermer, D.; Heathcock, C. *J. Org. Chem.* **1993**, *58*, 564. (d) Baran, P. S.; Corey, E. J. *J. Am. Chem. Soc.* **2002**, *124*, 7904−7905. (e) Schneekloth, J. S.; Kim, J.; Sorensen, E. J. *Tetrahedron* **2009**, *65*, 3096−3101. (f) Kim, J.; Schneekloth, J. S.; Sorensen, E. J. *Chem. Sci.* **2012**, *3*, 2849−2852.

(4) (a) Han, S.; Movassaghi, M. *J. Am. Chem. Soc.* **2011**, *133*, 10768−10771. (b) Qi, X.; Tambar, U. K. *J. Am. Chem. Soc.* **2011**, *133*, 10050−10053.

(5) Ji, Y.; He, X.; Peng, C.; Huang, W. *Org. Biomol. Chem.* **2019**, *17*, 2850−2864.

(6) (a) Rosen, G. M.; Tsai, P.; Barth, E. D.; Dorey, G.; Casara, P.; Spedding, M.; Halpern, H. J. *J. Org. Chem.* **2000**, *65*, 4460−4463. (b) Asao, N.; Sato, K.; Yamamoto, Y. *Tetrahedron Lett.* **2003**, *44*, 5675−5677. (c) Ramana, C. V.; Patel, P.; Vanka, K.; Miao, B.; Degterev, A. *Eur. J. Org. Chem.* **2010**, *2010*, 5955−5966. (d) Cikotiene, I. *Eur. J. Org. Chem.* **2012**, *2012*, 2766−2773. (e) Kumar, C. V. S.; Ramana, C. V. *Org. Lett.* **2014**, *16*, 4766−4769. (f) Marien, N.; Brigou, B.; Pinter, B.; De Proft, F.; Verniest, G. *Org. Lett.* **2015**, *17*, 270−273. (g) Kumar, C. V. S.; Ramana, C. V. *Org. Lett.* **2015**, *17*, 2870−2873.

(7) Wetzel, A.; Gagosz, F. *Angew. Chem., Int. Ed.* **2011**, *50*, 7354−7358.

(8) Selected reviews on DA-cyclopropanes in annulation reaction, see: (a) Mel'nikov, M.; Budynina, E.; Ivanovaa, O.; Trushkova, I. *Mendeleev Commun.* **2011**, *21*, 293−301. (b) Schneider, T.; Kaschel, J.; Werz, D. *Angew. Chem., Int. Ed.* **2014**, *53*, 5504−5523. (c) Grover, H.; Emmett, M.; Kerr, M. A. *Org. Biomol. Chem.* **2015**, *13*, 655−671.

(9) Selected reports on DA-cyclopropane cycloaddition reactions, see: (a) Yu, M.; Pagenkopf, B. L. *J. Am. Chem. Soc.* **2003**, *125*, 8122−8123. (b) Carson, C. A.; Kerr, M. A. *J. Org. Chem.* **2005**, *70*, 8242−8244. (c) Korotkov, V. S.; Larionov, O. V.; Hofmeister, A.; Magull, J.; de Meijere, A. *J. Org. Chem.* **2007**, *72*, 7504−7510. (d) Pohlhaus, P. D.; Sanders, S. D.; Parsons, A. T.; Li, W.; Johnson, J. S. *J. Am. Chem. Soc.* **2008**, *130*, 8642−8650. (e) Perreault, C.; Goudreau, S. R.; Zimmer, L. E.; Charette, A. B. *Org. Lett.* **2008**, *10*, 689−692. (f) Goldberg, A. F. G.; O'Connor, N.; Craig, R. A., II; Stoltz, B. M. *Org. Lett.* **2012**, *14*, 5314−5317. (g) Zhang, H. H.; Luo, Y.; Wang, H.; Chen, W.; Xu, P. F. *Org. Lett.* **2014**, *16*, 4896−4899. (h) Garve, L.; Pawliczek, M.; Jones, P.; Werz, D. *Chem. - Eur. J.* **2016**, *22*, 521−525. (i) Preindl, J.; Chakrabarty, S.; Waser, J. *Chem. Sci.* **2017**, *8*, 7112−7118. (j) Matsumoto, Y.; Nakatake, D.; Yazaki, R.; Ohshima, T. *Chem. - Eur. J.* **2018**, *24*, 6062−6066. (k) Augustin, A.; Busse, M.; Jones, P.; Werz, D. *Org. Lett.* **2018**, *20*, 820−823. (l) Chagarovskiy, A.; Vasin, V.; Kuznetsov, V.; Trushkov, I. *Angew. Chem., Int. Ed.* **2018**, *57*, 10338−10342. (m) Varshnaya, R.; Banerjee, P. *J. Org. Chem.* **2019**, *84*, 1614−1623. (n) Petzold, M.; Jones, P.; Werz, D. *Angew. Chem., Int. Ed.* **2019**, *58*, 6225−6229. (o) Xu, P.; Yu, J.; Zhou, F.; Zhou, J. *ACS Catal.* **2019**, *9*, 1820−1882.

(10) Reports on cycloaddition reaction with nitrones, see: (a) Young, I.; Kerr, M. *Angew. Chem., Int. Ed.* **2003**, *42*, 3023−3026. (b) Ganton, M. D.; Kerr, M. A. *J. Org. Chem.* **2004**, *69*, 8554−8557. (c) Young, I. S.; Kerr, M. A. *Org. Lett.* **2004**, *6*, 139−141. (d) Young, I. S.; Williams, J. L.; Kerr, M. A. *Org. Lett.* **2005**, *7*, 953−955. (e) Sapeta, K.; Kerr, M. *J. Org. Chem.* **2007**, *72*, 8597−8599. (f) Karadeolian, A.; Kerr, M. *J. Org. Chem.* **2007**, *72*, 10251−10253. (g) Stevens, A.; Palmer, C.; Pagenkopf, B. *Org. Lett.* **2011**, *13*, 1528−1531. (h) Humenny, W.; Kyriacou, P.; Sapeta, K.; Karadeolian, A.; Kerr, M. *Angew. Chem., Int. Ed.* **2012**, *51*, 11088−11091. (i) Gorbacheva, E. O.; Tabolin, A. A.; Novikov, R. A.; Khomutova, Y. A.; Nelyubina, Y. V.; Tomilov, Y. V.; Ioffe, S. L. *Org. Lett.* **2013**, *15*, 350−353. (j) Braun, C. M.; Congdon, E. A.; Nolin, K. A. *J. Org. Chem.* **2015**, *80*, 1979−1984. (k) Chidley, T.; Naresh, V.; Cheryl, A. C.; Kerr, M.; Pagenkopf, B. *Org. Lett.* **2016**, *18*, 2922−2925. (l) Xu, P.; Liu, J.; Shen, L.; Cao, Z.; Zhou, J. *Nat. Commun.* **2017**, *8*, 1619. (m) Xu, P.; Chen, C.; Liu, X.; Song, Y.; Zhou, F.; Zhou, J. *J. Org. Chem.* **2018**, *83*, 12763−12774.

(11) (a) Carson, C. A.; Kerr, M. A. *Angew. Chem.* **2006**, *118*, 6710−6713; *Angew. Chem., Int. Ed.* **2006**, *45*, 6560−6563. (b) Young, I. S.; Kerr, M. A. *J. Am. Chem. Soc.* **2007**, *129*, 1465−1469. (c) Morales, C.; Pagenkopf, B. *Org. Lett.* **2008**, *10*, 157−159. (d) Karadeolian, A.; Kerr, M. A. *Angew. Chem., Int. Ed.* **2010**, *49*, 1133−1135. (e) Zhang, H.; Curran, D. P. *J. Am. Chem. Soc.* **2011**, *133*, 10376−10378.

(12) Liu, R.; Ye, S.; Lu, C.; Zhuang, G.; Gao, J.; Jia, Y. *Angew. Chem., Int. Ed.* **2015**, *54*, 11205−11208.

DOI: 10.1021/acs.orglett.9b02035
Org. Lett. 2019, 21, 6221−6224

OL | Organic Letters

pubs.acs.org/OrgLett Letter

Interrupting the [Au]-Catalyzed Nitroalkyne Cycloisomerization: Trapping the Putative α-Oxo Gold Carbene with Benzo[c]isoxazole

Pawan S. Dhote and Chepuri V. Ramana*

Cite This: *Org. Lett.* 2021, 23, 2632–2637 Read Online

ACCESS | Metrics & More | Article Recommendations | Supporting Information

ABSTRACT: The [Au]-catalyzed nitroalkyne cycloisomerization of 2-alkynylnitrobenzenes leading to anthranils has been interrupted by possible trapping of the postulated intermediate α-oxo gold carbene with an external nucleophile such as benzo[c]isoxazole (anthranil). At the outset, this provides a simple synthesis of highly functionalized 3-acyl-(2-formylphenyl)-2*H*-indazoles with the sequential C−O, C−N, and N−N bond formations. This provides indirect support for the existence of α-oxo gold carbenes in the [Au]-catalyzed internal redox processes of nitroalkynes.

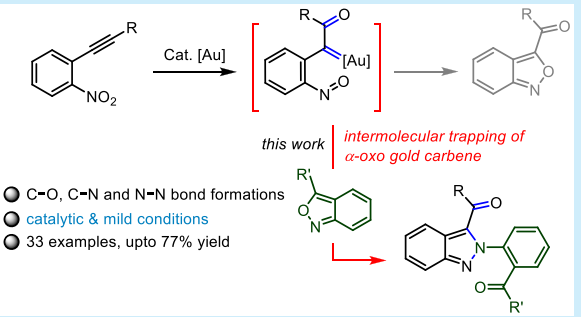

The 2*H*-indazole scaffold is one of the prominent pharmacophores well explored in medicinal chemistry with a good number of approved medicines spanning across a broad range of therapeutic applications.[1,2] The "Cadogan and Davis−Beirut reactions" that forge a 2*H*-indazole heterocyclic core via an intramolecular N−N bond formation are the two important reactions applied in the synthesis of this heterocyclic core.[3,4] In both the reactions, initially a nitro group undergoes either a reduction or an internal redox process leading to a reactive nitroso intermediate. In the case of the Davis−Beirut reaction, the intramolecular nucleophilic attack and/or a 5-centered 6π-electrocyclization of the nitroso intermediate results in an indazole *N*-oxide that undergoes either an internal redox reaction or deoxygenation. On the other hand, in the classical mechanism proposed for the Cadogan indazole synthesis, the nitroso intermediate further reduces to a nitrene that adds to the imine, though the possibility of the former process has also been established.[5] Despite their widespread utility, the harsh conditions/reagents employed for generating the reactive nitroso intermediates warrants the availability of milder reagents/conditions that are amicable for sensitive functional/protecting groups.

In this context, we speculated on the possibility of trapping the nitroso stabilized α-oxo gold carbene intermediates that are proposed in the catalytic cyclization of *o*-alkynylnitrobenzenes with *N*-centered nucleophiles.[6−9] The cycloisomerization of *o*-alkynylnitrobenzenes (trivially known as nitrotolans) leading to isatogens is one of the earliest redox neutral reactions, documented as early as in 1881 by Bayer during the course of his classic research on indigo.[6] In 2003, a seminal contribution by Yamamoto's group revealed the possibility of affecting this nitroalkyne cycloisomerization under gold catalysis.[7] Importantly, it has been revealed by Yamamoto's group that, depending upon the pendant substituent on the alkyne, the nitroalkyne cycloisomerization proceeds in complementary paths leading to either isatogen (when the substituent is aryl) and/or isomeric anthranil (exclusively with alky substituent). By isolating a nitroso-stabilized α-oxo alkyl iridium intermediate, Crabtree's group revealed that the overall process is a metal-mediated internal redox process leading to an α-oxo iridium carbene intermediate.[8] A similar mechanism even in gold(I\III)-catalyzed nitroalkyne internal redox processes with complementary regioselectivity during the initial oxygen transfer has been extended by Liu and our groups.[9]

These nitroso stabilized α-oxo gold carbene intermediates provide a handle for the carbene for exchange with N-centered nucleophiles[10] and also the reactive nitroso group in the proximity, for the subsequent N−N bond formation.[11] However, in this event, the carbene exchange process has to compete with the original intramolecular cyclization of the α-oxo gold carbene intermediate that leads to anthranil. As shown in Scheme 1, in the presence of anthranil **4** that is known to exchange with the goldcarbenes,[12] the reaction is expected to provide an imine that should undergo Davis-Beirut cyclization leading to the indazole **5** (or its *N*-oxide if it is sufficiently stable[13]) with simultaneous C−N and N−N bond formations.

Received: February 15, 2021
Published: March 19, 2021

https://doi.org/10.1021/acs.orglett.1c00539
Org. Lett. 2021, 23, 2632–2637

Scheme 1. Nitroalkyne Cycloisomerization and Associated Nitroso Stabilized α-Oxo Metal Carbene Intermediate and Possible Interruption with an External *N*-Based Nucleophile Leading to Indazoles

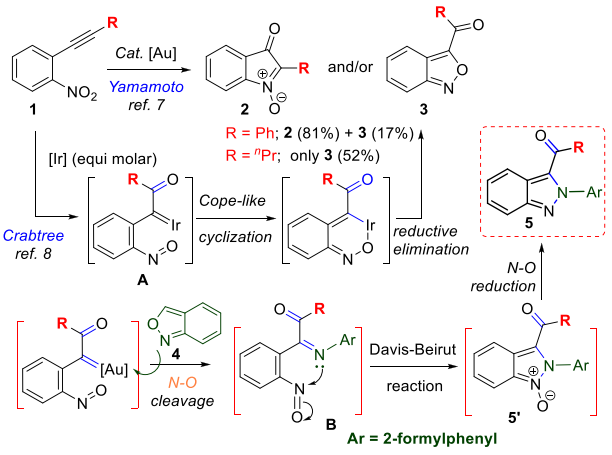

To examine these hypothetical possibilities, initially, employing 1-(but-1-yn-1-yl)-2-nitrobenzene (**1a**) as a substrate, we examined its cycloisomerization in the presence of anthranil **4a** following reported conditions using $AuBr_3$ (in toluene) and $Pd(CH_3CN)_2Cl_2$ (in acetonitrile) complexes. As shown in Table 1 (entries 1 and 2), with the palladium complex, isatogen **2a** was obtained exclusively.[14] On the other hand, with the $AuBr_3$,[7] the corresponding anthranil **3a** was mainly obtained with trace amounts of a new product, with the expected mass corresponding to the desired indazole **5aa**.

Table 1. Optimization of the Reaction Conditions[a]

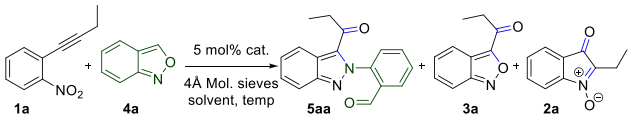

Entry	Catalyst	Solvent	Yield (%) 5aa[b]	Yield (%) 2a or 3a[b]
1	$AuBr_3$	PhMe	trace	64 (**3a**)
2	$Pd(CH_3CN)_2Cl_2$	MeCN	–	69 (**2a**)
3	$AuCl_3$	$ClCH_2CH_2Cl$	–	trace (**3a**)
4	$AuCl_3$	PhMe	54	12 (**3a**)
5	$AuCl_3$	MeCN	–	–
6	$AuCl_3$	1,4-Dioxane	–	–
7	$AuCl_3$	$PhCF_3$	44	13 (**3a**)
8	$AuCl_3$	PhCl	49	10 (**3a**)
9	$PicAuCl_2$	PhMe	42	10 (**3a**)
10	AuCl	PhMe	35	24 (**3a**)
11	$PPh_3AuCl/AgSbF_6$	PhMe	26	38 (**3a**)
12	IPrAuCl/AgOTf	PhMe	20	46 (**3a**)
13	$(ArO)_3PAuCl/AgNTf_2$	PhMe	27	42 (**3a**)
14[c]	$AuCl_3$	PhMe	57	10 (**3a**)
15[d]	**$AuCl_3$**	**PhMe**	**69**	**trace (3a)**

[a]In general, the reactions were carried out with 0.2 mmol of **1a** and 0.22 mmol of **4a** in 2 mL of solvent and 5 mol % of catalyst at rt with a reaction time of 3−4 h. [b]Isolated yield. [c]Reaction was carried at 80 °C. [d]Slow addition of **1a** through syringe pump at rt for 4 h.

Next, we examined the reactions with $AuCl_3$, which had shown superior reactivity over $AuBr_3$ in nitroalkyne cycloisomerizations.[15] However, in the prescribed 1,2-dichloroethane solvent, we got a poor conversion, resulting mainly with the formation of the anthranil **3a** in small amounts. Gratifyingly, when we switched the solvent to toluene, the uncharacterized product **5aa** that was encountered with $AuBr_3$ was obtained in 54% yield along with the anthranil **3a** (12%). Gratifyingly, the spectral data and single crystal X-ray crystal structure analysis of compound **5aa** revealed that it was the desired indazole and, importantly, it proved the point that the intermolecular trapping of gold carbene that results during the nitroalkyne cycloisomerization was possible. With these results, we next proceeded further to improve the yield of the reaction. As shown in Table 1, our initial attempts with changing the solvent were not encouraging (entries 5−8). This prompted us to explore the other gold(III) and cationic gold(I)-complexes in this pursuit. As shown, in Table 1 (entry 9), with dichloro(2-pyridinecarboxylato)gold(III) ($PicAuCl_2$, entry 9) the requisite indazole was obtained as a major product in moderate yields. Similarly, with AuCl and with other cationic gold(I)-complexes, the results are not encouraging (entries 10−13). In the majority of the cases, the cycloisomerization leading to anthranil **3a** was the major event, along with the formation of the requisite **5aa**. Gratifyingly, with $AuCl_3$, in toluene, when the reaction was heated to 80 °C, the yield of **5aa** was improved to 57% and the anthranil **3a** was also obtained in 10% yield (entry 14). Finally, when the reaction was carried out by slow addition of **1a** to a solution of **2a** and $AuCl_3$ catalyst at rt, the yield of **5aa** was improved to 69%, and the formation of the cycloisomerization product **3a** was also minimized (entry 15).

As illustrated in Scheme 2, a wide range of substituted nitroalkynes have been employed to examine the scope of the reaction and to understand how the substituents influence the outcome. Initially, we employed the substrates having different pendant substituents on the alkyne unit. As shown, changing the length of the side chain did not alter the reaction outcome, and it was also found that the protecting groups such as O-acetyl and O-TBS placed on this alkyl chain were intact. Interestingly, with the cyclopropyl substituted alkyne, the intramolecular cyclization was successfully completed and resulted in the requisite indazole **5ha** as a minor product and the corresponding anthranil **4h** as the major product. For the substrates **5ia**−**5la** having different substituents placed para to the alkyne unit, the outcome of the reaction was influenced. For example, when a carboxylate as well as cyano was present, the yield was 72% (**5ka**) and 77% (**5la**) revealing that the presence of an electron-withdrawing group (EWG) at this position had a stabilizing effect on the intermediate gold carbene. In contrast, when the substituent was fluorine, the yield was reduced to 47% (**5ia**), which indicates that σ-acceptors at this position are not compatible. When a methyl group **5ja** was present at this position, the yield was only 56%. It is noteworthy that the good yield was retained even when the reaction was carried out on 500 mg scale (**5aa**, 65% yield).

Next, we varied the substituents on the anthranil ring. When halogen-substituted anthranils were employed as the substrates, the reactions in general resulted in the corresponding indazoles **5ab**−**5ad** in low to moderate yields depending upon the position of the halogen atom. The yields are poor when the halogen is placed para to the nitrogen. On the other hand, with 5-methyl and 5-carboxymethyl anthranils **4e** and **4f** respectively, the corresponding indazoles were obtained in good to moderate yields. Interestingly, when a methoxy group is placed on the anthranil ring, there was no interception of the original

https://doi.org/10.1021/acs.orglett.1c00539
Org. Lett. 2021, 23, 2632−2637

Scheme 2. Reaction Scope and Limitations

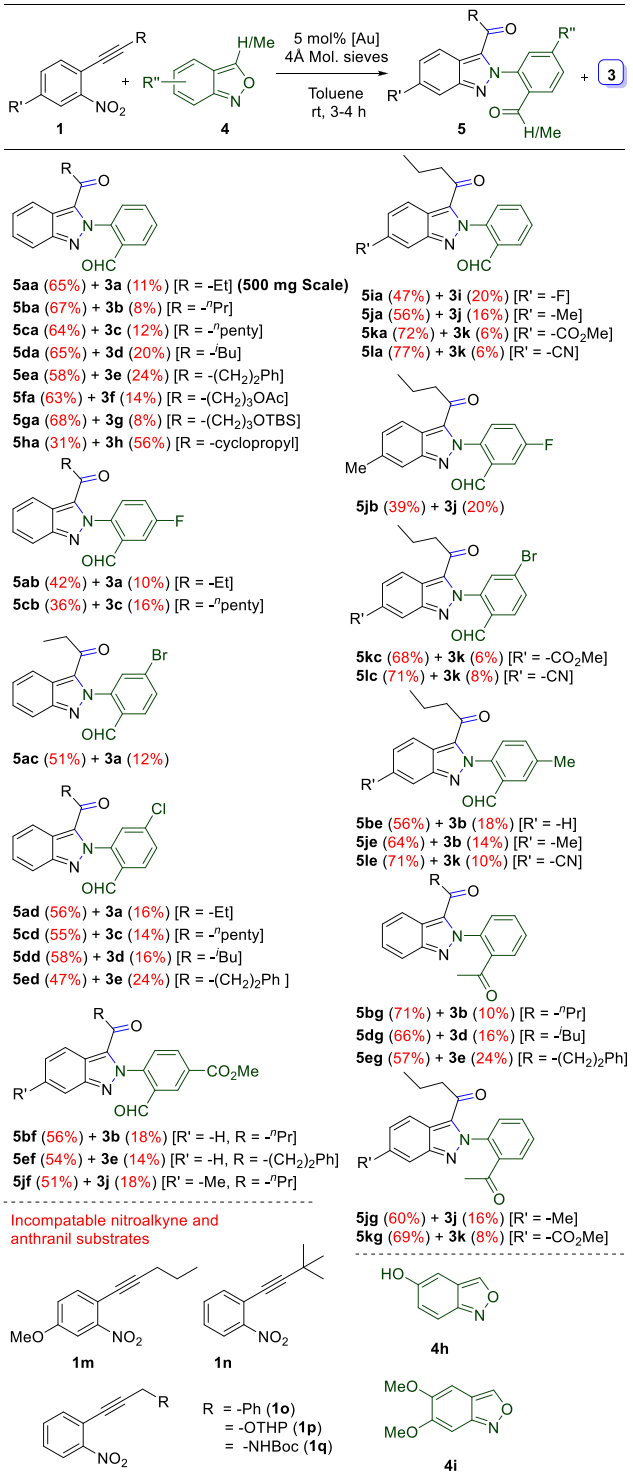

internal nitroalkyne redox process and the corresponding anthranil was obtained exclusively.[9a] Next, we examined the compatibility of a C3-methyl substituted anthranil **4g** employing different nitroalkynes. The results are encouraging, and the corresponding 2*H*-indazole containing an *o*-acyl group on the pendant aryl ring were obtained in moderate to good yields (**5bg**, **5cg**, **5dg**, **5jg**, and **5 kg**). In this case also, the nitroalkyne **1k** having the carboxylate group gave the best results. On the contrary, the nitroalkyne or the anthranil having methoxy or hydroxyl substitutes on the aryl ring were found to be incompatible and the reactions employing either of these substrates gave mainly the corresponding anthranil derivatives. In addition, when the alkyne end carries a bulky group or an alkyl chain having EWGs, the intramolecular cyclization is facile over the intermolecular carbene exchange, indicating that both steric and electronic factors play important roles. To show the utility, the selective homologation of the aldehyde group present in these products has been carried out employing the stable Wittig ylides (see Scheme S1, Supporting Information). The reactions are highly selective and proceed smoothly at rt to provide the corresponding *E*-olefins in excellent yields.

To probe whether this overall process involves the anthranil **3a** as an intermediate, control experiments have been carried out by employing **3a** as a substrate under the optimized conditions in the presence of **4a**. Even after prolonged reaction times, both **4a** and **3a** were intact, thus revealing that the internal redox cascade process was interrupted prior to the formation of **3a** and presumably by the carbene transfer from the intermediate α-oxo gold carbene to the nitrogen of anthranil **4a**. Next, the concern is about the possible intermolecular functionalization of alkyne with the anthranil **4** leading to an α-imino gold carbene[16] followed by oxygen transfer from the nitro group[17] (Scheme 3, eq 4) and finally

Scheme 3. Control Experiments to Support the Involvement of the α-Oxo Gold Carbene Intermediate (Eqs 1−3) and Alternative Possibility for the Formation of Indazole (Eq 4)

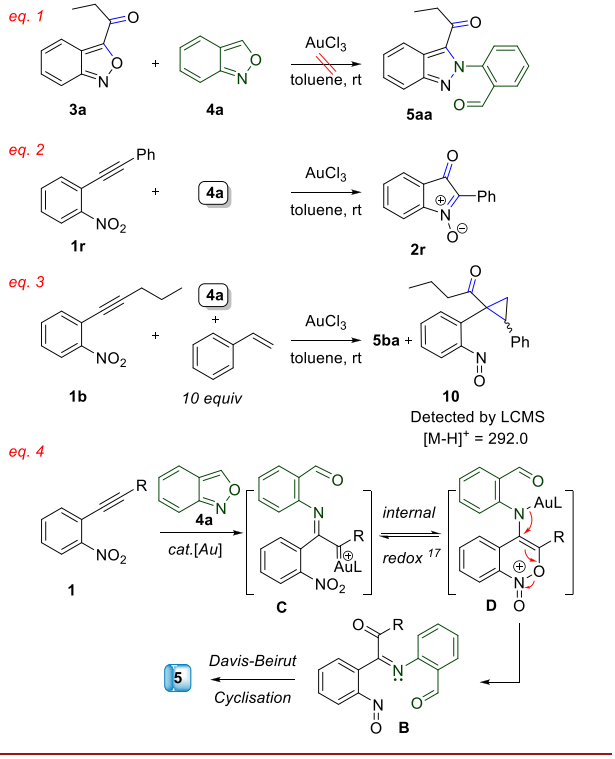

the N−N bond formation. As a control, the phenyl substituted nitroalkyne **1r**, when treated with **4a** under the optimized conditions (Scheme 3, eq 2), gave exclusively isatogen **2r** via 5-exo-dig cyclization. This indicated that the isomeric α-oxo gold carbene involved in this process prefers the intramolecular cyclization over the intermolecular carbene interception and importantly that the possibility of anthranil addition to the alkyne and subsequent α-imino gold carbene formation is not

https://doi.org/10.1021/acs.orglett.1c00539
Org. Lett. 2021, 23, 2632−2637

operational. An additional control experiment was conducted by carrying the reaction in the presence of excess styrene (known/used to trap the gold carbenes).[18] Although the expected cyclopropane product could not be isolated in reasonable amounts to characterize, the LCMS analysis showed its presence in the crude reaction mixture (Scheme 3, eq 3).

Further, competition experiments were done employing the alkynes **8a**–**8c**, which are known to be functionalized with the anthranil **4a** (leading to an α-imino gold carbene intermediate) under current conditions and also under the conditions\gold-complex reported for the same transformation.[19−21] As shown in Scheme 4, the reaction of **1a** and **4a** in the presence of

Scheme 4. Competition Experiments to Support the Involvement of the α-Oxo Gold Carbene Intermediate

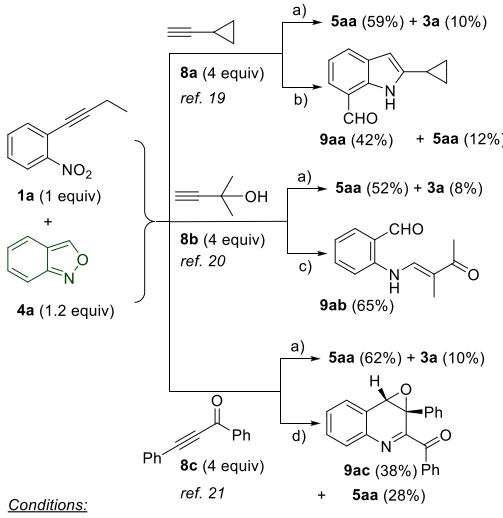

ethynyl cyclopropane (**8a**) under the prescribed conditions and Au[I]-catalyst/Ag-additive catalysts resulted in a mixture of the reported product **9aa** (42%) and indazole **5aa** (12%).[19] When the same reaction was carried out under the current conditions, it provided mainly the indazole **5aa** along with the anthranil **3a**. Similar results were obtained in the competition experiments employing alkyne **8b** or **8c**.[20,21] In general, with the reported complexes, the reaction between the anthranil **4a** and the alkyne **8** is facile, and with $AuCl_3$, the nitroalkyne redox process seems to be operating exclusively. Thus, these competition experiments clearly indicate that, unlike with the other complexes, it appears that $AuCl_3$ selectively activates the nitroalkyne **1a** over the competing terminal alkyne, and this provides indirect evidence for an internal oxygen transfer leading to an α-oxo gold carbene intermediate, and subsequent carbene transfer to the nitrogen present in the anthranil **4**.

In summary, a novel synthesis of functionalized 2*H*-indazoles is described, employing easily accessible *o*-nitroalkynes and anthranils under gold catalysis. At the outset, the current results provide indirect support for the proposed nitroso-stabilized α-oxo gold carbene intermediate in the nitroalkyne cycloisomerization leading to anthranil. In addition, this also provides a mild and catalytic approach for the availability of the key nitroso intermediates required in the Davis–Beirut cyclization with, importantly, one of the nitrogens having been incorporated externally.

■ ASSOCIATED CONTENT

Supporting Information

The Supporting Information is available free of charge at https://pubs.acs.org/doi/10.1021/acs.orglett.1c00539.

Characterization data ^{1}H, ^{13}C NMR/DEPT and HRMS spectra of all new compounds (PDF)

FAIR data, including the primary NMR FID files, for compounds **1a**, **1d**–**1f**, **1i**–**1m**, **2a**, **3a**, **3d**–**3g**, **3i**–**3m**, **5aa**–**5la**; **5ab**, **5cb**, **5jb**, **5kc**, **5lc**, **5ad**, **5cd**–**5ed**, **5be**, **5je**, **5le**, **5bf**, **5ef**, **5jf**, **5bg**, **5dg**, **5eg**, **5jg**, **5kg**, **7a**–**7c**, **8a**–**8c** (ZIP)

Accession Codes

CCDC 2050267 contains the supplementary crystallographic data for this paper. These data can be obtained free of charge via www.ccdc.cam.ac.uk/data_request/cif, or by emailing data_request@ccdc.cam.ac.uk, or by contacting The Cambridge Crystallographic Data Centre, 12 Union Road, Cambridge CB2 1EZ, UK; fax: +44 1223 336033.

■ AUTHOR INFORMATION

Corresponding Author

Chepuri V. Ramana − *Division of Organic Chemistry, CSIR-National Chemical Laboratory, Pune 411 008, India; Academy of Scientific and Innovative Research (AcSIR), Ghaziabad 201002, India;* orcid.org/0000-0001-5801-311X; Email: vr.chepuri@ncl.res.in

Author

Pawan S. Dhote − *Division of Organic Chemistry, CSIR-National Chemical Laboratory, Pune 411 008, India; Academy of Scientific and Innovative Research (AcSIR), Ghaziabad 201002, India*

Complete contact information is available at: https://pubs.acs.org/10.1021/acs.orglett.1c00539

Notes

The authors declare no competing financial interest.

■ ACKNOWLEDGMENTS

The authors acknowledge CSIR (India) for funding this project, DST-INSPIRE for a research fellowship to P.S.D., and Dr. Srinu Tothadi (CSIR-National Chemical Laboratory) for carrying the single crystal X-ray diffraction studies. The crystal structure for **5aa** has been deposited with the Cambridge Structural Database (CCDC 2050267).

■ REFERENCES

(1) (a) Denya, I.; Malan, S.; Joubert, J. Indazole derivatives and their therapeutic applications: a patent review (2013–2017). *Expert Opin. Ther. Pat.* **2018**, *28*, 441–453. (b) Zhang, S. G.; Liang, C. G.; Zhang, W. H. Recent Advances in Indazole-Containing Derivatives: Synthesis and Biological Perspectives. *Molecules* **2018**, *23*, 2783. (c) Gaikwad, D. D.; Chapolikar, A. D.; Devkate, C. G.; Warad, K. D.; Tayade, A. P.; Pawar, R. P.; Domb, A. J. Synthesis of indazole motifs and their medicinal importance: An overview. *Eur. J. Med. Chem.* **2015**, *90*, 707–731.

(2) (a) Janardhanan, J. C.; Bhaskaran, R. P.; Praveen, V. K.; Manoj, N.; Babu, B. P. Recent Advances in the Transition Metal Catalyzed

Synthesis of Indazoles. *Asian J. Org. Chem.* **2020**, *9*, 1410−1431. (b) Hassan, A. A.; Aly, A. A.; Tawfeek, H. N. *Indazoles: Synthesis and Bond-Forming Heterocyclization in Advances in Heterocyclic Chemistry*, Vol. *125*,; Scriven, E. F. V., Ramsden, C. A., Eds.; Academic Press: Cambridge, 2018; pp 235−300. (c) Schmidt, A.; Beutler, A.; Snovydovych, B. Recent advances in the chemistry of indazoles. *Eur. J. Org. Chem.* **2008**, *2008*, 4073−4095.

(3) Kaur, M.; Kumar, R. C-N and N-N bond formation *via* Reductive Cyclization: Progress in Cadogan/Cadogan-Sundberg Reaction. *ChemistrySelect* **2018**, *3*, 5330−5340.

(4) Zhu, J. S.; Haddadin, M. J.; Kurth, M. J. Davis−Beirut Reaction: Diverse Chemistries of Highly Reactive Nitroso Intermediates in Heterocycle Synthesis. *Acc. Chem. Res.* **2019**, *52*, 2256−2265.

(5) Zhu, J. S.; Li, C. J.; Tsui, K. Y.; Kraemer, N.; Son, J.-H.; Haddadin, M. J.; Tantillo, D. J.; Kurth, M. J. Accessing Multiple Classes of 2H-Indazoles: Mechanistic Implications for the Cadogan and Davis−Beirut Reactions. *J. Am. Chem. Soc.* **2019**, *141*, 6247−6253.

(6) Baeyer, A. Uber dieVerbindungen der Indigogruppe. *Ber. Dtsch. Chem. Ges.* **1881**, *14*, 1741−1746.

(7) Asao, N.; Sato, K.; Yamamoto, Y. $AuBr_3$-catalyzed cyclization of *o*-(alkynyl)nitrobenzenes. Efficient synthesis of isatogens and anthranils. *Tetrahedron Lett.* **2003**, *44*, 5675−5677.

(8) Li, X.; Incarvito, C. D.; Vogel, T.; Crabtree, R. H. Intramolecular Oxygen Transfer from Nitro Groups to C≡C Bonds Mediated by Iridium Hydrides. *Organometallics* **2005**, *24*, 3066−3073.

(9) (a) Jadhav, A. M.; Bhunia, S.; Liao, H.-Y.; Liu, R.-S. Gold-Catalyzed Stereoselective Synthesis of Azacyclic Compounds through a Redox/[2 + 2 + 1] Cycloaddition Cascade of Nitroalkyne Substrates. *J. Am. Chem. Soc.* **2011**, *133*, 1769−1771. (b) Patel, P.; Ramana, C. V. Divergent Pd(II) and Au(III) mediated nitroalkynol cycloisomerizations. *Org. Biomol. Chem.* **2011**, *9*, 7327−7334.

(10) For selected reviews on α-oxo gold carbenes: (a) Yeom, H.; Shin, S. Catalytic Access to α-Oxo Gold Carbenes by N-O Bond Oxidants. *Acc. Chem. Res.* **2014**, *47*, 966−977. (b) Zhang, L. A Non-Diazo Approach to α-Oxo Gold Carbenes *via* Gold-Catalyzed Alkyne Oxidation. *Acc. Chem. Res.* **2014**, *47*, 877−888. (c) Huple, D.; Ghorpade, S.; Liu, R. S. Recent Advances in Gold-Catalyzed N- and O-Functionalizations of Alkynes with Nitrones, Nitroso, Nitro and Nitroxy Species. *Adv. Synth. Catal.* **2016**, *358*, 1348−1367. (d) Zheng, Z.; Wang, Z.; Wang, Y.; Zhang, L. Au-Catalysed oxidative cyclisation. *Chem. Soc. Rev.* **2016**, *45*, 4448−4458. (e) Ye, L. W.; Zhu, X.; Sahani, R.; Xu, Y.; Qian, P. C.; Liu, R. S. Nitrene Transfer and Carbene Transfer in Gold Catalysis. *Chem. Rev.* **2020**, DOI: 10.1021/acs.chemrev.0c00348.

(11) For selected papers on the trapping of α-Oxo Gold Carbenes with N-centered nucleophiles, see: (a) Yeom, H.; Lee, J.; Shin, S. Gold-Catalyzed Waste-Free Generation and Reaction of Azomethine Ylides: Internal Redox/Dipolar Cycloaddition Cascade. *Angew. Chem., Int. Ed.* **2008**, *47*, 7040−7043. (b) Yeom, H. S.; Lee, Y.; Jeong, J.; So, E.; Hwang, S.; Lee, J. E.; Lee, S. S.; Shin, S. Stereoselective One-Pot Synthesis of 1-Aminoindanes and 5,6-Fused Azacycles Using a Gold-Catalyzed Redox-Pinacol-Mannich-Michael Cascade. *Angew. Chem., Int. Ed.* **2010**, *49*, 1611−1614. (c) Xiao, J.; Li, X. Gold α-Oxo Carbenoids in Catalysis: Catalytic Oxygen-Atom Transfer to Alkynes. *Angew. Chem., Int. Ed.* **2011**, *50*, 7226−7236. (d) He, W.; Li, C.; Zhang, L. An Efficient [2 + 2 + 1] Synthesis of 2,5-Disubstituted Oxazoles via Gold-Catalyzed Intermolecular Alkyne Oxidation. *J. Am. Chem. Soc.* **2011**, *133*, 8482−8485. (e) Xiao, Y.; Zhang, L. Synthesis of Bicyclic Imidazoles via [2 + 3] Cycloaddition between Nitriles and Regioselectively Generated α-Imino Gold Carbene Intermediates. *Org. Lett.* **2012**, *14*, 4662−4665. (f) Li, J.; Ji, K.; Zheng, R.; Nelson, J.; Zhang, L. Expanding the Horizon of Intermolecular Trapping of In-Situ Generated α-Oxo Gold Carbenes: Efficient Oxidative Union of Allylic Sulfides and Terminal Alkynes *via* C-C Bond Formation. *Chem. Commun.* **2014**, *50*, 4130−4133. (g) Mokar, B. D.; Huple, D. B.; Liu, R. S. Gold-catalyzed Intermolecular Oxidations of 2-Ketonyl-1-ethynyl Benzenes with *N*-Hydoxyanilines to Yield 2-Amino-indenones via Gold Carbene Intermediates. *Angew. Chem., Int. Ed.* **2016**, *55*, 11892−11896.

(12) (a) Mokar, B. D.; Jadhav, P. D.; Pandit, Y. B.; Liu, R. S. Gold-catalyzed (4 + 2)-annulations between α-alkyl alkenyl gold carbenes and benzisoxazoles with reactive alkyl groups. *Chem. Sci.* **2018**, *9*, 4488−4492. (b) Skaria, M.; Sharma, P.; Liu, R. S. Gold(I)-Catalyzed 1,3-Carbofunctionalizations of Anthranils with Vinyl Propargyl Esters To Yield 1,3-Dihydrobenzo[*c*]-isoxazoles. *Org. Lett.* **2019**, *21*, 2876−2879. (c) Kumar, R.; Singh, R.; Skaria, M.; Chen, L.; Cheng, M. J.; Liu, R. S. Gold-catalyzed (4 + 3)-annulations of 2-alkenyl-1-alkynylbenzenes with anthranils with alkyne- dependent chemoselectivity: skeletal rearrangement versus non-rearrangement. *Chem. Sci.* **2019**, *10*, 1201−1206.

(13) (a) Davies, I.; Guner, V.; Houk, K. Theoretical Evidence for Oxygenated Intermediates in the Reductive Cyclization of Nitrobenzenes. *Org. Lett.* **2004**, *6*, 743−746. (b) Pagar, V.; Jadhav, A.; Liu, R. S. Gold-Catalyzed Formal [3 + 3] and [4 + 2] Cycloaddition Reactions of Nitrosobenzenes with Alkenylgold Carbenoids. *J. Am. Chem. Soc.* **2011**, *133*, 20728−20731. (c) Schützner ová, E.; Krchňák, V. N-Oxide as an Intramolecular Oxidant in the Baeyer-Villiger Oxidation: Synthesis of 2-Alkyl-2*H*-indazol-3-yl Benzoates and 2-Alkyl-1,2-dihydro-3*H*-indazol-3-ones. *J. Org. Chem.* **2016**, *81*, 3585−3596. (d) Nykaza, T. V.; Harrison, T. S.; Ghosh, A.; Putnik, R.; Radosevich, A. T. A Biphilic Phosphetane Catalyzes N−N Bond-Forming Cadogan Heterocyclization via PIII/PV = O Redox Cycling. *J. Am. Chem. Soc.* **2017**, *139*, 6839−6842.

(14) Ramana, C. V.; Patel, P.; Vanka, K.; Miao, B.; Degterev, A. A Combined Experimental and Density Functional Theory Study on the Pd-Mediated Cycloisomerization of o-Alkynylnitrobenzenes − Synthesis of Isatogens and Their Evaluation as Modulators of ROS-Mediated Cell Death. *Eur. J. Org. Chem.* **2010**, *2010*, 5955−5966.

(15) (a) Liu, R. R.; Ye, S. C.; Lu, C. J.; Zhuang, G. L.; Gao, J. R.; Jia, Y. X. Dual Catalysis for the Redox Annulation of Nitroalkynes with Indoles: Enantioselective Construction of Indolin-3-ones Bearing Quaternary Stereocenters. *Angew. Chem., Int. Ed.* **2015**, *54*, 11205−11208. (b) Dhote, P. S.; Ramana, C. V. One-Pot Au[III]-/Lewis Acid Catalyzed Cycloisomerization of Nitroalkynes and [3 + 3]-Cycloaddition with Donor−Acceptor Cyclopropanes. *Org. Lett.* **2019**, *21*, 6221−6224.

(16) (a) Aguilar, E.; Santamaría, J. Gold-catalyzed heterocyclic syntheses through α-imino gold carbene complexes as intermediates. *Org. Chem. Front.* **2019**, *6*, 1513−1540. (b) Gao, Y.; Nie, J.; Huo, Y.; Hu, X. Q. Anthranils: Versatile Building Blocks in the Construction of C-N Bonds and N-heterocycles. *Org. Chem. Front.* **2020**, *7*, 1177−1196.

(17) (a) Yeom, H.; Lee, J.; Shin, S. Gold-Catalyzed Waste-Free Generation and Reaction of Azomethine Ylides: Internal Redox/Dipolar Cycloaddition Cascade. *Angew. Chem., Int. Ed.* **2008**, *47*, 7040−7043. (b) Yeom, H. S.; Lee, Y.; Lee, J. E.; Shin, S. Geometry-dependent divergence in the gold-catalyzed redox cascade cyclization of o-alkynylaryl ketoximes and nitrones leading to isoindoles. *Org. Biomol. Chem.* **2009**, *7*, 4744−4752. (c) Wetzel, A.; Gagosz, F. Gold-Catalyzed Transformation of 2-Alkynyl Arylazides: Efficient Access to the Valuable Pseudoindoxyl and Indolyl Frameworks. *Angew. Chem., Int. Ed.* **2011**, *50*, 7354−7358.

(18) (a) Johansson, M. J.; Gorin, D. J.; Staben, S. T.; Toste, F. D. *J. Am. Chem. Soc.* **2005**, *127*, 18002−18003. (b) Lopez, S.; Herrero-Gómez, E. H.; Pérez-Galán, P. P.; Nieto-Oberhuber, C. N.; Echavarren, A. E. *Angew. Chem., Int. Ed.* **2006**, *45*, 6029−6032.

(19) Jin, H.; Huang, L.; Xie, J.; Rudolph, M.; Rominger, F.; Hashmi, S. K. Gold-Catalyzed C-H Annulation of Anthranils with Alkynes: A Facile, Flexible, and Atom-Economical Synthesis of Unprotected 7-Acylindoles. *Angew. Chem., Int. Ed.* **2016**, *55*, 794−797.

(20) Skaria, M.; More, S.; Kuo, T. C.; Cheng, M. J.; Liu, R. S. Gold-catalyzed Iminations of Terminal Propargyl Alcohols with Anthranils with A typical Chemoselectivity for C(1)-Additions and 1,2-Carbon Migration. *Chem. - Eur. J.* **2020**, *26*, 3600−3608.

(21) Sahani, R. L.; Liu, R. S. Gold-Catalyzed [4 + 2] Annulation/Cyclization Cascades of Benzisoxazoles with Propiolate Derivatives to

https://doi.org/10.1021/acs.orglett.1c00539
Org. Lett. 2021, 23, 2632−2637

Access Highly Oxygenated Tetrahydroquinolines. *Angew. Chem., Int. Ed.* **2017**, *56*, 12736−12740.

https://doi.org/10.1021/acs.orglett.1c00539
Org. Lett. 2021, 23, 2632−2637

JOC The Journal of Organic Chemistry

pubs.acs.org/joc Note

Intermolecular Interception of α-Oxo Gold Carbenes of Nitroalkyne Cycloisomerization with 1,2-Benzo[*d*]isoxazole: Synthesis of Functionalized Quinazoline 1-Oxides

Pawan S. Dhote, Kishor A. Pund, and Chepuri V. Ramana*

Cite This: *J. Org. Chem.* 2021, 86, 10874–10882 Read Online

ACCESS | Metrics & More | Article Recommendations | Supporting Information

ABSTRACT: The known nitrogen-transfer reagent 1,2-benzo[*d*]-isoxazole has been used to trap the postulated α-oxo gold carbene intermediate involved in the [Au]-catalyzed internal redox process of 2-alkynylnitrobenzenes. This process led us to develop a general convergent method for the synthesis of highly functionalized quinazoline 1-oxides.

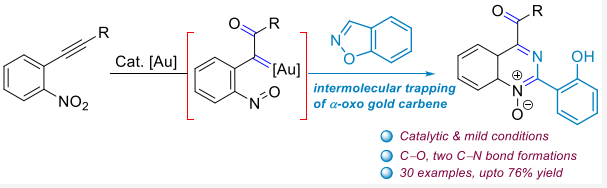

In recent years, homogeneous gold catalysis has taken a significant place in organic synthesis, in general, and in heterocyclic synthesis, in particular.[1] Specifically, the catalytic processes involving the reactive α-imino or α-oxo gold carbene intermediates represent an important advancement in this domain because of the versatile transformations that these intermediates undergo and the resulting product diversity.[2] In particular, the α-oxo gold carbene intermediates have attracted much attention, as they are easy to generate by inter- or intramolecular addition of nucleophilic oxygen donors to alkynes.[3] The exploited oxygen donors in this context include nitro compounds, nitrones, sulfoxides, pyridine *N*-oxides, and epoxides.

In 2003, employing *o*-alkynylnitrobenzenes, Yamamoto's group revealed the inaugural entry on the gold-catalyzed intramolecular oxygen atom transfer to alkyne that leads to either isatogen **2** or anthranil **3**.[4] The possibility of an α-oxo metal carbene after the initial internal nitroalkyne redox cyclization has been proposed by Crabtree's group in a similar transformation mediated by IrH complexes.[5] A similar possibility in the gold-catalyzed internal nitroalkynes redox process has been speculated by Liu and our groups.[6,7] The possible inter/intramolecular trapping of these speculated gold carbene intermediates with other nucleophiles that interrupt the subsequent intramolecular process is challenging and has been attempted with limited success.[7b,8] Recently, the carbene transfer from the α-oxo gold carbene **A** has been realized successfully by employing a benzo[*c*]isoxazole that resulted initially in an imine, which subsequently underwent a Davis–Beirut reaction giving highly functionalized indazoles.[9]

In continuation, we speculated a similar carbene exchange with the isomeric benzo[*d*]isoxazole **4** to synthesize the quinazoline 1-oxides. As shown in Scheme 1, the postulated [Au] → N carbene exchange of intermediate **A** with benzo[*d*]isoxazole **4** is expected to provide the imino-*o*-quinomethide **B**.[10] Subsequent nucleophilic addition of the nitroso group to quinomethide and deprotonation should lead to the quinazoline 1-oxide **5**.[11] Quinazoline 1-oxides are relatively unexplored in medicinal chemistry, which is quite surprising, as the parent quinazoline is one of the privileged skeletons in various drug discovery programs and is widely found in various natural products/approved drugs.[12] In general, these quinazoline-1-oxides are synthesized by N-oxidation, and there are no general methods documented for their convergent synthesis.[13] In this context, the development of novel synthetic routes to access quinazoline-1-oxides is an attractive task.

Our initial experiments in this regard started with the nitroalkyne **1a** and benzo[*d*]isoxazole **4a** as the substrates and examined the gold and palladium complexes that are commonly employed in the internal nitroalkyne redox process. In general, the reactions were carried out employing 1 equiv of 1-(but-1-yn-1-yl)-2-nitrobenzene (**1a**) and 1.1 equiv of benzo[*d*]isoxazole **4a** in suitable solvent at a given temperature in the presence of 5 mol % of catalyst. Table 1 saliently describes the exploratory experiments that were conducted in this context. When $AuBr_3$ was employed as a catalyst in toluene, it afforded the self-cycloisomerization product anthranil **3a**, along with a trace amount of a new product with an expected mass corresponding to the desired product **5aa**, while the reaction with $Pd(CH_3CN)_2Cl_2$ complex in acetonitrile gave isatogen **2a** exclusively.[7a,b] Next, $AuCl_3$[14] was employed in 1,2-dichloroethane, which results in the formation of anthranil **3a** in trace amounts (entry 3).[9] Gratifyingly, when

Received: May 25, 2021
Published: July 27, 2021

https://doi.org/10.1021/acs.joc.1c01221
J. Org. Chem. 2021, 86, 10874–10882

Scheme 1. Synthesis of Quinazoline 1-Oxides: Reported Methods and the Proposed Method via the Trapping of the Intermediate α-Oxo Gold Carbenes with 1,2-Benzo[*d*]isoxazole

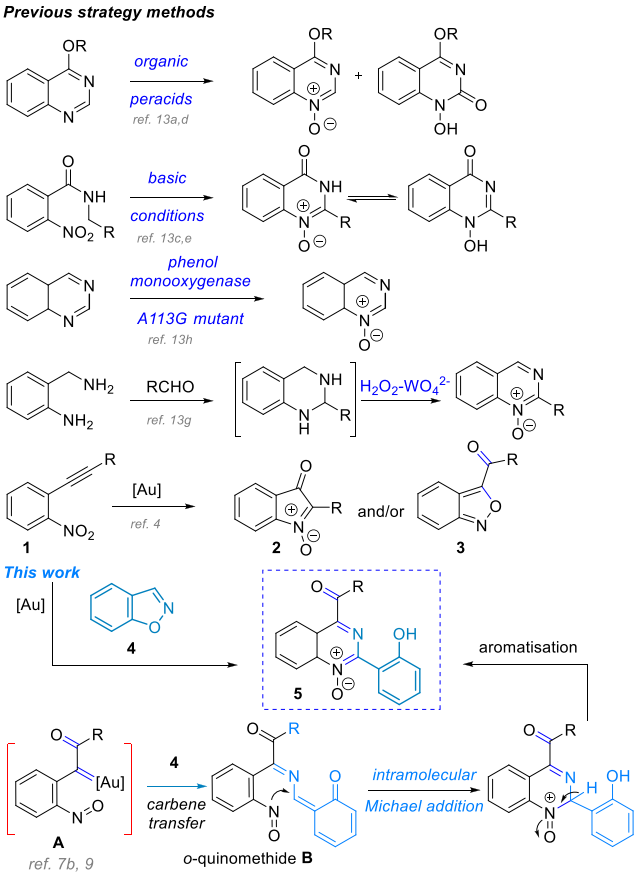

we switched to toluene as a solvent, it afforded the desired quinazoline 1-oxide **5aa** (62%) as the major product along with anthranil **3a** (10% yield) (entry 4).

Encouraged by these results, we screened different solvents. However, there was no net increase in the yield of **5aa** (entries 5−8). The changing of gold catalyst and the addition of silver salts did not improve the yields (entries 9−13). In all these cases, the anthranil **3a** was obtained in a major quantity along with requisite **5aa** obtained as a minor product. When AuCl was employed as a catalyst, a mixture of **5aa** and **3a** was obtained in equal proportions (entry 14). Heating the reaction to 80 °C improved the yield of **5aa** nominally (65%, entry 15). The yield of **5aa** was improved further to 73% when the reaction was carried out by the slow addition of **1a** to a solution of **4a** along with $AuCl_3$. In this case, the formation of cycloisomerization product **3a** was also minimized to trace amounts (entry 16). At this stage, the reaction with excess 1,2-benzo[*d*]isoxazole **4a** (3 equiv) under these conditions was tried. However, it did not improve the yield of the desired product (entry 17). A control experiment conducted without gold catalyst and by heating a mixture of **1a** and **4a** at 80 °C in toluene revealed that both of the starting compounds were intact as well as the essential role of the gold complex for the internal oxygen transfer (entry 18).

With the optimized conditions in hand, the scope of this reaction has been expanded by employing nitroalkyne substrates with varying substituents on the pendant alkyne

Table 1. Optimization of the Reaction Conditions.[a]

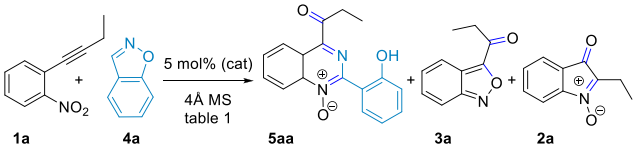

entry	catalyst	solvent	yield (%) 5aa[b] (%)	yield (%) 2a or 3a[b] (%)
1	$AuBr_3$	PhMe	trace	64 (**3a**)
2	$Pd(CH_3CN)_2Cl_2$	CH_3CN		66 (**2a**)
3	$AuCl_3$	$(CH_2)_2Cl_2$		trace (**3a**)
4	$AuCl_3$	PhMe	62	10 (**3a**)
5	$AuCl_3$	CH_3CN		
6	$AuCl_3$	1,4 Dioxane		
7	$AuCl_3$	$PhCF_3$	54	13 (**3a**)
8	$AuCl_3$	PhCl	59	10 (**3a**)
9	$PPh_3AuCl/AgSbF_6$	PhMe	26	32 (**3a**)
10	$PicAuCl_2$	PhMe	44	16 (**3a**)
11	$JohnPhosAuCl/AgSbF_6$	PhMe	49	19 (**3a**)
12	$IPrAuCl/AgNTf_2$	PhMe	36	26 (**3a**)
13	$BrettPhosAuCl/AgNTf_2$	PhMe	41	18 (**3a**)
14	AuCl	PhMe	38	24 (**3a**)
15[c]	$AuCl_3$	PhMe	65	6 (**3a**)
16[d]	**$AuCl_3$**	**PhMe**	**73**	**trace (3a)**
17[e]	$AuCl_3$	PhMe	72	trace (**3a**)
18[c]		PhMe		

[a]In general, the reactions were carried out with 0.2 mmol of **1a** and 0.22 mmol of **4a** in 2 mL of solvent and 5 mol % of catalyst at rt with a reaction time of 2−4 h. [b]Isolated yield. [c]Reaction was carried at 80 °C. [d]Addition of **1a** to solution of **4a** in solvent through a syringe pump for 4 h. [e]With 3 equiv (0.66 mmol) of **4a**.

unit (**1a**−**1i**, **1o**−**1r**) and also the phenyl-substituted one **1t** by placing different substituents *para* to the alkyne group (**1j**−**1n**) and also by changing the substituents on the 1,2-benzo[*d*]-isoxazole counterpart (**4a**−**4h**). As shown in Scheme 2, changing the length of the pendant alkyne unit did not alter the reaction outcome (**5aa**−**5ca**), whereas steric hindrance on the alkyne unit had an influence on the reaction outcome. For example, with the isobutyl substituent, the yield of the desired quinazoline 1-oxide was reduced to 60% (**5da**), and when a benzyl (**1o**) and *tert*-butyl (**1r**) group was present, there was no intermolecular interception and the intramolecular cyclization leading to corresponding anthranils was the main event. Similarly, when propargylic carbons bear an −I group such as −OTHP (**1p**) or −NHBoc (**1q**) the reactions led to a complex mixture from which a mixture of corresponding anthranils and/or isatogens could be isolated in small amounts. However, when the same groups are present on the homopropargylic position, their reactions with 1,2-benzo[*d*]-isoxazole **4a** proceeded smoothly and provided the corresponding quinazoline oxides in moderate to good yields. The examined scope with these substrates revealed the tolerance for various protecting group such as OAc, OTBS, OTHP, and OBn on the alkyl chain under current conditions. In addition, a gram-scale reaction was performed under the optimized conditions, and it was found that with 2 mol % of $AuCl_3$ the reactions proceeded well and provided the desired quinazoline 1-oxide **5ba** in 69%. Next, we examined the reactions with the substrates having electron withdrawing/donating groups such as $-CO_2Me$ (**1m**), $-NO_2$ (**1k**), −F (**1j**), and −Me (**1l**) *para*

https://doi.org/10.1021/acs.joc.1c01221
J. Org. Chem. 2021, 86, 10874−10882

Scheme 2. Reaction Scope[a]

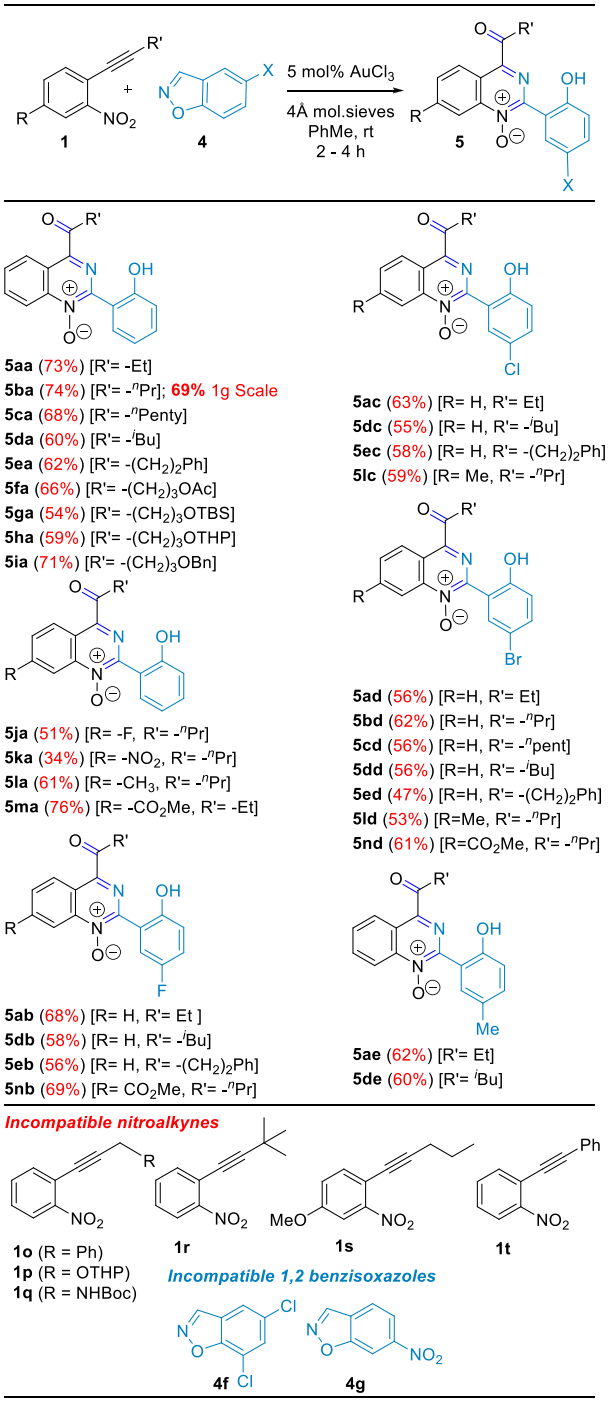

[a]For reaction conditions, see Table 1, entry 16. Isolated yields are reported after column chromatography.

to the alkyne unit. Interestingly, with the substrate having the $-CO_2Me$, the best reaction outcome was seen. On the other hand, with the substrate having the $-NO_2$ group, the intramolecular cyclization competed well and resulted in the requisite quinazoline *N*-oxide (**5ka**) in 34% yield, along with substantial amounts of anthranil/isatogen. With the substrates −F or −Me, the corresponding quinazoline *N*-oxides **5ja** (51%) and **5la** (61%), respectively, were obtained in moderate yields. Next, the 1,2-benzo[*d*]isoxazoles having substituents such as −F (**4b**), −Cl (**4c**), −Br (**4d**), and −Me (**4e**) were employed in the current reaction to examine how the electronic nature of the substituent *para* to the phenolic oxygen would influence the reaction outcome. In general, the reactions with these four 1,2-benzo[*d*]isoxazoles were found to be smooth and provided the corresponding heterocyclic products in moderate to good yields. In addition, the benzo[*d*]isoxazole having 5,7-dichloro (**4f**) or $-NO_2$ (**4g**) were found to be incompatible, and the reactions with these substrates resulted mainly in the anthranil formation. Some of the synthesized *N*-oxide derivatives were subjected for N−O bond reduction by using Zn dust in 30% aq NH_4Cl in THF to afford the corresponding quinazoline derivative in good yields (Scheme 3).[15]

Scheme 3. Defunctionalization to Quinazoline Scaffolds[a]

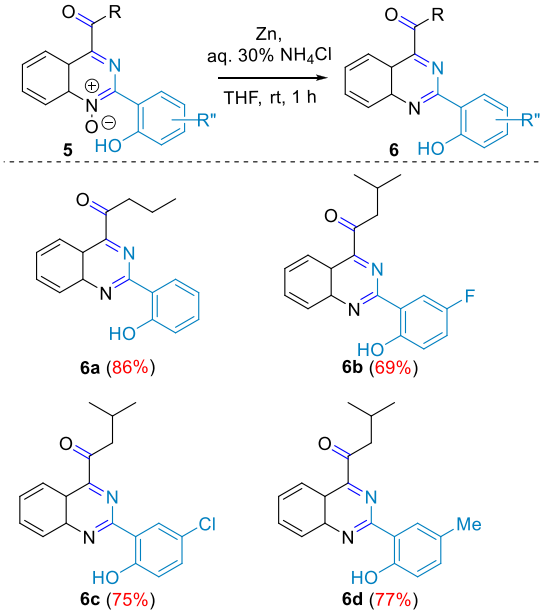

[a]Reaction conditions: **5** (0.16 mmol), Zn dust (0.32 mmol), aq 30% NH_4Cl/THF (1 mL, 1:1), rt, 1 h.

Having established the generality of the current reaction, we next proceeded further to learn about the possible involvement[16] of the α-oxo gold carbene intermediate and carbene transfer to a nitrogen center.[17] With 2-phenyethynylnitrobenzene **1t**, there was no interception by the 1,2-benzo[*d*]-isoxazoles and the reaction provided exclusively to isatogen (eq 1, Scheme 4). When 3-methylbenzo[*d*]isoxazole **4h** was used along with **1b**, the self-cycloisomerized product **3b** was obtained exclusively in 79% yield (eq 2, Scheme 4). This, taken together with the fact that 3-methyl-1,2-benzo[*d*]-isoxazole (**4h**) is not compatible in the current reaction, provided an indirect support for the initial N−O transfer to the alkyne. This ruled out the alternative possibility of the competing addition of the benzoxazole nitrogen to the alkyne, leading to an α-imino gold carbene and subsequent internal oxygen transfer.[10,18] Similar unsuccessful attempts in interrupting or trapping of the intermediates of the nitroalkyne cycloisomerization of 2-arylethynylnitrobenzenes such as **1t** reveal that the intermediate α-oxo gold carbene involved in this process is relatively unstable and/or the subsequent 6π-electrocyclization of this carbene is relatively faster.[6,8b,19] Next, competition experiments such as adding the nitroalkyne **1a** to a

https://doi.org/10.1021/acs.joc.1c01221
J. Org. Chem. 2021, 86, 10874−10882

Scheme 4. Control and Competition Experiments[a]

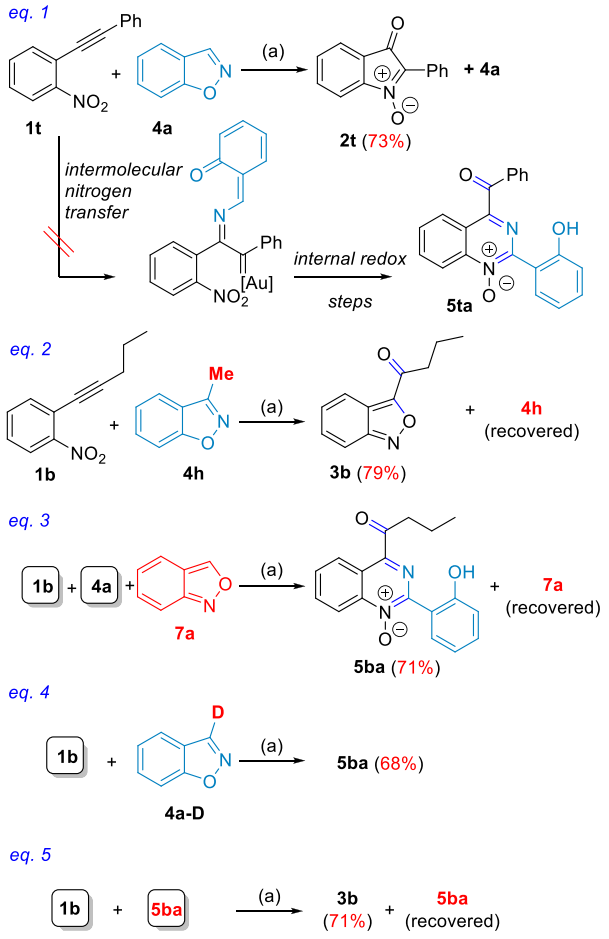

[a]Conditions: (a) = $AuCl_3$ (5 mol %), 4 Å MS, PhMe, rt, 4 h.

equimolar mixture of benzo[*d*]isoxazole **4a** and its regioisomer benzo[*c*]isoxazole **7a** under the current conditions resulted exclusively in quinazoline 1-oxide **5ba** (71% yield) along with the recovery of **7a**, revealing that the N-centered nucleophile of benzo[*d*]isoxazole is more reactive than the anthranil (eq 3, Scheme 4).[20] When deuterated (benzo[*d*]isoxazole-3-d) **4a-D**[21] was employed along with **1b**, there was no incorporation of the deuterated hydrogen in product **5ba** (eq 4, Scheme 4). This indicated that the aromatization step involves the removal of the hydrogen atom next to the imine. Finally, a control experiment that included treating an equimolar mixture of o-nitroalkyne **1b** and the quinazoline *N*-oxide **5ba** under the optimized conditions (in the absence of benzo[*d*]isoxazole) resulted exclusively in the cycloisomerized product anthranil **3a** (71%) with the recovery of *N*-oxide **5ba** (eq 5, Scheme 4). This result suggests that the obtained *N*-oxide products are stable and that there is no oxygen transfer from these *N*-oxides to the nitroalkyne that can potentially interrupt the initial nitroalkyne redoxcyclization.

To conclude, a novel methodology for the convergent synthesis of functionalized quinazoline 1-oxides has been developed. The overall process includes trapping of α-oxo gold carbene with benzo[*d*]isoxazole with the orchestration of sequential N−O bond cleavage and the formation of C−O and C−N bonds in concert. The current example demonstrates fine competition between inter- vs intramolecular heteroatom addition to alkynes *interalia* competition between the formation of α-imino vs α-oxo gold carbenes. It also revealed the opportunities with 1,2-benzo[*d*]isoxazoles to participate in the carbene transfer from the gold centers, apart from its established addition to alkynes leading to α-imino gold carbenes. Work in the direction of expanding the scope of the reaction with other nitrogen transfer agents in this regard is currently progressing in our lab.

EXPERIMENTAL SECTION

General Information. The reactions were carried out in anhydrous solvents under argon atmosphere in oven-dried glassware. All anhydrous solvents were distilled prior to use. Commercial reagents were used without any purification. Column chromatography was carried out by using silica gel (60−120, 100−200, 230−400 mesh). ^{1}H and ^{13}C NMR chemical shifts are reported in relative to chloroform-*d* (δ = 7.27) or TMS, and coupling constants (*J*) are reported in hertz (Hz). The following abbreviations have been used to designate signal multiplicity: s = singlet, d = doublet, t = triplet, q = quartet, sxt = sextet, hept = septet, m = multiplet, b = broad. High-resolution mass spectra (HRMS) were recorded on a Q Exactive Hybrid Quadrupole Orbitrap mass spectrometer, where the mass analyzer used for analysis is orbitrap and some compounds on electrospray ionization time-of-flight (ESI-TOF). Infrared (IR) spectra were measured in cm^{-1} using FT−IR spectrophotometer.

General Procedure for the Synthesis of Quinazoline 1-Oxide Derivatives. In general, all reactions were carried out employing 50 mg of nitroalkyne **1**. At rt, to a stirred solution of 1,2-benzo[*d*]-isoxazole **4** (1.1 equiv) in anhydrous toluene (1 mL) were added $AuCl_3$ (5 mol %) and 4 Å molecular sieves (40 mg), and a solution of nitroalkyne **1** (1 equiv) in anhydrous toluene (1 mL) was introduced via syringe pump over a period of 2−4 h. The stirring was continued until the complete disappearance of the starting nitroalkyne as indicated by TLC. The reaction mixture was concentrated under reduced pressure, and the resulting crude was purified by column chromatography to afford the products **5**.

*2-(2-Hydroxyphenyl)-4-propionylquinazoline 1-oxide (**5aa**):* R_f = 0.4 (20% EtOAc in petroleum ether); yield 61 mg (73%); orange solid; IR (neat): ν_{max} 2975, 2930, 1699, 1530, 1468, 1314, 1252, 1159, 755 cm^{-1}; ^{1}H NMR (500 MHz, $CDCl_3$): δ 10.41 (s, 1H), 9.05 (dd, *J* = 0.7, 8.5 Hz, 1H), 8.87 (d, *J* = 8.7 Hz, 1H), 8.07−8.15 (m, 2H), 7.88 (ddd, *J* = 1.2, 7.1, 8.5 Hz, 1H), 7.58 (ddd, *J* = 1.7, 7.0, 8.4 Hz, 1H), 7.09−7.22 (m, 2H), 3.42 (q, *J* = 7.2 Hz, 2H), 1.31 (t, *J* = 7.2 Hz, 3H), ppm; ^{13}C{^{1}H} NMR (125 MHz, $CDCl_3$) δ 202.3 (s), 160.3 (s), 152.1 (s), 148.7 (s), 144.6 (s), 135.7 (d), 133.7 (d), 133.0 (d), 130.9 (d), 127.6 (d), 121.2 (s), 120.5 (d), 120.4 (s),120.1 (d), 119.3 (d), 33.2 (t), 7.8 (q) ppm; HRMS (ESI) calcd for $C_{17}H_{15}N_2O_3$: 295.1077 [M + H]$^+$; found: 295.1073.

*2-(2-Hydroxyphenyl)-4-propionylquinazoline 1-oxide (**5ba**):* R_f = 0.4 (20% EtOAc in petroleum ether); yield 60 mg (74%); orange solid; IR (neat) ν_{max} 2975, 2930, 1699, 1530, 1468, 1314, 1252, 1159, 755 cm^{-1}; ^{1}H NMR (500 MHz, $CDCl_3$) δ 10.41 (s, 1H), 9.03 (dd, *J* = 0.7, 8.6 Hz, 1H), 8.06−8.16 (m, 2H), 8.84−8.92 (m, 1H), 7.88 (ddd, *J* = 1.2, 7.1, 8.5 Hz, 1H), 7.58 (ddd, *J* = 1.7, 7.0, 8.4 Hz, 1H), 7.10−7.24 (m, 2H), 3.35 (t, *J* = 7.3 Hz, 2H), 1.79−1.91 (m, 2H), 1.08 (t, *J* = 7.4 Hz, 3H) ppm; ^{13}C{^{1}H} NMR (125 MHz, $CDCl_3$) δ 201.8 (s), 160.3 (s),152.0 (s), 148.9 (s), 144.6 (s), 135.7 (d), 133.7 (d), 132.9 (d), 130.8 (d), 127.6 (d), 121.2 (s), 120.5 (d), 120.4 (s), 120.1 (d), 119.3 (d), 41.6 (t), 17.4 (t), 13.8 (q) ppm; HRMS (ESI) calcd for $C_{18}H_{17}N_2O_3$: 309.1239 [M + H]$^+$; found: 309.1248.

Procedure for 1 g Scale. At room temperature, to a solution of 1,2-benzo[*d*]isoxazole **4a** (632 mg, 5.81 mmol) in anhydrous toluene (20 mL) and 4 Å molecular sieves (800 mg) and $AuCl_3$ (32 mg) was added *o*-nitroalkyne **1b** (1g, 5.29 mmol) in anhydrous toluene (20 mL) via syringe pump over 6 h. The reaction was stirred at room tempreture until the completion as indicated by TLC. Usual workup followed by purification by column chromatography afforded compound **5ba** (1.13 g, 69% yield) as yellow solid.

*4-Hexanoyl-2-(2-hydroxyphenyl)quinazoline 1-oxide (**5ca**):* R_f = 0.5 (15% EtOAc in petroleum ether); yield 53 mg (68%); yellow

https://doi.org/10.1021/acs.joc.1c01221
J. Org. Chem. 2021, 86, 10874−10882

syrup; IR (neat) ν_{max} 2925, 2858, 1700, 1603, 1533, 1469, 1317, 1251, 1160, 759 cm^{-1}; ^1H NMR (400 MHz, $CDCl_3$) δ 10.42 (s, 1H), 9.02 (d, J = 8.5 Hz, 1H), 8.87 (d, J = 8.7 Hz, 1H), 8.04−8.17 (m, 2H), 7.83−7.94 (m, 1H), 7.51−7.65 (m, 1H), 7.08−7.22 (m, 2H), 3.36 (t, J = 7.4 Hz, 2H), 1.82 (t, J = 7.3 Hz, 2H), 1.38−1.45 (m, 4H), 0.94 (t, J = 7.1 Hz, 3H) ppm; $^{13}C\{^1H\}$ NMR (125 MHz, $CDCl_3$) δ 202.0 (s), 160.3 (s), 152.0 (s), 148.9 (s), 144.6 (s), 135.7 (d), 133.7 (d), 132.9 (d), 130.8 (d), 127.6 (d), 121.2 (s), 120.5 (d), 120.4 (s), 120.1 (d), 119.3 (d), 39.8 (t), 31.4 (t), 23.7 (t), 22.5 (t), 13.9 (q) ppm; HRMS (ESI) calcd for $C_{20}H_{21}N_2O_3$: 337.1547 $[M + H]^+$; found: 337.1549.

2-(2-Hydroxyphenyl)-4-(3-methylbutanoyl)quinazoline 1-oxide (**5da**): R_f = 0.5 (10% EtOAc in petroleum ether); yield 48 mg (60%); orange solid; IR (neat) ν_{max} 2958, 1700, 1603, 1534, 1320, 1253, 1163, 762 cm^{-1}; ^1H NMR (400 MHz, $CDCl_3$) δ 10.41 (s, 1H), 8.98−9.03 (m, 1H), 8.84−8.89 (m, 1H), 8.06−8.13 (m, 2H), 7.88 (ddd, J = 1.2, 7.1, 8.5 Hz, 1H), 7.59 (ddd, J = 1.7, 7.0, 8.4 Hz, 1H), 7.12−7.21 (m, 2H), 3.23 (d, J = 6.9 Hz, 2H), 2.38 (dt, J = 6.7, 13.4 Hz, 1H), 1.08 (s, 3H), 1.06 (s, 3H) ppm; $^{13}C\{^1H\}$ NMR (100 MHz, $CDCl_3$) δ 201.7 (s), 160.3 (s), 152.0 (s), 149.1 (s), 144.6 (s), 135.7 (d), 133.7 (d), 132.9 (d), 130.8 (d), 127.6 (d), 121.2 (s), 120.6 (d), 120.4 (s), 120.2 (d), 119.3 (d), 48.4 (t), 25.2 (d), 22.7 (q, 2C) ppm; HRMS (ESI) calcd for $C_{19}H_{19}N_2O_3$: 323.1390 $[M + H]^+$; found: 323.1388.

2-(2-Hydroxyphenyl)-4-(3-phenylpropanoyl)quinazoline 1-oxide (**5ea**): R_f = 0.4 (15% EtOAc in petroleum ether); yield 46 mg (62%); pale yellow solid; IR (neat) ν_{max} 3016, 2922, 2859, 1699, 1601, 1532, 1488, 1318, 1251, 757, 698 cm^{-1}; ^1H NMR (400 MHz, $CDCl_3$) δ 10.32 (s, 1H), 9.00 (dd, J = 1.4, 8.7 Hz, 1H), 8.81−8.87 (m, 1H), 8.08 (ddd, J = 1.1, 7.1, 8.7 Hz, 1H), 8.03 (dd, J = 1.8, 8.2 Hz, 1H), 7.83−7.88 (m, 1H), 7.56 (ddd, J = 1.8, 7.1, 8.5 Hz, 1H), 7.28 (d, J = 4.1 Hz, 3H), 7.25 (s, 1H), 7.18−7.22 (m, 1H), 7.15 (dd, J = 0.92, 8.2 Hz, 1H), 7.09−7.13 (m, 1H), 3.70 (t, J = 7.5 Hz, 2H), 3.14 (t, J = 7.5 Hz, 2H) ppm; $^{13}C\{^1H\}$ NMR (100 MHz, $CDCl_3$) δ 200.8 (s), 160.2 (s), 152.1 (s), 148.4 (s), 144.6 (s), 140.5 (s), 135.7 (d), 133.7 (d), 133.0 (d), 130.9 (d), 128.6 (d, 2C), 128.5 (d, 2C), 127.6 (d), 126.3 (d), 121.1 (s), 120.5 (d), 120.3 (s), 120.2 (d), 119.2 (d), 41.3 (t), 30.1 (t) ppm; HRMS (ESI) calcd for $C_{23}H_{19}N_2O_3$: 371.1390 $[M + H]^+$; found: 371.1393.

4-(4-Acetoxybutanoyl)-2-(2-hydroxyphenyl)quinazoline 1-oxide (**5fa**): R_f = 0.4 (20% EtOAc in petroleum ether); yield 49 mg (66%); yellow solid; IR (neat) ν_{max} 2954, 2928, 1726, 1530, 1468, 1239, 1067, 873, 753 cm^{-1}; ^1H NMR (400 MHz, $CDCl_3$) δ 10.32 (s, 1H), 9.07 (dd, J = 0.7, 8.5 Hz, 1H), 8.84−8.89 (m, 1H), 8.06−8.15 (m, 2H), 7.89 (ddd, J = 1.2, 7.1, 8.5 Hz, 1H), 7.59 (ddd, J = 1.7, 7.0, 8.4 Hz, 1H), 7.12−7.21 (m, 2H), 4.24 (t, J = 6.4 Hz, 2H), 3.48 (t, J = 7.1 Hz, 2H), 2.18 (quin, J = 6.7 Hz, 2H), 2.04 (s, 3H) ppm; $^{13}C\{^1H\}$ NMR (100 MHz, $CDCl_3$) δ 200.6 (s) 171.1 (s), 160.3 (s), 152.1 (s), 148.1 (s), 144.7 (s), 135.8 (d), 133.8 (d), 132.9 (d), 131.1 (d), 127.6 (d), 121.2 (s), 120.6 (d), 120.3 (s), 120.2 (d), 119.3 (d), 63.5 (t), 36.1 (t), 23.0 (t), 20.9 (q) ppm; HRMS (ESI) calcd for: $C_{20}H_{19}N_2O_5$: 367.1288 $[M + H]^+$; found: 367.1284.

4-(4-((tert-Butyldimethylsilyl)oxy)butanoyl)-2-(2-hydroxyphenyl)quinazoline 1-oxide (**5ga**): R_f = 0.4 (20% EtOAc in petroleum ether); yield 37 mg (54%); dark yellow syrup; IR (neat) ν_{max} 2929, 2860, 1699, 1602, 1531, 1469, 1315, 1252, 1103, 906, 760 cm^{-1}; ^1H NMR (400 MHz, $CDCl_3$) δ 10.42 (s, 1H), 9.03−9.09 (m, 1H), 8.84−8.89 (m, 1H), 8.07−8.15 (m, 2H), 7.84−7.91 (m, 1H), 7.54−7.61 (m, 1H), 7.16−7.19 (m, 1H), 7.10−7.15 (m, 1H), 3.78 (t, J = 6.1 Hz, 2H), 3.47 (t, J = 7.2 Hz, 2H), 2.05 (dt, J = 6.5, 13.4 Hz, 2H), 0.89 (s, 9H), 0.05 (s, 6H), ppm; $^{13}C\{^1H\}$ NMR (100 MHz, $CDCl_3$) δ 201.6 (s) 160.3 (s), 152.1 (s), 148.6 (s), 144.6 (s), 135.7 (d), 133.7 (d), 133.0 (d), 130.8 (d), 127.7 (d), 121.2 (s), 120.5 (d), 120.4 (s), 120.1 (d), 119.3 (d), 62.1 (t), 36.4 (t), 27.0 (t), 25.9 (q, 3C), 18.3 (s), −5.4 (q, 2C) ppm; HRMS (ESI) calcd for: $C_{24}H_{31}N_2O_4Si$: 439.2048 $[M + H]^+$; found: 439.2055.

2-(2-Hydroxyphenyl)-4-(4-((tetrahydro-2H-pyran-2-yl)oxy)-butanoyl)quinazoline 1-oxide (**5ha**): R_f = 0.4 (20% EtOAc in petroleum ether); yield 42 mg (59%); yellow solid; IR (neat) ν_{max} 2938, 2863, 1700, 1603, 1533, 1316, 1121, 1028, 756 cm^{-1}; ^1H NMR (400 MHz, $CDCl_3$) δ 10.42 (s, 1H), 9.06 (dd, J = 0.7, 8.6 Hz, 1H), 8.85−8.90 (m, 1H), 8.07−8.15 (m, 2H), 7.88 (ddd, J = 1.2, 7.1, 8.5 Hz, 1H), 7.58 (ddd, J = 1.7, 7.0, 8.4 Hz, 1H), 7.17 (dd, J = 0.9, 8.3 Hz, 1H), 7.13 (ddd, J = 1.1, 7.1, 8.1 Hz, 1H), 4.57 (t, J = 3.4 Hz, 1H), 3.89 (dt, J = 6.3, 9.7 Hz, 1H), 3.82 (ddd, J = 3.0, 8.1, 11.1 Hz, 1H), 3.41−3.59 (m, 4H), 2.14 (quin, J = 6.6 Hz, 2H), 1.61−1.76 (m, 2H), 1.53−1.61 (m, 2H), 1.43−1.49 (m, 2H) ppm; $^{13}C\{^1H\}$ NMR (100 MHz, $CDCl_3$) δ 201.5 (s), 160.3 (s), 152.0 (s), 148.7 (s), 144.6 (s), 135.6 (d), 133.7 (d), 133.0 (d), 130.8 (d), 127.7 (d), 121.2 (s), 120.5 (d), 120.4 (s), 120.1 (d), 119.2 (d), 98.9 (d), 66.5 (t), 62.4 (t), 36.8 (t), 30.6 (t), 25.4 (t), 24.4 (t), 19.6 (t) ppm; HRMS (ESI) calcd for: $C_{23}H_{25}N_2O_5$: 409.1758 $[M + H]^+$; found: 409.1757.

4-(4-(Benzyloxy)butanoyl)-2-(2-hydroxyphenyl)quinazoline 1-oxide (**5ia**): R_f = 0.4 (20% EtOAc in petroleum ether); yield 50 mg (71%); orange gummy solid; IR (neat) ν_{max} 2925, 2859, 1699, 1603, 1533, 1363, 1104, 749, 693 cm^{-1}; ^1H NMR (400 MHz, $CDCl_3$) δ 10.46 (s, 1H), 8.91−8.98 (m, 1H), 8.83 (dq, J = 0.6, 8.7 Hz, 1H), 8.11 (dd, J = 1.7, 8.1 Hz, 1H), 8.06 (ddd, J = 1.3, 7.1, 8.7 Hz, 1H), 7.76−7.82 (m, 1H), 7.58 (ddd, J = 1.7, 7.0, 8.4 Hz, 1H), 7.20−7.26 (m, 5H), 7.18 (dd, J = 0.9, 8.3 Hz, 1H), 7.10−7.15 (m, 1H), 4.43 (s, 2H), 3.62 (t, J = 6.0 Hz, 2H), 3.47 (t, J = 6.9 Hz, 2H), 2.13−2.21 (m, 2H) ppm; $^{13}C\{^1H\}$ NMR (100 MHz, $CDCl_3$) δ 201.4 (s), 160.3 (s), 151.9 (s), 148.9 (s), 144.5 (s), 138.1 (s), 135.5 (d), 133.7 (d), 133.0 (d), 130.7 (d), 128.3 (d, 2C), 127.8 (d), 127.7 (d), 127.5 (d, 2C), 121.2 (s), 120.5 (d), 120.4 (s), 120.1 (d), 119.1 (d), 72.9 (t), 69.3 (t), 36.8 (t), 24.7 (t) ppm; HRMS (ESI) calcd for: $C_{25}H_{23}N_2O_4$: 415.1652 $[M + H]^+$; found: 415.1660.

4-Butyryl-7-fluoro-2-(2-hydroxyphenyl)quinazoline 1-oxide (**5ja**): R_f = 0.4 (15% EtOAc in petroleum ether); yield 40 mg (51%); orange solid; IR (neat) ν_{max} 2962, 1700, 1603, 1536, 1489, 1322, 1252, 1159, 752 cm^{-1}; ^1H NMR (400 MHz, $CDCl_3$) δ 10.30 (s, 1H), 9.15 (dd, J = 5.6, 9.4 Hz, 1H), 8.51 (dd, J = 2.5, 9.3 Hz, 1H), 8.10 (dd, J = 1.5, 8.0 Hz, 1H), 7.57−7.65 (m, 2H), 7.12−7.20 (m, 2H), 3.35 (t, J = 7.2 Hz, 2H), 1.85 (sxt, J = 7.3 Hz, 2H), 1.07 (t, J = 7.4 Hz, 3H) ppm; $^{13}C\{^1H\}$ NMR (100 MHz, $CDCl_3$) δ 201.7 (s), 165.6 (ds, J_{C-F} = 262.3 Hz), 160.4 (s), 153.0 (s), 148.1 (ds, J_{C-F} = 1.4 Hz), 146.5 (ds, J_{C-F} = 12.3 Hz), 134.1 (d), 133.0 (d), 131.2 (dd, J_{C-F} = 10.8 Hz), 121.0 (dd, J_{C-F} = 24.7 Hz), 120.7 (d), 120.3 (d), 120.1 (s), 118.4 (s), 104.8 (dd, J_{C-F} = 26.9 Hz), 41.5 (d), 17.4 (d), 13.8 (q) ppm; HRMS (ESI) calcd for $C_{18}H_{16}N_2O_3$: 327.1139 $[M + H]^+$; found: 327.1141.

4-Butyryl-2-(2-hydroxyphenyl)-7-nitroquinazoline 1-oxide (**5ka**): R_f = 0.3 (25% EtOAc in petroleum ether); yield 26 mg (34%); yellow solid; IR (neat) ν_{max} 2924, 2853, 1695, 1602, 1538, 1465, 1348, 1073, 746 cm^{-1}; ^1H NMR (400 MHz, $CDCl_3$) δ 9.71 (s, 1H), 9.66 (dd, J = 0.5, 2.3 Hz, 1H), 9.35 (dd, J = 0.5, 9.2 Hz, 1H), 8.60 (dd, J = 2.3, 9.3 Hz, 1H), 8.09−8.14 (m, 1H), 7.60−7.66 (m, 1H), 7.15−7.22 (m, 2H), 3.38 (t, J = 7.2 Hz, 2H), 1.88 (sxt, J = 7.3 Hz, 2H), 1.09 (t, J = 7.4 Hz, 3H) ppm; $^{13}C\{^1H\}$ NMR (100 MHz, $CDCl_3$) δ 201.1 (s), 160.5 (s), 153.5 (s), 151.4 (s), 147.5 (s), 145.0 (s), 134.6 (d), 132.9 (d), 130.6 (d), 124.2 (d), 123.6 (s), 120.9 (d), 120.6 (d), 119.5 (s), 115.8 (d), 41.4 (t), 17.4 (t), 13.8 (q) ppm; HRMS (ESI) calcd for $C_{18}H_{16}N_3O_5$: 354.1084 $[M + H]^+$; found: 354.1090.

4-Butyryl-2-(2-hydroxyphenyl)-7-methylquinazoline 1-oxide (**5la**): R_f = 0.3 (20% EtOAc in petroleum ether); yield 48 mg (61%); yellow solid; IR (neat) ν_{max} 2961, 2929, 1702, 1605, 1523, 1488, 1328, 1255, 1165, 756 cm^{-1}; ^1H NMR (400 MHz, $CDCl_3$) δ 10.57 (s, 1H), 8.91 (d, J = 8.7 Hz, 1H), 8.66 (s, 1H), 8.10 (dd, J = 1.6, 8.0 Hz, 1H), 7.69 (dd, J = 1.6, 8.7 Hz, 1H), 7.58 (ddd, J = 1.7, 7.0, 8.4 Hz, 1H), 7.10−7.20 (m, 2H), 3.34 (t, J = 7.2 Hz, 2H), 2.71 (s, 3H), 1.85 (sxt, J = 7.3 Hz, 2H), 1.07 (t, J = 7.4 Hz, 3H) ppm; $^{13}C\{^1H\}$ NMR (100 MHz, $CDCl_3$) δ 202.0 (s), 160.3 (s), 152.1 (s), 148.6 (s), 147.9 (s), 144.7 (s), 133.6 (d), 132.9 (d, 2C), 127.3 (d), 120.6 (s), 120.5 (d), 120.1 (d), 119.4 (s), 118.3 (d), 41.6 (t), 22.7 (q), 17.4 (t), 13.8 (q) ppm; HRMS (ESI) calcd for $C_{19}H_{19}N_2O_3$: 500.2068 $[M + H]^+$; found: 500.2068.

2-(2-Hydroxyphenyl)-7-(methoxycarbonyl)-4-propionylquinazoline 1-oxide (**5ma**): R_f = 0.4 (20% EtOAc in petroleum ether); yield 58 mg (76%); yellow solid; IR (neat) ν_{max} 2939, 1720, 1605, 1529, 1447, 1281, 1177, 1051 754 cm^{-1}; ^1H NMR (400 MHz, $CDCl_3$) δ 10.14 (s, 1H), 9.42−9.46 (m, 1H), 9.14 (d, J = 8.9 Hz, 1H), 8.41−

https://doi.org/10.1021/acs.joc.1c01221
J. Org. Chem. 2021, 86, 10874−10882

8.46 (m, 1H), 8.10 (dd, J = 1.7, 8.1 Hz, 1H), 7.59 (td, J = 1.5, 7.7 Hz, 1H), 7.41−7.51 (m, 1H), 7.12−7.19 (m, 2H), 6.94−7.00 (m, 1H), 4.07 (s, 3H), 3.42 (q, J = 7.2 Hz, 2H), 1.32 (t, J = 7.1 Hz, 3H) ppm; $^{13}C\{^1H\}$ NMR (100 MHz, $CDCl_3$) δ 201.9 (s), 165.0 (s), 160.2 (s), 152.6 (s), 148.1 (s), 144.6 (s), 136.3 (s), 134.1 (d), 133.0 (d), 130.4 (d), 128.3 (d), 123.0 (s), 121.1 (d), 120.6 (d), 120.4 (d), 120.0 (d), 53.2 (q), 33.2 (t), 7.7 (q) ppm; HRMS (ESI) calcd for $C_{19}H_{17}N_2O_5$: 353.1132 $[M + H]^+$; found: 353.1134.

*2-(5-Fluoro-2-hydroxyphenyl)-4-propionylquinazoline 1-oxide (**5ab**):* R_f = 0.4 (20% EtOAc in petroleum ether); yield 61 mg (68%); dark yellow gummy solid; IR (neat) ν_{max}2236, 1703, 1507, 1432, 1143, 750 cm^{-1}; ^1H NMR (400 MHz, $CDCl_3$) δ 10.13 (s, 1H), 9.06 (d, J = 8.6 Hz, 1H), 8.86 (d, J = 8.9 Hz, 1H), 8.12 (td, J = 0.9, 7.9 Hz, 1H), 7.86−7.96 (m, 1H), 7.78 (dd, J = 3.1, 9.6 Hz, 1H), 7.28−7.34 (m, 1H), 7.12 (dd, J = 4.9, 9.0 Hz, 1H), 3.42 (q, J = 7.3 Hz, 2H), 1.32 (t, J = 7.2 Hz, 3H) ppm; $^{13}C\{^1H\}$ NMR (100 MHz, $CDCl_3$) δ 202.1 (s), 159.2 (s), 156.4 (s), 156.4 (s), 150.9 (s), 148.7 (s), 135.9 (d), 131.2 (d), 129.3 (s), 127.8 (d), 121.3 (s), 121.7 (dd, J_{C-F} = 8.4 Hz), 121.0 (dd, J_{C-F} = 23.6 Hz), 119.3 (d), 117.7 (dd, J_{C-F} = 25.2 Hz), 33.3 (t), 7.8 (q) ppm; HRMS (ESI) calcd for: $C_{17}H_{14}N_2O_3F$: 313.0983 $[M + H]^+$; found: 313.0984.

*2-(5-Fluoro-2-hydroxyphenyl)-4-(3-methylbutanoyl)quinazoline 1-oxide (**5db**):* R_f = 0.4 (20% EtOAc in petroleum ether); yield 49 mg (58%); yellow gummy solid; IR (neat) ν_{max}2958, 1699, 1535, 1477, 1243, 754 cm^{-1}; ^1H NMR (400 MHz, $CDCl_3$) δ 10.14 (s, 1H), 9.01 (dt, J = 0.6, 8.5, Hz, 1H), 8.81−8.90 (m, 1H), 8.12 (ddd, J = 1.3, 7.1, 8.7 Hz, 1H), 7.90 (ddd, J = 1.2, 7.1, 8.5 Hz, 1H), 7.77 (dd, J = 3.1, 9.6 Hz, 1H), 7.31 (ddd, J = 3.1, 7.6, 9.1 Hz, 1H), 7.12 (dd, J = 4.9, 9.0 Hz, 1H), 3.23 (d, J = 6.9 Hz, 2H), 2.33−2.43 (m, 1H), 1.08 (s, 3H), 1.07 (s, 3H) ppm; $^{13}C\{^1H\}$ NMR (100 MHz, $CDCl_3$) δ 201.4 (s), 157.5 (s), 156.4 (ds, J_{C-F} = 1.5 Hz), 155.1 (s), 150.8 (ds, J_{C-F} = 3.0 Hz), 149.2 (s), 144.6 (s), 135.9 (d), 131.1 (d), 127.7 (d), 121.7 (dd, J_{C-F} = 7.6 Hz), 121.3 (s), 121.0 (dd, J_{C-F} = 23.6 Hz), 119.3 (d), 117.6 (dd, J_{C-F} = 25.2 Hz), 48.4 (t), 25.1 (d), 22.7 (q, 2C) ppm; HRMS (ESI) calcd for: $C_{19}H_{18}N_2O_3F$: 341.1296 $[M + H]^+$; found: 341.1300.

*2-(5-Fluoro-2-hydroxyphenyl)-4-(3-phenylpropanoyl)-quinazoline 1-oxide (**5eb**):* R_f = 0.4 (20% EtOAc in petroleum ether); yield 43 mg (56%); yellow solid; IR (neat) ν_{max}3016, 2958, 1699, 1601, 1532, 1488, 1318, 1251, 757, 698 cm^{-1}; ^1H NMR (400 MHz, $CDCl_3$) δ 10.05 (s, 1H), 9.01 (dd, J = 0.7, 8.6 Hz, 1H), 8.84 (d, J = 8.4 Hz, 1H), 8.11 (ddd, J = 1.3, 7.1, 8.7 Hz, 1H), 7.89 (ddd, J = 1.2, 7.1, 8.5 Hz, 1H), 7.72 (dd, J = 3.1, 9.6 Hz, 1H), 7.27−7.34 (m, 5H), 7.15−7.20 (m, 1H), 7.11 (dd, J = 4.8, 9.1 Hz, 1H), 3.71 (t, J = 7.4 Hz, 2H), 3.17 (t, J = 7.4 Hz, 2H) ppm; $^{13}C\{^1H\}$ NMR (100 MHz, $CDCl_3$) δ 200.6 (s), 157.5 (s), 156.3 (ds, J_{C-F} = 1.5 Hz), 155.1 (s), 150.8 (s), 148.5 (s), 144.6 (s), 140.4 (s), 135.9 (d), 131.2 (d), 128.6 (d, 2C), 128.5 (d, 2C), 127.7 (d), 126.3 (d), 121.7 (dd, J_{C-F} = 7.6 Hz), 121.3 (s), 121.0 (dd, J_{C-F} = 23.6 Hz), 119.2 (d), 117.6 (dd, J_{C-F} = 25.2 Hz), 41.3 (t), 30.1 (t) ppm; HRMS (ESI) calcd for: $C_{23}H_{18}N_2O_3F$: 389.1296 $[M + H]^+$; found: 389.1300.

*4-Butyryl-2-(5-fluoro-2-hydroxyphenyl)-7-(methoxycarbonyl)-quinazoline 1-oxide (**5nb**):* R_f = 0.4 (20% EtOAc in petroleum ether); yield 54 mg (69%); orange gummy solid; IR (neat) ν_{max}2959, 1721, 1528, 1235, 1125, 748 cm^{-1}; ^1H NMR (400 MHz, $CDCl_3$) δ 9.78 (s, 1H), 9.40−9.47 (m, 1H), 9.08−9.17 (m, 1H), 8.44 (dd, J = 1.7, 8.8 Hz, 1H), 7.73−7.79 (m, 1H), 7.31 (ddd, J = 3.1, 7.5, 9.1 Hz, 1H), 7.11 (dd, J = 4.8, 9.1 Hz, 1H), 4.08 (s, 3H), 3.35 (t, J = 7.2 Hz, 2H), 1.82−1.90 (m, 2H), 1.09 (t, J = 7.4 Hz, 3H) ppm; $^{13}C\{^1H\}$ NMR (100 MHz, $CDCl_3$) δ 201.3 (s), 164.9 (s), 157.6 (s), 156.4 (ds, J_{C-F} = 1.5 Hz), 155.2 (s), 148.2 (s), 144.7 (s), 136.4 (s), 130.7 (d), 128.4 (d), 123.1 (s), 121.8 (dd, J_{C-F} = 8.4 Hz), 121.3 (dd, J_{C-F} = 23.6 Hz), 121.1 (d), 120.4 (s), 117.6 (dd, J_{C-F} = 25.2 Hz), 53.2 (q), 41.5 (t), 17.3 (t), 13.8 (q) ppm; HRMS (ESI) calcd for: $C_{20}H_{18}N_2O_5F$: 385.1194 $[M + H]^+$; found: 385.1196.

*2-(5-Fluoro-2-hydroxyphenyl)-4-propionylquinazoline 1-oxide (**5ac**):* R_f = 0.4 (20% EtOAc in petroleum ether); yield 59 mg (63%); dark yellow solid; IR (neat) ν_{max} 2932, 1706, 1603, 1532, 1469, 1321, 763 cm^{-1}; ^1H NMR (400 MHz, $CDCl_3$) δ 10.42 (s, 1H) 9.01−9.11 (m, 1H), 8.85 (d, J = 8.8 Hz, 1H), 8.12 (ddd, J = 1.2, 7.2, 8.6 Hz, 1H), 8.05 (d, J = 2.6 Hz, 1H), 7.86−7.96 (m, 1H), 7.51 (dd, J = 2.6, 8.9 Hz, 1H), 7.11 (d, J = 8.9 Hz, 1H), 3.42 (q, J = 7.1 Hz, 2H), 1.31 (t, J = 7.1 Hz, 3H) ppm; $^{13}C\{^1H\}$ NMR (100 MHz, $CDCl_3$) δ 202.1 (s), 158.9 (s), 150.8 (s), 149.0 (s), 144.6 (s), 135.9 (d), 133.6 (d), 131.8 (d), 131.2 (d), 127.7 (d), 125.0 (s), 122.0 (d), 121.5 (s), 121.3 (s), 119.3 (d), 33.3 (t), 7.7 (q) ppm; HRMS (ESI) calcd for: $C_{17}H_{14}N_2O_3Cl$: 329.0687 $[M + H]^+$; found: 329.0691.

*2-(5-Chloro-2-hydroxyphenyl)-4-(3-methylbutanoyl)quinazoline 1-oxide (**5dc**):* R_f = 0.4 (20% EtOAc in petroleum ether); yield 48 mg (55%); yellow gummy solid; IR (neat) ν_{max}2951, 1698, 1535, 1467, 1285, 754 cm^{-1}; ^1H NMR (400 MHz, $CDCl_3$) δ 10.43 (s, 1H), 9.00 (dt, J = 0.6, 8.5 Hz, 1H), 8.81−8.88 (m, 1H), 8.12 (ddd, J = 1.3, 7.1, 8.7 Hz, 1H), 8.04 (d, J = 2.6 Hz, 1H), 7.90 (ddd, J = 1.2, 7.1, 8.4 Hz, 1H), 7.51 (dd, J = 2.6, 8.9 Hz, 1H), 7.10 (d, J = 8.9 Hz, 1H), 3.22 (d, J = 6.9 Hz, 2H), 2.38 (dt, J = 6.7, 13.4 Hz, 1H), 1.09 (s, 3H), 1.08 (s, 3H) ppm; $^{13}C\{^1H\}$ NMR (100 MHz, $CDCl_3$) δ 201.5 (s), 158.9 (s), 150.7 (s), 149.3 (s), 144.6 (s), 135.9 (d), 133.6 (d), 131.9 (d), 131.2 (d), 127.7 (d), 125.0 (s), 122.0 (d), 121.5 (s), 121.3 (s), 119.3 (d), 48.5 (t), 25.3 (d), 22.7 (q, 2C) ppm; HRMS (ESI) calcd for: $C_{19}H_{18}N_2O_3Cl$: 357.1000 $[M + H]^+$; found: 357.1007.

*2-(5-Chloro-2-hydroxyphenyl)-4-(3-phenylpropanoyl)-quinazoline 1-oxide (**5ec**):* R_f = 0.4 (20% EtOAc in petroleum ether); yield 47 mg (58%); dark yellow solid; IR (neat) ν_{max}3018, 2925, 2859, 1703, 1606, 1318, 1251, 740, 689 cm^{-1}; ^1H NMR (400 MHz, $CDCl_3$) δ 10.33 (s, 1H), 8.99 (dt, J = 0.6, 8.5 Hz, 1H), 8.80−8.86 (m, 1H), 8.11 (ddd, J = 1.3, 7.1, 8.7 Hz, 1H), 8.02 (d, J = 2.6 Hz, 1H), 7.89 (ddd, J = 1.2, 7.1, 8.5 Hz, 1H), 7.51 (dd, J = 2.6, 8.8 Hz, 1H), 7.30 (d, J = 4.4 Hz, 4H), 7.19−7.23 (m, 1H), 7.10 (d, J = 8.9 Hz, 1H), 3.70 (t, J = 7.4 Hz, 2H), 3.18 (t, J = 7.4 Hz, 2H) ppm; $^{13}C\{^1H\}$ NMR (100 MHz, $CDCl_3$) δ 200.7 (s), 158.9 (s), 150.8 (s), 148.7 (s), 144.6 (s), 140.4 (s), 135.9 (d), 133.6 (d), 131.8 (d), 131.2 (d), 128.6 (d, 2C), 128.5 (d, 2C), 127.7 (d), 126.3 (d), 125.0 (s), 122.0 (d), 121.4 (s), 121.3 (s), 119.2 (d), 41.3 (t), 30.3 (t) ppm; HRMS (ESI) calcd for: $C_{23}H_{18}N_2O_3Cl$: 405.1000 $[M + H]^+$; found: 405.1005.

*4-Butyryl-2-(5-chloro-2-hydroxyphenyl)-7-methylquinazoline 1-oxide (**5lc**):* R_f = 0.4 (20% EtOAc in petroleum ether); yield 52 mg (59%); yellow gummy solid; IR (neat) ν_{max} 2124, 1704, 1367, 1163, 742, 660 cm^{-1}; ^1H NMR (400 MHz, $CDCl_3$) δ 10.58 (s, 1H), 8.90 (d, J = 8.6 Hz, 1H), 8.62−8.69 (m, 1H), 8.05 (d, J = 2.6 Hz, 1H), 7.72 (dd, J = 1.4, 8.7 Hz, 1H), 7.50 (dd, J = 2.6, 8.9 Hz, 1H), 7.10 (d, J = 8.9 Hz, 1H), 3.33 (t, J = 7.2 Hz, 2H), 2.72 (s, 3H), 1.81−1.91 (m, 2H), 1.09 (t, J = 7.4 Hz, 3H) ppm; $^{13}C\{^1H\}$ NMR (100 MHz, $CDCl_3$) δ 201.8 (s), 158.9 (s), 150.9 (s), 149.0 (s), 148.2 (s), 144.6 (s), 133.5 (d), 133.3 (d), 131.9 (d), 127.4 (d), 124.9 (s), 122.0 (d), 121.7 (s), 119.5 (s), 118.2 (d), 41.7 (t), 22.7 (q), 17.4 (t), 13.8 (q) ppm; HRMS (ESI) calcd for: $C_{19}H_{18}N_2O_3Cl$: 357.1000 $[M + H]^+$; found: 357.1007.

*2-(5-Bromo-2-hydroxyphenyl)-4-propionylquinazoline 1-oxide (**5ad**):* R_f = 0.4 (15% EtOAc in petroleum ether); yield 60 mg (56%); orange solid; IR (neat) ν_{max} 2926, 2855, 1690, 1601, 1534, 1464, 1251, 1116, 759 cm^{-1}; ^1H NMR (400 MHz, $CDCl_3$) δ 10.46 (s, 1H), 9.04 (dd, J = 0.7, 8.6 Hz, 1H), 8.83−8.87 (m, 1H), 8.19 (d, J = 2.5 Hz, 1H), 8.12 (ddd, J = 1.3, 7.1, 8.6 Hz, 1H), 7.91 (ddd, J = 1.2, 7.1, 8.4 Hz, 1H), 7.64 (dd, J = 2.5, 8.9 Hz, 1H), 7.05 (d, J = 8.7 Hz, 1H), 3.42 (q, J = 7.2 Hz, 2H), 1.33 (t, J = 7.2 Hz, 3H) ppm; $^{13}C\{^1H\}$ NMR (125 MHz, $CDCl_3$) δ 202.0 (s) 159.4 (s), 150.7 (s), 149.1 (s), 144.6 (s), 136.4 (d), 135.9 (d), 134.8 (d), 131.2 (d), 127.7 (d), 122.4 (d), 122.0 (s), 121.3 (s), 119.2 (d), 112.0 (s), 33.3 (t), 7.7 (q) ppm; HRMS (ESI) calcd for $C_{17}H_{14}BrN_2O_3$: 373.0182 $[M + H]^+$; found: 373.0185.

*2-(5-Bromo-2-hydroxyphenyl)-4-butyrylquinazoline 1-oxide (**5bd**):* R_f = 0.5 (15% EtOAc in petroleum ether); yield 63 mg (62%); dark yellow solid; IR (neat) ν_{max} 2925, 2866, 1699, 1600, 1531, 1466, 1323, 1246, 1155, 762 cm^{-1}; ^1H NMR (400 MHz, $CDCl_3$): δ 10.46 (s, 1H), 8.99−9.05 (m, 1H), 8.82−8.89 (m, 1H), 8.20 (d, J = 2.5 Hz, 1H), 8.12 (ddd, J = 1.3, 7.1, 8.7 Hz, 1H), 7.91 (ddd, J = 1.2, 7.1, 8.5 Hz, 1H), 7.64 (dd, J = 2.5, 8.7 Hz, 1H), 7.06 (d, J = 8.9 Hz, 1H), 3.34 (t, J = 7.2 Hz, 2H), 1.81−1.93 (m, 2H), 1.10 (t, J = 7.4 Hz, 3H) ppm; $^{13}C\{^1H\}$ NMR (100 MHz, $CDCl_3$): δ 201.6 (s), 159.4 (s), 150.7 (s), 149.2 (s), 144.6 (s), 136.4 (d), 135.9 (d), 134.9 (d), 131.2 (d), 127.7 (d), 122.0 (s), 121.3 (s), 119.3 (d), 112.0 (s),

https://doi.org/10.1021/acs.joc.1c01221
J. Org. Chem. 2021, 86, 10874−10882

41.7 (t), 17.5 (t), 13.8 (q) ppm; HRMS (ESI) calcd for $C_{18}H_{16}BrN_2O_3$: 387.0339 $[M + H]^+$; found: 387.0344.

*2-(5-Bromo-2-hydroxyphenyl)-4-hexanoylquinazoline 1-oxide (**5cd**):* R_f = 0.4 (15% EtOAc in petroleum ether); yield 53 mg (56%); dark yellow solid; IR (neat) ν_{max} 2927, 2862, 1694, 1600, 1530, 1469, 1251, 1079, 1022, 761 cm^{-1}; ^1H NMR (400 MHz, $CDCl_3$) δ 10.47 (s, 1H), 9.02 (dd, J = 0.7, 8.6 Hz, 1H), 8.82−8.88 (m, 1H), 8.20 (d, J = 2.5 Hz, 1H), 8.12 (ddd, J = 1.1, 7.1, 8.7 Hz, 1H), 7.91 (ddd, J = 1.1, 7.1, 8.4 Hz, 1H), 7.64 (dd, J = 2.5, 8.7 Hz, 1H), 7.06 (d, J = 8.9 Hz, 1H), 3.35 (t, J = 7.4 Hz, 2H), 1.84 (t, J = 7.4 Hz, 2H), 1.40−1.50 (m, 4H), 0.93−0.98 (m, 3H) ppm; $^{13}C\{^1H\}$-NMR (100 MHz, $CDCl_3$) δ 201.8 (s), 159.4 (s), 150.7 (s), 149.2 (s), 144.6 (s), 136.4 (d), 135.9 (d), 134.9 (d), 131.2 (d), 127.7 (d), 122.4 (d), 122.0 (s), 121.3 (s), 112.0 (s), 39.9 (t), 31.4 (t), 23.9 (t), 22.5 (t), 13.9 (q) ppm; HRMS (ESI) calcd for $C_{20}H_{20}BrN_2O_3$: 415.0652 $[M + H]^+$; found: 415.0654.

*2-(5-Bromo-2-hydroxyphenyl)-4-(3-methylbutanoyl)quinazoline 1-oxide (**5dd**):* R_f = 0.4 (15% EtOAc in petroleum ether); yield 55 mg (56%); orange solid; IR (neat) ν_{max} 2958, 2874, 1696, 1599, 1531, 1469, 1373, 1324, 1284, 1244, 1161, 762 cm^{-1}; ^1H NMR (500 MHz, $CDCl_3$) δ 10.48 (s, 1H), 9.01 (d, J = 7.6 Hz, 1H), 8.85 (d, J = 8.4 Hz, 1H), 8.19 (d, J = 3.05 Hz, 1H), 8.09−8.16 (m, 1H), 7.88−7.94 (m, 1H), 7.64 (dd, J = 2.7, 8.8 Hz, 1H), 7.05 (d, J = 9.1 Hz, 1H), 3.22 (d, J = 6.9 Hz, 2H), 2.38 (dt, J = 6.6, 13.5 Hz, 1H), 1.10 (s, 3H), 1.08 (s, 3H) ppm; $^{13}C\{^1H\}$ NMR (125 MHz, $CDCl_3$) δ 201.5 (s), 159.4 (s), 150.6 (s), 149.4 (s), 144.6 (s), 136.4 (d), 135.9 (d), 134.9 (d), 131.2 (d), 127.7 (d), 122.4 (d), 122.0 (s), 121.3 (s), 119.3 (d), 112.0 (s), 48.6 (t), 25.4 (s), 22.7 (t, 2C) ppm; HRMS (ESI) calcd for $C_{19}H_{18}BrN_2O_3$: 401.0495 $[M + H]^+$; found: 401.0497.

*2-(5-Bromo-2-hydroxyphenyl)-4-(3-phenylpropanoyl)-quinazoline 1-oxide (**5ed**):* R_f = 0.4 (20% EtOAc in petroleum ether); yield 44 mg (47%); pale yellow solid; IR (neat) ν_{max} 3016, 2916, 2859, 1699, 1599, 1531, 1467, 1369, 1283, 1152, 758, 698 cm^{-1}; ^1H NMR (400 MHz, $CDCl_3$) δ 10.38 (s, 1H), 8.99 (dd, J = 0.7, 8.6 Hz, 1H), 8.81−8.87 (m, 1H), 8.17 (d, J = 2.4 Hz, 1H), 8.11 (ddd, J = 1.3, 7.1, 8.7 Hz, 1H), 7.89 (ddd, J = 1.2, 7.1, 8.4 Hz, 1H), 7.64 (dd, J = 2.5, 8.9 Hz, 1H), 7.31 (d, J = 4.4 Hz, 4H), 7.19−7.24 (m, 1H), 7.05 (d, J = 8.7 Hz, 1H), 3.70 (t, J = 7.4 Hz, 2H), 3.18 (t, J = 7.4 Hz, 2H) ppm; $^{13}C\{^1H\}$ NMR (100 MHz, $CDCl_3$) δ 200.7 (s), 159.4 (s), 150.7 (s), 148.7 (s), 144.6 (s), 140.3 (s), 136.4 (d), 136.0 (d), 134.8 (d), 131.2 (d), 128.6 (d, 2C), 128.5 (d, 2C), 127.7 (d), 126.4 (d), 122.4 (d), 122.0 (s), 121.3 (s), 119.2 (d), 112.0 (s), 41.3 (t), 30.3 (t) ppm; HRMS (ESI) calcd for $C_{23}H_{18}BrN_2O_3$: 449.0495 $[M + H]^+$; found: 449.0504.

*2-(5-Bromo-2-hydroxyphenyl)-4-butyryl-7-methylquinazoline 1-oxide (**5ld**):* R_f = 0.4 (15% EtOAc in petroleum ether); yield 52 mg (53%); orange solid; IR (neat) ν_{max} 2962, 2928, 2874, 1701, 1596, 1532, 1468, 1288, 1167, 823, 754 cm^{-1}; ^1H NMR (400 MHz, $CDCl_3$) δ 10.62 (s, 1H), 8.83−8.95 (m, 1H), 8.65 (br. s., 1H), 8.17−8.22 (m, 1H), 7.72 (d, J = 8.7 Hz, 1 H), 7.60−7.66 (m, H), 7.01−7.08 (m, 1H), 3.30−3.37 (m, 2H), 2.72 (s, 3H), 1.82−1.91 (m, 2H), 1.06−1.12 (m, 3H) ppm; $^{13}C\{^1H\}$ NMR (100 MHz, $CDCl_3$) δ 13.8 (q), 17.5 (t), 22.7 (q), 41.7 (t), 111.9 (s), 118.3 (d), 119.6 (s), 122.2 (s), 122.4 (d), 127.4 (s), 133.3 (d), 134.9 (d), 136.3 (d), 144.6 (s), 148.3 (s), 149.0 (s), 150.8 (s), 159.4 (s), 201.8 (s) ppm; HRMS (ESI) calcd for $C_{19}H_{18}N_2O_3Br$: 401.0495 $[M + H]^+$; found: 401.0494.

*2-(5-Bromo-2-hydroxyphenyl)-4-butyryl-7-(methoxycarbonyl)-quinazoline 1-oxide (**5nd**):* R_f = 0.4 (20% EtOAc in petroleum ether); yield 55 mg (61%); orange gummy solid; IR (neat) ν_{max} 2959, 2680, 1723, 1567, 1435, 1235, 1132, 815, 755 cm^{-1}; ^1H NMR (400 MHz, $CDCl_3$) δ 10.11 (s, 1H), 9.45 (d, J = 1.1 Hz, 1H), 9.09−9.16 (m, 1H), 8.44−8.49 (m, 1H), 8.19 (d, J = 2.5 Hz, 1H), 7.66 (dd, J = 2.5, 8.7 Hz, 1H), 7.07 (d, J = 8.9 Hz, 1H), 4.08 (s, 3H), 3.35 (t, J = 7.2 Hz, 2H), 1.82−1.94 (m, 2H), 1.10 (t, J = 7.38 Hz, 3H) ppm; $^{13}C\{^1H\}$ NMR (100 MHz, $CDCl_3$) δ 201.3 (s), 164.9 (s), 159.4 (s), 151.3 (s), 148.5 (s), 144.6 (s), 136.7 (d), 136.5 (s), 134.8 (d), 130.8 (d), 128.4 (d), 123.2 (s), 122.5 (d), 121.7 (s), 121.1 (d), 112.2 (d), 53.2 (q), 41.6 (t), 17.5 (t), 13.8 (q) ppm; HRMS (ESI) calcd for $C_{20}H_{18}BrN_2O_5$: 445.0394 $[M + H]^+$; found: 445.0399.

*2-(2-Hydroxy-5-methylphenyl)-4-propionylquinazoline 1-oxide (**5ae**):* R_f = 0.4 (20% EtOAc in petroleum ether); yield 55 mg (62%); dark yellow gum; IR (neat) ν_{max}2931, 1701, 1530, 1481, 1248, 823, 755 cm^{-1}; ^1H NMR (400 MHz, $CDCl_3$) δ 10.13 (s, 1H), 8.98−9.06 (m, 1H), 8.81−8.90 (m, 1H), 8.09 (ddd, J = 1.3, 7.1, 8.7 Hz, 1H), 7.81−7.91 (m, 2H), 7.39 (dd, J = 2.2, 8.4 Hz, 1H), 7.07 (d, J = 8.4 Hz, 1H), 3.42 (q, J = 7.2 Hz, 2H), 2.44 (s, 3H), 1.32 (t, J = 7.2 Hz, 3H) ppm; $^{13}C\{^1H\}$ NMR (100 MHz, $CDCl_3$) δ 202.3 (s), 158.1 (s), 152.1 (s), 148.6 (s), 144.6 (s), 135.6 (d), 134.8 (d), 132.6 (d), 130.7 (d), 129.3 (s), 127.6 (d), 121.1 (s), 120.3 (d), 120.0 (s), 119.3 (d), 33.2 (t), 20.7 (q), 7.8 (q) ppm; HRMS (ESI) calcd for: $C_{18}H_{17}N_2O_3$: 309.1234 $[M + H]^+$; found: 309.1238.

*2-(2-Hydroxy-5-methylphenyl)-4-(3-methylbutanoyl)quinazoline 1-oxide (**5de**):* R_f = 0.4 (20% EtOAc in petroleum ether); yield 50 mg (60%); yellow gummy solid; IR (neat) ν_{max} 2957, 1695, 1531, 1479, 1161, 1067, 751 cm^{-1}; ^1H NMR (400 MHz, $CDCl_3$) δ 10.15 (s, 1H), 9.00 (dd, J = 0.8, 8.5 Hz, 1H), 8.81−8.92 (m, 1H), 8.06−8.15 (m, 1H), 7.84−7.90 (m, 2H), 7.37−7.42 (m, 1H), 7.08 (d, J = 8.4 Hz, 1H), 3.23 (d, J = 6.9 Hz, 2H), 2.44 (s, 3H), 2.39 (dt, J = 13.5, 6.8 Hz, 1H), 1.09 (s, 3 H),1.07 (s, 3H) ppm; $^{13}C\{^1H\}$ NMR (100 MHz, $CDCl_3$) δ 201.7 (s), 158.1 (s), 152.1 (s), 149.0 (s), 144.6 (s), 135.6 (d), 134.8 (d), 132.6 (d), 130.7 (d), 129.3 (s), 127.5 (d), 121.2 (s), 120.3 (d), 120.0 (s), 119.3 (d), 48.6 (t), 25.4 (q), 22.8 (q, 2C), 20.7 (d) ppm; HRMS (ESI) calcd for: $C_{20}H_{21}N_2O_3$: 337.1547 $[M + H]^+$; found: 337.1548.

General Procedure for N−O Bond Reduction. To a stirred solution of **5** (1 equiv) in THF at room temperature was added Zn dust (2 equiv) followed by 30% aq NH_4Cl solution. The reaction mixture was stirred until the disappearance of the starting material shown by TLC (i.e., 1 h). Then the usual workup followed by purification by column chromatography afforded compound **6**.

*2-(2-Hydroxyphenyl)-4-propionylquinazoline (**6a**).* R_f = 0.5 (10% EtOAc in petroleum ether); yield 41 mg (86%); dark yellow solid; IR (neat) ν_{max} 1703, 1547, 1471, 1254, 760 cm^{-1}; ^1H NMR (400 MHz, $CDCl_3$) δ 13.50 (s, 1H), 8.59−8.72 (m, 2H), 8.05 (dq, J = 0.6, 8.5 Hz, 1H), 7.96 (ddd, J = 1.4, 6.9, 8.4 Hz, 1H), 7.68 (ddd, J = 1.2, 6.9, 8.4 Hz, 1H), 7.46 (ddd, J = 1.8, 7.0, 8.4 Hz, 1H), 7.11 (dd, J = 0.9, 8.2 Hz, 1H), 7.04 (ddd, J = 1.2, 7.1, 8.1 Hz, 1H), 3.37 (t, J = 7.2 Hz, 2H), 1.83−1.95 (m, 2H), 1.11 (t, J = 7.4 Hz, 3H) ppm; $^{13}C\{^1H\}$ NMR (100 MHz, $CDCl_3$) δ 203.5 (s), 160.9 (s), 160.7 (s), 160.3 (s), 149.9 (s), 135.0 (d), 133.5 (d), 129.6 (d), 128.8 (d), 127.3 (d), 126.7 (d), 119.2 (d), 119.0 (s), 118.8 (s), 117.9 (d), 42.1 (t), 17.3 (t), 13.8 (q) ppm; HRMS (ESI) calcd for: $C_{18}H_{17}N_2O_2$: 293.1290 $[M + H]^+$; found: 293.1292.

*2-(5-Fluoro-2-hydroxyphenyl)-4-(3-methylbutanoyl)quinazoline (**6b**):* R_f = 0.5 (10% EtOAc in petroleum ether); yield 33 mg (69%); dark yellow gummy solid; IR (neat) ν_{max} 1707, 1547, 1475, 1248, 760 cm^{-1}; ^1H NMR (400 MHz, $CDCl_3$) δ 13.23 (s, 1H), 8.62−8.68 (m, 1H), 8.30 (dd, J = 3.2, 9.8 Hz, 1H), 8.03−8.09 (m, 1H), 7.98 (ddd, J = 1.4, 6.9, 8.4 Hz, 1H), 7.71 (ddd, J = 1.2, 6.9, 8.4 Hz, 1H), 7.17 (ddd, J = 3.2, 7.7, 9.0 Hz, 1H), 7.05 (dd, J = 4.7, 9.0 Hz, 1H), 3.25 (d, J = 6.9 Hz, 2H), 2.40 (dt, J = 6.7, 13.4 Hz, 1H), 1.11 (s, 3H), 1.10 (s, 3H) ppm; $^{13}C\{^1H\}$ NMR (100 MHz, $CDCl_3$) δ 203.1 (s), 160.7 (s), 159.8 (ds, J_{C-F} = 3.0 Hz), 156.9 (ds, J_{C-F} = 1.5 Hz), 154.6 (s), 149.8 (s), 135.2 (d), 129.2 (d), 127.4 (d), 126.7 (d), 120.5 (dd, J_{C-F} = 23.6 Hz), 119.1 (s), 119.0 (ds, J_{C-F} = 7.6 Hz), 118.9 (dd, J_{C-F} = 7.6 Hz), 114.7 (dd, J_{C-F} = 25.2 Hz), 49.0 (t), 24.9 (d), 22.8 (q, 2C) ppm; HRMS (ESI) calcd for: $C_{19}H_{18}N_2O_2F$: 325.1352 $[M + H]^+$; found: 325.1345.

*2-(5-Chloro-2-hydroxyphenyl)-4-(3-methylbutanoyl)quinazoline (**6c**).* R_f = 0.5 (10% EtOAc in petroleum ether); yield 36 mg (75%); yellow gummy solid; IR (neat) ν_{max}1703, 1536, 1462, 1212, 819, 759 cm^{-1}; ^1H NMR (400 MHz, $CDCl_3$) δ 13.45 (s, 1H), 8.64 (dt, J = 0.6, 8.5 Hz, 1H), 8.58 (d, J = 2.7 Hz, 1H), 8.02−8.08 (m, 1H), 7.99 (dd, J = 1.4, 6.9 Hz, 1H), 7.68−7.75 (m, 1H), 7.38 (dd, J = 2.7, 8.8 Hz, 1H), 7.05 (d, J = 8.7 Hz, 1H), 3.24 (d, J = 6.9 Hz, 2H), 2.41 (dt, J = 6.7, 13.5 Hz, 1H), 1.12 (s, 3H), 1.10 (s, 3H) ppm; $^{13}C\{^1H\}$ NMR (100 MHz, $CDCl_3$) δ 203.1 (s), 160.9 (s), 159.6 (s), 159.4 (s), 149.8 (s), 135.3 (d), 133.3 (d), 129.2 (d), 128.9 (d), 127.4 (d), 126.7 (d), 124.0 (s), 119.7 (s), 119.5 (d), 119.2 (s), 49.0 (t), 25.0 (d), 22.8 (q, 2C)

https://doi.org/10.1021/acs.joc.1c01221
J. Org. Chem. 2021, 86, 10874−10882

ppm; HRMS (ESI) calcd for: $C_{19}H_{18}N_2O_2Cl$: 341.1057 $[M + H]^+$; found: 341.1050.

*2-(2-Hydroxy-5-methylphenyl)-4-(3-methylbutanoyl)quinazoline (**6d**).* R_f = 0.5 (10% EtOAc in petroleum ether); yield 37 mg (77%); yellow gummy solid; IR (neat) ν_{max}1713, 1547, 1467, 1283, 810, 754 cm^{-1}; ^1H NMR (400 MHz, $CDCl_3$) δ 13.28 (s, 1H), 8.62 (dt, J = 0.7, 8.5 Hz, 1H), 8.42 (d, J = 1.9 Hz, 1H), 8.01−8.07 (m, 1H), 7.96 (dd, J = 1.4, 6.9 Hz, 1H), 7.67 (ddd, J = 1.2, 7.0, 8.3 Hz, 1H), 7.25−7.29 (m, 1H), 7.01 (d, J = 8.4 Hz, 1H), 3.25 (d, J = 6.9 Hz, 2H), 2.40−2.43 (m, 4H {methyl is merged}), 1.12 (s, 3H), 1.10 (s, 3H) ppm; $^{13}C\{^1H\}$NMR (100 MHz, $CDCl_3$) δ 203.4 (s), 160.7 (s), 160.6 (s), 158.7 (s), 150.0 (s), 135.0 (d), 134.5 (d), 129.4 (d), 128.7 (d), 128.2 (s), 127.4 (d), 126.6 (d), 118.9 (s), 118.3 (s), 117.8 (d), 49.1 (t), 25.1 (q), 22.8 (q, 2C), 20.8 (d) ppm; HRMS (ESI) calcd for: $C_{20}H_{21}N_2O_2$: 321.1603 $[M + H]^+$; found: 321.1591.

■ ASSOCIATED CONTENT

Supporting Information

The Supporting Information is available free of charge at https://pubs.acs.org/doi/10.1021/acs.joc.1c01221.

Characterization data, ^1H, $^{13}C\{^1H\}$, DEPT NMR, and HRMS spectra of all new compounds (PDF)

FAIR data, including the primary NMR FID files, for compounds **5aa**−**5ia**, **5ja**−**5ma**, **5ab**, **5db**, **5eb**, **5nb**, **5ac**, **5dc**, **5ec**, **5lc**, **5ad**−**5ed**, **5ld**, **5nd**, **5ae**, **5de**, and **6a**−**6d** (ZIP)

Accession Codes

CCDC 2077663 contains the supplementary crystallographic data for this paper. These data can be obtained free of charge via www.ccdc.cam.ac.uk/data_request/cif, or by emailing data_request@ccdc.cam.ac.uk, or by contacting The Cambridge Crystallographic Data Centre, 12 Union Road, Cambridge CB2 1EZ, UK; fax: +44 1223 336033.

■ AUTHOR INFORMATION

Corresponding Author

Chepuri V. Ramana − *Division of Organic Chemistry, CSIR-National Chemical Laboratory, Pune 411 008, India; Academy of Scientific and Innovative Research (AcSIR), Ghaziabad 201002, India;* orcid.org/0000-0001-5801-311X; Email: vr.chepuri@ncl.res.in

Authors

Pawan S. Dhote − *Division of Organic Chemistry, CSIR-National Chemical Laboratory, Pune 411 008, India; Academy of Scientific and Innovative Research (AcSIR), Ghaziabad 201002, India*

Kishor A. Pund − *Division of Organic Chemistry, CSIR-National Chemical Laboratory, Pune 411 008, India*

Complete contact information is available at: https://pubs.acs.org/10.1021/acs.joc.1c01221

Notes

The authors declare no competing financial interest.

■ ACKNOWLEDGMENTS

The authors acknowledge DST-SERB for funding this project and DST-INSPIRE for a research fellowship to P.S.D. and Dr. Srinu Tothadi (CSIR-National Chemical Laboratory) for carrying out the single-crystal X-ray diffraction studies. This work is dedicated to Professor Madhavarao Nagarajan on the occasion of his 70th birthday.

■ REFERENCES

(1) Selected books and reviews: (a) Dyker, G. An Eldorado for Homogeneous Catalysis? *Angew. Chem., Int. Ed.* **2000**, *39*, 4237−4239. (b) Stephen, A.; Hashmi, K. Homogeneous Catalysis by Gold. *Gold Bull.* **2004**, *37*, 51−65. (c) Hoffmann-Röder, A.; Krause, N. The Golden Gate to Catalysis. *Org. Biomol. Chem.* **2005**, *3*, 387−391. (d) Hashmi, A. S. K.; Hutchings, G. J. Gold Catalysis. *Angew. Chem., Int. Ed.* **2006**, *45*, 7896−7936. (e) Hashmi, A. S. K.; Toste, F. D. *Modern Gold Catalyzed Synthesis*; Wiley-VCH, 2012. (f) Toste, D.; Michelet, V. *Gold Catalysis: An Homogeneous Approach*; Imperial College Press, 2014. (g) Slaughter, L. M. *Homogeneous Gold Catalysis*; Springer, 2015. (h) Pflästerer, D.; Hashmi, A. S. K. Gold catalysis in total synthesis - recent achievements. *Chem. Soc. Rev.* **2016**, *45*, 1331−1367. (i) Hendrich, C. M.; Sekine, K.; Koshikawa, T.; Tanaka, K.; Hashmi, A. S. K. Homogeneous and Heterogeneous Gold Catalysis for Material Science. *Chem. Rev.* **2020**, DOI: 10.1021/acs.chemrev.0c00824. (j) Wang, T.; Hashmi, A. S. K. 1,2-Migrations onto Gold Carbene Centers. *Chem. Rev.* **2020**, DOI: 10.1021/acs.chemrev.0c00811. (k) Witzel, S.; Hashmi, A. S. K.; Xie, J. Light in gold Catalysis. *Chem. Rev.* **2021**, DOI: 10.1021/acs.chemrev.0c00841.

(2) (a) Ye, L.-W.; Zhu, X.-Q.; Sahani, R. L.; Xu, Y.; Qian, P.-C.; Liu, R.-S. Nitrene Transfer and Carbene Transfer in Gold Catalysis. *Chem. Rev.* **2020**, DOI: 10.1021/acs.chemrev.0c00348. (b) Tian, X.; Song, L.; Hashmi, A. S. K. α-Imino Gold Carbene Intermediates from Readily Accessible Sulfilimines: Intermolecular Access to Structural Diversity. *Chem. - Eur. J.* **2020**, *26*, 3197−3204. (c) Zhao, X.; Rudolph, M.; Asiri, A.; Hashmi, A. S. K. Easy access to pharmaceutically relevant heterocycles by catalytic reactions involving α-imino gold carbene intermediates. *Front. Chem. Sci. Eng.* **2020**, *14*, 317−349.

(3) (a) Yeom, H.; Shin, S. Catalytic Access to C-Oxo Gold Carbenes by N-O Bond Oxidants. *Acc. Chem. Res.* **2014**, *47*, 966−977. (b) Zhang, L. A Non-Diazo Approach to A-Oxo Gold Carbenes *via* Gold-Catalyzed Alkyne Oxidation. *Acc. Chem. Res.* **2014**, *47*, 877−888. (c) Huple, D.; Ghorpade, S.; Liu, R. S. Recent Advances in Gold-Catalyzed N- and O-Functionalizations of Alkynes with Nitrones, Nitroso, Nitro and Nitroxy Species. *Adv. Synth. Catal.* **2016**, *358*, 1348−1367. (d) Zheng, Z.; Wang, Z.; Wang, Y.; Zhang, L. Au-Catalysed oxidative cyclisation. *Chem. Soc. Rev.* **2016**, *45*, 4448−4458. (e) Bhunia, S.; Ghosh, P.; Patra, S. Gold-Catalyzed Oxidative Alkyne Functionalization by N-O/S-O/C-O Bond Oxidants. *Adv. Synth. Catal.* **2020**, *362*, 3664−3708. (f) Zheng, Z.; Ma, X.; Cheng, X.; Zhao, K.; Gutman, K.; Li, T.; Zhang, L. Homogeneous Gold-Catalyzed Oxidation Reactions. *Chem. Rev.* **2021**, DOI: 10.1021/acs.chemrev.0c00774.

(4) Asao, N.; Sato, K.; Yamamoto, Y. $AuBr_3$-catalyzed cyclization of *o*-(alkynyl)nitrobenzenes. Efficient synthesis of isatogens and anthranils. *Tetrahedron Lett.* **2003**, *44*, 5675−5677.

(5) Li, X.; Incarvito, C. D.; Vogel, T.; Crabtree, R. H. Intramolecular Oxygen Transfer from Nitro Groups to C≡C Bonds Mediated by Iridium Hydrides. *Organometallics* **2005**, *24*, 3066−3073.

(6) Jadhav, A. M.; Bhunia, S.; Liao, H.-Y.; Liu, R.-S. Gold-Catalyzed Stereoselective Synthesis of Azacyclic Compounds through a Redox/[2 + 2 + 1] Cycloaddition Cascade of Nitroalkyne Substrates. *J. Am. Chem. Soc.* **2011**, *133*, 1769−1771.

(7) (a) Ramana, C. V.; Patel, P.; Vanka, K.; Miao, B.; Degterev, A. A Combined Experimental and Density Functional Theory Study on the Pd-Mediated Cycloisomerization of *o*-Alkynylnitrobenzenes - Synthesis of Isatogens and Their Evaluation as Modulators of ROS-Mediated Cell Death. *Eur. J. Org. Chem.* **2010**, *2010*, 5955−5966. (b) Patel, P.; Ramana, C. V. Divergent Pd(II) and Au(III) mediated nitroalkynol cycloisomerizations. *Org. Biomol. Chem.* **2011**, *9*, 7327−7334.

(8) (a) Liu, R.-R.; Ye, S.-C.; Lu, C.-J.; Zhuang, G.-L.; Gao, J.-R.; Jia, Y.-X. Dual Catalysis for the Redox Annulation of Nitroalkynes with Indoles: Enantioselective Construction of Indolin-3-ones Bearing Quaternary Stereocenters. *Angew. Chem., Int. Ed.* **2015**, *54*, 11205−11208. (b) Zhou, S.; Liu, Q.; Bao, M.; Huang, J.; Wang, J.; Hua, W.; Xu, X. Gold(I)-catalyzed redox transformation of *o*-nitroalkynes with

indoles for the synthesis of 2,3′-biindole derivatives. *Org. Chem. Front.* **2021**, *8*, 1808−1816.
(9) Dhote, P. S.; Ramana, C. V. Interrupting the [Au]-Catalyzed Nitroalkyne Cycloisomerization - Trapping the Putative -Oxo Gold Carbene with Benzo[*c*]isoxazole. *Org. Lett.* **2021**, *23*, 2632−2637.
(10) (a) Zhou, A.-H.; He, Q.; Shu, C.; Yu, Y.-F.; Liu, S.; Zhao, T.; Zhang, W.; Lu, X. Atom-economic generation of gold carbenes: gold-catalyzed formal [3 + 2] cycloaddition between ynamides and isoxazoles. *Chem. Sci.* **2015**, *6*, 1265−1271. (b) Jadhav, P. D.; Lu, X.; Liu, R. S. Gold-catalyzed [5 + 2]- and [5 + 1]-Annulations between Ynamides and 1,2-Benzisoxazoles with Ligand-Controlled Chemoselectivity. *ACS Catal.* **2018**, *8*, 9697−9701. (c) Xu, W.; Zhao, J.; Li, X.; Liu, X. Selective [5 + 1] and [5 + 2] Cycloaddition of Ynamides or Propargyl Esters with Benzo[*d*]isoxazoles *via* Gold Catalysis. *J. Org. Chem.* **2018**, *83*, 15470−15485. (d) Reviews: Hu, F.; Szostak, M. Recent Developments in the Synthesis and Reactivity of Isoxazoles: Metal Catalysis and Beyond. *Adv. Synth. Catal.* **2015**, *357*, 2583−2614. (e) Li, L.; Tan, T.; Zhang, Y.; Liu, X.; Ye, L. Recent advances in transition-metal-catalyzed reactions of alkynes with isoxazoles. *Org. Biomol. Chem.* **2017**, *15*, 8483−8492. (f) Sahani, R.; Ye, L.; Liu, R. S. Synthesis of nitrogen-containing molecules *via* transition metal-catalyzed reactions on isoxazoles, anthranils and benzoisoxazoles. *Adv. Organomet. Chem.* **2020**, *73*, 195−251. (g) Li, L.; Luo, W.-F.; Ye, L.-W. Recent Progress in the Gold-Catalyzed Annulations of Ynamides with Isoxazole Derivatives via α-Imino Gold Carbenes. *Synlett* **2021**, DOI: 10.1055/a-1344-5998.
(11) (a) Osipov, D. V.; Osyanin, V. A.; Klimochkin, Y. N. *ortho*-Quinone methides as Key Intermediates in Cascade Heterocyclizations. *Russ. Chem. Rev.* **2017**, *86*, 625−687. (b) Yang, X.; Wang, L.; Hu, F.; Xu, L.; Li, S. Redox-Triggered Switchable Synthesis of 3,4-Dihydroquinolin-2(1H)-one Derivatives *via* Hydride Transfer/N-Dealkylation/N-Acylation. *Org. Lett.* **2021**, *23*, 358−364.
(12) (a) Mfuh, A. M.; Larionov, O. V. Heterocyclic N-Oxides - An Emerging Class of Therapeutic Agents. *Curr. Med. Chem.* **2015**, *22*, 2819−2857. (b) Khan, I.; Zaib, S.; Batool, S.; Abbas, N.; Ashraf, Z.; Iqbal, J.; Saeed, A. Quinazolines and Quinazolinones as Ubiquitous Structural Fragments in Medicinal Chemistry: An Update on the Development of Synthetic Methods and Pharmacological Diversification. *Bioorg. Med. Chem.* **2016**, *24*, 2361−2381.
(13) (a) Yamanaka, H. Reaction of 4-Alkoxyquinazolines with Organic Peracid. *Chem. Pharm. Bull.* **1959**, *7*, 152−158. (b) Sternbach, L. H.; Kaiser, S.; Reeder, E. Quinazoline 3-Oxide Structure of Compounds Previously Described in the Literature as 3.1.4-Benzoxadiazepines. *J. Am. Chem. Soc.* **1960**, *82*, 475−480. (c) Tennant, G. Heterocyclic N-oxides. Part IV. A General Route to 2-n-alkyl-3, 4-dihydro-3-oxoquinoxalines and their 1-Oxides. *J. Chem. Soc. C* **1966**, 2285−2287. (d) Higashino, T.; Amano, T.; Tamura, Y.; Katsumata, N.; Washizu, Y.; Ono, T.; Hayashi, E. On N-Oxidation of 4-Alkyl-, 4-Phenyl-quinazoline and Reaction of 4-Methylquinazoline 1-Oxide. *Chem. Pharm. Bull.* **1972**, *20*, 1874−1882. (e) Spence, T. W. M.; Tennant, G. The chemistry of Nitro-Compounds. Part II. The Scope and Mechanism of the Base-Catalysed Transformations of some N, N-disubstituted *o*-Nitrobenzamides. *J. Chem. Soc., Perkin Trans. 1* **1972**, 97−102. (f) Murashima, T.; Tamai, R.; Fujita, K.; Uno, H.; Ono, N. Ambident Reactivity of Nitro Heteroaromatic Anions. *Tetrahedron Lett.* **1996**, *37*, 8391−8394. (g) Coşkun, N.; Çetin, M. A New Regioselective Synthesis and Ambient Light Photochemistry of Quinazolin-1-oxides. *Tetrahedron* **2007**, *63*, 2966−2972. (h) Petkevičius, V.; Vaitekūnas, J.; Vaitkus, D.; Č·nas, N.; Meškys, R. Tailoring a Soluble Diiron Monooxygenase for Synthesis of Aromatic *N*-oxides. *Catalysts* **2019**, *9*, 356.
(14) For the first use of $AuCl_3$ in homogeneous gold catalysis, see: (a) Hashmi, A. S. K.; Schwarz, L.; Choi, J.; Frost, T. A New Gold-Catalyzed C-C Bond Formation. *Angew. Chem., Int. Ed.* **2000**, *39*, 2285−2288. (b) Hashmi, A. S. K.; Frost, T.; Bats, J. Highly Selective Gold-Catalyzed Arene Synthesis. *J. Am. Chem. Soc.* **2000**, *122*, 11553−11554.
(15) (a) Aoyagi, Y.; Abe, T.; Ohta, A. Facile and Efficient Deoxygenation of Aromatic N-Oxides with Zinc and Aqueous Ammonium Chloride. *Synthesis* **1997**, *1997*, 891−894. (b) Fulopova, V.; Cziesla, L.; Fleming, M.; Lu, Y.; Voelker, A.; Krchnak, V. Traceless Solid-Phase Synthesis of Trisubstituted Quinazolines. *ACS Comb. Sci.* **2015**, *17*, 470−473.
(16) For mechanistic studies in gold catalysis, see: (a) Hashmi, A. S. K. Homogeneous Gold Catalysis Beyond Assumptions and Proposals - Characterised Intermediates. *Angew. Chem., Int. Ed.* **2010**, *49*, 5232−5241. (b) Lauterbach, T.; Asiri, A.; Hashmi, A. S. K. Organometallic Intermediates of Gold Catalysis. *Adv. Organomet. Chem.* **2014**, *62*, 261−297.
(17) (a) Yeom, H.-S.; Lee, J.-E.; Shin, S. Gold-Catalyzed Waste-Free Generation and Reaction of Azomethine Ylides: Internal Redox/Dipolar Cycloaddition Cascade. *Angew. Chem., Int. Ed.* **2008**, *47*, 7040−7043. (b) Yeom, H.-S.; Lee, Y.; Lee, J.-E.; Shin, S. Geometry-Dependent Divergence in the Gold-Catalyzed Redox Cascade Cyclization of *o*-alkynylaryl Ketoximes and Nitrones leading to Isoindoles. *Org. Biomol. Chem.* **2009**, *7*, 4744−4752. (c) Wetzel, A.; Gagosz, F. Gold-Catalyzed Transformation of 2-Alkynyl Arylazides: Efficient Access to the Valuable Pseudoindoxyl and Indolyl Frameworks. *Angew. Chem., Int. Ed.* **2011**, *50*, 7354−7358.
(18) (a) Aguilar, E.; Santamaría, J. Gold-Catalyzed Heterocyclic Syntheses through α-Imino Gold Carbene Complexes as Intermediates. *Org. Chem. Front.* **2019**, *6*, 1513−1540. (b) Gao, Y.; Nie, J.; Huo, Y.; Hu, X. Q. Anthranils: Versatile Building Blocks in the Construction of C-N Bonds and N-heterocycles. *Org. Chem. Front.* **2020**, *7*, 1177−1196.
(19) (a) Lu, B.; Li, C.; Zhang, L. Gold-Catalyzed Highly Regioselective Oxidation of C-C Triple Bonds without Acid Additives: Propargyl Moieties as Masked α,β-Unsaturated Carbonyls. *J. Am. Chem. Soc.* **2010**, *132*, 14070−14072. (b) Schulz, J.; Jašíková, L.; Škríba, A.; Roithová, J. Role of Gold(I) α-Oxo Carbenes in the Oxidation Reactions of Alkynes Catalyzed by Gold(I) Complexes. *J. Am. Chem. Soc.* **2014**, *136*, 11513−11523.
(20) Zhang, S. A Reliable and Efficient First Principles-Based Method for Predicting pKa Values. 4. Organic Bases. *J. Comput. Chem.* **2012**, *33*, 2469−2482.
(21) Manetsch, R.; Zheng, L.; Reymond, M.; Woggon, W. D.; Reymond, J. L. A Catalytic Antibody against a Tocopherol Cyclase Inhibitor. *Chem. - Eur. J.* **2004**, *10*, 2487−2506.

https://doi.org/10.1021/acs.joc.1c01221
J. Org. Chem. 2021, 86, 10874−10882

frontiers in Chemistry

ORIGINAL RESEARCH
published: 09 July 2021
doi: 10.3389/fchem.2021.689780

Gold-Catalyzed Complementary Nitroalkyne Internal Redox Process: A DFT Study

K. Vipin Raj[1,2], *Pawan S. Dhote*[2,3], *Kumar Vanka*[1,2]* *and Chepuri V. Ramana*[2,3]*

[1]*Physical and Materials Chemistry Division, CSIR-National Chemical Laboratory, Pune, India,* [2]*Academy of Scientific and Innovative Research (AcSIR), Ghaziabad, India,* [3]*Organic Chemistry Division, CSIR-National Chemical Laboratory, Pune, India*

Gold-catalysis, in this century, is one of the most emerging and promising new areas of research in organic synthesis. During the last two decades, a wide range of distinct synthetic methodologies have been unveiled employing homogeneous gold catalysis and aptly applied in the synthesis of numerous natural products and biologically active molecules. Among these, the reactions involving α-oxo gold carbene/α-imino gold carbene intermediates are of contemporary interest, in view of their synthetic potential and also due to the need to understand the bonding involved in these complexes. In this manuscript, we document the theoretical investigations on the regio-selectivity dependence of substitution on the gold-catalyzed cycloisomerization of *o*-nitroarylalkyne derivatives. We have also studied the relative stabilities of α-oxo gold carbene intermediates.

Keywords: gold-catalysis, internal redox, cycloisomerization, α-oxo gold carbene, DFT calculation

OPEN ACCESS

Edited by:
Soumyajit Roy,
Indian Institute of Science Education and Research Kolkata, India

Reviewed by:
Alain Rafael Puente Santiago,
The University of Texas at El Paso, United States
Jian-Ping Zou,
Nanchang Hangkong University, China

***Correspondence:**
Chepuri V. Ramana
vr.chepuri@ncl.res.in
Kumar Vanka
k.vanka@ncl.res.in

Specialty section:
This article was submitted to Catalysis and Photocatalysis, a section of the journal Frontiers in Chemistry

Received: *01 April 2021*
Accepted: *10 June 2021*
Published: *09 July 2021*

Citation:
Vipin Raj K, Dhote PS, Vanka K and Ramana CV (2021) Gold-Catalyzed Complementary Nitroalkyne Internal Redox Process: A DFT Study. Front. Chem. 9:689780. doi: 10.3389/fchem.2021.689780

INTRODUCTION

Gold catalyzed reactions have been increasingly emerging in the literature over the past few decades (Hashmi, 2007; Pflästerera and Hashmi, 2015). The majority of these reactions are based on the propensity of gold complexes to act as carbophilic Lewis acids in the activation of carbon–carbon multiple bonds, thus allowing the formation of new C–C and C–hetero atom bonds by inter-/intramolecular addition of nucleophiles across the Au-complexed multiple bonds (Corma et al., 2011). An interesting class of gold-catalyzed reactions that needs a mention in this context are the catalytic internal redox cyclisation's (Xiao and Li, 2011; Zhang, 2014; Yeom and Shin, 2014). The oxygen atom transfer to alkynes catalyzed by gold complexes is a well-known addition–elimination process employing nucleophilic oxygen atom donors such as nitro (Asao et al., 2003; Li et al., 2005; Ramana et al., 2010), amine-/pyridine *N*-oxides (Cui et al., 2009; Nosel et al., 2013), nitrone (Heom et al., 2008; Pati and Liu, 2009; Chen et al., 2011), sulfoxides (Shapiro and Toste, 2007; Lu et al., 2013), and epoxides (Hashmi et al., 2008; Lin et al., 2008), reacting with the activated alkynes.

The Au-catalyzed cycloisomerizaton of nitrotolans documented by Yamamoto and co-workers in 2003 (**Scheme 1**, Eq. 1) (Asao et al., 2003), is an important advancement to synthesize 2-arylisatogens. Interestingly, when the pendant alkyne substituent is an alkyl group, the internal redox process proceeds in a complementary mode resulting in the formation of a benzo[*c*]isoxazole, trivially known as anthranil. A mechanism founded upon the addition of the oxygen of the nitro group in a 6-*endo*-dig fashion has been postulated as the key step involved for the intramolecular redox process. Initially, it has been proposed that the resulting gold-ate complex **A** undergoes protonolysis followed by ring opening with water to produce a nitrosobenzene. There exist two possibilities for the subsequent dehydrative cyclization leading to isatogens (*path a*) or anthranil

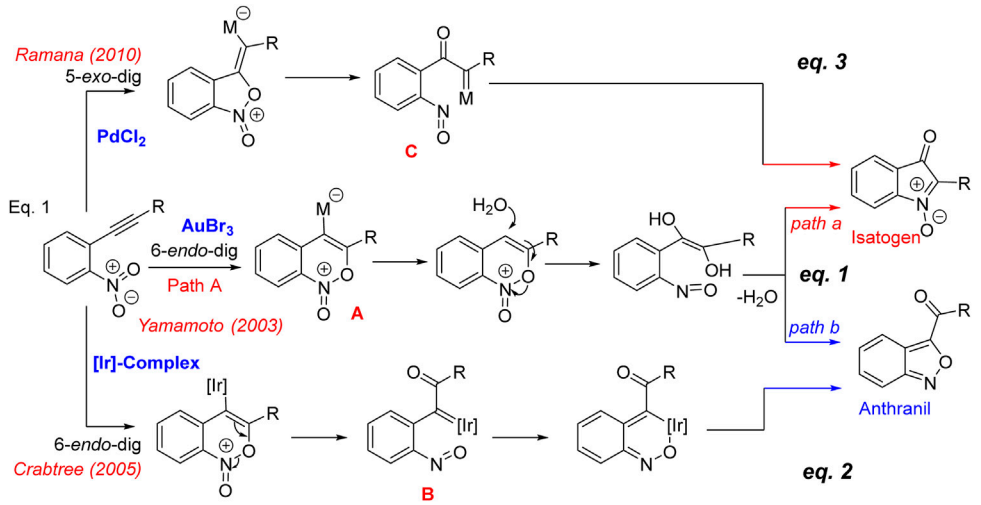

SCHEME 1 | Mechanism of nitroalkyne cycloisomerization.

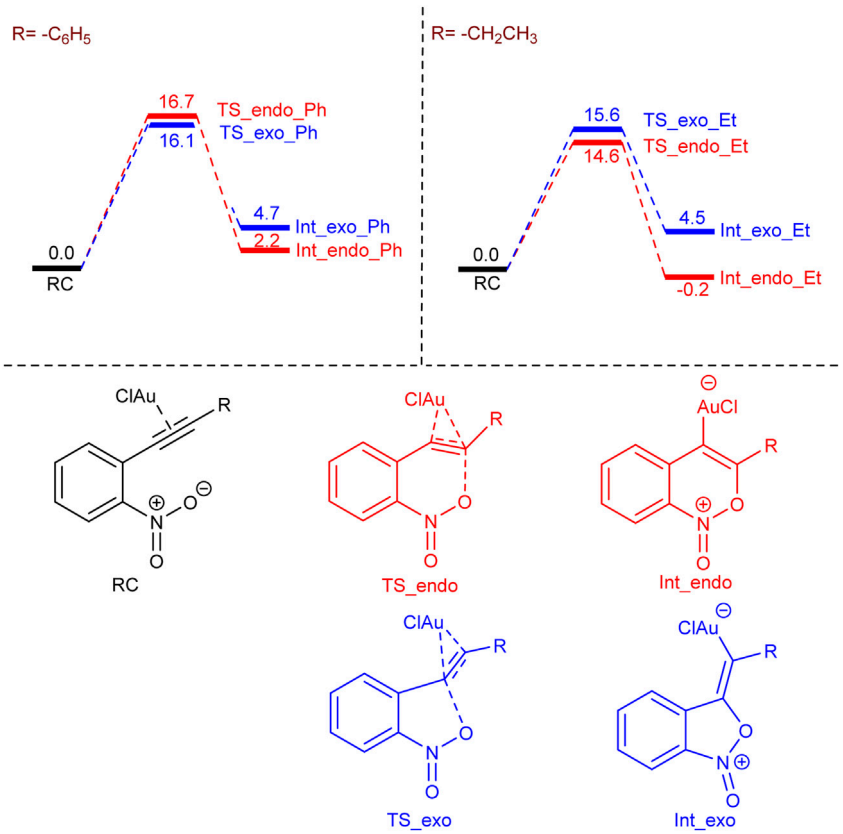

SCHEME 2 | The free energy profile for the formation of *-endo* and *-exo* intermediates for –phenyl and –ethyl substitutions. Values are in kcal/mol.

(*path b*). Though this explains the possible paths, it does not account for why these paths are substituent dependent. In a later report, Crabtree's group has documented (**Scheme 1**, Eq. 2) a similar nitroalkynes cycloisomerization by iridium hydrides leading to anthranils (Li et al., 2005). With the help of single crystal structural analysis, it has been proved that there exists an

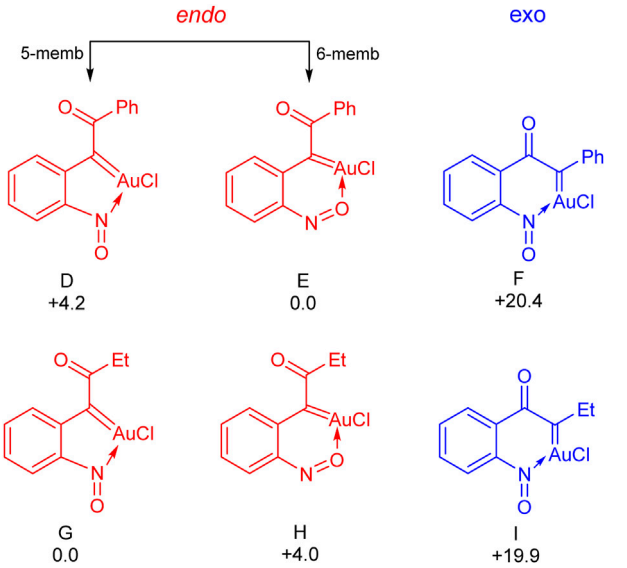

FIGURE 1 | The relative free energies of α-oxo gold carbenes with respect to the most stable one (E for the phenyl substitution and G for the ethyl substitution). Values are in kcal/mol.

intermediate iridium(III) nitroso complex **B**, which results after the initial oxygen transfer from nitro to alkyne in a 6-*endo*-dig fashion. In this context, as a part of the total synthesis of the pseudoindoxyl class of natural products (Ramana et al., 2010; Patel et al., 2013), we have speculated on the possibility of complementing this process by employing Pd-complexes which was successfully realized to come up with a general method for the synthesis of 2-aryl and 2-alkyl isatogens *via* an internal nitro-alkyne redox process (**Scheme 1**, Eq. 3) (Ramana et al., 2010). We have also studied in detail the mechanistic aspects with density functional theory (DFT) and reasoned that the formation of an α-oxo metal carbenoid **C** occurs by the 5-*exo*-dig mode of cyclization of the nitro group on the alkyne, which subsequently undergoes a 6n-electro cyclization to isatogen. In this manuscript, we document the DFT calculations on the [Au]-catalysed complementary nitroalkyne redox process that leads to α-oxo gold carbenes **B** and **C**, especially focusing on the energies associated with oxygen transfer and carbene transfer. This has been undertaken considering the importance of gold catalyzed processes that proceed through the α-imino and/or α-oxo gold carbenes and their promising applications in the heterocyclic synthesis (Aguilar and Santamaría, 2019; Zhang, 2014). These processes in general proceed through the carbene and/or nitrene transfer from the [Au]-centre (Ye, 2020). However, in case of the Au-carbenes **B** and **C**, such a transfer is challenging, as the internal electrocyclization along with the nitroso group is highly favored with either of them. The possibility of trapping these reactive intermediates has been attempted with internal and external nucleophiles. However, on both instances, it has been realized that the intramolecular process leading to isatogens or anthranil has exclusively taken place and the products obtained are from the reaction of the nucleophile employed with the isatogen. Thus, a qualitative understanding of the relative energies of **B** and **C** and the energies associated in their formation is expected to provide some clues on the possible trapping.

RESULTS AND DISCUSSION

In order to understand the selectivity (*endo* or *exo*) dependence on the substitution (alkyl or aromatic) on the nitro alkyne, we have performed density functional theory (DFT) calculations using the Turbomole 7.2 program package (TURBOMOLE V7.2, 2017). We have chosen the ethyl ($-CH_2CH_3$) and phenyl ($-C_6H_5$) groups as the representatives for alkyl and aromatic substitutions and considered AuCl as the catalyst instead of $AuCl_3$, in accordance with previously reported work (Straub, 2004). The *endo* or *exo* selectivity arises due to the two different possibilities of oxygen (of the nitro group) attack on the C–C triple bond (see **Scheme 2**), and our calculations indicate that the *exo* transition state (TS_exo_Ph) is favorable by 0.6 kcal/mol over the *endo* transition state (TS_endo_Ph) for phenyl substitution (see **Scheme 2**). In contrast, the *endo* transition state (TS_endo_Et) is favorable by 1.0 kcal/mol over the *exo* transition (TS_exo_Et) state for ethyl substitution, which corroborates with the experimental observations. Furthermore, in the case of ethyl substitution, the *endo* intermediate (Int_endo_Et) is more preferable than the *exo* intermediate (Int_exo_Et) by 4.7 kcal/mol, but in the case of phenyl substitution, the *exo* intermediate (Int_exo_Ph) is less favorable than the *endo* intermediate (Int_endo_Ph) by 2.5 kcal/mol. In other words, the *endo* pathway to form the first intermediate is favorable both kinetically and thermodynamically for the ethyl substitution, but the *exo* pathway is only kinetically favorable for the phenyl substitution.

Next, the energies of the six different possible oxo gold carbenes (D to I in **Figure 1**) have been calculated to see their relative stability. As shown in **Figure 1**, depending upon the heteroatom of the nitroso group involved in the coordination, there exists two possibilities for the oxo gold carbene resulting from the 6-*endo* dig path – with the nitrogen atom, a five–membered coordination (D and G for Ph and Et respectively) and six-membered coordination with the oxygen atom (E and H for Ph and Et respectively). Interestingly, with both phenyl and ethyl, the [Au]-carbenes derived from the 6-*endo* dig path are more stable. In case of the phenyl, E, the six-membered coordination is more stable than the D, five-membered coordination, by 4.2 kcal/mol. However, with the ethyl substituent, this was seen to be exactly reversed. G, the five-membered coordination was seen to be more stable than H, the six-membered coordination, by 4.0 kcal/mol. When it comes to the 5-*exo* dig path, in both the ethyl (19.9 kcal/mol unfavourable compared to G) and phenyl (20.4 kcal/mol unfavourable compared to E) cases, the energies associated with resulting carbenes reveal that they are unfavourable.

Overall, these preliminary calculations indicate that the α-oxo gold carbenes resulting from the 6-*endo*-dig mode of oxygen transfer are favored in general, though the energies associated

with this process vary with respect to the substituent. For example, as discussed already, the formation of the first intermediate *via* the 6-*endo*-dig mode is kinetically and thermodynamically favourable for ethyl substitution. However, the corresponding mode is only thermodynamically favourable for phenyl substitution. This indicates that energies associated with the internal oxygen transfer lead to the α-oxo gold carbene B and also, given its comparable stability, that the chances of the carbene transfer from this reactive intermediate are greater.

CONCLUSION

To conclude, DFT calculations on the internal oxygen transfer of the Au-catalyzed *o*-nitroalkyne cycloisomerization reactions have been carried out to understand the relative energies associated with the oxygen transfer and the energies of the resulting α-oxo gold carbenes. These calculations clearly reveal that the α-oxo gold carbenes resulting from the 6-*endo* dig addition of the oxygen to the alkyne is thermodynamically stable, when compared to the alternative α-oxo gold carbene that results from the 5-*exo* dig addition. Our calculations also suggest that the substitutions on the *o*-nitroalkynes have a significant role in altering the regio-selectivity of the reaction.

COMPUTATIONAL DETAILS

All the calculations in this study have been performed with density functional theory (DFT), with the aid of the Turbomole 7.2 suite of programs (TURBOMOLE V7.2, 2017), using the M06-2X functional (Zhao and Truhlar, 2008). The def-TZVP basis set has been employed (Schäfer et al., 1994; Eichkorn et al., 1997). The resolution of identity (RI) (Eichkorn et al., 1995), along with the multipole accelerated resolution of identity (marij) (Sierka et al., 2003) approximations have been employed for an accurate and efficient treatment of the electronic Coulomb term in the DFT calculations. Solvent correction were incorporated with optimization calculations using the COSMO model (Klamt and Schüürmann, 1993), with toluene ($\varepsilon = 2.374$) as the solvent. The values reported are ΔG values, with zero-point energy corrections, internal energy and entropic contributions were included through frequency calculations on the optimized minima, with the temperature taken to be 298.15 K. Harmonic frequency calculations were performed for all stationary points to confirm them as a local minima or transition state structures. The XYZ coordinates of the optimized geometries of all the structures are provided in the **Supplementary Material**.

DATA AVAILABILITY STATEMENT

The original contributions presented in the study are included in the article/**Supplementary Material**, further inquiries can be directed to the corresponding author.

AUTHOR CONTRIBUTIONS

CR and KV: Problem Identification and Manuscript Writing. KVR: DFT Calculations and Assistance in Manuscript Writing and PD Support for DFT and Assistance in Manuscript Writing.

ACKNOWLEDGMENTS

KVR wishes to acknowledge CSIR for providing senior research fellowship. KVR and KV also acknowledge the Multi-Scale simulation and Modeling project (MSM) for the computational facilities. The support and the resources provided by 'PARAM Brahma Facility' under the National Supercomputing Mission, Government of India at the Indian Institute of Science Education and Research (IISER) Pune are gratefully acknowledged. PD acknowledges DST-INSPIRE for a research fellowship and CR acknowledge CSIR (India) for funding this project.

SUPPLEMENTARY MATERIAL

The Supplementary Material for this article can be found online at: https://www.frontiersin.org/articles/10.3389/fchem.2021.689780/full#supplementary-material

REFERENCES

Aguilar, E., and Santamaría, J. (2019). Gold-catalyzed Heterocyclic Syntheses through α-imino Gold Carbene Complexes as Intermediates. *Org. Chem. Front.* 6, 1513–1540. doi:10.1039/C9QO00243J

Asao, N., Sato, K., and Yamamoto, Y. (2003). AuBr3-catalyzed Cyclization of O-(alkynyl)nitrobenzenes. Efficient Synthesis of Isatogens and Anthranils. *Tetrahedron Lett.* 44, 5675–5677. doi:10.1016/S0040-4039(03)01357-1

Chen, D., Song, G. Y., Jia, A. Q., and Li, X. W. (2011). Gold- and Iodine-Mediated Internal Oxygen Transfer of Nitrone- and Sulfoxide-Functionalized Alkynes. *J. Org. Chem.* 76, 8488–8494. doi:10.1021/jo201347r

Corma, A., Leyva-Pérez, A., and Sabater, M. J. (2011). Gold-Catalyzed Carbon–Heteroatom Bond-Forming Reactions. *Chem. Rev.* 111 (3), 1657–1712. doi:10.1021/cr100414u

Cui, L., Peng, Y., and Zhang, L. (2009). A Two-step, Formal [4 + 2] Approach toward Piperidin-4-Ones via Au Catalysis. *J. Am. Chem. Soc.* 131, 8394–8395. doi:10.1021/ja903531g

Eichkorn, K., Treutler, O., Öhm, H., Häser, M., Ahlrichs, R., Öhm, H., et al. (1995). Auxiliary Basis Sets to Approximate Coulomb Potentials. *Chem. Phys. Lett.* 240, 283–290. doi:10.1016/0009-2614(95)00621-A

Eichkorn, K., Weigend, F., Treutler, O., and Ahlrichs, R. (1997). Auxiliary Basis Sets for Main Row Atoms and Transition Metals and Their Use to Approximate Coulomb Potentials. *Theor. Chem. Acc. Theor. Comput. Model. (Theoretica Chim. Acta)*. 97, 119–124. doi:10.1007/s002140050244

Hashmi, A. S. K., Bührle, M., Salathé, R., and Bats, J. W. (2008). Gold Catalysis: Synthesis of 3-Acylindenes from 2-Alkynylaryl Epoxides. *Adv. Synth. Adv. Synth. Catal.* 350, 2059–2064. doi:10.1002/adsc.200800385

Hashmi, A. S. K. (2007). Gold-Catalyzed Organic Reactions. *Chem. Rev.* 107, 3180–3211. doi:10.1021/cr000436x

Heom, H. S., Lee, J. E., and Shin, S. (2008). Gold-Catalyzed Waste-free Generation and Reaction of Azomethine Ylides: Internal Redox/Dipolar Cycloaddition Cascade. *Angew. Chem. Int. Ed.* 47, 7040–7043. doi:10.1002/anie.200802802

Klamt, A., and Schüürmann, G. (1993). COSMO: a New Approach to Dielectric Screening in Solvents with Explicit Expressions for the Screening Energy and its Gradient. *J. Chem. Soc. Perkin Trans.* 2, 799–805. doi:10.1039/P29930000799

Li, X., Incarvito, C. D., Vogel, T., and Crabtree, R. H. (2005). Intramolecular Oxygen Transfer from Nitro Groups to C:C Bonds Mediated by Iridium Hydrides. *Organometallics*. 24, 3066–3073. doi:10.1021/om050116+

Lin, G.-Y., Li, C.-W., Hung, S.-H., and Liu, R.-S. (2008). Diversity in Gold- and Silver-Catalyzed Cycloisomerization of Epoxide–Alkyne Functionalities. *Org. Lett.* 10, 5059–5062. doi:10.1021/ol802047g

Lu, B., Li, Y., Wang, Y., Aue, D. H., Luo, Y., and Zhang, L. (2013). [3,3]-Sigmatropic Rearrangement versus Carbene Formation in Gold-Catalyzed Transformations of Alkynyl Aryl Sulfoxides: Mechanistic Studies and Expanded Reaction Scope. *J. Am. Chem. Soc.* 135, 8512–8524. doi:10.1021/ja401343p

Nösel, P., dos Santos Comprido, L. N. T., Lauterbach, M., Rominger, F., and Hashmi, A. S. K. (2013). 1,6-Carbene Transfer: Gold-Catalyzed Oxidative Diyne Cyclizations. *J. Am. Chem. Soc.* 135, 15662–15666. doi:10.1021/ja4085385

Patel, P., Reddy, B. N. P., and Ramana, C. V. (2013). The Synthesis of the central Tricyclic Core of the Isatisine A: Harmonious Orchestration of [metal]-Catalyzed Reactions in a Sequence. *Tetrahedron*. 70, 510–516. doi:10.1016/j.tet.2013.11.026

Pati, K., and Liu, R. S. (2009). Efficient Syntheses of α-pyridones and 3(2H)-Isoquinolones through Ruthenium-Catalyzed Cycloisomerization of 3-En-5-Ynyl and O-Alkynylphenyl Nitrones Chem. *Commun*.14, 5233–5235. doi:10.1039/B910773H

Pflästerera, D., and Hashmi, S. (2015). Gold Catalysis in Total Synthesis – Recent Achievements. *Chem. Soc. Rev*. 45, 1331–1367. doi:10.1039/C5CS00721F

Ramana, C. V., Patel, P., Vanka, K., Miao, B. C., and Degterev, A. (2010). A Combined Experimental and Density Functional Theory Study on the Pd-Mediated Cycloisomerization of O-Alkynylnitrobenzenes—Synthesis of Isatogens and Their Evaluation as Modulators of ROS-Mediated Cell Death. *Eur. J. Org. Chem.* 2010 (31):5955–5966. doi:10.1002/ejoc.201000769

Schäfer, A., Huber, C., and Ahlrichs, R. (1994). Fully Optimized Contracted Gaussian Basis Sets of Triple Zeta Valence Quality for Atoms Li to Kr. *J. Chem. Phys.* 100, 5829–5835. doi:10.1063/1.467146

Shapiro, N. D., and Toste, F. D. (2007). Rearrangement of Alkynyl Sulfoxides Catalyzed by Gold(I) Complexes. *J. Am. Chem. Soc.* 129, 4160–4161. doi:10.1021/ja070789e

Sierka, M., Hogekamp, A., and Ahlrichs, R. (2003). Fast Evaluation of the Coulomb Potential for Electron Densities Using Multipole Accelerated Resolution of Identity Approximation. *J. Chem. Phys.* 118, 9136–9148. doi:10.1063/1.1567253

Straub, B. F. (2004). Gold(i) or Gold(iii) as Active Species in AuCl3-Catalyzed Cyclization/cycloaddition Reactions? *Chem. Commun.* 2004, 1726–1728. doi:10.1039/B404876H

TURBOMOLE V7.2 (2017). A development of University of Karlsruhe and Forschungszentrum Karlsruhe GmbH, 1989-2007, TURBOMOLE GmbH, since 2007. Available at: http://www.turbomole.com (Accessed May 18, 2018)

Xiao, J., and Li, X. (2011). Gold α-Oxo Carbenoids in Catalysis: Catalytic Oxygen-Atom Transfer to Alkynes, *Angew. Chem. Int. Ed.* 50, 7226–7236. doi:10.1002/anie.201100148

Ye, L. W., Zhu, X., Sahani, R., Xu, Y., Qian, P. C., and Liu, R. S. (2020). Nitrene Transfer and Carbene Transfer in Gold Catalysis. *Chem. Rev.* 2020, 121. doi:10.1021/acs.chemrev.0c00348

Yeom, H.-S., and Shin, S. (2014). Catalytic Access to α-Oxo Gold Carbenes by N-O Bond Oxidants. *Acc. Chem. Res.* 47, 966–977. doi:10.1021/ar4001839

Zhang, L. (2014). A Non-diazo Approach to α-Oxo Gold Carbenes via Gold-Catalyzed Alkyne Oxidation. *Acc. Chem. Res.* 47, 877–888. doi:10.1021/ar400181x

Zhao, Y., and Truhlar, D. G. (2008). The M06 Suite of Density Functionals for Main Group Thermochemistry, Thermochemical Kinetics, Noncovalent Interactions, Excited States, and Transition Elements: Two New Functionals and Systematic Testing of Four M06-Class Functionals and 12 Other Functionals. *Theor. Chem. Account.* 120, 215–241. doi:10.1007/s00214-007-0310-x

Conflict of Interest: The authors declare that the research was conducted in the absence of any commercial or financial relationships that could be construed as a potential conflict of interest.

Personal Account

DOI: 10.1002/tcr.202100111

THE CHEMICAL RECORD

Gold-Catalysed Nitroalkyne Cycloisomerization – Synthetic Utility

Pawan S. Dhote,[a, b] Swapnil V. Halnor,[a, b] and Chepuri V. Ramana*[a, b]

Dedicated to Professor Christian Bruneau for his outstanding contribution to catalysis

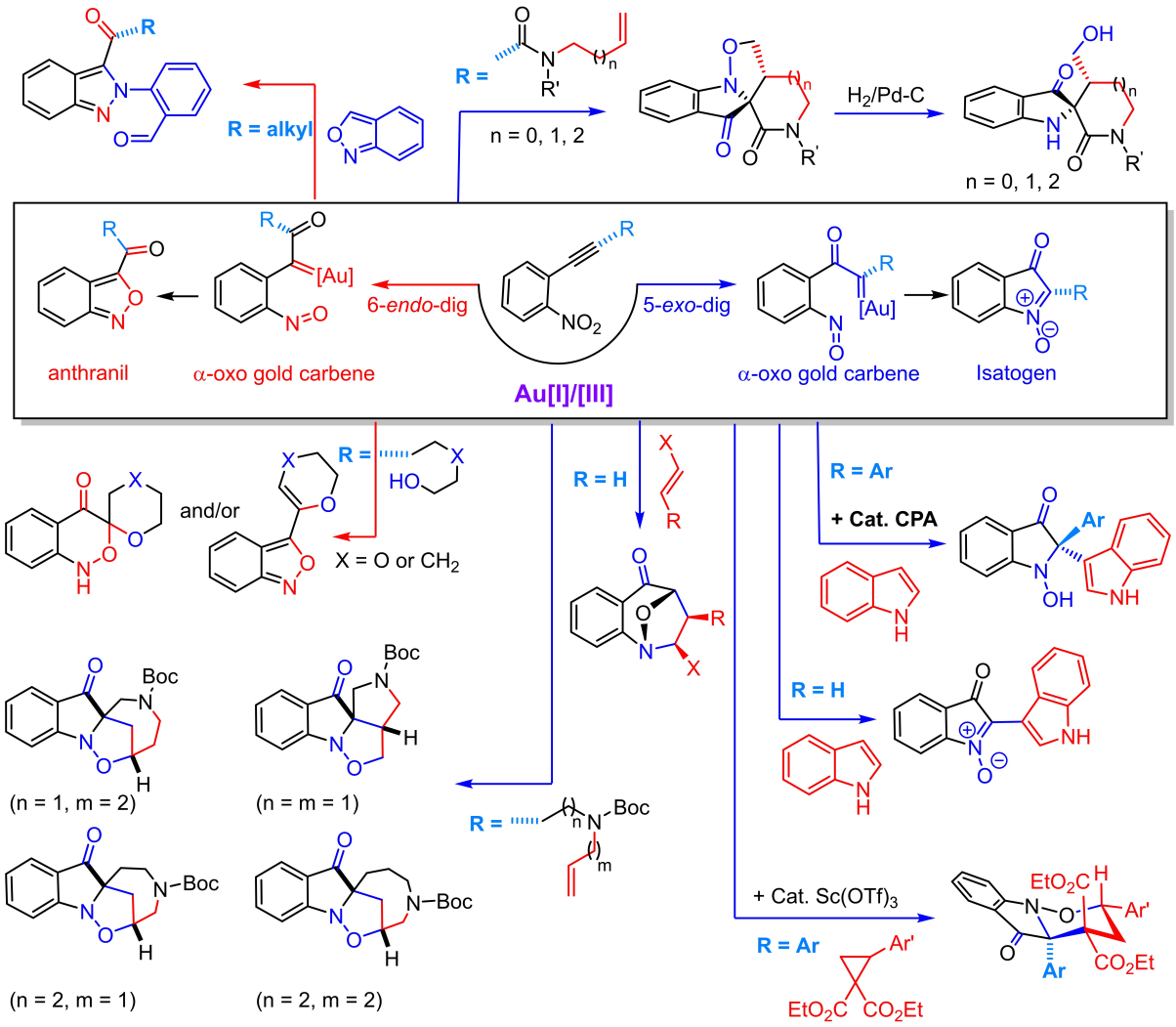

Abstract: The gold-catalysed intramolecular redox cyclization of *o*-alkynylnitrobenzens documented by Professors Naoki Asao and Yoshinori Yamamoto is an important discovery that has opened two complementary research domains. Advancing this cyclization with other metals as well as developing new methods around the products that result from this reaction is one aspect that has seen growing interest. On the other hand, the idea of generating α-oxo gold carbenes *via* oxygen transfer to alkynes has established another important aspect in gold-catalysis. In this account, we will be dealing with the first aspect, which revolves around the internal redox cyclization of nitroalkynes (trivially called as nitroalkyne cycloisomerization), focusing mainly on the gold-complexes and the synthetic methods developed around it from our group and from other groups, and also providing the details of similar transformations documented with other metals so that the complementary reactivity/diversity of these transformations could be appreciated.

Keywords: Gold-Catalysis, Internal Redox Cyclization, α-Oxo Gold Carbene, Isatogen, Anthranil

1. Introduction

Catalysis with gold-complexes is one of the remarkable areas that has emerged in this millennium and has grown exponentially in a short span of two decades, maintaining its presence in a majority of the fundamental reaction classes that are known to be mediated by acids/bases and other metal complexes.[1] This includes simple electrophilic cyclizations/cycloisomerizations, rearrangements to diverse cycloadditions, cyclopropanation to glycosylations, oxidations and internal redox processes, aryl couplings and C–H functionalization, to name a few. This, taken together with the distinct and unprecedented organic transformations that are reported with gold-complexes, demonstrates that catalytic transformations by gold-complexes have gained popularity as reliable transforms in the retrosynthetic design of target molecules of natural and unnatural origin.[2] In particular, the high carbophilicity/π-electrophilic activation of gold-complexes has been explored in the intra and intermolecular functionalization of C–C multiple bonds to forge a wide range of carbocyclic and heterocyclic skeletons in a regio-/stereo- and enantioselective manner.[3]

A particularly interesting class of gold-catalysed reactions is the catalytic internal nitroalkyne redox cyclization.[4] The cyclization of *o*-arylalkynylnitrobenzenes reported by the group of Professors Naoki Asao and Yoshinori Yamamoto from Tohoku University was one of the early examples for the gold (III)-catalysed nitro-alkyne redox process – which has provided a practical alternative for the synthesis of the 2-aryl-3-oxo-3*H*-indole 1-oxide unit (trivially known as isatogens) (Figure 1).[5]

[a] *P. S. Dhote, S. V. Halnor, Dr. C. V. Ramana*
Organic Chemistry Division
CSIR- National Chemical Laboratory,
Dr.Homi Bhabha Road, Pune-411008, India
E-mail: vr.chepuri@ncl.res.in
[b] *P. S. Dhote, S. V. Halnor, Dr. C. V. Ramana*
Academy of Scientific and Innovative Research (AcSIR),
Ghaziabad-201002, India

This indeed opened a new domain in gold-catalysis that comprised of the gold-catalysed oxygen atom transfer to alkynes employing nucleophilic oxygen atom donors such as amine-/pyridine *N*-oxides, nitrone, sulfoxides and epoxides for the generation of reactive α-oxo gold carbene intermediates.[6] Taken together with the α-imino gold carbene intermediates, this has been regarded as an important advancement in gold catalysis due to versatile transformations these intermediates undergo and the resulting product diversity.[7]

In the following sections, will be described a brief compilation of methods that have been documented for the nitroalkyne cycloisomerization until recently, followed by the mechanistic aspects of the gold-catalysed nitroalkyne cycloisomerization and subsequent synthetic exploration of the gold-catalysed nitroalkyne cycloisomerization, by combining it with the nucleophilic additions and cycloadditions in the synthesis of complex heterocyclic scaffolds.

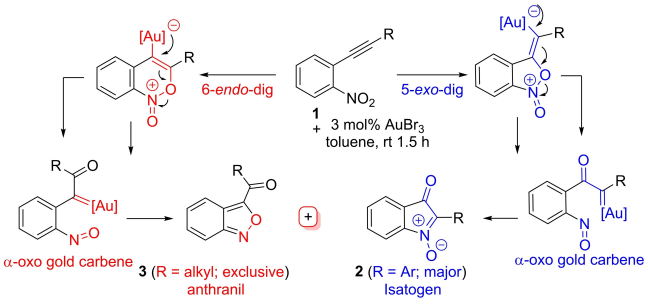

Figure 1. Yamamoto's Gold-Catalysed Nitroalkyne Cycloisomerization and Substrate Dependent Complementary Redox Cyclization and the Key Reactive α-Oxo Gold Carbene Intermediates Proposed Later.

2. Nitroalkyne Cycloisomerization Leading to Isatogens

2.1. Documented Before Yamamoto's 2003 Disclosure

The cyclization of *o*-alkynylnitrobenzens is one of earliest redox processes to be documented in organic synthesis. In dealing with the synthesis of indigo, in 1881, Bayer reported the cycloisomerization of *o*-nitrophenylpropiolates 4 in cold concentrated sulphuric acid leading to 2-carboxy-3-oxo-3*H*-indole 1-oxide 5.[8] The central bicyclic core of this is trivially called an isatogen (isatin + gen), since they are isomeric to isatin. Later, Pfeiffer and Ruggli have explored this class of compounds systematically and provided some important advancements for the *o*-nitroalkyne cycloisomerization, which includes the pyridine-mediated internal redoxycyclization either under photochemical or thermal conditions (Scheme 1) or the use of nitrosobenzene to promote the cycloisomerization, which takes several days to form the isatogens.[9]

In 1969, Bond and Hooper revealed that during the preparation of unsymmetrical diaryl acetylenes employing Cu-(I) 2-nitrophenylacetylide **8** under Castro-Stephens coupling conditions, in some instances, prolonged heating of the reaction in pyridine gave the corresponding isatogens **10** directly (Scheme 2). The yields and the time of the reaction varied with respect to the substituents present on the aryl ring.[10]

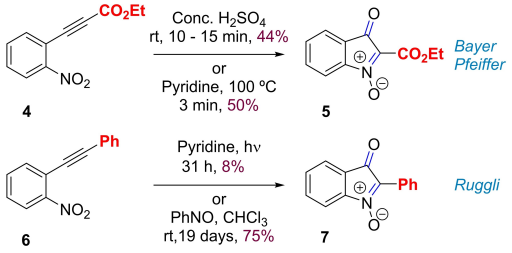

Scheme 1. Acid/Base-Mediated Nitroalkyne Cycloisomerization.

Along similar lines, Rosen and co-workers documented a one-pot protocol that comprises of carrying Sonogashira coupling of *o*-iodonitrobenzene derivatives **11** with (hetero) arylacetylenes **12a** in neat triethyl amine and continuing the reaction for 3–4 days at rt (Scheme 3).[11a] This has been applied aptly for the synthesis of various 2-(hetero)aryl

Mr. Pawan Dhote was born in Nagpur, Maharashtra, India in 1993. He received his B.Sc. (Chemistry) from Fergusson College, Pune in 2014, and M.Sc (Organic Chemistry) in 2016 from Department of Chemistry, Savitribai Phule Pune University (formerly known as University of Pune), Maharashtra, India. Later, in 2017 he joined the group of Dr. C. V. Ramana at CSIR- National Chemical Laboratory, Pune, India as DST-INSPIRE Fellow. Currently, he is working on gold catalysed o-nitroalkyne/o-azidoalkyne reactions.

Mr. Swapnil V. Halnor was born in Maharashtra, India in 1993. He obtained his B.Sc. (Chemistry) from Abasaheb Garware College, Pune in 2014, and M.Sc (Organic Chemistry) from Department of Chemistry, Savitribai Phule Pune University (formerly known as University of Pune), Maharashtra, India, in 2016. He joined the group of Dr. C.V. Ramana at CSIR-National Chemical Laboratory, Pune, India as a CSIR-Junior Research Fellow in 2018 and is currently working on the total synthesis of natural products using gold catalysis.

Dr. Ramana obtained his MSc. from Andhra University, Waltair (1991) and PhD from University of Hyderabad under the supervision of Professor M. Nagarajan (Synthetic Carbohydrate Chemistry). From 1998 to 2001 he was associated with Professor Andrea Vasella at ETH Zurich as a post-doctoral researcher (glycosidase inhibitors). From May 2001 onwards, he had been associated with CSIR-National Chemical Laboratory. At NCL, the focus of Ramana's group includes small molecules synthesis by employing transition metal complexes, developing new catalytic methods and process development for APIs and Agrochemicals. He is a recipient CSIR Young Scientist award in Chemical Sciences (2003) and CNR Rao National Prize in Chemical Sciences (2017). He is the fellow of Indian Academy of Sciences (2014, Bangalore).

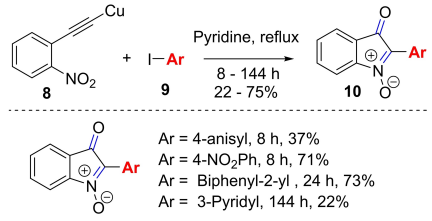

Scheme 2. A one-pot Castro-Stephen's coupling and Nitroalkyne Cyclo-isomerization.

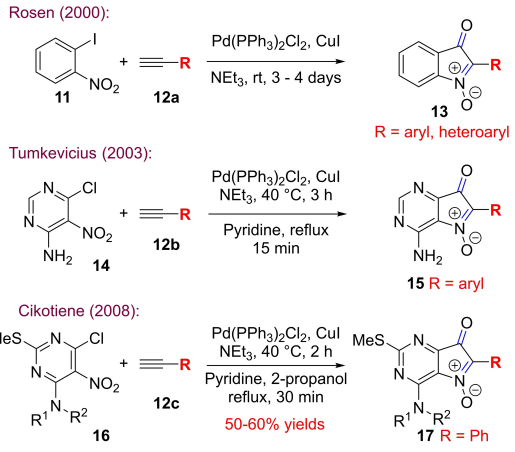

Scheme 3. One-pot Sonogashira Coupling – Nitroalkyne Cycloisomerization.

isatogens **13**. However, when an alkyl group such as a methyl was present on the alkyne end, the corresponding 2-methylisatogen was obtained in poor yields. Although, the role of the original [Pd]-catalyst over the cyclization is not very clear, the facile nitroalkyne cycloisomerization at rt indicates that the phosphine free Pd(II)-salts resulting after the initial Sonogashira coupling may be responsible. Interestingly, a similar protocol with 6-chloro-5-nitropyrimidine derivatives **14**/**16** required separate heating in neat pyridine to carry out the requisite nitroalkyne cycloisomerization.[11b,c]

2.2. Reported After Yamamoto's 2003 Disclosure

In 2009, Söderberg and co-workers reported a regiospecific synthesis of isatins **19** from 1-iodo-2-nitro-benzenes under Pd catalysis (Scheme 4). The optimal reaction conditions were 5 mol% $PdCl_2(PPh_3)_2$ in acetone at 60 °C.[12] Both electron rich as well as electron deficient substitutions on the aromatic unit were well tolerated. However, only in two cases, the corresponding 2-bromoisatogens were isolated in good yields. Control experiments revealed that switching to dichloromethane with the same catalyst at reflux gave the bromoisatogen **20** in excellent yields. Considering this, it has been

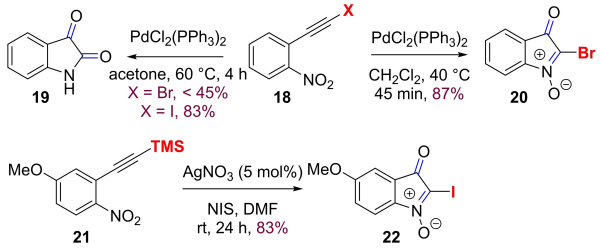

Scheme 4. Pd-/Ag-Catalysed Nitroalkyne Cyloisomerizations.

assumed that 2-haloisatogens are involved *en-route* to the isatins formation. Interestingly, when the Pd-complex was replaced with $AuBr_3$ in CH_2Cl_2, the bromoalkyne **18** was found to be unchanged even after 5 days. In the same report, it has been also shown that the attempted conversion of the TMS-alkyne **21** to corresponding iodoalkyne with $AgNO_3$/NIS gave the isatogen **22** exclusively.

In 2015, Harrity and co-workers have generalized the Söderberg's Ag-catalysed nitroalkyne cycloisomerization of iodoalkynes **23** employing Cu-catalysts in THF at reflux (Scheme 5). Substrates having an electron donating group on the aryl unit were compatible under low catalyst loading that is, 25 mol% of CuBr.DMS complex. Whereas with electron withdrawing groups the reaction underwent slow cyclization, requiring stoichiometric amounts of $Cu(CH_3CN)BF_4$. As expected, when $PdCl_2(PPh_3)_2$ was used as a catalyst isatin **19** was obtained exclusively. It was also interesting to note that a similar observation was made when 1 equiv. of CuBr.DMS was employed.The utility of these products has been examined by a cross coupling of the iodo at the C2 position with a wide range of alternative heterocyclic derivatives.[13]

In 2018, Song and group developed a copper-catalysed cycloisomerization of non-prefunctionalized nitroalkynes **25** for the synthesis of C2-tetrasubstituted indolin-3 ones **28** with $BrCF_2CO_2R$ **26** (Scheme 6). In this protocol, diboron acts as the reductant, rendering a fluorine-containing non-carbon quaternary centre in mild to excellent yields. Later, the same

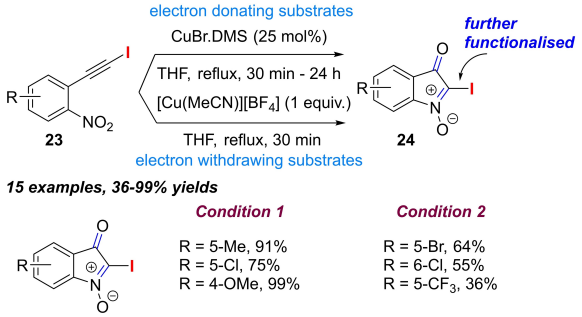

Scheme 5. Cu–Catalysed Cycloisomerization of 2-Nitrophenyliodoacetylene.

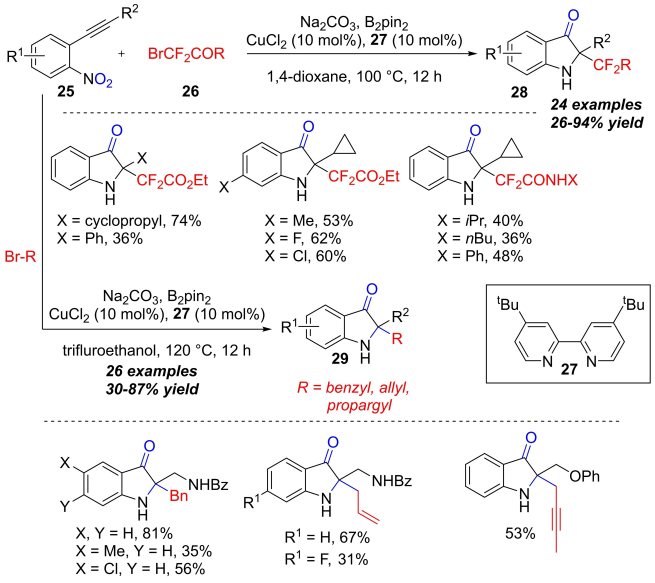

Scheme 6. Cu/B_2pin_2-Catalysed Cycloisomerization of *o*-Nitroalkynes for the Synthesis of C2-Tetrasubstituted Indolin-3-ones.

group employed different radical sources such as allyl, benzyl and propargyl bromides to synthesize diverse C2-quaternary indolin-3-ones **29** (Scheme 6).[14]

Following this, Peng's group developed a CuH-catalysed reductive cyclization of *o*-alkynylnitroarene **30** for the diasterospecific synthesis of 3-hydroxyindoline **31** and 2-aryl-3H-indol-3-one scaffolds **32** in a one pot operation (Scheme 7). The standard catalytic operation involved treatment of **30** in the presence of $CuCl_2$/dppf (ligand) (10 mol%) along with $Me(EtO)_2SiH$/LiOMe (4 equiv.) at room temperature to deliver 3-hydroxyindoline derivative **31**. When the reaction was continued with added silica gel at 80 °C for 12 h under O_2, it provided the 2-aryl-3*H*-indol-3-ones **32**. The reaction mechanism involves the formation of the LCu–H active catalyst that promotes the key nitroalkyne cycloisomerization resulting in the isatogen, which upon reduction by hydrosilane furnishes 2-aryl-3H-indol-3-one, the further reduction of which gives the 3- hydroxyindoline **31**.[15]

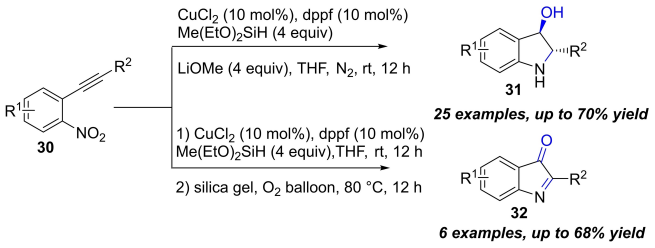

Scheme 7. Cu–H Catalysed Synthesis of 3-hydroxyindolines and 2-aryl-3*H*-indol-3-ones.

3. Gold-Catalysed Nitroalkyne Cycloisomerization & Involvement of α-Oxo Gold Carbenes

In 2003, Yamamoto and co-workers reported a substrate dependent gold(III)-catalysed cycloisomerization of *o*-alkynylnitrobenzenes **33** (Scheme 8).[5] When the pendant alkyne substituent was an aryl, isatogen **34** was obtained as the major product, along with the isomeric benzo[*c*]isoxazole, which is trivially known as anthranil **35**. Interestingly, when an alkyl group such as *tert*-butyl is placed on the alkyne, the corresponding anthranils **35** were obtained exclusively in good yields.

As mentioned above, this is an important development, as it is the first report on a catalytic internal nitroalkyne redox process to be documented. In addition, it also indicated an alternative possibility with the nitroalkyne cycloisomerization to synthesize anthranils, which otherwise were known to provide the isatogens. Importantly, subsequent findings revealed that this gold-catalysed internal oxygen transfer to alkynes leads to reactive α-oxo gold carbenes, which are otherwise synthesized *via* carbene transfer to the gold complexes. The initial mechanistic path proposed by Yamamoto is founded upon the addition of the oxygen from the nitro group in a 6-*endo*-dig fashion, which results in the formation of **33-A**. The resulting aurate complex undergoes protonolysis to afford **33-B** followed by ring opening with water to produce a nitrosobenzene adduct **33-C**. At this stage, there exist two possibilities for the subsequent dehydrative cyclization, either leading to isatogens **34** (Scheme 8, ***path a***) or anthranil **35** (Scheme 8, ***path b***). Though this explained the possible paths for the two isomeric products, however, it did not account for why these paths were substituent dependent.

In 2005, Crabtree's group studied the nitroalkyne cycloisomerization that leads to anthranil, using stoichiometric amounts of iridium hydride complex **36** (Scheme 9). With the help of single crystal structural analysis, it has been speculated that there exists an intermediate nitroso stabilized α-oxo

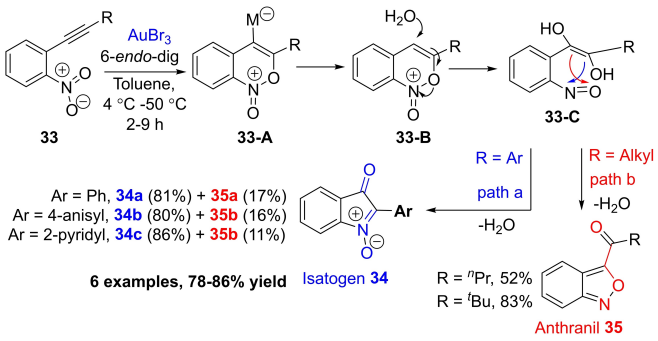

Scheme 8. Gold(III)-Catalysed Redox Cyclization of *o*-Alkynylnitrobenzenes.

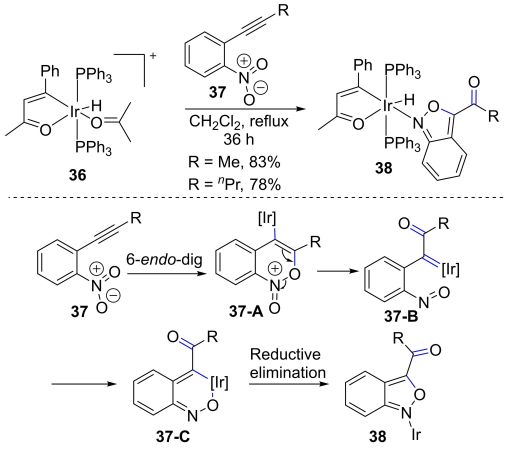

Scheme 9. Iridium(III) Hydride Complex Mediated Nitroalkyne Cycloisomerization.

iridium(III) complex **37-B**, which results after the initial oxygen transfer from nitro to alkyne in a 6-*endo*-dig fashion.[16]

In 2010, as a part of the total synthesis of Isatisine A, we speculated about the possibility of a palladium-catalysed nitroalkyne cycloisomerization to synthesize both 2-aryl and 2-alkyl isatogens (Scheme 10) and executed the same successfully with a $PdCl_2(CH_3CN)_2$ complex in acetonitrile.[17] Though our initial hypothesis was a halopalladation of the alkyne and subsequent oxygen transfer from the nitro to vinyl-[Pd] intermediate, the detailed density functional theory (DFT) calculations revealed that the reaction path involves the formation of the α-oxo palladium carbene **39-B** *via* the internal oxygen transfer from nitro to [Pd]-complex alkyne in a 5-*exo*-dig fashion. The intermediate metal carbene subsequently undergoes 6π-electrocyclization leading to isatogen **40**. Subsequent examination of the substrate scope demonstrated this as a general method for the synthesis of 2-aryl and 2-alkylisatogens. Indeed, this has been employed as the key tool in our total synthesis of Isatisine A and Trigonoliimine C.[18]

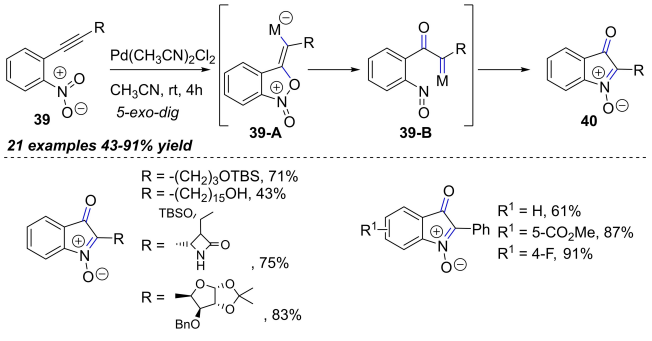

Scheme 10. [Pd]-Catalysed Nitroalkyne Cycloisomerization.

After a year, Liu and co-workers reported the PPh_3AuNTf_2-catalysed internal nitroalkyne redox cyclization/[3 + 2]-cycloaddition comprising of 1-ethynyl-2-nitrobenzenes **41** and alkenes **42** to form complex azacyclic compounds **43** in a stereoselective manner (Scheme 11).[19] The use of $AuCl_3$, $PtCl_2$/CO gave inseparable mixture of products. Whereas, $ClAuP(^tBu)_2$(o-biphenyl)/$AgNTf_2$ and IPrAuCl/$AgNTf_2$ [5 mol%; IPr = 1,3-bis(diisopropylphenyl)imidazol-2-ylidene] gave separable diastereomeric mixture of cycloaddition products.

The mechanism for this transformation involves the formation of α-oxo gold carbene **41-A** *via* a 5-*exo* dig cyclization and N–O bond cleavage. Next, the resulting gold carbene undergoes an internal redox reaction giving the enol core **41-B**, which upon [3 + 2]-cycloaddition with an external alkene **42** in a concerted *exo*-manner results in the bridged bicyclic compound **43** selectively. The scope of this cyclization-cycloaddition cascade was demonstrated by using various electron-rich olefins, along with electron rich and electron deficient nitroalkynes. Interestingly, as a part of control experiments, this group revised the mechanism for the formation of anthranil previously reported by Yamamoto, and described the possible involvement of α-oxo gold carbene.

Recently, Xu's group showed that these intermediate terminal α-oxo gold carbenes could be trapped with indoles.[20] This group developed a simple method for the synthesis of 2-indolylisatogens **46** *via* a PPh_3AuNTf_2-catalysed cascade reaction of *o*-alkynylnitrobenzene **44** with indoles **45** (Scheme 12). The reaction proceeds through the formation of

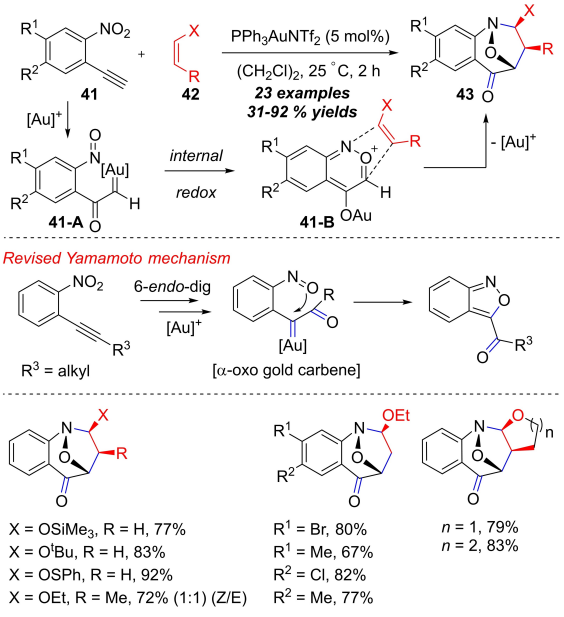

Scheme 11. [Au]-Catalysed Stereoselective Synthesis of Azacyclic Compounds and Revised Mechanism.

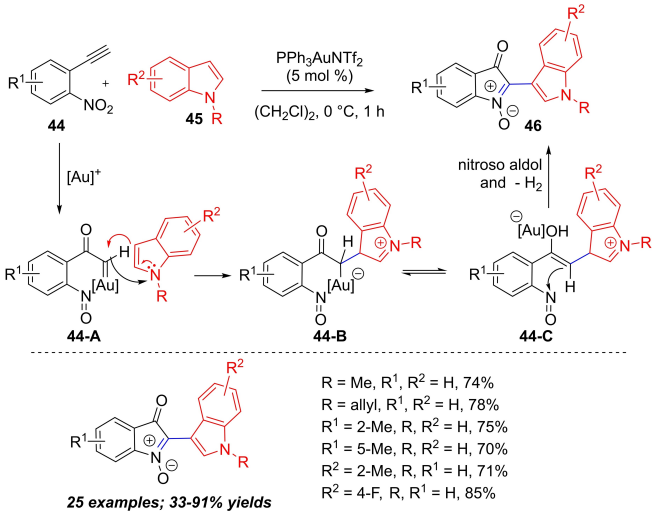

Scheme 12. Gold(I)-Catalysed Redox Transformation of o-Alkynylnitrobenzene with Indoles.

gold carbene intermediate **44-A** *via* 5-*exo*-dig cyclization of *o*-alkynylnitrobenzene, followed by addition of C3 of indole, which on internal redox forms enolate and subsequent cyclization yields 2-indolyl derivatives **46**. The gold-complexes such as $AuCl_3$, $(ArO)_3PAuNTf_2$, $IPrAuCl/AgNTf_2$ are found to be to not promising.

In parallel to Liu's work, we have also speculated on the possible involvement of α-oxo gold carbenes during investigations that were aimed at the possible interruption of these metal catalysed cycloisomerization processes with internal nucleophiles such as –OH.[21] As shown in Scheme 13, depending upon the catalyst employed and the proximity of the –OH group, the formation of the *spiro*-indolin-3-one **48** and *spiro*-benzoxazinone **49** was observed with the Pd-complex. On the other hand, when $AuBr_3$ was employed as catalyst, in case of substrate **47b**, the *spiro*-benzoxazinone **51** and anthranil derivative **52** were obtained in equal proportion and with **47c**, *spiro*-benzoxazinone **54** was obtained exclusively. The diversity in the product formation has explained by possible complementary 5-*exo*/6-*endo* dig cyclizations operating respectively with Pd- and Au-complexes, and by the nature of the intermediate nitroso-stabilized metal carbenoids involved in the reaction (Scheme 14). The formation of *spiro*-benzoxazinone **49** with substrate **47a** has been explained by invoking the possible insertion of the carbene across the –OH. However, the products obtained from the $AuBr_3$-cyclization revealed that such trapping of the intermediate α-oxo gold carbene is not operational and the protodeauration is operational at least in case of the cycloisomerization of substrate **47a**.

However, Wang and co-workers documented a similar [Pd]-catalysed cycloisomerization of *o*-alkylnylnitrobenzenes **55** having an internal nitrogen-nucleophile leading to *N,N'*-ketal spiropseudoindoxyl derivatives **56** (Scheme 15).[22] This

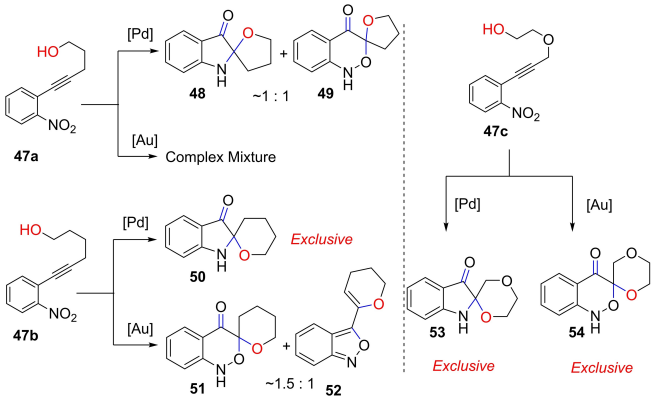

Scheme 13. Interrupting the [Pd]-/[Au]-Catalysed Nitroalkyneredox Process with Internal Nucleophile.

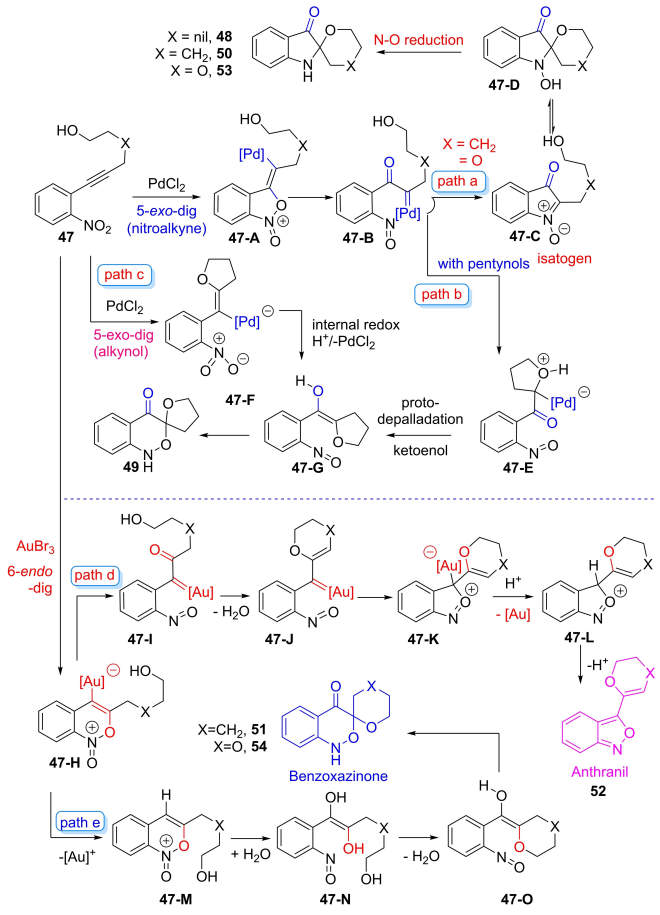

Scheme 14. Mechanism of [Pd]-/[Au]-Catalysed Nitroalkyneredox Process with Internal Nucleophile.

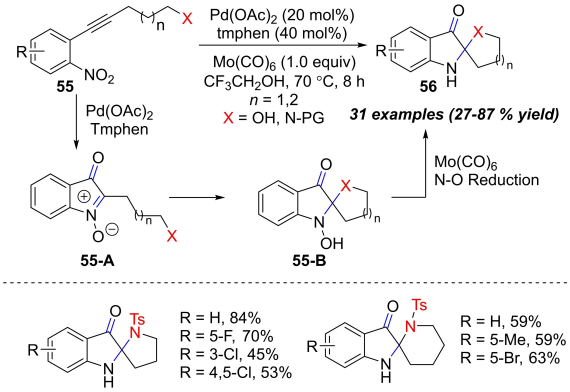

Scheme 15. Synthesis of *N,N'*-ketal Spiropseudoindoxyl Derivatives.

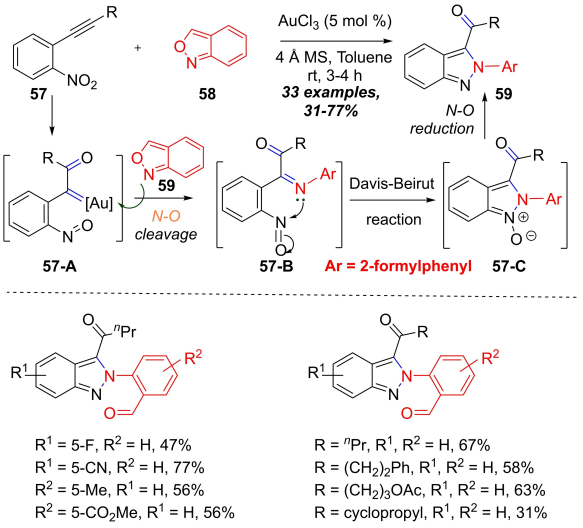

Scheme 16. Interrupting the Nitroalkyne Cycloisomerization by Anthranils.

transformation has been optimized employing different palladium catalysts [$Pd(OAc)_2$, $Pd(TFA)_2$, $PdCl_2(dppf)$ and $Pd(CH_3CN)_2Cl_2$], along with various ligands/reductants, to come up with the optimized conditions that comprise of employing $Pd(OAc)_2$ (20.0 mol%) along with the tmphen ligand (40.0 mol%) and $Mo(CO)_6$ reductant.The proposed mechanism consists of a 5-*exo* dig cyclization to isatogens **55-A** followed by an intramolecular nucleophilic addition of the amine and subsequent $Mo(CO)_6$-mediated reductive cleavage of the N–O bond.

A successful intermolecular trapping of intermediate α-oxo gold carbene in this nitroalkyne cycloisomerization, especially one that leads to anthranils, has been documented recently from our group.[23] We speculated that in the presence of a nitrogen donor such as benzo[*c*]isoxazole (anthranil) **58** (which is an established nitrogen donor to metal coordinated alkynes and results in a α-oxo/imino gold carbene and also participates in carbene transfer reactions from the gold carbenes with equal ease[24]) the intermediate α-oxo carbene that results during the cycloisomerization of nitroalkyne **57** should transfer the carbene to nitrogen (in competition with the original internal 6π-electron cyclization) to form an intermediate imine. Subsequent Davis-Beirut cyclization would lead to 3-acyl-(2-formylphenyl)-2H-indazoles **59** (Scheme 16). This has been successfully realized with simple $AuCl_3$ as a catalyst in toluene at rt resulting in the indazole derivatives **59**. The beauty of this reaction is that the overall process comprises of sequential cleavage of three N–O bonds and the formation of C–O, C–N and N–N bonds in concert. The scope of this reaction has been explored with a wide range of anthranils/nitroalkynes. As a control, various Pt, Pd and Au-complexes, along with a range of Ag additives, have been screened and it has been realized that either they resulted in poor conversion/yields or ended up in complex intractable mixtures. Control experiments revealed that the alternative path that comprises of the initial formation of α-imino gold carbene *via* addition of anthranil to the alkyne first and subsequent internal oxygen transfer from the nitro group is not in operation. At the outset, these studies provided an indirect support for the presence of a reactive α-oxo gold carbene in these internal nitroalkyne cycloisomerizations.

4. Synthetic Utility of [Au]-Catalyzed Nitralkyne Redox Cycloisomerization

From the above discussion, it is evident that Yamamoto's report on [Au]-catalyzed nitroalkyne cycloisomerization leading to the synthesis of isatogens has reinitiated this area. The ready functionalization of these isatogens at the C2-position, either by nucleophilic addition or by cycloaddition, generates the synthetically demanding 2,2-disubstituted 1,2-dihydro-3*H*-indolin-3-one (trivially known as pseudoindoxyl - a subgroup of indole class of alkaloids bears this name) skeleton, which is one of the key aspects that has been inspired the researchers. This is evident from the appearance of various Pd, Ag, Hg and Cu-complexes in the pursuit of developing regioselective nitroalkyne cycloisomerizations. Yet, the cyclizations with [Au]-complexes are more attractive, since they are facile at rt. The added advantage with the [Au]-complexes is their Lewis acidity, which can be used for post functionalization of the resulting isatogens and also gives a provision to employ other Lewis acids in the same-pot to develop novel cascade and/or one-pot operations. In the following sections, various reports documented in this context are summarized briefly.

4.1. Cascade Transformations by Combining the [Au]-Catalysed Nitroalkyne Cycloisomerization with Nucleophilic Additions

The intermolecular functionalization of isatogens with external nucleophiles such as amino acids and alcohols has been studied in detail by Hooper's group (Scheme 17).[25a] The addition of Grignard reagents or anions derived from the active methylene groups were documented earlier by Marchetti and Greci groups respectively.[25b,c] As a part of the total synthesis of Isatisine A, we documented the $InCl_3$-mediated addition of C3

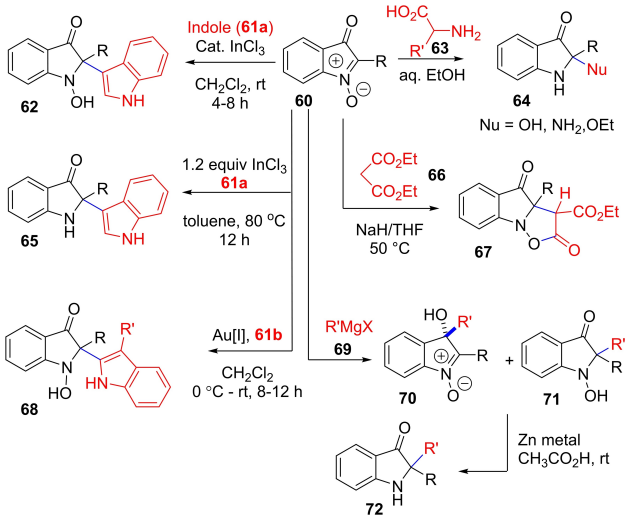

Scheme 17. Nucleophilic Addition to Isatogens.

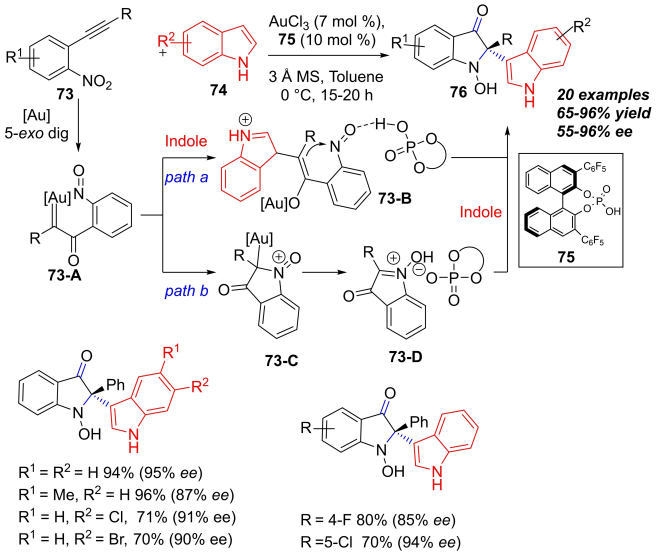

Scheme 18. Asymmetric Addition of Indole to in-situ prepared Isatogens *via* gold (III) Catalysed Nitroalkyne Cycloisomerization

of indoles and also a [Au]-catalysed addition of C2 of indole selectively at the nitrone carbon of the isatogens in dealing with the total synthesis of Trigonoliimine C. The reaction of isatogens with allyl- and propargyl bromides under Barbier conditions has also been examined by our group in the context of the ongoing total synthesis of Austamide. However, it was not regiospecific (unpublished results).

A successful merger of [Au]-catalysed cycloisomerization with indole addition in an asymmetric manner has been accomplished by Jia's group (Scheme 18).[26] In 2015, Jia and co-workers documented a gold(III) and chiral phosphoric acid-catalysed enantioselective construction of *N*-hydroxyindolin-3-ones **76** bearing a C2 quaternary stereocenter. In general, o-nitroalkyne **73** and indole **74** were reacted in the presence of $AuCl_3$ (7 mol%) and chiral phosphoric acid **75** (10 mol%) in toluene at 0 °C to expedite this redox annulation.

Interestingly, the use of 3 Å molecular sieves was found to be important, increasing both yield and enantioselectivity of *N*-hydroxyindolin-3-one derivatives **76**. Their proposed redox annulation pathway comprises of an initial internal oxygen transfer in a 5-*exo*-dig leading to the α-*oxo* gold carbene **73-A** and subsequent internal cyclization to isatogen **73-C** and then nucleophilic attack of indole on the chiral ion pair **73-D** to form indoline-3-one derivatives **76**. Another possibility that comprises of the intermolecular interception of the gold carbene **73-A** with indole followed by cyclization has been also invoked; however, control experiments revealed that a stepwise protocol involving isatogen as the intermediate was operating.

4.2. Cascade Transformations by Combining the [Au]-Catalysed Nitralkyne Cycloisomerization with Cycloaddition Reactions

Though isatogens are known for more than 140 years, the cycloaddition reactions with isatogens were reported very recently.[27] In 2001, Greci and co-workers have the [3+2]-dipolar cycloaddition of 2-phenylisatogen **77** with maleamide derivatives **78** (4 equiv.) in refluxing toluene (Scheme 19). The reactions proceeded smoothly and provided a mixture of *exo*-/*endo*-isomers **79** in good yields.[27a]

Later, in 2003,[27b] the same group carried out the cycloaddition of 2-phenylisatogen in neat ethyl acrylate, methyl crotonate, and ethyl cinnamate at 80 °C. Interestingly, in the case of ethyl acrylate, the cycloaddition was found to be non-selective and delivered all the four possible isomers **81 a–d**. Whereas with ethyl crotonate or ethyl cinnamate having *trans*-configuration, the cycloaddition reaction proceeded with complete regio- and stereoselectivity and provided a single product **83**. The *ab initio* calculations have revealed that the product distribution may be influenced by kinetic rather than thermochemical factors. In 2015,[28] our group documented a one-pot [3+2]-cycloaddition of isatogens with olefins fol-

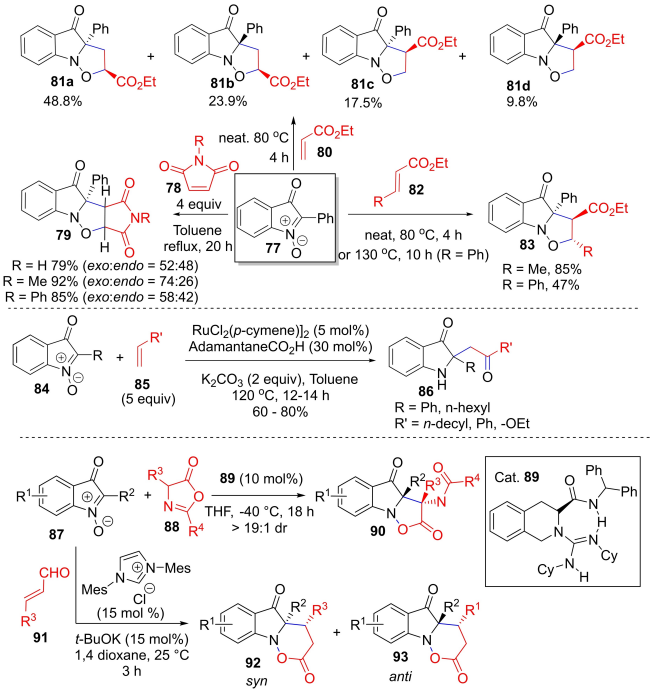

Scheme 19. Documented Cycloaddition Reactions of Isatogens.

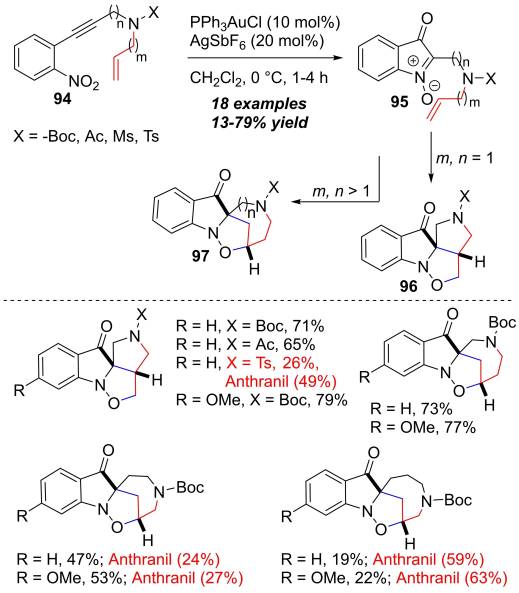

Scheme 20. Gold(I)-Catalysed Cycloisomerization of o-Nitroenynamides and Intramolecular [3+2] Cycloaddition with Olefin.

lowed by [Ru]-catalysed redox neutral cleavage, resulting in β-amino ketones or ester **86**; when a vinyl ether was used. Control experiments revealed that the cycloaddition was regio- and stereoselective. Very recently, Liu and co-workers documented an organocatalytic asymmetric formal [3+2] cycloaddition of isatogens with azalactones **88** to construct indolin-3-one derivatives **90**.[29a] Meanwhile, Du and co-workers reported a NHC-catalysed [3+3]-cycloaddition of isatogen with acryl aldehyde derivatives **91**.[29b]

As a part of our ongoing program on the total synthesis of Austamide, one of the early approaches comprised of constructing the tricyclic core by employing a gold-catalyzed nitroalkyne cycloisomerization with intramolecular [3+2]-cycloadditions. However, one major concern was competition between the isatogen *vs* anthranil formation in gold-catalysed cycloisomerization in general. Especially when the substituent on the alkyne end was an alkyl group, the exclusive formation of anthranil was observed. In this context, we hypothesized that the presence of an electron withdrawing group such as nitrogen on a pendant chain would promote the 5-*exo* mode of cyclization *inter alia* isatogen formation.[30]

With this proposal, as shown in Scheme 20, the gold(I)-catalysed cycloisomerization of *o*-nitroenynamides **94** led mainly to isatogen **95** and subsequent regioselective [3+2] cycloaddition with suitably positioned internal olefins yielded products **96/97** in moderate to good yields. This transformation was examined with the majority of the Au complexes and (with or without Ag additives) found to be compatible, with variations mainly in the isolated yields. Only for the cases of the reactions where $AgNO_3$ or $AgCO_3$ were employed as additives, the starting nitroalkyne was found to be intact. The regioselectivity in cycloaddition for the construction of tricyclic core depends on varying the chain length of the olefin unit. As such, propargyl-*N*-allyl derivatives (m, n = 1) underwent this two-step protocol to give isoxazolidines **96** exclusively, whereas with propargyl-*N*-butenyl (m > 1) or when increasing the length of the carbon chain before nitrogen atom from the alkyne unit (n > 1) the [4,2,1]-bridged bicyclic products **97** with endo-selectivity were observed. The scope of the reaction was proved by varying the substituents on the aryl ring, chain length on olefin unit and different protecting groups. In the case of *N*-Ms and *N*-Ts, anthranil derivatives were also formed along with isatogen/cycloaddition products.

In parallel to our report, Verniest's group reported a similar Au(III)-catalysed cycloisomerization of *o*-nitrophenyl-propiolamides **98** and subsequent intramolecular dipolar cycloaddition with alkenes afforded the tetracyclic core (Scheme 21).[31] The strained heterocycle underwent N–O bond reduction by hydrogenative cleavage, which provided the tricyclic C2-spiropseudoindoxyl product **99** as a single diastereomer. Interestingly, DFT studies revealed that these transformations do not involve the gold carbene **98-B**. A mechanism founded upon the participation of the amide oxygen in the ring opening *via* the formation of an oxirane core **98-C**, which subsequently converted to isatogen **98-D** and underwent intramolecular [3+2]-cycloaddition. Interestingly, the estab-

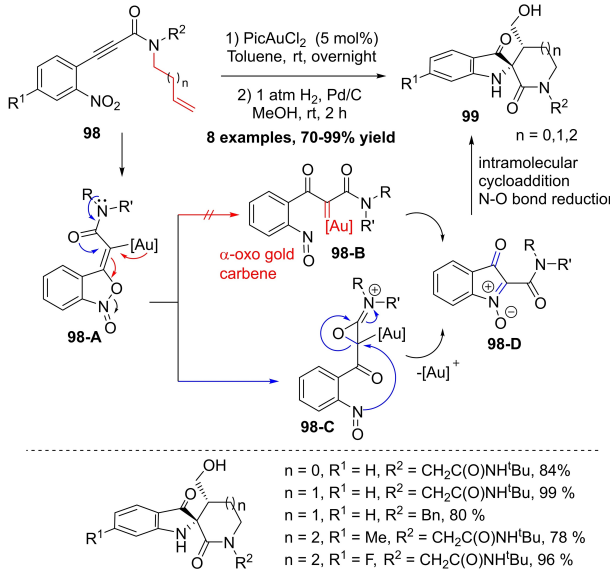

Scheme 21. Gold (III)- Catalyzed Synthesis of Tricyclic core of C2-Spiropseudoindoxyl.

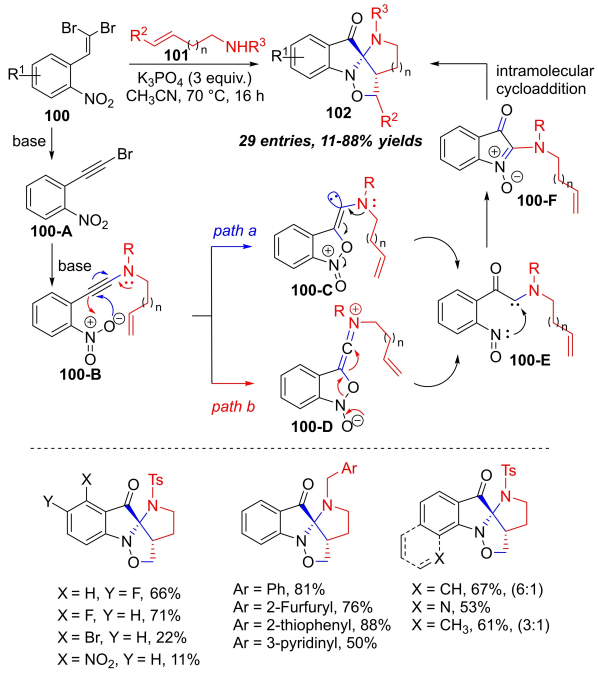

Scheme 22. Metal free Cyclization of o-Nitroaryl Ynamides and Ynamines.

lished Au(I), Au(III) and Pd(II)-complexes were found to be less selective and resulted either in poor product yields or complex mixtures. In the substrate-scope exploration, electron-donating and –halogens on the aryl unit, electron-rich and -poor groups on the amide nitrogen atom were well-tolerated in this cascade protocol.

In 2018, the same group developed a metal free cascade reaction between 1-dibromovinyl-2-nitro substituted arenes **100** and secondary amines **101**, resulting in the formation of spiropseudoindoxyls **102** in a one pot protocol (Scheme 22).[32] The proposed reaction mechanism involved the formation of bromoalkyne **100-A**, followed by the loss of HBr to form ynamide **100-B** through an addition/elimination sequence. This ynamide undergoes two distinct pathways, where path a proceeds *via* attack of oxygen of nitro group to β-position of alkyne and subsequent cyclization forms stabilised carbene **100-E**. Whereas, in path b, attack of the ynamide on oxygen of nitro group results in the formation of carbene **100-E**. Next, the nucleophilic attack of the nitroso nitrogen at the carbene and further isomerisation affords 2-amino isatogen **100-F**, followed by intramolecular [3+2] cycloaddition, which provide the tetracyclic compounds **102** in good yields. The QTAIM (quantum theory of atoms in molecules) and ELF (electron localization function) studies revealed that a single-electron transfer from the nitro group plays an important role in the cycloisomerization process. In the substrate scope exploration, electron-donating and -withdrawing groups on the aryl unit, and the protecting group of the amine nitrogen atom, were well-tolerated to construct the respective pseudoindoxyl core.

In 2019, our group developed a one pot, two step protocol for the synthesis of pseudoindoxyl derivatives **105** from o-nitroalkynylbenzene **103** comprising of isatogen formation and its $Sc(OTf)_3$ mediated [3+3]cycloaddition with donor acceptor cyclopropane (DAC) **104** (Scheme 23).[33] Initial optimization studies have revealed that the Au(I), Pd, Pt-complexes, along with the Lewis acid as additive were found to be less compatible and ended with the formation of isatogen, along with product **105**, in maximum cases. This cycloaddition reaction is highly distereoselective, where, in case of 2-arylisatogens, both nitroalkyne cycloisomerization and cycloaddition were facile in a one pot manner; whereas, in 2-alkylisatogens, both the steps were conducted separately. Various electron rich/deficient groups on the aryl unit of both DAC and nitroalkyne were compatible. The competition experiments between olefins and DAC shows interesting cycloadduct formation. For example, when *N*-allyl propargylamide derived nitroalkyne was treated with a gold/Lewis acid catalyst along with DAC, it was found that after the isatogen formation, it underwent [3+2]-cycloaddition with the pendant allyl group. Moreover, during the reaction with electron rich/electron deficient olefins added externally along with DAC, the cycloadduct formed *via* [3+3]-cycloaddition was seen to be preferred over the classical [3+2]-cycloaddition of isatogens.

In 2020, Deng's group demonstrated the $Cu(0)/PPh_3$-Catalysed cascade bis-heteroannulation reaction by employing various *o*-nitroalkynes **106** and methylketoximes **107** leading

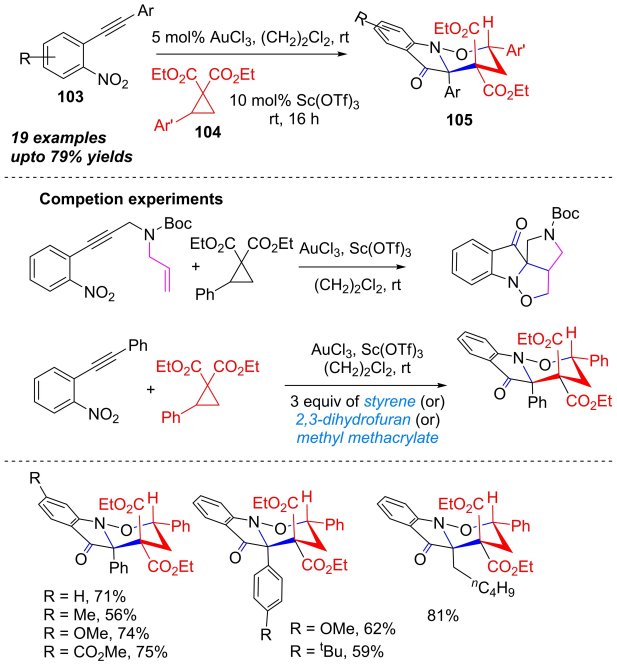

Scheme 23. Gold(III)/$Sc(OTf)_3$-Catalysed Cycloisomerization and [3+3] Cycloaddition with Donor -Acceptor Cyclopropane.

to the pyrazofused pseudoindoxyl compounds **108** with broad substrate scope and functional-group tolerance (Scheme 24).[34] A standard catalytic operation involved treatment of o-nitro-alkynes **106** with methylketoximes **107** in the presence of Cu metal (50 mol%)/PPh_3 (2 equiv.) to deliver the pyrazolo[1,5-a]indolone product **108**. The use of Cu(I) or Cu(II)-catalyst along with PPh_3 as reductant were found to be non-compatible

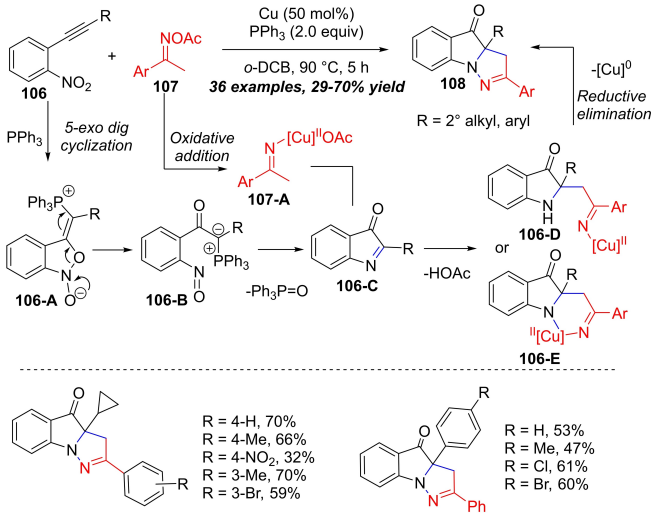

Scheme 24. Cu(0)-Mediated Reductive Bis-heteroannulations Reaction.

and ended up in low yields of *bis*-heteroannulation product **108**. In the proposed reaction mechanism, first, a nucleophilic attack of the PPh_3 base to an alkyne moiety gave **106-A**, and on cyclization/intramolecular charge transfer/deoxygenation further gave indol-3-one **106-C**. Later, oxidative addition of Cu(0) into the N–O bond of oxime acetate led to migratory insertion across the C=N bond, with final reductive elimination with N–N bond formation to afford **108**.

5. Conclusions

In summary, the internal redox cyclization of *o*-alkynylnitro benzenes with metal complexes in general, and with gold-complexes, in particular, is relatively unexplored, as the efforts are mainly focused on utilization of end products. The substrate dependent complementary formation of isatogens or anthranils is the unique feature of the gold-complexes. From the examples provided, it becomes apparent that the focus had been mainly on manipulating Au-complexes/ligands and also alkyne substituents to arrive at isatogens exclusively. This was mainly because of the presence of a reactive nitrone and a carbonyl group in conjugation to the same. The Lewis-acidity of gold complexes allowed post modification of these reactive units *via* nucleophilic additions or cycloadditions. However, the nucleophiles or the dipolarophiles used are limited in number and still this domain is open for further exploration. In addition, the complementary path that provides the anthranil, which revealed the existence of α-oxo metal carbenes in the reaction path, has been relatively unexplored. The singular contributions in this regard were: using these resulting anthranils (with Hg-complexes)[35] for further nitrogen transfer to alkynes and our recent contribution on trapping the corresponding α-oxo gold carbene with an external anthranil. The recent disclosure on affecting this transformation with iodo[36] or under electrochemical conditions[37] provides an opportunity to study the internal redox cyclisation trans-formation in parallel. In addition, the involvement of an α-oxo gold carbene in case of isatogen synthesis has been not yet fully established, as there are some instances where DFT calcu-lations revealed alternative possibilities. Taken together with expanding the scope of the complementary nitroalkyne cyclo-isomerization reactions, this important question remain un-answered and would certainly attract a great deal of attention in the near future.

Acknowledgements

The work documented in this personal account is a result of dedicated hard work and innovative ideas by CVR's students. CVR is grateful to Dr. Pitambar Patel (one who started the

work on *o*-nitroalkyne), Dr. C. V. Suneel Kumar, and Dr. B. Narendraprasad Reddy. CVR would like to thank Dr. Kumar Vanka for doing computational studies and Prof. Alexi Degtrev for carrying out biological activity. We would also like to thank CSIR (India) for a generous research funding as well as for a research fellowship to SVH and DST-INSPIRE for a research fellowship to PSD.

References

[1] Selected reviews/book chapter on gold-catalysed reaction: a) S. K. Hashmi, G. J. Hutchings, *Angew. Chem. Int. Ed.* **2006**, *45*, 7896–7936; *Angew. Chem.* **2006**, *118*, 8064–8105; b) S. K. Hashmi, *Chem. Rev.* **2007**, *107*, 3180–3211; c) N. T. Patil, Y. Yamamoto, *Chem. Rev.* **2008**, 108, 3395–3442; d) S. Shin, *Gold*-Catalyzed *Carbene Transfer Reactions*, Springer, Cham. **2014**, 357, pp. 25–62.

[2] Selected reviews on gold-catalysed reaction in total synthesis: a) M. Rudolph, S. K. Hashmi, *Chem. Soc. Rev.* **2012**, *41*, 2448–2462; b) Y. Zhang, T. Luo, Z. Yang, *Nat. Prod. Rep.* **2014**, *31*, 489–503; c) D. Pflästerera, S. K. Hashmi, *Chem. Soc. Rev.* **2016**, *45*, 1331–1367; d) W. Li, B. Yu, *Chem. Soc. Rev.* **2018**, *47*, 7954–7984; e) P. Toullec, V. Michelet, *Isr. J. Chem.* **2018**, 58, 578–585.

[3] a) W. Zia, D. Toste, *Chem. Soc. Rev.* **2016**, *45*, 4567–4589; b) Y. Li, W. Li, J. Zhang, *Chem. Eur. J.* **2017**, *23*, 467–512; c) C. Praveen, *Asian J. Org. Chem.* **2020**, *9*, 1953–1998.

[4] Selected reviews on gold-catalysed internal redox processes: a) D. Garayalde, C. Nevado, *ACS Catal.* **2012**, *2*, 1462–1479; b) L. M. Zhang, *Acc. Chem. Res.* **2014**, *47*, 877–888; c) H. S. Yeom, S. Shin, *Acc. Chem. Res.* **2014**, *47*, 966–977.

[5] N. Asao, K. Sato, Y. Yamamoto, *Tetrahedron Lett.* **2003**, *44*, 5675–5677.

[6] J. Xiao, X. Li, *Angew. Chem. Int. Ed.* **2011**, *50*, 7226–7236; *Angew. Chem.* **2011**, *123*, 7364–7375.

[7] a) E. Aguilar, J. Santamaría, *Org. Chem. Front.* **2019**, *6*, 1513–1540; b) L. W. Ye, X. Zhu, R. Sahani, Y. Xu, P. C. Qian, R. S. Liu, *Chem. Rev.* **2020**, DOI: 10.1021/acs.chemrev.0c00348.

[8] A. Baeyer, *Ber. Dtsch. Chem. Ges.* **1881**, *14*, 1741–1746.

[9] a) P. Pfeiffer, J. Liebigs, *Ann. Chem.* **1916**, *411*, 72; b) P. Ruggli, E. Casper, B. Hegedus, *Helu. Chim. Acta.* **1937**, *20*, 250.

[10] C. C. Bond, M. Hooper, *J. Chem. Soc. (C)*, **1969**, 2453–2460.

[11] a) G. M. Rosen, P. Tsai, E. D. Barth, G. Dorey, P. Casara, M. Spedding, H. J. Halpern, *J. Org. Chem.* **2000**, *65*, 4460–4463; b) I. Susvilo, A. Brukstus, S. Tumkevicius, *Synlett* **2003**, *8*, 1151–1152; c) I. Cikotiene, E. Pudziuvelyte, A. Brukstus, *J. Heterocycl. Chem.* **2008**, *45*, 1615–1620.

[12] B. C. G. Söderberg, S. P. Gorugantula, C. R. Howerton, J. L. Petersen, S. W. Dantale, *Tetrahedron* **2009**, *65*, 7357–7363.

[13] E. J. M. Maduli, S. J. Edeson, S. Swanson, P. A. Procopiou, J. P. A. Harrity, *Org. Lett.* **2015**, *17*, 390–392.

[14] a) W. Fu, Q. Song, *Org. Lett.* **2018**, *20*, 393–396; b) W. Fu, Y. Zhou, Q. Song, *Chem. Asian J.* **2018**, *13*, 2511–2515.

[15] H. Peng, J. Ma, L. Duan, G. Zhang, B. Yin, *Org. Lett.* **2019**, *21*, 6194–6198.

[16] X. Li, C. D. Incarvito, T. Vogel, R. H. Crabtree, *Organometallics* **2005**, *24*, 3066–3073.

[17] C. V. Ramana, P. Patel, K. Vanka, B. Miao, A. Degterev, *Eur. J. Org. Chem.* **2010**, 5955–5966.

[18] a) P. Patel, C. V. Ramana, *J. Org. Chem.* **2012**, *77*, 10509–10515; b) B. N. Reddy, C. V. Ramana, *Chem. Commun.* **2013**, *49*, 9767–9769.

[19] A. M. Jadhav, S. Bhunia, H. Y. Liao, R. S. Liu, *J. Am. Chem. Soc.* **2011**, *133*, 1769–1771.

[20] S. Zhou, Q. Liu, M. Bao, J. Huang, J. Wang, W. Hua, X. Xu, *Org. Chem. Front.* **2021**, *8*, 1808–1816.

[21] P. Patel, C. V. Ramana, *Org. Biomol. Chem.* **2011**, *9*, 7327–7334.

[22] L. W. Chen, J. L. Xie, H. J. Song, Y. X. Liu, Y. C. Gub, Q. M. Wang, *Org. Chem. Front.* **2017**, *4*, 1731–1735.

[23] P. S. Dhote, C. V. Ramana, *Org. Lett.* **2021**, DOI:10.1021/acs.orglett.1c00539.

[24] Y. Gao, J. Nie, Y. Huo, X. Q. Hu, *Org. Chem. Front.* **2020**, *7*, 1177–1196.

[25] a) J. E. Bunney, M. Hooper, *Tetrahedron Lett.* **1966**, 3857–3860; b) C. Berti, M. Colonna, L. Greci, L. Marchetti, *Tetrahedron* **1975**, *31*, 1745–1753; c) C. Berti, L. Greci, L. Marchetti, *J. Chem. Soc.-Perkin Trans.* **1979**, 233–236.

[26] R. R. Liu, S. C. Ye, C. J. Lu, G. L. Zhuang, J. R. Gao, Y. X. Jia, *Angew. Chem. Int. Ed.* **2015**, *54*, 11205–11208; *Angew. Chem.* 2015, 127, 11357–11360.

[27] a) L. Greci, G. Tommasi, P. Bruni, P. Sgarabotto, L. Righi, *Eur. J. Org. Chem.* **2001**, 3147–3153; b) P. Astolfi, P. Bruni, L. Greci, P. Stipa, L. Righi, C. Rizzoli, *Eur. J. Org. Chem.* **2003**, 2626–2634.

[28] C. V. S. Kumar, C. V. Ramana, *Org. Lett.* **2015**, *17*, 2870–2873.

[29] a) L. Xie, Y. Li, S. Dong, X. Feng, X. Liu, *Chem. Commun.* **2021**, *57*, 239–242; b) J. Xu, S. Hu, Y. Lu, Y. Dong, W. Tang, T. Lu, D. Du, *Adv. Synth. Catal.* **2015**, *357*, 923–927.

[30] C. V. S. Kumar, C. V. Ramana, *Org. Lett.* **2014**, *16*, 4766–4769.

[31] N. Marien, B. Brigou, B. Pinter, F. Proft, G. Verniest, *Org. Lett.* **2015**, *17*, 270–273.

[32] N. Marien, B. N. Reddy, F. Vleeschouwer, S. Goderis, K. Hecke, G. Verniest, *Angew. Chem. Int. Ed.* **2018**, *57*, 5660–5664; *Angew. Chem.* **2018**,*130*, 5762–5766.

[33] P. S. Dhote, C. V. Ramana, *Org. Lett.* **2019**, *21*, 6221–6224.

[34] H. Meng, Z. Xu, Z. Qu, H. Huang, G. J. Deng, *Org. Lett.* **2020**, *22*, 6117–6121.

[35] M. Zhenga, K. Chena, S. Zhu, *Synthesis* **2017**, *49*, 4173–4182.

[36] I. Cikotiene, *Eur. J. Org. Chem.* **2012**, 2766–2773.

[37] L. W. Wang, Y. F. Feng, H. M. Lin, H. T. Tang, Y. M. Pan, *J. Org. Chem.* **2021**, DOI:10.1021/acs.joc.1c00012.

Manuscript received: April 1, 2021
Revised manuscript received: May 9, 2021
Version of record online: ■■ ■■, ■■■■

PERSONAL ACCOUNT

The [Au]-catalysed cyclization of *o*-alkynylnitrobenzenes is an important transformation presumably proceeding through the reactive α-oxo gold carbenes (for ready carbene transfer) and results in the end products those can be further functionalized. This has been amply explored in developing the cascade transformations that delivered known natural products scaffolds.

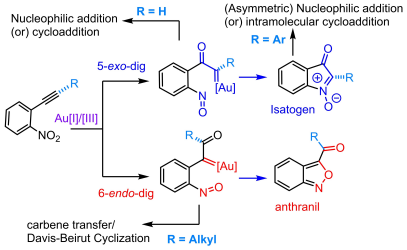

*P. S. Dhote, S. V. Halnor, Dr. C. V. Ramana**

1 – 14

Gold-Catalysed Nitroalkyne Cycloisomerization – Synthetic Utility

Organic & Biomolecular Chemistry

ROYAL SOCIETY OF CHEMISTRY

REVIEW

View Article Online
View Journal | View Issue

Cite this: *Org. Biomol. Chem.*, 2021, **19**, 7970

Total synthesis of the pseudoindoxyl class of natural products

Pawan S. Dhote, [a,b] Pitambar Patel, [c,b] Kumar Vanka [d,b] and Chepuri V. Ramana *[a,b]

The pseudoindoxyl sub-structural motif, amongst the large set of the indole class of alkaloids, represents a unique subset of the oxygenated indole class of the alkaloid family. A majority of this class of natural products contains complex bridged/polycyclic scaffolds with interesting biological profiles. They are thus attractive synthetic targets. Starting from 1963, twenty-eight natural products having the pseudoindoxyl scaffold have been isolated, among which the synthesis of 13 natural products has been accomplished. In this review, we highlight the completed as well as the formal total synthesis of the natural products with a spiro-pseudoindoxyl ring, with a focus on their development. The challenges and the future perspective based on the recent developments in the field will also be discussed. We strongly believe that this review will not only update but also attract the attention of researchers in dealing with the synthesis of pseudoindoxyl compounds.

Received 2nd July 2021,
Accepted 17th August 2021

DOI: 10.1039/d1ob01285a

rsc.li/obc

[a]*Organic Chemistry Division, CSIR-National Chemical Laboratory Dr Homi Bhabha Road, Pune-411008, India. E-mail: vr.chepuri@ncl.res.in*
[b]*Academy of Scientific and Innovative Research (AcSIR), Ghaziabad-201002, India*
[c]*CSIR-North East Institute of Science and Technology, Assam-785006, India*
[d]*Physical Chemistry Division, CSIR-National Chemical Laboratory Dr Homi Bhabha Road, Pune-411008, India*

1. Introduction

Indole and its derivatives are highly abundant scaffolds found in several natural products and pharmaceuticals with significant biological activities.[1] Among these scaffolds, natural products with the pseudoindoxyl moiety occupy a special place in the indole alkaloid family, in particular, those containing a spirocyclic quaternary center at the C2-position. The term

Pawan S. Dhote

Pawan S. Dhote was born in Nagpur, Maharashtra, India in 1993. He received his B.Sc. (chemistry) from Fergusson College, Pune in 2014, and M.Sc. (organic chemistry) in 2016 from the Department of Chemistry, Savitribai Phule Pune University (formerly known as the University of Pune), Maharashtra, India. Later, in 2017, he joined the group of Dr Chepuri V. Ramana at CSIR-National Chemical Laboratory, Pune, India as a DST-INSPIRE Fellow. Currently, he is working on gold catalysed o*-nitroalkyne/*o*-azidoalkyne reactions and their applications in the total syntheses of natural products.*

Pitambar Patel

Pitambar Patel received his bachelor's and master's degrees from Sambalpur University, Sambalpur, India. Then he received his PhD degree in organic chemistry under the guidance of Dr Chepuri V. Ramana at CSIR-NCL, Pune. This was followed by a postdoctoral stint at the Institute for Basic Science, KAIST, South Korea, under Professor Sukbok Chang. He is currently a SERB Research Scientist (SRS) at the CSIR-North East Institute of Science and Technology, Jorhat, India. His research interests include the application of transition metal catalysis in the synthesis of small bioactive heterocycles and natural products. He also works on natural product isolation and on studies of their bioactivity.

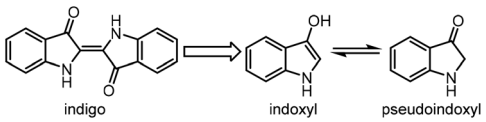

Fig. 1 Indigo degradation leading to indoxyl and pseudoindoxyl.

pseudoindoxyl has had its own association with the father of indole chemistry, Adolf Bayer. The term indoxyl (3-hydroxyindole) that was isomeric with oxindole was coined by Baeyer in 1882 for an intermediate product of indigo degradation (Fig. 1).[2] However, as this compound showed the characteristic reactions of both phenols and ketones and since the concept of keto–enol tautomerism had not yet been put forward, due to ambiguity about the position of one of the hydrogen atoms in indoxyl, it was believed that both the enolic and ketonic forms were two different compounds. In addition to this, it was also strongly believed that the indoxyl occurred solely in the stable enolic form (3-hydroxyindole) and the ketonic form was labile and unstable, and hence this was called "pseudoindoxyl".

Starting from 1947, several natural products bearing the pseudoindoxyl scaffold have been isolated (Fig. 2). Some of the pseudoindoxyl natural products have been found to possess high biological activity, such as duocarmycin (antitumour antibiotic),[3] (−)-isatisine A (anti-HIV),[4] melokhanine E (antimicrobial, MIC = 2 μM against *P. aeruginosa* and 5 μM against *E. faecalis*),[5] mitragynine pseudoindoxyl (μ-opioid agonist),[6] rupicoline (anti-cholinesterasic activity)[7] and trigonoliimine C (anti-cancer).[8] Subsequently, various synthetic methodologies to construct the pseudoindoxyl core and also the total syntheses of various pseudoindoxyl natural products have been reported by many research groups across the globe, despite their challenging structural features. To date, close to twenty-eight pseudoindoxyl natural products have been isolated, among which the total syntheses of thirteen natural products **1–13** have been accomplished (Fig. 2). However, the total syntheses of the remaining 15 pseudoindoxyl natural products (compound **14–28**) are yet to be reported.

The synthesis of the related structure, a spiropseudoindoxyl bearing a spirocyclic stereocenter at the C3 position, has been very well addressed in many reviews.[9] Coming to the construction of the pseudoindoxyl moiety, there are limited reported methods on their synthesis, as this skeleton seems to be an underappreciated structure in the field of medicinal and organic chemistry. An extensive compilation, especially focusing on the synthetic methods for forging the spiropseudoindoxyl moiety, has been provided by Huang and Verniest and co-workers.[10] On the other hand, there is no review that has appeared on the various approaches for the total synthesis of natural products bearing the pseudoindoxyl structural unit. This has prompted us to compile the details of the total syntheses of the pseudoindoxyl class of natural products, illustrating the strategy level innovations in each total synthesis, with an emphasis on the creativity required for constructing this structural unit.

The proposed biosynthetic pathway for the formation of these pseudoindoxyl scaffolds involves oxidative rearrangement of the corresponding indole compounds (Fig. 3). There is a debate on whether these compounds are naturally occurring secondary metabolites or artefacts (formed *via* air mediated auto-oxidation of the related indole derivative) resulting during the isolation of the plant material. Although numerous synthetic methods have been developed for the construction of the spiro-pseudoindoxyl unit, the most common

Kumar Vanka

Kumar Vanka did his undergraduate studies (BSc) at the Indian Institute of Technology, Kharagpur, India, and then received his MSc and PhD degrees in computational chemistry under the guidance of Professor Tom Ziegler at the University of Calgary, Canada. This was followed by a postdoctoral stint at the University of Kansas, USA, under Professor Ward Thompson. He has been a scientist at the National Chemical Laboratory (CSIR-NCL), India, since December 2007 and is currently a Principal Scientist there. His research interests include computational studies of reaction mechanisms relevant to organic, inorganic and organometallic chemistry and investigations into the origins of life on Earth and in the universe.

Chepuri V. Ramana

Dr Chepuri V. Ramana obtained his MSc from Andhra University, Waltair (1991) and PhD from the University of Hyderabad under the supervision of Professor M. Nagarajan (synthetic carbohydrate chemistry). From 1998 to 2001 he was associated with Professor Andrea Vasella at ETH Zurich as a post-doctoral researcher (glycosidase inhibitors). From May 2001 onwards, he has been associated with CSIR-National Chemical Laboratory. At NCL, the focus of Ramana's group is on small molecule synthesis by employing transition metal complexes, developing new catalytic methods and process development for APIs and agrochemicals. He is a recipient of the CSIR Young Scientist Award in Chemical Sciences (2003) and the CNR Rao National Prize in Chemical Sciences (2017). He is a fellow of the Indian Academy of Sciences (2014, Bengaluru).

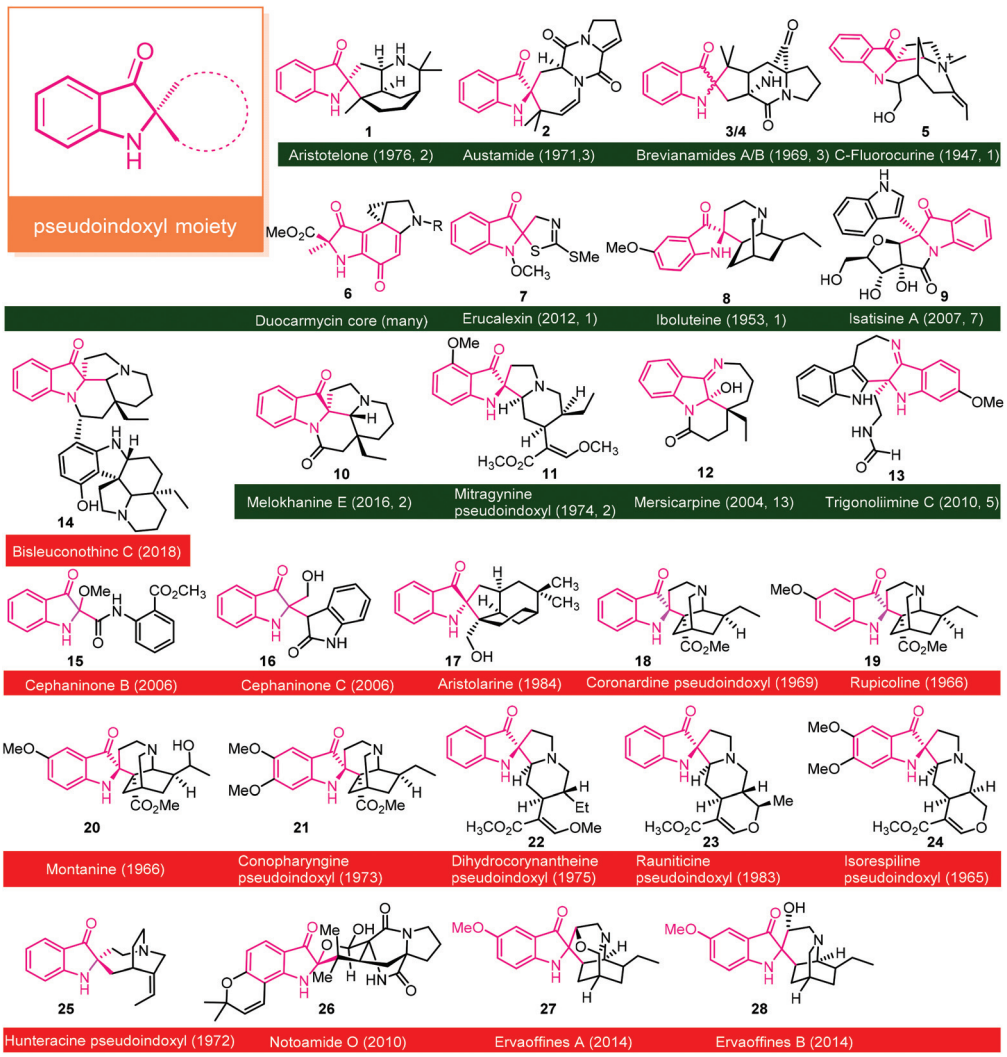

Fig. 2 Natural products with the pseudoindoxyl core (isolation year, the number of total syntheses reported).

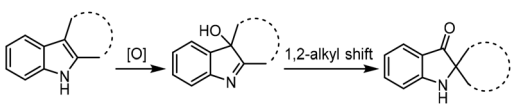

Fig. 3 Biosynthetic pathway for the pseudoindoxyl molecule.

approach for their synthesis comprises a two-step oxidative rearrangement of the corresponding 2,3-disubstituted indole derivative, involving the oxidation of the indole followed by a 1,2-alkyl rearrangement. The details of the isolation and total synthesis of thirteen molecules (**1–13**) by different research groups using different strategies are described below in chronological order. Since the syntheses of fifteen molecules **14–28** are not reported, only related references pertaining to their isolation have been mentioned.[11] Owing to the existence of several book chapters and reviews on the topic of the total synthesis of duocarmycin (**6**) and its derivatives, this review will not cover its synthesis.[12]

2. Total synthesis of pseudoindoxyl natural products

2.1 (+)-Aristotelone

(+)-Aristotelone (**1**) was isolated from *Aristotelia chilensis* by Silva and co-workers in 1976.[13] It is a spiro-pseudoindoxyl natural product with a 6/5/5/6/6 pentacyclic core and a 5/5 spirocyclic unit. Borschberg and Heathcock groups reported the synthesis of aristotelone (**1**), using the biogenetic partner aristoteline (**29**) as the common starting point and employing the classical two-step oxidative rearrangement as the key protocol. Borschberg's group had extensively studied the oxidative transformation of (+)-aristotelone (**1**) by the oxidative transformation of (+)-aristoteline (**29**) (Scheme 1), which comprises synthesizing **1** as well as its constitutional isomer: another natural product tasmanine, both proceeding *via* another natural product serratoline.[14] Interestingly, the oxidation of aristoteline with *m*-CBPA either in petroleum ether or dichloromethane was not diastereoselective, whereas when the same

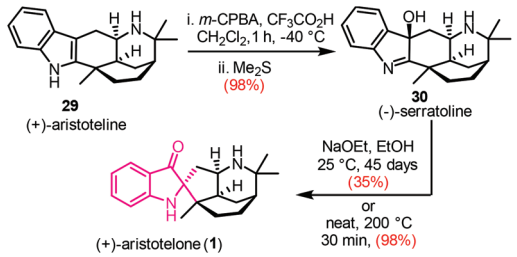

Scheme 1 Borschberg's synthesis of (+)-aristotelone (**1**).

reaction was conducted in the presence of TFA, serratoline (**30**) was obtained exclusively in quantitative yields. This has been explained by the strong *cis*-directing effect of the protonated piperidine N-atom during the oxygen transfer from the peracid. When treated with NaOEt in EtOH at 25 °C, serratoline was transformed very slowly into the alkaloid (+)-aristotelone (**1**), with 16% yield after 13 days and 35% after 45 days. However, when heated at 200 °C for 30 min, **1** was obtained in quantitative yields. The same group has also documented the borontrifluoride·etherate mediated inter conversion of (+)-aristotelone (**1**) to tasmanine.

Later, Heathcock's group reported the synthesis of *Aristotelia* alkaloids (+)-**29**, (−)-**30**, (+)-**1**. As shown in Scheme 2,[15] employing the method of Stevens and Kenney,[16] (1*S*)-(−)-β-pinene (**31**) and 3-indolylacetonitrile (**32**) were coupled by a $Hg(NO_3)_2$-mediated Ritter reaction followed by the reduction of the resulting imine with $NaBH_4$ to give (+)-makomakine (**33**). An intramolecular Friedel–Crafts reaction afforded (+)-aristoteline (**29**), which was oxidized by reaction with oxygen in the presence of Adam's catalyst. Reduction of the intermediate hydroperoxide delivered alkaloid (−)-**30**. Aristotelone (+)-**1** was produced in 97% yield by the base mediated oxidative rearrangement of **30**.

2.2 Austamide

Austamide (**2**) is a toxic metabolite isolated in 1971 by Steyn from toxic maize-meal cultures of *Aspergillus ustus* CSIR 1128.[17] Structurally, it contains a pentacyclic skeleton featuring a spiro-pseudoindoxyl chromophore having two stereogenic quaternary carbon centers, with one at the spiro ring junction. The Kishi and Corey groups reported the total synthesis of austamide using the pentacyclic indole derivative **40** as the advanced intermediate, which upon oxidation followed by 1,2-alkyl migration, results in the key spiropseudoindoxyl derivative.

As shown in Scheme 3, in 1978, Kishi's group studied the oxidative rearrangement of indole **40** to *trans*-tetrahydroaustamide (**42**) which has been postulated as a possible biosynthetic pathway for austamide (**2**) (Scheme 3).[18] The synthesis started with the reduction of 3,3-dimethyl-4-pentynoic acid (**34**) and protection with benzyl bromide afforded alkyne **35** which upon treatment with *o*-iodoaniline in DMF in the presence of cuprous iodide and triethylamine gave indole, and was further converted to gramine **36**. Condensation of compound **36** with L-proline derivative **37** afforded amido-malonate derivative **38**. Deprotection of the carbobenzyloxy group and refluxing in xylene solvent gave the cyclized diketopiperazine product in 7 : 1 diastereometric mixture with **39** as the major stereoisomer. Compound **39** then was converted to the eight membered compound *trans*-**40** over four steps that include deprotection, NaH catalysed cyclisation and subsequent hydrolysis/decarboxylation. Compound **40** was converted into hydroxyl indoline **41** with *m*-CPBA, which, on acid mediated pinacol-type rearrangement, afforded *trans*-tetrahydroaustamide **42** in 40% yield over the last two steps.

A year later, a successful completion of the stereospecific total synthesis of (±)-austamide (**2**) was documented by this group (Scheme 4).[19] The diketopiperazine ester **38** was hydrolysed/decarboxylated, with the deprotection of the benzyl

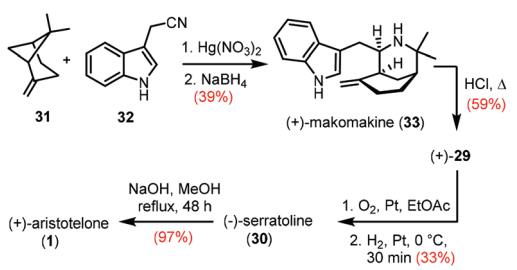

Scheme 2 Heathcock's total synthesis of (+)-aristotelone (**1**).

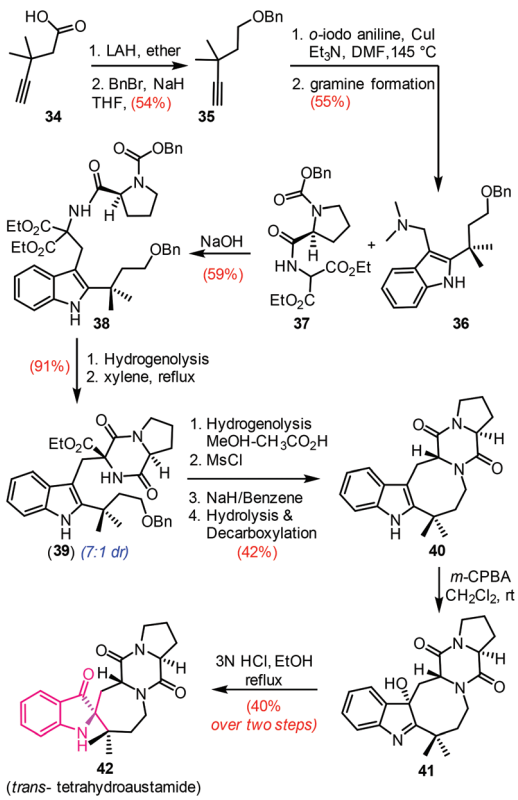

Scheme 3 Kishi's oxidative rearrangement to *trans*-tetrahydroaustamide (**42**).

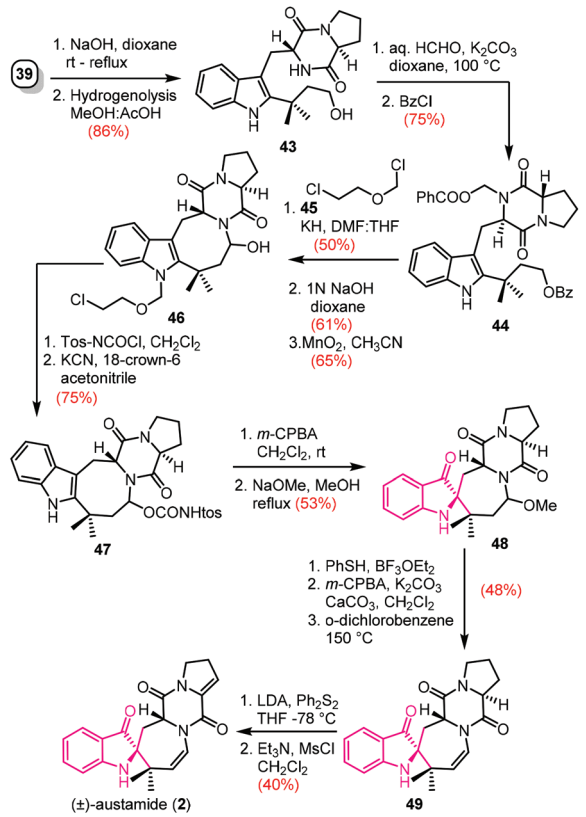

Scheme 4 Kishi's total synthesis of (±)-austamide (**2**).

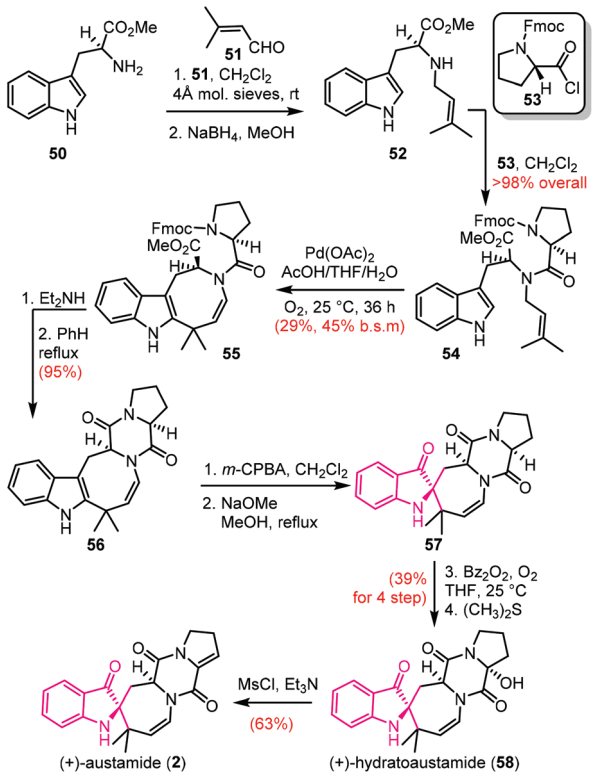

Scheme 5 Corey's enantioselective total synthesis of (+)-austamide (**2**).

group by hydrogenolysis affording alcohol **43**. Compound **43** was hydroxy-methylated, followed by benzoylation of the newly formed primary hydroxyl group to afford benzoate **44**. Alkylation of the indole N-atom of **44** with 2-chloroethyl-chloromethyl ether **45**, and basic hydrolysis/oxidation provided the protected *N*-acyl-*N*,*O*-hemiacetal compound **46**. The use of the chloroethoxymethyl protecting group is an important development in this sequence, as without indole *N*-protection, the oxidation results in the formation of a hemi-aminal involving the N-atom of indole. Also, the easy deprotection of this chloroethoxymethyl group by refluxing with KCN in acetonitrile in the presence of 18-crown-6 offered compatible conditions for a sensitive protecting group such as tosyl carbamate. Next, the methoxy-indoxyl compound **48** was successively obtained *via* deprotection and base catalysed oxidative rearrangement in 53% overall yield from compound **47**. Treatment of compound **48** with thiophenol with subsequent oxidation to sulfoxide, followed by its *in situ* pyrolysis resulted in *trans*-dihydroaustamide **49**. The reaction of compound **49** with LDA formed a dianion, which was quenched by diphenyl disulphide, giving the tertiary alcohol as a mixture of stereoisomers. Subsequent dehydration in the presence of trimethylamine and MsCl gave (±)-austamide **2**.

Based on the multistage, [Pd]-mediated transformation to the tricyclic core, the Corey group accomplished the first enantioselective total synthesis of (+)-austamide **2** and (+)-hydratoaustamide **58** from the common intermediate **56**. As depicted in Scheme 5, the commercially available (*S*)-tryptophan methyl ester (**50**) was converted to the Schiff base with aldehyde **51**, followed by reduction of the imine afforded compound **52**. Fmoc-(*S*)-prolyl chloride (**53**), on reaction with **52**, produced the coupled amide **54**. The key steps in this protocol involved the palladium-mediated conversion of the *N*-prenylated tryptophan derivative **54** to the eight membered tricycle core indoloazocine **55**. Removal of the Fmoc group and cyclisation gave the diketopiperazine (DKP) **56** in 95% yield. The synthesis of (+)-**2** was accomplished in five steps from **56**. The treatment of compound **56** under Kishi's oxidative rearrangement sequence gave the pentacyclic spirocyclic spiro-pseudoindoxyl core, which, upon radical-initiated α-hydroxylation followed by dehydration in the proline subunit, furnished the desired (+)-austamide (**2**).[20]

2.3 Brevianamides A and B

Brevianamides A (**3**) and B (**4**) were isolated by Birch and Wright in 1969 from *Penicillium brevicompactum* and were the first known bicyclo[2.2.2]diazaoctane alkaloids.[21] William's group reported the first total synthesis of (±)-brevianamide B (**4**), which was a breakthrough achievement in the history of brevianamide B synthesis.[22] Their total synthesis featured a biomimetic-intramolecular Diels–Alder (IMDA) reaction, and an intramolecular S_N2' cyclisation reaction for the construction of the complex anti-bicyclo[2.2.2]diazaoctane core. In 2009, Williams described the various strategies developed to prepare a bicyclo[2.2.2]diazaoctane core, which was found in a vast

number of prenylated alkaloids in a seminal review on the total synthesis of these particular natural products.[23] In this context, we only describe the recent total synthesis of pseudoindoxyl brevianamides A (**3**) and B (**4**) from 2009 onwards by different research groups. However, most of the approaches documented follow a similar strategy for the construction of the spiro-pseudoindoxyl core: oxidation followed by the 1,2-alkyl migration of the respective indole derivative.

Simpkins's group employed a double cationic cyclisation for the construction of the diketopiperazine core using the Seebach 'self-reproduction of chirality' method (Scheme 6).[24]

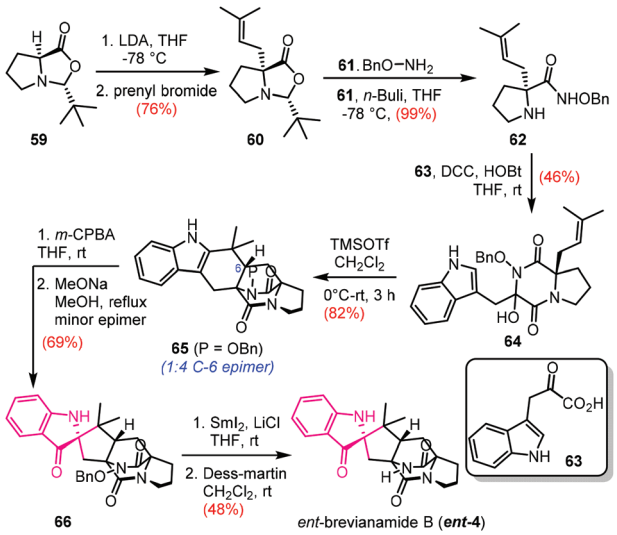

Scheme 6 Simpkins's total synthesis of *ent*-brevianamide B (**4**).

The total synthesis of **4** began with Seebach proline acetal **59**, which was prenylated, followed by the oxazolone opening with lithiated benzyl amine **61** to give proline amide **62**. Classical acid-amine coupling of the indole pyruvic acid **63** with **62** afforded cyclized hydroxy product **64**. This cyclisation arose due to the high nucleophilic character of the hydroxamic acid nitrogen. Cyclisation of **64** using TMSOTf gave **65** with a 1 : 4 C-6 *epimeric* mixture. The separated minor diastereomer **65** was subjected to peracid oxidation and basic pinacol-type rearrangement to afford spiro-indoxyl compound **66**. Reductive cleavage of the N-OBn bond resulted in concomitant indoxyl reduction and, on Dess–Martin oxidation, gave *ent*-brevianamide B (***ent*-4**).

The formal synthesis of **4** in 12 steps was reported by Scheerer's group, using the stereoselective IMDA cycloaddition of intermediate pyrazinone **70** with nitroacrylate-derived dienophiles **71** to provide the bicyclo[2.2.2]diazoctane core (Scheme 7).[25] Pyrazinone **70** was prepared from proline-derived diketopiperazine **68** by enolisation followed by aldol addition to indole carboxaldehyde **67**. The intermediate β-alkoxy adduct was acylated and then base-mediated elimination gave exocyclic diene **69**, which on subsequent isomerization yielded diketopiperazadiene **70**. The intermolecular cycloaddition of **70** with nitroacrylate **71** at ambient temperature provided two regioisomeric cycloadducts **72** and **73** (1 : 4 ratio) in 84% combined yield. The 1 : 4 mixture was exposed to DBU, which afforded elimination to two isomeric unsaturated ester products. Major isomer **75** having the desired regiochemistry was subjected for hydrogenation, which resulted in a 1 : 1 mixture of the *syn*- and *anti*-fused products **76** and **77**. Ester **77** was treated with excess MeMgBr to afford tertiary alcohol **78**, which upon acid hydrolysis gave lactam **79**. Finally,

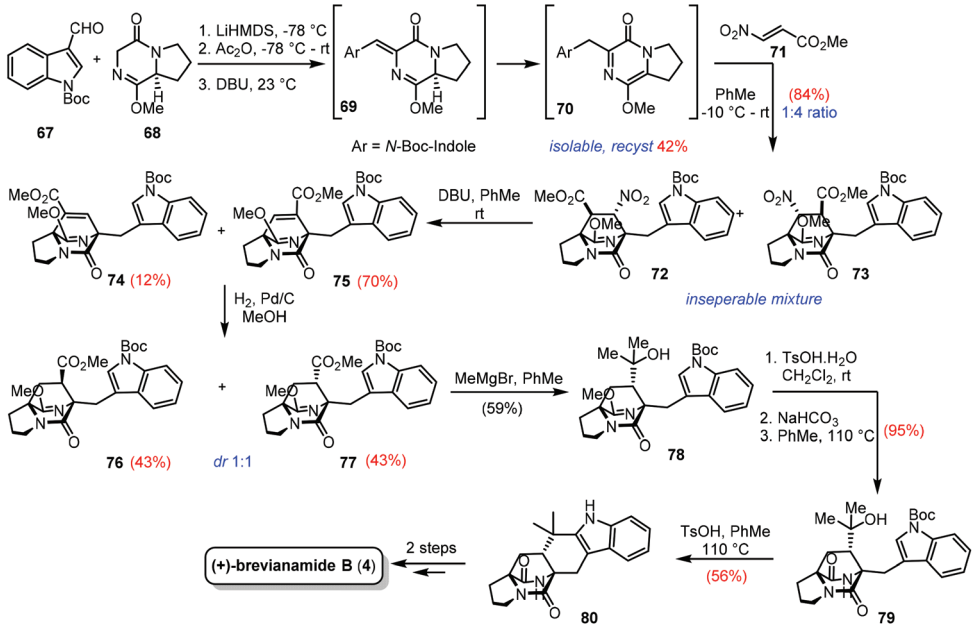

Scheme 7 Scheerer's formal synthesis of (+)-brevianamide B (**4**).

the *p*-TSA mediated Boc-deprotection and Friedel–Crafts cyclization of the indole on the derived tertiary carbocation gave annulated natural product **4** in 83% yield.

Recently, Lawrence and co-workers reported the first biomimetic total synthesis of (+)-brevianamide A (**3**) in 7 steps with 7.2% overall yield (Scheme 8), which implicated a bioinspired cascade transformation of the linearly fused (−)-dehydro-brevianamide E (**91**) into a topologically complex, bridged-spiro-fused structure of (+)-brevianamide A (**3**).[26] Both brevianamides A (**3**) and B (**4**) are diastereoisomers, but despite the similarity in their structures, there are no reports on the synthesis of **3**, because of problems associated with the reactivity and regioselectivity. The synthesis of the (+)-dehydrodeoxybrevianamide E (**89**), in a linear sequence of five steps, commenced with the phthaloyl protection of commercially available L-tryptophan methyl ester **81**. Danishefsky's reverse prenylation using B-prenyl-9-borabicyclo[3.3.1]nonane **84** afforded intermediate **85** in 69% overall yield. Lithium carboxylate **86** was exposed to a one pot-acyl chloride formation and further imine acylation reaction with dehydroproline **87** gave *N*-acyl enamine **88**. Removal of the phthaloyl group has been done with less nucleophilic reagents. On the other hand, the same pot spontaneous cyclisation afforded (+)-**89** with an overall yield of 34%. The oxidation of **89** with *m*-CPBA gave two diastereomers **90** and **91**, which were used to prepare both unnatural-(−) and natural-(+) enantiomers of brevianamide A and B. Exposure of dehydrobrevianamide E (**91**) to LiOH in water led to a domino retro-5-*exo-trig*/[1,2]-alkyl shift/Diels–Alder reaction sequence to afford (+)-brevianamide A (**3**) and (+)-brevianamide B (**4**) in a combined 63% yield with 93 : 7 diastereomeric ratio, which closely matches with the isolation ratio. The unnatural (−)-enantiomers of brevianamide A (**3**) and B (**4**) were similarly accessed by subjecting the minor diastereomer **90** to the same reaction conditions. The intramolecular Diels–Alder reaction produces (−)-**3** and (−)-**4** in 60% combined yield.

2.4 C-Fluorocurine

C-Fluorocurine (**5**) is a calabash curare pseudoindoxyl alkaloid containing a C20 monoquaternary center isolated from the *Strychnos guianensis* stembark.[27] It has a hollow sphere type of geometry in ring E with the group inside, showing the effect of strong trans-annular interaction in NMR. To date, there are no reports on the total synthesis of **5**. However, the racemic synthesis of 19,20-dihydronorfluorocurine (**100**) has been documented by Boekelheide's group (Scheme 9) in 1972.[28] The synthesis began with the formation of tetracyclic ketone **95** by the condensation of 3,4-dihydro-β-carbonine **92** and ethyl α-ethylacetoacetate **93** and formaldehyde followed by the acid hydrolysis of intermediate tetracyclic esters **94**. Subsequently, tetracyclic ketone **95** was subjected to a sequence of Wittig olefination and acid hydrolysis to install aldehyde moiety **97** with inversion in configuration at the 3-ethyl group. The Corey–Chaykovsky reaction conditions were employed to obtain

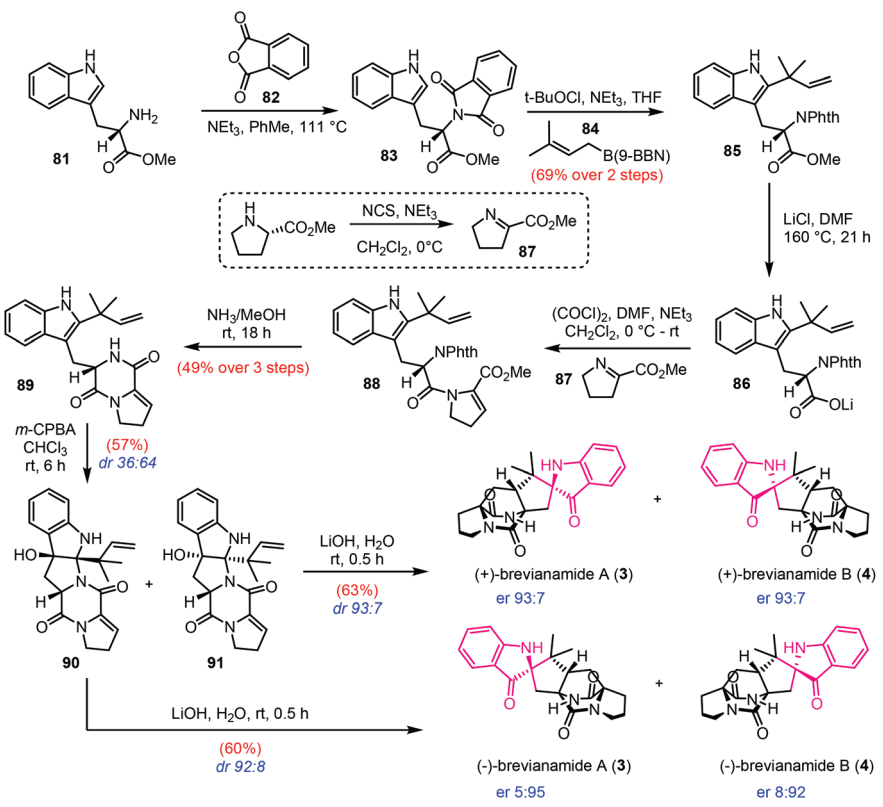

Scheme 8 Lawrence's biomimetic total synthesis of (+)-**3**, (+)-**4**, (−)-**3**, and (−)-**4**.

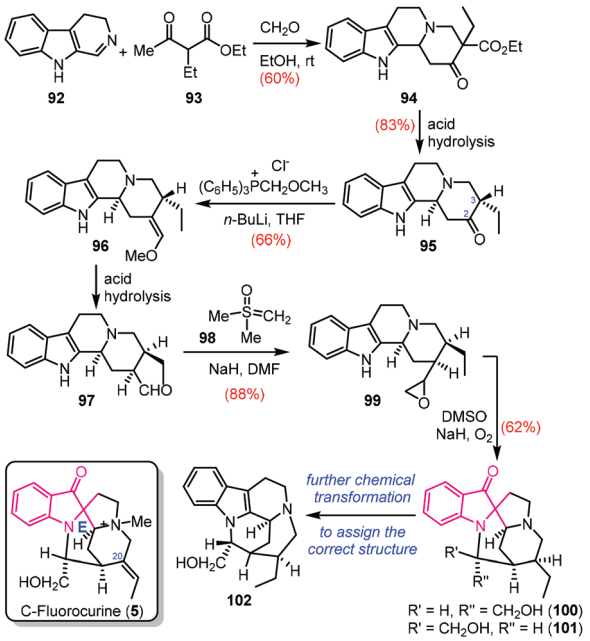

Scheme 9 Boekelheide's total synthesis of (±)-19,20-dihydronorfluorocurine (**100**).

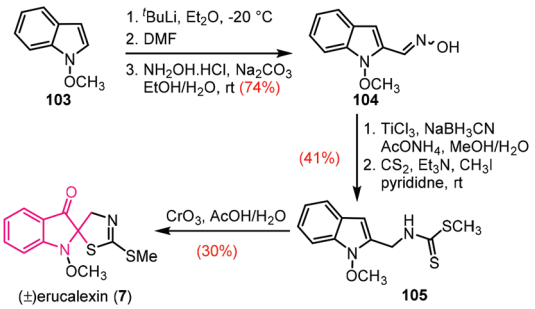

Scheme 10 Predras' total synthesis of (±)-erucalexin (**7**).

epoxide **99**. Surprisingly, only one isomer predominated, which was confirmed by thin layer chromatography, with the fractional crystallization of the product showing a sharp melting point. The oxidative rearrangement and cyclisation for the construction on the E ring occurred in one pot from compound **99** in the presence of NaH in DMSO solvent under an oxygen atmosphere. Whether the product forms **100** or its epimer **101** was a matter of confusion, since it lacked the natural material for comparison. This led to further chemical modification to the natural product 19,20-dihyronormavacurine (**102**); subsequent matching with the spectral isolation data led to the conclusion that the pseudoindoxyl derivative was a racemic 19,20-dihydronorfluorocurine (**100**).

2.5 (+)-Erucalexin

(+)-Erucalexin (**7**) was isolated from the wild crucifer dog mustard (*Erucastrum gallicum* L.) by Pedras *et al.*[29] It has a unique carbon substituent at the C-2 of 3-oxindole, instead of the common C-3 substitution found in all cruciferous phytoalexins. The chemical structure of **7** represents the spiro[2*H*-indole-2,5′(4′*H*)-thiazol]-3-one, showing an intriguing rearrangement in its biosynthetic pathway. Its biological activity is of interest: it shows activity against *S. sclerotiorum* and *Rhizoctonia solani*, the two most important pathogens of oilseeds and vegetable crucifer. In view of its intriguing structural feature and promising antifungal activity, the group of Predras and team in 2006 reported the first biomimetic synthesis of (±)-erucalexin (Scheme 10).[30] The synthesis commenced with the C2–H deprotonation of 1-methoxyindole **103** using *t*-BuLi, followed by quenching with DMF to afford 1-methoxyindole-2-carboxaldehyde, which, on reaction with hydroxyl-amine, gave oxime **104** in 74% yield. Reduction of **104** was followed by *in situ* conversion to its biosynthetic precursor 1-methoxyisobrassin **105** by standard treatment with CS_2 and CH_3I. After an extensive optimization of the reaction parameters for oxidative cyclization of **105**, CrO_3 was found to be a suitable oxidant in the acetic acid–water system to afford the desired (±)erucalexin (**7**) in moderate yield (30%).

2.6 Iboluteine

Iboga type alkaloids are mostly isolated from the *Tabernanthe* or the *tabernaemontana species* of plant belonging to the *Apocynaceae* family.[31] Iboluteine (**8**) is the one of the members of this alkaloid family containing the pseudoindoxyl core. Catalytic oxidation of ibogaine (**115**) alkaloid (isolated from the root extract of *T.iboga*), followed by reduction and alkaline rearrangement led to its formation.[32] To date, many research groups have focused on the total synthesis of **115** since its isolation. Great efforts have been made by Büchi[33] to this end. Jana,[34] and Zhao groups have independently reported the total synthesis of **115**. However, there is only one total synthesis for iboluteine (**8**) by Zhao and team that featured 12-methoxytabertinggin (**114**) as a key precursor for the biomimetic transformation into other iboga-type alkaloids such as **8** and **115**, as depicted in Scheme 11.[35]

The synthesis began with the one pot cascade Pictet–Spengler condensation/intramolecular ammonolysis reaction of 5-methoxytryptamine (**106**) with **107** to afford lactam **108**. Boc-protection of indole nitrogen followed by the intermolecular aldol reaction of **109** with **110** gave compound **111**. Mesylation of the resulting sec –OH group, followed by elimination and hydrogenation gave single isomer **112**. Reduction of the ester group by LAH and subsequent acidic treatment afforded keto alcohol **113**. Classical Swern-oxidation of **113** followed by the intramolecular aldol condensation reaction furnished compound **114**. Furthermore, reduction of α,β-unsaturated ketone **114** with zinc in acetic acid led to the cleavage of the C–N bond, which, on subsequent intramolecular Michael addition followed by Wolff–Kishner reduction, afforded a mixture of ibogaine **115** and *epi*-ibogaine **116** in 34% overall yield. The obtained ibogaine **115** was oxidized to ibogaine hydroxyindolenine **117** by using DMDO. Under basic conditions, compound **117** underwent a pinacol-

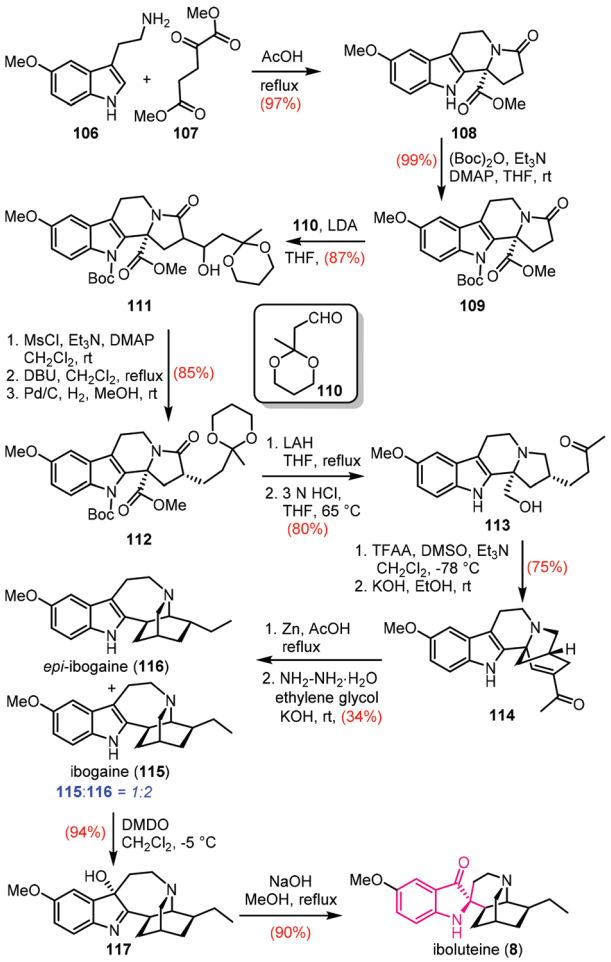

Scheme 11 Zhao's total synthesis of (±)-iboluteine (**8**).

type ring contraction rearrangement to furnish the desired spiropseudoindoxyl product iboluteine (**8**) in 90% yield.

2.7 Isatisine A

Isatisine A (**9**) was isolated in 2007 by Chen's team from the leaves of *Isatis Indigotica fort* (Cruciferae).[4] Its acetonide **126** was isolated first as an artefact and showed moderate anti-HIV activity with EC_{50} = 37.8 μM and selectivity index = 7.98, as well as cytotoxicity against C8166 cancer cell lines. The structural features of **9** include a fused pentacyclic framework containing a densely substituted furan subunit, and five contiguous stereo-centers with a pseudoindoxyl core. In view of their fascinating structures and biological significance, its total synthesis has attracted considerable attention from the synthetic community since its isolation. In 2010, Kerr and co-workers reported the first total synthesis of (+)-isatisine A (**9**) and revised its absolute configuration.[36] To date, there are seven total syntheses of both (+)-isatisine A and (−)-isatisine A combined. In addition to this, one report on the synthesis of 13-deoxyisatisine A **162** has also been reported in the literature.

The inaugural synthesis of isatisine A (**9**) was reported by Kerr's group, which commenced with the Lewis acid-catalysed Johnson tetrahydrofuran synthesis using indole-2-carboxaldehyde (**118**) and the homo-chiral (*S*)-vinylcyclopropane diester (**119**) to obtain the THF-derivative **120** in 89% yield as a mixture of the 2,5-*cis*:2,5-*trans* (furan numbering) isomers. The pendant vinyl group was converted to primary alcohol **121** in three steps, *via* dihyroxylation, oxidative cleavage, and reduction. Elimination of one ester moiety by making it an allyl ester through hydrogenesis/Mitsunobu conditions and [Pd]-mediated debenzylative allylation gave enolate **122**. Simple dihydroxylation afforded the single diastereomer, which, on acetonide formation with the concomitant removal of the silyl ether gave acetonide **124**. Removal of the *N*-tosyl group and treatment with *m*-CPBA gave the crude oxidation product which, on isolation and treatment with indole and camphor sulphonic acid (CSA), afforded isatisine acetonide **126**. Simple acid hydrolysis produced natural product **9** in 82% yield. The total synthesis of (+)-isatisine A (**9**) was achieved in 14 steps from homochiral cyclopropane **119** in an overall yield of 5.8% (Scheme 12). The specific rotation of synthetic acetonide **126** and the synthetic isatisine A (**9**) was found to be $[\alpha]_D^{25}$

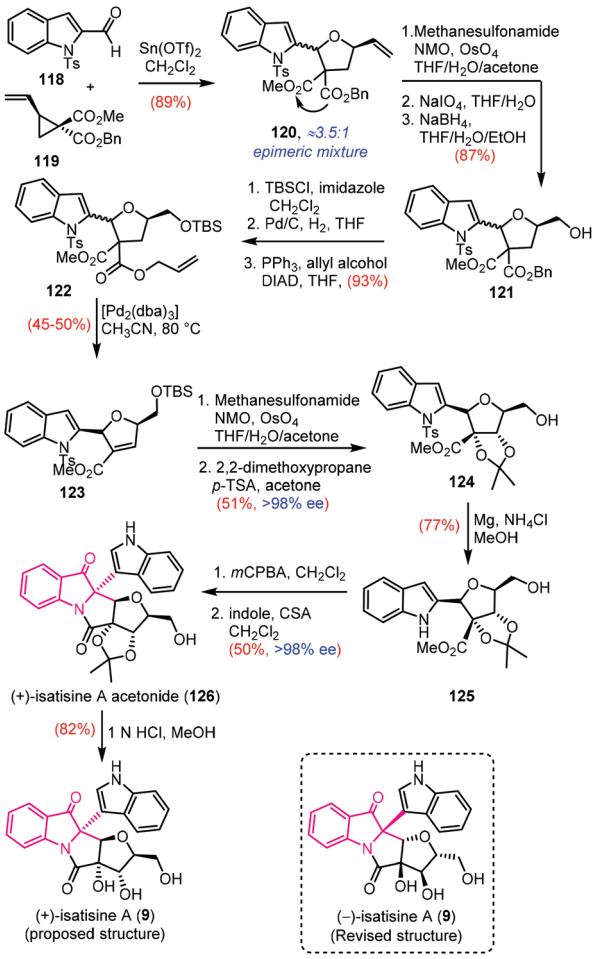

Scheme 12 Kerr's total synthesis of (+)-isatisine A (**9**).

= +271 and $[\alpha]_D^{25}$ = +274, respectively. However, the specific rotation of **126** in the isolation paper is $[\alpha]_D^{25}$ = −283 (*c* = 0.46, MeOH), which is equal and opposite in value to the synthesized compound. Based on this, Kerr *et al.* revised the structure of (−)-isatisine A from C2(R), C9(S), C10(R), C12(S), C13(S), to C2(S), C9(R), C10(S), C12(R), C13(R), as shown in Scheme 12. Later, in the same year, Kerr *et al.* disclosed a full documentation on their various approaches towards the synthesis of isatisine A.[37]

In 2011, Panek and co-workers reported the total synthesis of (+)-isatisine A (**9**), based on a silyl-directed Mukaiyama-type [3 + 2] annulation, for the construction of a fully substituted furan core. On the other hand, the tetracyclic pseudoindoxyl core was built by using modified Buchwald amidation conditions (Scheme 13).[38] The total synthesis of **9** was accomplished in 13 steps with a 6.9% overall yield. The synthesis began with the construction of fully substituted furan **129** through the Mukaiyama-type [3 + 2]-annulation of silane anti-**127** with 2-bromocinnamyl aldehyde **128**. Selective

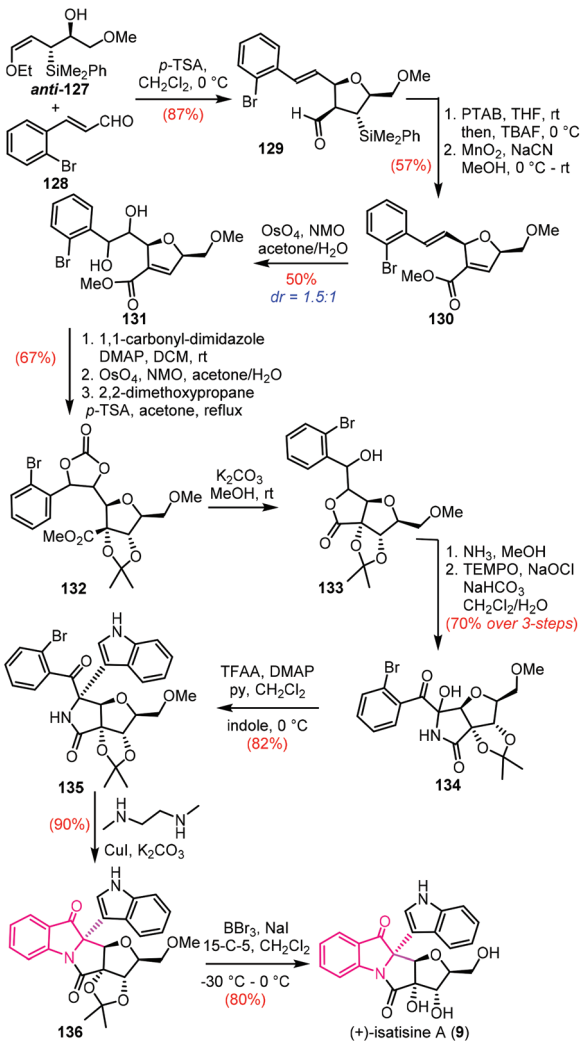

Scheme 13 Panek's enantioselective total synthesis of (+)-isatisine A (**9**).

α-bromination of the conjugated olefin, followed by elimination, gave an α,β-unsaturated aldehyde which, on oxidation with MnO_2 in the presence of NaCN, afforded α,β-unsaturated ester **130** in 57% yield over 2 steps. A styrene like olefin of **130** was selectively dihydroxylated and produced a 1.5 : 1 mixture of diastereomers. Subsequent to this, there was a carbonate conversion of diols and stereoselective dihydroxylation of the α,β-unsaturated ester, which, on acetonide protection, afforded intermediate **132** in 67% yield (3 steps). Carbonate removal and cleavage of the methyl ester led to the formation of an intermediate of dihydroxy acid, which underwent lactonisation to **133**. Lactone opening by ammonia, followed by TEMPO-mediated oxidation and subsequent cyclisation gave a key intermediate hemiaminal **134**. The Lewis acid catalysed formation of iminium ion and addition of indole from the less hindered convex face of the bicycle failed to produce the desired adduct. The use of TFAA made aminal a good leaving group, and the subsequent addition of indole afforded **135** in 82% yield as a single stereoisomer. A modified Buchwald intramolecular amidation using a CuI-mediated coupling led to the generation of tetracyclic intermediate **136** and further deprotection of the methyl ether and acetonide in one pot provided (+)-isatisine A (**9**) in 80% yield. In 2015, the group published their second report on the total synthesis of isatisine A and discussed the various difficulties faced during the synthesis.[39]

In the same year, Liang reported the total synthesis of (−)-isatisine A (**9**), the natural enantiomer of the alkaloid.[40] The key features included the unprecedented intramolecular *C*-glycosylation of an indole and oxidative ring contraction using common and inexpensive building blocks such as indole and D-ribose (Scheme 14). However, the construction of the pseudoindoxyl core of the molecule is similar to that of Kerr's approach. The reaction commences with an aldol reaction between the enolate of **137** and **138** (the sugar part), and subsequent benzoylation and Lewis acid cyclisation produced *C*-gycosylation compound **140**. The synthesis of dicarbonyl derivative **141** without affecting the anomeric center was carried out in the presence of SeO_2 in 1,4-dioxane. When compound **141** was treated with hydrogen peroxide in the presence of potassium carbonate, it underwent ring contraction to tetracyclic core **142**. The one pot debenzoylation and the ring opening of **142** have been carried out by treatment with NaOMe in MeOH/THF. Further removal of two benzyl groups by hydrogenolysis afforded a triol, which was then selectively protected as ketal to give **143**. The oxidation of chloroindole afforded the epoxide, which was opened by a primary alcohol to produce a pair of diastereomers. These were treated further by using Kerr's procedure, and (−)-isatisine A acetonide **126** was obtained in 36.0% yield. The acid hydrolysis of **126** afforded (−)-**9** in 88% yield.

In early 2012, Xie's group reported the biomimetic synthesis of (−)-isatisine A (**9**) in 8 steps with an overall yield of 8.6% from the known glucal **144**.[41] The key steps involved the nucleophilic addition to obtain the pseudoindoxyl unit and an unprecedented biomimetic benzylic-ester rearrangement. As

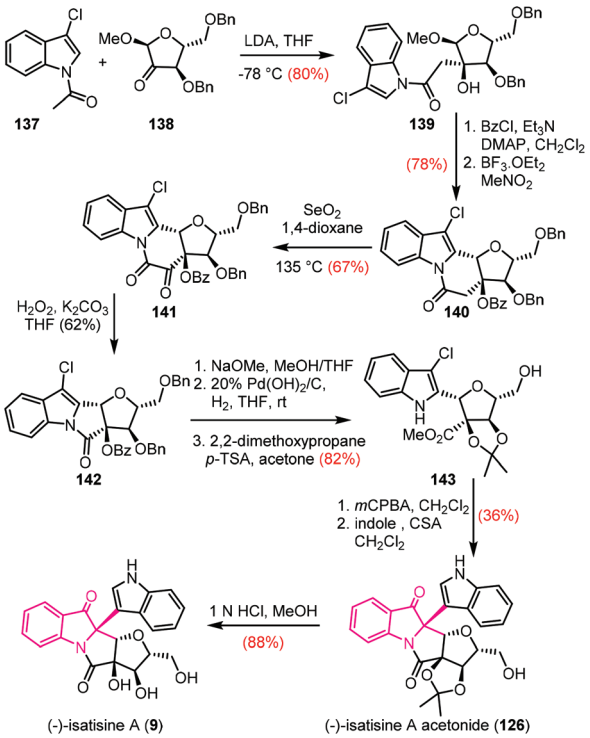

Scheme 14 Liang's total synthesis of (–)-isatisine A (**9**).

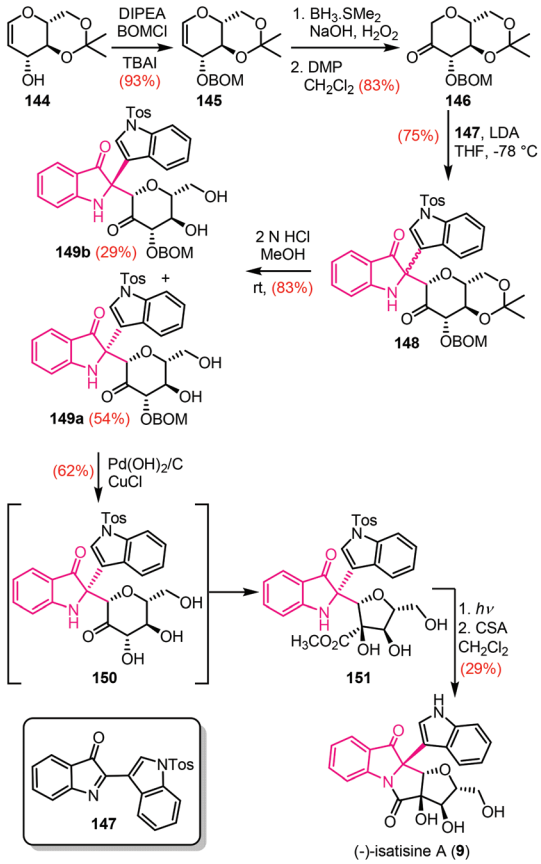

Scheme 15 Xie's total synthesis of (–)-isatisine A (**9**).

shown in Scheme 15, the BOM-protection of alcohol **144**, followed by hydroboration of enol ether and DMP oxidation, afforded compound **146**. Nucleophilic coupling with substrate **147** proved to be challenging due to the steric hindrance. With extensive trials, ketone **146** was treated with LDA for 0.5 h at −78.0 °C and then coupled with electrophilic **147**, providing ketone **148** as a diastereomeric mixture in 75% yield. Acetonide deprotection led to the formation of **149a** and **149b**. Spectroscopic analysis found **149a** to be the major product in 54.0% yield and **149b** was found to be the minor product in 29% yield. Based on the configuration of C2 in the product and Kerr's report, compound **149a** was hydrogenated to afford unstable triol **150**, which underwent *in situ* Cu-mediated oxidation and benzylic ester rearrangement to **151** with good chemo- and diastereoselectivity. Photo-induced deprotection of the Tos-group and treatment with CSA in CH_2Cl_2 at room temperature furnished the desired product (–)-**9**. It was observed that compound **149b** also gives (–)-isatisine A (**9**) in 16% yield by using the same protocol, which shows that the separation of two diastereomers was unnecessary. Using the same reaction strategy, the mixture of **149a** and **149b** produced (–)-isatisine A (**9**) in 18% yield. One more paper on the total synthesis of (–)-isatasine A (**9**) by the Xie group, which provides the reaction strategy in detail with their trials and failures, described earlier, was reported in 2015.[42]

In the year 2012, Ramana's group reported the synthesis of 13-deoxy isatisine A (**162**), employing the in-house developed $InCl_3$ mediated selective *C*3-indolylation of isatogen to furnish the requisite pseudoindoxyl core (Scheme 16).[43] The synthesis began from the known lactone **152**, which on TBS protection of the primary alcohol followed by reaction with TMS acetylene in the presence of a base gave hemiacetal **153**. One step deoxygenation and TBS deprotection of **153** was achieved using $BF_3{\cdot}OEt_2$ and Et_3SiH to furnish β-alkyne derivative **154** exclusively in 61% yield. Next, benzyl protection of the primary hydroxy group and the subsequent Sonogashira coupling with 2-nitro iodobenzene gave intermediate **156**, which was subjected to acid-mediated acetonide deprotection to give diol compound **157**. Synthesis of ester derivative **158** from **157** was carried out in a three step sequence with 56% yield, involving the selective oxidation of the primary alcohol to an aldehyde, which was further oxidised to carboxylic acid followed by esterification of the acid group. The Pd(II)-catalysed *o*-nitroalkyne cycloisomerisation of **158** gave the key isatogen intermediate **159** in 59% yield. The $InCl_3$ mediated selective alkylation of isatogen **159** with indole afforded the requisite pseudoindoxyl core **160** in 53% yield. Next, ester hydrolysis and subsequent acid amine coupling generated tetracyclic core **161**. Finally, debenzylation of **161** using $TiCl_4$ gave the 13-deoxy isatisine A (**162**) in 88% yield.

Later in the same year, this group reported the total synthesis of (–)-**9** starting from D-ribose involving four consecutive metal-catalysed/mediated transformation at the final steps.[44] The key reactions are Pd-catalysed isatogen synthesis followed

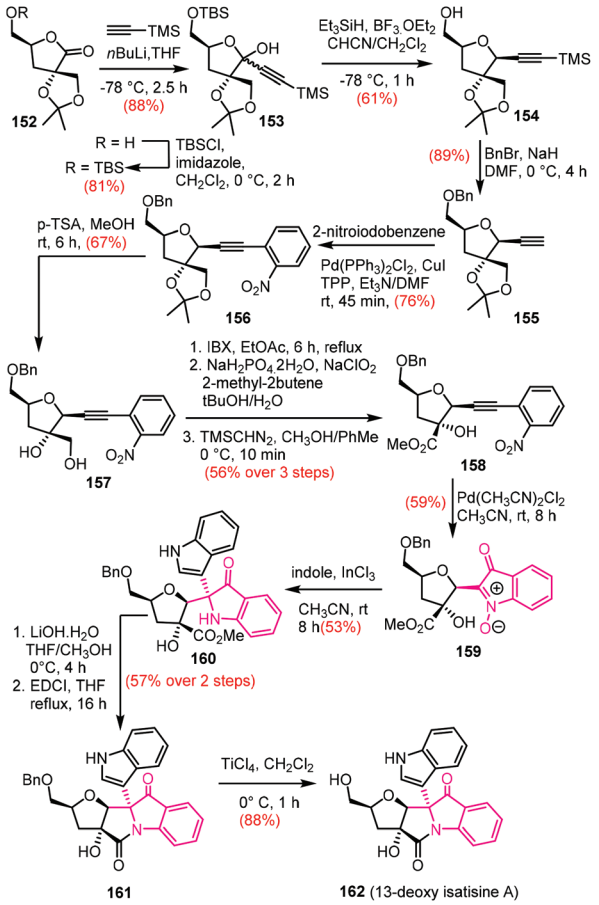

Scheme 16 Ramana's total synthesis of 13-deoxy isatisine A (**162**).

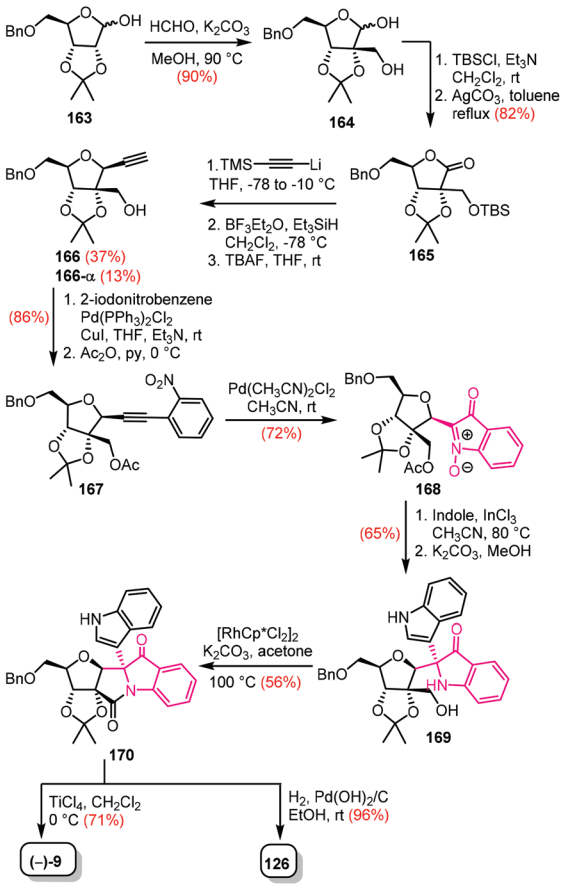

Scheme 17 Ramana's total synthesis of (–)-isatisine A (**9**).

by the In-mediated selective addition of indole to isatogen to get the pseudoindoxyl unit, and subsequent [Rh]-catalysed dehydrogenative N-heterocyclisation of amino alcohol to γ-lactam to give the tetracyclic core of isatisine A (Scheme 17). The starting lactone **165** was prepared from readily available, inexpensive D-ribose by employing a 3-step protocol. The addition of trimethylsilylethynyllithium to **165**, followed by the reduction of crude hemiketal and subsequent C-TMS deprotection furnished β-alkyne **166** (37%) along with α-anomer **166-α** (13%) in a ratio of ~3 : 1. Next, the Sonogashira coupling of **166** with 2-iodonitrobenzene, followed by acetate protection of the free –OH group resulted in *o*-nitroalkyne **167**. [Pd]-Mediated nitroalkyne cycloisomerisation gave isatogen **168** in good yield. The key stereoselective addition of indole to **168** was carried out in the presence of $InCl_3$, followed by acetate deprotection by treatment with K_2CO_3 in methanol, which gave the amino-alcohol **169** in 65% yield. Oxidative lactamisation of **169** using $[Cp^*RhCl_2]_2$ and catalytic potassium carbonate afforded the lactam compound **170**, which, on deprotection of the benzyl and acetonide groups using $TiCl_4$, resulted in the isolation of (–)-isatasine A (**9**) in 71% yield. On the other hand, selective debenzylation using hydrogenolysis conditions afforded the acetonide of (–)-isatisine A (**126**) in 96% yield.

2.8 Melokhanine E

In 2016, Cheng and co-workers documented the isolation of melokhanine E (**10**), a pseudoindoxyl alkaloid, from the twigs and leaves of *Melodinus khasianus*.[5] Melokhanine E possesses a 6/5/5/6/6 pentacyclic structure and exhibited superior broad-spectrum activity (MIC = 2 μM against *P. aeruginosa* and 5 μM against *E. faecalis*). The compound (–)-(**10**), was biogenetically derived from an eburnane type indole alkaloid (+)-eburnamonine. In the light of their unique structure and promising biological activity, they have been privileged motifs for synthetic and medicinal chemists since their isolation.

In 2019, Zhu's group reported the first total synthesis of (–)-melokhanine E **10** and its congeners, which featured an α-iminol rearrangement, and an integrated oxidation/diastereoselective cyclisation sequence with the desired C20/C21 *cis* stereochemistry (Scheme 18).[45] The synthesis commenced with the Upjohn dihydroxylation of diastereoselective pure compound **172**, which was synthesized from 3-cyclopentenecarboxylic acid (**171**) in six steps, affording diol **173** in 89% yield as a single diastereomer. Saponification and α-imino rearrangement gave spiroindoline-3-one **174** in excellent yield. Diketone **175** was made by the classical Swern oxidation, which, upon highly stereoselective lactamization, provided the pentacyclic **176** in 58.0% overall yield. Hydrolysis followed by

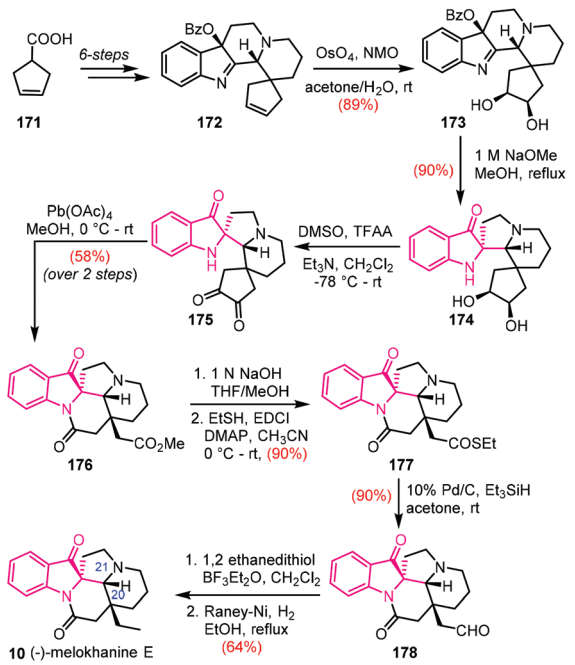

Scheme 18 Zhu's total synthesis of (–)-melokhanine E (**10**).

EDCI coupling with ethanethiol generated thioester **177**. Fukuyama reduction gave aldehyde **178**, which was converted *via* the 1,3-dithiolane intermediate into (–)-**10** in good overall yield.

Recently, the Pierce group disclosed a 12-step convergent synthesis of the indole alkaloid (±)-**10** with 11% overall yield.[46] As shown in Scheme 19, the synthetic approach involves a formal [3 + 2] cycloaddition of two reactive precursors having a 1,3-dipole, and an imine species cyclopropane substrate, for the stereoselective formation of the natural product. Spirocyclic cyclopropane **180** and piperidine derivative **183** were synthesized by a known sequence with some modifications from anthranilic acid (**179**) and delta-valerolactam (**181**) in 4 and 6 steps respectively.[47] The coupling of indolinone **180** and piperidine derivative **183** proved to be more challenging, due to the steric bulk on both the coupling partners, as well as deactivation of the nucleophile *via* resonance of the 3-keto functionality of the indolinone. After extensive trials, suitable conditions for amide coupling were found to involve 2 equiv. of collidine in the presence of 0.33 equiv. of triphosgene in the CH_2Cl_2 solvent for 3.5 h, at 40 °C, furnishing **184** in 45% yield. Coupled biscyclopropane **184** was subjected for the key cycloaddition step with MgI_2 under microwave conditions, which promoted the spirocycle opening and the thermolysis of the Boc-carbamate to form the reactive imine intermediate which subsequently underwent the formal [3 + 2] cycloaddition affording the (±)-melokhanine (**10**) in 88% yield as a single, detectable diastereomer.

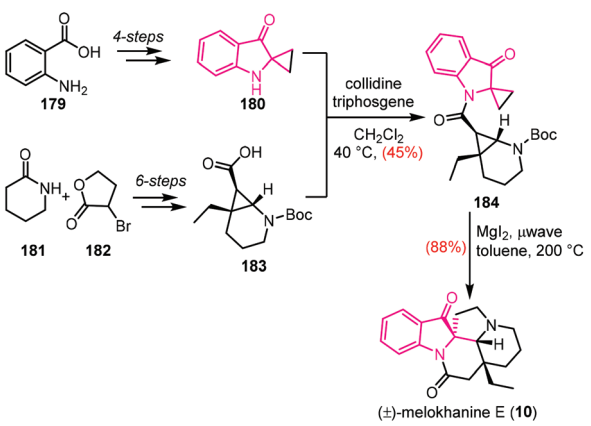

Scheme 19 Pierce's racemic total synthesis of (±)-melokhanine E (**10**).

2.9 Mitragynine pseudoindoxyl

Mitragynine pseudoindoxyl (**11**), is a pentacyclic spiro pseudoindoxyl alkaloid isolated from the leaves of the Thai folk medicine *Mitragyna speciosa* Korth, along with mitragynine.[48] The biotransformation of this natural alkaloid by the fungus *Helminthosporum* sp., provided the metabolites mitragynine pseudoindoxyl and hydroxy mitragynine pseudoindoxyl, which were found to be quite active pharmacologically. It is a μ-opioid receptor agonist and δ-opioid receptor antagonist and acts as a G protein biased agonist at the μ-opioid receptor and vas deferens through the δ-receptor in mice. It is a more potent analgesic than morphine and as potent as enkephalin.[49] To date, there are two reports of the semi-synthesis of **11** from mitragynine and one report of the synthesis of its 11-methoxy derivative (**198**). In all the cases, the spiropseudoindoxyl unit was synthesized from the corresponding indole derivative *via* its selective hydroxylation, followed by a Wagner–Meerwein type 1,2-alkyl rearrangement of the hydroxyindolenines.

In 1996, Sakai and co-workers, while analyzing the CD spectra of pseudoindoxyl alkaloids, described the synthesis of the mitragynine pseudoindoxyl starting from mitragynine **185**, in a very low yield (Scheme 20).[50] Oxidation of **185** with one equivalent of lead tetraacetate afforded 7-acetoxyindolenine derivative **186** in 50% yield. The sodium methoxide mediated rearrangement of **186** furnished spiro-pseudoindoxyl molecule **11** as a single isomer in 11% yield along with **187**.

Majumdar *et al.* reported the semi-synthesis of (±)-mitragynine pseudoindoxyl (**11**) starting from mitragynine, similar to Sakai's synthesis with improved yields (Scheme 21).[55] Oxidation of **185** with PIFA gave hydroxyindolenine derivative **187** in 57% yield. Treatment of **187** with $Zn(OTf)_2$ in toluene under reflux conditions formed spiro-pseudoindoxyl molecule **11** in 39% yield.

In 2012, Sorenson and co-workers reported a highly diastereoselective synthesis of the 11-methoxy mitragynine pseudoindoxyl **198** (Scheme 22).[51] The synthesis featured a simple and efficient method that involved combining mechanistic elements of both the Ugi and Houben–Hoesch reactions and introducing the intramolecular addition of arenes having at least one π-donor atom, in addition to the N-atom, to electrophilic nitrilium ions, in a three-component coupling of arenes, isocyanide, and ketone. The total synthesis started

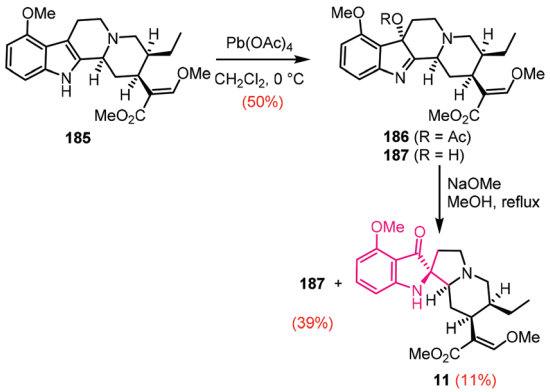

Scheme 20 Sakai's synthesis of the (±)-mitragynine pseudoindoxyl (**11**).

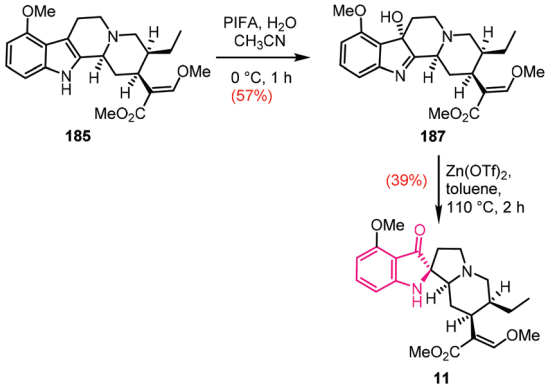

Scheme 21 Majumdar's synthesis of (±)-mitragynine pseudoindoxyl (**11**).

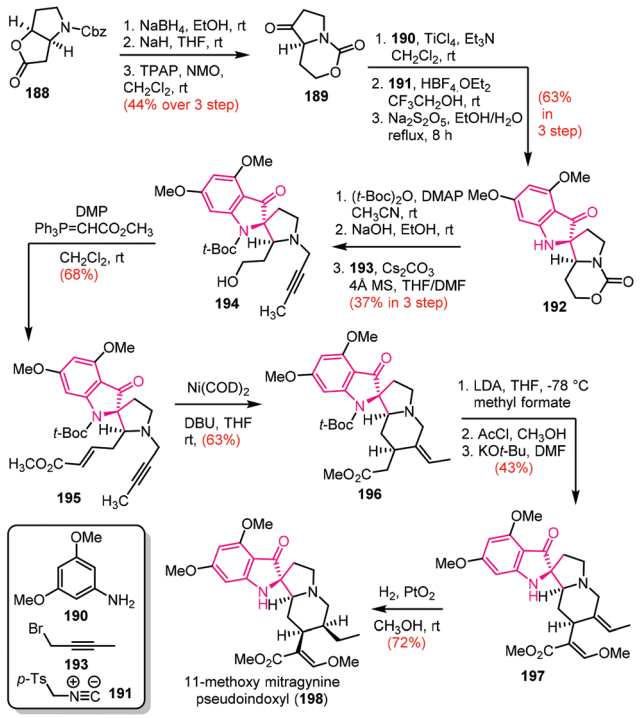

Scheme 22 Sorensen's total synthesis of (±)-11-methoxy mitragynine pseudoindoxyl (**198**).

with a three-step conversion of the Cbz-derivative of Geissman–Waiss lactone **188** to bicyclic lactone **189**, involving the reductive cleavage of the lactone ring, followed by formation of the cyclic carbamate, and subsequent Ley–Griffith oxidation, leading to desired ketone **189**. The key steps for the formation of pseudoindoxyl core **192** from **189** took place in three steps. This involved *in situ* imine formation by condensation of **189** with **191**, followed by exposure to the combined action of the fluoroboric acid diethyl ether complex and tosylmethyl isocyanide, resulting in the spiro-fused tosylmethyl imine intermediate, which, on heating in a mixture of ethanol and water containing sodium metabisulphite, afforded a hydrolysis product as a single diastereomer **192** in 63% overall yield.

Then, lactone **192** was converted to ester compound **195** through a 4-step sequence involving *N*-protection, cyclic carbamate cleavage, *N*-alkylation and oxidative homologation. Diastereoselective, reductive cyclisation of **195** by treatment with bis(cyclooctadiene)nickel(0) and 1,8-diazabicycloundec-7-ene gave piperidine tetracyclic derivative **196** in 63% yield. The conversion of compound **196** to **197** *via* a three step protocol has been reported by the groups of Takayama,[52] Cook[53] and Ma.[54] Finally, hydrogenation of the *exo*-olefin in the presence of Adam's catalyst led, in complete diastereo face-selective fashion, to the 11-methoxy mitragynine **198**, in 72% yield.

2.10 Mersicarpine

Mersicarpine (**12**), isolated from the *Kopsia* species of the flowering plant, by Kam and co-workers in 2004, has an unusual tetracyclic structure bearing a seven membered cyclic imine and fused δ-lactam around a tertiary hydroxyl group.[56] Due to its unique structure, mersicarpine has received considerable attention from synthetic chemists. Both racemic and enantiomeric synthesis of mersicarpine (**12**) have been documented employing common cyclic intermediate **206**, which, upon functional group modification, led to **12**.

The first total synthesis of (±)-mersicarpine (**12**) was reported by Kerr and co-workers in 2008, featuring $Mn(OAc)_2$ catalysed malanoic radical cyclisation and indole oxidation (Scheme 23).[57] In addition, they also studied the dramatic chemical shift variance in the ^{1}H NMR spectra of **12** with respect to solvent acidity. The synthesis began with the acylation of indoline **199** followed by DDQ-oxidation to **200**. The Michael addition of acetylacetone to **200** and $Mn(OAc)_2$-mediated malanoic radical cyclisation delivered δ-lactam **201** in good yield. The fragmentation of **201** through *retro*-Claisen condensation produced methylketone **202**, which upon conjugate addition with acrylonitrile, afforded compound **203**. Subsequent reduction and a two step dehydration protocol afforded olefin **205**. Hydrogenation of both olefin and nitrile, followed by Boc-protection, resulted in carbamate **206**. Compound **207**, bearing the key pseudoindoxyl unit, was achieved by the oxidation of **206** with the *in situ* prepared dimethyl dioxirane, to afford a 1 : 1 mixture of diastereomers, which may be due to the epimerizable nature of the hemiaminal. The final step, amine deprotection and presumed imine formation, gave a single compound (±)-**12** in 80% yield.

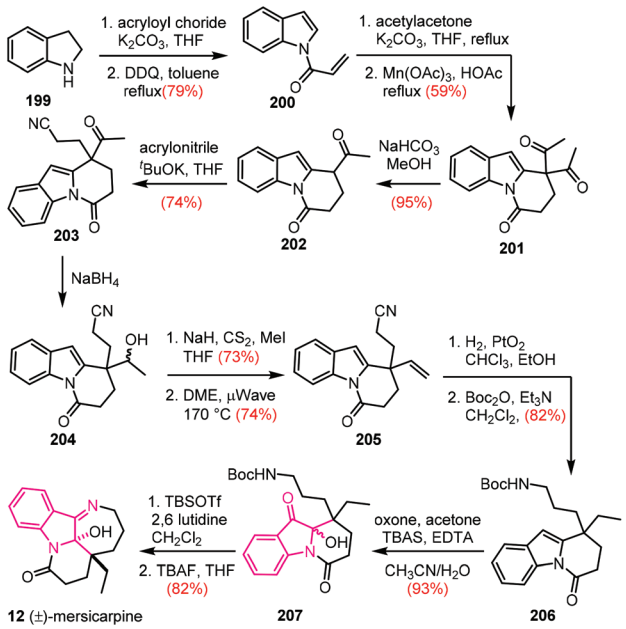

Scheme 23 Kerr's total synthesis of (±)-mersicarpine (**12**).

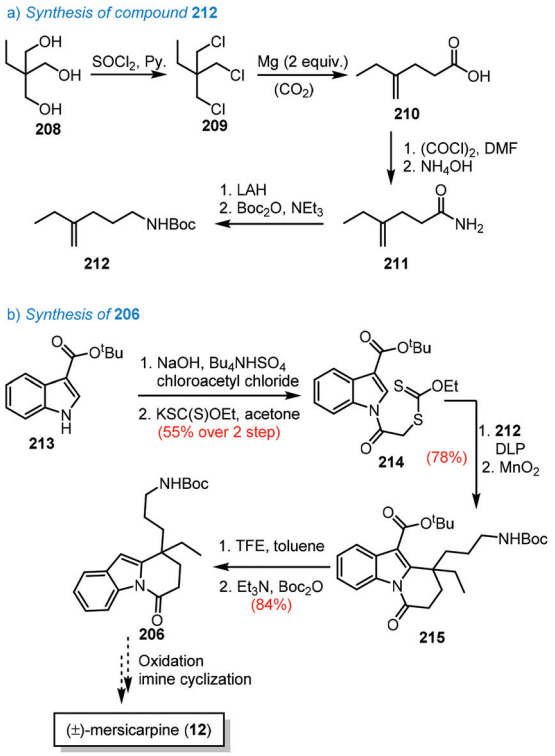

Scheme 24 Zard's formal synthesis of (±)-mersicarpine (**12**).

A year later, Zard and co-workers disclosed the formal total synthesis of (±)-mersicarpine (**12**) by synthesizing Kerr's intermediate **206**. The synthetic approach for **206** includes an impressive intermolecular radical addition/cyclisation cascade to construct the lactam core with a six membered ring (Scheme 24).[58] The synthesis commenced with the preparation of xanthate **214** bearing an electron withdrawing *tert*-butoxycarbonyl group at the 3-position of indole **213**. Acylation of **213**, followed by nucleophilic substitution by the potassium *O*-ethyl xanthate salt, afforded xanthate **214**. The other radical coupling partner olefin **212** was synthesised from triol **208**, in a 6-step sequence reported by Shalaby and co-workers.[59] The radical cascade of xanthate **214** and olefin **212** in the presence of lauroyl peroxide (DLP) proceeded normally to afford **215** *via* radical addition and subsequent 6-exo cyclisation to the indole ring. A one-pot removal of the *tert*-butyl ester group and decarboxylation followed by reprotection of the amine as its *tert*-butyl carbamate provided **206** in 84% yield and thus finishing the formal synthesis of (±)-mersicarpine **12**.

In 2010, Fukuyama reported the first enantiocontrolled total synthesis of (−)-mersicarpine **12** in 10 steps from known ketoester **217**, featuring an Eschenmoser–Tanabe-type fragmentation, to form chiral alkyne unit **220**. The facile synthesis of the indole core was effected by the combination of Sonogashira coupling and [Au]-catalysed cyclisation (Scheme 25).[60] The synthesis commenced with the preparation of known asymmetric ketoester **217** developed by d'Angelo and co-workers.[61] IBX-oxidation, followed by the epoxidation of the enone, afforded epoxy-ketone **218**. Semicarbazone **219** was formed, and was oxidized with lead tetraacetate to form the 1,3,4-oxadiazoline intermediate, which underwent an Eschenmoser–Tanabe type fragmentation to furnish compound **220**. Reduction of aldehyde, and further Sonogashira coupling with *o*-iodoaniline, followed by [Au]-catalysed indole formation afforded **222** in good yield. Installation of the N-atom at the 3-position of indole by treatment with a diazo-compound and subsequent lactamisation followed by mesylation of the hydroxyl group afforded **224**. Hydrogenolysis of **224** to 3-aminoindole **225**, followed by autoxidation with sodium bicarbonate under refluxing solvent conditions with methyl sulfide provided (−)-mersicarpine **12** in 96% yield over three steps.

The DIBAL-H mediated reductive ring expansion reaction of cyclic ketoxime **229** for the construction of the azepinoindole core of mersicarpine was revealed by Tokuyama's team in 2012 (Scheme 26).[62] This concise total synthesis of (−)-**12**, accomplished in 9-steps (was a six-pot process from known ketoester **217**) in 30% overall yield. The synthesis was initiated with the formation of tricyclic oxime **229**, from optically active cyclohexanone **217**. The Fisher-indole protocol afforded tricyclic indole **227**. Later, the DDQ-mediated regioselective benzylic oxidation and subsequent oxime formation provided keto-oxime **229**. The key step, a one pot protocol to construct the characteristic azepinoindole skeleton involves the treatment of **229** with DIBAL-H, leading to ring expansion *via* the classical Beckmann rearrangement, along with ester reduction to give the unstable azepinoindole, which was rapidly protected to give Cbz-carbamate **230**. Compound **230** was subjected to the TPAP/NMO-mediated cyclic lactam formation. The 2-steps of the Fukayama autoxidation subsequent to this afforded natural product (−)-**12** in 30% overall yield.

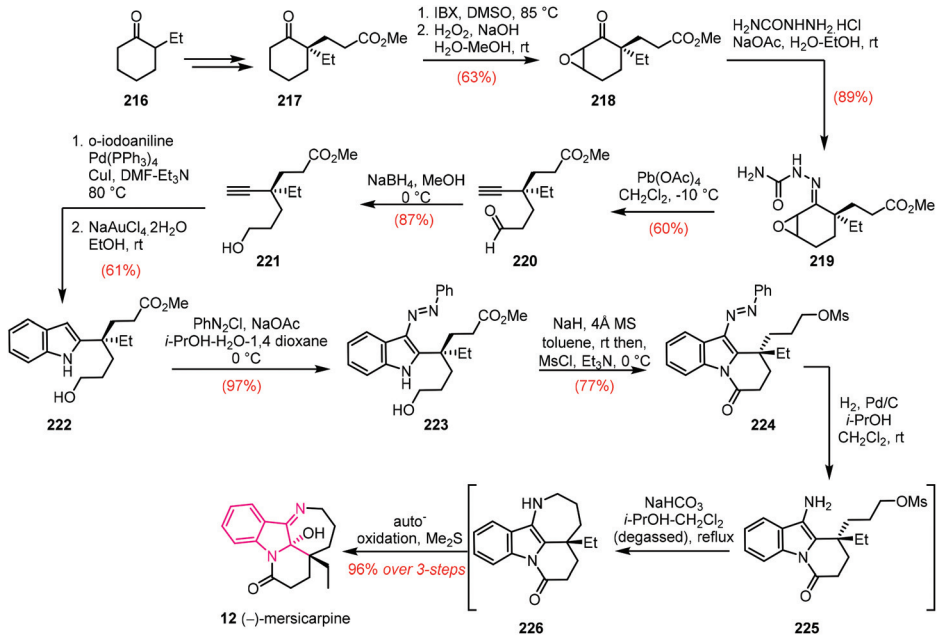

Scheme 25 Fukuyama's total synthesis of (–)-mersicarpine (**12**).

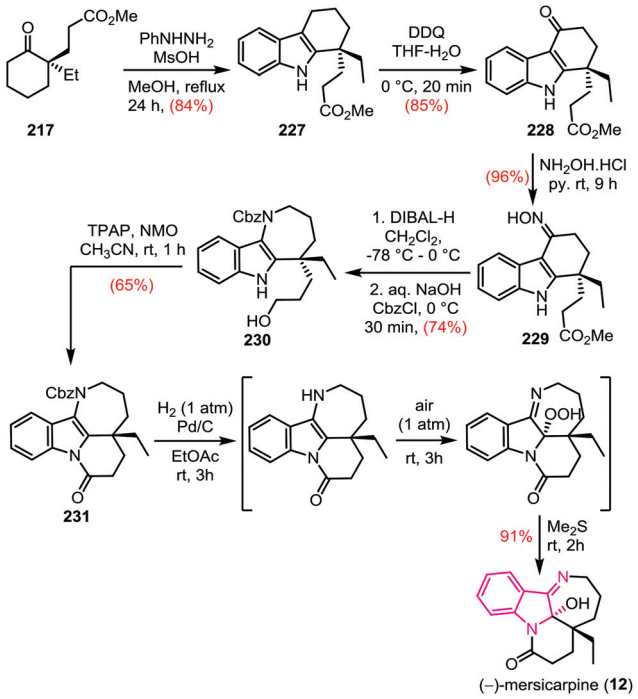

Scheme 26 Tokuyama's total synthesis of (–)-mersicarpine (**12**).

Next year, the same group published a detailed report on various approaches used for the total synthesis of mersicarpine (**12**).[63] As the final synthetic route for **12** is the same as discussed above, it will not be discussed further.

Han and co-workers reported an alternative synthetic route for common cyclic intermediate **206**, which led to (±)-**12** in nine steps, utilizing the in house developed $Al(OTf)_3$-catalysed nucleophilic addition of the silyl enol ether to the carbocation species generated *in situ* from a tertiary alcohol (Scheme 27).[64] The synthesis was initiated with the formation of tricyclic tertiary alcohol **236**, using a three step sequence from commercially available indole **232** and succinic anhydride (**233**). The other reactive partner, silyl enol ether **240**, was prepared *via* the Mitsunobu reaction of 1-hydroxypropan-2-one (**237**) and *tert*-butyl *o*-tosylcarbamate (**238**), followed by the TMSOTf-mediated enol formation in two steps. The strategic step to tricyclic **241** involves the $Al(OTf)_3$-catalysed nucleophilic addition of silyl-enol ether **240** to the *in situ* formed carbocation species from tertiary alcohol **236**. Importantly, under the above conditions, the addition of various other nucleophiles such as indole, pyrrole, and furan to **236** was carried out successfully in good yields. Removal of the O-Ts– group, followed by reduction, led to compound **206**, which further followed Kerr's protocol to form (±)-**12**.

In 2014, the same group disclosed their various efforts towards the construction of a quaternary carbon center *via* nucleophilic addition of the silyl enol ether to the carbocation species generated *in situ* from a tertiary alcohol and its application in the total synthesis of **12** (Scheme 28).[65] Compound **206** was synthesized as per their previous report.[66] Next, the oxidation of **206** using Kerr's conditions gave **207**. Without purification, compound **207** was treated with TfOH to afford mersicarpine **12** in 43% yield. However, treatment of **207** with TFA in CH_2Cl_2 solvent followed by replacing CH_2Cl_2 with EtOAc solvent and stirring overnight afforded 58% of **12**. Thus, starting from indole and succinic anhydride, compound **12** was synthesized in 8 linear steps with 14% overall yields.

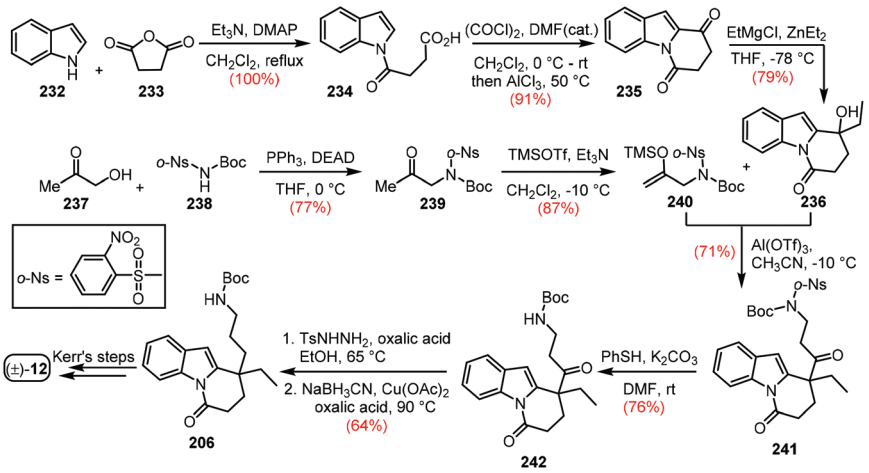

Scheme 27 Han's formal synthesis of (±)-mersicarpine (**12**).

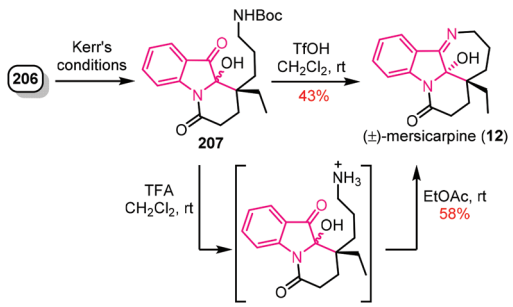

Scheme 28 Han's synthesis of (±)-mersicarpine (**12**).

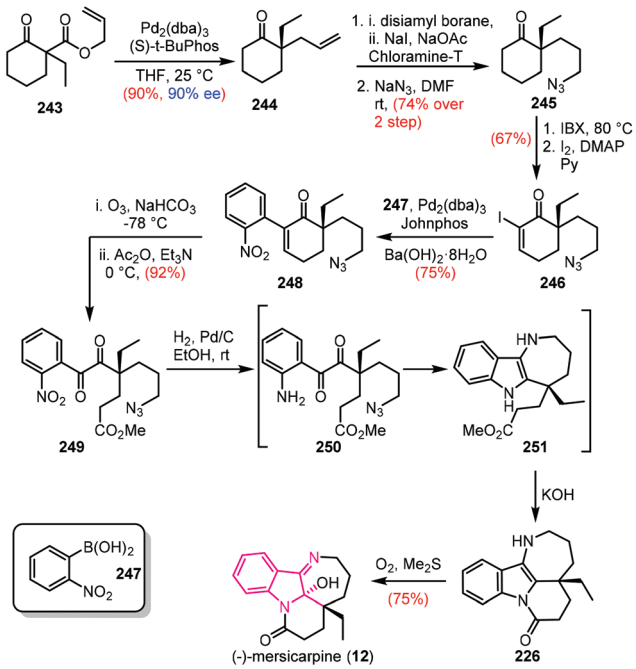

Scheme 29 Zhu's total synthesis of (−)-mersicarpine (**12**).

Zhu and team disclosed the enantioselective total synthesis of (−)-mersicarpine **12** in 2013, featuring the Suzuki–Miyaura coupling reaction to couple two fragments, incorporating key intermediate **246** and an unprecedented oxidation/reduction/cyclisation protocol for the construction of the mersicarpine skeleton from substituted cyclohexenone **248** (Scheme 29).[67] The synthesis was initiated with the [Pd]-catalysed enantioselective decarboxylative allylation of β-ketoester **243** to (*S*)-2-allyl-2-ethylcyclohexanone (**244**) in 90% yield with 92% ee. A hydroboration/iodination sequence led to the conversion to alkyl azide **245**. Oxidation of **245** to enone and further iodination afforded the vinyl iodide **246**. The Suzuki–Miyaura coupling of **246** with **247** provided the functionalized cyclohexenone **248** in 75% yields. Next, oxonolysis followed by the addition of Ac_2O and Et_3N afforded diketone ester **249**. After extensive trials and efforts, the hydrogenation of the diketone ester gave **251**, which underwent lactamisation to unstable tetracycle **226**. On autoxidation, this afforded (−)-**12** in a relatively good yield. Furthermore, compound **249** was successfully employed in the total synthesis of (−)-scholarisine G, (+)-melodinine E, (−)-leuconoxine, and (−)-leuconolam.

Later in 2015, the same group reported both the racemic and enantioselective synthesis of **248**, as well as (S)-**249**, and showed the application of (S)-**249** in the total synthesis of (−)-mersicarpine, (−)-scholarisine G, (+)-melodinine E, (−)-leuconoxine, (−)-leuconolam, (−)-leuconodine A and C, and (+)-leuconodine F. However, their approach for the synthesis of (−)-mersicarpine (**12**) was the same as the earlier report.[68]

The application of the carbamate functionality enabled a carbocationic species bearing a masked amine, which was utilized by Liang and co-workers for the total synthesis of (±)-mersicarpine **12** (Scheme 30).[69] The key features involved the intramolecular Friedel–Crafts alkylation with the carbamate functionality enabled carbocation for the construction of a δ-lactam having a quaternary carbon center of mersicarpine. The synthesis commenced from the formation of carbamate **255** from compound **252**. The Grignard reaction with a ketone

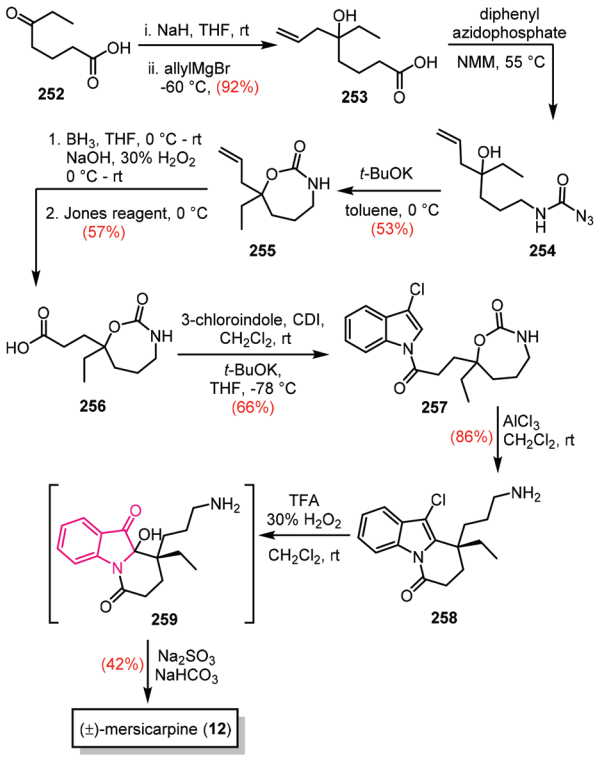

Scheme 30 Liang's total synthesis of (±)-mersicarpine (**12**).

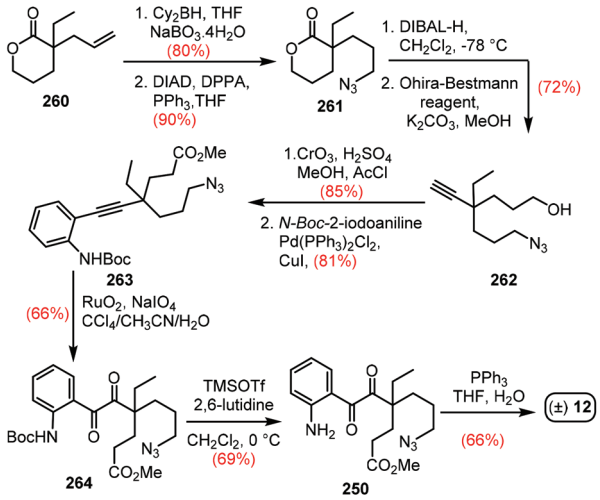

Scheme 31 Liang's total synthesis of (±)-mersicarpine (**12**).

after deactivating the carboxylic acid led to compound **253**, which was further converted to azide **254**. Substrate **254** under basic conditions underwent the Curtius rearrangement to generate the isocyanate intermediate, which was captured by a tertiary alcohol to form carbamate **255** in 53% yield over 2 steps. Hydroboration/oxidation of **255** followed by the Jones oxidation afforded acid **256**. A classical CDI coupling of acid **256** and 3-chloro indole afforded amide **257**. The $AlCl_3$-catalysed intramolecular Friedel–Crafts alkylation formed the carbocation *in situ* through the decarboxylation of carbamate, leading to δ-lactam **258**, whose upon further oxidation and subsequent imine formation provided the (±)-mersicarpine **12** in 42% yield.

In the next year, the same group reported the convergent synthesis of (±)-mersicarpine (**12**), along with the synthesis of leuconoxine, leuconodine, melodinine E, and leuconolam by controlling the specific cyclisation sequence through the Staudinger reaction, using common intermediate **250** (Scheme 31).[70] The synthesis commenced by the construction of **262** from known lactone **260**. Hydroboration–oxidation followed by the Mitsunobu reaction using DPPA converted compound **260** to **261**. Lactol formation followed, which on Ohira–Bestmann homologation, afforded alkyne **262**. Oxidation followed by Fischer esterification provided the coupling partner for the Sonogashira coupling with *t*-butyl-(2-iodophenyl)carbamate to furnish compound **263**. Diketone **264** was formed by a ruthenium catalysed oxidation, which, on deprotection of the Boc-group, afforded compound **250**. Treatment of **250** under Staudinger aza-witting reaction conditions in a mixed solvent of THF and water furnished the (±)-mersicarpine (**12**) in 66% yield.

The biosynthetically inspired total synthesis of (−)-mersicarpine (**12**) was reported by Dai and co-workers in 2014 (Scheme 32).[71] The key steps involve a Witkop–Winterfeldt oxidative indole cleavage, which, on transannular cyclization, provided the mersicarpine skeleton in one pot. The total synthesis began with the Boc-protection followed by α-carboxylation and ethylation of **265** to the allyl ketocaboxylate **266**. Pd-Mediated decarboxylative allylation followed by Boc-removal resulted in **267**. Transformation to azidoketone **268** was then done in 3-steps *via* hydroboration/oxidation, mesylation and S_N2 azide displacement. Oxidative Witkop–Winterfeldt indole cleavage by *m*-CPBA afforded lactum **269a**, which underwent transannular cyclisation to provide unstable tricyclic hemiaminal **269** as a 2 : 1 diastereomeric mixture. Compound **273**, on treatment with PPh_3, smoothly underwent the Staudinger-aza-witting

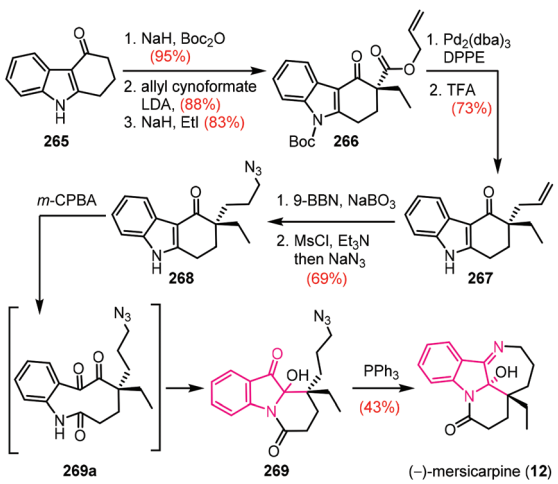

Scheme 32 Dai's total synthesis of (−)-mersicarpine (**12**).

process to afford **12** as a single diastereomer in 43% yield. Additionally, compound **269** was further functionalised to achieve the total synthesis of leuconodines B and D, leuconoxine, melodinine E, leuconolam, and rhazinilam.

Gaich and co-workers disclosed the formal synthesis of the racemic mersicarpine **12** in eight isolated steps, with 6% overall yield, from commercial β-ketoester **270** (Scheme 33).[72] The synthesis commenced with the allylation of **270**, and NBS-promoted bromoketone synthesis, followed by refluxing in Me_2S to provide β-ketosulfide **271** in two steps. Compound **271** was subjected to the Gassman indole protocol to afford 3-(methylthio)indole **272** in 77% yield. α,β-Unsaturated nitrile **274** was prepared from **272** in a 4-step sequence through the selective deprotection of the sulfide group, DIBAL-H reduction, Parikh–Doering reaction and Witting olefination. Reduction of the olefin of **274** with Mg/MeOH afforded compound **275**. Compound **275** was converted to Kerr's intermediate **206** by a 4-step protocol *via* reduction of the cyanide group, which was trapped *in situ* by Boc_2O followed by hydroboration and δ-lactam formation. Furthermore, the Kerr's procedure was followed to afford the (±)-mersicarpine (**12**).

Later, in 2017, Luo and co-workers reported the tandem [3 + 2]-cycloaddition/rearrangement/oxidation sequence for the total synthesis of (−)-mersicarpine **12** in a 4-step protocol, from known intermediate **277** (Scheme 34).[73] Surprisingly, the group accidentally noticed the formation of (−)-mersicarpine (**12**) during their total synthesis of (−)-rhazinal. The synthesis commenced from the preparation of enantiopure known compound **277** in a 7-step sequence from cyclohexanone **276**, reported by the Fukuyama group. A one pot Pd-catalysed indole formation and subsequent Heck reaction afforded compound **278** in 75.0% yield. Sequential lactam formation followed by mesylation afforded compound **279**, which was subjected for azidation to form compound **280**. Here, the actual

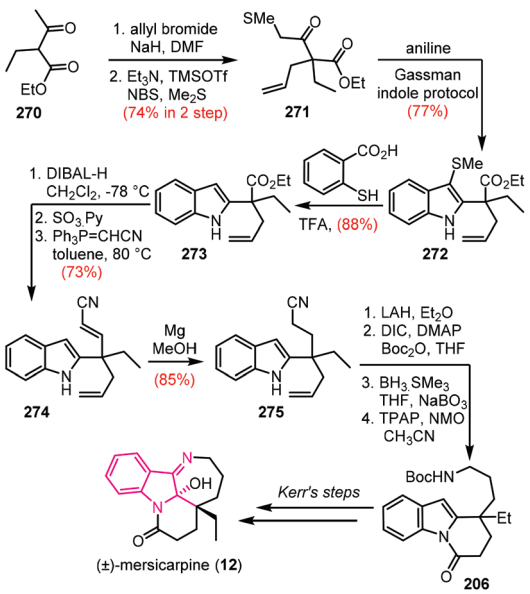

Scheme 33 Gaich's formal synthesis of (±)-mersicarpine (**12**).

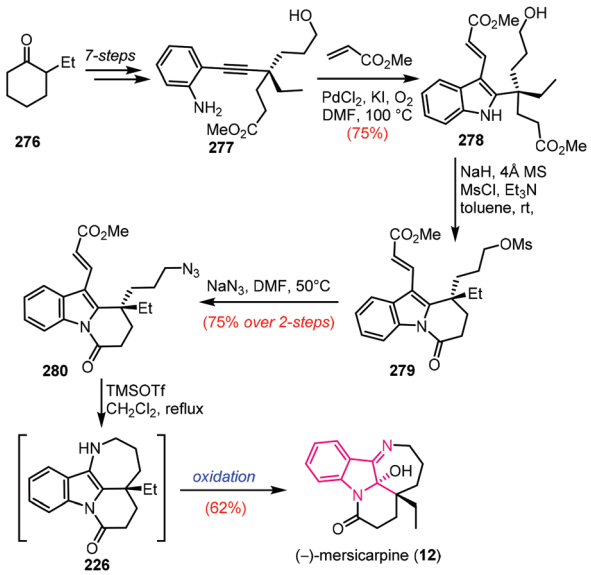

Scheme 34 Luo's total synthesis of (−)-mersicarpine (**12**).

target was the conversion of **280** to the pentacyclic core of (−)-rhazinal *via* intramolecular formal [4+1] cycloaddition of azidodienes. During the screening process, when compound **280** was treated with TMSOTf under heating conditions, it led to the unexpected (−)-mersicarpine (**12**) in very low yield. This was possibly formed by a 1,3-dipolar cycloaddition leading to triazoline, which underwent subsequent rearrangement and further oxidation in the presence of oxygen. Finally, performing the same reaction in the presence of an oxygen atmosphere gave 63% yield of (−)-**12**.

In 2019, Wang and co-workers reported an enantioselective total synthesis of (−)-mersicarpine **12** using the Smith-modified Madelung indole synthesis from 2-methylaniline (**282**) and chiral lactone (+)-**260** (Scheme 35).[74] The synthesis began with the formation of the optically active allylated lactone **260** from an intermolecular palladium-catalysed asymmetric decarboxylative allylic alkylation of lactone **281**. The key Smith-modified Madelung indole synthesis involved the preparation of *N*-silylated *o*-toluidine from **282a** and without isolation; the intermediate was exposed to *n*-BuLi solution, which upon the slow addition of (+)-**260**, led to the acylation/heteroatom Peterson olefination/isomerization/protonation cascade and afforded chiral indole **284** in 85% yield. Conversion of hydroxy to azido *via* a Mitsunobu reaction followed by hydroboration–oxidation of the olefin group afforded compound **285**. Next, the TPAP/NMO-mediated lactamisation afforded the *N*-acyl indole (**286**), which, upon Kerr's protocol of oxone mediated indole oxidation, formed compound **269**, which was earlier reported by Dai's group during their synthesis of **12**. Finally, the TPP mediated Staudinger aza-Wittig cyclization of **269** gave the enantiopure (−)-mersicarpine (**12**) in 64% yield. The author also reported the synthesis of (−)-scholarisine G, (+)-melodinine E and (−)-leuconoxine starting from azide intermediate **286**.

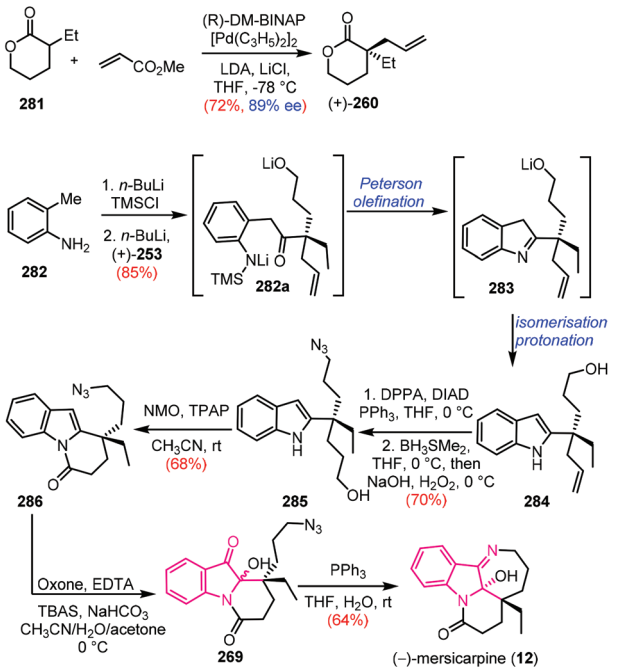

Scheme 35 Wang's total synthesis of (–)-mersicarpine (**12**).

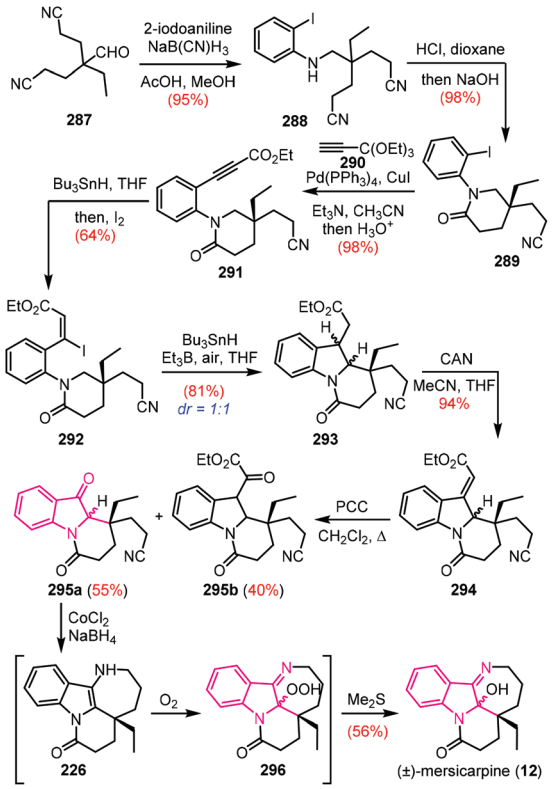

Scheme 36 Beaudry's total synthesis of (±)-mersicarpine (**12**).

Recently in 2019, Beaudry's group reported the total synthesis of leuconoxine, melodinine E, and mersicarpine (**12**) from a common indoline architecture, which was constructed by using a radical 1,5 hydrogen shift followed by a 5-*exo-trig* cyclisation (Scheme 36).[75] The synthesis commenced with the reductive amination of **287** and 2-iodoaniline to give **288**. Acid hydrolysis led to an amidine intermediate, which, on hydrolysis, with a base gave *N*-iodophenyl lactam **289**, and further Sonogashira coupling with alkyne **290** afforded **291**. Hydrostannation of propyolate **291** followed by iodination gave **292** as a single regioisomer. Radical cyclisation of **292** through 1,5-HAT (hydrogen atom transfer) and subsequent 5-*exo-trig* cyclisation led to indoline **293** in good yield as a 1 : 1 mixture of *trans*-indoline diastereomers. Ceric ammonium nitrate (CAN) mediated chemo-selective oxidation of **293** gave desired unsaturated ester **294**. The initial attempt of oxidative cleavage of **294** using standard reagents such as O_3 and RuO_4 does not provide the required 3-indolinone derivative **295a**. Finally, the oxidative cleavage of unsaturated ester **294** was carried out employing PCC to furnish desired compound **295a** along with minor amounts of undesired indole glyoxylate **295b** in 55% and 40% yields respectively. Selective reduction of the nitrile group in **295a** apparently generates the amine, which underwent cyclization to the corresponding enamine, followed by auto oxidation of the indole ring by oxygen, and the reduction of peroxide to furnish (±)-mersicarpine (**12**). In the same report, the total synthesis of leuconoxine and melodinine E was accomplished starting from **293** by selectively converting it to the corresponding indole derivative followed by further functional group manipulation.

2.11 Trigonoliimines C

Trigonoliimines A–C belong to the class of bis-indole alkaloids with an unprecedented pentacyclic skeleton isolated from the leaves of *Trigonostemon lii* collected in the Yunan province of China in 2010.[76] The biosynthesis of these alkaloids that commenced with the coupling of tryptamine and kynuramine was proposed. In addition, they also reported the anti-HIV-1 activity of the trigonoliimines and revealed a modest anti-HIV activity for trigonoliimine A (EC_{50} = 0.95 μg mL^{-1}). Trigonoliimine C (**13**) was the first to be synthesized in this family and was reported by the groups of Tambar (racemic), Movassaghi (enantioselective), and Ramana (racemic), whereas Hao's group reported the biomimetic synthesis of the pentacyclic core of trigonoliimine C (**320**).[8,77–80] However, Tambar, Movassaghi and Hao have had a similar approach for the synthesis of the key pseudoindoxyl moiety, which involves the selective mono oxidation of the 2,2′-bis-tryptamine followed by an acid mediated 1,2-alkyl rearrangement strategy. On the other hand, Ramana *et al.* have employed an Au-catalysed selective addition of tryptamine to the nitrone group to obtain the pseudoindoxyl core.

In 2011, Tambar's group reported the first total synthesis of (±)-trigonoliimine C **13**, which was a benchmark achievement in the history of trigonoliimine synthesis (Scheme 37).[77] They hypothesized the biogenetic pathway for the family of these alkaloids that involves an oxidative aryl–aryl coupling of two tryptamine derivatives to form an unsymmetrical 2,2′-binary

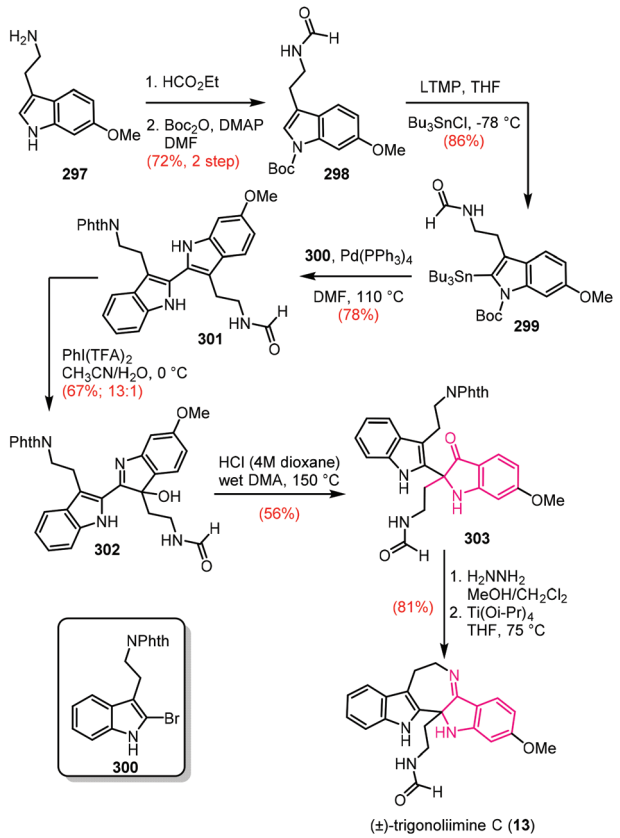

Scheme 37 Tambar's total synthesis of (±)-trigonoliimine C (**13**).

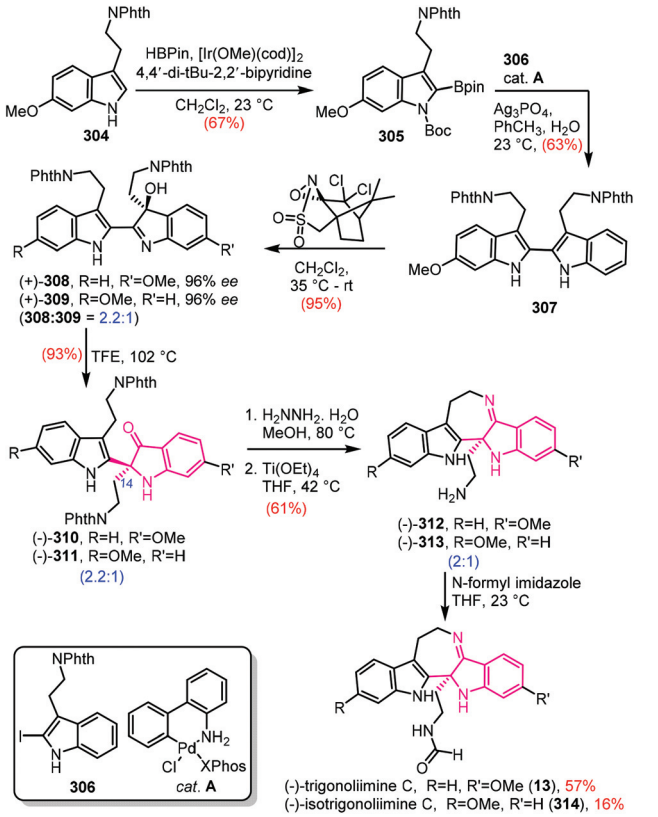

Scheme 38 Movassaghi's total synthesis of (−)-trigonoliimine C (**13**).

tryptamine moiety, which is converted to trigonoliimine scaffolds A–C through a series of selective oxidative rearrangements. With this biosynthetic hypothesis in mind, their total synthesis started with the synthesis of the Boc-protected 6-methoxytryptamine **298** in 2 steps from 6-methoxytryptamine (**297**) in 72% yield. Compound **298** was then subjected to a Boc-directed lithiation/stannylation sequence, to produce stannylindole **299**, which, upon Stille coupling with 2-bromotryptamine **300**, afforded compound **301** in 78% yield. The selective mono oxidation of **301** with $PhI(TFA)_2$ in acetonitrile and water solvent at 0 °C produced desired hydroxyindolenine **302** as the major product, along with a minor amount of the undesired product in a 13 : 1 ratio. The Wagner–Meerwein [1,2]-shift of **302** by using Brønsted acid HCl, along with *N*,*N*-dimethylacetamide as the solvent, formed key pseudoindoxyl **303**. This rearrangement addressed the major synthetic challenges for accessing the dense polycyclic scaffold and the fully substituted tertiary carbinamine stereocenter. Finally, the removal of the phthalimide and subsequent $Ti(Oi\text{-}Pr)_4$ mediated cyclisation afforded (±)-trigonoliimine C (**13**) in 81% yield over two steps.

Immediately after Tambar's report, Movassaghi and coworkers also reported the enantioselective total synthesis of (−)-trigonoliimine C (**13**) and revised its absolute stereochemistry of '14S' to '14R' as depicted in Scheme 38.[78] The synthetic approach for the key pseudoindoxyl core and the pentacyclic framework was similar to that of the Tambar group. The total synthesis began with the iridium catalysed *C*2-borylation of the 6-methoxytryptamine derivative **304**, followed by the Suzuki–Miyaura cross coupling of boronate **305** with 2-iodo-tryptamine **306** using a palladium-based precatalyst and silver phosphate as an additive to afford bis-tryptamine **307**. Treatment of **307** with Davis' oxaziridine provided an inseparable mixture of hydroxyindolenines (+)-**308** and (+)-**309** in 95% yield with 96% enantiomeric excess. A Wagner–Meerwein type 1,2-alkyl rearrangement of hydroxyindolenines (+)-**308** and (+)-**309** in trifluoroethanol resulted in the selective formation of pseudoindoxyl (−)-**310** and (−)-**311** (2.2 : 1) in 93% combined yield with high enantioselectivity. The di-Phth group was cleaved using excess hydrazine, followed by intramolecular dehydrative cyclisation, providing the cyclic imine **312**/**313**. Finally, *N*-formylation of the pendant 1°-amine group with *N*-formyl imidazole, followed by silica gel chromatography separation, provided (−)-**13** and its epimer (−)-**314** in 57% and 16% yields, respectively.

Later, in 2014, the same group reported the enantioselective total synthesis of **13**, as well as the stereochemical assignment and biological activity of all trigonoliimines, using the earlier described strategy with improved yields.[8] They reported that trigonoliimines A–C showed weak anticancer activity against HeLa and U-97 cells.

In the same year, Hao and co-workers achieved the biomimetic oxidative rearrangement of the bistryptamine framework into the core ring system of trigonoliimine C **320** (Scheme 39).[79] The synthesis began with the dimerization of *N*-phthaloyl tryptamine **315** to afford 2,2′-biindolyl **316**. After extensive effort, it was found that compound **316** oxidized with *in situ* generated dimethyldioxirane and provided desired **317** as a major product in 70% yield, along with 10% of 3,3′-dihydroxybisindole **316**. Compound **317** was subsequently subjected to a pinacol type rearrangement with a HCO_2H-saturated toluene mixture, affording compound **318**. Finally, removal of both the Phth-group followed by formylation with ethyl formate efficiently converted compound **319** into the core ring system of trigonoliimine C (**320**).

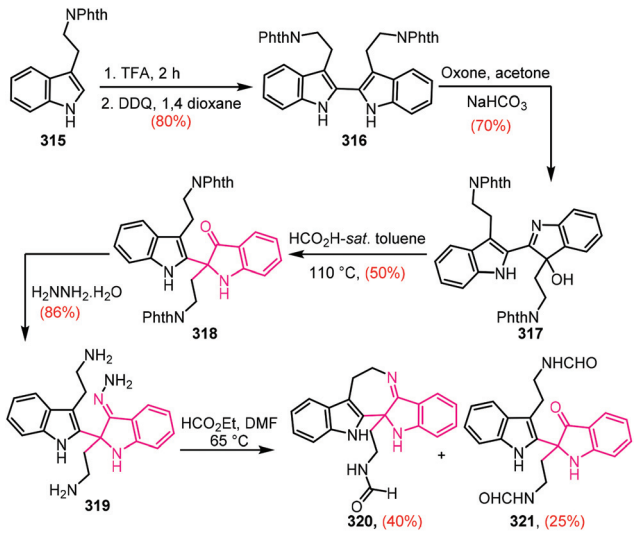

Scheme 39 Hao's biomimetic synthesis to make the core of trigonoliimine C.

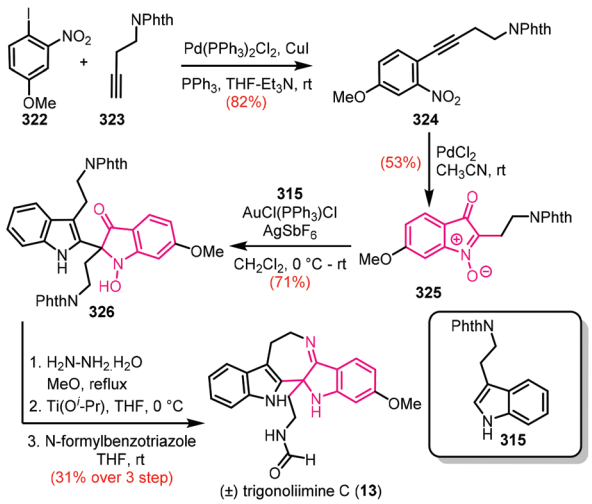

Scheme 40 Ramana's total synthesis of (±)-trigonoliimine C (**13**).

Table 1 Methods employed for the construction of the central pseudoindoxyl core

Key intermediate	Reagent	Natural product
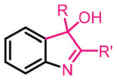	Acid/base semi pinacol rearrangement	Aristotelone, austamide brevianamide A/B, ibuluteine melokhanine E, mitragynine pseudoindoxyl, trigonoliimine C, erucalexin, isatisine A, mersicarpine
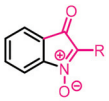	R′ addition (*C*2-alkylations)	Isatisine A, trigonoliimine C
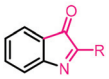		
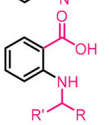	Base/Ac_2O	Mitragynine pseudoindoxyl, melokhanine E
	[Cu]-Catalysed C–N bond formation	Isatisine A

In 2013, Ramana *et al.* accomplished the total synthesis of **13** by employing three catalytic transformations, including Pd-mediated cycloisomerisation, [Au]-catalysed addition of protected tryptamine to isatogen and reduction of N–OH to the N–H group (Scheme 40).[80] The synthesis was commenced with the Sonogashira coupling of **322** with commercially available alkyne **323** affording **324** in 82% yield. Next, Pd-mediated cycloisomerisation of **324** led to the formation of isatogen **325** and further, in house developed [Au]-catalysed addition of *N*-phthalimido tryptamine **315** to **326** afforded *N*-hydroxyl indol-3-one in 71% yield. Conversion of **326** to natural product **13** occurred in 31% overall yield, through a three step protocol, which included the removal of both the Phth-group with concomitant N–OH reduction with hydrazine, intramolecular imine formation and *N*-formylation.

3. Conclusion and outlook

This review demonstrates how the total syntheses of challenging complex pseudoindoxyl natural products have been successfully achieved during the last 60 years. The various approaches described above for the construction of the pseudoindoxyl core can be summarized into four types. In the first and most widely employed approach, the oxidation of the corresponding 2,3-substituted indole derivative followed by 1,2-alkyl migration gives the required pseudoindoxyl core. This approach is suitable for both spiro and 2,2-disubstituted pseudoindoxyl molecules and hence it has attracted the most attention and plays an important role in total synthesis. The second approach is the regioselective *C*2-alkylation of the isatogen derivative leading to the 2,2-disubstituted pseudoindoxyl core.

The third approach comprises a base mediated formation of the C2–C3 bond from 2-cyano aniline or 2-carboxylic acid aniline derivatives furnishing the required pseudoindoxyl core. The fourth approach is the intramolecular amination of the corresponding aryl bromide derivative (Table 1). Despite this, the total synthesis of many pseudoindoxyl natural products has not yet been reported. Some of the reasons for this are: (i) the bio-activity of the pseudoindoxyl class of natural products has not been well explored; (ii) limited funding for research in total synthesis; and (iii) limited and inefficient synthetic methods for the construction of the pseudoindoxyl unit. In fact, the biological activity of only a few molecules has been explored, whereas the activity of a majority of pseudoindoxyl molecules has not been explored. Further improvement of the existing synthetic methods as well as the development of novel and flexible approaches for making the pseudoindoxyl core is needed to meet this challenge. With the advancement of natural product chemistry, more molecules with pseudoindoxyl skeletons will be isolated and identified along with their biological activity in the near future. This will drive synthetic chemistry across the globe to develop more efficient and concise synthetic methods and strategies. We hope that this review will inspire synthetic chemists to re-evaluate and develop new, efficient synthetic strategies for noteworthy divergent syntheses.

Conflicts of interest

There are no conflicts to declare.

Acknowledgements

P. S. D. and P. P. thank DST-INSPIRE for the research fellowship and K. V. and C. V. R. thank CSIR for research funding.

Notes and references

1 (*a*) N. K. Kaushik, N. Kaushik, P. Attri, N. Kumar, C. H. Kim, A. K. Verma and E. H. Choi, *Molecules*, 2013, **18**, 6620–6662; (*b*) M. Ishikura, T. Abe, T. Choshi and S. Hibino, *Nat. Prod. Rep.*, 2015, **32**, 1389–1471; (*c*) E. Stempel and T. Gaich, *Acc. Chem. Res.*, 2016, **49**, 2390–2402.

2 A. Baeyer and V. Drewsen, *Ber. Dtsch. Chem. Ges.*, 1882, **15**, 2856–2864.

3 K. Gomi, E. Kobayashi, K. Miyoshi, T. Ashizawa, A. Okamoto, T. Ogawa, S. Katsumata, A. Mihara, M. Okabe and T. Hirata, *Jpn. J. Cancer Res.*, 1992, **83**, 113–120.

4 J. F. Liu, Z. Y. Jiang, R. R. Wang, Y. T. Zheng, J. J. Chen, X. M. Zhang and Y. B. Ma, *Org. Lett.*, 2007, **9**, 4127–4129.

5 G.-G. Cheng, D. Li, B. Hou, X.-N. Li, Y.-Y. Chen, P.-K. Lunga, A. Khan, Y.-P. Liu, Z.-L. Zuo and X.-D. Luo, *J. Nat. Prod.*, 2016, **79**, 2158–2166.

6 L. T. Yamamoto, S. Horie, H. Takayama, N. Aimi, S. Sakai, S. Yano, J. Shan, P. K. T. Pang, D. Ponglux and K. Watanabe, *Gen. Pharmacol.*, 1999, **33**, 73–81.

7 M. T. Andrade, J. A. Lima, A. C. Pinto, C. M. Rezende, M. P. Carvalho and R. A. Epifanio, *Bioorg. Med. Chem.*, 2005, **13**, 4092–4095.

8 S. Han, K. C. Morrison, P. J. Hergenrother and M. Movassaghi, *J. Org. Chem.*, 2014, **79**, 473–486.

9 For selective reviews, see: (*a*) N. R. Ball-Jones, J. J. Badillo and A. K. Franz, *Org. Biomol. Chem.*, 2012, **10**, 5165–5181; (*b*) D. Cheng, Y. Ishihara, B. Tan and C. F. Barbas III, *ACS Catal.*, 2014, **4**, 743–762; (*c*) B. Yu, D. Q. Yu and H. M. Liu, *Eur. J. Med. Chem.*, 2015, **97**, 673–698; (*d*) T. L. Pavlovska, R. G. Redkin, V. V. Lipson and D. V. Atamanuk, *Mol. Divers.*, 2016, **20**, 299–344; (*e*) G.-J. Mei and F. Shi, *Chem. Commun.*, 2018, **54**, 6607–6621; (*f*) X. Fang and C. J. Wang, *Org. Biomol. Chem.*, 2018, **16**, 2591–2601.

10 (*a*) Y. Ji, X. He, C. Peng and W. Huang, *Org. Biomol. Chem.*, 2019, **17**, 2850–2864; (*b*) N. Marien, B. N. Reddy and G. Verniest, *Targets in Heterocyclic Systems*, 2017, (10.17374/targets.2018.21.308).

11 Isolation references for.(*a*) Bisleuconothic C – A. E. Nugroho, W. Zhang, Y. Hirasawa, Y. Tang, C. P. Wong, T. Kaneda, A. H. A. Hadi and H. Morita, *J. Nat. Prod.*, 2018, **81**, 2600–2604; (*b*) Cephaninone B/C – (i) P. Wu and C. Jao, *J. Nat. Prod.*, 2006, **69**, 1467–1470; (ii) C. Chang, Y. Hsu, Y. Wu and T. Chuang, *Int. J. Mol. Sci.*, 2015, **16**, 3980–3989; (*c*) Aristolarine – M. Hesse and R. Kyburz, *Helv. Chim. Acta*, 1984, **67**, 91; (*d*) Coronordine pseudoindoxyl – B. Hwang, J. A. Weisbach, B. Douglas, R. Raffauf, M. P. Cava and K. Bessho, *J. Org. Chem.*, 1969, **34**, 412–415; (*e*) Rupicoline & montanine – C. Niemann and J. W. Kessel, *J. Org. Chem.*, 1966, **31**, 2265–2269; (*f*) Conopharyngine pseudoindoxyl – P. A. Crooks and B. Robinson, *J. Pharm. Pharmacol.*, 1973, **25**, 820–823; (*g*) Dihydrocorynantheine pseudoindoxyl – J. D. Phillipson and S. R. Hemingway, *Phytochemistry*, 1975, **14**, 1855–1863; (*h*) Raunticine pseudoindoxyl – J. D. Phillipson and N. Supavita, *Phytochemistry*, 1983, **22**, 1809–1813; (*i*) For Isorespiline pseudoindoxyl – K. Kilminister and B. Webb, *Phytochemistry*, 1972, **11**, 389–391; (*j*) Hunteracine pseudoindoxyl – R. H. Burnell, A. Chapelle and M. F. Khalil, *Can. J. Chem.*, 1974, **52**, 2327–2330; (*k*) Notoamide O – S. Tsukamoto, H. Umaoka, K. Yoshikawa, T. Ikeda and H. Hirota, *J. Nat. Prod.*, 2010, **73**, 1438–1440; (*l*) Ervaoffines A/B – B.-Q. Tang, W.-J. Wang, X.-J. Huang, G.-Q. Li, L. Wang, R.-W. Jiang, T.-T. Yang, L. Shi, X.-Q. Zhang and W.-C. Ye, *J. Nat. Prod.*, 2014, **77**, 1839–1846.

12 (*a*) D. L. Boger, C. W. Boyce, R. M. Garbaccio and J. A. Goldberg, *Chem. Rev.*, 1997, **97**, 787–828; (*b*) J. Sakata and H. Tokuyama, in *Cutting-Edge Organic Synthesis and Chemical Biology of Bioactive Molecules*, Springer, Singapore, 2019, pp. 101–124.

13 D. S. Bhakuni, M. Silva, S. A. Matlin and P. G. Sammes, *Phytochemistry*, 1976, **15**, 574–575.

14 (*a*) R. Guller and H.-J. Borschberg, *Tetrahedron: Asymmetry*, 1992, **3**, 1197–1204; (*b*) R. Guller and H.-J. Borschberg, *Helv. Chim. Acta*, 1993, **76**, 1847–1862; (*c*) H.-J. Borschberg, *Tetrahedron Lett.*, 1994, **35**, 865–868.
15 C. Heathcock and D. Stoermer, *J. Org. Chem.*, 1993, **58**, 564–568.
16 R. V. Stevens and P. M. Kenney, *J. Chem. Soc., Chem. Commun.*, 1983, 384–386.
17 P. S. Steyn, *Tetrahedron Lett.*, 1971, **36**, 3331–3334.
18 A. J. Hutchison and Y. Kishi, *Tetrahedron Lett.*, 1978, **6**, 539–542.
19 A. J. Hutchison and Y. Kishi, *J. Am. Chem. Soc.*, 1979, **101**, 6786–6788.
20 P. S. Baran and E. J. Corey, *J. Am. Chem. Soc.*, 2002, **124**, 7904–7095.
21 A. J. Birch and J. J. Wright, *J. Chem. Soc. D*, 1969, 644b–645.
22 (*a*) R. Williams and T. Glinka, *Tetrahedron Lett.*, 1986, **27**, 3581–3584; (*b*) R. Williams, T. Glinka and E. Kwast, *J. Am. Chem. Soc.*, 1988, **110**, 5927–5929; (*c*) L. A. Adams, M. W. N. Valente and R. M. Williams, *Tetrahedron*, 2006, **62**, 5195–5200.
23 K. Miller and R. M. Williams, *Chem. Soc. Rev.*, 2009, **38**, 3160–3174.
24 F. Frebault and N. Sipkins, *Tetrahedron*, 2010, **66**, 6585–6596.
25 J. Robins, K. Kim and J. Scheerer, *J. Org. Chem.*, 2016, **81**, 2293–2301.
26 R. C. Godfrey, N. J. Green, G. S. Nichol and A. L. Lawrence, *Nat. Chem.*, 2020, **12**, 615–619.
27 H. Schmid and P. Karrer, *Helv. Chim. Acta*, 1947, **30**, 2081–2091.
28 D. O'Rell and V. Boekelheide, *J. Am. Chem. Soc.*, 1972, **94**, 3205–3212.
29 (*a*) M. S. C. Pedras and D. P. O. Okinyo, *Chem. Commun.*, 2006, 1848–1850; (*b*) M. S. C. Pedras and V. K. Sharma-Mamillapalle, *Bioorg. Med. Chem.*, 2012, **20**, 3991–3996.
30 M. S. C. Pedras, M. Suchy and P. W. K. Ahiahonu, *Org. Biomol. Chem.*, 2006, **4**, 691–701.
31 (*a*) R. Goutarel and M. Janot, *Ann. Pharm. Fr.*, 1953, **11**, 272–274; (*b*) D. F. Dickel, C. L. Holden, R. C. Maxfield, L. E. Paszek and W. I. Taylor, *J. Am. Chem. Soc.*, 1958, **80**, 123–125.
32 (*a*) M. Goutarel, M.-M. Janot, F. Mathys and V. Prelog, *Helv. Chim. Acta*, 1950, **39**, 742; (*b*) M. F. Bartlett, D. F. Dickel and W. I. Taylor, *J. Am. Chem. Soc.*, 1958, **80**, 126–136.
33 (*a*) G. Büchi, D. L. Coffen, K. Kocsis, P. E. Sonnet and F. E. Ziegler, *J. Am. Chem. Soc.*, 1965, **87**, 2073–2075; (*b*) G. Büchi, D. L. Coffen, K. Kocsis, P. E. Sonnet and F. E. Ziegler, *J. Am. Chem. Soc.*, 1966, **88**, 3099–3109.
34 G. K. Jana, S. Paul and S. Sinha, *Org. Prep. Proced. Int.*, 2011, **43**, 541–573.
35 G. Zhao, X. Xie, S. Tang and X. She, *Org. Lett.*, 2016, **18**, 2447–2450.
36 A. Karadeolian and M. A. Kerr, *Angew. Chem., Int. Ed.*, 2010, **49**, 1133–1135.
37 A. Karadeolian and M. A. Kerr, *J. Org. Chem.*, 2010, **75**, 6830–6841.
38 J. Lee and J. S. Panek, *Org. Lett.*, 2011, **13**, 502–505.
39 J. Lee and J. S. Panek, *J. Org. Chem.*, 2015, **80**, 2959–2971.
40 X. Zhang, T. Mu, F. Zhan, L. Ma and G. Liang, *Angew. Chem., Int. Ed.*, 2011, **50**, 6164–6166.
41 W. Wu, M. Xiao, J. Wang, Y. Li and Z. Xie, *Org. Lett.*, 2012, **14**, 1624–1627.
42 M. Xiao, W. Wu, L. Wei, X. Jin, X. Yao and Z. Xie, *Tetrahedron*, 2015, **71**, 3705–3714.
43 C. V. S. Kumar, V. G. Puranik and C. V. Ramana, *Chem. – Eur. J.*, 2012, **18**, 9601–9611.
44 (*a*) P. Patel and C. V. Ramana, *J. Org. Chem.*, 2012, **77**, 10509–10515; (*b*) P. Patel, B. N. Reddy and C. V. Ramana, *Tetrahedron*, 2014, **70**, 510–516.
45 G. Li, C. Piemontesi, Q. Wang and J. Zhu, *Angew. Chem., Int. Ed.*, 2019, **58**, 2870–2874.
46 A. Cholewczynski, P. Williams and J. Pierce, *Org. Lett.*, 2020, **22**, 714–717.
47 (*a*) F. De Simone, J. Gertsch and J. Waser, *Angew. Chem.,Int. Ed.*, 2010, **49**, 5767–5770; (*b*) M. Kawada, Y. Kawano, H. Sugihara, S. Takei and I. Imada, *Chem. Pharm. Bull.*, 1981, **29**, 1900–1911.
48 J. E. Zarembo, B. Douglas, J. Valenta and J. A. Weisbach, *J. Pharm. Sci.*, 1974, **63**, 1407–1415.
49 H. Takayama, H. Ishikawa, M. Kitajima and S. Horie, *J. Med. Chem.*, 2002, **45**, 1949–1956.
50 (*a*) H. Takayama, M. Kurihara, S. Subhadhirasakul, M. Kitajima, N. Aimi and S. Sakai, *Heterocycles*, 1996, **42**, 87–92; (*b*) H. Takayama, H. Ishikawa, M. Kurihara, M. Kitajima, N. Aimi, D. Ponglux, F. Koyama, K. Matsumoto, T. Moriyama, L. T. Yamamoto, K. Watanabe, T. Murayama and S. Horie, *J. Med. Chem.*, 2002, **45**, 1949–1956.
51 J. Kim, J. Schneekloth and E. Sorenson, *Chem. Sci.*, 2012, **3**, 2849–2852.
52 H. Takayama, N. Aimi and S. Sakai, *Yakugaku Zasshi*, 2000, **120**, 959–967.
53 (*a*) J. Ma, W. Yin, H. Zhou and J. M. Cook, *Org. Lett.*, 2007, **9**, 3491–3494; (*b*) J. Ma, W. Yin, H. Zhou, X. Liao and J. M. Cook, *J. Org. Chem.*, 2009, **74**, 264–273.
54 X. Sun and D. Ma, *Chem. – Asian J.*, 2011, **6**, 2158–2165.
55 A. Varadi, G. F. Marrone, T. C. Palmer, A. Narayan, M. R. Szabo, V. Le Rouzic, S. G. Grinnell, J. J. Subrath, E. Warner, S. Kalra, A. Hunkele, J. Pagirsky, S. O. Eans, J. M. Medina, J. Xu, Y. X. Pan, A. Borics, G. W. Pasternak, J. P. McLaughlin and S. Majumdar, *J. Med. Chem.*, 2016, **59**, 8381–8397.
56 T. S. Kam, G. Subramaniam, K. H. Lim and Y. M. Choo, *Tetrahedron Lett.*, 2004, **45**, 5995–5998.
57 J. Magolan, C. A. Carson and M. A. Kerr, *Org. Lett.*, 2008, **10**, 1437–1440.
58 A. Biechy and S. Z. Zard, *Org. Lett.*, 2009, **11**, 2800–2803.
59 E. L. McCaffery and S. W. Shalaby, *J. Organomet. Chem.*, 1967, **8**, 17.
60 R. Nakajima, T. Ogino, S. Yokoshima and T. Fukuyama, *J. Am. Chem. Soc.*, 2010, **132**, 1236–1237.

61 D. Desmaeele and J. d'Angelo, *J. Org. Chem.*, 1994, **59**, 2292–2303.
62 Y. Iwama, K. Okano, K. Sugimoto and H. Tokuyama, *Org. Lett.*, 2012, **14**, 2320–2322.
63 Y. Iwama, K. Okano, K. Sugimoto and H. Tokuyama, *Chem. – Eur. J.*, 2013, **19**, 9325–9334.
64 X. Zhong, Y. Li and F. S. Han, *Chem. – Eur. J.*, 2012, **18**, 9784–9788.
65 X. Zhong, S. Qi, Y. Li, J. Zhang and F. S. Han, *Tetrahedron*, 2014, **71**, 3734–3740.
66 X. Zhong, Y. Li and F. S. Han, *Chem. – Eur. J.*, 2012, **18**, 9784–9788.
67 Z. Xu, Q. Wang and J. Zhu, *J. Am. Chem. Soc.*, 2013, **135**, 19127–19130.
68 Z. Xu, Q. Wang and J. Zhu, *J. Am. Chem. Soc.*, 2015, **137**, 6712–6724.
69 Z. Lv, Z. Li and G. Liang, *Org. Lett.*, 2014, **16**, 1653–1655.
70 Z. Li, Q. Geng, Z. Lv, B. P. Pritchett, K. Baba, Y. Numajiri, B. M. Stoltz and G. Liang, *Org. Chem. Front.*, 2015, **2**, 236–240.
71 Y. Yang, Y. Bai, S. Sun and M. Dai, *Org. Lett.*, 2014, **16**, 6216–6219.
72 M. Pfaffenbach and T. Gaich, *Eur. J. Org. Chem.*, 2015, 3427–3429.
73 Y. Zhang, Y. Xue and T. Luo, *Tetrahedron*, 2017, **73**, 4201–4205.
74 Y. Liu and H. Wang, *Chem. Commun.*, 2019, **55**, 3544–3547.
75 R. Kim, A. J. Ferreira and C. Beaudry, *Angew. Chem., Int. Ed.*, 2019, **58**, 12595–12598.
76 C. J. Tan, Y. T. Di, Y. H. Wang, Y. Zhang, Y. K. Si, Q. Zhang, S. Gao, X. J. Hu, X. Fang, S. F. Li and X. J. Hao, *Org. Lett.*, 2010, **12**, 2370–2373.
77 X. Qi, H. Bao and U. K. Tambar, *J. Am. Chem. Soc.*, 2011, **133**, 10050–10053.
78 S. Han and M. Movassaghi, *J. Am. Chem. Soc.*, 2011, **133**, 10768–10771.
79 S. Liu and X. J. Hao, *Tetrahedron Lett.*, 2011, **52**, 5640–5642.
80 B. N. Reddy and C. V. Ramana, *Chem. Commun.*, 2013, **49**, 9767–9769.